Universidad San Jorge

Escuela de Arquitectura y Tecnología

ANÁLISIS DE ESCENARIOS DE CLIMA FUTURO E IMPACTO DEL CAMBIO CLIMÁTICO SOBRE LOS VIÑEDOS DEL TERRITORIO ESPAÑOL IBÉRICO-BALEAR

TESIS DOCTORAL

Emma Gaitán Fernández

Villanueva de Gállego. 2022

Universidad San Jorge

Escuela de Arquitectura y Tecnología

ANÁLISIS DE ESCENARIOS DE CLIMA FUTURO E IMPACTO DEL CAMBIO CLIMÁTICO SOBRE LOS VIÑEDOS DEL TERRITORIO ESPAÑOL IBÉRICO-BALEAR

TESIS DOCTORAL

Emma Gaitán Fernández

Villanueva de Gállego. 2022

Directora de Tesis

Mª Rosa Pino Otín

AGRADECIMIENTOS

Lo que obtienes al alcanzar tus metas no es tan importante como en lo que te conviertes

(Henry David Thoreau)

Llegar al final de este viaje no solo supone alcanzar una meta que creía casi imposible, sino que durante el proceso he coleccionado muchos momentos y enseñanzas que ya son una parte de mí. Por ello no quería dejar de agradecer a todos los que han contribuido a ello:

A Rosa, por ser el motor que ha movido este trabajo, con su apoyo y sus palabras de aliento en los momentos en los que quise tirar la toalla y su optimismo en las épocas de mayor entusiasmo.

A mis compañeros en la Fundación para la Investigación del Clima, no solo por lo que aprendo de ellos cada día, sino también por los buenos momentos que pasamos juntos. En especial a Robert y Javier, por darme siempre el empujoncito que necesitaba en aquellos momentos en que estaba atascada. Sus consejos y buenas palabras son un tesoro.

A Jaime y Luis, por creer en mí desde el principio y darme la maravillosa oportunidad de seguir creciendo día a día.

A mis padres, Federico y Conchi, por ser referentes en mi vida y no cortarme nunca las alas para alcanzar mis sueños. A mi hermana, Ana, mi apoyo incondicional.

A mi familia (Cristian, Leo y Vera), mi mayor logro, cuyo apoyo y amor me ha acompañado durante todo el proceso. Sin ellos esto no habría sido posible.

¡Gracias! a todos los que de alguna manera han contribuido a que haya llegado a la meta.

RESUMEN

El cultivo de la vid es una práctica ancestral en regiones mediterráneas como España y la región de Aragón en particular. Las características climáticas actuales de esta región la convierten en una zona especialmente óptima para su cultivo siendo un referente mundial. En el contexto actual de calentamiento global, las alteraciones climáticas esperadas (aumento de las temperaturas, variaciones en los regímenes pluviométricos e intensificación de los eventos extremos) pueden suponer un gran peligro para la idoneidad climática que caracteriza a la región. Por lo tanto, es esencial llevar a cabo estudios precisos que evalúen el impacto del cambio climático a escala local y orientados al sector vitícola en particular.

Con el fin de evaluar el impacto del cambio climático en el sector vitícola aragonés (como caso de estudio particular) así como en el español (Península y Baleares) se han considerado tres aspectos: variaciones en el clima promedio (temperatura y precipitación), variaciones en eventos extremos (olas de calor y frío así como episodios de sequía) e indicadores bioclimáticos de interés vitícola.

Para ello, se han generado por primera vez escenarios de clima futuro a escala local de temperatura, precipitación, olas de calor y frío, indicadores de sequía e indicadores bioclimáticos basados en nueve *Earth System Models* (ESMs) y dos *Representative Concentration Pathway* (RCP4.5 y RCP8.5) pertenecientes a la quinta fase del *Coupled Model Intercomparison Project* (CMIP5). Para la generación de escenarios a escala local se ha empleado una metodología de *downscaling* estadístico en dos pasos desarrollada por la Fundación para la Investigación del Clima (FIC) y que aporta un valor añadido a la toma de decisiones en materia de adaptación al cambio climático.

Como indicadores de sequía se han utilizado el Índice estandarizado de Precipitación (SPI) y el Índice estandarizado de Precipitación y Evapotranspiración (SPEI). Como indicadores bioclimáticos se han empleado el Índice de Huglin (HI), el Índice de frío (CI), el Índice de sequedad (DI) y el Índice hidrotérmico. Como complemento, se calcularon dos indicadores combinados: el Sistema de Clasificación Climática Multicriterio (Sistema MCC) y el Índice Compuesto (CompI).

Los resultados de temperatura y precipitación van en línea con las tendencias observadas en las últimas décadas: aumentos progresivos de temperatura (siendo más intensos en los meses estivales) y variaciones en el régimen pluviométrico a nivel de concentración (es decir, misma cantidad de precipitación registrada en menos tiempo).

En promedio para todo el territorio, a finales de siglo y bajo el escenario más desfavorable, se espera que las temperaturas experimenten sus mayores ascensos en los meses de verano, pudiendo aumentar hasta 7 ºC en el caso de las temperaturas máximas y 5.8 ºC en las temperaturas mínimas. Estos aumentos harán que la meseta sur, la costa mediterránea y las Islas Baleares superen fácilmente los 38 ºC. Los ascensos menos acusados se esperan en los meses de invierno (hasta 4 ºC) tanto para la temperatura máxima como la mínima.

Los episodios de olas de calor se espera que aumenten, en promedio para la región y bajo el escenario RCP8.5 a finales de siglo, su intensidad media en más de 2 ºC (superándose los 38.8 ºC) y su intensidad máxima en 3.6 ºC (lo que supondrían temperaturas por encima de los 41 ºC). Además se espera que la duración de la misma aumente hasta alcanzar de 12 a 20 días, en función del área a la que afecten. Por el

contrario, los episodios de olas de frío se mantendrán en la ocurrencia e intensidad actual.

Respecto a los episodios de sequía, los resultados difieren según se analice el SPI (basado exclusivamente en precipitación) o el SPEI (considerando el efecto de la temperatura a través de la Evapotranspiración). En el primero de los casos, no se aprecian cambios de interés y la región se mantendrá en valores normales de alternancia de periodos secos y húmedos. En el segundo de los casos, bajo el RCP8.5, se aprecia como toda la región tiende hacía episodios de sequía cada vez más intensos y extensos en el tiempo, sufriendo episodios de sequía de severos a extremos.

A nivel de territorio, la meseta sur peninsular, especialmente Andalucía, Extremadura y Murcia, junto con el Valle del Ebro serán las regiones más afectadas desde el punto de vista climático. Por un lado, son las zonas donde se espera que se alcancen los incrementos y las temperaturas más elevadas y por otro lado, son zonas bastante secas, con poca pluviometría. La combinación de ambas características hyará que estas regiones sufran fuertes episodios de sequía severa.

El hecho de que una de las zonas dónde se esperan que los cambios de temperatura sean más acusados sea el Valle del Ebro, es crucial para Aragón. Esta zona es la más poblada y de mayor concentración socioeconómica de la región lo que puede suponer un gran riesgo para la salud, la mortalidad, la movilidad y el bienestar socioeconómico entre otros factores.

En base a los resultados obtenidos para los indicadores bioclimáticos se espera que los indicadores térmicos (HI y CI) tiendan a aumentar a lo largo del siglo XXI, mientras que la escasez de agua (DI) será más pronunciada. Las tendencias encontradas no tienen la misma repercusión en todo el territorio. En el sur de la península, con valores de HI superiores a 3500°C y de CI por encima de 20°C y DI por debajo de -200 mm, la continuidad del sector vitivinícola en su estado actual se ve seriamente amenazada, con una disminución de los años climáticamente óptimos como muestran los valores de CompI. Por el contrario, el norte peninsular y las zonas montañosas, a pesar de los aumentos previstos, con HI inferiores a 2500°C, noches frescas (IC inferior a 15°C) y un aporte hídrico suficiente (DI superior a 150 mm) mejoran considerablemente su aptitud climática (CompI) aunque se mantiene el riesgo de enfermedad de mildiu debido al aumento de la temperatura y la humedad.

Disponer de información climática de calidad (basada en proyecciones climáticas robustas y fiables) ajustada a las características micro climáticas de la región y considerando los efectos climáticos que pueden tener implicaciones en el sector vitícola, supone una información de valor añadido imprescindible en la toma de decisiones para la adaptación al cambio climático.

Índice

1. INTRODUCCIÓN Y ANTECEDENTES

1.1 CAMBIO CLIMÁTICO Y MODELIZACIÓN CLIMÁTICA

El cambio climático es, sin lugar a dudas, uno de los grandes retos a los que se enfrenta la humanidad en el próximo futuro a nivel planetario. Desde que se crea en 1998 el IPCC (Panel Intergubernamental sobre Cambio Climático por sus siglas en inglés) con el fin de aunar esfuerzos en la lucha frente al cambio climático, se han podido hacer evaluaciones integrales del estado de los conocimientos científicos, técnicos y socioeconómicos sobre el cambio climático, sus causas, posibles repercusiones y estrategias de respuesta. Ha sido el encargado de unificar la metodología de trabajo así como la definición de los nuevos escenarios de clima futuro que han de ser utilizados por los centros de investigación en las simulaciones climáticas.

Los distintos informes de evaluación presentados por el IPCC destacan detalladamente los cambios en el clima ya registrados. Los datos observados no dejan lugar a dudas: se esperan cambios en los patrones de precipitación, aumento de las temperaturas, cambios en la ocurrencia de eventos extremos, alteraciones en las fechas de los ciclos fenológicos de los cultivos, eventos de sequía y olas de calor y frío más intensos y alteraciones en la aparición de enfermedades en cultivos, entre otros- Esto pone de manifiesto la necesidad de adaptarse a la nueva realidad climática y estar preparados para los cambios que se espera que ocurran en el futuro.

Las primeras conclusiones presentadas por el sexto informe del IPCC6, por sus siglas en inglés) (IPCC, 2021a y b) son contundentes respecto a la realidad actual (e indiscutible) de emergencia climática. Estas conclusiones, centradas en las bases físicas del clima, ponen de manifiesto cómo esta situación además está directamente ligada a la actividad humana, de manera que no hay ninguna región del planeta que no se haya visto afectada por algún efecto relacionado con el cambio climático.

Hay dos puntos clave en los que el informe es tajante: "la temperatura de la superficie global continuará incrementándose al menos hasta mitad de siglo teniendo en cuenta todos los escenarios posibles de emisiones" y “Es inequívoco que la actividad humana ha calentado la atmósfera, el océano y la superficie terrestre". Esto significa que, incluso en el escenario menos desfavorable, la temperatura seguirá en ascenso, ya que serán necesarios como mínimo 30 años para poder encauzar el daño ocasionado por las actividades humanas desarrolladas en las últimas décadas. Estas conclusiones no pretenden ser alarmistas, sino remarcar que, igual que la actividad humana es la principal causante del estado actual, también es la única que puede frenarla y que está a tiempo de ello.

Actuar contra el cambio climático es un reto realmente importante. Muchos de los cambios observados en las últimas décadas no tienen precedentes de situaciones similares (IPCC, 2021a y b) por lo que las medidas a adoptar no están definidas. Para hacer frente a esta problemática se tienen tres vías de trabajo. En primer lugar, diseñar medidas de mitigación a gran escala, que sean inminentes y contundentes a la hora de reducir su impacto. A continuación, adoptar medidas de adaptación adecuadas a cada sector y a su problemática particular y por último, entender la investigación como una herramienta de apoyo para adaptarse al cambio climático.

En las últimas décadas la comunidad científica ha centrado gran parte de sus esfuerzos en simular el clima futuro a través del desarrollo de Modelos Climáticos (MC), los cuales

pretenden representar el comportamiento e interacciones entre los distintos componentes del sistema climático y su evolución en las próximas décadas. Las proyecciones climáticas simuladas por los MCs son los pilares en los que se basarán los estudios de evaluación de impactos y se sustentarán las medidas de adaptación. Por tanto, disponer de un conjunto fiable y robusto de proyecciones climáticas es el punto de partida en cualquier estudio relacionado con el impacto que el cambio climático pueda tener en cualquier sector.

Son varios aspectos los que han de tenerse en cuenta en el estudio del impacto del cambio climático: 1) variaciones en las condiciones climáticas medias de la región, 2) alteraciones en la frecuencia de ocurrencia e intensidad de los eventos extremos y 3) consecuencias de dichas modificaciones climáticas. Los impactos como consecuencia del cambio climático no afectan de forma homogénea a todas las regiones por lo que es esencial que estos estudios se realicen a escala local considerando las distintas condiciones micro meteorológicas que coexisten dentro de una misma región.

Las proyecciones climáticas de variables como la temperatura y la precipitación proporcionan una visión del impacto general del cambio climático como consecuencia del calentamiento global. A partir de esta información, se evalúan variables extremas (como las olas de calor y los episodios de sequía) que proporcionan información sobre eventos que no ocurren con tanta frecuencia y que completan la visión en conjunto del cambio climático en una región, ya que se dispondrá de información promedio junto con información de extremos. Pero esta información no es suficiente para evaluar el impacto del cambio climático en la vid y se requiere de información climática adaptada a sus requerimientos heliotérmicos e hídricos, los cuáles se evalúan mediante indicadores bioclimáticos (Huglin 1978; Maglhaes 2008; Malherio et al., 2010).

En base a lo anteriormente expuesto, determinar la relación entre clima y viñedo y evaluar su **evolución futura**, cobra un especial interés en regiones como España donde el sector vitícola no es solo importante en términos de biodiversidad sino también socioeconómicos.

España es una de las regiones más afectada por los efectos del cambio climático. Se espera que en las próximas décadas la temperatura media ascienda en todo el territorio español entre 2 y 4 °C y que se produzcan ligeros cambios en la cantidad de precipitación acumulada anualmente. Los eventos de precipitación serán más concentrados en el tiempo (es decir, misma cantidad pero precipitada en menos días), y los fenómenos extremos serán cada vez más intensos (Porter and Semenov, 2005; Gaitán et al., 2019, 2020). Estas alteraciones climáticas supondrán un aumento de la demanda de regadío (Doll 2002), un aumento en la ocurrencia de enfermedades y plagas (Alig et al., 2002) así como cambios en la zonificación vitícola (Malheiro et al., 2010) entre otros impactos. Esto significa que eventos tales como olas de calor, sequías o precipitaciones extremas, entre otros, se producirán de forma más recurrente aumentándose considerablemente el riesgo socio-económico asociado a su presencia.

Existen varios estudios centrados en técnicas de regionalización o *downscaling* de temperatura para España (Ribalaygua et al., 2013a, 2013b; Frías et al., 2005; Hervada-Sala et al., 2000; Turco et al., 2014) pero estos no abordan la problemática de los eventos extremos de temperatura (ya sean días con temperaturas muy altas/muy bajas u olas de calor/frio). Los pocos estudios que existen relacionados con este aspecto se

centran en estudiar eventos históricos (Fernández-Montes and Rodrigo 2012; Fonseca et al., 2016). En el caso concreto de Aragón, hay pocos estudios que hayan desarrollado escenarios a escala local de temperatura y estos, en general, no contemplan situaciones extremas ni usan modelos pertenecientes a la quinta fase del Proyecto de Intercomparación de Modelos acoplados (CMIP5, en sus siglas en inglés, *Coupled Model Intercomparison Project*) (Buerger et al., 2007; Goncalves et al., 2014; Ribalaygua et al., 2013a).

Respecto a la generación de escenarios futuros de precipitaciones a escala local, existen estudios que generan proyecciones de precipitación en base a distintas técnicas de *downscaling* y conjunto de modelos climáticos para España (Osca et al., 2013; Turco et al., 2011; Barrera-Escoda et al., 2014) aunque la mayoría con modelos anteriores al CMIP5. El resto de estudios basados en modelos del CMIP5 se centran en regiones concretas como una cuenca hidrográfica (Miró et al., 2021), la región mediterránea (Monjo et al., 2016) o toda la península y lo hacen en base a modelos regionales generados en el *proyecto Coordinated Downscaling Experiment - European Domain* EURO-CORDEX (Lorenzo and Alvarez, 2021).

Por tanto, hasta donde sabemos no existía hasta la fecha ningún estudio para Aragón en base a CMIP5 y mediante *downscaling* estadístico que simule proyecciones climáticas ni de temperatura ni de precipitación. A nivel peninsular existen diversos estudios publicados sobre proyecciones climáticas en base al CMIP5. La mayoría de dichos estudios utilizan las salidas directas de los modelos o las salidas de EURO-CORDEX, por lo que no utilizan una metodología estadística.

1.1.1. Los modelos climáticos: herramienta para la simulación del clima

A día de hoy la herramienta más potente en la simulación del clima futuro son los modelos climáticos (MCs). Los MCs resuelven las ecuaciones fundamentales de las leyes y principios de la física que rigen los procesos en cada componente del sistema climático global (atmósfera, hidrosfera, criosfera, litosfera y biosfera), como los intercambios de energía y de masa, mediante métodos numéricos (figura 1). Los MCs están compuestos por diferentes módulos, cada uno de los cuales reproduce los procesos de cada componente del sistema climático, siendo los principales módulos atmosféricos (AGCM, de sus siglas en inglés) y los oceánicos (OGCM, de sus siglas en inglés).

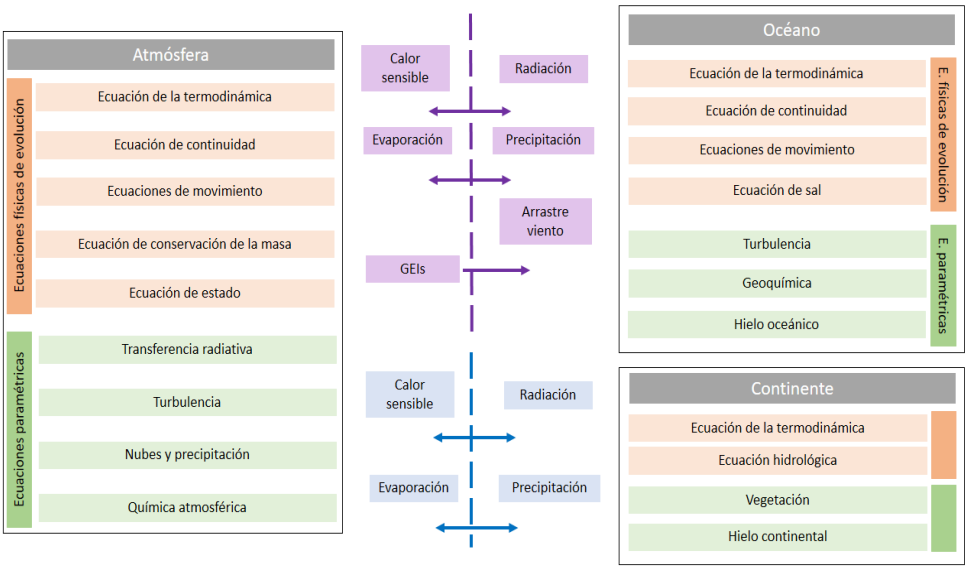

Figura 1. Esquema de ecuaciones y procesos físicos simulados por un MC. Elaboración propia.

Estas ecuaciones son ecuaciones en derivadas parciales, es decir, no lineales y no es posible hallar una solución analítica, por lo que en muchas ocasiones es preciso recurrir al análisis numérico para determinar una solución aproximada. Para poder resolverlas, los MCs consideran un espacio tridimensional discretizado en una cuadrícula (150km x 150km en la atmósfera y 100km x100km en el océano), así como la evolución temporal (diaria). En cada punto de la cuadrícula, se representan los valores de las variables del modelo y se resuelven las ecuaciones fundamentales obteniendo valores de las variables meteorológicas para un cierto instante en el futuro. Aquellos procesos que la rejilla del modelo no puede representar explícitamente (porque son de menor escala) se parametrizan, es decir, se estudian como si fueran variables derivadas a partir de otras y no como variables independientes (por ejemplo, la precipitación convectiva, la microfísica de las nubes, los flujos de la capa límite planetaria etc.) (figura 2).

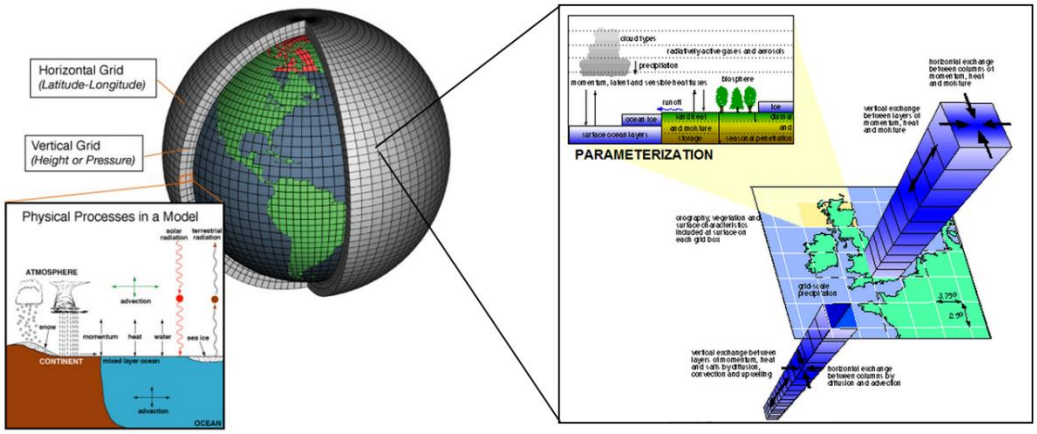

Figura 2. Figura esquemática de un MC y del concepto de rejilla espacial. Fuentes: National Oceanic and Atmospheric Administration (NOAA) y Climate Research Unit (CRU), 2000.

Por lo tanto, las características que van a definir el comportamiento de un MC serán la resolución espacial, el nivel de parametrización definido y la complejidad computacional en la ejecución del modelo, diferenciando aquellos modelos simples de los más complejos.

Los MCs han evolucionado mucho desde los años sesenta. De los modelos más simples (condicionados por las limitaciones computacionales y la simple representación de los procesos físicos a escala bidimensional) pasando por los modelos de circulación general (representación tridimensional del sistema atmósfera-océano así como la mejora en la capacidad computacional) hasta llegar a los más actuales.

La última generación de modelos climáticos son los *Earth System Models* (ESM), que describen los procesos que tienen lugar dentro y entre la atmósfera, el océano, la criosfera y la biosfera marina y terrestre. A parte de simular las ecuaciones físicas que rigen el comportamiento de la atmósfera y del océano, estos modelos además recogen los mecanismos químicos y biológicos que gobiernan a los elementos del sistema terrestre e incluyen erupciones volcánicas y variaciones de la radiación solar entrante.

Otro de los avances incluidos en los ESMs es la representación del ciclo del carbono, permitiendo el cálculo interactivo de las emisiones atmosféricas de CO_2 o similares. También pueden incluir otros componentes, como la química de la atmósfera, las capas de hielo, la vegetación dinámica, el ciclo del nitrógeno, modelos urbanos o de cultivos, etc. El principal avance frente a los MCs utilizados anteriormente es que permiten la interacción del sistema con el ciclo del carbono y tienen en cuenta la bioquímica y la biogeología marina (figura 3).

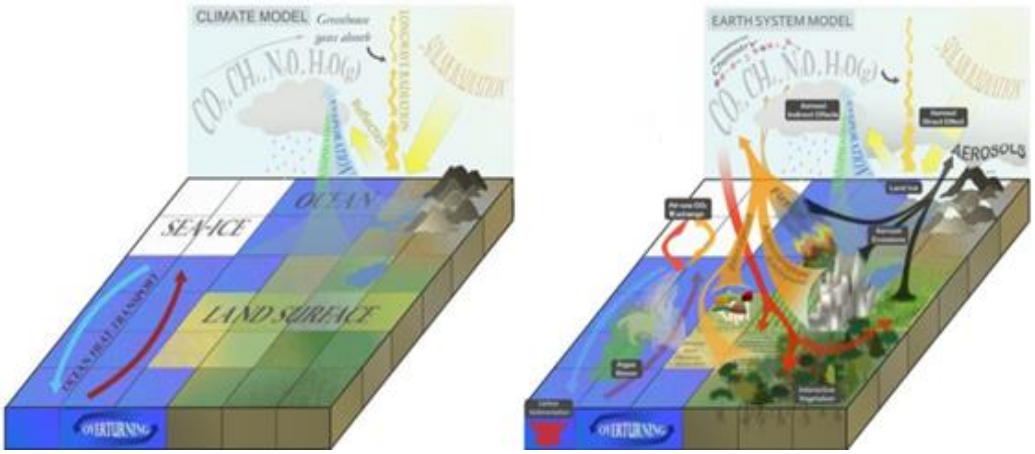

Figura 3. Características principales de los MCs y de los ESMs. Fuente: Heavens et al. 2013

Cada nueva generación de modelos climáticos está vinculada a una nueva fase del IPCC que establece las líneas de desarrollo generales que todos los centros responsables de los modelos han de tener en cuenta. Por ejemplo: rango de tamaños en las rejillas, cobertura espacial y temporal, variables mínimas a simular y número mínimo de escenarios de emisiones con los que trabajar, entre otros. Es por eso por lo que según se han ido sucediendo las distintas fases del IPCC, se ha ido modificando la manera en que se definen los escenarios de emisiones sobre los que se construyen las simulaciones o escenarios climáticos futuros. Los ESMs son la base del ***Climate Model***

Intercomparison Project en sus fases quinta CMIP5 (Taylor et al., 2012) y sexta CMIP6 (Eyring et al., 2016) y constituyen los conjuntos más actuales de experimentos coordinados de modelos climáticos disponibles. El CMIP es el organismo encargado de hacer públicos los resultados de los múltiples modelos en formato estandarizado y sus distintas fases van surgiendo de forma paralela al IPCC. Además, entre sus otros objetivos, se encuentra comprender los cambios climáticos pasados, presentes y futuros derivados de la variabilidad natural no forzada o en respuesta a cambios en el forzamiento radiativo en un contexto multimodelo. Esta comprensión incluye la evaluación del rendimiento de los modelos durante el periodo histórico y la cuantificación de las causas de la dispersión en las proyecciones futuras.

Según el IPCC (IPCC 2013: Glosario) un ***escenario climático*** es:

> "una representación plausible y a menudo simplificada del clima futuro, basada en un conjunto internamente coherente de relaciones climatológicas, que se construye para ser utilizada de forma explícita en la investigación de las consecuencias potenciales del cambio climático antropogénico, y que sirve de insumo para las simulaciones de los impactos"

De manera que un ***escenario de cambio climático*** será la diferencia entre un escenario climático concreto y el clima actual.

Los escenarios climáticos se definen por la necesidad de evaluar cómo y cuánto se verá afectado el clima futuro a consecuencia de la actividad humana (actividad antropogénica).

Hay dos formas de evaluar la influencia de la actividad humana. Por un lado, considerarla responsable de una emisión futura de gases de efecto invernadero y otras sustancias, entonces hablaremos de ***escenarios de emisiones*** o por otro lado, considerando el efecto final de las emisiones, es decir, el forzamiento radiativo. En este caso, hablaremos de **escenarios de forzamiento radiativo.**

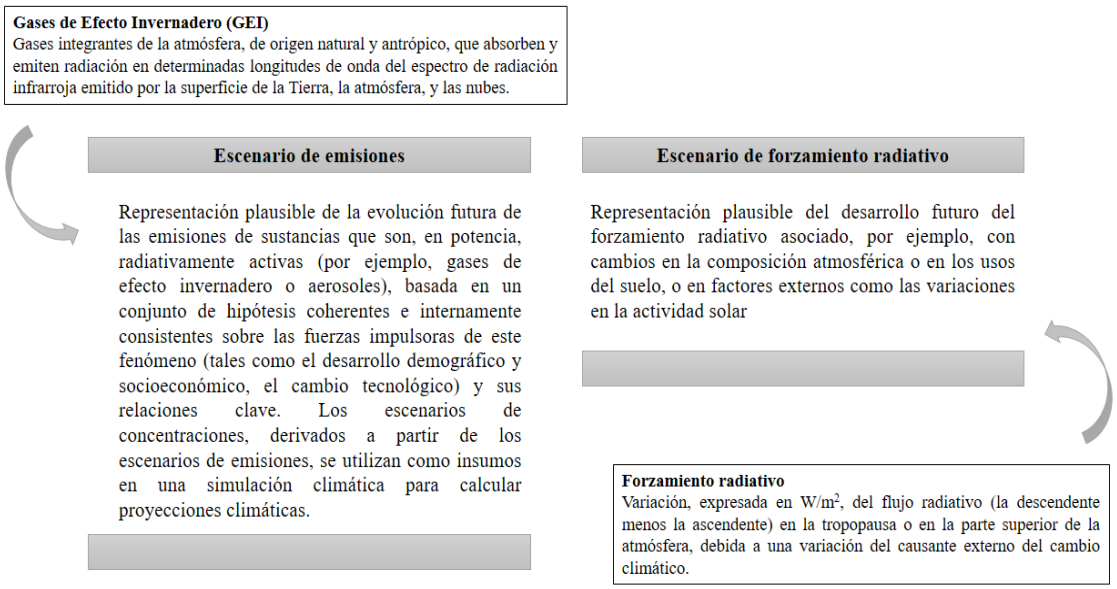

Figura 4. Diferencias entre escenario de emisiones y escenario de forzamiento radiativo. Definiciones extraídas del Glosario del IPCC (IPCC, 2013: Glosario)

El concepto de escenario de emisiones fue usado hasta el Cuarto informe del IPCC (IPCC 2007), de manera que en el Quinto informe (IPCC 2013) se ha trabajado con los escenarios de forzamiento radiativo.

Los escenarios futuros asociados al quinto informe del IPCC son los ***Representative Concentration Pathways (RCPs)***, definiéndose cuatro escenarios (en función del forzamiento radiativo alcanzado en 2100): RCP2.6, **RCP4.5**, RCP6.0 y **RCP8.5**. Estos escenarios se agrupan en lo que el IPCC denomina "Tier 1", aquellos RCPs que han de ser sí o sí simulados por todos los ESMs, y "Tier 2", aquellos que son opcionales. Al primer grupo pertenecerían los RCPs 4.5 y 8.5 y al segundo el resto; aunque la mayoría de los modelos proporcionan información de al menos RCP 2.6, 4.5 y 8.5.

El nombre de los RCPs viene dado por dos de sus características principales:

1) ***Representative***. Los RCPs se basan en escenarios de emisiones ya existentes, es decir, cada RCP representa un conjunto de escenarios de emisiones ya existentes (diferentes maneras de emitir gases de efecto invernadero y otras sustancias) con un mismo forzamiento radiativo en el 2100. Por lo que el RCP debe ser compatible tanto con escenarios extremos como con escenarios medios.

2) ***Concentration Pathway***. Este término hace hincapié en que los RCPs son la herramienta para la generación de escenarios de emisiones, y no escenarios en sí mismos, ya que, si bien recogen las distintas componentes de los forzamientos radiativos, no son un conjunto completo de proyecciones climáticas, socioeconómicas y de emisión.

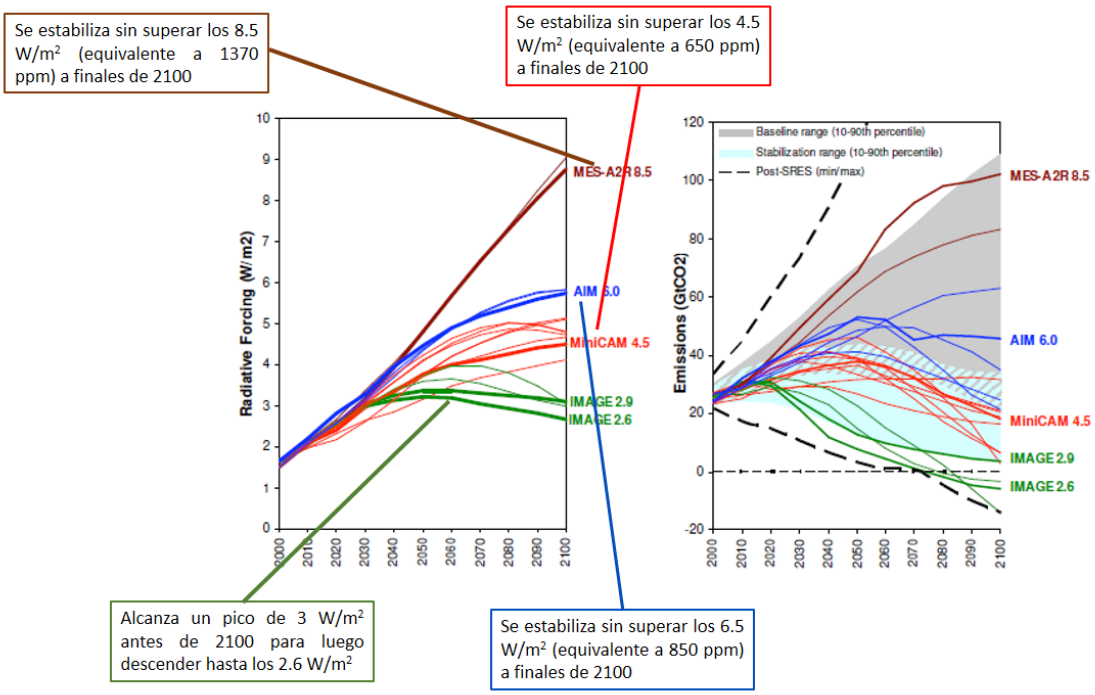

Figura 5. Esquema de los forzamientos radiativos y los escenarios de emisiones de CO_2 bajo distintos RCPs. (Figura basada en IPCC 2014)

Por lo tanto, para simular el clima futuro, se establecen hipótesis de cómo puede ser en el futuro el forzamiento radiativo según evolucione la sociedad. Bajo estas hipótesis se corren los MCs y se obtienen los escenarios climáticos.

A pesar de que los modelos climáticos suelen reproducir de forma adecuada las características generales de la atmósfera presentan ciertas limitaciones, de manera que tienen dificultades a la hora de simular fenómenos de pequeña escala o muy locales como consecuencia 1) de su insuficiente resolución espacial (2-3º), 2) la topografía está descrita con poco detalle dejándose fuera algunos forzamientos relacionados con la misma y 3) los procesos recogidos mediante parametrizaciones directas se ajustan de manera estadística para todo el planeta pudiendo ser ineficientes en regiones concretas.

1.1.2. Necesidad de pasar de escala global a escala local

Dado que en la mayor parte de los estudios de evaluación de impactos es necesaria la presencia de escenarios climáticos con resolución local de variables cercanas a la superficie terrestre (temperatura a 2 m., precipitación, etc.), surge la necesidad de adaptar la información proporcionada por los ESMs (de baja resolución espacial) a la información requerida por los modelos de impacto (de mayor resolución espacial-local en superficie).

Los estudios más recientes ponen de manifiesto la existencia de un cambio climático global, pero estas alteraciones no afectan de la misma manera a todas las regiones del mundo y dentro de una misma región, se observan cambios significativos ente puntos muy próximos.

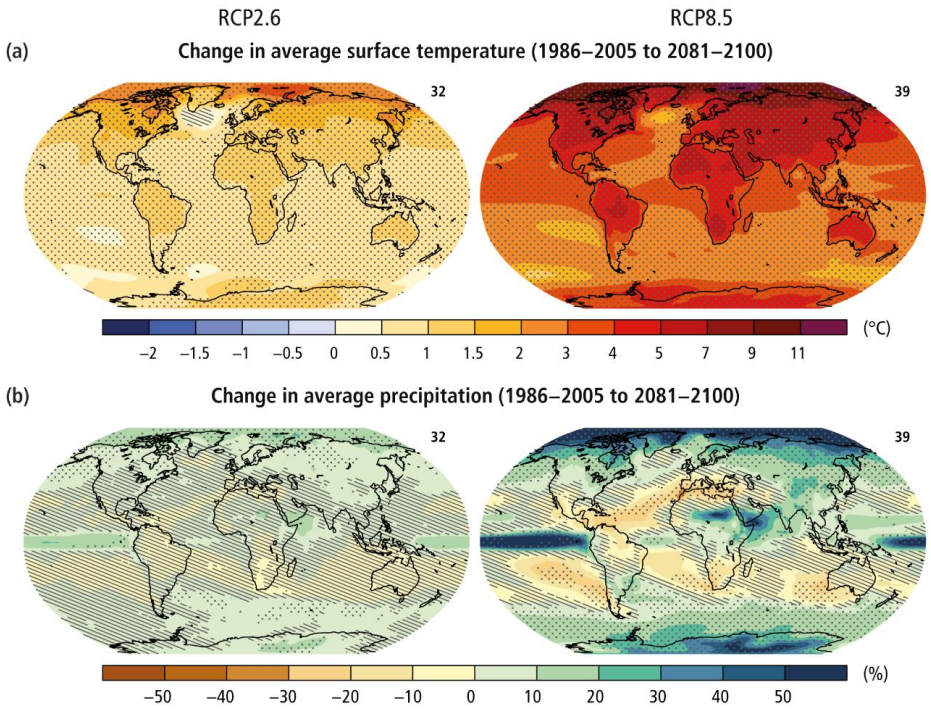

Figura 6. Cambio en la temperatura media de la superficie (a) y en la precipitación media (b) basados en las proyecciones de la media multimodelo para 2081-2100 en relación con 1986-2005 bajo los escenarios RCP2.6 (izquierda) y RCP8.5 (derecha). El número de modelos utilizados para calcular la media multimodelo se indica en la esquina superior derecha de cada panel. El punteado muestra las regiones en las que el cambio proyectado es grande en comparación con la variabilidad interna natural, y en las que al menos el 90% de los modelos coinciden en el signo del cambio. El rayado muestra las regiones en las que el cambio previsto es inferior a una desviación estándar de la variabilidad interna natural. Fuente: IPCC5 Report

En muchos casos, conocer la evolución del clima en una región o como promedio en una celda de un MC (200km x 200km) no es suficiente, necesitándose información a escala mucho más local. Este proceso de reducción de escala es conocido como ***regionalización o downscaling.*** En estos procesos se combina la información proporcionada por un MC con información más detallada como la topografía, la meteorología local, los usos del suelo etc.

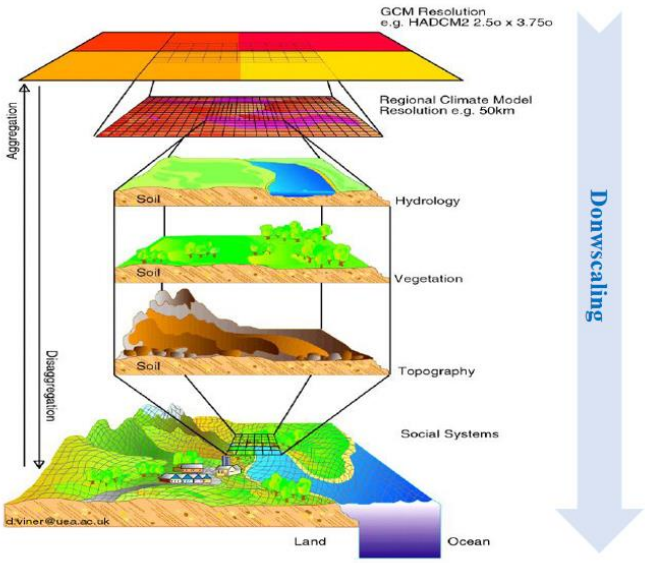

Figura 7. Figura esquemática de regionalización o downscaling (Fuente: David Viner, Climatic Research Unit, University of East Anglia, UK, 2000)

Existen múltiples técnicas de *downscaling*, desde las más básicas basadas en aplicar algún tipo de tratamiento estadístico a las distintas salidas de los modelos climáticos (denominadas MOS, *Model Output Statistics*) hasta las más avanzadas, fundamentadas en procesos físicos. Dentro de estas últimas se encuentran las técnicas de *downscaling* dinámico y *downscaling* estadístico:

- ***Downscaling estadístico***: se obtienen relaciones empíricas entre variables a gran escala (configuraciones atmosféricas de baja resolución, denominadas predictores) procedentes de los Modelos Climáticos y variables de alta resolución en superficie cuya simulación se quiere obtener (denominadas predictandos).
- ***Downscaling dinámico***: se incrementa la resolución del modelo en la zona de interés mediante anidando un modelo climático regional (RCM, por sus siglas en inglés) en las condiciones de contorno del modelo climático global o realizando una técnica de “zoom” de la rejilla del propio modelo climático global.

Cada técnica tiene ciertas ventajas e inconvenientes que hacen que una sea más apropiada que otra en función de las características del estudio en el que se vayan a utilizar. En términos generales el *downscaling* dinámico tiene una base física más fuerte y no requiere de una base de datos observados histórica frente al *downscaling* estadístico que exige asumir la hipótesis de que las relaciones detectadas en el pasado se mantendrán en el futuro, pudiendo provocar efectos de sobreajuste. Además requiere de una base de datos observados histórica, lo que supone un factor muy limitante en

aquellas regiones con pocas observaciones. Por otro lado, el *downscaling* estadístico permite recoger la micrometeorología local (siendo la mejor técnica en zonas de compleja orografía) y generar un mayor número de proyecciones climáticas (facilitando la cuantificación de la incertidumbre). Sin olvidar que su coste computacional es muy bajo, mientras que el elevado coste computacional de los modelos dinámicos restringe considerablemente el número de proyecciones climáticas a generar y su resolución espacial (en torno a los 25km) mantiene alguno de los problemas asociados a la resolución de los modelos climáticos

downscaling dinámico versus downscaling estadístico

Dinámico		Estadístico	
Ventajas	Inconvenientes	Ventajas	Inconvenientes
❑ Simula mecanismos climáticos. ❑ No realiza asunciones *a priori* sobre cómo están relacionados el clima presente y el futuro. ❑ Herramientas científicas permanentemente actualizadas.	❑ Los resultados son sensibles a las parametrizaciones iniciales. ❑ El posible sesgo existente en los MCGs se puede propagar a la escala local. ❑ Son modelos costosos en términos computacionales y de tiempo.	❑ Poco costosos en términos computacionales y de tiempo. ❑ Permite evaluar los resultados climáticos sobre un grupo de MCGs y sobre diversos escenarios. ❑ Puede corregir los sesgos propios de los MCGs.	❑ No incorpora mecanismos climáticos. ❑ No está ajustado para capturar varianzas o eventos extremos. ❑ Asume que las relaciones entre el clima local y el de gran escala permanecen constantes.
Aplicaciones		Aplicaciones	
❑ Áreas geográficas pobres en datos meteorológicos. ❑ Relaciona los resultados con procesos climáticos. ❑ Estudios asociados con extremos climáticos y variabilidad no-lineal.		❑ Regiones ricas en datos meteorológicos. ❑ Permite comparar el clima presente y el futuro de forma consistente. ❑ Medias climáticas, y ciertos rangos de variabilidad.	

Figura 8. Características principales de las distintas técnicas de *downscaling*. Elaboración propia.

En base a sus ventajas y desventajas, las técnicas estadísticas serán las más adecuadas en aquellas regiones ricas en datos meteorológicos y con una orografía compleja, gran diversidad climática y ocurrencia de fenómenos de pequeña escala (como la precipitación convectiva), mientras que las dinámicas serán de gran utilidad en aquellas regiones pobres en datos observados y sin una meteorología muy local (fenómenos micro meteorológicos fuera del alcance de la rejilla del modelo).

1.1.3. Datos necesarios para llevar a cabo el *downscaling* estadístico

❖ <u>Datos observados procedentes de estaciones meteorológicas</u>

Las técnicas de *downscaling* estadístico requieren de datos meteorológicos observados ubicados en la zona sobre la que se realiza el estudio. Estos datos deben cumplir unos estándares mínimos de calidad por lo que:

1) han de pasar por distintos controles que aseguren su fiabilidad. Todas las series de datos se ven sometidas a distintos tests que detectan inhomogeneidades, datos anómalos y huecos, desestimándose aquellas series que no los superen.

2) deben tener una extensión mínima de 5 años. Aunque lo deseable es que su extensión sea lo mayor posible alcanzando los 30-50 años en muchas zonas esto no es posible.

3) lo ideal es que cubran la mayor extensión del territorio y que lo hagan de forma lo más homogénea posible.

- Reanálisis

Un reanálisis es un conjunto de estimaciones históricas sobre una malla regular de variables meteorológicas y oceánicas generado por modelos avanzados de predicción climática y oceánica mediante técnicas de simulación de datos. Los modelos se aplican sobre un conjunto de datos observados procedentes, no solo de observatorios meteorológicos, sino de múltiples fuentes de datos observados como las boyas marinas, los globos sonda, los radiosondeos, los satélites y los radares.

El reanálisis ha de ser sometido a un proceso de calidad que permita eliminar aquellos valores que no sean coherentes como, por ejemplo, precipitaciones negativas, áreas sin datos, humedades relativas superiores al 100% o temperaturas mínimas superiores a las máximas.

Los MCs necesitan ser validados frente a una base de datos observados completa, es decir, sin datos faltantes. Por lo que el uso de un reanálisis es imprescindible para poder aplicar el proceso de validación de los modelos.

- Modelos Climáticos

El último set de datos que se requiere son los modelos climáticos. Las técnicas estadísticas, debido a su rapidez computacional, permiten trabajar con un número elevado de modelos climáticos (n) y RCPs (m), por lo que se obtendrá un conjunto de (n x m) proyecciones climáticas. Los MCs se corren de forma continua desde el pasado hacía el futuro, una vez que se simula el periodo de control, la ejecución se separa en tantas ejecuciones como RCPs se consideren. De cada modelo climático se dispone, por tanto, de una simulación de control denominada “Historical” para el periodo 1951-2005 y de entre 2 y 4 RCPs para el periodo 2006-2100.

Al igual que se hace con los datos observados y con el reanálisis, las simulaciones de control también han de someterse a controles de calidad para evitar la presencia de datos incoherentes.

La salida de control o Historical es imprescindible, no solo, para la generación de las simulaciones futuras, sino también para evaluar el comportamiento de cada modelo climático simulando el clima actual durante el proceso de validación.

1.1.4. Procesos de verificación y validación

Antes de proceder a generar las proyecciones climáticas a escala local, se llevan a cabo dos procesos que permiten evaluar el comportamiento de la metodología y el funcionamiento de cada modelo climático, información que ha de tenerse en cuenta e incluirse en las simulaciones futuras. Ambos procesos se realizan a escala local, es decir, en cada punto donde hay datos de un observatorio meteorológico.

- Verificación de la metodología

El proceso de verificación permite evaluar cómo de buena es la metodología de *downscaling* empleada a la hora de simular el clima actual, generalmente los últimos 30-50 años, según las bases de datos empleadas. Para ello, se comparan las series simuladas de los datos del reanálisis mediante *downscaling*, con los datos observados para un periodo común.

Durante el proceso de verificación han de tenerse en cuenta algunos aspectos:

1) Se han de simular correctamente tanto los valores medios como los extremos.

2) Se ha de simular correctamente tanto la escala climática (promedios de 30 años) como la diaria (cambios de un día a otro).

3) Aplicar estudios de robustez como análisis de años cálidos/fríos o secos/húmedos. Lo que se pretende con este análisis es comprobar que si los años elegidos para simular son cálidos (secos) la metodología es capaz de simular años fríos (húmedos) y viceversa.

4) Para poder realizar este proceso, la resolución espacial y temporal del reanálisis ha de adecuarse a la del modelo climático con el que se va a trabajar posteriormente. La resolución espacial de los reanálisis suele ser más fina que la de los MCs por lo que su rejilla se "relajará" a la resolución del MC extrapolando. En el caso de la resolución temporal se utilizará la diaria.

5) Dado que cada dato de la serie simulada por *downscaling* del reanálisis se corresponde con un día con fecha real, es posible comparar dichas series con los datos observados aunque no existen observaciones para todos los días del periodo, ya que las comparaciones se hacen día a día. Este aspecto es fundamental, ya que sugiere que se están reproduciendo de forma satisfactoria las relaciones físicas entre predictores y predictandos.

- Validación de los modelos climáticos

En general, los MCs tienden a simular un clima más frío, cálido, húmedo o seco de lo que éste es en realidad y además, no simulan de la misma manera todas las regiones del planeta. Esta diferencia entre modelos a la hora de simular el clima actual es consecuencia de las características de cada modelo, de las condiciones de contorno establecidas y de las parametrizaciones asumidas. Por lo tanto, determinar como de bueno es un MC simulando el clima de la región de estudio es una información clave a tener en cuenta en la generación de las proyecciones climáticas futuras. El proceso mediante el cual se evalúa a los MCs se conoce como validación y consiste en comparar las series simuladas mediante *downscaling* a partir de la salida de control (Historical) del MC con las series simuladas mediante *downscaling* a partir del reanálisis para un periodo común.

En contra de lo que ocurría en el caso de la verificación, en la validación no se pueden comparar las series simuladas día a día, ya que la salida de control no pretende simular un día concreto sino las características climáticas generales, por lo que la comparativa ha de hacerse a escala climática (en periodos de mínimo 30 años).

1.1.5. Proyecciones climáticas futuras

Una vez finalizados ambos procesos, si los resultados son buenos y se han descartado aquellos MCs que no funcionan adecuadamente en la zona de estudio, se proceden a generar las proyecciones climáticas futuras.

Por cada MC y RCP se tiene una simulación futura diaria hasta el 2100 sobre la que se va a aplicar el *downscaling*, obteniéndose así un abanico de proyecciones futuras diarias a escala local o regionalizadas. Aunque las series regionalizadas ofrecen datos diarios, su interpretación ha de hacerse a escala climática (periodos de al menos 30 años) y nunca sobre fechas concretas.

Las series simuladas pueden ser utilizadas desde dos enfoques:

1) atendiendo a los cambios esperados respecto al periodo de control. Para ello se analizará la diferencia de la variable a analizar entre un periodo futuro (por ejemplo, 2041-2070) y el periodo de control (por ejemplo, 1971-2000). Esta información proporciona una idea de cómo va a ser el cambio esperado de dicha variable.

2) atendiendo a los valores absolutos alcanzados. En ciertos estudios de impactos es necesario evaluar los valores que va a alcanzar una variable (por ejemplo, saber si la temperatura superará cierto umbral) más que la magnitud del cambio esperado.

Por ejemplo, si para un cultivo la temperatura máxima es crítica cuando se superan los 40 ºC en una época del año concreto, necesitaremos saber la evolución de la temperatura máxima en valor absoluto mejor que la variación de dicha variable. Saber que la variación esperada de temperatura máxima será de, por ejemplo, 2.5ºC no nos informa de si se superará el umbral crítico. En función de la aplicación que se le vaya a dar a las simulaciones futuras, se escogerá un formato u otro.

En el caso de que sea necesario trabajar con valores absolutos, es necesario corregir el error sistemático sobre las series simuladas. Para poder corregir dicho error, primero se han de cuantificar las incertidumbres asociadas al proceso de *downscaling*.

1.1.6. Incertidumbres asociadas al proceso de *downscaling*. Corrección del error sistemático

A lo largo del proceso de *downscaling* van surgiendo ciertas incertidumbres, es decir, estados de conocimiento incompleto como, por ejemplo, imprecisión de los datos, ambigüedad en la definición de un concepto o una proyección incierta de la conducta humana.

Estas incertidumbres pueden dividirse en cuatro grandes grupos asociados a los forzamientos radiativos futuros, a la técnica de *downscaling* empleada, a los modelos climáticos y a la variabilidad natural del sistema climático y su ocurrencia de forma encadenada por lo que reciben el nombre de ***cascada de incertidumbres***.

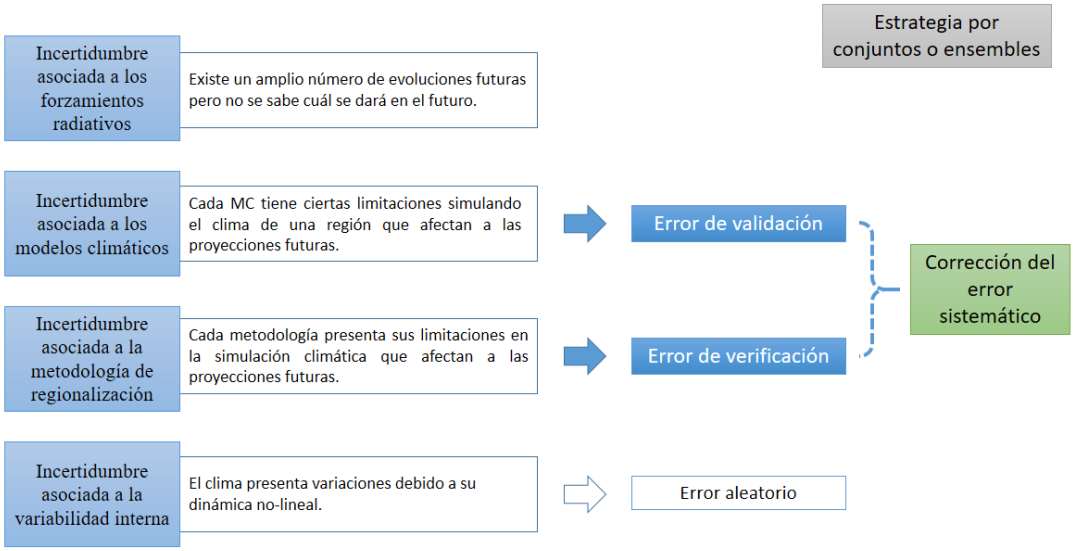

Figura 9. Esquema de las incertidumbres asociadas al proceso de *downscaling*. Elaboración propia.

Conocer estas incertidumbres es muy importante a la hora de manejar los escenarios climáticos futuros. A mayor incertidumbre, mayor ha de ser la cautela y flexibilidad con la que se manejen los escenarios. Cuantificar las incertidumbres es un proceso muy complejo pero imprescindible para un análisis correcto de los escenarios.

Se puede intentar minimizar el efecto de la incertidumbre mediante la corrección del error sistemático. El error sistemático se puede definir como el error que se comete al simular cierta variable con respecto a su valor observado. En este caso, el error sistemático es la combinación del error de verificación (asociado a la metodología de *downscaling*) y el error de validación (asociado a cada uno de los distintos MCs). El error asociado a la variabilidad climática y al forzamiento radiativo elegido se denominan errores de impredecibilidad (no son cuantificables) y no se incluyen en el error sistemático ya que no son medibles.

El error sistemático no se calcula directamente en el proceso de generación de proyecciones climáticas futuras a escala diaria ya que la manera en la que se calcula varía, no solo en función de la variable, sino también depende de la escala temporal a considerar (diaria, mensual, estacional o anual).

1.1.7. Limitaciones de los escenarios climáticos futuros

Los escenarios de clima futuros son estimaciones que pretenden dan una idea de cómo será el clima pero en ningún caso son predicciones categóricas y presentan ciertas limitaciones que han de tenerse siempre en cuenta:

1) no todas las variables se simulan con la misma robustez. Por ejemplo, las simulaciones de temperatura presentan mayor fiabilidad que las de precipitación ya que esta última variable presenta una variabilidad interna mucho mayor que dificulta su simulación.

2) al ser un estudio local, es decir, considerando la información proporcionada por los datos observados es muy importante que la información de partida sea de calidad y que

el observatorio esté ubicado lo más cerca posible y mejor correlacionado, climáticamente hablando, con el punto donde se quiere hacer el estudio.

3) ninguna proyección climática (asociada a una combinación MC-RCPs) es más probable que otra por lo que cuanto mayor sea el número de combinaciones MC-RCP más amplio será el abanico de proyecciones climáticas con el que trabajar y poder cuantificar las incertidumbres en las proyecciones.

1.1.8. Simulaciones futuras de variables derivadas

Una vez que se han generado series de temperatura y precipitación futuras a escala local, estas suponen el input para el cálculo de las variables derivadas de interés, como por ejemplo, episodios de olas de calor, índices de sequía o indicadores bioclimáticos.

El cálculo de las variables derivadas también lleva un proceso de verificación en el que se comparan los resultados obtenidos al calcular las variables en base a datos observados con las variables obtenidas sobre las series simuladas del reanálisis.

1.1.9. Consideraciones finales a la modelización climática

Mediante las técnicas de *downscaling* es posible adaptar la salida de los modelos climáticos (con resolución media de 200 km) a escala local y en el caso de las técnicas estadísticas incorporar información meteorológica mediante datos observados. Al final del proceso, se obtienen series simuladas diarias a escala local para todo el siglo XXI de temperatura (máxima y mínima) y precipitación. El número de proyecciones climáticas depende de la cantidad de modelos climáticos y RCPs considerados pero lo ideal es trabajar con el mayor número de ellos posibles.

Finalmente, para que la robustez de las proyecciones climáticas sea lo mayor posible es importante que se trabaje a escala local y diaria, que se utilicen los MCs más actuales a fecha de la realización del estudio y que se hagan estudios de verificación y validación completos que permitan evaluar las incertidumbres y calcular el error sistemático.

1.2 EL RETO DE LOS EVENTOS EXTREMOS

Existe un amplio consenso en la literatura científica en cuanto a que los efectos más graves del calentamiento global estarán relacionados no solo con un cambio en el clima medio, sino especialmente con un aumento de la frecuencia e intensidad de los fenómenos extremos (como los huracanes, las sequías y las olas de calor, entre otros) como se refleja en las conclusiones del IPCC y en estudios independientes (Cook et al., 2013). Por su ubicación al sur de Europa, hay dos fenómenos extremos con fuerte impacto en el territorio español: las olas de calor y los episodios de sequía.

Las olas de calor (definidas como un periodo de x días consecutivos con temperaturas extremas) son una forma de tiempo extremo que aumentará en frecuencia, intensidad y duración bajo la influencia de un clima cambiante durante los próximos años (IPCC 2013; Field et al., 2012). Los fenómenos de temperaturas extremas pueden afectar a muchos aspectos de la vida humana como la mortalidad, la salud, el confort o la agricultura y la hidrología (García-Herrera et al., 2005; Roldán et al., 2016) y de forma considerable al viñedo, ya que una larga exposición de la vid a altas temperaturas puede ocasionarle estrés térmico o suponer el achicharramiento de las hojas y/o el fruto.

El efecto que las altas temperaturas tienen sobre diversos sectores es un tema de gran interés científico, aunque en la literatura es difícil encontrar estudios que presenten proyecciones climáticas a escala local. La mayoría de estos estudios incluyen información sobre temperaturas extremas como herramienta para explorar el impacto de dichos extremos en un sector determinado (Tobias et al., 2014; Roldán et al. 2016; Royé et al., 2021) pero no hacen una evaluación propia de las mismas.

A nivel europeo existen tanto estudios sobre temperaturas extremas actuales (Soares et al., 2012; Seubert et al., 2014) como futuras. Estos últimos, o no están basados en CMIP5 (Estrella and Menzel 2013; Hertig et al., 2010) o están en base a EURO-CORDEX (Carvalho et al., 2021). Respecto a las olas de calor y eventos extremos, hay más cantidad de estudios publicados pero la gran mayoría abarcan áreas completas como toda Europa (Schoetter et al., 2015; Vautard et al., 2013), la región mediterránea (Zittis et al., 2016) o todo un país (Kim et al., 2018; Planton et al., 2008) quedándose Aragón fuera de casi todos ellos. En España los últimos estudios publicados sobre olas de calor (Lorenzo et al., 2021; Pereira et al., 2021) y altas temperaturas (Pereira et al., 2017; Lorenzo and Alvarez 2022) se basan principalmente en modelos provenientes de EURO-CORDEX.

La sequía, por otra parte, es probablemente uno de los fenómenos climáticos extremos con mayor impacto en la población mundial y que puede afectar a millones de personas cada año en todo el planeta (Bryant 1993; Wilhite 2000). Los episodios de sequía tienen graves efectos en la disponibilidad de agua y, por tanto, en actividades económicas como el turismo y la agricultura (Lesk et al., 2016) o profundos impactos en la salud humana (Stanke et al., 2013) y en los ecosistemas (Alary et al., 2014) que pueden persistir en el tiempo (Dai 2011).

Según las conclusiones aportada por el IPCC (IPCC 2014), el análisis del régimen de precipitaciones (Calbo, 2010; Lavaysse et al., 2012), las sequías (Burke and Brown, 2008; Lopez-Bustins et al, 2013) y las temperaturas extremas que aumentan

drásticamente la evapotranspiración (ET) (Rebetez et al., 2006) y disminuyen la humedad del suelo (Sheffield and Wood 2008) sugieren que los episodios de sequía podrían ser más graves en todo el mundo a lo largo del siglo XXI (Dai 2013).

Los escenarios de sequía publicados para España también son escasos: o bien proceden de estudios realizados con anterioridad al IPCC5 y en áreas muy reducidas (López-Bustins et al., 2013) o bien utilizan modelos del IPCC5 pero emplean información de *downscaling* dinámico proveniente de EURO-CORDEX (Collados-Lara et al., 2018; Marcos-García et al., 2017) u otros modelos dinámicos (Ojeda et al., 2021). En ambos casos Aragón es una zona que no están bien representando debido a la escala espacial de dichos estudios que no permite considerar con detalle las características climáticas de menor escala que condicionan a Aragón.

En este contexto, la mayoría de las zonas europeas y la región mediterránea parecen ser puntos calientes regionales destacados del cambio climático en los que se espera un aumento de la ocurrencia de eventos extremos (Beniston et al., 2007; Skaugen et al., 2004). En España, al igual que en el resto de Europa (Feyen and Dankers, 2009), se han producido diferentes series de sequías importantes en las últimas décadas. Además, la literatura parece indicar una tendencia al aumento de la escasez de agua meteorológica en la Península Ibérica, ya sea por un aumento de la frecuencia de los episodios de sequía o por un cambio en el régimen de precipitaciones (Fragoso et al., 2018; Gallego et al., 2011; García-Barrón et al., 2011; Machado et al., 2011; Ojeda et al., 2017; Vicente-Serrano et al., 2004). Esto hace necesario el desarrollo de escenarios futuros de sequías a escala local que sean adecuados para evaluar los impactos del cambio climático.

Por ello, la comunidad científica y las instituciones están dedicando muchos esfuerzos a entender, identificar, documentar y monitorizar estos fenómenos de forma más exhaustiva.

Uno de los grandes retos a los que se enfrenta la comunidad científica es la simulación de eventos meteorológicos o climáticos extremos, y no solo porque son variables que se mantienen fuera de los rangos promedios o porque se tiene menos información histórica que permita evaluar su ocurrencia, sino porque en muchos casos existen varias definiciones para un mismo evento, lo que dificulta su análisis y seguimiento. Un fenómeno extremo es fácil de reconocer, pero difícil de definir.

Según el glosario del IPCC (IPCC 2013: Glosario), se define un ***evento meteorológico o climático extremo*** como:

> "fenómeno meteorológico raro en determinado lugar y época del año. Aunque las definiciones de raro son diversas, la rareza normal de un fenómeno meteorológico extremo sería igual o superior a los percentiles 10º o 90º de la estimación de la función de densidad de probabilidad observada."

distinguiendo entre fenómenos simples (aquellos eventos meteorológicos locales e individuales que exceden un umbral crítico en una escala continuada) y fenómenos complejos (tiempo severo asociado a un fenómeno climático particular como consecuencia de una combinación crítica de variables).

Los extremos eventos no pueden describirse en función de una única variable ya que vienen definidos por gran cantidad de atributos. Desgraciadamente, la naturaleza multidimensional de estos fenómenos suele pasarse por alto, ya que se establecen rankings basados en un único atributo, perdiéndose información muy valiosa para su estudio.

Díaz and Murnane (2008), propusieron una taxonomía simple que permite analizar el evento en función de su rareza, severidad y duración del evento (figura 10).

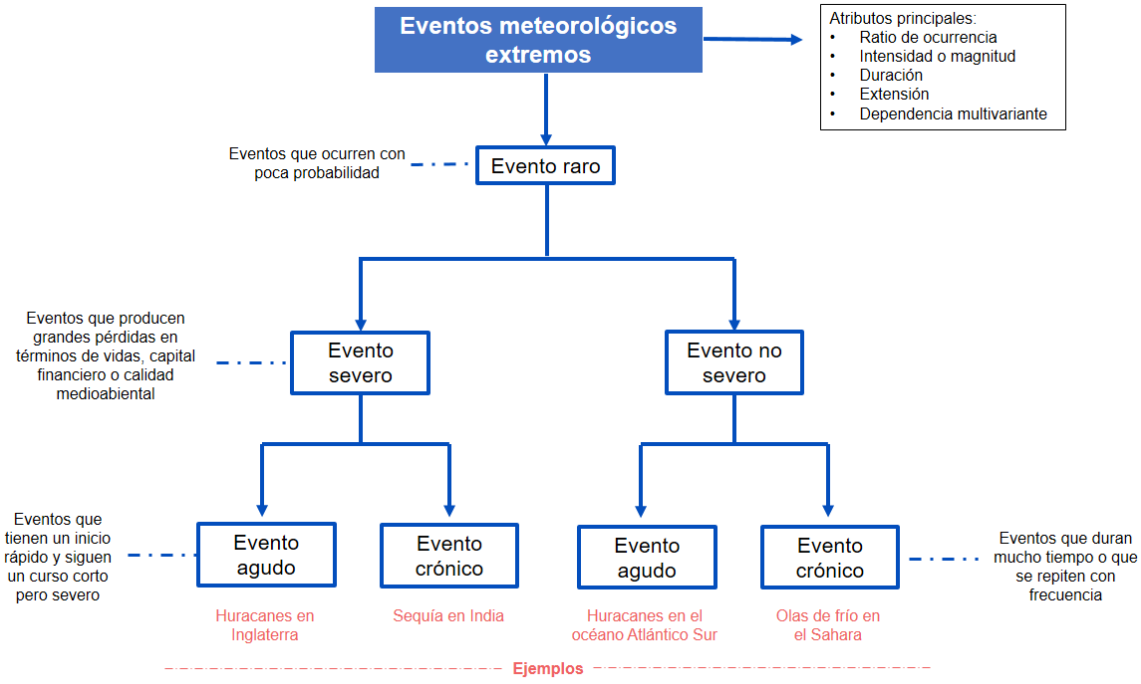

Figura 10. Clasificación de los eventos meteorológicos extremos en función del grado de severidad. Elaboración propia basado en Díaz y Mumane, 2008.

Una de las preguntas más recurrentes dentro de la comunidad científica es ¿qué procesos pueden propiciar la aparición de un fenómeno extremo? Stephenson 2008, propone dos orígenes:

1) El principio evolutivo, es decir, el evento extremo no ocurre de forma estacionaria sino que evolucionan de otros eventos menos extremos hasta su completo desarrollo.

2) El principio estacionario. Eventos extremos casi estacionarios, como las temperaturas, presentan una ratio de cambio en su amplitud igual cero. Esta característica implica que existe un balance entre la tendencia de los forzamientos y las disipaciones.

Además, hay ciertos procesos que pueden dar lugar y/o favorecen la formación de eventos extremos. Por ejemplo, el rápido crecimiento de un sistema debido a inestabilidades, el desplazamiento de sistemas sinópticos a nuevas localizaciones o su aparición en diferentes épocas del año. También la coincidencia temporal y espacial de varios fenómenos que de forma individual no son considerados extremos pero que

combinados aumentan su intensidad o cambios en la persistencia u ocurrencia de los fenómenos que pasan a ser crónicos, entre otros. La clave se encuentra en entender cómo estos procesos han actuado en el pasado y como se comportarán en el futuro.
Según el IPCC6 (IPCC 2021a y b), la ocurrencia de eventos extremos no tiene precedente en los registros observados y se espera que esta aumente en las próximas décadas como consecuencia del calentamiento global, de manera que cada leve aumento tiene un impacto importante. En los últimos años se ha reforzado la evidencia de que ciertos fenómenos extremos se han recrudecido como consecuencia de la influencia humana:

- En todas las regiones se ha observado un aumento en los episodios de calor, especialmente las zonas continentales provocando un fuerte impacto en la salud y el bienestar general. Estos episodios ocurren de forma más regular, ampliando su periodo de aparición.
- Se ha observado un aumento en el número de días y noches cálidas y un descenso en el número de días y noches frías.
- El cambio climático también juega un papel importante en la ocurrencia de eventos de lluvia extremos, siendo cada vez más intensos y localizados espacial y temporalmente. Se espera que estos eventos se intensifiquen en torno a un 7% por cada 1ºC de calentamiento global.
- En el lado opuesto, ha aumentado el área afectada por sequías, cada vez más severas y prolongadas.

Los datos observados son claros al respecto: el número de eventos extremos ha crecido en casi todas las regiones del mundo, siendo muy pocas aquellas en las que ha disminuido. El siguiente paso, para poder predecir los fenómenos extremos de la mejor forma posible, es saber cuántos de esos fenómenos son debido a la variabilidad natural del sistema climático y qué porcentaje consecuencia de la actividad humana.

Para responder esta pregunta, se aplican estudios de “atribución” que permiten evaluar si la intensidad y/o frecuencia de un evento extremo ha cambiado o cambiará como consecuencia del cambio climático. En este tipo de estudios hay que lidiar con ciertas limitaciones que dificultan los trabajos de atribución. En primer lugar, la calidad de los datos observados, que normalmente son muy cortos para recoger fenómenos meteorológicos con periodos de ocurrencia de más de 30/50 años. En segundo lugar, la dificultad de los modelos para simular un evento extremo concreto y finalmente, cómo de bien los modelos conocen los procesos físicos que rigen dicho evento y de qué manera se verán alterados por el cambio climático. En aquellos eventos donde se vean bien representadas todas las condiciones, el grado de confiabilidad será mayor y viceversa.

La importancia de poder evaluar el impacto que el cambio climático tiene en la ocurrencia y características de estos fenómenos es una pieza clave para poder simularlos con el mayor grado de confiabilidad posible. Es tanto el interés en avanzar en este aspecto que desde el 2011 se publica de forma anual el informe “Explicando los eventos extremos desde una perspectiva climática” publicado como suplemento especial dentro del Boletín de la Sociedad Meteorológica Americana (BAMS de sus siglas en inglés), donde se recogen decenas de estudios de atribución. Por desgracia a

día de hoy sabemos que el cambio climático es una causa más, añadida a las ya existentes, de aparición de eventos extremos pero no podemos saber si es “la causa”.

Conocer el comportamiento futuro de los fenómenos extremos de mayor impacto en la región considerada en este estudio como las olas de calor y de frío y las sequías con gran efecto en el sector vinícola es de gran importancia para minimizar los impactos negativos y evaluar el riesgo asociado a cada fenómeno. El riesgo asociado a un episodio extremo puede entenderse como la combinación entre las características naturales del propio fenómeno (duración, intensidad, extensión), la vulnerabilidad de la sociedad frente a dicho fenómeno y la capacidad de prevención frente a dicho fenómeno (figura 11).

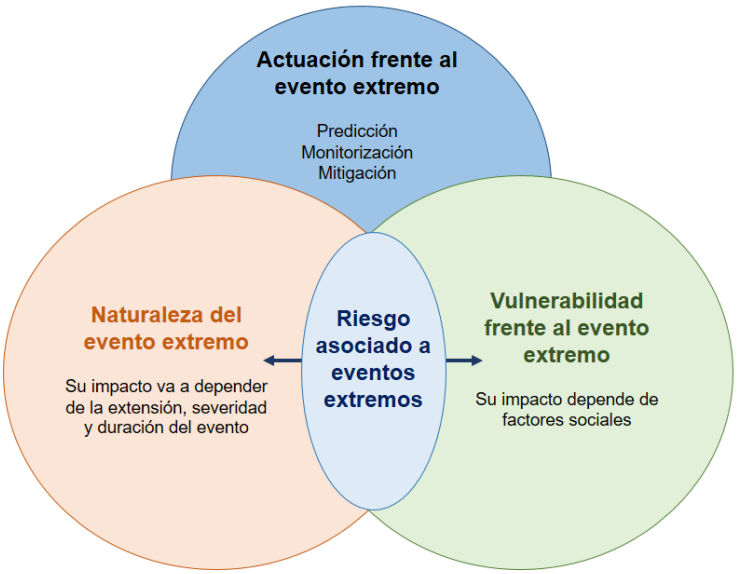

Figura 11. Riesgo asociado a un evento meteorológico extremo en base a los elementos que lo condicionan. Elaboración propia.

1.2.1. Episodios de olas de calor y frío

Existen muchas y muy variadas formas de definir una ***ola de calor***. Por ejemplo:

- Según la Agencia Estatal de Meteorología (AEMET) una ola de calor es “un episodio de al menos tres días consecutivos, en que como mínimo el 10% de las estaciones consideradas registran máximas por encima del percentil del 95% de su serie de temperaturas máximas diarias de los meses de julio y agosto del periodo 1971-2000”.
- La Organización Meteorológica Mundial (WMO, de sus siglas en inglés) lo define como “un evento extremo condicionado por un marcado calentamiento del aire o por una invasión de aire cálido sobre una extensa región y con una duración desde pocos días a varias semanas”.
- El IPCC lo define como “un periodo de calor anormal e incómodo”.
- EURO-CORDEX considera que un episodio de ola de calor es “un periodo de al menos tres días consecutivos en los que la temperatura máxima diaria supere el percentil 99 de las temperaturas máximas diarias de los meses de mayo a septiembre para el periodo de control de 1971 a 2000”.

Además de las anteriormente citadas, una ola de calor se puede definir en función de los datos que se manejan o del sector en el que se vayan a analizar. Por ejemplo, algunas definiciones se han utilizado para identificar olas de calor en una serie temporal de datos de temperatura (Smith et al., 2013). En otras ocasiones la elección de la definición de ola de calor puede influir tanto en las tendencias proyectadas (Smith et al., 2013) como en las estimaciones de los riesgos durante los eventos (Anderson and Bell 2009; Chen et al., 2016; Kent et al., 2014).

Según las recomendaciones de la WMO (2010), una definición práctica y cualitativa de una ola de calor debe considerar la existencia de un tiempo caluroso marcado y no habitual en una región durante al menos dos días consecutivos en el periodo caluroso del año, basándose en las condiciones climáticas locales, con condiciones térmicas registradas por encima de determinados umbrales.

Por otra parte, y a grandes rasgos, una ***ola de frío*** puede definirse como un acontecimiento meteorológico caracterizado por un fuerte descenso de la temperatura del aire cerca de la superficie que conduce a valores extremadamente bajos. Otras definiciones manejadas por organismos nacionales e internacionales son:

- AEMET define una ola de frío como “un episodio de al menos tres días consecutivos, en que como mínimo el 10% de las estaciones consideradas registran mínimas por debajo del percentil del 5% de su serie de temperaturas mínimas diarias de los meses de enero y febrero del periodo 1971-2000”
- La WMO define un episodio de ola de frío como “un enfriamiento marcado del aire o una invasión de aire muy frío en una zona amplia”.
- Según el IPCC, una ola de frío es un evento que suele causar problemas y graves impactos en la población, especialmente en las altitudes del norte.
- EURO-CORDEX define un episodio de ola de frío como “un periodo de al menos tres días consecutivos en los que la temperatura mínima diaria no supere el percentil 1 de las temperaturas mínimas diarias de los meses de octubre a abril para el periodo de control de 1971 a 2000”.

Las directrices marcadas por la WMO recomiendan considerar un episodio de ola de frío como "un tiempo frío marcado e inusual que se caracteriza por un descenso brusco y significativo de las temperaturas del aire cerca de la superficie (máximas, mínimas y medias diarias) en una zona amplia y que persiste por debajo de ciertos umbrales durante al menos dos días consecutivos durante la estación fría".

Según recomienda la WMO (2015) en su guía *“The Guidelines on the definition and monitoring of extreme weather and Climate Events”*, los episodios de ola de calor y frío han de evaluarse atendiendo a las siguientes características:

- Duración media: número medio de días que duró la ola de calor.
- Intensidad media: valor medio de la temperatura durante la ola de calor.
- Intensidad máxima: valor máximo que alcanzó la temperatura durante la ola de calor.
- Extensión espacial: área ocupada por la ola de calor.

Los episodios de ola de calor y ola de frío se calculan en base a las características climáticas de cada punto, por lo que el umbral (el valor de temperatura) que determina

si un día es demasiado cálido (o frío) no es fijo y no debe ser tomado como referencia fuera del punto para el que ha sido determinado.

1.2.2. Episodios de sequía

Las sequías son otro de los eventos climáticos más extremos y persistentes y uno de los episodios menos entendidos ya que su propia naturaleza intrínseca lo convierte en un fenómeno de gran complejidad (Hagman 1984). Además, es uno de los fenómenos naturales que más afectan a la sociedad ya que su impacto no siempre es cuantificable en el mismo momento en el que se detecta el fenómeno como sí ocurre con otros fenómenos meteorológicos tales como los huracanes, los terremotos o las inundaciones (Bryant 1991; Wilhite 1992). Por este motivo, es uno de los temas más recurrentes en la comunidad científica (Scheffield et al., 2012; Dai 2013; Spinoni et al., 2015) y desde las instituciones se están haciendo grandes esfuerzos por construir una base de datos de sequía que permitan ayudar a cuantificar el fenómeno como el *European Drought Observatory* (www.ge.uio.no/de) donde se recopila información del *Combined Drought Index*, CDI (Sepulcre-Canto et al., 2012) y del *European Drought Impact Inventory*, EDII (Stahl et al., 2012) o el *National Drought Mitigation Center* que realiza un inventario semanal de las condiciones de sequía en US a través de varios índices de sequía. En España se ha generado una base de datos del SPEI (Vicente-Serrano et al., 2017).

Las características que hacen que esté fenómeno sea más complejo de cuantificar son:

1) Los fenómenos de sequía suelen acumularse en el tiempo, desde pocos meses a años, y sus efectos siguen repercutiendo en algunos sectores incluso años después de que haya terminado el episodio.

2) No hay una definición estándar y global que determine un fenómeno de sequía, sino que hay cientos de definiciones generalmente relacionadas con las características climáticas y socioeconómicos de la región para la que se define (Wilhite and Glantz 1985).

3) A diferencia de otros fenómenos como los tornados o los terremotos, los episodios de sequía no causan pérdidas de vida ni daños estructurales sino que sus efectos son más silenciosos, por lo que muchos servicios de protección civil colocan a este fenómeno en el ranking de los más peligrosos (Bryant 1991). Las consecuencias de la sequía también dependen de su uso socioeconómico por lo que tienen una componente social y otra cultural (Hayes 2011). Como ejemplo, se produce escasez de agua debido al aumento de la población, a los usos agrícolas, usos energéticos o al consumo en sectores industriales (Bates et al., 2008).

4) Debido a que los efectos asociados a un episodio de sequía pueden perdurar, e incluso, intensificarse con el paso de los meses, en la mayoría de las ocasiones no se cuantifican adecuadamente debido a la falta de registros históricos (Hayes 2011). Además, es complicado por los múltiples mecanismos que lo causan y por su operacionabilidad a diferentes escalas espaciales y temporales convirtiéndola en uno de los fenómenos más difíciles de monitorizar y manejar (Wilhite 1992).

Atendiendo exclusivamente al punto de vista meteorológico, un ***episodio de sequía*** es (Wilhite 2000):

> "la interrupción durante un tiempo prolongado de los patrones normales de la circulación global"

siendo contadas las ocasiones en las que este fenómeno se analiza exclusivamente desde esta perspectiva, sino que en general se amplía el concepto considerando el impacto que este fenómeno tiene en otros sectores. Es por esto, que se habla de cuatro tipos de sequía cuyos efectos van encadenándose: sequía meteorológica, agrícola, hidrológica y socioeconómica (figura 12).

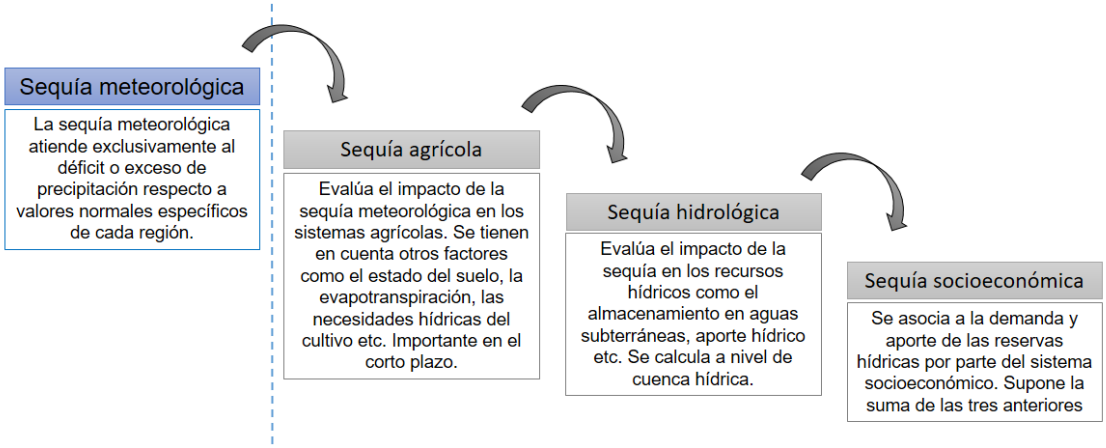

Figura 12. Tipos de sequía según el sector en el que impacten y las componentes que se vean afectadas. Elaboración propia.

Además del sector al que más afectan, estos tipos de sequía difieren entre sí por la duración, intensidad y extensión espacial del fenómeno (Hayes et al., 2010). Además pueden ser analizadas desde dos puntos de vista: conceptual u operacional (Wilhite and Glantz 1985). Si se evalúa la sequía conceptualmente, solo se tiene en cuenta el fenómeno físico que supone, es decir, alteraciones en el régimen pluviométrico, pero si se evalúa operacionalmente, se intenta definir características de dicho fenómeno como el comienzo y el fin del episodio, la recurrencia o la intensidad. Todas ellas informaciones muy útiles para intentar predecir estos fenómenos.

Como la sequía meteorológica por definición es una alteración de los valores normales de precipitación, es un fenómeno que se da en cualquier tipo de clima, independientemente de que presente un régimen pluviométrico elevado o escaso. No ha de confundirse con la aridez, fenómeno de escasez de precipitaciones permanente y que es propio de una región y no una alteración temporal. Aunque la sequía meteorológica hace referencia solo a las precipitaciones, la presencia de ciertos factores como las rachas de viento fuerte (McVivar et al., 2012a), el contenido de agua (Willet et al., 2014), la nubosidad y la duración solar (Wild et al., 2013) o las altas temperaturas (Cook et al., 2014; Livneh and Hoerling 2016, Huo et al., 2017; Hartman et al., 2013) pueden contribuir a su intensificación. Por otro lado, el impacto de la sequía no va a ser el mismo y dependerá del estado en el que se encuentren los recursos hídricos y las necesidades socioeconómicas en el momento en el que se produce el fenómeno.

Sequías de la misma magnitud pueden tener efectos muy diferentes en función de la época del año y el lugar en el que ocurran.

Son muchos los sectores interesados en evaluar la presencia de episodios de sequía y sus impactos, como por ejemplo, efecto en desastres naturales (Carroll et al., 2009) o ecológicos (Lewis et al., 2011; Choat et al., 2012), influencia en incendios forestales (Gudmundson et al., 2014; Westerling et al., 2006), en el abastecimiento de agua y la gestión de recursos hídricos (Pedro-Monzonis et al., 2015; Hoerling et al., 2014; Seager et al., 2015), en la agricultura (Tsakiris et al., 2010; Lesk et al., 2016) y la ganadería (Alary et al., 2014; Clark et al., 2016), sin olvidar el impacto social y económico (García-Herrera et al., 2010; Cheesman 2016; Stanke et al., 2013).

No existe una magnitud física ni un instrumento que permita medir la sequía, por lo que la manera en la que se analizan los episodios de sequía es a través de ***indicadores o índices de sequía***, definidos como (Hayes et al., 2000, Hayes 2006):

"un indicador directo basado en información climática que resume en un único valor las características principales del fenómeno facilitando su uso frente a valores puros de las variables meteorológicas. Un índice es útil si proporciona una evaluación clara, simple y cuantitativa de las características principales de la sequía"

Los índices de sequía suelen ser ajustados a la zona de estudio y a las necesidades de evaluación del fenómeno por lo que existe una gran variedad de ellos. En las últimas décadas se ha producido un gran avance en el desarrollo de estos índices. Se definen índices basados exclusivamente en la precipitación como el SPI (McKee et al., 1993), el RAI (Van-Rooy 1965), el DSI (Bryant et al 1992), el NRI (Gommes and Petrassi 1994) o el DFI (Gonzalez and Valdes 2006). Otros combinan la precipitación con el efecto de la temperatura como el SPEI (Vicente-Serrano et al., 2010a) y el RDI (Tsakaris and Vangelis 2005; Thomas et al 2015) o el *aridity index* (Subrahmanyam and Subramaniam, 1964). Finalmente, otros índices aumentan su complejidad incluyendo variables como como la cobertura nubosa, el *stream* flow (SWSI, Nagarajan 2003), la humedad del suelo (SPDI, Palmer 1965) o la vegetación (NDVI, Nagarajan 2003).

Son varios los estudios que han intentado recopilar todos ellos (Zagar 2011; Niemeyer 2008; Wilhite and Glatz 1985) con el fin de poner en común todo lo existen referente a indicadores de sequía, pero la selección de un indicador u otro no es tan sencilla ya que hay que tener en cuenta la disponibilidad de datos para su cálculo, el uso que se le va a dar a la información y si se va a aplicar a una región u otra (necesidad de índices normalizados). Con el fin de acotar el uso de indicadores y dar una ruta de trabajo a los interesados, son múltiples las guías que organismos, como el IPCC o la WMO, generan con directrices para el cálculo de sequías. En una de ellas, *"The Lincoln declaration on Drought Indices"* (Hayes et al., 2010) se determinó que el Índice de Precipitación Estandarizado (SPI) es, probablemente, el único índice valido para cualquier región del mundo y escala temporal.

En el contexto de calentamiento global actual, es evidente que el aumento de las temperaturas ha llevado a una aceleración del proceso hidrológico. Por un lado, aumenta la energía disponible mediante la evapotranspiración, por otro, aumenta la capacidad de almacenamiento calorífico por parte de la atmósfera a razón teórica de un

7% por cada incremento de 1 ºC (Trenberth 2011) y por último, la energía disponible en la superficie aumenta más despacio. La conjunción de todos los aspectos provoca alteraciones en la humedad disponible y por ende en la precipitación global, lo que se traduce en periodos secos, especialmente en verano (Vicente-Serrano et al., 2010b).

El SPI, es un índice que se calcula exclusivamente en base a la precipitación. Atendiendo a lo anterior, Vicente-Serrano et al. (2010a), definieron el Índice estandarizado de precipitación y evapotranspiración (SPEI) que supone una modificación del SPI mediante la introducción de la evapotranspiración.

Ambos índices (SPI y SPEI) son índices estandarizados (permiten comparar regiones entre sí fácilmente), permiten evaluar, mediante su comparativa, la influencia de la temperatura en los episodios de sequía y han sido ampliamente aplicados en la zona de estudio. Por todo ello, son los índices más adecuados para alcanzar los objetivos planteados en este estudio. Además, pueden representarse a diferentes escalas en función del alcance del estudio (figura 13).

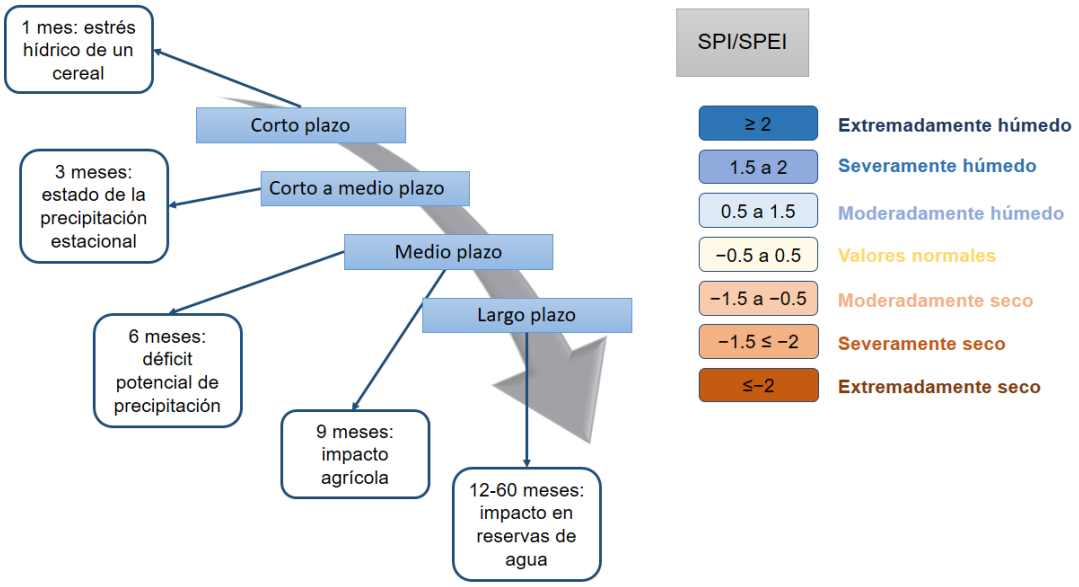

Figura 13. Escala de intensidades usada para evaluar el SPI/SPEI así como implicaciones de la sequía según la escala temporal considerada. Elaboración propia.

El ***Índice de precipitación estandarizado*** (SPI) fue desarrollado por Mckee et al. (1993) y se basa en dos supuestos: que la variabilidad de la precipitación es mayor que la de la temperatura y la evapotranspiración potencial (ETP), y que el resto de las variables son estacionarias en el tiempo. El ***valor del SPI*** se define como:

> "un valor numérico que representa el número de desviaciones estándar de la precipitación, en el periodo de acumulación en cuestión, respecto a la media, una vez transformada la distribución original de la precipitación en una distribución normal (es decir, media de cero y desviación estándar de 1)"

Los valores del SPI pueden interpretarse como el número de desviaciones típicas en que la anomalía observada se desvía de la media a largo plazo.

El ***Índice de evapotranspiración y de precipitación estandarizado*** (SPEI), desarrollado por Vicente-Serrano et al., 2010a y revisado por Begueria et al., 2014, es una variante del SPI. Tiene mayor potencial como índice de sequía ya que considera el balance climático (a través de la diferencia entre la precipitación mensual y la ETP). Se define el ***valor del SPEI*** como:

"un valor numérico que representa el número de desviaciones estándar del balance climático (precipitación menos ETP), en el periodo de acumulación en cuestión, respecto a la media, una vez transformada la distribución original de la precipitación en una distribución normal (es decir, media de cero y desviación estándar de 1)"

Los valores del SPEI pueden interpretarse de la misma manera que los del SPI (número de desviaciones estándar en que la anomalía observada se desvía de la media a largo plazo).

Para el cálculo del SPI se utiliza la distribución Gamma con el fin de ajustarse a la serie de precipitación original (WMO, 2012) y en el caso del SPEI se utiliza la distribución log-logística (Vicente-Serrano et al., 2015; Vicente-Serrano and Beguería, 2016). Los parámetros de estas distribuciones se obtienen por el método de momentos ponderados probabilísticos insesgados (Vicente-Serrano and Beguería, 2016). La escala de valores de SPI y SPEI utilizada en el estudio puede verse en la figura 13.

1.3 EL IMPACTO DEL CAMBIO CLIMÁTICO SOBRE EL CULTIVO DE LA VID: INDICADORES BIOCLIMÁTICOS

El sector agrícola en general y el vitícola en particular, es uno de los más vulnerables al cambio climático. El impacto del cambio climático no afecta de la misma manera a todas las regiones ni cultivos por igual, por lo que es esencial que se evalué a escala local. Para alcanzar este objetivo es necesario disponer de información climática proyectada a escala local (por ejemplo, temperatura y precipitación), evaluar el impacto que dichas proyecciones suponen para el sector vitícola (mediante indicadores bioclimáticos) e identificar los posibles riesgos a los que ha de hacer frente el sector en las próximas décadas.

A día de hoy, España es una de las regiones más apropiadas para cultivar vinos de alta calidad por sus características climáticas y edafológicas (Van Leeuwen et al., 2004; Sotés et al., 2012). Aunque en general el viñedo europeo se cultiva entre 100 y 300 m de altura, las características climáticas del territorio ibérico-balear hacen posible que se cultiven algunas variedades hasta los 1000m, ampliándose considerable el rango de variedades de uvas y por ende de tipos y calidades de vinos que se pueden obtener. Desgraciadamente, estas condiciones pueden verse modificadas en el futuro (Deque et al., 2012; Lorenzo et al., 2013).

A grandes rasgos, los vinos españoles pueden agruparse en continentales (tipo Rioja o Valdepeñas), atlánticos húmedos (tipo Alabariño o Chacolí) y mediterráneos (Penedés). Estos factores propios y únicos de cada una de las distintas regiones donde se cultivan vinos españoles, dan lugar a las Denominaciones de Origen (DOs). Las DOs españolas constituyen el sistema utilizado en España para el reconocimiento de una calidad diferenciada, consecuencia de unas características propias y diferenciables debidas al medio geográfico en el que se producen las materias primas.

La importancia que el sector vitícola tiene para un país como España se reflejan en las cifras (FEV, 2021): es el primer viñedo del mundo con 949.565 ha de vid, lo que supone un 13% del total mundial; es el tercer productor mundial con una producción media anual de vino y mosto de entre 40 y 42 millones de hectolitros; es el primer exportador mundial en volumen (21 millones de hectolitros en 2019) y el tercero en valor (2.700 millones de euros exportados en 2019. Tres de cada cinco botellas comercializadas en el mundo proceden de Europa y España es responsable del 25% de la producción de vino europeo. Además, es líder en viñedo ecológico, con 121.000 ha responsables de una producción de más de 400.000 toneladas de uvas de vinificación (FEV, 2021).

En España hay cerca de 4300 bodegas (de las cuales más de 3000 son exportadoras) que venden vinos españoles en más de 198 países. Estas cifras demuestran que el sector vitícola aporta un gran valor a la economía, generando y manteniendo más de 427.000 empleos (FEV, 2021). Esto es especialmente relevante en zonas rurales pues permite luchar contra el despoblamiento rural y fomentar el turismo gastronómico, principalmente a través de los museos y bodegas que conforman la Red de Rutas del Vino de España.

Organismos nacionales como la Federación Española del Vino, el Observatorio Español del Vino o la Organización Interprofesional del Mercado del Vino, junto con internacionales como la Organización Internacional del Vino están poniendo mucho

esfuerzo y recursos en elaborar un plan de acción frente al cambio climático, intentando identificar las necesidades del sector con el fin de establecer ciertas directrices, recomendaciones y buenas prácticas que velen por el futuro del sector vitícola español. Estos esfuerzos se ven reflejados en los más 170 millones al año que se invierte en proyectos de I+D+i (FEV, 2021).

1.3.1. Clima y vid

La vid es una planta leñosa perteneciente a las Vitáceas que comprende 19 géneros, de los cuáles únicamente el género *Vitis* es cultivado. Este género se divide a su vez en *Euvitis* y *Muscadina*. La mayoría de las vides cultivadas pertenecen al género *Euvitis* y se cultivan, principalmente en Asia Oriental, América y Europa. En las dos primeras regiones se dan más de 20 especies, mientras que en Europa se cultiva, exclusivamente, la especie *Vitis vinífera.*

Debido al considerable aumento en el número de hectáreas de vides cultivadas en regiones como Australia, Estados Unidos, Chile, Sudáfrica y Nueva Zelanda, la industria vitícola europea ha visto la necesidad de ir un paso más allá para hacer frente a sus crecientes "competidores", probando nuevas variedades y mejorando las técnicas de cultivo.

Tradicionalmente las zonas más óptimas para el cultivo de la vid se han ubicado entre los 30-50^{0}N y los 20-50°S coincidiendo con aquellas regiones que presentan temperaturas promedio anuales entre los 10 y los 20°C.

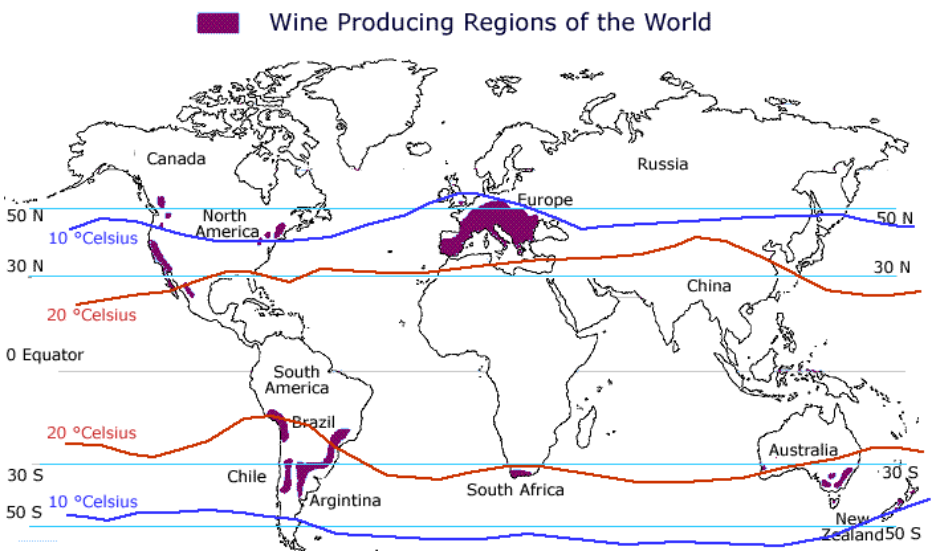

Figura 14. Localización de las principales regiones vitícolas del mundo (en color morado). En líneas generales, se sitúan entre los 30-50 ºN y los 20-50 ºS. Estos límites se corresponden con las isotermas 10 y 20 ºC en ambos hemisferios. Fuente: Sallis et al, 2009:3.

Estas regiones presentan un clima base (unas características climáticas promedio) que las convierten en idóneas para su cultivo con una producción óptima de la vid dando lugar a vinos equilibrados y de calidad. Si el clima base es demasiado frío, se obtienen vinos desequilibrados como consecuencia de la escasa maduración de la uva. Por el contrario, si el clima es demasiado cálido, también se obtienen vinos desequilibrados, pero en este caso por sobre maduración de la uva (figura 15). El clima base determina

qué variedades de vid encajan en cada región y el estilo de vino que podrá producir, y la variabilidad climática es la encargada de diferenciar unas añadas de otras dentro de un mismo viñedo.

La variabilidad climática es una característica intrínseca del clima y desde siempre los viticultores han ido adaptándose de forma gradual a las condiciones medioambientales locales y regionales y a sus variaciones (Jones et al., 2012). Por tanto, el clima promedio y la variabilidad climática son los factores medioambientales que más influyen en la calidad y producción del vino (Spellman 1999; David 2000; Santos et al., 2011).

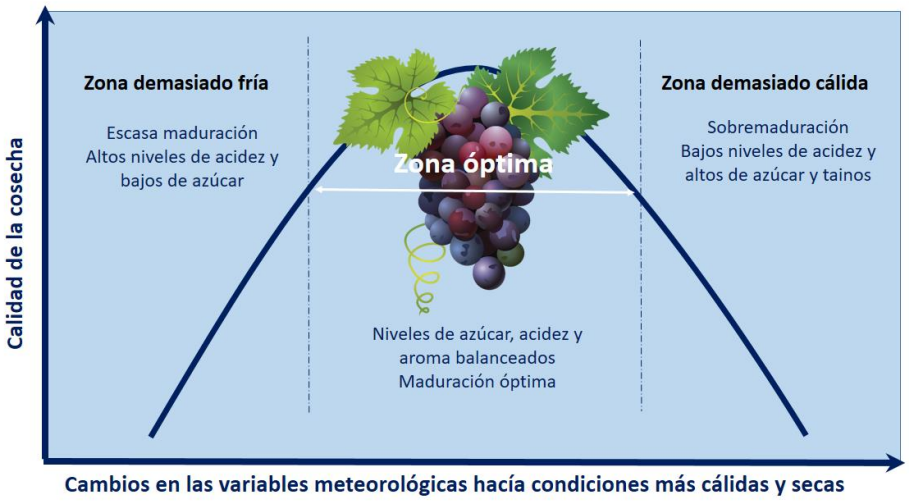

Figura 15. Calidad de la cosecha en función de las condiciones climáticas (basada en PricewaterhouseCoopers, 2009)

La vid es muy sensible al clima (Kenny 1993; Winkler 1974; Gladstones 1992; Jones 2006; Meier 2007; White 2006) y a las condiciones atmosféricas en un gran rango de escalas temporales (Santos et al., 2019), desde impactos a corto plazo (heladas, rachas de viento y granizo), a medio plazo (sequías e inundaciones) y a largo plazo (tendencias climáticas). Por otro lado, las variables climáticas influyen en aspectos como el crecimiento y la productividad de la vid, rigen la fotosíntesis, son el aporte de agua o determinan la coloración, entre otros (Carbonneau 2003). Además, posibles alteraciones en los requerimientos climáticos (heliotérmicos e hídricos) tienen un fuerte impacto en las características organolépticas finales de la uva (acidez, azúcar, color, etc) y por ende, en las características finales del vino. Por consiguiente, cambios en patrones meteorológicos y/o climáticos son la consecuencia de los efectos del cambio climático que pueden derivar en impactos para el sector vitícola (Schultz 2000; Jones et al., 2005a).

Está demostrado que el cambio climático afecta al viñedo (Kenny and Harrinson 1992; Jones 2006) y los resultados mostrados por las proyecciones climáticas parecen apuntar a una tendencia hacía impactos cada vez más fuertes (Meehl 2007) y un desplazamiento de las zonas óptimas para el cultivo de la vid hacía los Polos de unos 20º hacía el 2050 (Kenny and Harrinson 1993; Tate 2001). Se espera que los efectos del cambio climático afecten al viñedo, no solo de forma global sino dentro de cada añada, modificando los estados fenológicos y la definición de “gestión tradicional” del viñedo.

Son varios los estudios que han analizado la relación clima-viñedo en territorio español durante las últimas décadas (Santos et al., 2012; Malheiro et al 2010; Ramos et al.,

2008; Lorenzo et al., 2013; Fraga et al., 2014, Ramos et al., 2008; Moral et al., 2015) o han realizado una clasificación climática para el pasado (Blanco-Ward 2007; Moral et al., 2015). En los últimos años, además, se ha añadido el esfuerzo de utilizar proyecciones climáticas para estudiar las relaciones clima futuro-viñedo (Lorenzo et al., 2013, 2015) y proyectar zonificaciones climáticas mediante distintos indicadores (Blanco-Ward 2007; Lorenzo et al., 2012; Fraga et al., 2012, 2013; Resco et al., 2016; Santos et al., 2019).

1.3.2. La vid: ¿cómo le influyen las variables meteorológicas?

La vid es una planta perenne caracterizada por presentar ciclos de vida anuales interdependientes, es decir, las condiciones de un ciclo condicionan las características que tendrá el siguiente. El ciclo biológico de la vid engloba el ciclo vegetativo y el ciclo reproductor, de manera que ambos son simultáneos en el tiempo (figura 16). Dentro de las distintas etapas, el periodo de maduración es el más importante, ya que es el momento en el que se fijan las características organolépticas finales de la uva (acidez, color y aroma) y que definen su calidad, alcanzándose los niveles óptimos de azúcar y alcohol.

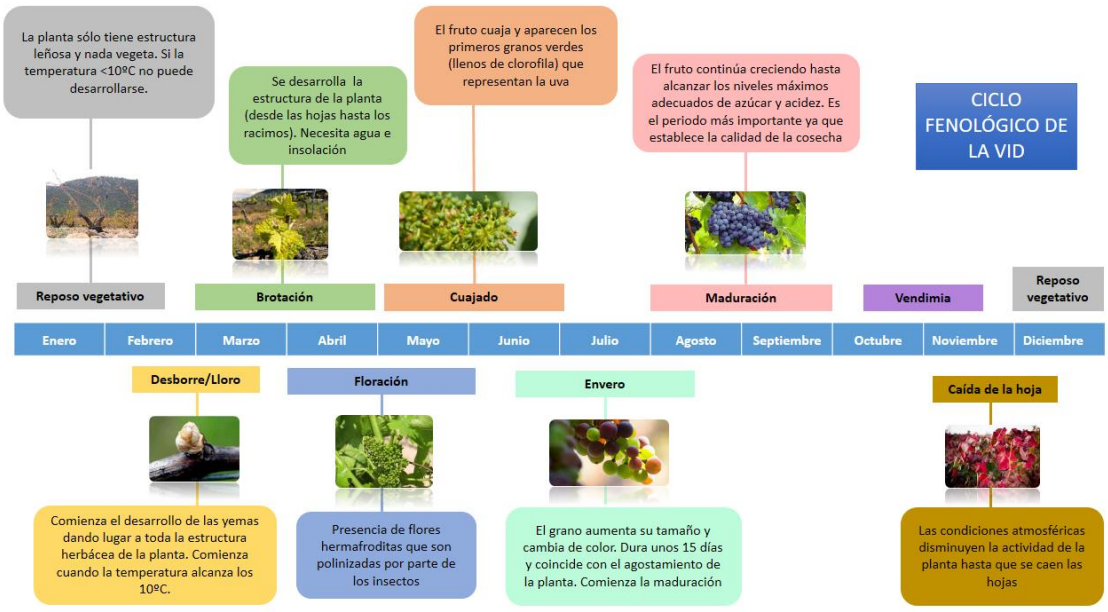

Figura 16. Etapas fenológicas de la vid. Elaboración propia.

Las distintas variables meteorológicas van a jugar un papel importante en el correcto desarrollo de la vid, de manera que es necesario que se den las condiciones térmicas e hídricas idóneas en cada una de ellas (Magalhaes 2008; Makra et al., 2009). Mientras que la temperatura afecta principalmente a la calidad de la uva (Jones and Davis 2000; Santos et al., 2011) y al equilibrio del vino mediante una correcta maduración, la radiación y la precipitación tienen efectos en la cantidad de la cosecha ya que son factores a tener en cuenta en la gestión del viñedo (Lopes et al., 2008).

Aunque el calor y la insolación son dos variables que aportan múltiples beneficios en el correcto desarrollo de la vid, un exceso de ambos puede convertirlos en perjudiciales. En el aporte justo de calor, agua e insolación está la clave para el éxito productivo y

cualitativo de la vid, de manera que cada variable meteorológica está ligada a la vid de diferente manera.

En términos generales, las condiciones más favorables para la vid son aquellas en las que la temperatura óptima en el periodo de crecimiento se sitúa entre los 12-22 ºC (Jones et al., 2006) y la temperatura media en el periodo vegetativo entre los 20 y 30 ºC (Gouveia et al., 2011) asegurándose una adecuada acumulación de calor en el periodo de maduración (White et al., 2006; Holland and Smith, 2014). Respecto a la precipitación, se requieren entre 350 y 600 mm anuales para obtener vinos de calidad (Hidalgo et al., 2012). Además, este cultivo es muy exigente en cuanto a las horas solares, necesitando entre 10 (en octubre) y 15 horas (junio y julio). En cuanto a la presencia de enfermedades, la humedad relativa máxima juega un papel esencial en los meses de mayo y junio (favoreciendo enfermedades criptogámicas como el mildiu, el oídium y la botritis), lo ideal son valores entre el 60 y el 70%.

A continuación, se analiza el papel que juega cada variable meteorológica en el desarrollo de la vid.

- Temperatura

Como se ha comentado, la temperatura es la variable que más impacto tiene en el ciclo de la vid. En cada una de las etapas fenológicas es necesario que se den unos valores térmicos concretos para que la baya se desarrolle correctamente ya que tanto la composición metabólica como la fisiológica de la uva están fuertemente relacionadas con ella (Jones et al., 2012).

En términos generales, la actividad de la planta y por tanto su desarrollo comienza cuando las temperaturas alcanzan los 10ºC (normalmente en primavera). Una vez alcanzado o superado dicho umbral (denominado cero vegetativo) la planta se mantiene en desarrollo hasta que las temperaturas vuelven a situarse por debajo de dicho umbral (normalmente en otoño). Este periodo de tiempo se denomina periodo activo de la vid. La parte radicular de la vid tiene un periodo activo algo más largo que la parte aérea, esto se debe a que el suelo alcanza el cero vegetativo antes que el aire y el descenso de temperaturas es más lento llegando de nuevo a ese umbral con posterioridad. Estos valores varían de una variedad a otra e incluso hay algunas variedades que pueden dar señales de desarrollo una vez alcanzados los 0 ºC pero en términos generales se acepta el umbral de 10 ºC para el cero vegetativo y el periodo de abril a octubre como el periodo activo.

La temperatura juega un papel especialmente importante en las siguientes etapas fenológicas:

1) Salida de dormancia de yemas latentes. Tras varios días consecutivos con temperatura mínima inferior a un umbral establecido en función de la variedad, las yemas despiertan de su reposo vegetativo. Ocurre en invierno.

2) Desborre. Las yemas brotan a partir de un umbral, normalmente 10 ºC.

3) Floración. Esta etapa es altamente dependiente de las temperaturas.

4) Maduración. Este es el periodo más importante y determina la calidad de la cosecha. Los procesos que ocurren en esta etapa se producen a nivel de baya y es por eso que

cada variedad necesita que durante la maduración que la temperatura se mantenga dentro de unos valores concretos (figura 17) (Jones et al., 2006).

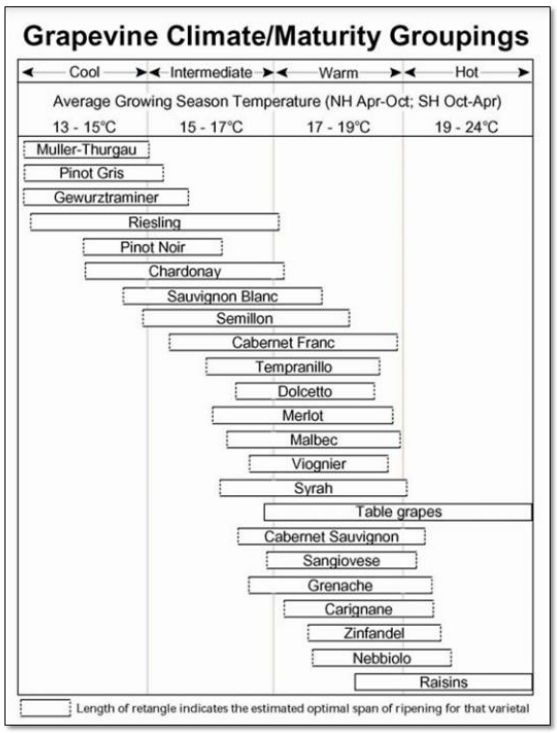

Figura 17. Umbrales de temperatura durante la época de crecimiento para diferentes variedades de uva. Fuente: Jones 2006.

Temperaturas muy elevadas en este periodo (en función de los requerimientos de cada variedad) ponen en riesgo la calidad de la uva. Los impactos en la baya por altas temperaturas varían si éstas se producen en combinación con otros factores (como la humedad relativa) y en función del momento del día en que se consideren (figura 18).

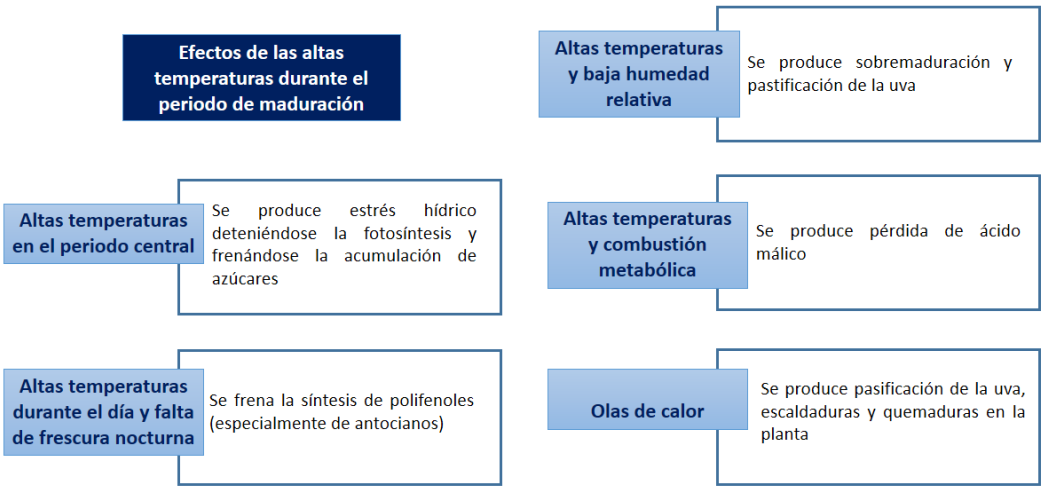

Figura 18. Efectos asociadas a las altas temperaturas registradas durante el periodo de maduración. Elaboración propia.

En general, temperaturas altas son sinónimo de calidad del vino. Pero esta afirmación no es 100% cierta ya que las temperaturas extremas (tanto altas como bajas) también pueden afectar al viñedo de forma negativa. Además, cada variedad tolera de forma diferente las altas temperaturas (Moutinho-Pereira et al., 2007). El mayor problema relacionado con altas temperaturas es la posible desecación de las partes aéreas de la planta e incluso su muerte. Mientras que temperaturas muy bajas pueden llegar a helar los órganos herbáceos o limitar el desarrollo de la planta (figura 19).

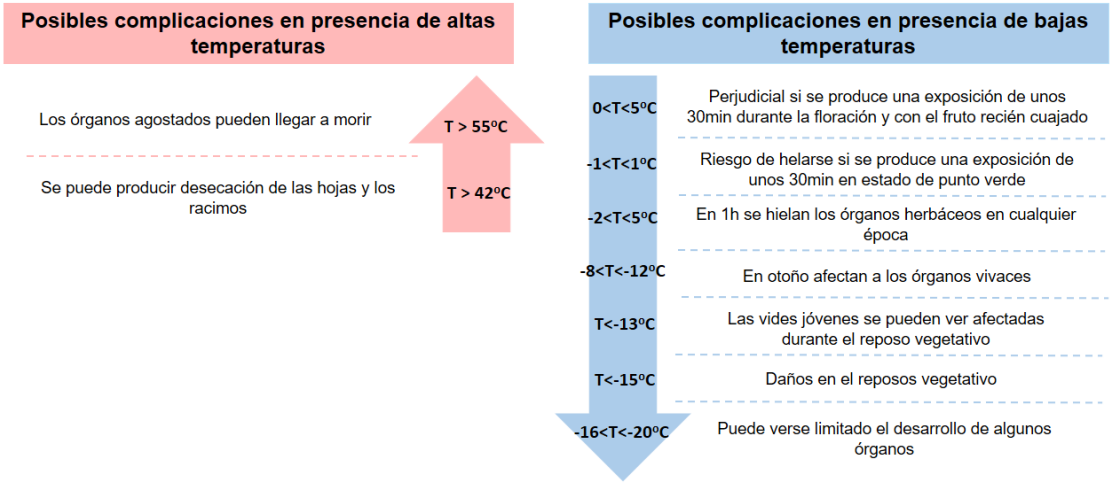

Figura 19. Posibles complicaciones que pueden presentarse en la vid bajo condiciones extremas de temperatura. Elaboración propia.

Las diferencias genéticas, morfológicas y fisiológicas entre variedades propician que su adaptación al cambio climático sea diferente en cada caso. Variedades con una baja demanda termal (pocas necesidades de acumulación de calor con un rango pequeño de oscilación) tendrán más complicado adaptarse, las variedades que necesiten poca demanda termal pero tengan un rango alto de oscilación tendrán un margen medio de adaptación, mientras que aquellas variedades con una alta demanda termal tendrán más fácil adaptarse al cambio climático. En general, las variedades de uva blancas tienen una demanda termal más baja que las tintas.

- <u>Pluviometría</u>

El 80% de la vid es agua, por lo que es esencial para su constitución ya que la usa para el transporte de nutrientes, para transpirar y para refrigerarse. Por lo tanto, mantener el aporte hídrico es esencial para que el viñedo viva. Ha de tenerse en cuenta que la vid no requiere el mismo aporte hídrico en todas las etapas fenológicas, por lo que es igual o más importante conocer la evolución pluviométrica dentro del año que la precipitación anual total. Tanto un exceso como un defecto de agua en momentos clave pueden ser perjudicial para la vid (figura 20).

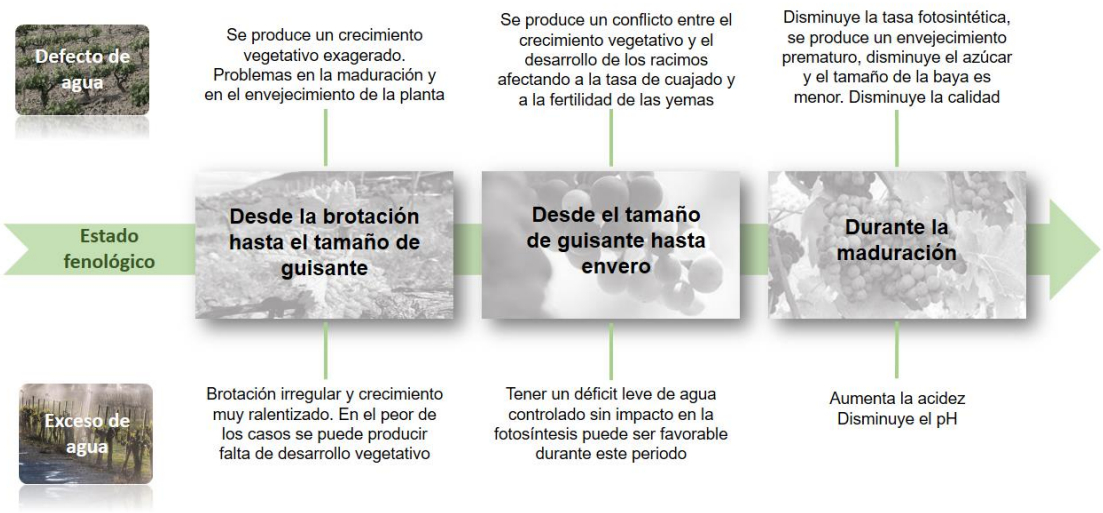

Figura 20. Consecuencias de déficit o exceso de agua en función de la etapa fenológica en la que se produzca. Elaboración propia.

- <u>Humedad relativa</u>

La humedad relativa no es una variable que influya en la vid tanto como la precipitación o como la temperatura. Pero valores de humedad muy altos o bajos pueden resultar perjudiciales para la planta. Si la humedad relativa es alta (>80%) puede favorecer la proliferación de ciertas enfermedades mientras que situaciones de estrés hídrico acompañadas de humedades bajas (<40%) resultan críticas para la vid. Humedades relativas de entre el 60-70% son las óptimas, ya que favorecen la actividad fotosintética.

- <u>Insolación</u>

La vid necesita de un cierto número de horas de sol para su crecimiento, siendo muy exigente durante las etapas de floración y maduración. En términos generales, la vid necesita entre 10 y 14 horas de sol para su óptimo desarrollo.

- <u>Fenómenos meteorológicos extremos adversos</u>

Aunque la vid es una planta que se adapta muy fácilmente al estrés medioambiental, los fenómenos extremos la pueden llegar a afectar irreversiblemente (Hidalgo 2012; Easterling 2000; Jones et al., 2005; Menzel et al., 2011).

Dentro de los fenómenos extremos hay algunos que resultan especialmente perjudiciales para la vid como los episodios de olas de calor, los episodios de sequía y los episodios de granizo y heladas. Las consecuencias de su aparición van a depender del momento del ciclo biológico de la vid en que aparezcan (figura 21).

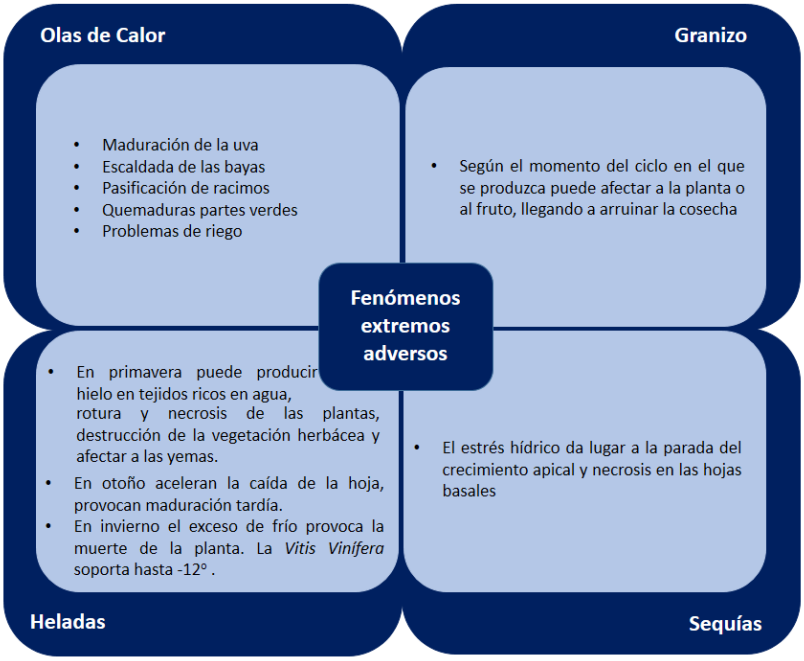

Figura 21. Fenómenos extremos con mayor impacto en el viñedo y las posibles consecuencias asociadas a su aparición. Elaboración propia.

Además de las variables meteorológicas anteriormente expuestas y que varían día a día, hay otros factores que van a influir en el buen desarrollo del viñedo: los factores geográficos (ubicación, continentalidad, orientación etc.); los factores climáticos (las características promedio de una región contribuyen a la idoneidad climática para el cultivo de la vid) y los factores socio-económicos (técnicas de manejo de la finca, elección adecuada del cultivo etc.) (figura 22).

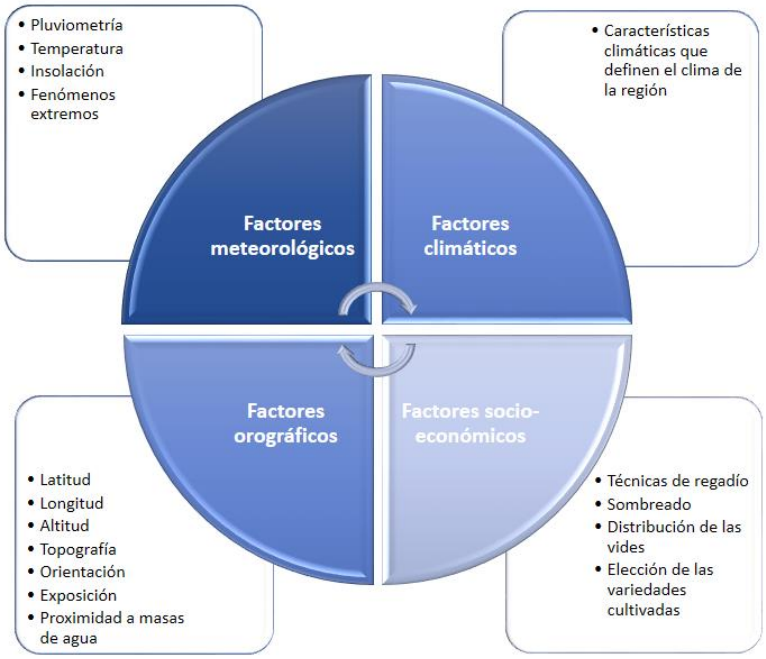

Figura 22. Combinación de factores que condicionan el cultivo y la producción vitícola. Elaboración propia.

1.3.3. Cambio Climático y viñedos

Durante las últimas décadas los cambios en las condiciones climáticas como consecuencia del cambio climático (aumento de las temperaturas, alteraciones en el régimen pluviométrico, alteraciones en la ETP o aumento en las concentraciones de CO_2), han afectado de forma directa a los viñedos a lo largo de todo el mundo. Son múltiples los estudios que recopilan los cambios que los productores vitícolas han experimentado en sus fincas (Battaglini et al., 2009; Alonso and O'Neill, 2011) y que tienen relación directa con los requerimientos heliotérmicos e hídricos que la vid necesita para un crecimiento óptimo, observándose cambios en cualquier tipo de clima.

Entre los principales cambios que se han reportado, a nivel de finca, destacan cambios en la viabilidad de una zona para cultivar ciertos tipos de variedades, cambios en la distribución geográfica (Schultz, 2000), cambios en el régimen hídrico y por tanto en las necesidades de riego (Ruml et al., 2012), variaciones en las secuencias de plagas y enfermedades (Gouevia et al., 2011), alteraciones de los parámetros edafológicos, aumento de las temperaturas durante la época de crecimiento (Fraga et al., 2012; Santos et al., 2012; Duchene and Schneider, 2005; Neumann and Matzarakis, 2011) y baja predictibilidad y regularidad de la cosecha y la calidad del vino (Schlutz 2000; Jones et al., 2005a).

Entre los principales cambios observados a nivel de baya y vino, los más reportados fueron: cambios en la composición química de la uva y del vino, cambios en las características organolépticas (Orduna 2010; Bureau et al., 2000), cambios en la secuencia de las etapas fenológicas (Jones et al., 2005), especialmente en la época de brotación, comienzo de la cosecha., y en comienzo de maduración (Stock et al., 2005; Ganichot 2002; Duchene and Schneider 2005; Sigler 2008; Petgen 2007; Duchene et al., 2010; García de Cortazar Atauri 2006; Webb et al., 2007; Pieri 2010; Koufus et al., 2014, 2017; Ramos et al., 2008). También un aumento de los eventos extremos con el peligro que su ocurrencia supone para la seguridad de la cosecha (Kerry and Harrinson, 1992; Jones et al., 2005).

A nivel español, junto con los impactos ya mencionados, se ha observado un descenso en la superficie vitícola en el noreste peninsular como consecuencia del estrés hídrico (Camps and Ramos, 2012), un aumento de la demanda de regadío (Alonso and O'Neill, 2011) y una reducción de la esperanza de vida de la vid en un 30%. Según un estudio de la Universidad de la Rioja (Andrés et al., 2020), el 90% de los profesionales asociados a alguna Denominación de Origen han notado los efectos del cambio climático y el 56% consideran que esos impactos les están afectando de forma considerable. Entre los riesgos climáticos que más les afectan sitúan a las heladas, los pedriscos, las sequías y las olas de calor.

Todos los cambios anteriormente citados suponen impactos económicos asociados a la actividad del viñedo, que dependiendo de la región donde se hayan observado han supuesto un impacto positivo o negativo. Por ejemplo, el aumento de las temperaturas mínimas durante la maduración ha supuesto un descenso en la calidad de ciertos vinos procedentes de la Península Ibérica (Fraga et al., 2012; Malheiro et al., 2010; Kenny and Harrinson 1992; Koundouras et al., 1999; Santos et al., 2010b) y el aumento de las temperaturas máximas ha supuesto una degradación de las características organolépticas en muchas de las principales regiones vitícolas (Orduna 2010; Buttrose

et al., 1971; Downey et al., 2006; Bureau et al., 2000). Mientras que esas mismas variaciones térmicas han favorecido la producción vitícola y la mejora en la calidad del vino en regiones frías (Gouveia et al., 2011), ver figuras 23 y 24. En resumen, los cambios asociados al impacto del cambio climático, tanto a nivel de planta, finca o socioeconómico, no son proporcionales en todo el territorio (Hannah et al., 2013).

De todas las alteraciones ocasionadas por el cambio climático, hay tres que destacan especialmente: aumento del CO_2, alteraciones en el régimen pluviométrico y aumento de las temperaturas. Debido a su ubicación en el sur de Europa, España se espera que sea una de las regiones más afectadas por los efectos del cambio climático, especialmente por este aumento de las temperaturas y el estrés hídrico lo que hace urgente determinar la relación entre clima y viñedo y evaluar su evolución futura.

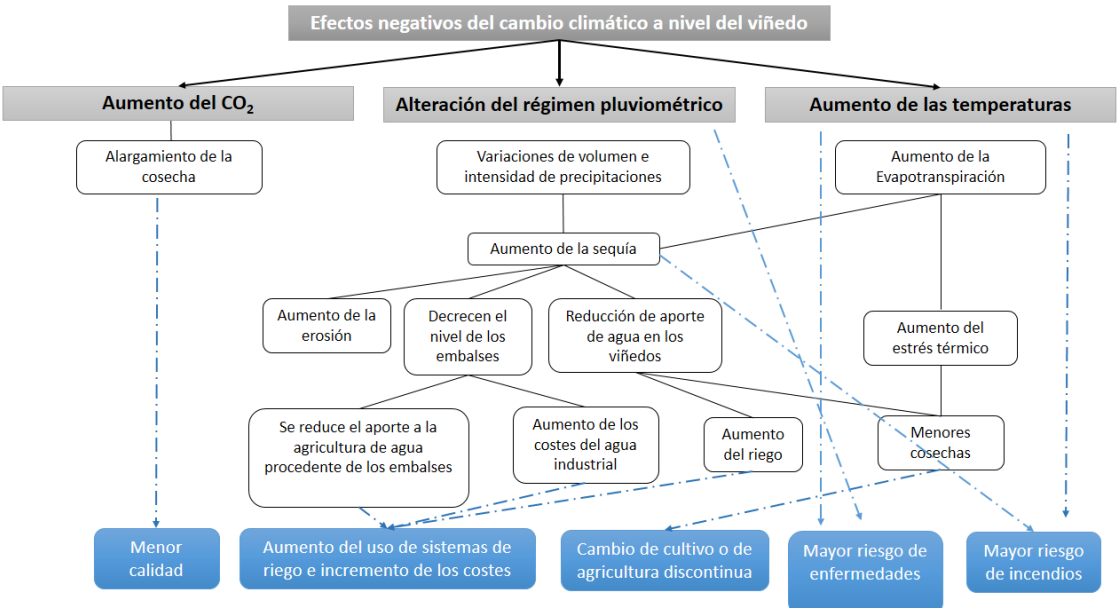

Figura 23. Efectos negativos del cambio climático a nivel viñedo relacionados con el aumento de CO_2, con alteraciones en el régimen pluviométrico y con el aumento de las temperaturas. Elaboración propia.

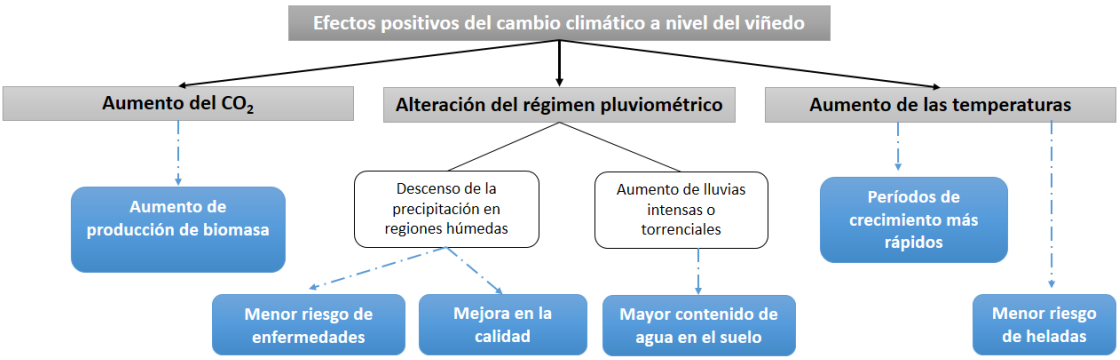

Figura 24. Efectos positivos del cambio climático a nivel viñedo relacionados con el aumento de CO_2, con alteraciones en el régimen pluviométrico y con el aumento de las temperaturas. Elaboración propia.

1.3.4. Indicadores bioclimáticos como herramientas para el estudio del viñedo

La manera en la que es posible evaluar la relación entre clima/meteorología y los distintos factores que afectan a la vid y al conjunto de la producción vitícola, es a partir de los indicadores bioclimáticos (Fregoni 2003). Un indicador o índice bioclimático es un parámetro que mide una variable en función de sus valores climáticos promedios. A través de una selección de indicadores bioclimáticos se pueden estudiar distintos factores de interés vitícola como la idoneidad climática de una región para cultivar la vid, el tipo de variedad más idóneo o la posibilidad de aparición de ciertas pestes y/o enfermedades.

En líneas generales, los estudios clásicos utilizan **índices individuales** calculados en base a la temperatura y la precipitación y derivados de ellos. A continuación se enumeran los relevantes:

Impactos evaluados	Referencias
Las heladas y las sequías	Carbonneau and Tonietto, 1998; Tonietto 1999; Carbonneau 2003; Jones et al., 2005a; Duchene and Schneider 2005; Wang et al., 2020; Karoglan et al., 2018; Bois et al., 2014
Eventos extremos	Eastering et al., 2000b; Martinez-Casanovas et al., 2002; Michael et al., 2005
Producción de la uva	Bindi et al., 1996; Tate 2001; Maxwell et al., 2016; Holland and Smith 2005; Cafarra et al., 2012
Potencial agroclimático	Chuine et al., 2004; García de Cortazar Atauri 2006; Barbeau 2007; Bois 2007; Bellia et al 2008; Hunter et al. 2010; Neethling et al., 2012; Bonnefoy et al. 2013
Actividad enológica	Schultz 2000; Webb et al., 2007
Idoneidad climática de la región	Gladstones 1992; Fregoni 2003; Jones 2006
Precios del vino	Combris et al., 1997; Ashenfelter et al., 1995
Daño económico	Bernetti et al., 2012; De Salvo et al., 2013

Figura 25. Recopilación de estudios sobre impactos del cambio climático. Elaboración propia

Entre los indicadores individuales más utilizados destacan la temperatura y la precipitación durante la época de crecimiento, la temperatura y la amplitud térmica diaria durante la maduración, los días con temperaturas muy extremas, ocurrencia de heladas, los grados día o distintos índices de clasificación climática como Winkler (Winkler et al 1994) o Huglin (Huglin 1978).

Estudios más recientes ponen de manifiesto la necesidad de trabajar con **índices combinados** ya que representan de forma más completa la clasificación y discriminación vitícola (Ibacache, 2010) y permiten caracterizar la calidad del vino (Huglin 1978; Maglhaes 2008). Esta forma de trabajar se engloba dentro del concepto de zonificación vitícola y es el primer paso para evaluar el potencial vitícola de una región (Malherio et al., 2010). Entre los más utilizados se encuentran el CatI (Fraga et al., 2014), índice de Zuluaga (Westphalen and Maluf 2000) o el Grape Water Index (Teixeira et al., 2012), entre otros.

Tonietto y Carbonneau definieron en 2003 el *Geoviticulture Multicriteria Climatic Classification (MCC) System*, siendo el primer estudio que plantea una metodología para describir de forma macro climática la variabilidad vitícola de una región. El MCC System se basa en la combinación de tres índices complementarios entre sí y que aportaban

tanto información heliotérmica como hídrica: *Huglin Index, Cool night Index y Dryness Index*. Esta clasificación supuso el punto de partida para comparar y establecer grupos de regiones similares de forma más eficiente que la que se venía usando hasta la fecha, que normalmente solo incluía un único índice y que se ha comprobado que recoge de forma más que suficiente la variabilidad vitícola (Blanco-Ward et al., 2007). El uso del MCC System como clasificación vitícola está muy extendido y muestra de ellos son las múltiples regiones en las que se ha aplicado y en las que se utiliza como herramienta de adaptación al cambio climático (Fraga et al., 2014; Irimia et al., 2013; Tonietto et al., 2010; Vukovic et al., 2010).

Por lo tanto, los índices bioclimáticos son herramientas que permiten evaluar cómo ciertas variables pueden afectar a la vid en distintos momentos de su ciclo vegetativo y cómo pueden condicionar las características de las uvas y de los tipos de vino. Disponer de esta información es de gran utilidad para realizar una óptima planificación del viñedo, no solo en las actividades temporales (es decir, año a año) sino en actividades que han de planificarse a medio-largo plazo (como por ejemplo, elegir variables más resilientes a las nuevas condiciones climáticas o trasladar el viñedo a localidades más altas).

1.3.5. Denominaciones de Origen

Una DO permite identificar un producto originario de un lugar determinado cuyascaracterísticas principales y diferenciadoras son exclusivamente consecuencia del medio geográfico en que se producen, de los factores humanos y naturales que intervienen en su desarrollo y de las fases de producción que se realizan en dicha zona geográfica.

Las DOs es el sistema que se utiliza en España para reconocer la calidad diferenciada de un vino. A través del Consejo Regulador se entregan las calificaciones de DOs a aquellos vinos que, por su materia prima y su forma de ser elaborados y envasados, solo pueden ser generados en una determinada región.

Para que un vino sea reconocido con el distintivo de DO debe cumplir, además de las características propias de la región donde se elaboran, que sea reconocido en el mercado y que haya sido reconocido como vino de la zona durante mínimo 5 años. Existe una denominación de origen más exclusiva, la Denominación de Origen Calificada (DOCa.), que se concede a aquellos vinos que además de cumplir los requisitos de DO cumplen otras condiciones como los controles de calidad a los que se someten y las condiciones de su comercialización (figura 26).

Requisitos para que un vino obtenga la Denominación de Origen

1. Vinos elaborados en la región de la DO con uvas procedentes exclusivamente de esa región
2. Poseer características especiales y una calidad que solo se consigue gracias al medio geográfico en el que se elaboran.
3. Gozar de gran prestigio por su origen en el mercado
4. Haber trascurrido al menos cinco años desde que el vino se reconoce como producto propio de la zona

Requisitos para que un vino obtenga la Denominación de Origen Calificada

1. Poseer, al menos, 10 años de reconocimiento de Denominación de Origen
2. Pasar un sistema de control en todos los procesos de la cadena que certifiquen la calidad y cantidad de los vinos
3. Debe existir una delimitación cartográfica de los terrenos aptos para la elaboración de vinos con derecho de DOCa
4. Todo el vino producido debe venderse embotellado.

Figura 26. Requisitos necesarios para que un vino se distinguido como DO o DOca. Elaboración propia.

Desde la primera DO legalmente certificada, la Denominación de Origen Jerez-Xérés-Sherry en 1935, hasta el 2021, el número de zonas con certificación de DO ha ascendido hasta 101. En lo referente a las DOCa solo hay dos que cumplen esos requisitos: Rioja (localizada en La Rioja, País Vasco y Navarra) y Priorat (en Cataluña). Se pueden encontrar alguna DO en todo el territorio español como se aprecia en la figura 27.

Listado de Denominaciones de Origen

Andalucía
Condado de Huelva, Jérez-Xérès-Sherry, Granada, Málaga, Manzanilla-Sanlúcar de Barrameda, Montilla-Moriles, Lebrija y Sierras de Málaga

Castilla-La Mancha
Almansa, Calzadilla, Campo de la Guardia, Casa del Blanco, Dehesa del Carrizal, Dominio de Valdepusa, El Vicario, Finca Élez, Guijoso, La Jaraba, La Mancha, Los Cerrillos, Manchuela, Méntrida, Mondéjar, Pago Florentino, Ribera del Júcar, Uclés, Valdepeñas y Vallegarcía

Islas Baleares
Binissalem y Pla i Llevant

Aragón
Aylés, Calatayud, Campo de Borja, Cariñena y Somontano

Cataluña
Alella, Cataluña, Conca de Barberà, Costers del Segre, Empordá, Montsant, Penedés, Pla de Bages, Priorat, Tarragona y Terra Alta

Galicia
Monterrei, Rías Baixas, Ribeira Sacra, Ribeiro y Valdeorras

Cantabria
Costa de Cantabria, Liébana

Extremadura
Ribera del Guadiana

Islas Canarias
Abona, El Hierro, Islas Canarias, Gran Canaria, La Gomera, La Palma, Lanzarote, Tacoronte-Acentejo, Valle Güimar, Valle de la Orotava e Ycoden-Daute-Isora

Comunidad Valenciana
Alicante, Chozas Carrascal, El Terrazo, Los Balagueses, Utiel-Requena, Valencia y Vera de Estenas

Principado de Asturias
Cangas

Madrid
Vinos de Madrid

Castilla y León
Abadía-Retuerta, Arlanza, Arribes, Bierzo, Cebreros, Cigales, Dehesa Peñalba, León, Ribera del Duero, Rueda, Sierra de Salamanca, Tierra del Vino de Zamora, Toro, Ureña, Valles de Benavente y Valtiendas

Navarra
Bolandín, Navarra, Pago de Arínzano, Pago de Otazu y Pago de Irache

Murcia
Bullas y Yecla

País Vasco
Chacolí de Álava, Chacolí de Bizkaia y Chacolí de Getaria

Cava
Cataluña, La Rioja, Aragón, País Vasco, Navarra, Castilla y León, Comunidad Valenciana y Extremadura

Jumilla
Murcia y Castilla – La Mancha

Figura 27. Listado de DO clasificado por comunidades autónomas. Elaboración propia.

2. JUSTIFICACIÓN Y OBJETIVOS

De todo lo dicho anteriormente se desprende que el cambio climático supone nuevos retos para la Península Ibérica que repercutirán en el sector vitícola español lo que hace imprescindible disponer de información climática local predicha de calidad.

Ya existían varios estudios de *downscaling* específicamente sobre la temperatura en España (Brands et al., 2011b; Frías et al., 2005; Frías et al., 2010; Hervada-Sala et al., 2000; Miró et al., 2016; Turco et al., 2014), pero muy pocos estudios han explorado las temperaturas extremas en este territorio, tanto a nivel histórico (Fernández-Montes y Rodrigo, 2012; Fonseca et al., 2016) como a futuro (Pereira et al.2017; Lorenzo et al., 2021, Pereira et al., 2021, Lorenzo and Alvarez, 2022).

Pero como ya se ha visto, solo unos pocos estudios han desarrollado **escenarios** de temperatura en la región de Aragón (noreste de España) (Buerger et al., 2007; Goncalves et al., 2014; Ribalaygua et al., 2013a), pero ninguno de ellos desarrolló escenarios de temperaturas extremas u olas de calor. Sólo (Barrera-Escoda et al., 2014) desarrolló escenarios de temperaturas extremas en la cuenca del Ebro. Ese estudio mostró que el aumento previsto del número de noches tropicales y de las temperaturas extremas podría tener un efecto negativo sobre la salud humana y las condiciones de confort. Otros estudios también han analizado los posibles impactos del cambio climático en esta región sobre la salud humana (Roldán et al., 2016). Ambos estudios utilizaron los modelos climáticos asociados al 4º informe de evaluación del IPCC y no al 5º como es nuestro caso.

Los escenarios de sequía en España también son escasos y no informan del impacto que estos extremos supondrán para la región.

En el caso de las temperaturas extremas, se han realizado varios estudios que exploran las temperaturas extremas actuales (Kuglitsch et al., 2010) y futuras en Europa (Carvalho et al., 2021). Sin embargo, o se basan en modelos anteriores al CMIP5 o usan *downscaling* dinámico.

Aunque muchos modelos climáticos tienen dificultades para reproducir adecuadamente los extremos climáticos, como las olas de calor (Stegehuis et al., 2015), unos pocos estudios han informado sobre escenarios de olas de calor en Europa (Fischer and Schar 2010; Schoetter et al., 2015), o situados en la región mediterránea (Zittis et al., 2016), en Francia (Planton et al., 2008), Italia (Tomozeiu et al., 2007) o Finlandia (Kim et al., 2018). Schoetter et al. (2015) y Kim et al. (2018) son uno de los pocos estudios que ya utilizan los modelos del IPPC5. Como parte del Experimento Europeo Coordinado de Desescalado Regional (EURO-CORDEX) (Giorgi et al., 2009), la iniciativa EURO-CORDEX proporciona proyecciones climáticas regionales para Europa. Vautard et al., (2013) utilizó el proyecto EURO-CORDEX para simular olas de calor a escala regional europea, proporcionando una reducción de escala de las simulaciones CMIP5. Estos estudios a escala europea sólo incluían algunas localidades de España, pero no Aragón.

La industria vitícola es un ejemplo de globalización (Anderson 2003, Hussein et al., 2008) con el desarrollo de nuevas regiones de consumo y producción, expansión del comercio internacional y de innovación tecnológica. Las medidas llevadas a cabo por la industria para reducir los impactos del cambio climático (Galbreath 2014, Alonso and O'Neill 2011, Lereboullet et al., 2013a) refuerzan la necesidad de disponer de información climática (Lemos et al., 2012) y estrategias de comunicación con la industria (Lemos et al., 2012; Holland et al. 2010).

A pesar de que son muchos los indicios e informes sobre los efectos que el cambio climático ya ha ocasionado en el sector vitícola así como el esfuerzo llevado a cabo por la comunidad científica para identificar las relaciones entre variables meteorológicas y vid y el impacto que dichos cambios tienen en el futuro, siguen siendo escasos los estudios enfocados a analizar cómo los productores y los agricultores vitícolas pueden adaptarse a dichos cambios (Holland et al. 2010).

Desde el punto de vista de nuestro territorio y aunque existen estudios que evalúan el impacto del cambio climático en los viñedos del territorio español ibérico-peninsular, la mayoría lo hacen en base a proyecciones climáticas dinámicas (que no han tenido en cuenta la climatología local), salidas directas de los modelos climáticos o un número reducido de localizaciones españolas ya que forman parte de estudios que abarcan áreas geográficas más extensas. No existe hasta la fecha ningún estudio que evalúe el impacto del cambio climático en los viñedos del territorio ibero-español mediante índices bioclimáticos calculados en base a proyecciones climáticas regionalizadas a escala local con una técnica de *downscaling* estadístico (considerando la climatología local) generadas a partir de modelos climáticos pertenecientes a la quinta fase del CMIP.

Por tanto, **los escenarios de olas de calor/frío y sequía** en Aragón a escala local así como **los escenarios de indicadores bioclimáticos de interés vitícola** en territorio Ibérico-peninsular español no han sido obtenidos hasta la fecha, lo que justifica los objetivos de esta tesis pues es imprescindible disponer de escenarios locales para determinar el impacto del cambio climático en la realidad ambiental o socioeconómica de cada región para tomar decisiones de adaptación al cambio climático. La manera en la que se han generado proyecciones de temperatura y precipitación a escala local en base a modelos CMIP5 cubre una laguna de información climática en la región de Aragón. Finalmente, y dado que la industria vitícola aragonesa se puede beneficiar de las prácticas y soluciones llevadas a cabo por regiones climáticas similares, se justifica la necesidad de ampliar el estudio de indicadores vitícolas a todo el territorio ibérico-peninsular.

OBJETIVO:

Por lo tanto, **el objetivo** principal de este estudio es generar escenarios de clima futuro a escala local en España para el siglo XXI de temperatura y precipitación así como de eventos entremos de olas de calor/frío y sequías a fin de disponer de las bases climatológicas para calcular índices bioclimáticos que puedan valorar a escala local el impacto vitícola. Este estudio permitirá evaluar la idoneidad de la zona de estudio para el cultivo vitícola, así como determinar qué zonas van a perder potencial vitícola y cuáles van a ganarlo, lo que supondrá una información de gran utilidad para definir posibles medidas de adaptación del sector vitícola frente al cambio climático.

Para ello, se han planteado los siguientes **objetivos secundarios**:

a) Generación de escenarios para el Siglo XXI de temperatura y precipitación para Aragón a escala local en base a modelos pertenecientes al CMIP5 usando una metodología de *downscaling* estadístico basado en un método de análogos en dos pasos (Ribalaygua et al., 2013a). Como escenario futuro se han escogido los RCPs 4.5 y 8.5 como representación de una situación de evolución futura promedio y extrema.

b) Generación de escenarios de olas de calor/frío y sequías para Aragón a partir de las series de temperatura y precipitación generadas en el objetivo anterior.

c) Ampliar la generación de escenarios de temperatura y precipitación, así como los escenarios de olas de calor/frío y sequías para todo el territorio español ibérico-balear como base metodológica a la generación de índices bioclimáticos para todo el territorio.

d) Finalmente, en base a estas proyecciones de temperatura y precipitación, la generación de escenarios futuros de seis indicadores bioclimáticos a escala local: índice de Huglin, Índice de sequedad, Índice de frescor nocturno, Índice hidrotérmico de Branas, Bernon and Levadoux, Sistema de clasificación vitícola "Geoviticulture Multicriteria Climatic Classification" y el Índice CompI. para todo el territorio Ibérico-balear español.

3. METODOLOGÍAS

Atendiendo a los objetivos expuestos en el apartado anterior la tesis ha constado de tres fases principales. Una primera fase en la que se han generado los escenarios de temperatura y precipitación regionalizados para Aragón y evaluado los cambios esperados en dichas variables y cómo afectarán al territorio. Posteriormente, y utilizando las series regionalizadas en la primera fase, se han generado escenarios futuros de episodios de olas de calor/frío y sequía para Aragón y los impactos asociados a dichos eventos extremos. Finalmente, se ha procedido a calcular diversos indicadores climáticos de interés vitícola para todo el territorio español ibérico-balear (Figura 28).

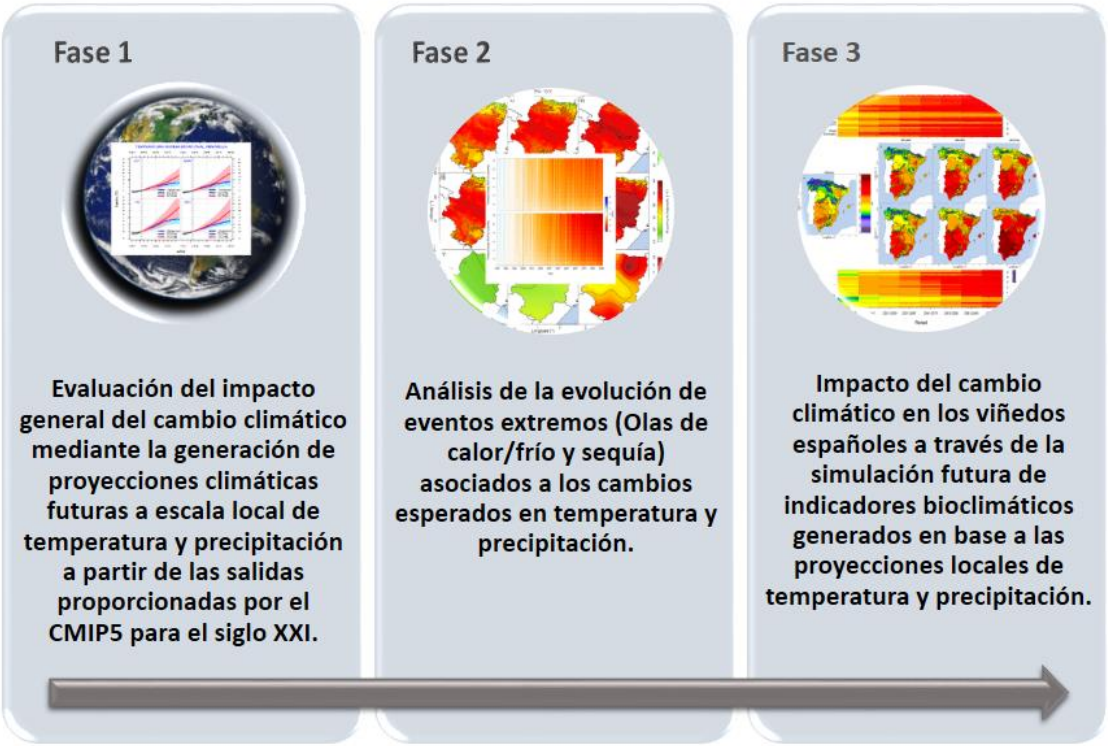

Figura 28. Fases desarrolladas a lo largo del estudio. Elaboración propia.

Tras el desarrollo de las fases 1 y 2 y como punto de partida para contextualizar la fase 3, se han generado escenarios de temperatura y precipitación así como escenarios de olas de calor/frío y sequía para todo el territorio español ibérico-peninsular. Esta información supone un complemento al estudio realizado en dichas fases y permite obtener una visión total del impacto climático y extremo en términos térmicos y pluviométricos.

3.1. Generación de escenarios de clima futuro de temperatura y precipitación

Teniendo en cuenta los puntos analizados en el apartado de introducción sobre modelización climática y considerando las características orográficas y climáticas de la zona de estudio así como la disponibilidad de datos observados, se ha elegido una metodología de *downscaling* estadístico basada en dos pasos (Ribalaygua et al., 2013a) como herramienta para la generación de las proyecciones climáticas de temperatura y precipitación.

3.1.1. Metodología de *downscaling* estadístico en dos pasos

Esta metodología consta de dos pasos: estratificación analógica y funciones de transferencia que permitan establecer relaciones entre los predictores (campos atmosféricos de baja resolución) y los predictandos (variables en superficie). La manera de trabajar en el segundo paso va a depender de la variable a simular.

- Primer paso: estratificación analógica

El primer paso consiste en una estratificación analógica basada en la hipótesis de que los patrones atmosféricos "análogos" (predictores) deben causar efectos locales "análogos" (predictores), lo que significa que se seleccionan los días más parecidos al día que se va simular (Benestad et al., 2007; Zorita y von Storch, 1999). La similitud entre dos días cualesquiera se midió utilizando una distancia pseudoeuclidiana entre los campos a gran escala utilizados como predictores entre cada día análogo y el día problema. Para cada predictor, se calculó y estandarizó la distancia euclidiana ponderada sustituyéndose por el percentil más cercano de una población de referencia de distancias euclidianas ponderadas para ese predictor. Este método es adecuado para reproducir las relaciones no lineales entre los predictores y los predictandos, pero no sirve para simular valores fuera del rango de valores observados (Imbert y Benestad, 2005). Es por esto que se procede a realizar un segundo paso.

- Segundo paso: funciones de transferencia

El comportamiento estadístico de cada variable (temperatura y precipitación en este caso) es muy diferente y, por tanto, el segundo paso depende de la variable.

1) Para estimar las temperaturas mínimas y máximas diarias, se realiza, por cada variable, una regresión lineal múltiple con selección automática de predictores sobre el conjunto de análogos seleccionado en el paso 1. Las relaciones lineales se aplican sobre un conjunto de predictores potenciales, compuesto por los valores de las variables atmosféricas en la vertical del punto (espesores) para el que se quiere estimar la temperatura en superficie, un indicador de la duración de la noche en el día en cuestión y un promedio ponderado de las temperaturas de los días anteriores. Una vez establecida la relación lineal existente entre los predictores seleccionados y el predictando (temperatura mínima o máxima), se aplica dicha relación a los valores de los predictores del día problema para estimar el valor del predictando en dicho día.

2) Para estimar la precipitación, en primer lugar, cada grupo de m días problema se regionaliza mediante el primer paso (m se elige como el número de días de un mes concreto). A continuación, y para cada día problema de estos m días, se obtiene una cantidad de precipitación preliminar promediando la cantidad de lluvia de sus n días más análogos, por lo que las m fechas problema se ordenan de mayor a menor por cantidad de precipitación preliminar. Para asignar la cantidad de lluvia final, tomamos cada una de las cantidades de lluvia de los $m \times n$ días análogos y las ordenamos y agrupamos en m grupos. Es decir, las m cantidades de precipitación final también se ordenan, al igual que las m fechas problema (que se ordenan previamente a partir de la precipitación preliminar). A continuación, ambas se vinculan: cada cantidad ordenada se asigna a cada una de las m fechas ordenadas.

Finalizados ambos pasos se tiene un conjunto de 18 proyecciones climáticas (9 ESMs x 2RCPs) de temperatura mínima, temperatura máxima y precipitación en cada uno de los observatorios considerados en el estudio. Será lo que llamemos proyecciones climáticas "brutas", es decir, no se les ha corregido el posible error sistemático asociado al método empleado.

3.1.2. Procesos de verificación y validación

Una vez que se han generado escenarios climáticos de precipitación y temperatura a escala local, se ha llevado a cabo un proceso de verificación (comparativa entre series simuladas a partir del reanálisis frente a datos observados) y un proceso de validación (comparativa entre series simuladas a partir del Historical de cada ESMs frente a series simuladas a partir del reanálisis). Los datos obtenidos en ambos procesos serán de utilidad para cuantificar y corregir el error sistemático consecuencia del método empleado.

3.1.3. Corrección del error sistemático

A las series "brutas" de proyecciones de temperatura y precipitación se les aplica un método de corrección de error sistemático con el fin de que su uso a nivel absoluto (y no como incremento) sea fiable y robusto.

En este caso, se ha empleado un método que permite corregir los datos de forma proporcional, es decir, a aquellos valores que presenten un mayor error se les aplica una corrección mayor y viceversa. La magnitud del error se obtiene: 1) comparando la función de distribución de los valores observados frente a la función de distribución de los valores simulados en base al ERA-40 (error 1 o de verificación) y 2) comparando la función de distribución de los valores simulados en base al ERA-40 con la función de distribución correspondiente a los valores simulados en base al Historical para cada modelo empleado (error 2 o de validación). En este caso, se emplea la función de distribución acumulada empírica (ECDF).

Al comparar las dos funciones entre sí se pueden establecer relaciones de proporcionalidad (no lineales) entre ambas, siendo las diferencias obtenidas las que nos permiten corregir el error entre ambos grupos. Una vez obtenidos los errores 1 y 2, estos se combinan y se aplican sobre la variable a corregir.

Una vez finalizado todo el proceso, los escenarios de clima futuro de temperatura y precipitación suponen un conjunto de proyecciones climáticas fiables y robustas que sirven de base para estudios de eventos extremos e indicadores bioclimáticos.

3.2. Generación de escenarios de clima futuro de valores extremos

3.2.1. Olas de calor/frío

Teniendo en cuenta las diferentes definiciones planteadas para cuantificar las olas de calor y frío propuestas por los diferentes organismos oficiales nacionales e internacionales comentadas en la introducción, y considerando las características climáticas de la zona de estudio, se ha aplicado la siguiente definición de ***ola de calor*** en este estudio (figura 29):

"al menos tres días consecutivos con temperatura máxima superior al percentil 95 obtenido de su serie de temperatura máxima observada y calculado entre los meses de junio a septiembre durante el periodo 1980-2000".

Figura 29. Definición de ola de calor y frío empleada en este estudio. Elaboración propia.

y se ha considerado como un episodio de ***ola de frío*** como (figura 29):

"al menos tres días consecutivos con temperatura mínima inferior al percentil 5 obtenido de su serie de temperatura mínima observada y calculado entre los meses de noviembre a abril durante el periodo 1980-2000"

Los resultados obtenidos se han analizado en base a varias consideraciones: intensidad media y máxima, duración y extensión espacial del evento.

3.2.2. Episodios de sequía

Después de un extensivo análisis sobre indicadores de sequía y atendiendo a las características climáticas de la región de estudio se han seleccionado el SPI y el SPEI como indicadores idóneos para evaluar la sequía meteorológica en Aragón. Por un lado, la definición de ambos indicadores permite su comparativa entre regiones y periodos temporales, por otro, el SPEI fue desarrollado y testado precisamente en Aragón por Vicente-Serrano et al. 2010. Además, el SPEI al incluir el efecto de la temperatura permite llevar a cabo un estudio de la importancia que tiene en el balance hídrico, punto muy importante en el contexto actual de calentamiento global.

Para evaluar los resultados se ha tenido en cuenta la intensidad de los indicadores así como su extensión espacial, además se ha considerado de interés calcular los valores de ambos índices a 6, 12, 24 y 60 meses abarcando situaciones de corto a largo plazo.

3.3. Generación de escenarios de clima futuro de indicadores bioclimáticos

Una vez obtenida una idea clara del impacto del cambio climático en el clima medio y en la ocurrencia de eventos extremos en Aragón se procede a evaluar qué implicaciones pueden tener estas alteraciones climáticas en el cultivo de la vid. En esta fase del estudio, se ha ampliado el área de análisis a todo el territorio Ibérico-Peninsular. El motivo de ampliar el área se debe a que los resultados obtenidos en otras regiones del país pueden se orientativas para los viticultores aragoneses a la hora de tomar medidas de adaptación frente a los problemas asociados al cambio climático.

La cantidad de indicadores vitícolas a emplear es muy extensa, pero en base a la literatura científica y al enfoque que se le quería dar al estudio (basado en el clima promedio y no en extremos) se han elegido como indicadores bioclimáticos: índice de Huglin, Índice de

sequedad, Índice de frescor nocturno, Índice hidrotérmico de Branas, Bernon and Levadoux, Sistema de clasificación vitícola “Geoviticulture Multicriteria Climatic Classification” y el Índice Compl.

A continuación, se expone la definición de cada uno de los índices propuestos.

- **<u>Índice de Huglin (HI)</u>**

El Índice de Huglin es un índice termal basado en grados días, es decir en el concepto de acumulación de calor. Este índice se utiliza para evaluar la demanda térmica y radiativa básica de la uva durante el periodo de crecimiento que garantice una completa y adecuada maduración.

Cada variedad de uva requiere una acumulación de calor determinada para que la maduración se produzca de forma óptima (Tonietto, 1999). Según los valores obtenidos de HI, el clima variará entre muy frío o muy cálido:

ÍNDICE DE HUGLIN (HI)

$$\sum_{Abril}^{Sept.} \frac{(\bar{T}-10)(T_{max}-10)}{2} * k$$

$\bar{T} \equiv$ temperatura media (ºC)
$T_{max} \equiv$ temperatura máxima (ºC)
$k_{(mes)} \equiv (0,0,0,0.1,0.3,0.5,0.5,0.5,0.5,0,0,0)$

Categoría	Umbrales	Características	Observaciones
0	≤1200	---	Regiones demasiado frías para el cultivo de la vid.
1	1200-1500	HI-3: muy frío	Regiones al límite de la vid. Alcanzan la madurez solo las variedades muy tempranas. Especialmente las blancas.
2	1500-1800	HI-2: frío	Estas regiones permiten el crecimiento de un amplio rango de variedades, tanto blancas como tintas.
3	1800-2100	HI-1: templado	Alcanzan la madurez las variedades tardías.
4	2100-2400	HI+1: templado cálido	No debería existir limitaciones heliotérmicas y casi cualquier variedad puede madurar.
5	2400-2700	HI+2: cálido	En estas regiones se superan las condiciones heliotérmicas incluso para las variedades más tardías. Riesgo de estrés térmico.
6	2700-3000	HI+3: muy cálido	No existe limitación heliotérmica. Pueden darse hasta dos maduraciones en un mismo ciclo. Riesgo muy elevado de estrés térmico.
7	≥ 3000	---	Regiones demasiado cálidas para el cultivo de la vid.

Figura 30. Índice de Huglin: definición matemática, escala de intensidades e implicaciones asociadas a cada categoría. Elaboración propia.

- **<u>Índice de sequedad (Dryness Index DI)</u>**

El Índice de sequedad (DI) evalúa la disponibilidad de agua en el suelo proporcionando información sobre las condiciones de estrés hídrico. Según diversos estudios (Blanco-Ward et al., 2007; Vanderlinden et al., 2004; Brixner et al., 2014) y concretamente Fonseca et al (2012), se eligió la fórmula de Hargreaves para el cálculo del DI en lugar de otras formulaciones más complejas en el cálculo de la ETP.

ÍNDICE DE SEQUEDAD (DI)

$$\sum_{April}^{Sept.} (Wo + P - Tv - Es)$$

P ≡ precipitación (mm)
Wo ≡ reserva de agua en suelo inicial (mm) = 200
T_v ≡ Transpiración potencial en el viñedo (mm) = ETP*k
Es ≡ Evaporación directa a través del suelo (mm) = (ETP/N)*(1-k)*JPm
JPm=P/5

Categoría	Umbrales	Características	Observaciones
5	> 150	DI-2: húmedo	Regiones húmedas o con ausencia de sequía, presentan un alto nivel de disponibilidad de agua en el balance hídrico. Un exceso de humedad puede resultar perjudicial para ciertas variedades, mermando la calidad de la cosecha.
4	150-50	DI-1: subhúmedo	Regiones con ausencia de sequía pero los valores hídricos que la definen solo muestran que se ha alcanzado un mínimo de disponibilidad hídrica con ciertas condiciones de restricciones para los meses de verano.
3	50 – (-100)	DI+1: moderadamente seco	Bajo estas carcaterísicas la vid tiene que hacer frente a ciertas condiciones potenciales de sequía. Aunque situaciones de leve sequía durante la maduración son beneficiosas puede resultar perjudicial para ciertas variedades.
2	(-100)- (-200)	DI+2: seco	Regiones con condiciones de sequía leve.
1	≤ -200	DI+3: muy seco	Problemas debidos al estrés hídrico y en la mayoría de los casos se requerirá aporte de agua extra.

Figura 31. Índice de sequedad: definición matemática, escala de intensidades e implicaciones asociadas a cada categoría. Elaboración propia.

- **Índice de frescor nocturno (Cool night Index CI)**

El índice de frescor nocturno (CI) es un índice termal basado en la temperatura nocturna durante el periodo de maduración (septiembre en el HN). Temperaturas nocturnas moderadamente bajas junto con temperaturas diurnas altas favorecen la producción de vinos de alta calidad ya que se favorece la síntesis de algunas componentes fenológicas.

ÍNDICE DE FRESCOR NOCTURNO (CI)

$\bar{T}_{min}$ (sept)

T_{min} ≡ temperatura mínima (ºC)

Categoría	Umbrales	Características	Observaciones
5	≥25	---	Regiones con temperaturas nocturnas demasiado cálidas para favorecer la maduración.
4	18 -25	CI1: noches cálidas	Regiones con un periodo de maduración de la uva con altas temperaturas nocturnas para todas las variedades, pudiéndose verse afectados el color y el potencial aromático de las bayas.
3	14 -18	CI2: noches templadas	Regiones donde las variedades tardías madurarán en condiciones de más bajas temperaturas que aquellas variedades tempranas.
2	12 -14	CI3: noches frías	En condiciones de noches frías, la maduración puede ocurrir en temperaturas más frescas de las que requieren ciertos tipos de variedades, aunque siguen siendo condiciones favorables.
1	6-12	CI4: noches muy frías	Estas condiciones pueden ser positivas para aquellas variedades que, debido a su potencial heliotérmico, garanticen un buen nivel de maduración de la uva.
0	≤6	---	Regiones con temperaturas nocturnas demasiado frías para favorecer la maduración.

Figura 32. Índice de frescor nocturno: definición matemática, escala de intensidades e implicaciones asociadas a cada categoría. Elaboración propia.

- **Índice hidrotérmico de Branas, Bernon and Levadoux (HyI)**

El índice hidrotérmico de Branas, Bernon and Levadoux es un índice que combina el efecto de la humedad del aire (a través de la precipitación) y la temperatura en la época de crecimiento con el fin de evaluar el riesgo de exposición de la uva a ciertas enfermedades como el Mildiu.

Índice hidrotérmico de Branas, Bernon and Levadoux (HyI)

$$\sum_{April}^{Aug} (\bar{T} * P)$$

$\bar{T} \equiv$ temperatura media (ºC)
P $\equiv$ precipitación (mm)

Categoría	Umbrales	Características
1	< 2500	Bajo riesgo
2	2500-5100	Riesgo medio
3	5100-7500	Riesgo alto
4	>7500	Riesgo muy alto

Figura 33. Índice hidrotérmico de Branas, Bernon y Levadoux: definición matemática, escala de intensidades e implicaciones asociadas a cada categoría. Elaboración propia.

- **<u>CompI Index</u>**

El ***CompI Index*** (Malheiro et al., 2010) es un índice que permite evaluar la adecuación climática para el crecimiento de la uva. El CompI es el porcentaje de años óptimos para el cultivo de la vid para un periodo dado. Se entiende por año óptimo aquel año en el que se alcanzan unos umbrales críticos de los índices HI, DI, HyI y unas condiciones de temperatura mínima.

CompI Index (CompI)

$$\frac{nº\ años\ óptimos}{nº\ años\ del\ periodo}$$

Umbrales	Condiciones para que se de un año óptimo	Observaciones
0.0-0.2	HI ≥ 900 ºC DI ≥ -100mm HyI ≤ 7500ºC·mm T_{min} > -17 ºC (siempre)	% de años óptimos para la viticultura del periodo considerado
0.2-0.4		
0.4-0.6		
0.6-0.8		
0.8-1.0		

Figura 34. CompI Index: definición matemática, escala de intensidades e implicaciones asociadas a cada categoría. Elaboración propia.

- **<u>The Geoviticulture Multicriteria Climatic Classification (MCC) System</u>**

El sistema MCC se desarrolló para mejorar la caracterización del clima vitícola en las regiones productoras de vino del mundo. Se trata de un sistema de clasificación climática de las regiones vitícolas basado en la integración de las diferentes clases de tres índices climáticos -DI, HI y CI-. De este modo, se establece el clima vitícola de cada región y se pueden clasificar y agrupar las regiones. Así, el sistema permite la identificación de análogos climáticos. Permite evaluar una región vitícola desde el punto de vista del clima vitícola, del grupo climático y del clima vitícola con variabilidad intra-anual (Tonietto and Carbonneau 2004).

MCC System	Combinación de HI, DI and CI

Combinación de categorías que resultan óptimas para el cultivo de la vid	Combinación de categorías que resultan óptimas para el cultivo de la vid
HI-3, HI-2, HI + 1 CI + 1; CI +2 DI-1, DI + 1	CI-2, CI-1 DI + 2, DI + 3

Figura 35. MCC System: definición matemática, escala de intensidades e implicaciones asociadas a cada categoría. Elaboración propia.

Para el análisis de los resultados se ha optado por varios enfoques complementarios entre sí:

- Enfoque 1: por un lado, se analizan los resultados a nivel de mapa (interpolado en base a todos los observatorios disponibles para el estudio) y por otro, se analiza la información agrupada por DOs. De esta manera, se puede optar por evaluar directamente la DO que se quiere consultar y comparar con otras DOs de características similares. También permite evaluar qué regiones del territorio serán óptimas o dejarán de serlo para un tipo de variedad o vino en particular o bien comparar regiones climáticas parecidas con maneras de producir similares y establecer sinergias entre ellas.
- Enfoque 2: los valores de los indicadores se han representado de dos maneras: en valores absolutos y categorizados. Las categorías en las que se mueven los indicadores son bastante amplias por lo que no es lo mismo que una región se encuentre en el límite superior de la categoría que en el inferior. Por ejemplo, si los valores del DI se sitúan dentro del rango [-100,50] dos observatorios con valores en ese rango pertenecerán a esa categoría pero desde el punto visto de aporte hídrico no es lo mismo tener DI= -90 que DI= 45. De ahí la importancia de evaluar ambas escalas simultáneamente.

3.4. Datos y área de estudio

3.4.1. Área de estudio

El estudio se ha llevado a cabo sobre dos regiones. La primera parte, en la que se ha evaluado el impacto del cambio climático a través de las variables meteorológicas primarias (temperatura y precipitación) y los eventos extremos asociadas a las mismas (olas de calor/frío y eventos de sequía, respectivamente), se ha ejecutado principalmente sobre Aragón y se ha complementado con información para toda España. En la segunda parte se ha evaluado el impacto del cambio climático sobre los viñedos a través de indicadores bioclimáticos, a nivel de territorio español ibérico-balear. Esto ha permitido, por un lado, evaluar cómo se verán afectados los viñedos aragoneses y por otro, poder comparar dichos resultados con los obtenidos en otras regiones ibérico-baleares. Disponer de información en un territorio más extenso permite considerar qué medidas de adaptación están tomando otras regiones con características climáticas y vitícolas similares a las nuestras y considerar su implantación.

Características físicas y climáticas de Aragón

Aragón se encuentra ubicado en la zona noreste de la Península Ibérica (España) y ocupa una extensión de aproximadamente 47,720 km^2 (340 km de largo por 240 km de ancho). Por su localización (figura 36), Aragón se encuentra en una zona con clima mediterráneo del oeste, presentando inviernos muy fríos y veranos muy cálidos y secos así como escasa pluviometría. Sin embargo, la gran diferencia de altitudes, más de 3000m de diferencia entre los valles (como el valle del Ebro) y las zonas montañosas (Los Pirineos) junto con la orografía específica de la zona (la cuenca hidrográfica del Ebro en el valle y la cadenas montañosas, los Pirineos al norte y la Cordillera Ibérica al sur del valle, respectivamente) hacen que las características climáticas se modifiquen localmente. Estas modificaciones climáticas locales explican ciertas características típicas de la región como son: la sequedad del terreno a lo largo de las riberas del río Ebro, la presencia de patrones de lluvia aleatorios, un alto contraste térmico entre el invierno y el verano como consecuencia de las fuertes características continentales de la región y los típicos vientos "mistral" del noreste, que son frecuentes en la región.

Las temperaturas medias anuales de Aragón varían entre la zona del valle del Ebro cuya temperatura media se sitúa en torno a los 15 ºC y las zonas más altas con temperaturas medias de apenas 7 ºC. Un rasgo característico de la región es su alta amplitud térmica anual, ya que en algunas zonas del territorio puede oscilar entre temperatura negativas en los meses de inverno y temperaturas superiores a los 35 ºC en los meses estivales, aunque en promedio la amplitud térmica anual se sitúa en torno a los 12 ºC.

Una característica importante de la región es la escasa precipitación, la cual se distribuye claramente conforme al relieve como demuestran las isoyetas, que se disponen en círculos concéntricos que van disminuyendo desde las zonas de montaña hasta el centro de la región. Aunque la precipitación total media anual del territorio aragonés se sitúa en torno a los 550 mm, hay regiones cuya media está por debajo de estos valores (por ejemplo, en el sector central de la depresión del Ebro). Sólo en los Pirineos y, en menor medida, en la Cordillera Ibérica, las precipitaciones alcanzan valores importantes, 1800-2000 mm y muestran valores positivos de balance hídrico (considerando la diferencia entre precipitación y la ETP).

Por otro lado, más del 60% de la región presenta valores medios de ETP superiores a 1100 mm, mostrando un balance hídrico negativo, a lo que contribuye no sólo la escasez de precipitaciones sino también el fuerte viento ("Cierzo") característico del Valle del Ebro (López et al., 2007). Así, el 70% del territorio aragonés se considera semiárido de acuerdo al valor del índice propuesto por el Programa de Naciones Unidas para el Medio Ambiente (inferior a 0,5) e incluso el 30% del territorio presenta valores del índice de 0,3. (Cherlet et al., 2018).

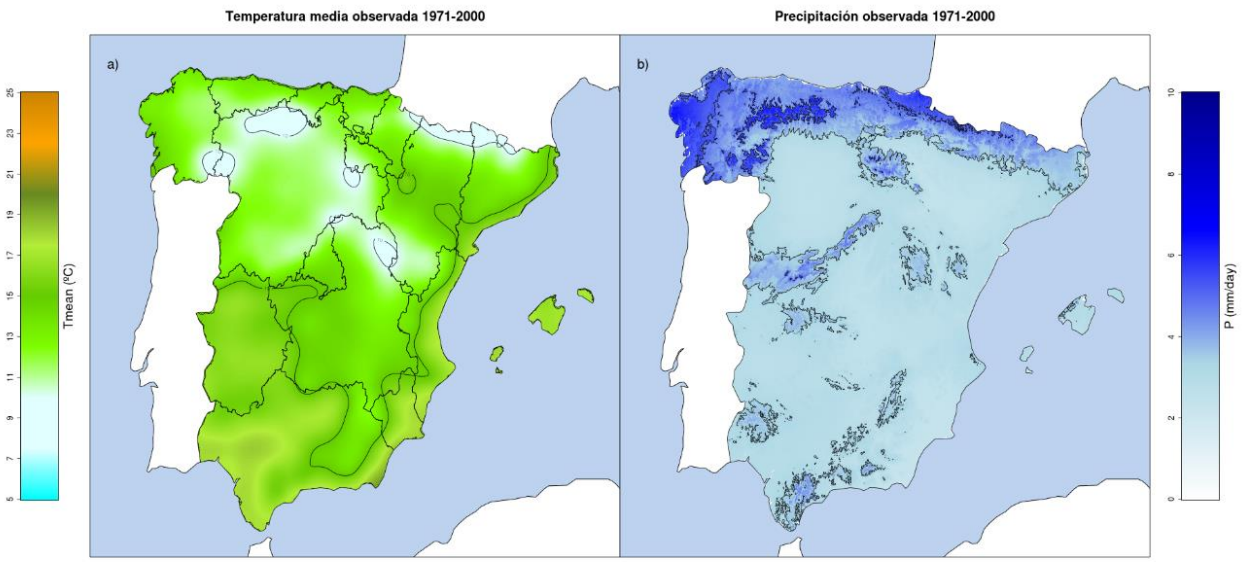

Figura 36. a) Temperatura media observada y b) precipitación media diaria observada en el territorio español Ibérico-balear en el periodo 1971-2000. Elaboración propia.

Características físicas y climáticas del territorio español Ibérico-balear

El territorio español peninsular y las Islas Baleares considerado en el estudio abarca un área de 588.294 km2 (figura 36). Debido a su ubicación próxima a grandes masas de agua y por su compleja orografía (desde el nivel del mar hasta picos que superan los 3400 km) el clima español es muy variado y complejo, de manera que se pueden contar hasta 13 regiones climáticas según la clasificación de Köppen, y múltiples microclimas.

El clima de la España ibérico-balear depende de su situación en el extremo suroccidental de Europa y de su compleja orografía mientras que las islas Baleares se encuentran en el Mediterráneo occidental cerca de la península ibérica y son relativamente montañosas. Este espacio geográfico está afectado climáticamente por los vientos dominantes provenientes del Atlántico y las borrascas asociadas al frente polar, las altas presiones relacionadas con los anticiclones de las Azores y centroeuropeos, las bajas norteafricanas, la influencia del Mediterráneo y las advecciones de masas de aire frío centroeuropeo y ártico.

Las precipitaciones medias totales anuales en la Península disminuyen, en general, de norte a sur y de oeste a este. Los máximos pluviométricos se presentan en el norte peninsular (costa Atlántica) mientras que los valores mínimos se encuentran en el sureste peninsular (litoral de Almería y Murcia). Las precipitaciones son más abundantes, en general, en otoño e invierno y escasas en verano. La mayor parte del territorio presenta sequía estival y son relativamente frecuentes los chubascos intensos asociados a inestabilidad y la nubosidad convectiva, sobre todo en las regiones mediterráneas y del suroeste peninsular.

Respecto a las temperaturas, las más bajas se producen en el mes de enero y las más altas en julio. En invierno, en las zonas de montaña y en el interior peninsular hay frecuentes heladas y se pueden alcanzar temperaturas mínimas muy bajas, tanto los días anticiclónicos con fuerte irradiación nocturna como los días de advecciones frías árticas o centroeuropeas. Independientemente de las altas cumbres, se alcanzan temperaturas

invernales muy bajas en valles intramontanos del Pirineo aragones-catalán, del sistema Ibérico y de la vertiente sur de la cordillera Cantábrica. En verano las máximas temperaturas se alcanzan en zonas del centro del valle del Guadalquivir y del sur de Extremadura. En el litoral galaico-cantábrico las temperaturas veraniegas son relativamente suaves y la interacción de las brisas marinas con los montes costeros origina algunos días de llovizna; en el litoral mediterráneo el verano se caracteriza por la fuerte insolación, la humedad relativa alta con sensación de bochorno y el largo periodo de sequía, aunque pueden producirse algunas tormentas.

Los factores fundamentales del paisaje vegetal son el clima, el suelo y la geomorfología. La mayor parte de Galicia, la cornisa cantábrica y los Pirineos, pertenecen a la región biogeográfica Eurosiberiana (normalmente sin sequía estival), mientras que el resto de la Península y Baleares pertenecen a la región mediterránea.

3.4.2. Bases de datos empleadas

Para llevar a cabo un estudio de análisis de impacto del cambio climático en base a las metodologías que hemos seleccionado, es necesario disponer de dos grupos de datos: datos observados en superficie y datos atmosféricos (reanálisis y modelos climáticos). En la figura 37, se muestra, a modo resumen, en qué parte del proceso se requiere cada base de datos.

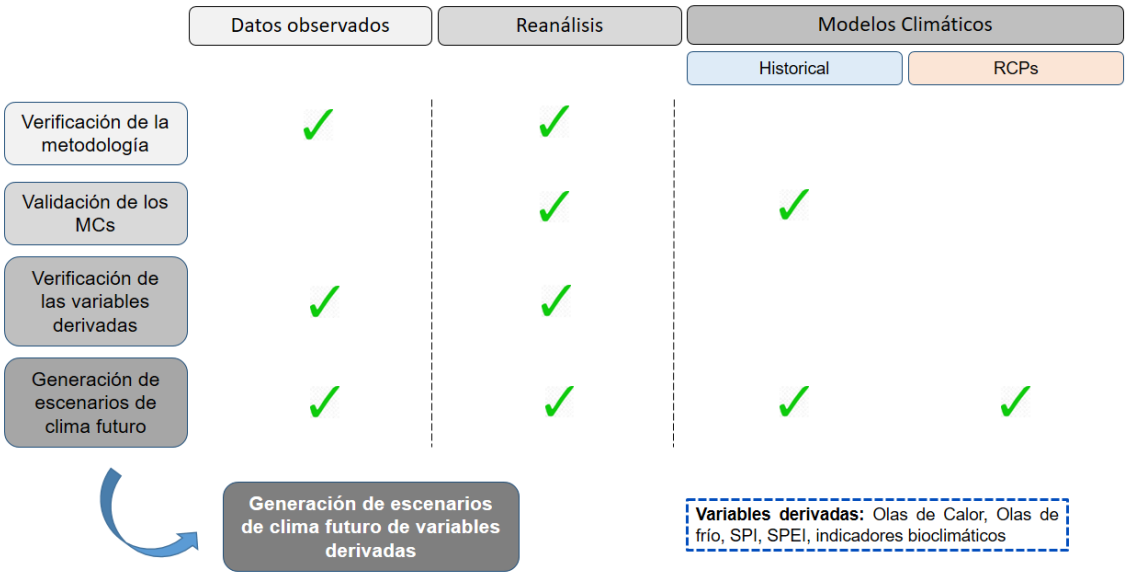

Figura 37. Esquema de las bases de datos necesarias para la generación de escenarios de clima futuro de indicadores bioclimáticos y fenómenos extremos así como los procesos en los que son necesarias. Elaboración propia.

<u>Base de datos observados en superficie (campos predictandos)</u>

- Base de datos empleados en el estudio propio de Aragón

El conjunto de datos observacionales utilizado en el presente estudio consiste en una serie temporal de las temperaturas máximas y mínimas diarias así como de precipitación, obtenidas de la extensa red de observatorios instrumentales de AEMET (http://www.aemet.es) y distribuidos de forma bastante homogénea, por todo el territorio de Aragón.

Estos observatorios están sometidos a un estricto control de calidad de los datos, que incluye la detección y corrección de múltiples puntos críticos en las series temporales climáticas a largo plazo, la cobertura de las lagunas, la evaluación de la homogeneidad de las series climáticas y la corrección de las inhomogeneidades encontradas.

Para garantizar la calidad de los datos, se descartaron las estaciones con un gran número de lagunas de datos o sin al menos 15 años de registros diarios. En segundo lugar, se analizó el conjunto de datos para detectar la presencia de puntos de datos extremos que pudieran considerarse observaciones sospechosas o errores de transcripción (consideramos que los puntos de datos eran extremos si se separaban de la media mensual en más de cuatro veces el valor de la desviación estándar). En tercer lugar, se verificó que los datos no contuvieran inhomogeneidades que pudieran introducir un sesgo en los registros que no estuvieran relacionados con el clima.

El primer conjunto de datos (compuesto por 103 observatorios) se utilizó para analizar y elaborar los escenarios climáticos regionales de temperaturas máximas y mínimas (figura 38a, puntos rojos). De estos 103 observatorios, los que tenían al menos el 75% de los datos de temperatura máxima recogidos de junio a septiembre (es decir, el periodo de referencia para el cálculo de las olas de calor) entre 1980 y 2000 y los observatorios que tenían al menos el 75% de los datos de temperatura mínima recogidos de noviembre a abril (es decir, el periodo de referencia para el cálculo de las olas de frío) entre 1980 y 2000 configuran un segundo conjunto de datos seleccionados para el estudio de los eventos extremos de olas de calor y frío, respectivamente. En ambos casos, el número de observatorios fue de 71 (figura 38b).

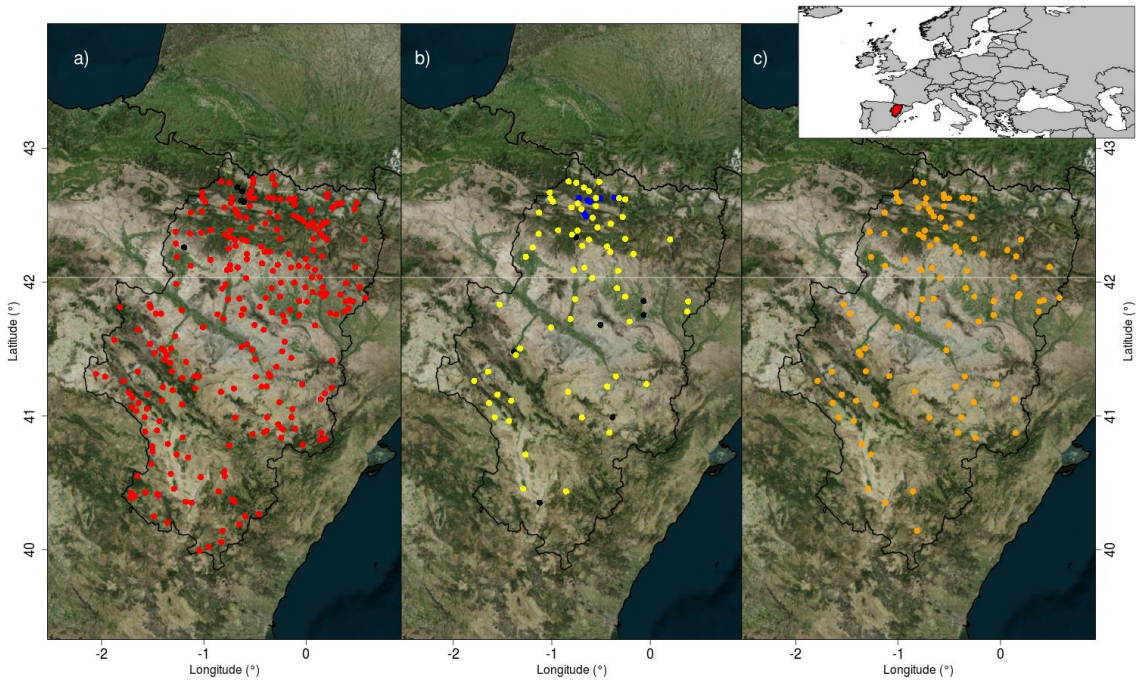

Figura 38. a) Ubicación de los observatorios de temperatura (en rojo) y de precipitación (en rojo y negro) utilizados para la generación de los escenarios futuros, b) localización de los escenarios utilizados en el cálculo de olas de calor y frío (en amarillo), solo para olas de calor (en negro) y solo para olas de frío (en azul), c) localización de los escenarios utilizados en el cálculo de los indicadores de sequía (puntos naranjas). Elaboración propia.

Para la simulación de futuros escenarios climáticos de **precipitación**, se utilizó un primer conjunto de 263 estaciones (figura 38a, puntos rojos y negro). De estas 263 estaciones, sólo se utilizaron para la simulación de los índices de sequía las que tenían datos para ambas variables, temperatura y precipitación (figura 38c).

- Base de datos empleados en el estudio propio del territorio español ibérico-balear

Al igual que en el caso de estudio de Aragón, los datos empleados provienen de la red de observatorios instrumentales de AEMET y cumple los mismo requisitos de calidad que se describen en el apartado anterior. Esta base de datos ha sido empleada en numerosos estudios de generación de escenarios climáticos futuros en este área (Gaitan et al., 2019; Gaitan et al., 2020; Gomez-Martinez et al., 2021; Monjo et al., 2016; Ribalaygua et al., 2013b). En el estudio se han utilizado un total de 1778 observatorios con datos tanto de temperatura como de precipitación, cubriendo ampliamente todo el territorio estudiado (figura 39).

Para el análisis de los resultados por DOs, se han elegido aquellos observatorios que se encuentran dentro del territorio clasificado como tal (figura 39). En total, hay 789 observatorios dentro de 59 DOs situadas en el territorio ibérico-balear. Se dejan fuera del presente estudio las DOs en las que no se encontraron observatorios con información de temperatura y precipitación simultáneamente o con información meteorológica escasa, lo que supuso sólo alrededor del 1,3% del total de la superficie ocupada por las DOs.

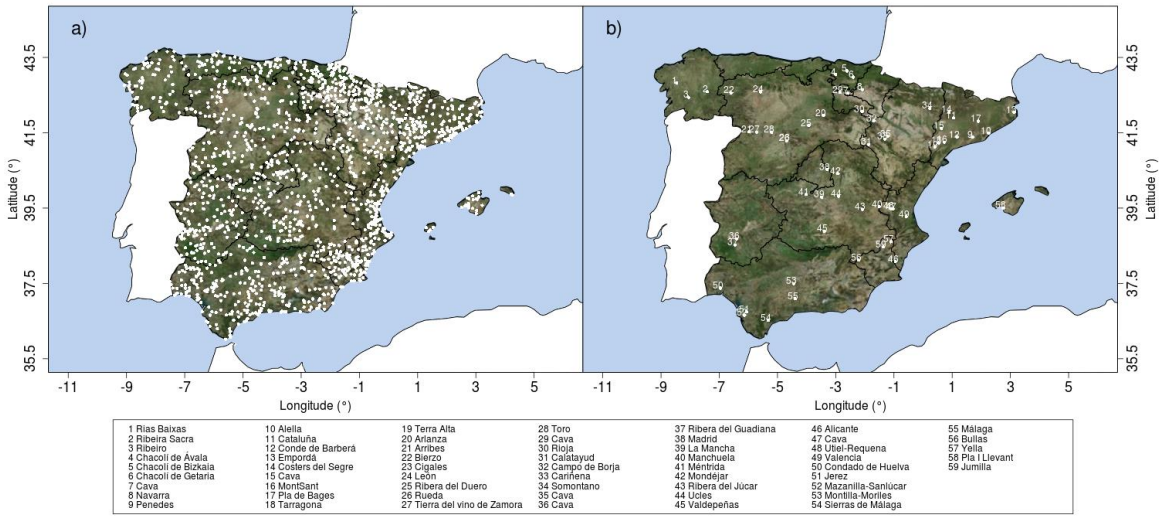

Figura 39. a) Estaciones meteorológicas empleadas en el estudio vitícola así como b) localización de las DOs seleccionadas para su análisis climático. Elaboración propia.

<u>Datos atmosféricos (campos predictores)</u>

- Reanálisis Europeo ERA-40

Para estudiar el comportamiento de las simulaciones históricas del modelo CMIP5, se utilizó el conjunto de datos de reanálisis del Centro Europeo de Previsiones Meteorológicas a Medio Plazo (ECMWF ERA-40; http://www.ecmwf.int/research/era/do/get/) (Uppala et al., 2005) para el periodo 1958-2000 con una resolución temporal de 6 horas y una resolución espacial de 125 km. Para la

verificación de la metodología, fue necesario reducir la escala temporal y espacial del reanálisis para poder comparar tanto ERA-40 como las simulaciones del modelo climático (Ribalaygua et al., 2013a; Ribalaygua et al., 2013b). Los límites geográficos de la ventana atmosférica utilizada fueron las latitudes 31,5°N a 55,1°N y las longitudes 27,0°W a 14,6°E, cubriendo no sólo el área geográfica en estudio sino también las zonas atmosféricas circundantes que ejercen una influencia meteorológica en toda la Península Ibérica (Ribalaygua et al., 2013a). El uso del conjunto de datos ERA-40 nos ha permitido comparar estos nuevos resultados con los publicados por Ribalaygua et al 2013b basados en modelos del CMIP3.

- Modelos climáticos globales pertenecientes al CMIP5

En el presente estudio, se trabajó con un conjunto de nueve modelos climáticos que pertenecen al CMIP5 y que fueron proporcionados por los archivos del Programa de Diagnóstico e Intercomparación de Modelos Climáticos (PCMDI) (Tabla 1). El número de modelos elegidos se limitó a la disponibilidad de datos con frecuencias temporales diarias. Todos los modelos eran ESM.

Para generar los campos predictores de los modelos, tomamos los valores diarios de varios campos de interés a gran escala (es decir, altura geopotencial, humedad específica y viento) en diferentes niveles de presión para los nueve ESMs mostrados en la tabla 1 asociados a la CMIP5 (Taylor et al., 2012). Además, utilizamos un experimento histórico (Taylor et al., 2012) que generó simulaciones del pasado siglo XX y que fue útil para la evaluación del rendimiento del modelo frente al clima actual. Por último, se consideraron dos escenarios o RCPs (Moss et al., 2010), concretamente el escenario RCP8.5 "alto" y el escenario RCP4.5 "intermedio", ambos correspondientes a diferentes rangos posibles de forzamiento radiativo alcanzado en el año 2100 respecto a los valores de la era preindustrial (4,5 y 8,5 W/m2, respectivamente).

Modelo climático	Resolución espacial/temporal	Centro de investigación responsable	Referencias
GFDL-ESM2M	2ºx2,5º daily	National Oceanic and Atmospheric Administration (NOAA), E.E.U.U.	Dunne et al. (2012)
CanESM2	2,8ºx2,8º daily	Canadian Centre for Climate Modeling and Analysis (CC-CMA), Canadá.	Chylek et al. (2011)
CNRM-CM5	1,4ºx1,4º daily	CNRM (Centre National de Recherches Meteorologiques), Meteo-France, Francia.	Voldoire et al. (2013)
BCC-CSM1-1	1,4ºx1,4º daily	Beijing Climate Center (BCC), China Meteorological Administration, China.	Xiao-Ge et al. (2013)
HADGEM2-CC	1,87ºx1,25º daily	Met Office Hadley Center, United Kingdom.	Collins et al. (2008)
MIROC-ESM-CHEM	2,8ºx2,8º daily	Japan Agency for marine-Earth Science and Technology (JAMSTEC), Atmosphere and Ocean Research Institute (AORI), and National Institute for Environmental Studies (NIES), Japan.	Watanabe et al. (2011)
MPI-ESM-MR	1,8ºx1,8º daily	Max-Planck Institute for Meteorology (MPI-M), Germany.	Raddatz et al. (2007); Marsland et al. (2003)
MRI-CGCM3	1,2ºx1,2º daily	Meteorological Research Institute (MRI), Japan.	Yukimoto et al. (2011)
NorESM1-M	2,5ºx1,9º daily	Norwegian Climate Centre (NCC), Norway.	Bentsen et al. (2012); Iversen et al. (2012)

Tabla 1. Información sobre los nueve modelos climáticos pertenecía al CMIP5. Los modelos fueron suministrados por el Programa de Diagnóstico e Intercomparación de Modelos Climáticos (PCMDI).

3.4.3. Denominaciones de Origen

De las 101 DO totales se ha trabajado finalmente con 54 DOs de ellas (figura 39). Se han seleccionado aquellas DOs de las que se tienen datos históricos de temperatura y precipitación procedentes de observatorios ubicados en el área denominada para cada DO. Así mismo también se han quedado fuera del estudio algunas DOs que no estaban incluidas en el mapa de la base de datos del Ministerio de Agricultura, Pesca y Alimentación, MAPA, en el momento de su consulta y aquellas que a pesar de tener datos meteorológicos estos no han pasado los filtros mínimos de calidad. Las DOs canarias se han dejado fuera del estudio ya que debido a su ubicación geográfica, se rigen por patrones atmosféricos diferentes a los utilizados en Península y Baleares y requieren de un estudio propio considerando sus particularidades climáticas.

4. RESULTADOS

Resultado 1
Proyecciones climáticas futuras de temperatura y de episodios de olas de calor y de frío para Aragón (España) en base a las salidas de modelos pertenecientes al CMIP5

Projection of temperatures and heat and cold waves for Aragón (Spain) using a two-step statistical downscaling of CMIP5 model outputs

Abstract

Heat- and cold-wave scenarios and temperature scenarios during the 21st century were obtained for Aragón (Spain), using, for the first time, nine Earth System Models (ESM) and two Representative Concentration Pathway (RCP) scenarios – RCP4.5 and RCP8.5 - belonging to the 5th Coupled Model Intercomparison Project (CMIP5).

Local climate heat-wave scenarios show an increase of its mean intensity close to 2 ºC (reaching temperatures of up to 38.8 ºC) and an average increase of the maximum intensity of 3.6 ºC (temperature of up to 41.5 ºC) with respect to a historic period (1971–2000) for the RCP8.5 scenario at the end of the century. The duration of heat waves will increase by 7 days at the end of the century (total average duration of 12 days). The future intensity and duration of cold-wave episodes will remain stable.

Local climate change scenarios for daily maximum temperatures show a gradual increase throughout the 21st century. The greatest increases will occur during the summer at the end of the century, reaching values of up to 7 ºC for the RCP 8.5 scenario. The minimum temperature increases show similar behaviours to the maximum temperatures, but with less marked increases (3 ºC and 5.6 ºC for the RCP4.5 and RCP8.5 scenarios respectively in summer at the end of the century).

The highest temperatures and the intensity of the heat waves will be especially intense in the Ebro Valley, the most populated area. In addition, the Pyrenees will suffer the longest heat waves, especially at the end of the century, and the greatest increases in maximum temperatures.

The downscaling of the CMIP5 models, offers accurate scenarios -both spatially and temporally- of extreme temperatures and heat and cold waves, useful for decision-making for local adaptation to climate change but also as a reference for other European regions.

1. Introduction

There is widespread agreement in the scientific literature that the most severe effects of global warming will be related not only to a change in the mean climate, but especially to an increase in the frequency and intensity of extreme events, such as floods, droughts and heat waves as is reflected in the conclusions provided by the Intergovernmental Panel on Climate Change (IPCC) and in independent studies (Cook et al. 2013). Heat waves (i.e., a period of consecutive days with extreme hot temperatures) are one form of extreme weather that is likely to increase in frequency, intensity and duration under the influence of a changing climate during upcoming years (IPCC, 2013; Field et al., 2012). Extreme temperature events can impact many aspects of human life, such as mortality, health, comfort, agriculture and hydrology (Garcia-Herrera et al., 2005; Roldan et al., 2016). For example, in 2003, an extraordinary ‘‘mega heat wave’’ occurred in Central Europe, which had important consequences on society.

One of the main problems when evaluating extreme episodes of temperature (that is, cold or heat waves) is that there are no universal definitions of these phenomena. Some

definitions use a fixed term (5 days > 30 ºC or 3 days > 35 ºC in the case of a heat wave); some include humidity, spatial extent or accumulated heat ((Anderson and Bell, 2009; Russo et al., 2017; Suparta and Yatim, 2017); some set their threshold according to a specific percentile (Anderson and Bell, 2009; Kent et al., 2014; Smith et al., 2013); and some are based on combined indexes of different meteorological variables, such as World Meteorological Organization member guidelines (WMO, 2010).

Although large-scale and small-scale processes involved in the development of European heat waves, such as interactions between land surface and atmosphere and the influence of large-scale atmospheric circulation, are not fully understood (Vautard et al., 2013), climate models could be a suitable tool for providing accurate heat-wave assessments for future adaptation strategies.

Global climate models (GCMs) are fundamental tools for the study of future climate, and they are able to provide data to estimate large-scale aspects of climate change, to drive regional climate models or to be used directly by impact models. GCM outputs are also used for projections of temperature extremes around the world (Dosio, 2017; Gross et al., 2017; Jeong et al., 2016; Saeed et al., 2017; Sillmann et al., 2014).

Recently, efforts to reduce model uncertainty have led to a new generation of global climate models called Earth system models (ESM) that integrate the individual parts of the climate system (atmosphere, ocean, land and sea ice) and the exchange of energy and mass between them (Knutti and Sedlacek, 2013). They also include chemical processes, land use, plant and ocean ecology and an interactive carbon cycle, which enables integration of biochemical processes into the models (Heavens et al. 2013). These models are the basis of the fifth phase of the Coupled Model Intercomparison Project (CMIP5) (Taylor et al., 2012), constituting the most current set of coordinated climate model experiments (Brands et al., 2013; Carvalho et al., 2017; Chen et al., 2016; Perez et al., 2014)

The CMIP5 models and their predecessors have become an important resource for climate scientists and others investigating possible future impacts. However, the spatial resolution of these models remains too low for many impact assessments at a local scale, on which policy and management decisions need to be made. These models are run at coarse spatial resolutions, which is also a major limitation in projecting extreme events because projections of climate extremes and simulations of heat-wave characteristics on regional scales are very sensitive to spatial resolution and the interpretation of gridded outputs (Chen et al., 2016).

The deficiency in scale is addressed through downscaling techniques involving either statistical approaches or dynamic approaches. In the statistical approach, high-resolution predictands (surface variables) are obtained by applying relationships that are identified from the observed climate data to these predictands and to large-scale predictors of GCM outputs (Asong et al., 2016; Benestad et al., 2007; Semenov and Stratonovitch, 2010). In dynamical downscaling, a time-varying regional climate model (RCM) of atmospheric boundary conditions is nested within the GCM (Giorgi and Gutowski, 2015; Giorgi and Mearns, 1991;). Both methods have been widely used and both have advantages and disadvantages. The main advantages of statistical downscaling techniques are that they are computationally inexpensive, they provide local information and they allow quantifying the uncertainty associated to the downscaling process and to the climatic models.

Several studies have been carried out to explore present temperature extremes in Europe (Soares et al., 2012) and in the Mediterranean region (Kuglitsch et al., 2010; Seubert et al., 2014), and other studies have developed scenarios of temperature extremes in the same areas (Estrella and Menzel, 2013; Hertig et al., 2010; Lavaysse et al., 2012). However, none of them have applied the downscaling CMIP5 models.

Although many climate models have difficulties in properly reproducing climate extremes, such as heat-wave conditions (Stegehuis et al., 2015), a few studies have reported on heat-wave scenarios in Europe (Fischer and Schar, 2010; Schoetter et al., 2015), or located in in the Mediterranean region (Zittis et al., 2016), in France (Planton et al., 2008), Italy (Tomozeiu et al., 2007) or Finland (Kim et al., 2018). Schoetter (2015) and Kim (2018) are one of the few studies that already uses the models from the IPPC5. As a part of the European Coordinated Regional Downscaling Experiment (EUROCORDEX) (Giorgi, 2009), the EUROCORDEX initiative provides regional climate projections for Europe. (Vautard et al., 2013) used the EUROCORDEX project to simulate heat waves at the European regional scale, providing a downscaling of CMIP5 simulations. These European-scale studies only featured a few locations in Spain. Several downscaling studies have been specifically conducted on temperature in Spain (Brands et al., 2011b; Frias et al., 2005; Frias et al., 2010; Hervada-Sala et al., 2000; Miro et al., 2016; Turco et al., 2014), but very few studies have explored temperature extremes in Spain (Fernandez-Montes and Rodrigo, 2012; Fonseca et al., 2016) and they do it in past periods (1925–2006 and 1986–2005, respectively).

Only a few studies have developed temperature scenarios in the Aragón region (northeastern Spain) (Buerger et al., 2007; Goncalves et al., 2014; Ribalaygua et al., 2013a), but none of them developed temperature-extreme or heat-wave scenarios. Only (Barrera-Escoda et al., 2014) developed scenarios of extreme temperatures in the Ebro basin. That study showed that the projected increase in the number of tropical nights and extreme temperatures could have a negative effect on human health and comfort conditions. Other studies have also analysed the possible impacts of climate change in this region on human health (Roldan et al., 2016). Both studies used the climate models associated to the 4th assessment report of the IPCC.

Aragón is characterised by a highly complex topography that causes large climate gradients. Downscaling techniques were required to capture these orographic features, allowing for the areas that were most vulnerable to extreme changes to be identified. Statistical downscaling is particularly recommended for areas with complex topography (Kattenberg and Amer Meteorol, 1996). Nevertheless, downscaling of CMIP5 simulations has not been used to date, and heat-wave scenarios cannot be found in this sensible area of Spain.

Therefore, the objectives of this study were:

- Generate local heat- and cold-wave scenarios of the 21st century to downscale GCMs from CMIP5 using a statistical methodology in the area of Aragón, Spain.
- In addition, generate new climate scenarios using CMIP5 models for Aragón to simulate the future daily maximum and minimum temperatures in order to analyse the differences with respect to the scenarios we generated in 2013 for the 21st

century using the Special Report on Emissions Scenarios, SRES (IPCC, 2000) previous to CMIP5.

Aragón, moreover, is a representative territory of different European climates, from the low-land areas in the centre of Aragón (the Ebro River Basin) to the mountain regions in the north (the Pyrenees) which makes it a good indicator of future European climate changes. Finally, an original two-step analogue / regression statistical downscaling method developed by the Climate Research Foundation was carried out.

The information used in the present study was based on the most current data available. It was useful for identifying the areas that were most vulnerable to extreme temperature changes in Aragón, and for helping decision makers to design mitigation and adaptation strategies in response to territorial environmental impacts derived from climate change.

2. Material and Methods

2.1 Study area and datasets

2.1.1 Study area

The present study was carried out in the region of Aragón (Fig.R1.1), which is located in the northeast part of the Iberian Peninsula in Spain and which has an area of approximately 47,720 km^2 (340 km length and 240 km width). Because of its location, Aragón falls within the Western Mediterranean climate area, with cool winters and hot, dry summers. However, the extreme altitude differences of over 3,000 m between the plains (the Ebro River Basin) and the mountains (the Pyrenees), together with the specific topography of the Ebro River Basin and the mountain chains (the Pyrenees to the north of the basin and the Iberian Mountains to the south), modify the local climate. As a result, the climate characteristics of the area are somewhat different from a standard Western Mediterranean climate, and they typically consist of dryness of the land along the banks of the Ebro River, random rain patterns, high thermal contrast between winter and summer as a consequence of the strong continental characteristics of the region and the typical northeast “mistral” winds, which are frequent in the region.

2.1.2. Surface observation dataset (predictands)

The observational dataset used in the present study consists of a time series of the daily maximum and minimum temperatures distributed, quite homogeneously, throughout the Aragón territory (Fig.R1.1). This dataset it is the same as the one used in a previous study (Ribalaygua et al., 2013a) in order to facilitate comparison of the results.

Data were obtained from the extensive network of instrumental observatories owned by the Spanish Meteorological Agency (AEMET) (http://www.aemet.es). The stations are subject to strict data quality control, which includes detecting and correcting multiple aberrant points in the long-term climate time series, covering the gaps, assessing the homogeneity of the climate series and correcting any inhomogeneities found. This process was carried out by the Aragón Government (López et al., 2007) to guarantee the quality of the data, stations with a large number of data gaps or without at least 15 years of daily records were discarded. Second, we analysed the dataset for the presence of extreme data points that could be considered suspect observations or transcription errors (we considered data points to be extreme if they were separated from the monthly average by more than four times the value of the standard deviation). Third, we verified that the data did not contain

inhomogeneities that could introduce bias into any records that were not related to the climate, (Ribalaygua et al. 2013a)

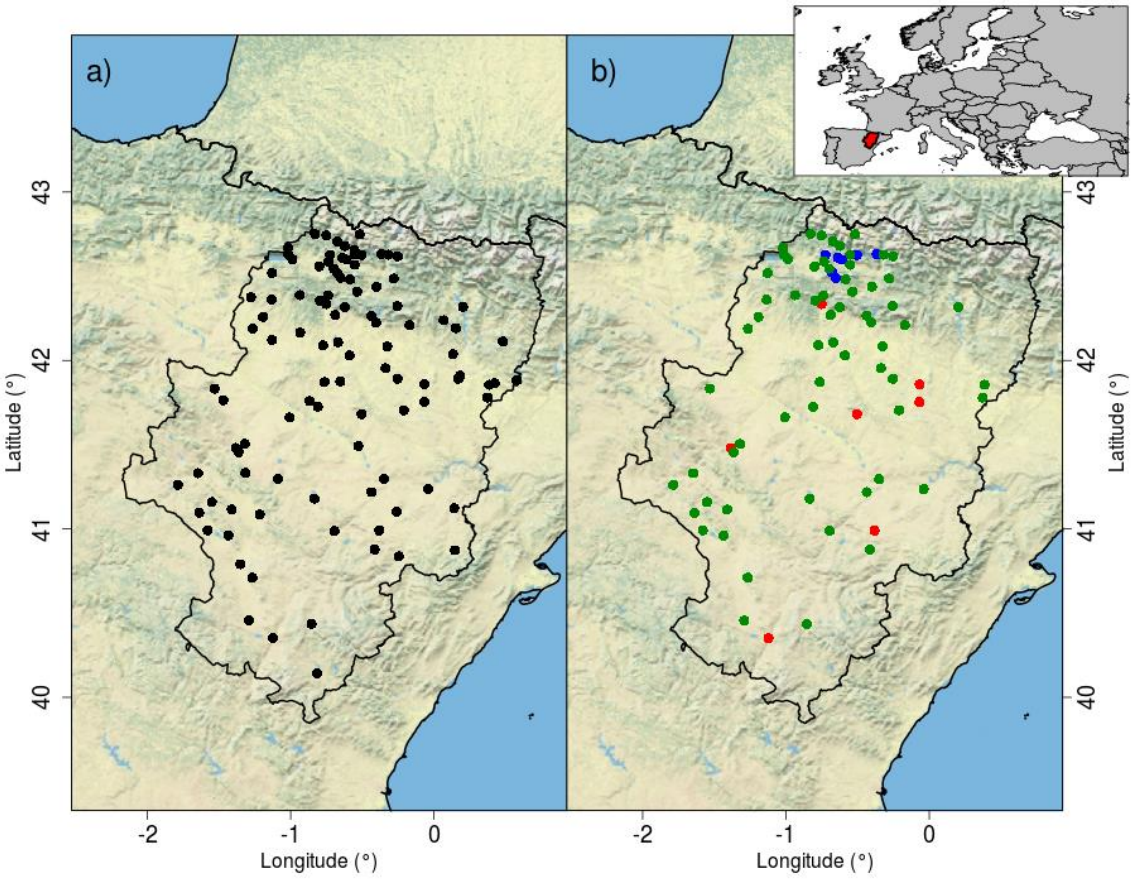

Figure R1.1. Location of the study Area: Aragon (Spain) in Europe. Points indicate the stations used in the study. a) Stations of temperature (103) used in the generation of climate regional scenarios of maximum and minimum temperature (verification, validation and scenarios). b) Stations used exclusively on the generation of heat waves (7, red), used exclusively on the generation of cold waves (7, blue) and those used in both extreme events (64, green). "(Map source: OpenStreetMap)"

The first set of data (composed of 103 stations) was used to analyse and produce the regional climate scenarios of maximum and minimum temperatures (Fig. R1.1a). Of these 103 stations, those that had at least 75% of maximum temperature data collected from June to September (i.e., the reference period for the calculation of heat waves) between 1980 and 2000 and stations that had at least 75% of minimum temperature data collected from November to April (that is, the reference period for the calculation of cold waves) between 1980 and 2000 perform a second set of data selected for the study of extreme events. In both cases, the number of observatories was 71 (Fig.R1.1b).

2.1.3. Atmospheric dataset (predictors)

2.1.3.1 Reanalysis

As a reference dataset, we used the reanalysis from the European Centre for Medium-Range Weather Forecasts (ECMWF ERA-40; http://www.ecmwf.int/research/era/do/get/era-40) (Uppala et al., 2005) for the period 1958–2000. For the atmospheric window, we used geographical limits from 31.5°N to 55.1°N latitude and from 27.0°W to 14.6°E longitude, covering not only the geographic area under study, but also the surrounding atmosphere areas, which exert a meteorological influence all over the Iberian Peninsula (Ribalaygua et al., 2013a).

For verification of the methodology, it was necessary to reduce the temporal (six hourly) and spatial (125 km) scale of the reanalysis to that of the different climate models in order to compare both, ERA-40 and the climate model simulations (Ribalaygua et al., 2013a; Ribalaygua et al., 2013b).

2.1.3.2. Climate model data

In the present study, we worked with a set of nine climate models that belong to the CMIP5 and that were provided by the Program for Climate Model Diagnosis and Intercomparison (PCMDI) archives (Table R1.1). The number of models chosen was limited to the availability of data with daily time frequencies. All of the models were ESMs.

To generate the model predictor fields, we took the daily values of several large-scale fields of interest (that is, geopotential height, specific humidity and wind) at different pressure levels for the nine ESMs showed in the table R1 associated with the CMIP5 (Taylor et al., 2012). Moreover, we used an historical experiment (Taylor et al., 2012) which generated simulations of the past 20th century and which was useful for the evaluation of model performance against the present climate. Finally, the representative concentration pathway (RCP) families were considered (Moss et al., 2010), specifically the RCP8.5 'high' scenario and the RCP4.5 'intermediate' scenario, both of which corresponded to different possible ranges of radiative forcing reached in the year 2100 with respect to values of the pre-industrial era (4.5 and 8.5 W/m^2, respectively).

2.2 Methodologies

2.2.1 *Description of the downscaling methodology*

The methodology of statistical downscaling used in this study was chosen according to three main advantages:

1) Allows easier quantification of the main uncertainties associated with the generation of future climate scenarios (van der Linden and Mitchell, 2009).

2) It is a key for the achievement of climate simulations that are consistent with observations which, in turn, are physically coherent (Ribalaygua et al., 2013b).

3) Provides local detail, which is useful information because nearby data points in space can evolve under different future climate conditions (Ribalaygua et al., 2013b).

A two-step analogue / regression statistical downscaling method that was developed by the Climate Research Foundation (FIC) (Ribalaygua et al., 2013b) was applied to obtain future scenarios of the maximum and minimum temperatures at a local scale in the region of Aragón. This methodology consisted of a two-step analogue / regression statistical method, which has been used in national and international projects with good verification results. In the present paper, we present a summary of the two-step method (more details can be found in Ribalaygua et al., 2013b).

GFDL-ESM2M	2ºx2,5º daily	National Oceanic and Atmospheric Administration (NOAA), E.E.U.U.	Dunne et al. (2012)
CanESM2	2,8ºx2,8º daily	Canadian Centre for Climate Modeling and Analysis (CC-CMA), Canadá.	Chylek et al. (2011)
CNRM-CM5	1,4ºx1,4º daily	CNRM (Centre National de Recherches Meteorologiques), Meteo-France, Francia.	Voldoire et al. (2013)
BCC-CSM1-1	1,4ºx1,4º daily	Beijing Climate Center (BCC), China Meteorological Administration, China.	Xiao-Ge et al. (2013)
HADGEM2-CC	1,87ºx1,25º daily	Met Office Hadley Center, United Kingdom.	Collins et al. (2008)
MIROC-ESM-CHEM	2,8ºx2,8º daily	Japan Agency for marine-Earth Science and Technology (JAMSTEC), Atmosphere and Ocean Research Institute (AORI), and National Institute for Environmental Studies (NIES), Japan.	Watanabe et al. (2011)
MPI-ESM-MR	1,8ºx1,8º daily	Max-Planck Institute for Meteorology (MPI-M), Germany.	Raddatz et al. (2007); Marsland et al. (2003)
MRI-CGCM3	1,2ºx1,2º daily	Meteorological Research Institute (MRI), Japan.	Yukimoto et al. (2011)
NorESM1-M	2,5ºx1,9º daily	Norwegian Climate Centre (NCC), Norway.	Bentsen et al. (2012); Iversen et al. (2013)

Table R1.1. Information about the nine climate models belonged to the 5 Coupled Model Intercomparison Project (CMIP5) corresponding to the fifth report of the IPCC. Models were supplied by the Program for Climate Model Diagnosis and Intercomparison (PCMDI) archives.

The first step was analogous stratification. An analogue method was applied based on the hypothesis that 'analogue' atmospheric patterns (predictors) should cause analogue local effects (predictands), which means that the number of days that were most similar to the day to be downscaled were selected (Benestad et al., 2007; Zorita and von Storch, 1999). The similarity between any two days was measured using a pseudo-Euclidean distance between the large-scale fields used as predictors. For each predictor, the weighted Euclidean distance was calculated and standardised by substituting it with the closest percentile of a reference population of weighted Euclidean distances for that predictor. This method is a good method for reproducing nonlinear relationships between predictors and the predictands, but it could not be used to simulate values outside of the range of observed

values ((Imbert and Benestad, 2005). In order to overcome this problem and to obtain a better simulation, a second step was required.

The second step focuses on temperature. To determine the temperature, a multiple linear regression analysis for the selected number of most analogous days was performed for each station and for each problem day. From a group of potential predictors, the linear regression selected those with the highest correlation, using a forward and backward stepwise approach.

About the accuracy in simulating temperatures of our downscaling technique, in our previous work about climate change in Aragón (Ribalayagua et al., 2013a) we achieved an average bias below 0.1 ºC" (Ribalaygua et al., 2013a).

2.2.2. Validation and climate simulation of temperature

In order to determine the ability of each ESM to simulate the predictor fields, absolute and relative temperatures from the downscaled ESM simulation of the historical experiment was compared with the downscaled ERA-40 simulation (previously verified against the observations) during a common historical period (1958–2000).

Due to the characteristics of the ESMs, the validation process presents certain limitations. First, as climate models do not reproduce day-to-day meteorology, validation cannot be performed on a daily scale and it must be done using climate statistics over long periods of time, resulting in a loss of information on climate variability. Second, we could not compare the climate characteristics obtained from the ESM historical simulation with those obtained from the observations because the latter had missing data and large gaps; therefore, we had to compare ESMs simulations with simulations from the reanlaysis of a dataset (previously validated in the verification process). Both sources of error should be considered in the final uncertainty analysis.

As error measures, bias and standard deviation were analysed on a seasonal scale for both maximum and minimum temperatures. An ensemble strategy was used to quantify the uncertainties inherent in future climate projections (IPCC, 2013). For each scenario (i.e., RCP4.5 and RCP8.5), an ensemble of the approved downscaled ESMs was used to estimate the mean change (compared to 1976-2005) and to quantify the main contributions to the uncertainty.

Future local climate scenarios for maximum and minimum temperature, for nine GCMs and two RCPs have been produced at the daily scale. To draw the temperature maps, we used Thin Plate Spline regression (TPS) from the R-Package "fields" (Nychka et al., 2015).

2.2.3. Definition of hot- and cold-wave episodes

There are many and varied terms used to define a heat wave. For example, the AEMET defines a heat wave as an "episode of at least three consecutive days, in which at least 10% of the stations considered record maximums above the 95% percentile of their series of maxima daily temperatures of the months of July and August of the period 1971–2000." The WMO defines a heat wave as an extreme event with marked warmed of the air or the invasion of very warm air over a large area, it usually last from a few days to a few weeks." The IPCC defines a heat wave as "a period [of] abnormally and uncomfortably hot weather". Those definitions are not the only ones accepted in the scientific literature. Some heat-wave definitions have been used to identify heat waves in a time series of temperature data

(Smith et al., 2013;), and the choice of the heat wave definition can influence both projected heat-wave trends (Smith et al., 2013) and estimates of health risks during events (Anderson and Bell, 2009; Chen, et al. 2015, Kent, et al. 2014).

According to the recommendations of the WMO (WMO, 2010), a practical and qualitative definition of a heat wave must consider marked and unusual hot weather over a region during at least two consecutive days in the hot period of the year, based on local climate conditions, with thermal conditions recorded above given thresholds. On the basis of these recommendations and the characteristics of the Aragón climatology, we defined a heat wave as follows: at least three consecutive days with a maximum temperature above the 95th percentile of the maximum temperature series and calculated between the months of June to September during the period 1980–2000.

In broad terms, a cold wave can be defined as a meteorological event characterised by a sharp drop of air temperature near the surface, leading to extremely low values. According to the IPCC 2007, (Parry et al., 2007) a cold wave is an event that often causes problems and severe impacts on the population, especially in northern altitudes. However, there is still a lack of a clear and consistent definition for cold-wave events in the world.

In the WMO's Meteoterm vocabulary, a cold wave is defined as "marked cooling of the air, or the invasion of very cold air, over a large area." For the AEMET, a cold wave is "an episode of at least three consecutive days, in which at least 10% of the considered stations register minimums below the 5% percentile of their series of minima daily temperatures for the months of January and February of the period 1971–2000". The WMO's members guideline define a cold wave as "marked and unusual cold weather characterised by a sharp and significant drop of air temperatures near the surface (max, min and daily average) over a large area and persisting below certain thresholds for at least two consecutive days during the cold season".

Considering the climate characteristics of Aragón, we defined a cold wave as follows: at least three consecutive days with a minimum temperature below the fifth percentile of a minimum temperature series and calculated between the months of November to April during the period 1980–2000.

To better identify a heat or cold wave, we evaluated average duration, maximum intensity and average intensity as it is recommended by the WMO in the Guidelines on the definition and monitoring of extreme weather and Climate Events. The average duration refers to the average number of days the heat wave lasted. The average intensity represents the average value of the temperature during the heat wave. The maximum intensity is equal to the maximum value that the temperature reached during the heat wave.

2.2.4. Verification and simulation of heat and cold waves

In order to assess the capacity of the downscaling methodology to simulate heat and cold waves observed in the past, we evaluated how the downscaling methodology simulated the 95th percentile of maximum temperatures and the 5th percentile of minimum temperatures, which are the thresholds that indicate the existence of an episode of a heat and cold wave, respectively. In addition, we analysed the intensity of the wave (average and maximum) and the average duration, comparing the heat and cold waves calculated from the simulated ERA-40 temperature series with those obtained from the observed series. Verification of the maximum and minimum temperatures can be seen in a previous

study by Ribalaygua (Ribalaygua et al., 2013a). The statistical measures used in the verification processes were the bias, the standard deviation and the Pearson correlation (Murray et al., 2009) at the daily scale. The statistical measures were calculated using R-cran package computing software (R Development Core Team 2010).

From the ESM simulated temperature series (nine ESMs and two RCPs), we determined the heat- and cold-wave episodes that were expected in Aragón during the upcoming decades of the 21st century. The heat- and cold-wave scenarios were compared to a historical period (1976–2005) to analyse the future changes with respect to the actual situation of these extreme events.

3. Results

3.1. Validation of the CMIP5 model statistical downscaling to predict temperatures

The seasonal bias that result from a comparison between the ERA-40 temperature simulations and the historical temperature simulations for each ESM for a common period (1958-2000) are shown in Fig. R1.2 for absolute temperatures (that is, the difference between simulated Historical ESM data and simulated ERA-40 data). For both the maximum and minimum temperatures, the obtained bias was around tenths of a degree in all months, so they were very close to zero. The error was not above half of a degree for any of the cases. Therefore, the results showed that the ESMs were capable of adequately simulating both the maximum and the minimum temperatures on annual and seasonal scales.

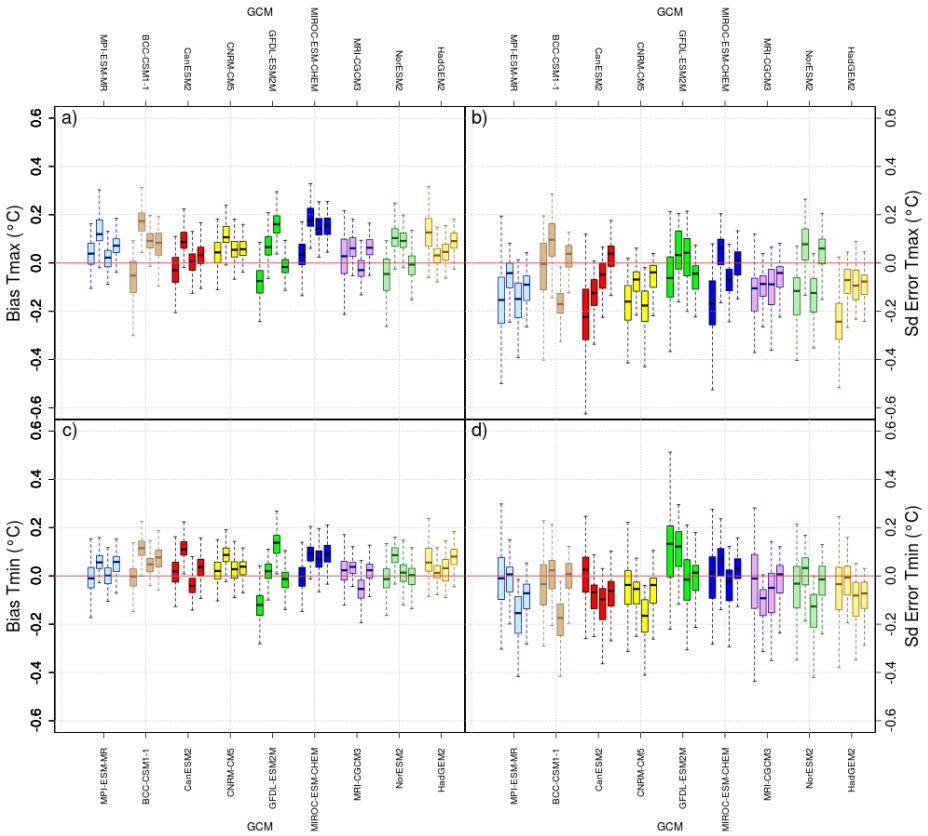

Figure R1.2. Validation of the GCMs used for the simulation of temperatures. Absolute Bias for a) maximum and c) minimum temperature and absolute standard deviations for b) maximum and d) minimum temperature, between the results obtained by downscaling the Historical scenario of each GCM used in the study with those obtained by downscaling the reanalysis ERA-40 for a common period (1958-2000). There are four boxplots, representing a season of the year (winter, spring, summer and autumn), for each GCM.

3.2. Local climate scenarios to predict future temperatures

Fig. R1.3 and R1.4 show local climate-change scenarios for future daily maximum and minimum temperatures respectively, which have been predicted on the basis of the nine models (see Table R1.1). Fig. R1.3 and 4 allowed for the establishment of a general view of the changes expected in Aragón. In addition, Fig. R1.5 and R1.6 represent the summer maximum and winter minimum temperature changes expected for the periods 2041–2070 and 2071-2100 as presentation of mid- and end-century expected changes, which were calculated according to the scenarios RCP4.5 and RCP8.5.

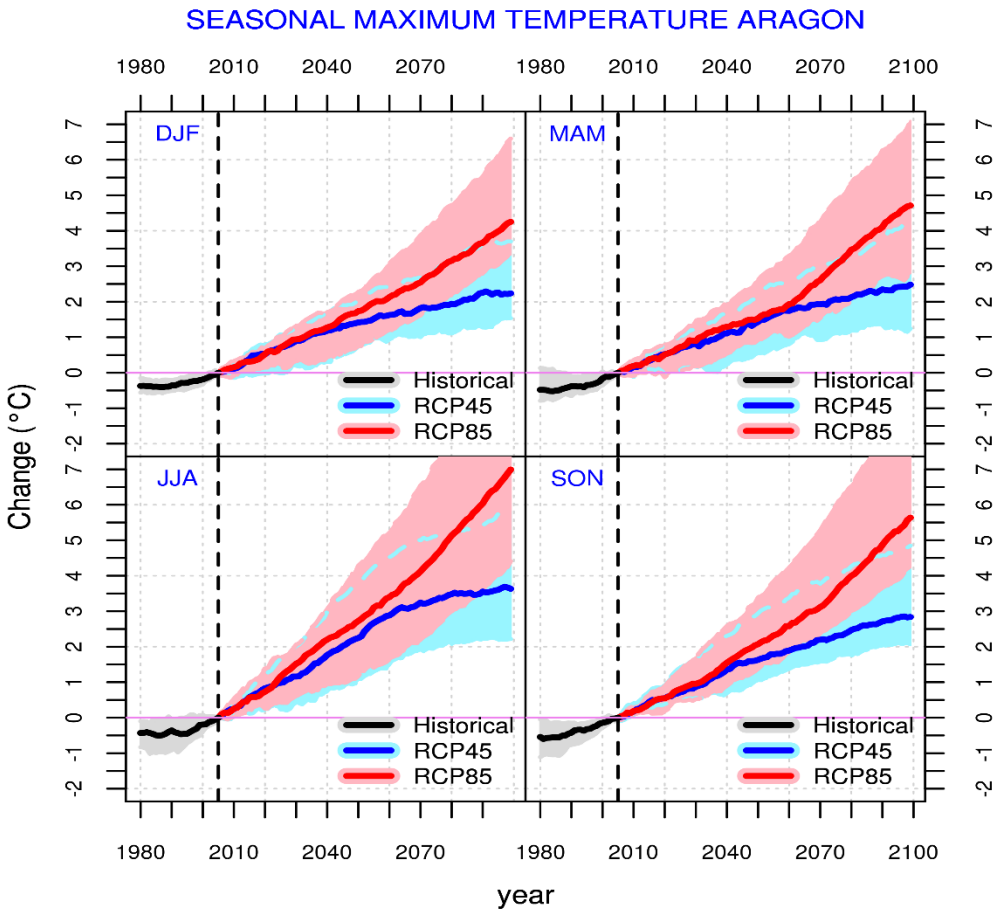

Figure R1.3. For the four seasons (winter, spring, summer and autumn) simulated maximum temperature for the twenty-first century displayed as absolute increase against the value simulated for the 1976–2005 Historical period. The vertical dotted line marks the end of the Historical data (2005). Data grouped for every RCP simulation of every global climate model used and for the last 30 years of every station. The ensemble median (solid lines) and the 10th–90th percentile (shaded areas) values are displayed

Expected changes in the average temperature for the rest of the seasons of the year can be found in the supplementary material for maximum temperatures increase (Fig. S1.1–S1.3) and minimum temperatures increase (Fig S1.4-S1.6). In addition, Fig S1.7- S1.9 showed the maximum and S1.10-S1.12, minimum temperatures expected in this century.

Fig.R1.3 shows a gradual increase in the maximum temperatures throughout the 21st century. During the mid-century, the least significant changes are expected during the winter and springs months (around 1.5 and 1.7 ºC for the RCP4.5 and RCP8.5, respectively), and the most significant changes are expected for the summer months, with

values of 2.1 ºC for the RCP4.5 and 2.7 ºC for the RCP8.5. At the end of the century, the expected changes are more marked and differ notably between the two RCPs. During winter and spring months, the expected values are around 2.3 ºC and 2.4 ºC for the RPC4.5 and 4.3 ºC and 4.7 ºC for the RCP8.5, respectively. The greatest changes are expected for summer months, reaching values of 7 ºC for the RCP8.5 and 3.6 ºC for the RCP4.5.

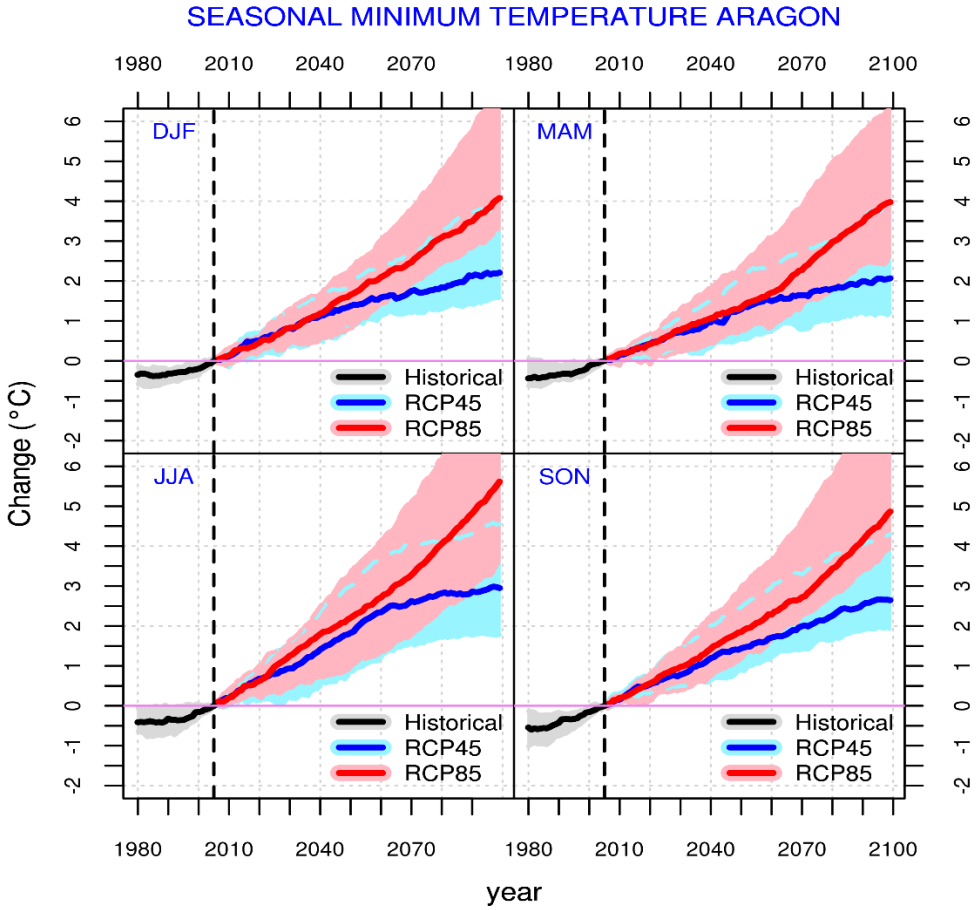

Figure R1.4. For the four seasons (winter, spring, summer and autumn) simulated minimum temperature for the twenty-first century displayed as absolute increase against the value simulated for the 1976–2005 Historical period. The vertical dotted line marks the end of the Historical data (2005). Data grouped for every RCP simulation of every global climate model used and for the last 30 years of every station. The ensemble median (solid lines) and the 10th–90th percentile (shaded areas) values are displayed

The areas most affected by the maximum temperature increases are expected to be the Pyrenees and the areas in the southwest and north of Aragón during all the 21ª century for the months of summer, spring and autumn, especially in the RCP8.5 scenario (Fig. R1.5). In contrast, in the winter months, the highest temperature increases at the end of the century are expected in the Pyrenees area and the Ebro Valley (Fig S1.1).

Scenarios of maximum temperatures of the 21st century (Fig R1.5 and Fig S1.7-S1.9) point that expected maximum temperatures are not proportional to the expected increases shown before (Fig R1.5 and Fig S1.1-S1.3).

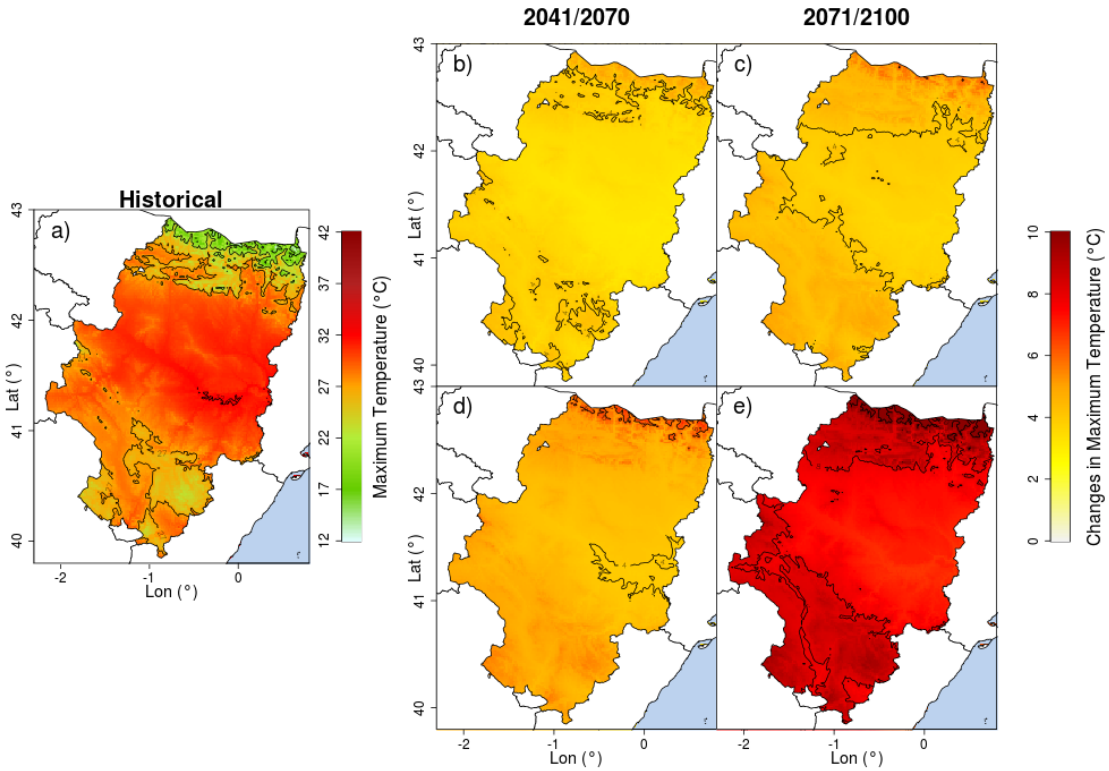

Figure R1.5. Geographical representation of the expected changes of maximum temperature in summer for the periods 2041-2070 and 2071-2100 respect to the reference Historical Period (1976-2005). Both emissions scenarios are represented: RCP4.5 (figures b and c) and RCP8.5 (figures d and e). Figure 5a represents the Historical absolute temperature for the period 1976-2005.

The evolution of the minimum temperature increases throughout the 21st century demonstrate similar behaviours to the maximum temperatures, but with less marked increases, especially at the end of the century (Fig. R1.6 and S1.4-S1.6). By the middle of the century, all of the seasons of the year, except for the summer, are expected to show increases in the minimum temperature of less than 2.0 ºC, and even in the spring, the increases are expected to be close to 1.0–1.2 ºC. The summer months are expected to show the greatest increases in minimum temperatures, varying from 1.8 ºC for the RCP4.5 to 2.3 ºC for the RCP8.5. At the end of the century, increases in the minimum temperatures during the summer months are expected to range from 3.0 ºC (RCP4.5) to 5.6 ºC (RCP8.5. Winter months are expected to show an increase between 2.8 ºC and 4.1 ºC, spring months between 2.1 ºC and 4 ºC and autumn months between 2.6 ºC and 5 ºC for the RCP4.5 and RCP8.5 scenarios, respectively.

The increases in the minimum temperature in are expected to be quite homogeneous throughout the region and the seasons according to the RCP4.5. In contrast, according to RCP8.5 (Fig. R1.6c, d), these changes will be more pronounced in the Ebro Valley at the end of the 21st century. The highest minimum temperatures are expected to be recorded in the central zone of Aragón during all seasons of the year (see supporting information, S1.10-S1.12).

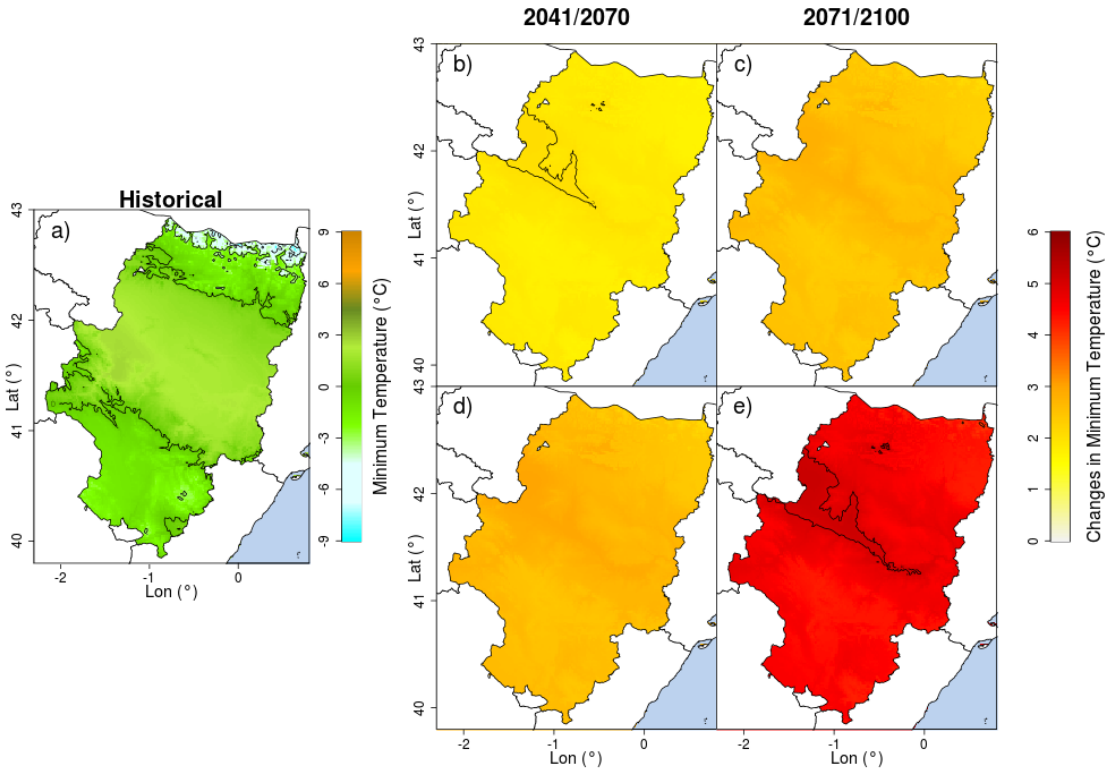

Figure R1.6. Geographical representation of the expected changes of minimum temperature in winter for the periods 2041-2070 and 2071-2100 respect to the reference Historical Period (1976-2005). Both emissions scenarios are represented: RCP4.5 (up, figures b and c and RCP8.5 (figures d and e). Figure 6a represents the Historical absolute temperature for the period 1976-2005.

3.3. Verification of hot- and cold-wave episodes

To verify the simulation of both of heat waves and cold waves, we compared the wave episodes obtained from ERA-40 simulations against the episodes recorded by the observations.

The first step was to verify that the methodology correctly simulated both percentiles, the 95th percentile of the maximum temperature and the 5th percentile of the minimum temperature. Both cases have been well simulated by applying the downscaling methodology to the ERA-40 series (Fig. R1.7). Data from the simulated ERA-40 series and the observed series were very close, and the error committed by simulating the ERA-40 series respect to the observed one was very low, especially in the 95th percentile. For example, we found error values around 0.36 ºC for summer months and around 0.69 ºC for the winter months in the 95th percentile, and 0.6 ºC for summer months and around 0.68 ºC for the winter months in the 5th percentile.

Regarding the verification of the identification parameters of a heat wave, Fig. R1.8 shows the results obtained for the duration of a heat wave, its temporary occurrence and its average intensity (maximum intensity is not shown here, but it was also taken into account in the present study and can be seen in Support Information (S1.13)).

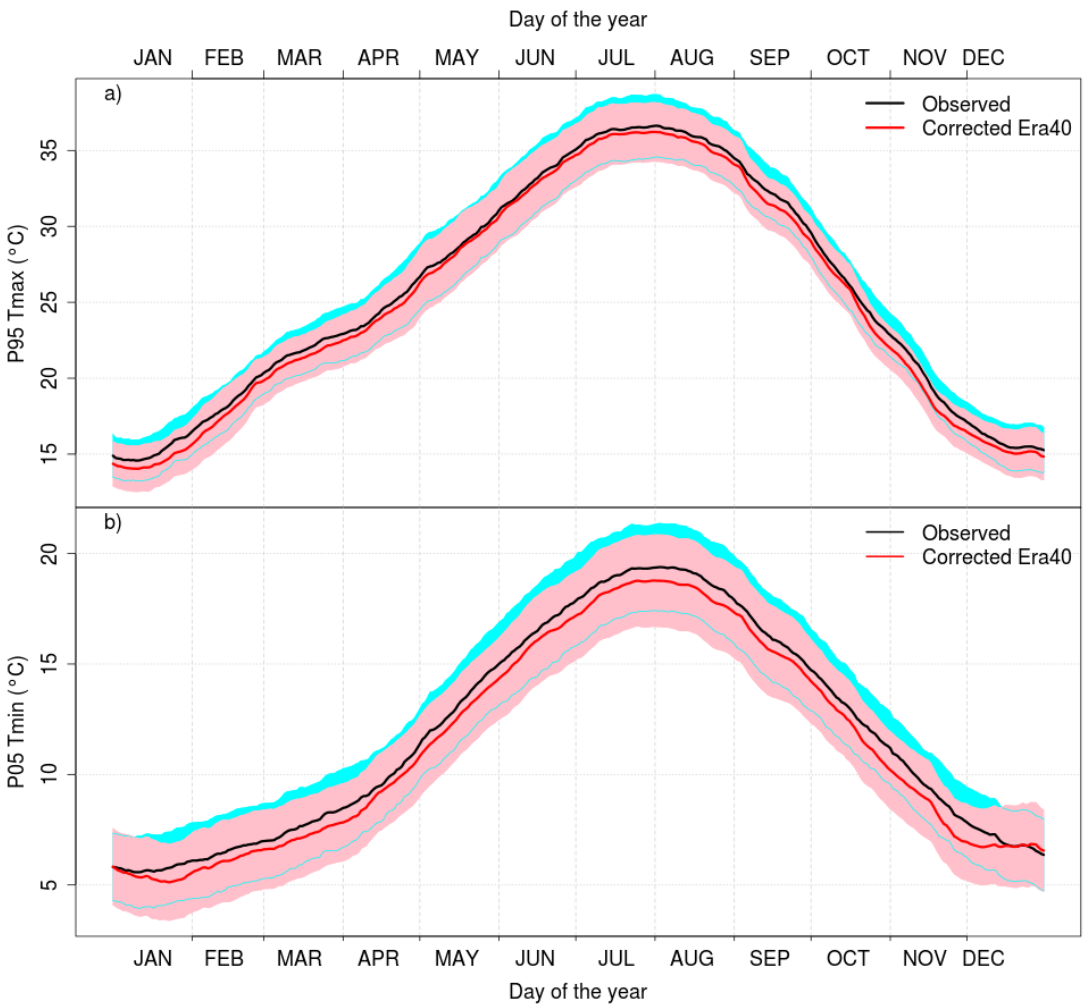

Figure R1.7. Results of the verification process obtained for a) the 95th percentile of maximum temperature and b) the 05th percentile of minimum temperature comparing the results obtained by downscaling the reanalysis ERA-40 (black) along the observations (red) for a common (1980-2000). The solid lines represent the median and the shaded areas the 10-90th percentile of the values.

As can be seen in Fig. R1.8a and b the average intensity of observed heat waves and ERA-40 simulations are very similar in the 71 observatories. We found a high correlation between the average intensity of a heat wave and the results from the observed and the simulated ERA-40 scenarios (p = 0.9889). A similarly high correlation was obtained in terms of the maximum intensity of a heat wave (p= 0.9883, not shown here).

Regarding to the average duration of heat waves episodes, Fig. R1.8c and d showed a similar pattern of temporal and spatial distribution and a strong correlation (p = 0.8976). For example, both datasets showed a clear signal of heat waves during the years 1982, 1987, 1990, 1994 and 1998, and they both showed no heat wave during the years 1986, 1987, 1996 and 1997.

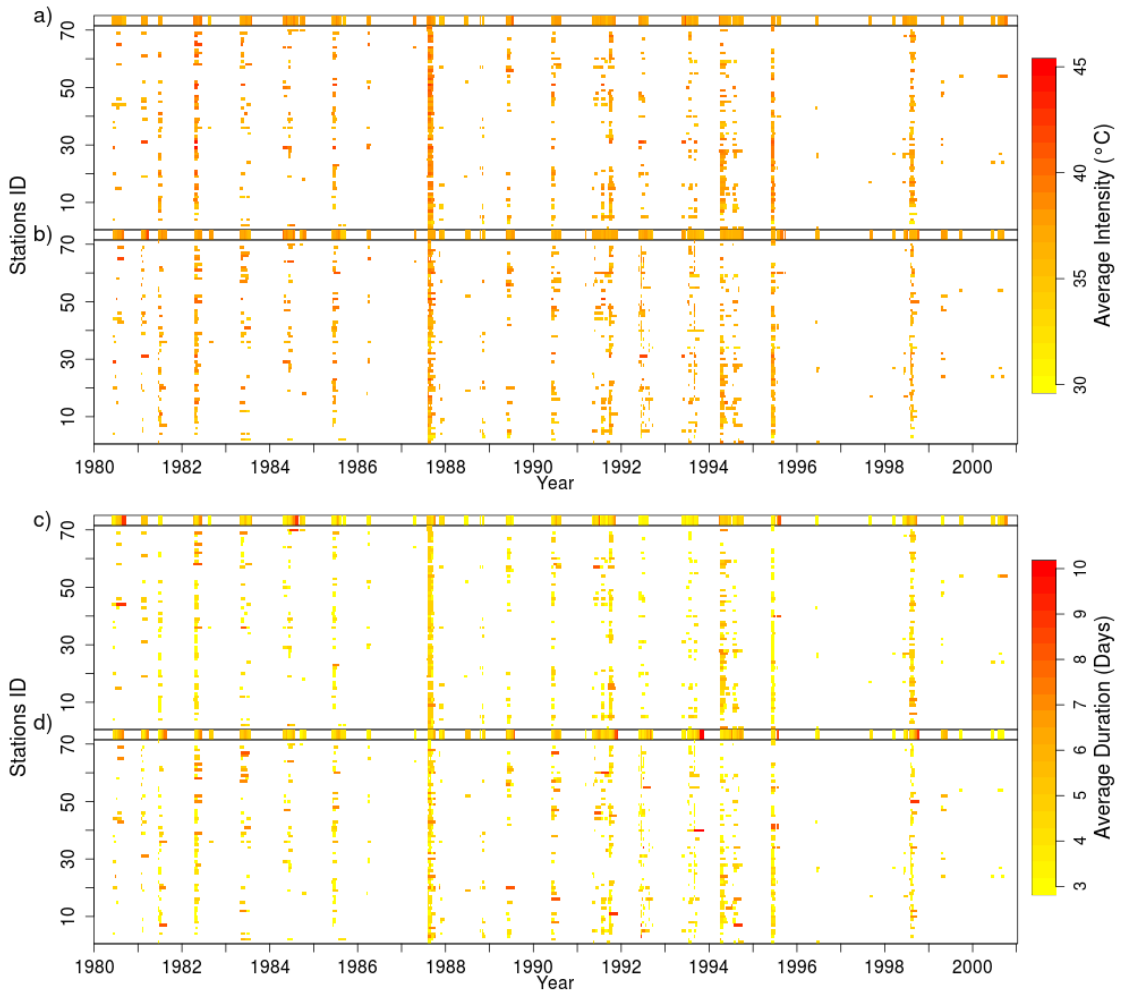

Figure R1.8. Results of the verification process for heat waves obtained comparing the simulated heat waves for the reanalysis Era-40 along the observed heat waves for a common period (1980-2000). a) Average intensity of the heat waves registered in the 71 stations used in the study against b) the average intensity obtained by downscaling of the reanalysis ERA-40 in these stations for the period 1980-2000. The color of each pixel shows the average intensity that corresponds to each heat wave (ºC), each column represents one year of the considered period and each row one station. The upper row shows the mean of the average intensity from the whole observatories. Down, c) and d) same as a) and b) but for the duration of the heat waves. The color of each pixel shows the duration corresponding to each heat wave (number of days).

Similar results are present in Fig. R1.9 for cold waves. In this case, the correlation obtained between the average duration of the observed cold waves (Fig R1.9c) and those simulated for ERA-40 (Fig R1.9d) was p = 0.8593, which was lower than the p-value obtained for heat waves. The correlations of the intensities between both groups of data were strong (p = 0.8849 and p = 0.792 for maximum intensity and average intensity, respectively), but lower than those obtained for the heat waves. The cold-wave pattern (that is, duration, average intensities and maximum intensities) were very similar in both datasets, marking episodes of cold waves during the same time periods.

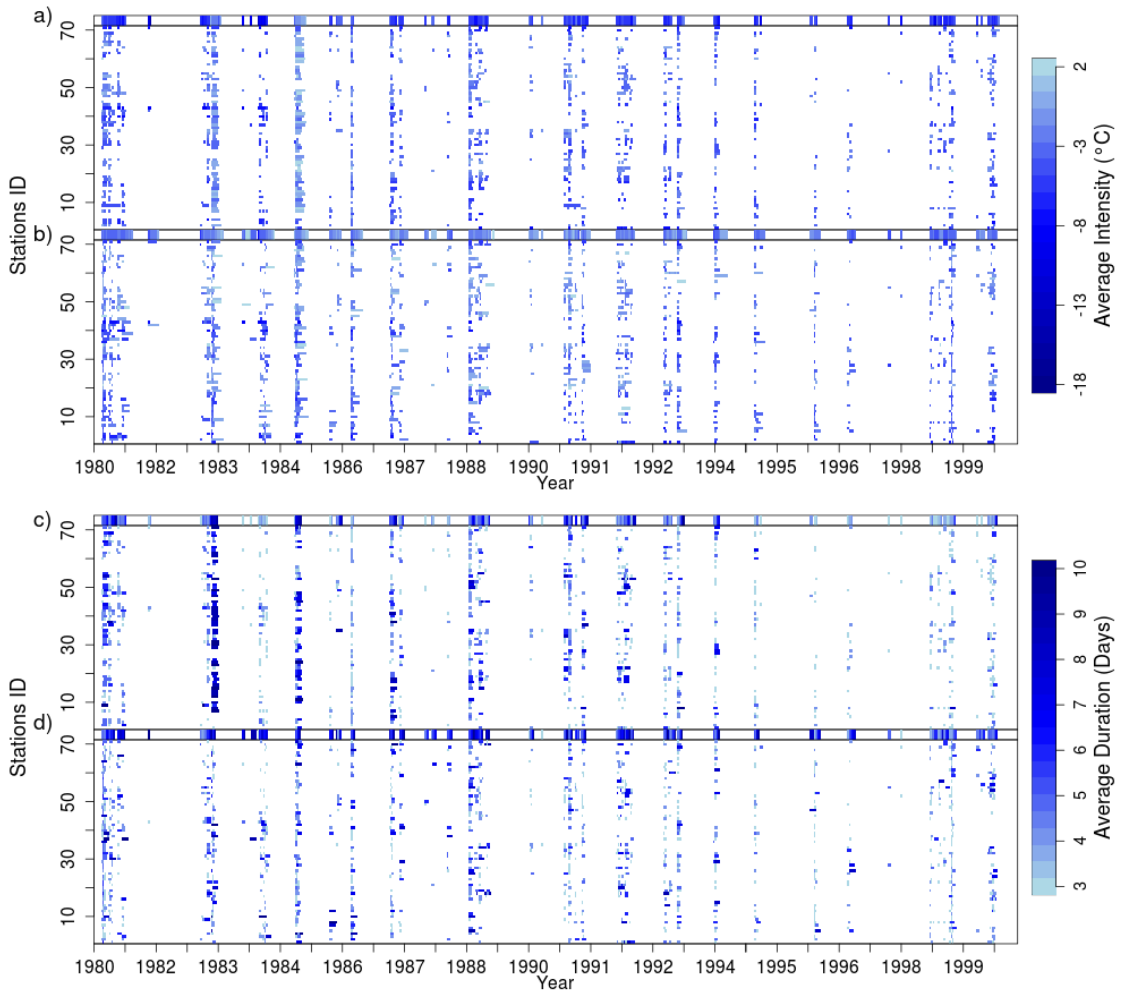

Figure R1. 9. Results of the verification process for cold waves obtained comparing the simulated cold waves for the reanalysis Era-40 along the observed cold waves for a common period (1980-2000). a) Average intensity of the heat waves registered in the 71 stations used in the study against b) the average intensity obtained by downscaling of the reanalysis ERA-40 in these stations for the period 1980-2000. The color of each pixel shows the average intensity that corresponds to each cold wave (ºC), each column represents one year of the considered period and each row one station. The upper row shows the mean of the average intensity from the whole observatories. Down, c) and d) same as a) and b) but for the duration of the cold wave. The color of each pixel shows the duration corresponding to each cold wave (number of days)

3.4. Local future climate scenarios of hot- and cold-waves episodes

Fig. R1.10 and R1.11 show the climate scenarios for heat waves in Aragón according to the RCP4.5 and the RCP8.5scenarios, respectively. The figures show the temporal evolution (from historical data to 2100) for three main features of the heat waves: average intensity (first row), maximum intensity (second row) and average duration (third row). The temporal periods analysed were 1976–2005 (historical; first column), 2041–2070 (second column) and 2071–2100 (third column). These periods were chosen as representative of the present, mid-century and end-century periods. Fig. R1.12 and R1.13 show the same information but for cold waves.

In addition, in Support information heat and cold waves are represented as increments in temperature for heat waves (S1.15 and S1.16 for RCP4.5 and the RCP8.5 scenarios, respectively) and for cold waves (S1.17 and S1.18 for RCP4.5 and the RCP8.5 scenarios, respectively).

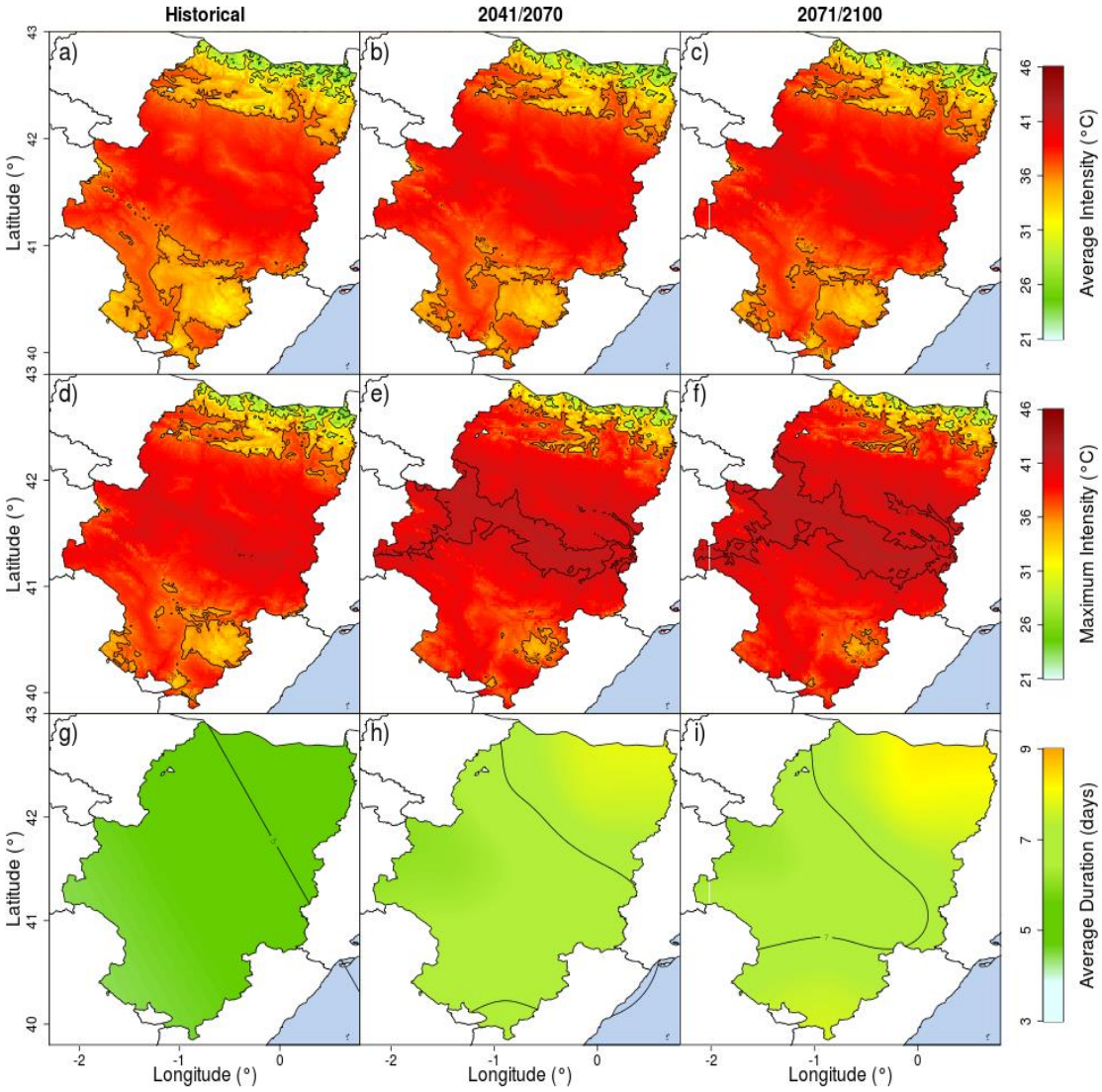

Figure R1.10. Geographical representation of the expected evolution of the heat waves for Aragon in the periods 2041-2070 and 2071-2100 compared to the reference Historical Period (1971-2000) in terms of absolute values according to the RCP4.5. The rows show the three parameters analyzed in the study (average intensity, maximum intensity and duration) and the columns the three temporal periods (Historical, 2041-2070 and 2071-2100). The maps are generated by interpolating the available stations over the entire territory.

During the coming decades, an increase in the duration of heat waves is expected. According to the RPC4.5, sharp increases in the average intensity of heat waves are not expected with respect to the values corresponding to the historical period (an average of approximately 0.8 ºC). This means that a mean intensity of 37.6 ºC is expected at mid-century and 37.8 ºC at the end of the century. According to the RCP8.5, the average intensity would increase an average of approximately 1–1.2 ºC during the middle of the century (reaching 38 ºC) and close to 2 ºC at the end of the century (reaching 38.8 ºC).

In the case of the maximum intensity of the heat waves, the average increases with respect to the expected historical period were somewhat more pronounced than those expected for the average intensity, especially in the case of RCP8.5. According to RCP4.5, average increases of 1.4 ºC and 1.7 ºC (reaching 39.3 ºC and 39.6 ºC) are expected in the maximum intensity during the middle and end of the century, respectively. In the case of RCP8.5, those average increases are expected to rise to 2 ºC and 3.6 ºC (reaching 39.9 ºC and 41.5 ºC) during the middle and end of the century, respectively.

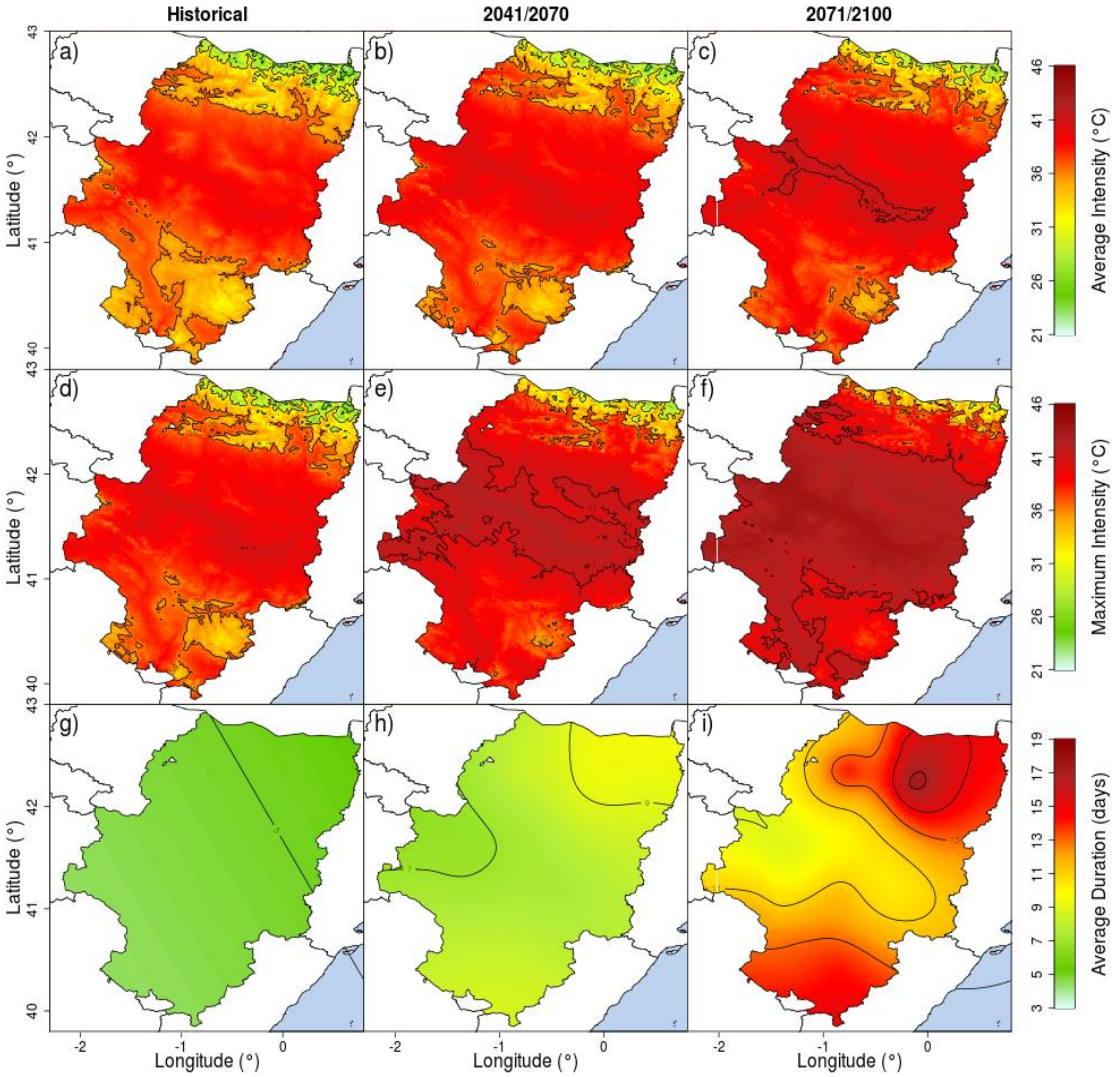

Figure R1.11. Geographical representation of the expected evolution of the heat waves for Aragon in the periods 2041-2070 and 2071-2100 compared to the reference Historical Period (1971-2000) in terms of absolute values according to the RCP8.5. The rows show the three parameters analyzed in the study (average intensity, maximum intensity and duration) and the columns the three temporal periods (Historical, 2041-2070 and 2071-2100). The maps are generated by interpolating the available stations over the entire territory.

Note that for the average (maximum) intensity, there was a difference between observatories, such that in some of them the intensity could reach 46 ºC (48 ºC), while in other parts of the region it would not exceed 32 ºC (34 ºC) according to the RCP8.5.

The average and maximum intensity of the heat waves will be especially intense in the Ebro Valley in the middle of the century, and it will spread throughout the entire territory toward the end of the century, except for the Pyrenean area further north.

According to RCP4.5, an average increase in the number of days that lasts a heat waves (duration) compared to the historical period of about 2 days is expected during mid-century (2041-2070), with a maximum increase of 11 days, which would mean that the average duration of heat waves it would be around 7 days, with durations that vary between 4 and 18 days according to the station. At the end of the century, very sharp variations are not expected with respect to half a century. Results from the RCP8.5 predict that the average duration of heat waves will increase by 3 days in the middle of the century and by 7 days

at the end of the century, which means that heat waves would have an average duration of between 8 and 12 days, respectively. Note that according to the RCP8.5 scenario, some observatories are expected to experience sharp increases during the historic period of up to 16 and 44 days for the period 2041-2070 and 2071-2100 respectively, so there would be observatories where the consecutive days that exceed the “hot-day” threshold would be 23 and 52 days, for the same periods.

In this case, the Pyrenees to the north and the Iberian to the south of Aragón are the zones that would suffer longer heat waves; although, as we have seen, they would be the least affected by the intensity of the expected heat waves.

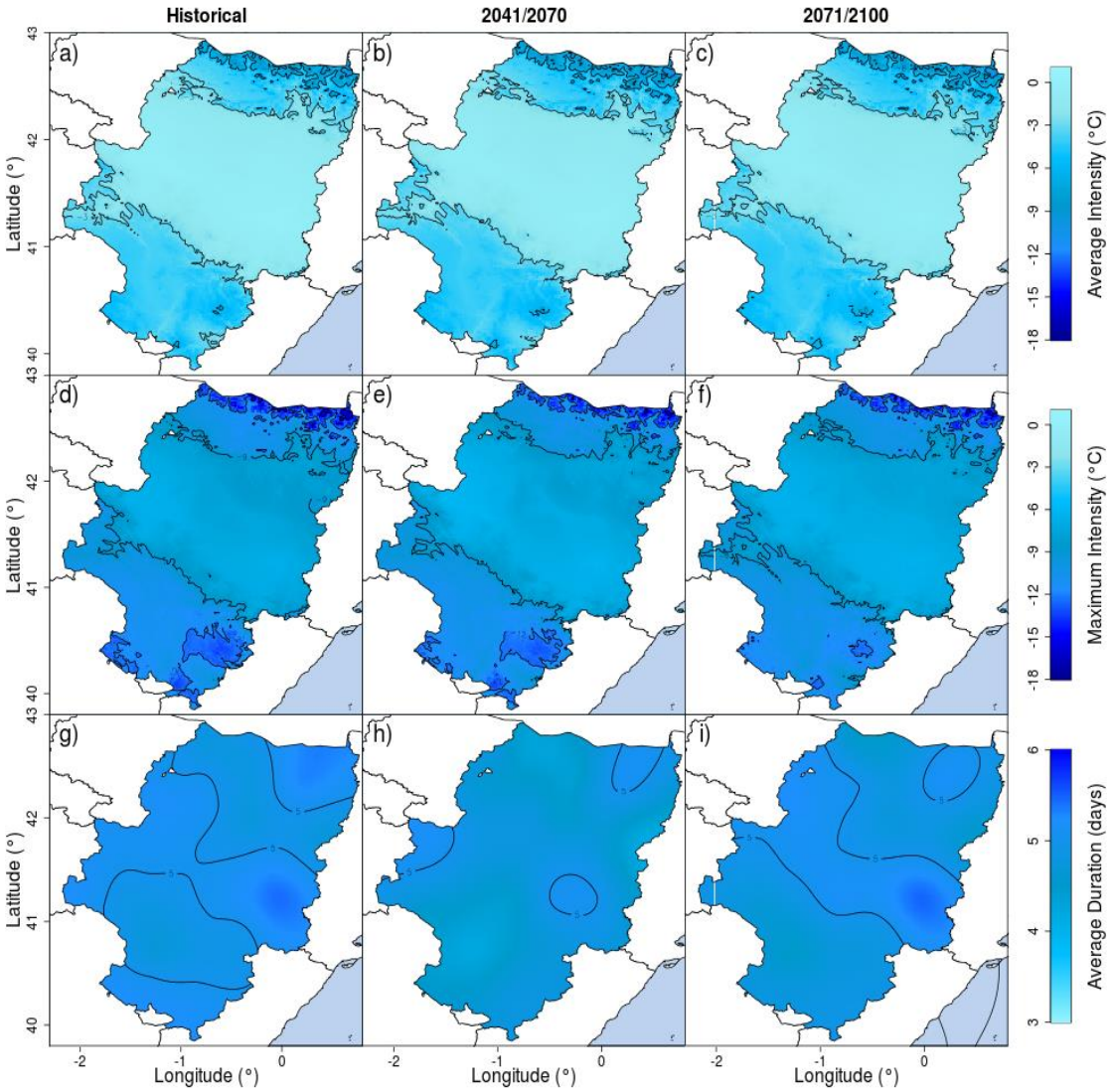

Figure R1.12. Geographical representation of the expected evolution of the cold waves for Aragon in the periods 2041-2070 and 2071-2100 compared to the reference Historical Period (1971-2000) in terms of absolute values according to the RCP4.5. The rows show the three parameters analyzed in the study (average intensity, maximum intensity and duration) and the columns the three temporal periods (Historical, 2041-2070 and 20712100). The maps are generated interpolating the available observatories over the entire territory.

On the other hand, the episodes of cold waves would not change either the average or maximum intensity values (see Fig. R1.12 and Fig. S1.17 for the RCP4.5 scenario and Fig. R1.13 and Fig. S1.18 for the RCP8.5). The variations of average intensity with respect to the historic period are, on average, ± 0.5 ºC, and in some observatories they could reach ± 1.0–1.5 ºC, independent of the RCP.

A similar pattern is expected for the maximum intensity of the cold waves (Fig. R1.12b and R1.13b), with few variations with respect to the historical period and similar patterns to those expected for the mean intensity. The north and the south of the territory are the regions that are expected to be the most affected by the intensity of the cold waves.

During the upcoming decades, an increase in the duration of cold-wave episodes is not expected. Both RCP4.5 (Fig. R1.12h and Fig. S1.17h) and RCP8.5 (Fig. R1.13h and Fig. S1.18h) predict that by the middle of the century, the average duration of cold waves will remain around 4 to 5 days, with episodes of 3 to 7 days in the middle of the century and 11 days at the end of the century. This would mean that the average duration of cold waves would not be modified with respect to the historical period, unlike what is expected in the case of heat waves, and in the most severe cases, the increase would be about three days at the end of the century. No differences of this pattern are expected in the territory.

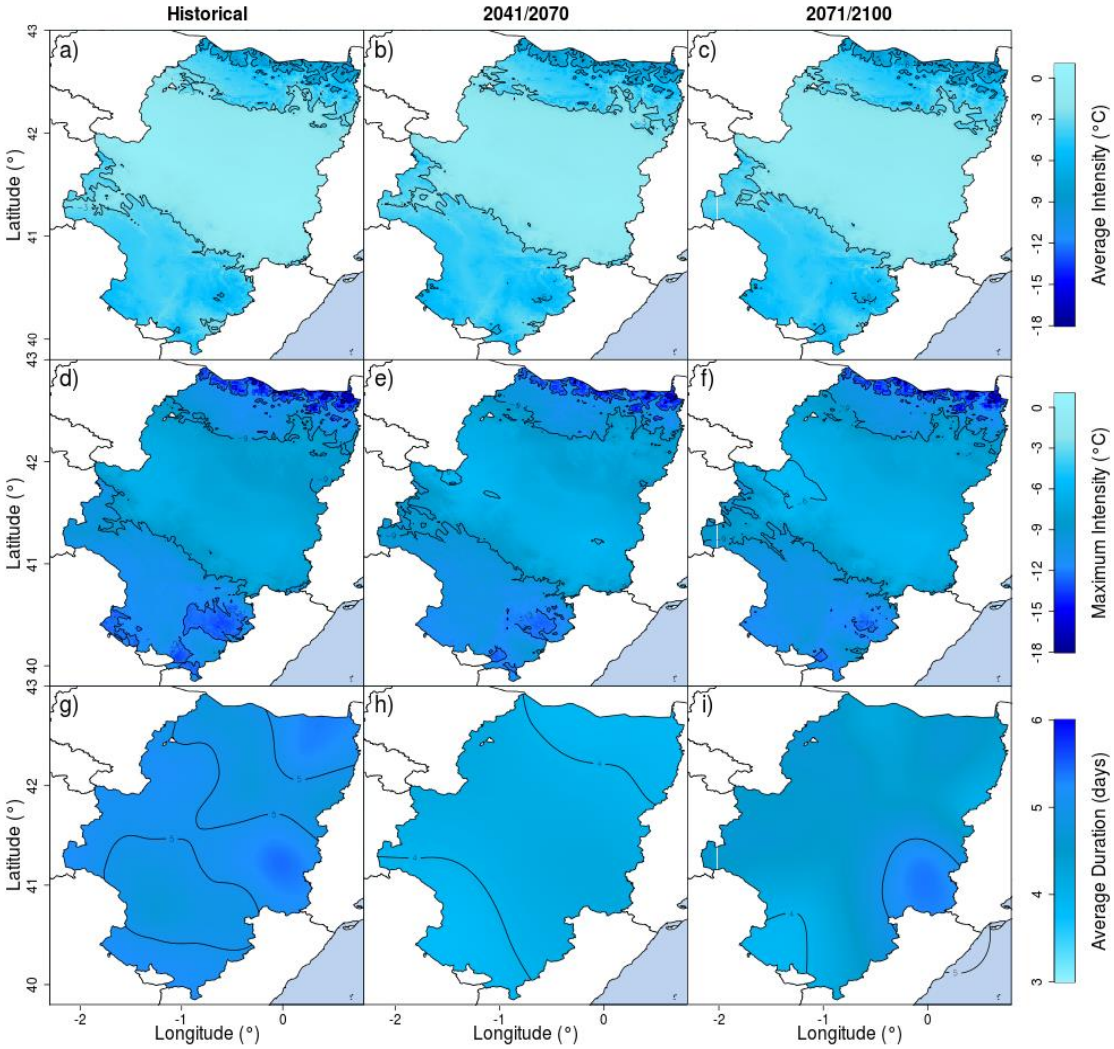

Figure R1.13. Geographical representation of the expected evolution of the cold waves for Aragon in the periods 2041-2070 and 2071-2100 compared to the reference Historical Period (1971-2000) in terms of absolute values according to the RCP8.5. The rows show the three parameters analyzed in the study (average intensity, maximum intensity and duration) and the columns the three temporal periods (Historical, 2041-2070 and 20712100). The maps are generated interpolating the available observatories over the entire territory.

4. Discussion

In the present study, heat- and cold-wave scenarios for the 21st century were obtained for the first time in the region of Aragón, Spain, using new ESMs belonging to the CMIP5. In

addition, the climate scenarios for temperatures in this region were reconstructed with the new ESMs in order to assess differences with respect to the models used prior to CMIP5. These results offer one of the best snapshots of future climate change based on currently available data on the risks that extreme temperatures can cause in the Aragón region, both spatially and temporally.

4.1. Considerations of the temperature scenarios

The new models used in the present study to obtain climate scenarios in Aragón are ESMs, not climate models. The improvements incorporated in the ESMs allow for greater precision in the simulation of climate variables, which provides evidence that the results of the validation are good.

The validation of the ESMs was good for both maximum and minimum temperatures. The differences between seasonal means were practically negligible (below a few tenths of a degree in temperature), and the differences between seasonal standard deviations were almost always below the reference values for every ESM (the standard deviation of the downscaled reanalysis data).

The validation results obtained in the present study show lower error rates than those obtained by the scenarios described in the fourth IPCC report and presented in previous studies (Ribalaygua et al., 2013a). In that case, the error was 1 ºC, and even in some models (for example, the CNCM3 model in the summer), it was around 1.5 ºC; in contrast, the results presented here did not reach such high values. Likewise, the values of the standard deviation are lower than those obtained in the previous study (5–10% in the present study vs. 15–20% in a previous study (Ribalaygua et al., 2013a).

Another key point that justifies the generation of new climate scenarios for Aragón is the current designation of climate scenarios provided by IPCC experts—that is, RCPs. Therefore, obtaining local climate scenarios that are based on the most current information is a priority.

The results obtained in the present study, both in the validation process and in the verification process, allow for the maximum and minimum temperature scenarios to be possibly used in subsequent studies of extreme events and bioclimatic variables. Future climate scenarios (maximum and minimum temperatures) show an evolution toward warmer climates throughout the Aragón region. These results agree with those obtained from the CMIP5 models by the IPCC (IPCC, 2013) and by the AEMET (www.Aemet.es). Previous data collected by other authors and assembled by the IPCC (IPCC, 2013) expect that the greatest temperature increases will occur during the summer months. The results of the present study showed that increases in temperature (both maximum and minimum) were less marked than those published by the AEMET (for example, our results showed changes of 3.6 and 7 ºC at the end of the century, while the AEMET results predicted changes of 4.1 and 8.2 ºC under RPC4.5 and RCP8.5 scenarios, respectively), although both our results and the AEMET results suggest that the summer months will be the time during which the most abrupt changes in temperature will be observed, while the winter months will be the time during which the least abrupt changes will be observed.

Results presented by the IPCC came from the ESMs, so they do not have the added value of applying downscaling techniques to obtain results at a local scale. On the other hand, one of the advantages of working with climate-change scenarios is to have the widest range

of future projections (using the greatest possible number of climate scenarios and downscaling methodologies). Therefore, the scenarios generated by the AEMET are complementary to those presented here because different statistical downscaling methodologies, as well as different ESMs, have been applied.

Similar processes were carried out in the generation of climate scenarios for Spain published by the AEMET (www.Aemet.es) and in the EsTcena project (Brands et al., 2013; Brands et al., 2011a). Results that were generated by different centres were presented on the basis of different methodologies, including the one used in the present study.

We compared the new scenarios that were based on the models of the fifth report of the IPCC with those published by Ribalaygua (Ribalaygua et al., 2013a), which correspond to the fourth report of the IPCC. We observed that the most recent scenarios trended toward higher temperatures than what was expected in (Ribalaygua et al., 2013a), with greater increases occurring during summer months compared to winter months. For example, for the summer months, the new results expect that for the period 2071–2100, the maximum temperature in the most extreme case will reach up to 7 ºC, while those presented by Ribalaygua (Ribalaygua et al., 2013a) for the same period were estimated to reach 5 ºC. However, both studies agreed that the northwest and southwest regions would be the most affected by these variations.

In both cases, maximum and minimum temperatures, in view of the validation results and in the face of the same reanalysis of ERA-40, it is justified that the scenarios generated for the fifth IPCC report are more precise than those that already exist for the Aragón region. Having a range of climate-scenario projections in Aragón facilitates the evaluation of extreme phenomena of interest, such as heat and cold waves, which have strong impacts in the region.

4.2. Consideration about the simulation of heat and cold waves

Our results allow for the simulation of episodes of heat and cold waves throughout the 21st century and prove the validity of the simulations, as is evident by the good verification and validation results. As the methodology is able to adequately simulate the 95th percentile of maximum temperatures and the 5th percentile of minimum temperatures, it is assumed that the thresholds that define the heat or cold waves are being simulated in an appropriate way.

The downscaling methodology that was used was able to successfully simulate heat and cold waves reported by the observations, as shown by the results of the verification process. The ESMs were also successful at simulating the maximum and minimum temperatures during the validation process. However, in the verification process of heat and cold waves, were identified some limitations that must be considered in the simulation of future scenarios:

1) There were gaps in the observed series. The lack of data in the observed series reduced the length of observed data compared to the reanalysed ERA-40 series (that is, the full series without gaps) for the same period of time. Therefore, the number of days included in the 95th percentile (or 5th percentile) of the maximum (or minimum) temperature was greater in the ERA-40 series compared to the observed series.

2) In general, downscaling techniques tend to soften the simulated temperature series with respect to the observed values, which implies that certain episodes of hot or cold waves

are softened in their duration or intensity compared to the observed data and would therefore be classified differently. In the present study, it was appreciated that the average and maximum intensities of the observed cold and heat waves was greater than that simulated for the ERA-40 reanalysis.

In summary, the uncertainties associated with both verification and validation must be considered when interpreting future scenarios.

The results of this study about heat and cold waves are consistent with the results published by both the IPCC (IPCC, 2013) and the AEMET (www.Aemet.es). All models agree that the number of days considered as “hot days” will increase in the coming decades and, therefore, the heat waves will be more frequent. On the other hand, the number of “cold days” will be maintained and, in some cases, will even decrease so, on the contrary of what is expected for heat waves, the frequency of cold waves will remain at its current frequency.

What is stated in the previous paragraph is plausible with one of the main theoretical conclusions about the trend of temperatures reported by the IPCC (IPCC 2013), which is based on the change in the probability of reaching certain temperature values. The probability distribution of temperatures can either move to warmer climates without undergoing changes, can be extended or a combination of both. The third situation is the one that has been observed in recent decades in different studies (Hansen et al., 2012) IPCC, 2001) and is the most plausible situation in the context of the observed data. The new distribution of temperatures implies a less pronounced change in the colder temperatures of the series, a much more marked change in the warmer temperatures and a greater number of warm extreme events. These conclusions support the results anticipated for the coming decades—i.e., the maintenance of cold waves (in number and intensity) and an increase of heat waves.

Regarding the territory of Aragón, the scenarios obtained in the present study indicate that the Ebro valley, the most populated area in the region, will observe the highest maximum temperatures, especially at the end of the century and in the summer (around 40 ºC), as well as the greatest intensity of heat waves. This can have important impacts on the health of the population. The health risks associated with heat waves are well known, both in terms of mortality (Robine et al., 2008; Roldan et al., 2016) and mobility (Lin et al., 2009; Steul et al., 2018), as well as health costs (Roldan et al., 2015). Moreover, these extreme events will cause significant socio-economic impacts because a large part of Aragonese industry and farming is situated in this zone (Olesen et al., 2011).

In addition, the Pyrenees will suffer the longest heat waves (but not the most intense ones), especially at the end of the century, and the greatest increases in maximum temperatures with respect to the values recorded during the historical period (1971–2000). The northern zone is where the greatest intensity of cold waves will also be located, although their durations will not change much compared to the current cold waves. Therefore, it is the heat that is the most outstanding future risk for these ecosystems.

Changes in temperature (even if they are moderate) and warming are potential risks to this rich ecological area, which is characterised by a diversity of species and a wealth of native plants and animals, giving rise to national parks such as Ordesa and Monte Perdido (high mountains). Therefore, these areas are particularly vulnerable to any changes in climate

that could lead to radical alterations in habitats or cause losses in their rich biodiversity, as has been previously described (Kulakowski et al., 2017).

Furthermore, the Pyrenees area decides the amount of water available for urban and agricultural use, with a direct effect on hydrology and agriculture in the Ebro Valley. Changes in temperature and snow accumulation could seriously threaten the sustainability and the equilibrium between available resources and water demand. On the other hand, abrupt temperature changes can lead to accelerated thawing that could cause flooding in populated areas near the river, a risk that has been well evaluated in the literature (Gobiet et al., 2014; Guerreiro et al., 2018) and that will demand new and innovative adaptation strategies (De Martino et al., 2012).

Finally, the disappearance of snow due to a rise in temperature in the area could lead to a negative impact on the winter tourism industry and the Pyrenean ski resorts, which are currently an important part of the region's economy, especially in the Pyrenean valleys (Gilaberte-Burdalo et al., 2014; Gilaberte-Burdalo et al., 2017; Lopez-Moreno et al., 2011; Pons et al., 2015).

5. Conclusions

Our study of data from Aragón, Spain, is the first to simulate episodes of heat and cold waves throughout the 21st century in a valid way, based on the good verification and validation results. In addition, we used climate models to obtain more precise climate scenarios for the temperatures in this territory compared to previously available scenarios.

The use of ESMs from the fifth report of the IPCC and a methodology of downscaling has proven to be effective, allowing us to obtain greater precision in the simulation of the climate variables in this territory and to predict a realistic picture of the risks that extreme temperatures can cause in the Aragón region, both spatially and temporally. The climate scenarios predict higher maximum temperatures compared to previous scenarios. The greatest increases will occur during summer at the end of the century, reaching values of up to 7 ºC in the most unfavourable scenario.

Climate heat- and cold-wave scenarios showed that heat waves will be longer and more intense in upcoming decades. However, intensity and duration of cold waves will not change much compared to the current cold waves. The temperatures and heat-wave intensities will be especially high in the Ebro Valley, the most populated area. However, the Pyrenees will suffer the longest heat waves, especially at the end of the century, and the greatest increases in maximum temperatures.

The present study provides useful information coming from the downscaling for the first time in Aragón of models from IPCC5 to support decision-making and in the development of specific measures to prevent socio-economic, environmental and human health impacts due climate change in Aragón, a territory that can be a good indicator of the impacts of climate change in southern Europe.

Material suplementario Resultado 1

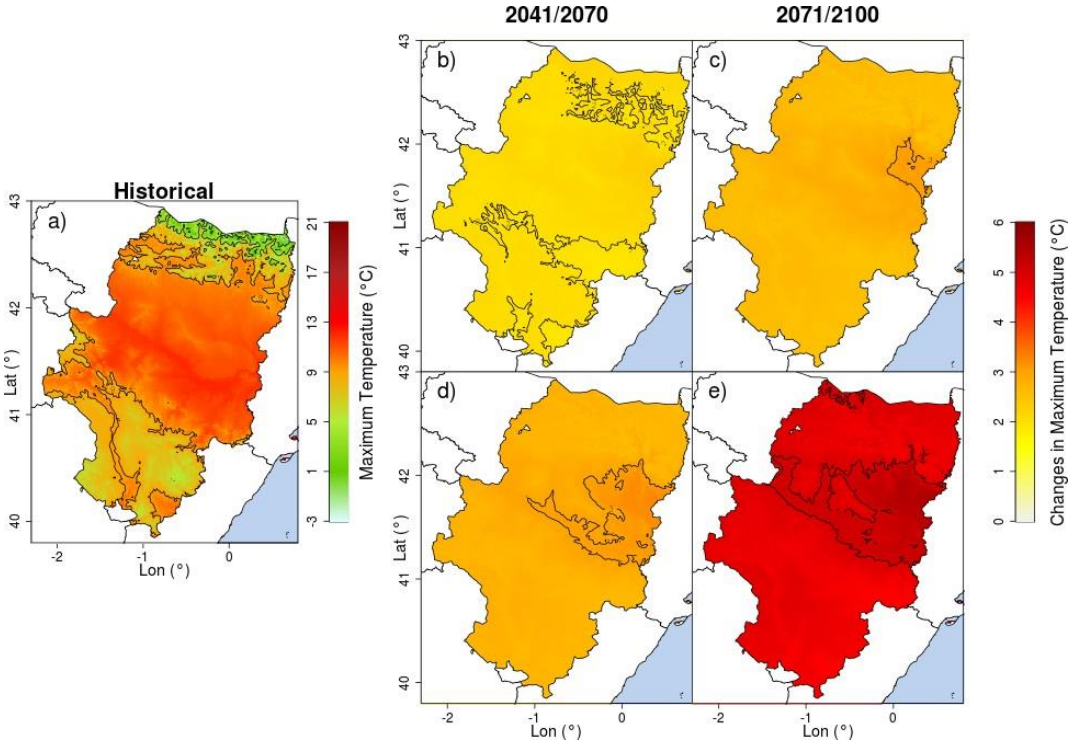

Figure S1.1. Geographical representation of the expected changes of maximum temperature in winter for the periods 2040-2070 and 2070-2100 compared to the reference Historical Period (1976-2005) according to both emissions scenarios, RCP4.5 (figures b and c) and RCP8 (figures d and e). Figure a represents the Historical absolute maximum temperature

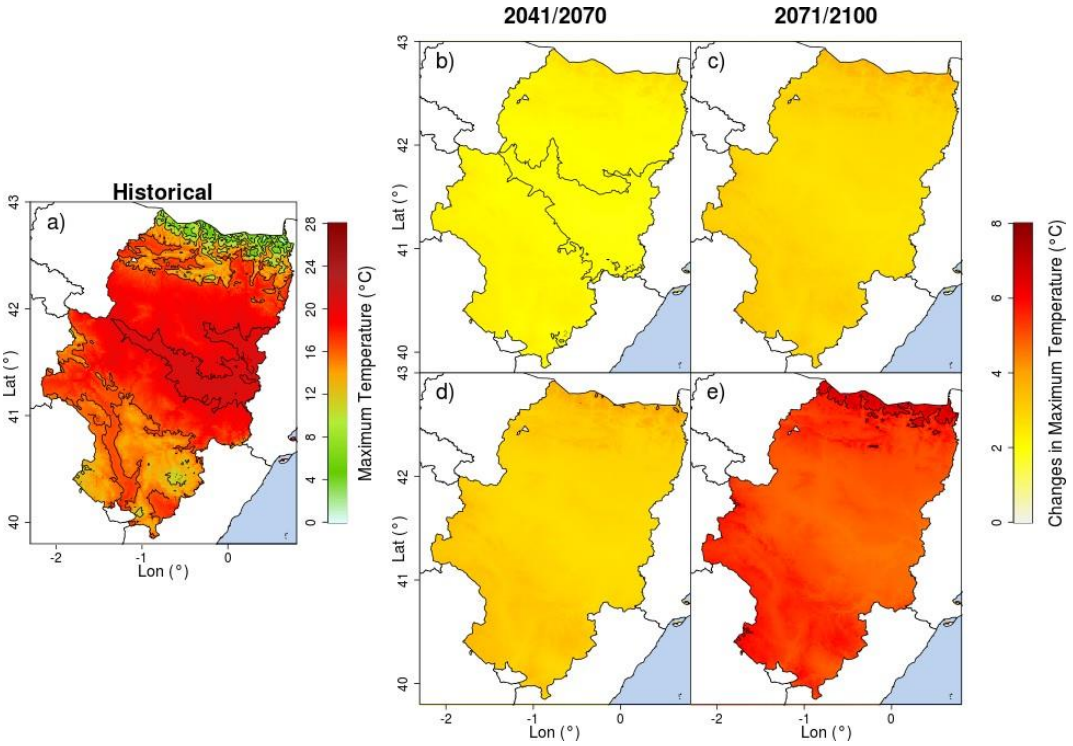

Figure S1.2. Geographical representation of the expected changes of maximum temperature in spring for the periods 2040-2070 and 2070-2100 compared to the reference Historical Period (1976-2005) according to both emissions scenarios, RCP4.5 (figures b and c) and RCP8 (figures d and e). Figure a represents the Historical absolute maximum temperature.

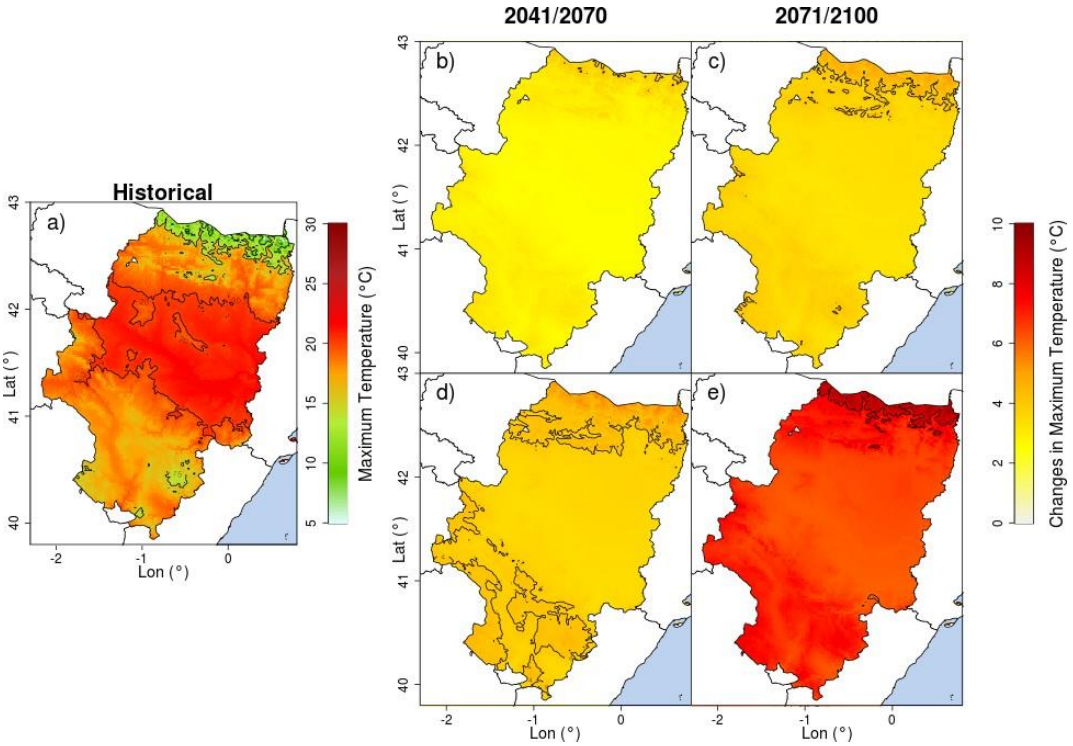

Figure S1.3. Geographical representation of the expected changes of maximum temperature in autumn for the periods 2040-2070 and 2070-2100 compared to the reference HistoricalPeriod (1976-2005) according to both emissions scenarios, RCP4.5 (figures b and c) and RCP8 (figures d and e). Figure a represents the Historical absolute maximum temperature.

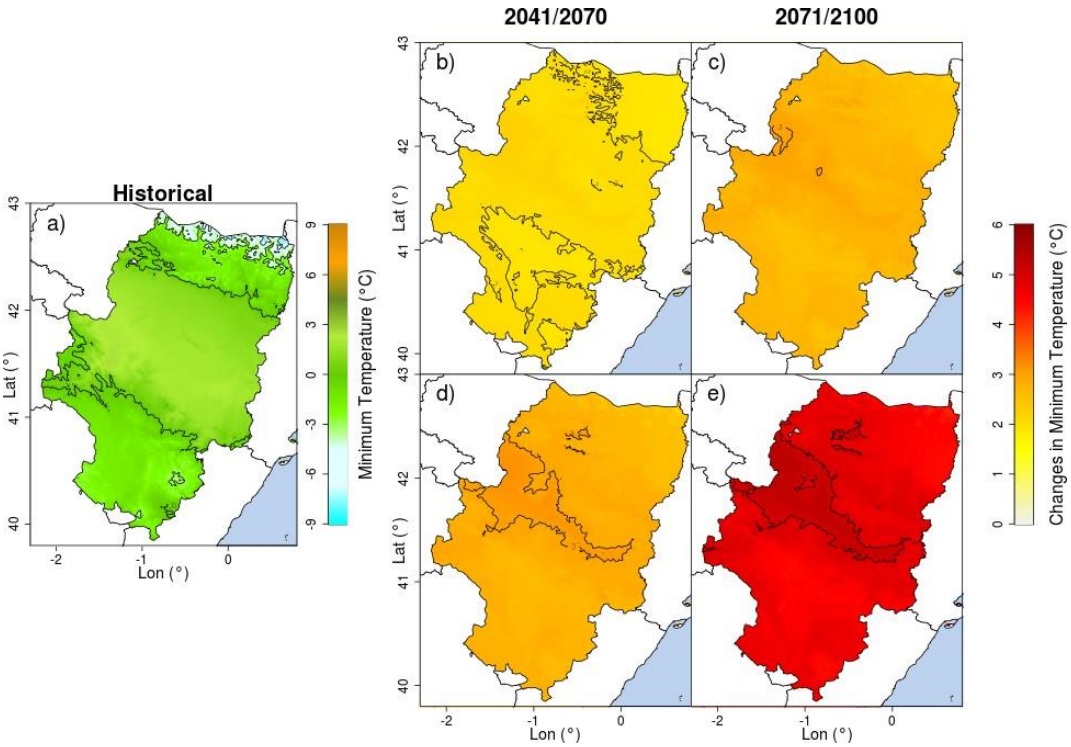

Figure S1.4. Geographical representation of the expected changes of minimum temperature in winter for the periods 2040-2070 and 2070-2100 compared to the reference Historical Period (1976-2005) according to both emissions scenarios, , RCP4.5 (figures b and c) and RCP8 (figures d and e). Figure a represents the Historical absolute minimum temperature.

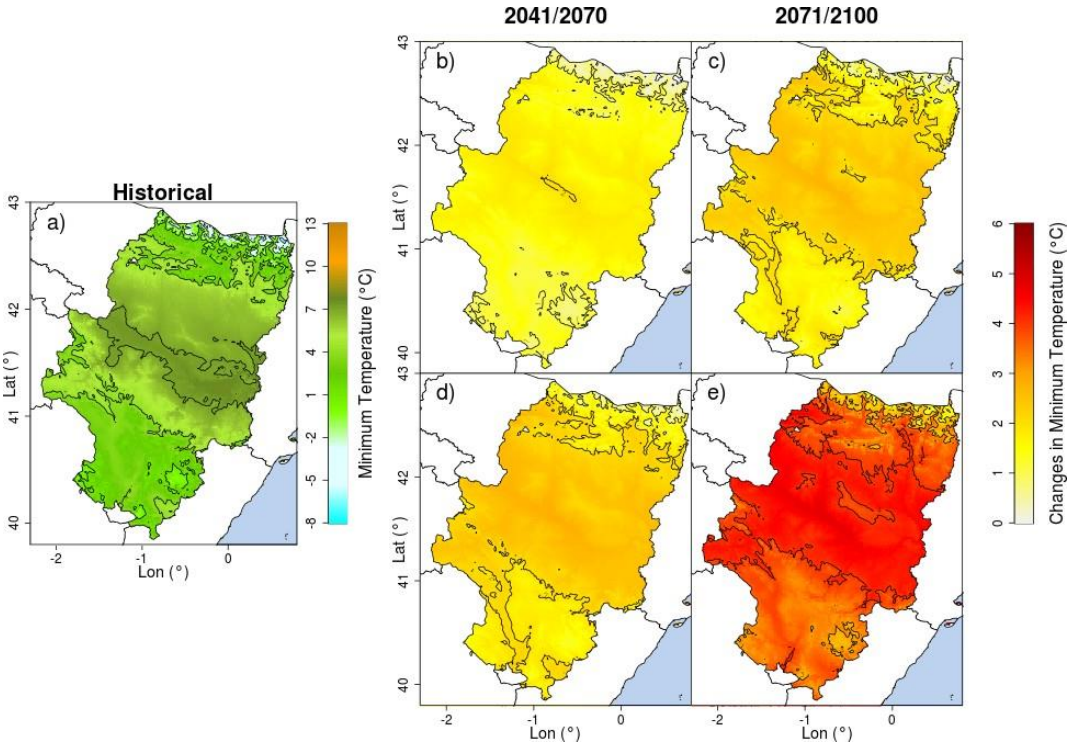

Figure S1.5. Geographical representation of the expected changes of minimum temperature in spring for the periods 2040-2070 and 2070-2100 compared to the reference Historical Period (1976-2005) according to both emissions scenarios, , RCP4.5 (figures b and c) and RCP8 (figures d and e). Figure a represents the Historical absolute minimum temperature.

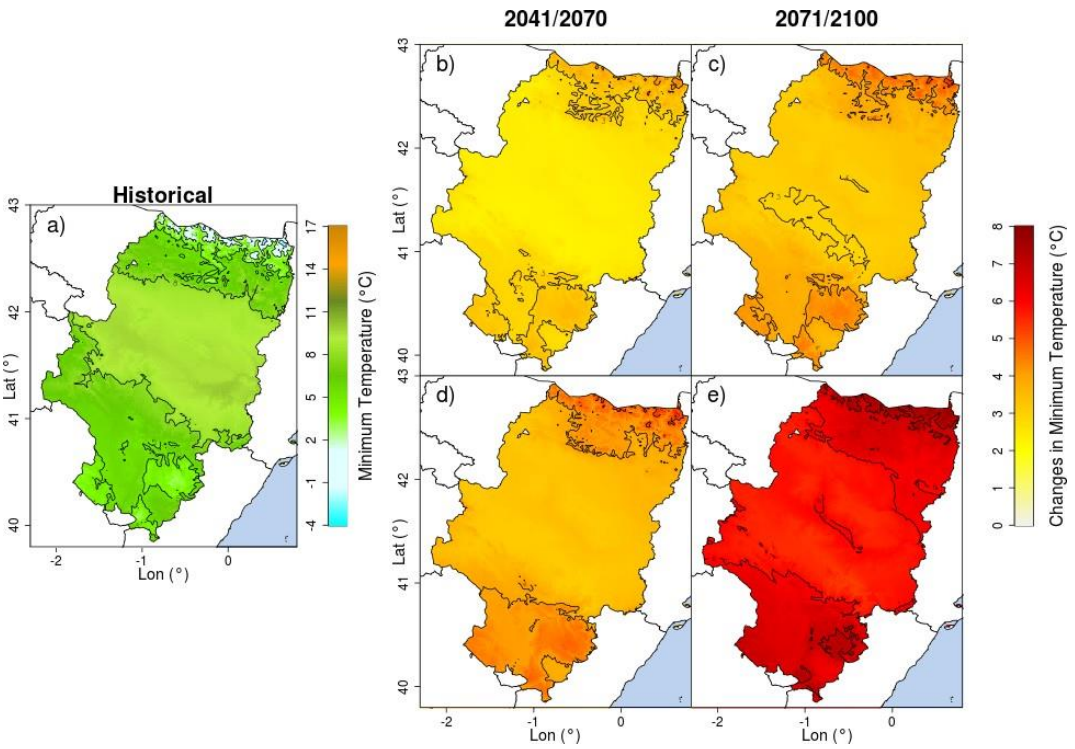

Figure S1.6. Geographical representation of the expected changes of minimum temperature in autumn for the periods 2040-2070 and 2070-2100 compared to the reference HistoricalPeriod (1976-2005) according to both emissions scenarios, RCP4.5 (figures b and c) and RCP8 (figures d and e). Figure a represents the Historical absolute minimum temperature.

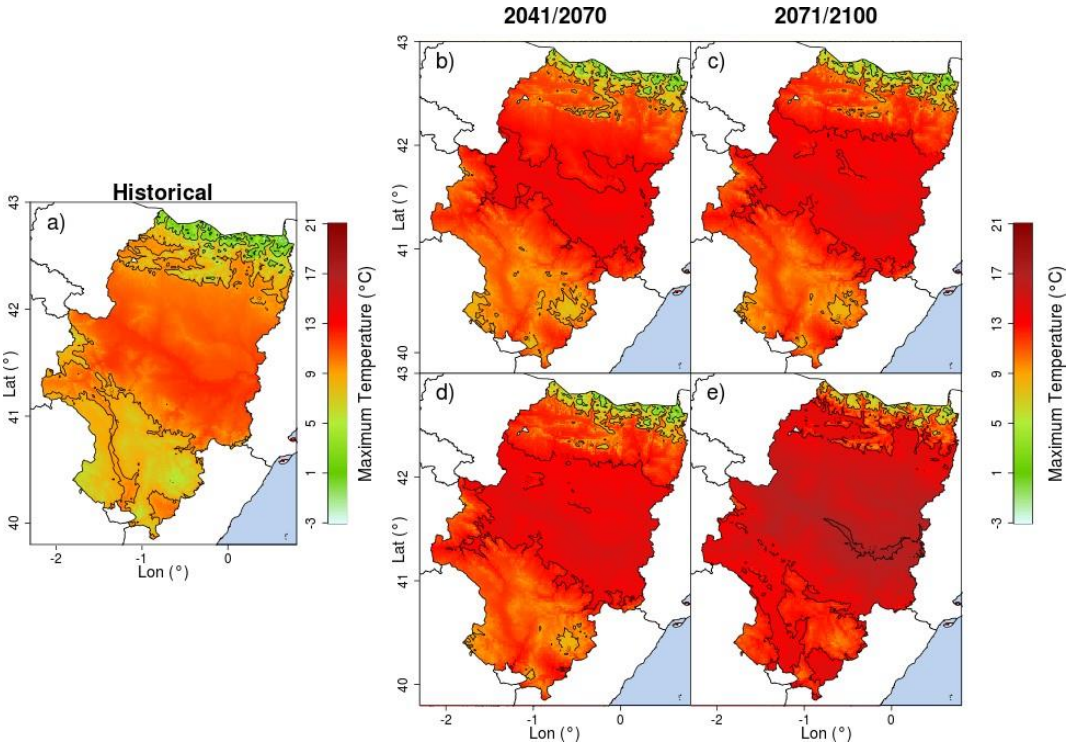

Figure S1.7. Geographical representation of the expected maximum temperature in winter for theperiods 2040-2070 and 2070-2100 compared to the reference Historical Period (1976- 2005) according to both emissions scenarios, RCP4.5 (figures b and c) and RCP8 (figures d and e). Figure a represents the Historical absolute maximum temperature.

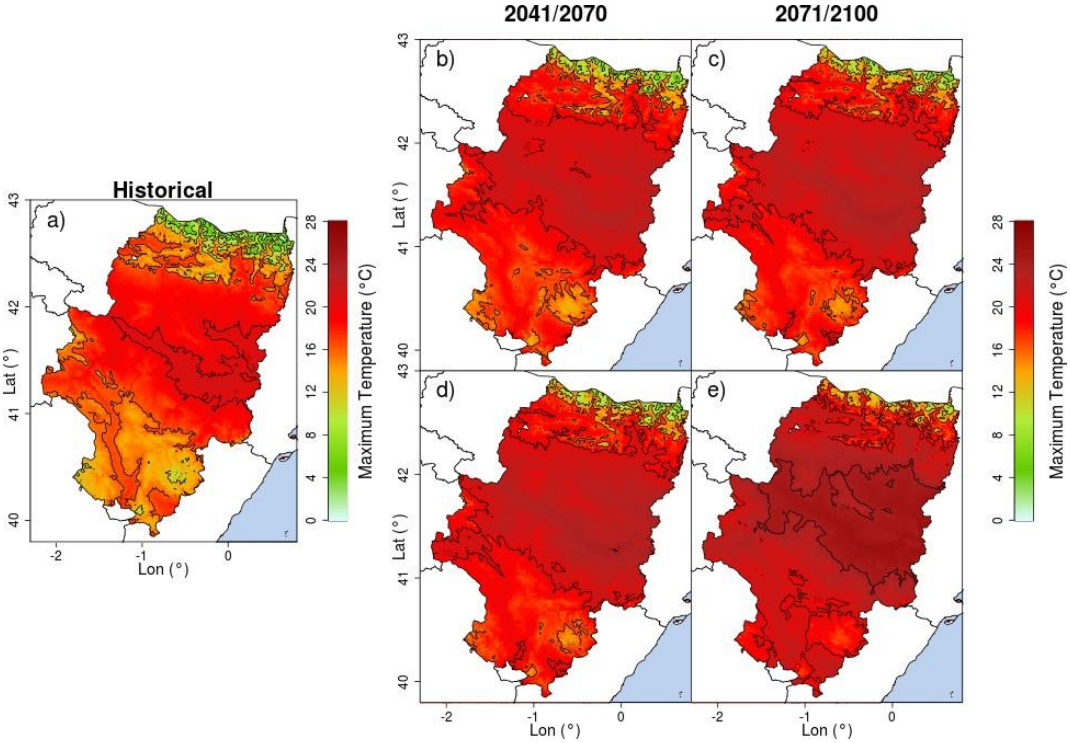

Figure S1.8. Geographical representation of the expected máximum temperature in spring for theperiods 2040-2070 and 2070-2100 compared to the reference Historical Period (1976- 2005) according to both emissions scenarios, RCP4.5 (figures b and c) and RCP8 (figures d and e). Figure a represents the Historical absolute maximum temperature

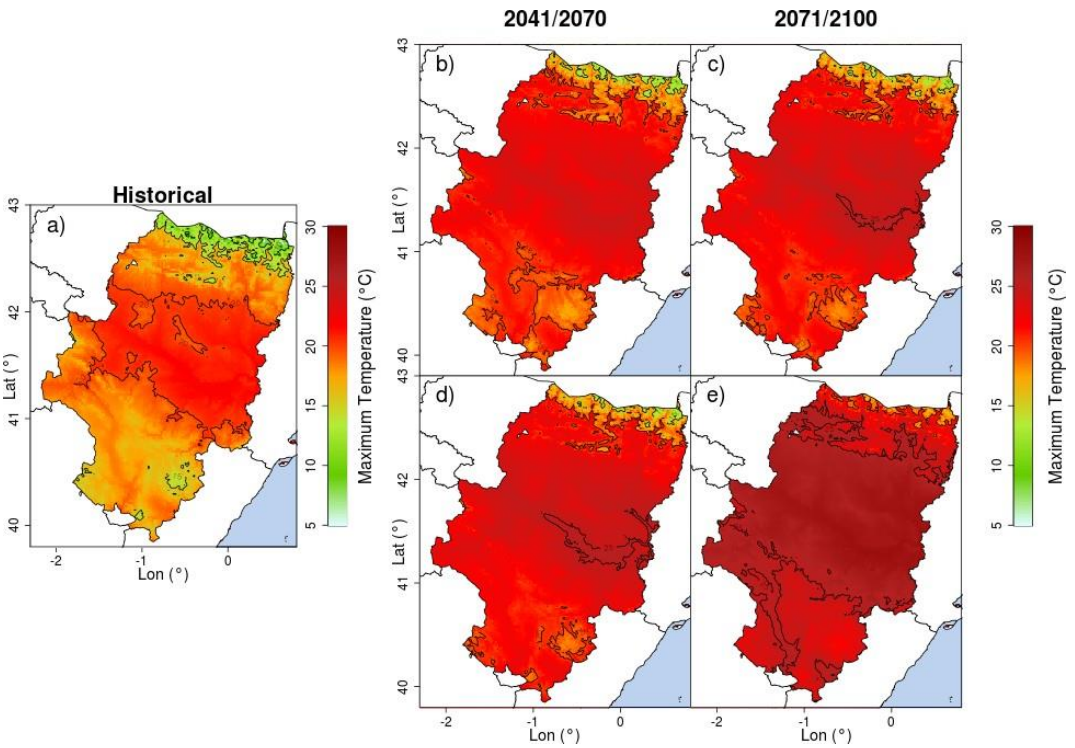

Figure S1.9. Geographical representation of the expected máximum temperature in autumn for the periods 2040-2070 and 2070-2100 compared to the reference Historical Period (1976-2005) according to both emissions scenarios, RCP4.5 (figures b and c) and RCP8(figures d and e). Figure a represents the Historical absolute maximum temperature

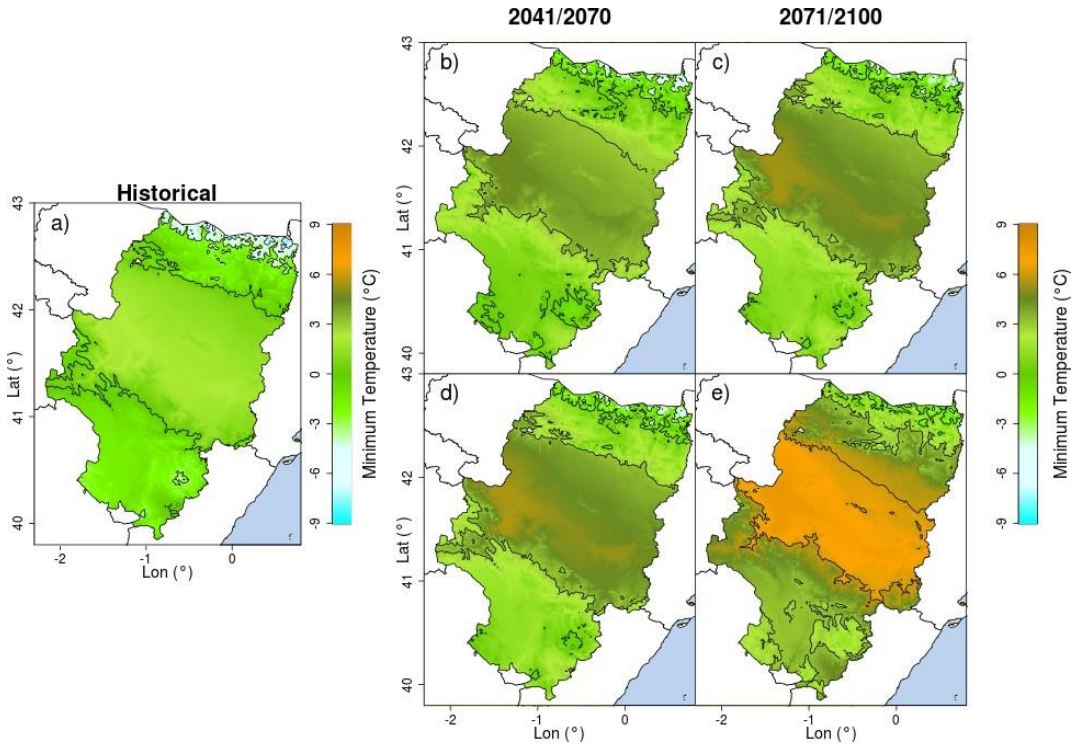

Figure S1.10. Geographical representation of the expected minimum temperature in winter for the periods 2040-2070 and 2070-2100 compared to the reference Historical Period (1976-2005) according to both emissions scenarios, RCP4.5 (figures b and c) and RCP8(figures d and e). Figure a represents the Historical absolute mínimum temperature

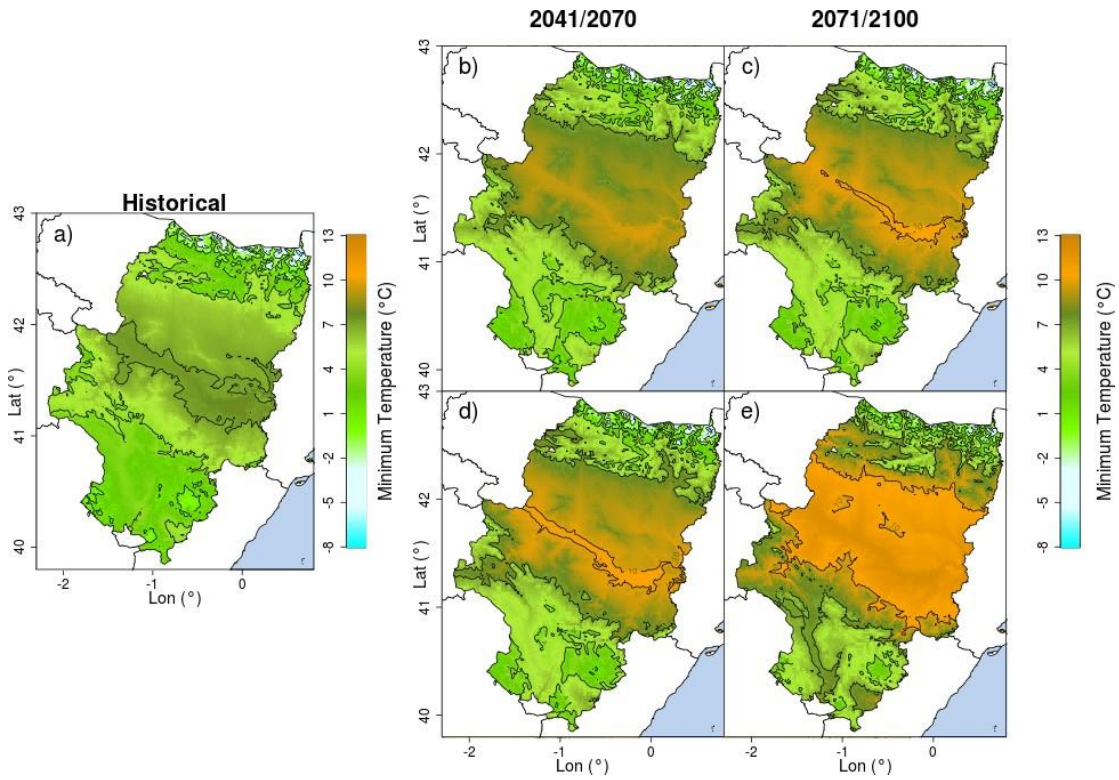

Figure S1.11. Geographical representation of the expected minimum temperature in spring for the periods 2040-2070 and 2070-2100 compared to the reference Historical Period (1976-2005) according to both emissions scenarios, RCP4.5 (figures b and c) and RCP8(figures d and e). Figure a represents the Historical absolute mínimum temperature

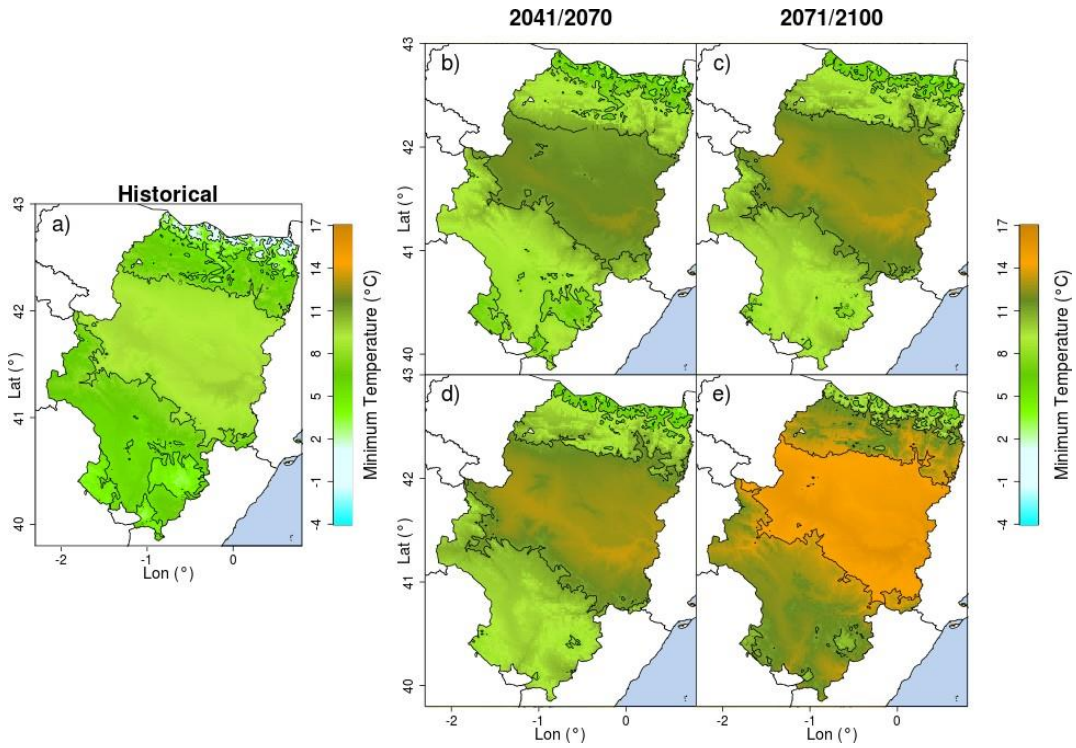

Figure S1.12. Geographical representation of the expected minimum temperature in autumn forthe periods 2040-2070 and 2070-2100 compared to the reference Historical Period (1976-2005) according to both emissions scenarios, RCP4.5 (figures b and c) and RCP8(figures d and e). Figure a represents the Historical absolute mínimum temperature

Figure S1.13. Results of the verification process for heat waves obtained comparing the simulated heat waves for the reanalysis Era40 along the observed heat waves for a common period (1980-2000). a) maximum intensity of the heat waves registered in the 71 observatories used in the study against b) the maximum intensity obtained by downscaling of the reanalysis Era40 in these observatories for the period 1980-2000. The colour of each pixel shows the maximum intensity that corresponds to each heat wave (ºC). The upper row shows the mean of the maximum intensity from the whole observatories.

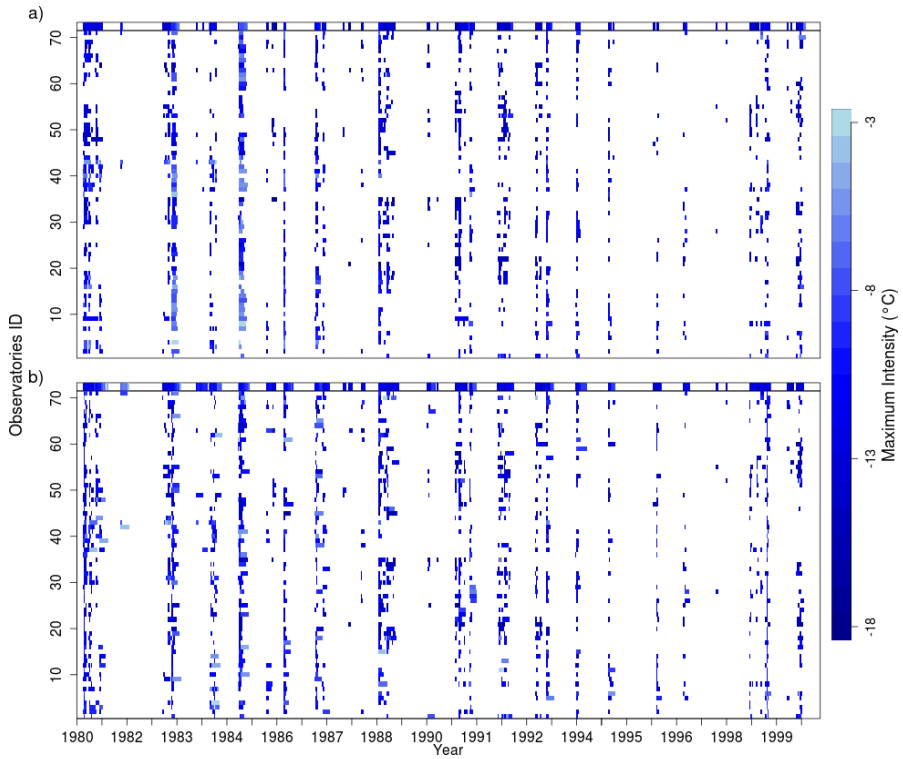

Figure S1.14. Results of the verification process for cold waves obtained comparing the simulatedheat waves for the reanalysis Era40 along the observed cold waves for a common period(1980-2000). a) maximum intensity of the heat waves registered in the 71 observatoriesused in the study against b) the maximum intensity obtained by downscaling of the reanalysis Era40 in these observatories for the period 1980-2000. The colour of each pixel shows the maximum intensity that corresponds to each cold wave (ºC). The upperrow shows the mean of the maximum intensity from the whole observatories.

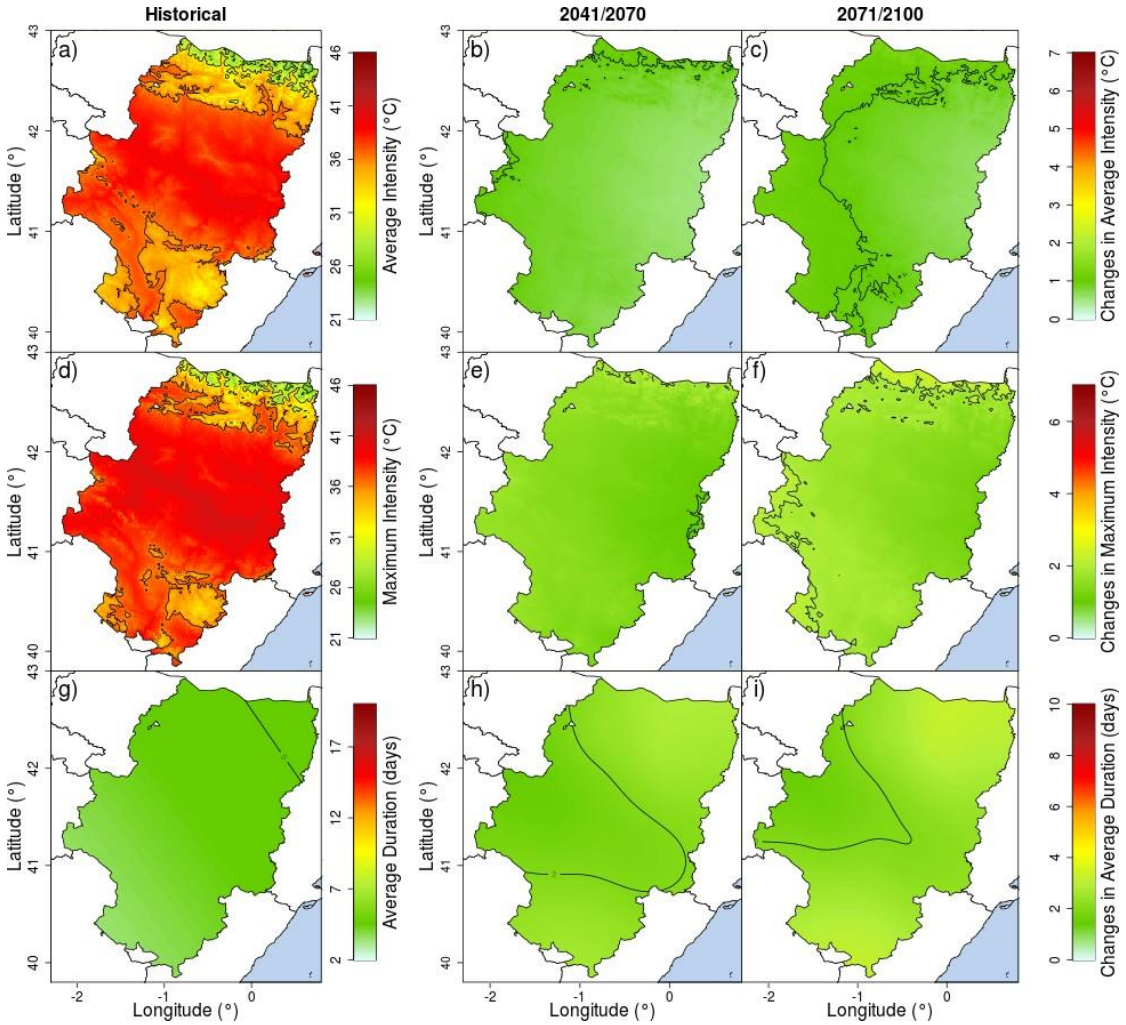

Figure S1.15. Geographical representation of the expected evolution of the heat waves for Aragon in the periods 2041-2070 and 2071-2100 in terms of increments values respect to the reference Historical Period (1971-2000) according to the RCP4.5. The rows showthe three parameters analyzed in the study (average intensity, maximum intensity and duration) and the columns the three temporal periods (Historical, 2041-2070 and 2071- 2100). The maps are generated interpolating the available observatories over the entireterritory.

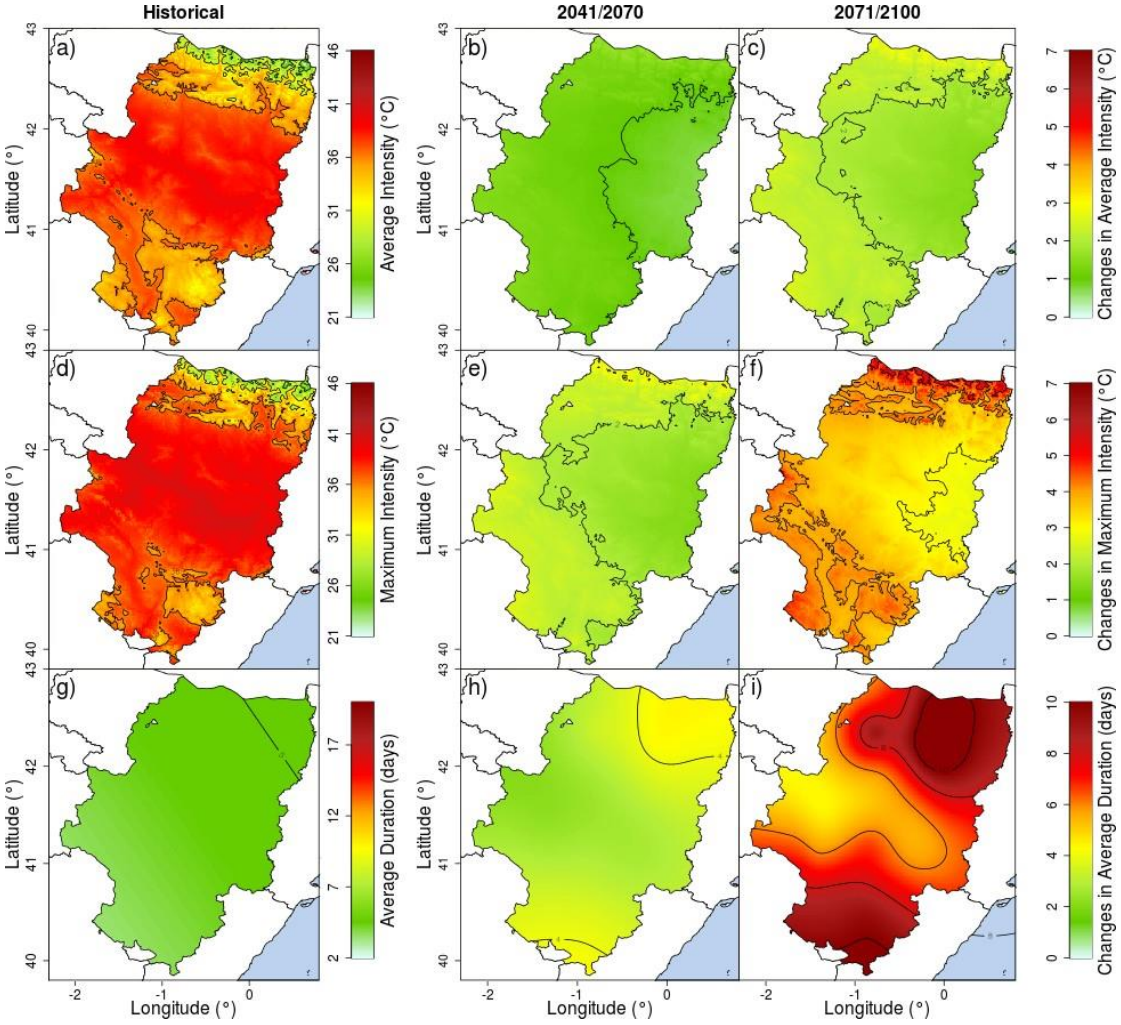

Figure S1.16. Geographical representation of the expected evolution of the heat waves for Aragon in the periods 2041-2070 and 2071-2100 in terms of increments values respect to the reference Historical Period (1971-2000) according to the RCP8.5. The rows showthe three parameters analyzed in the study (average intensity, maximum intensity and duration) and the columns the three temporal periods (Historical, 2041-2070 and 2071- 2100). The maps are generated interpolating the available observatories over the entireterritory.

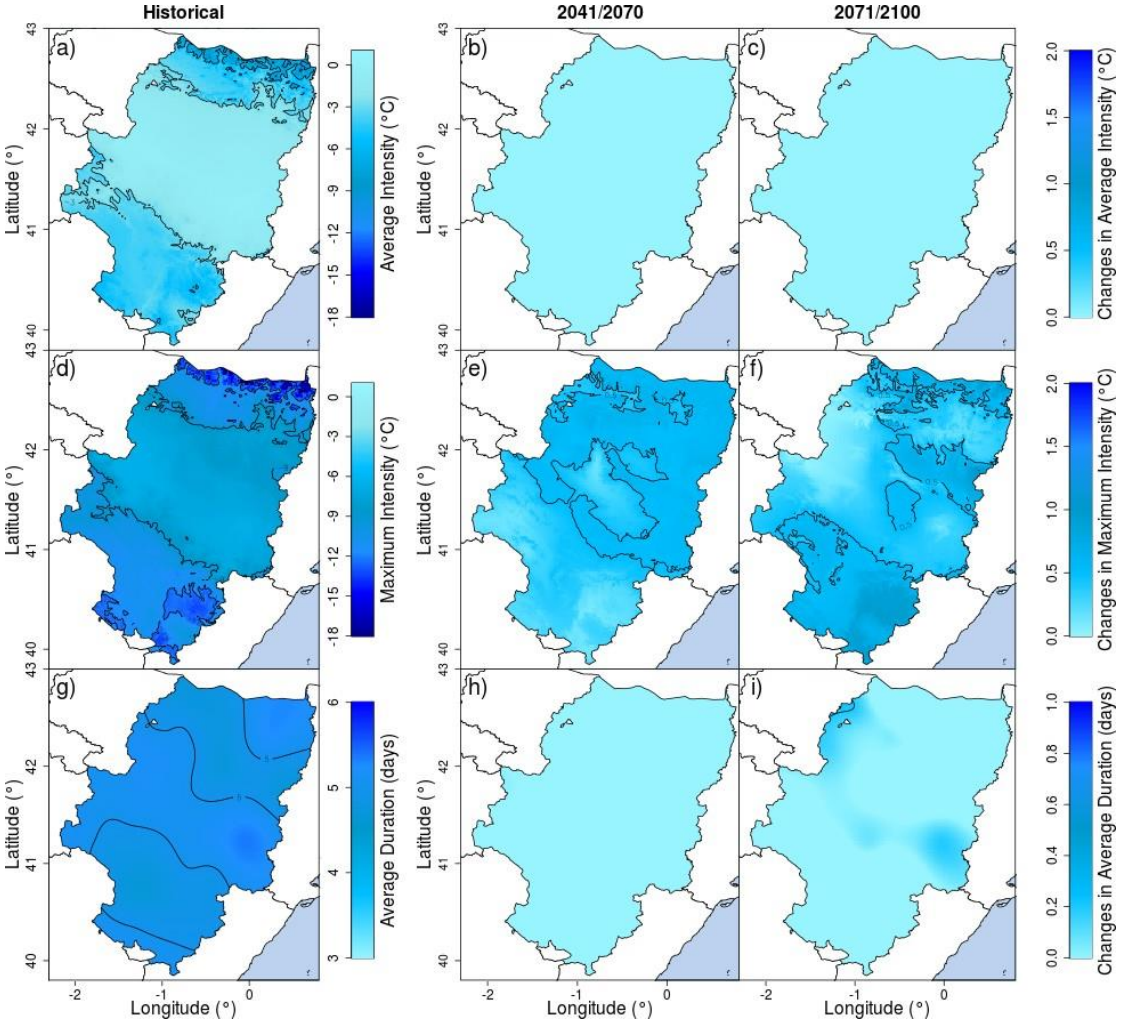

Figure S1.17. Geographical representation of the expected evolution of the cold waves for Aragon in the periods 2041-2070 and 2071-2100 in terms of increments values respect to the reference Historical Period (1971-2000) according to the RCP4.5. The rows showthe three parameters analyzed in the study (average intensity, maximum intensity and duration) and the columns the three temporal periods (Historical, 2041-2070 and 2071- 2100). The maps are generated interpolating the available observatories over the entireterritory.

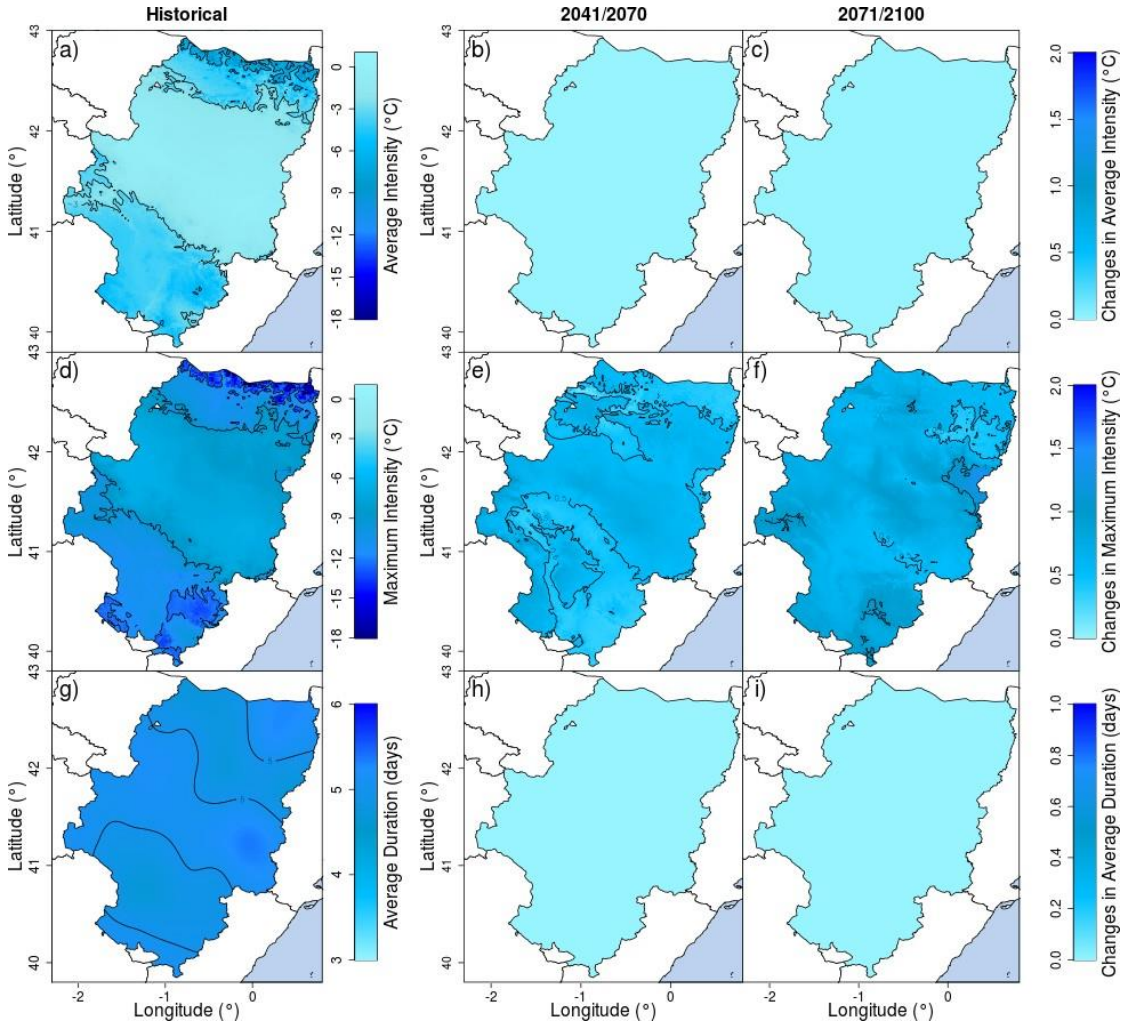

Figure S1.18. Geographical representation of the expected evolution of the cold waves for Aragon in the periods 2041-2070 and 2071-2100 in terms of increments values respect to the reference Historical Period (1971-2000) according to the RCP8.5. The rows showthe three parameters analyzed in the study (average intensity, maximum intensity and duration) and the columns the three temporal periods (Historical, 2041-2070 and 2071- 2100). The maps are generated interpolating the available observatories over the entireterritory.

Anexo R1. Escenarios de temperatura y olas de calor y frío para Península Ibérica y Baleares

En el Anexo Resultado 1 se recogen los resultados de las proyecciones climáticas para todo el territorio español (Península e Islas Baleares) de temperatura (máxima y mínima) y episodios de olas de frío y calor.

En las figuras AR1.1 a AR1.4 se muestran los resultados obtenidos para temperatura máxima y temperatura mínima en base a los escenarios RCP4.5 y RCP8.5. Suponen una representación espacial de la evolución esperada de cada variable en los periodos 2041-2070 y 2071-2100 comparados con el periodo de referencia (1976-2005) bajo el escenario considerado. Las filas muestran las cuatro estaciones del año (invierno, primavera, verano y otoño) y las columnas los tres periodos temporales (Historical, 2041-2070 and 2071-2100).

En las figuras AR1.5 a AR1.8 se muestran los resultados obtenidos para los episodios de olas de calor y frío en base a los escenarios RCP4.5 y RCP8.5. Suponen una representación espacial de la evolución esperada de cada variable en los periodos 2041-2070 y 2071-2100 comparados con el periodo de referencia (1976-2005) bajo el escenario considerado. Las filas muestran las características principales (intensidad media, intensidad máxima y duración media) y las columnas los tres periodos temporales (Historical, 2041-2070 and 2071-2100).

Los mapas se han generado interpolando todos los observatorios disponibles en el estudio.

En base a los resultados obtenidos y en promedio a todo el territorio (habrá zonas donde los cambios proyectados serán más o menos intensos) se espera:

- Un aumento gradual de las temperaturas medias (entre 2 y 4 ºC en función del escenario considerado y la zona del territorio), siendo los meses estivales los que experimentarán los ascensos más acusados.
- Un aumento en las temperaturas máximas a finales de siglo de entre 3.8 y 7 ºC en los meses estivales (dependiendo del RCP considerado) que son los más críticos en cuanto a esta variable. Estos aumentos suponen temperaturas superiores a 38 ºC en toda la mitad sur peninsular, la zona Mediterránea y las Islas Baleares. Aunque en el resto del año los ascensos se esperan algo menos acusados, siguen siendo elevados. En los meses de invierno se esperan aumentos de entre 2 y 4 ºC, en los meses de primavera entre 2.8 y 5 ºC y en los meses de otoño entre 3y 6 ºC. Estos resultados corresponden con el periodo 2071-2100 bajo el escenario RCP8.5.
- Los aumentos esperados en las temperaturas máximas tienen como consecuencia que los episodios de olas de calor sean cada vez más intensos y aparezcan con más frecuencia. Además de ser más persistentes. La costa Mediterránea se verá especialmente afectada por situaciones de olas de calor, las cuales podrán abarcar hasta 20 días a finales de siglo en el caso más desfavorable.
- Los mayores aumentos en temperatura mínima se esperan en los meses de verano y otoño, especialmente en la Costa Mediterránea. En promedio, los

aumentos esperados oscilan entre 3 y 5.8 ºC en los meses de verano y otoño y entre 2 y 4 ºC en los meses de invierno y primavera.

- Aunque se esperan cambios considerables en las temperaturas mínimas medias, no se esperan grandes cambios en los extremos, por lo que no se aprecian alteraciones importantes de los episodios de olas de frío futuros respecto a los actuales.

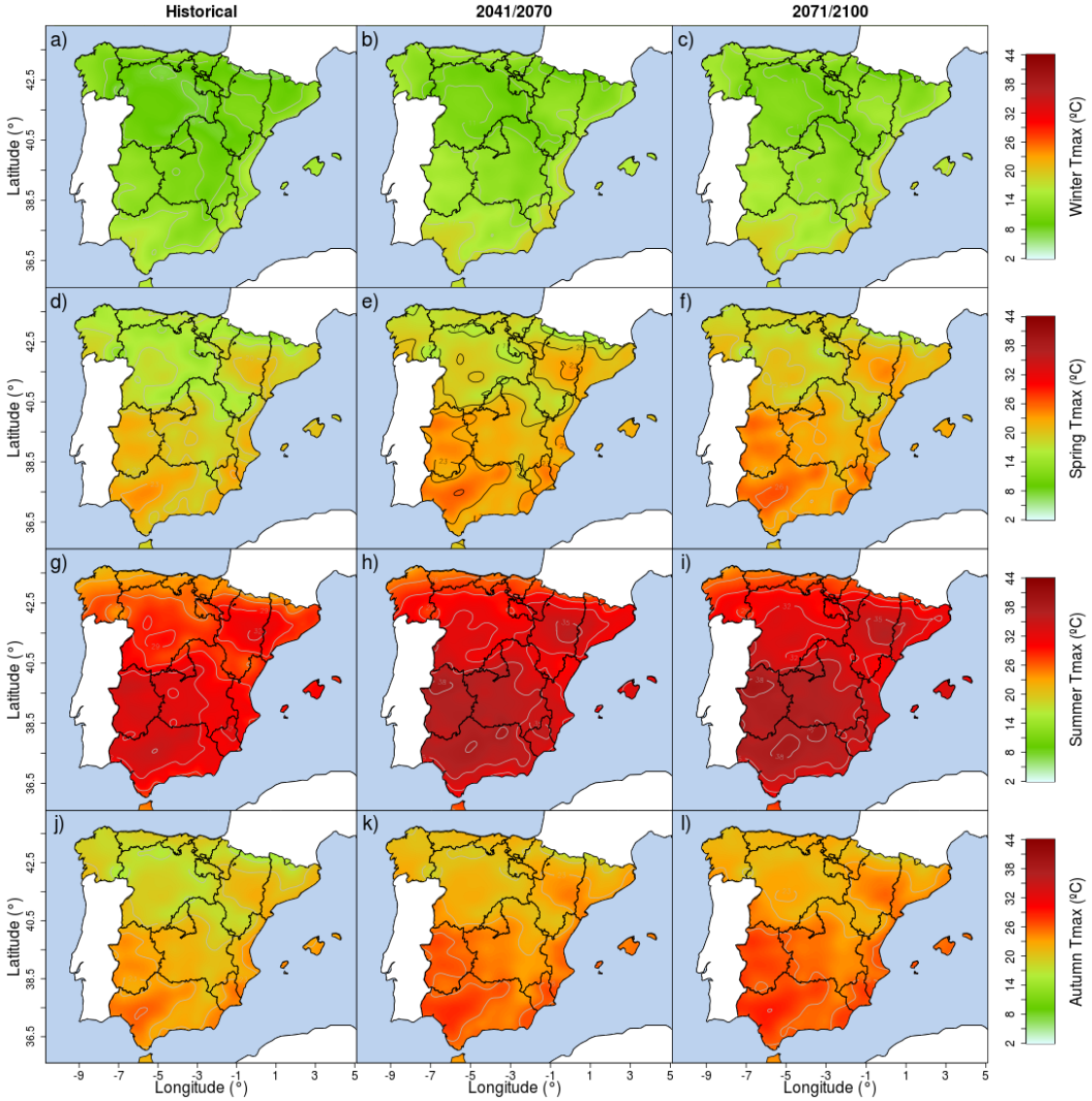

Figura AR1.1. Representación espacial de la evolución esperada de la Temperatura Máxima en los periodos 2041-2070 y 2071-2100 comparados con el periodo de referencia (1976-2005) según el escenario RCP4.5. Las filas muestran las cuatro estaciones del año (invierno, primavera, verano y otoño) y las columnas los tres periodos temporales (Historical, 2041-2070 and 2071-2100). Los mapas se han generado interpolando todos los observatorios disponibles en el estudio.

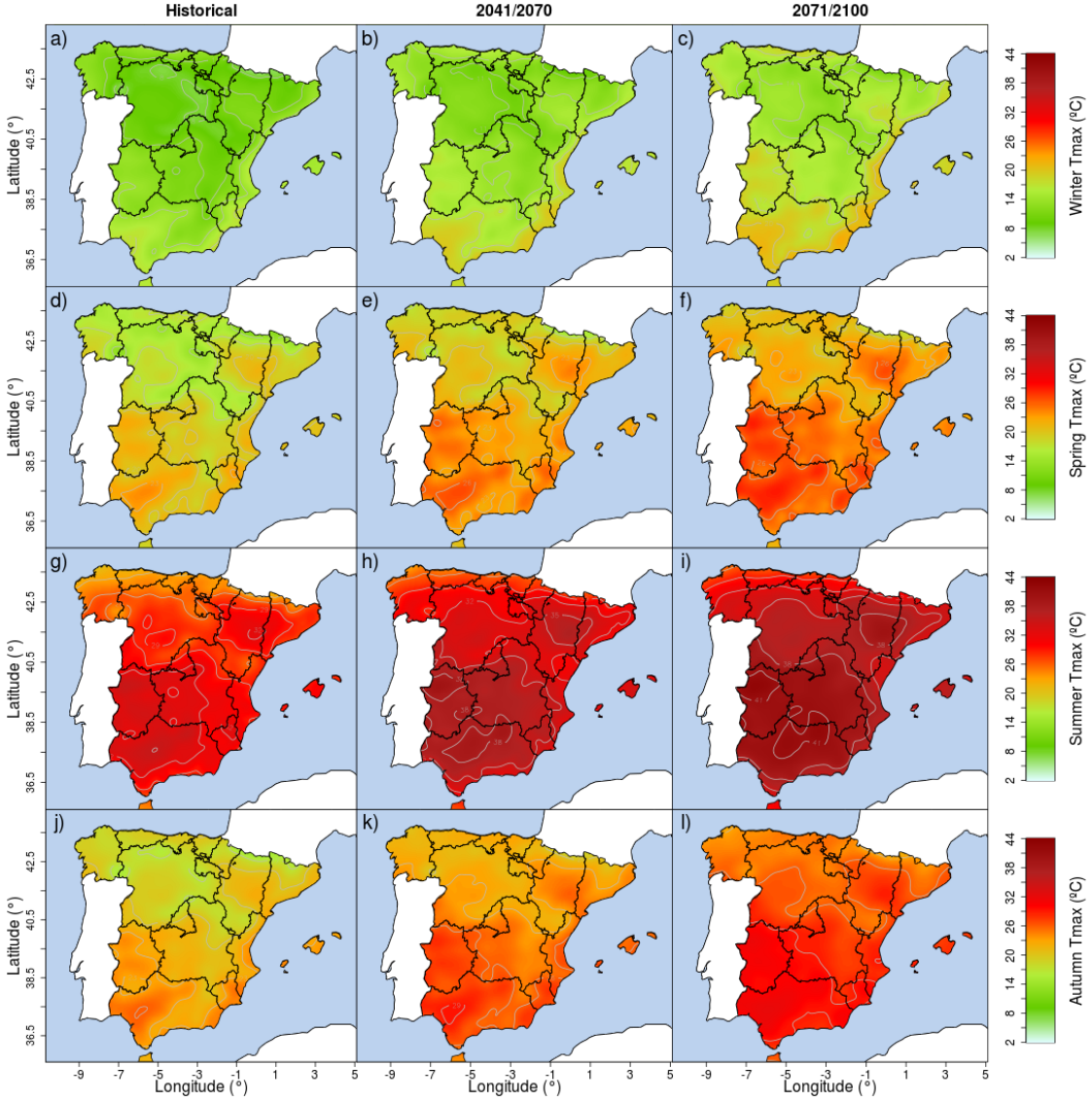

Figura AR1.2. Representación espacial de la evolución esperada de la Temperatura Máxima en los periodos 2041-2070 y 2071-2100 comparados con el periodo de referencia (1976-2005) según el escenario RCP8.5. Las filas muestran las cuatro estaciones del año (invierno, primavera, verano y otoño) y las columnas los tres periodos temporales (Historical, 2041-2070 and 2071-2100). Los mapas se han generado interpolando todos los observatorios disponibles en el estudio.

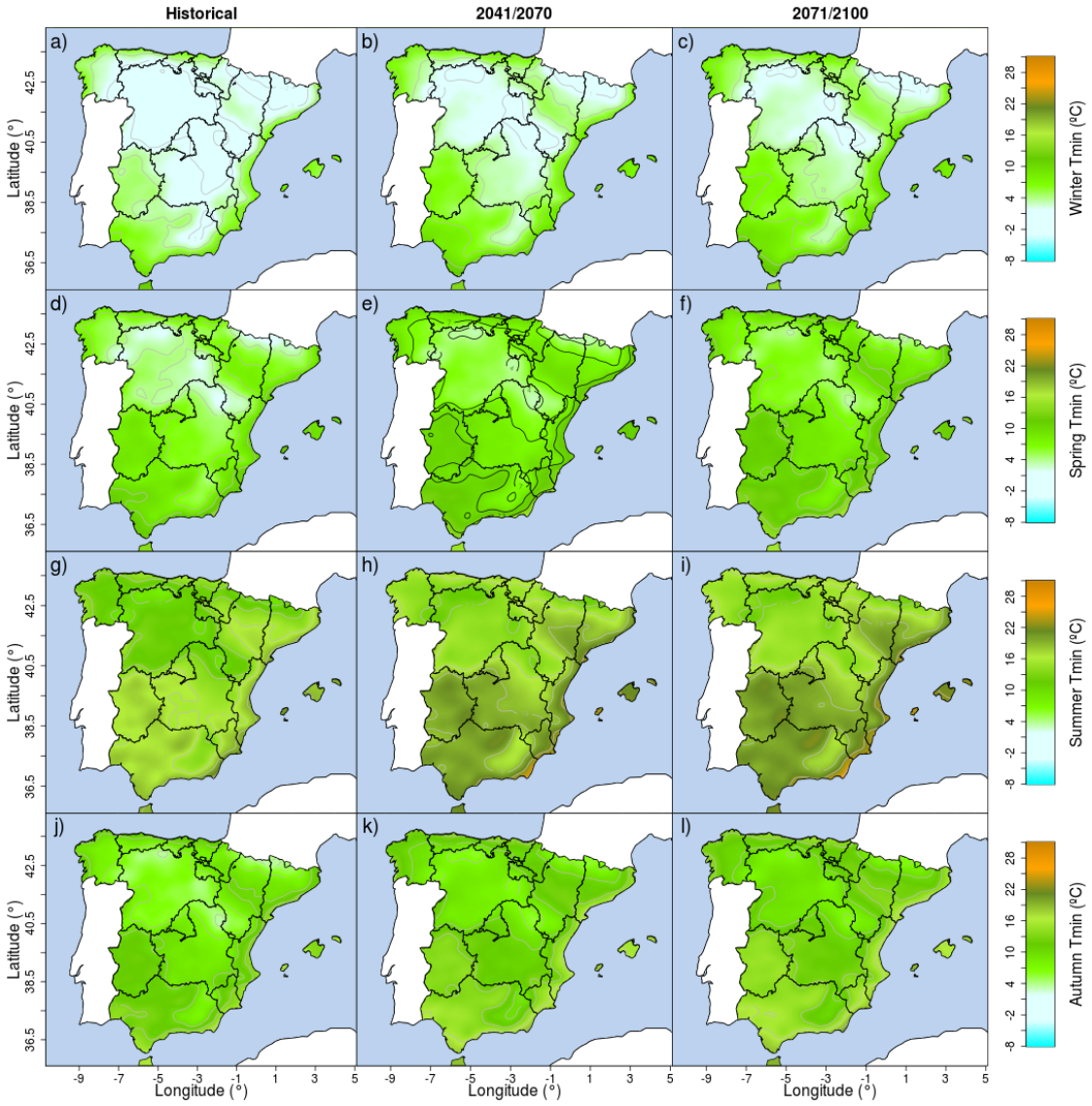

Figura AR1.3. Representación espacial de la evolución esperada de la Temperatura Mínima en los periodos 2041-2070 y 2071-2100 comparados con el periodo de referencia (1976-2005) según el escenario RCP4.5. Las filas muestran las cuatro estaciones del año (invierno, primavera, verano y otoño) y las columnas los tres periodos temporales (Historical, 2041-2070 and 2071-2100). Los mapas se han generado interpolando todos los observatorios disponibles en el estudio.

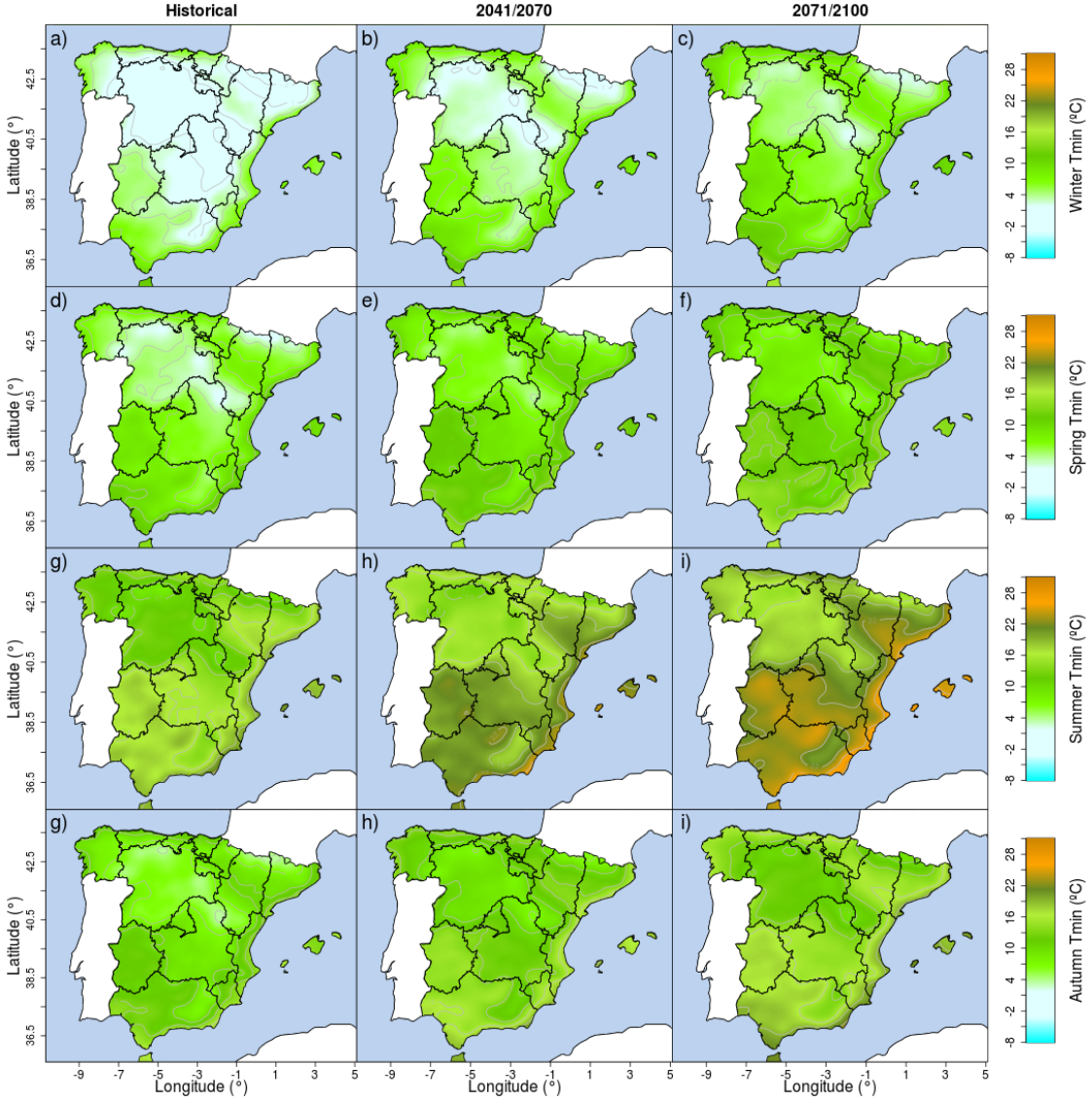

Figura AR1.4. Representación espacial de la evolución esperada de la Temperatura Mínima en los periodos 2041-2070 y 2071-2100 comparados con el periodo de referencia (1976-2005) según el escenario RCP8.5. Las filas muestran las cuatro estaciones del año (invierno, primavera, verano y otoño) y las columnas los tres periodos temporales (Historical, 2041-2070 and 2071-2100). Los mapas se han generado interpolando todos los observatorios disponibles en el estudio.

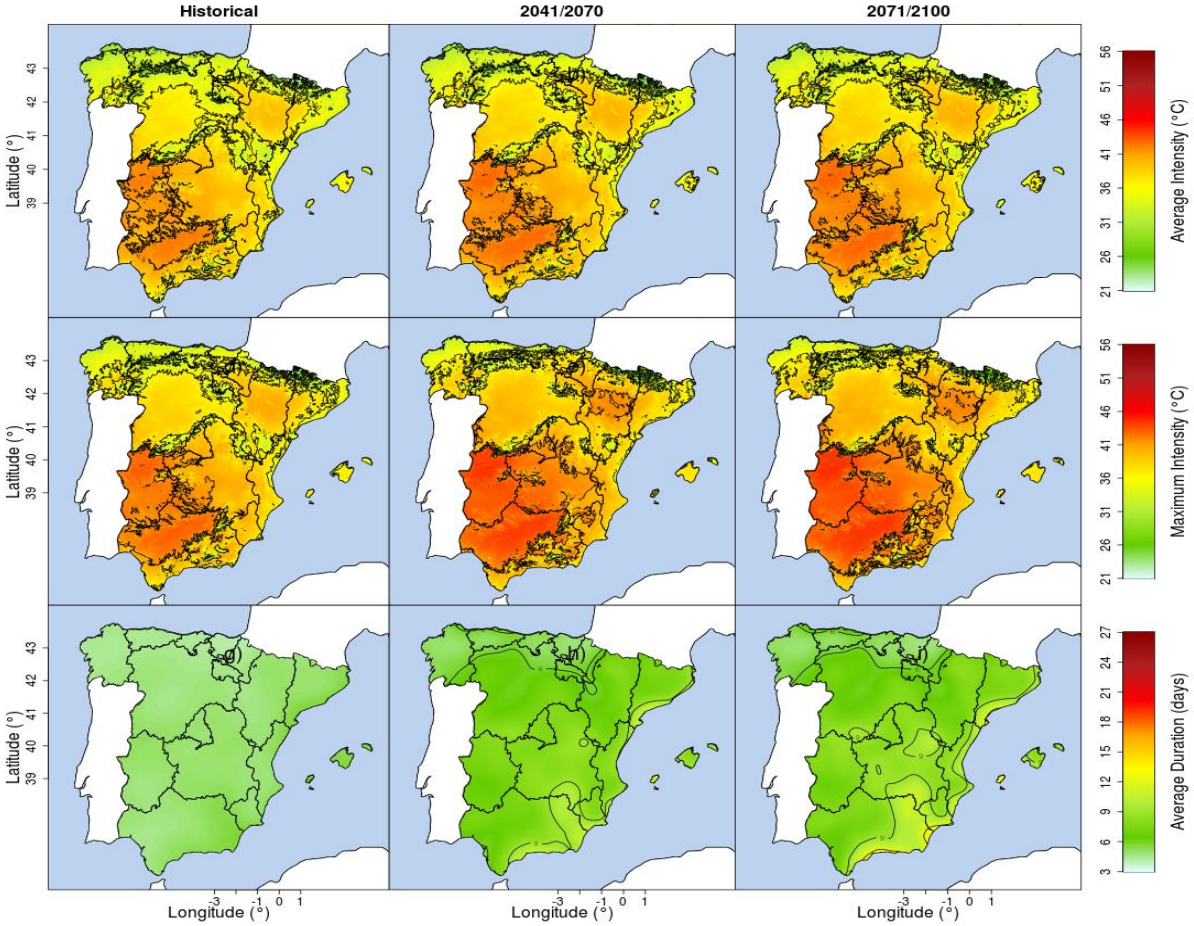

Figure AR1.5. Representación espacial de la evolución esperada de las olas de calor en los periodos 2041-2070 y 2071-2100 comparados con el periodo de referencia (1976-2005) según el escenario RCP4.5. Las filas muestran las características principales (intensidad media, intensidad máxima y duración media) y las columnas los tres periodos temporales (Historical, 2041-2070 and 2071-2100). Los mapas se han generado interpolando todos los observatorios disponibles en el estudio.

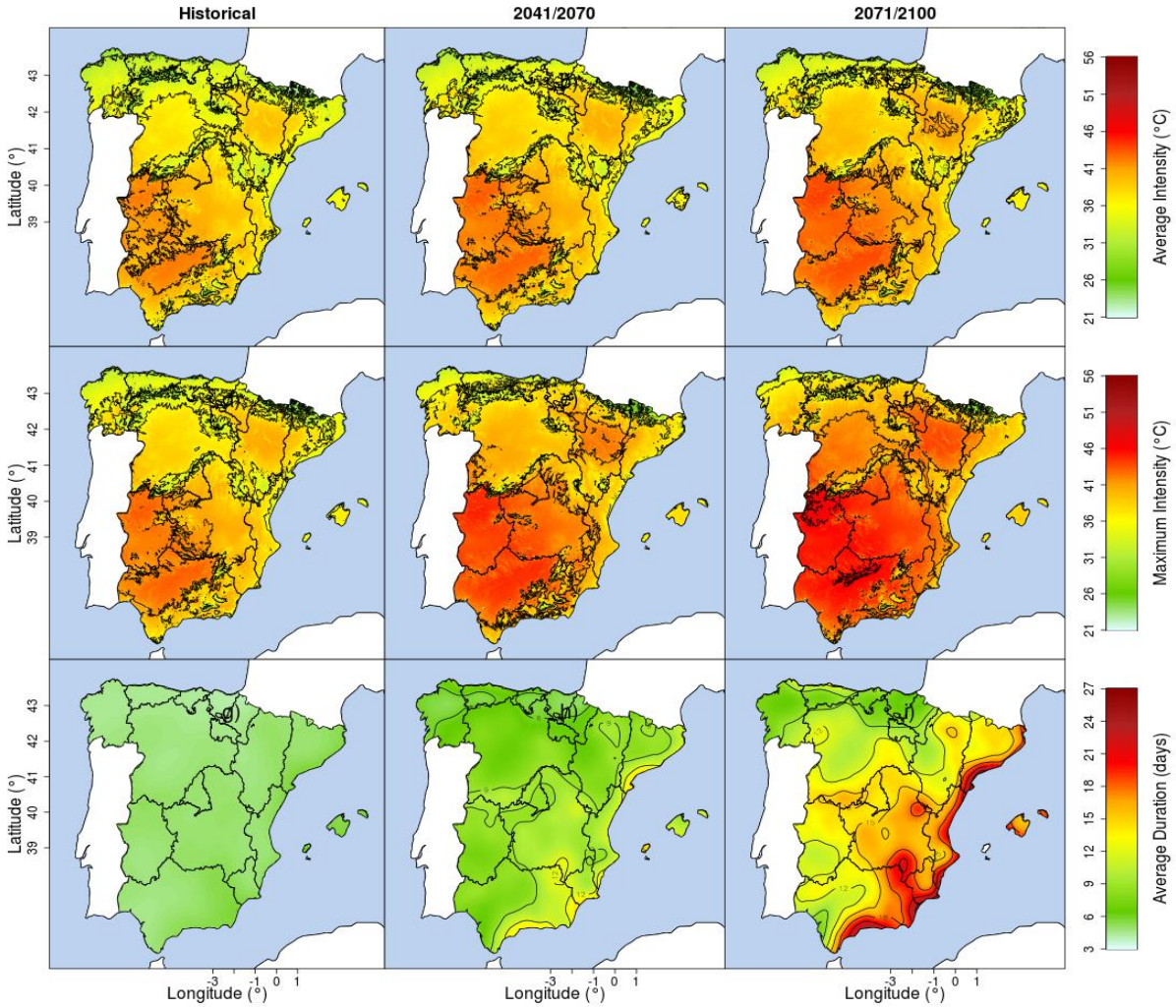

Figure AR1.6. Representación espacial de la evolución esperada de las olas de calor en los periodos 2041-2070 y 2071-2100 comparados con el periodo de referencia (1976-2005) según el escenario RCP8.5. Las filas muestran las características principales (intensidad media, intensidad máxima y duración media) y las columnas los tres periodos temporales (Historical, 2041-2070 and 2071-2100). Los mapas se han generado interpolando todos los observatorios disponibles en el estudio.

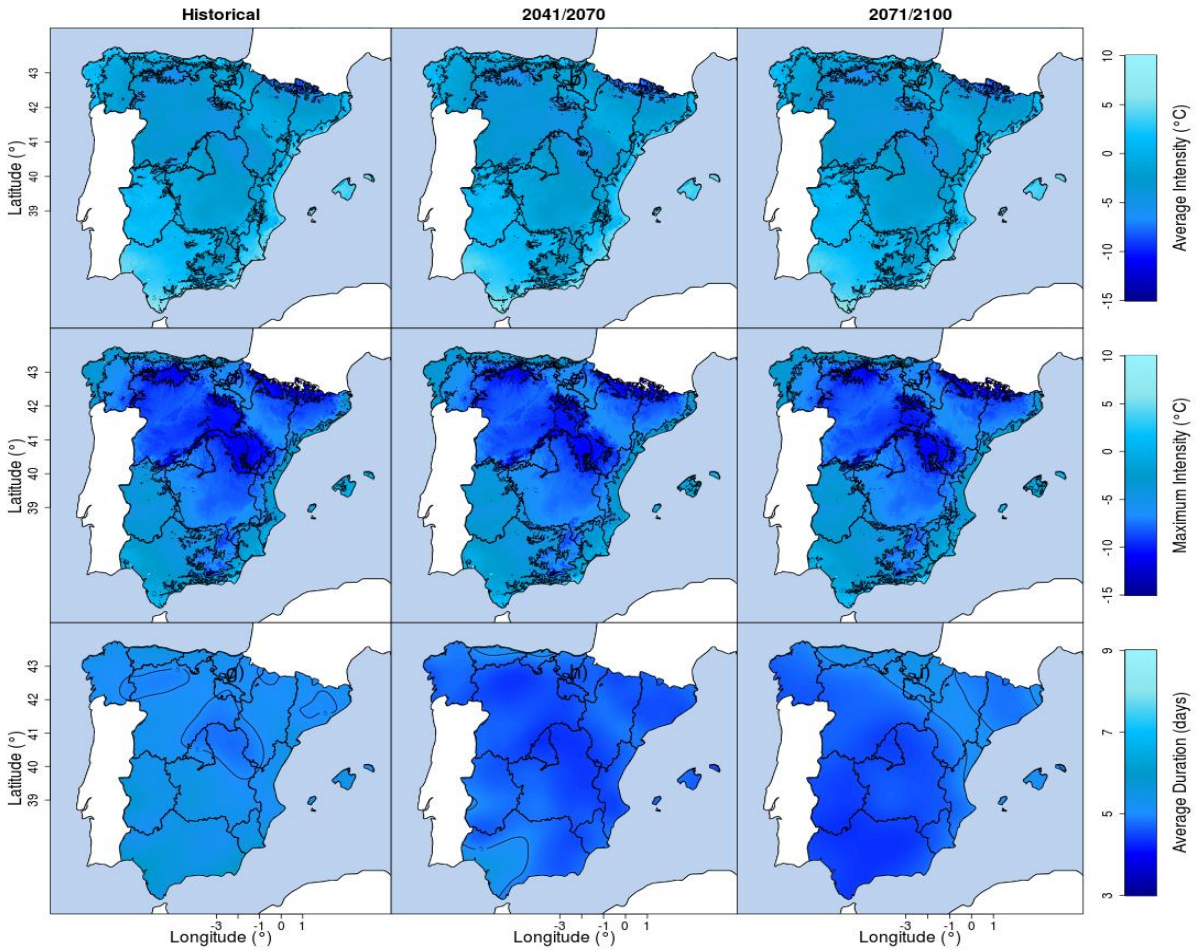

Figure AR1.7. Representación espacial de la evolución esperada de las olas de frío en los periodos 2041-2070 y 2071-2100 comparados con el periodo de referencia (1976-2005) según el escenario RCP4.5. Las filas muestran las características principales (intensidad media, intensidad máxima y duración media) y las columnas los tres periodos temporales (Historical, 2041-2070 and 2071-2100). Los mapas se han generado interpolando todos los observatorios disponibles en el estudio.

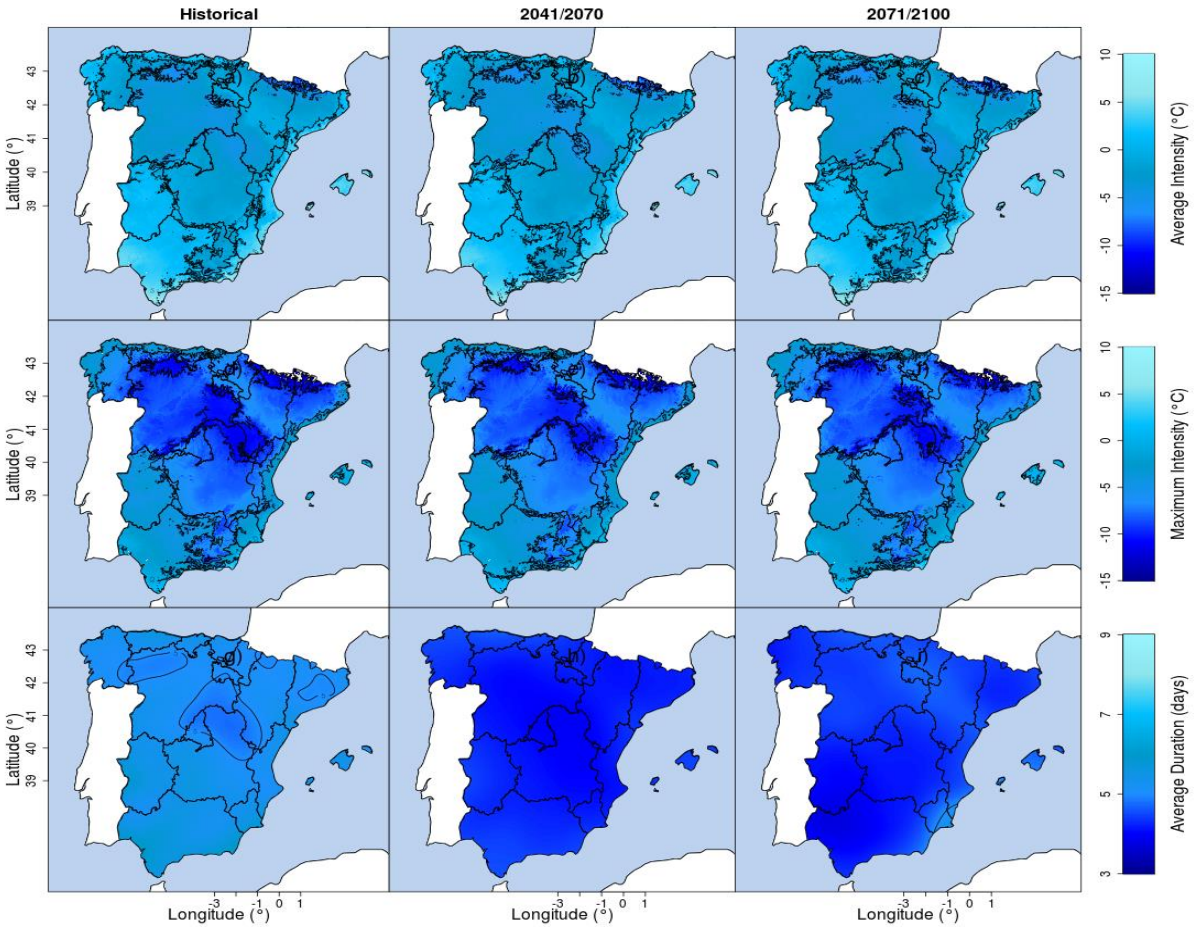

Figure AR1.8. Representación espacial de la evolución esperada de las olas de frío en los periodos 2041-2070 y 2071-2100 comparados con el periodo de referencia (1976-2005) según el escenario RCP8.5. Las filas muestran las características principales (intensidad media, intensidad máxima y duración media) y las columnas los tres periodos temporales (Historical, 2041-2070 and 2071-2100). Los mapas se han generado interpolando todos los observatorios disponibles en el estudio.

Resultado 2
Impacto del cambio climático en la ocurrencia de eventos de sequía de Aragón (NE de España)

Impact of climate change on drought in Aragon (NE Spain)

Abstract

Droughts are one of the extreme climatic phenomena with the greatest and most persistent impact on health, economic activities and ecosystems and are poorly understood due to their complexity. The exacerbation of global warming throughout this century probably will cause an increase in droughts, so accurate studies of future projections at a local level, not done so far, are essential.

Climate change scenarios of drought indexes for the region of Aragon (Spain) based on nine Earth System Models (ESMs) and two Representative Concentration Pathways (RCPs) corresponding to the fifth phase of the Coupled Model Intercomparison Project (CMIP5) have been generated for the first time. Meteorological Drought episodes were analysed from three main aspects: magnitude (index values), duration and spatial extent. The evolution of drought is also represented in a novel way, allowing identification, simultaneously, of the intensity of the episodes as well as their duration in different periods of accumulation and, for the first time, at the observatory level.

Future meteorological drought scenarios based on the Standardized Precipitation Index (SPI) hardly show variations in water balance with respect to normal values. However, the Standardized Precipitation Evapotranspiration Index (SPEI) which, in addition to precipitation, considers evapotranspiration, shows a clear trend towards increasingly intense periods of drought, especially when considering cumulative periods and those at the end of the century.

Representation of the territory of the drought indexes reflects that the most populated areas (Ebro Valley and SW of the region), will suffer the longest and most intense drought episodes. These results are key in the development of specific measures for adapting to climate change.

1. Introduction

Drought is probably one of the extreme climatic phenomena with the greatest impact on the world's population and that can affect millions of people every year around the planet (Bryant, 1991; Wilhite, 2000). It also has serious effects on the availability of water and therefore on economic activities such as agriculture (Lesk et al., 2016) and tourism and profound impacts on human health (Stanke et al., 2013) and ecosystems (Alary et al., 2014) that may persist over time. (Dai, 2011). However, drought is a phenomenon that is not well understood due to its complexity and lack of historical records (Wilhite, 2000) and because it depends on numerous factors.

For this reason, the scientific community and institutions are putting a lot of effort into understanding, identifying, documenting and monitoring this phenomenon more exhaustively. Examples are the drought databases of the European Drought Observatory, the National Drought Mitigation Center and, the historical database of the Standardized Precipitation Evapotranspiration Index (SPEI) (http://spei.csic.es/database.html).

1.1 Droughts types and indexes

Precipitation is the primary controlling factor of drought but other meteorological phenomena, such as temperature (Cook et al., 2014; Hao et al., 2017; Livneh and Hoerling, 2016), wind (McVicar et al., 2012a) and relative humidity (Willett et al., 2014), can modulate its intensity (Bates et al., 2008). Through potential evapotranspiration (PET), it is possible to evaluate the amount of water that would evaporate and transpire if there was enough water available, which is very important in the evaluation of meteorological droughts.

Because drought affects so many different aspects (environmental, economic, social, health), a single 'drought' does not really exist. Drought is often classified into four types (Wilhite, 2000; Wilhite et al., 1985): meteorological, agricultural, hydrological and socioeconomic drought.

The main subject of the current study is meteorological drought, a type of drought characterized by below-normal precipitation over a period of months to years and that should be defined as a condition relative to the normal local condition (Dai, 2011; Paparrizos et al., 2018; Wilhite, 2000).

On the other hand, to characterize droughts, standardized drought indexes are used in the literature. These indexes are direct indicators based on climate information, defined so that the results are comparable in time and space since droughts of the same magnitude can have very different effects depending on the time of year and the place where they occur (Hayes et al., 1999; Vicente-Serrano, 2016; Wilhite, 2000).

Some of these indexes are well established and have been used to monitor climatic conditions across different locations; these include the Palmer Drought Severity Index (PDSI; Palmer, 1965) and Standardized Precipitation Index (SPI; McKee et al., 1993), for example. The Lincoln Declaration on Drought Indexes (Hayes et al., 2011) determined that SPI is the only index, from the point of view of meteorological drought, valid for any region of the world and any time scale, being one of the most used in Europe (Spinoni et al., 2015). It is able to provide better spatial standardization than PDSI (Lloyd-Hughes and Saunders, 2002) and indicate drought initiation and termination because they are implicit parts of the index (Sonmez et al., 2005).

SPI, however, presents some limitations such as that it neglects the effect of temperature increase and, therefore, the effect that an increase in PET (Vicente-Serrano et al., 2010a) or in the atmospheric evaporative demand (AED) (Vicente-Serrano et al, 2020) can have on droughts, which may affect prediction of the impact of global warming in future drought conditions. It should be noted, however, that other meteorological variables as wind speed, solar radiation and air humidity, can also affect PET changes linked to climate change.

To avoid this problem, (Vicente-Serrano et al., 2010a) proposed a new climatic drought index, SPEI, which considers the difference between monthly precipitation and AED. Thus, SPEI best reflects climate change as it makes a more realistic measurement of water availability by incorporating the effect of temperature on changes in evaporation demand as does PDSI. On the other hand, it maintains the multi-temporal nature and simplicity of SPI (Marcos-Garcia et al., 2017).

According to the latest report of the Intergovernmental Panel on Climate Change (IPCC, 2014a), analysis of the precipitation regime (Calbo, 2010; Lavaysse et al., 2012), droughts (Burke and Brown, 2008; Lopez-Bustins et al., 2013) and the extreme temperatures that drastically increase evapotranspiration (ET) (Rebetez et al., 2006) and decrease soil moisture (Sheffield and Wood, 2008) suggest that drought episodes could become more severe around the world in the 21st century (Dai, 2013).

There are some studies that emphasize that future projections of drought may overestimate drought episodes if future soil moisture (Berg et al., 2017) and runoff (Yang et al., 2018) simulations are not taken into account (Berg and Sheffield, 2018), which can affect AED. In addition, recent studies highlight the need to include CO2 concentration in the analysis of AED under climate conditions since an increase of the CO_2 acts contributing to the increase in temperatures that in turn affect the Vapour-Pressure Deficit (VPD). On the other hand, CO_2 could increase water use efficiency by plants reducing AED and therefore mitigate the drying (Dai et al., 2018; Roderick et al., 2015). In this context, most European areas and the Mediterranean region seem to be prominent regional climate change hotspots where an increment in the occurrence of extreme events is expected (Beniston et al., 2007; Skaugen et al., 2004). Specifically, a possible rise in the intensity and frequency of extreme drought events is expected (Forzieri et al., 2014; Hoerling et al., 2012; Iglesias et al., 2007; Marcos-Garcia et al., 2017; Paparrizos et al., 2018), especially in the summer months (Vicente-Serrano et al., 2010c), and will have significant environmental, social and economic impacts (Blenkinsop and Fowler, 2007).

The global climate models used today reproduce temperature trends very well, but the level of precision for large-scale precipitation patterns is lower than for temperature (IPCC, 2014b). This has caused the climatic projections of droughts to show great uncertainty and therefore we cannot know with precision the effects of climatic change on drought severity at the regional level in the future (Burke and Brown, 2008). This is especially problematic in areas with high precipitation variability, such as the Mediterranean region, where the drought patterns derived from the results of global climate models are not consistent (Vicente-Serrano et al., 2004).

1.2 Drought in NE Spain (Aragón)

In Spain, as in the rest of Europe (Feyen and Dankers, 2009), different series of major droughts have been happening in recent decades. In addition, the literature seems to indicate a trend towards an increase in meteorological water scarcity in the Iberian Peninsula, either due to an increase in the frequency of drought episodes or due to a change in the precipitation regime (Fragoso et al., 2018; Gallego et al., 2011; Garcia-Barron et al., 2011; Machado et al., 2011; Ojeda et al., 2017; Vicente-Serrano et al., 2004). This makes necessary studies at a local level and the development of future scenarios of droughts which are adequate as possible for evaluating the local impacts of climate change.

Drought scenarios in Spain are also scarce: either they are from studies conducted prior to the Fifth Assessment Report of the United Nations Intergovernmental Panel on Climate Change (IPCC5) and in very small areas (Lopez-Bustins et al., 2013) or they use IPCC5 models but use dynamic downscaling information from the European Coordinated Regional Downscaling Experiment (EUROCORDEX; (Collados-Lara et al.,

2018; Marcos-Garcia et al., 2017). The latter also evaluates only SPI and SPEI at the 12-month scale. However, these studies agree that the combined use of SPI and SPEI is adequate for studying drought episodes in the future (Lopez-Bustins et al., 2013; Marcos-Garcia et al., 2017).

The combined study of both indexes, SPEI and SPI could be an effective formula for an adequate study of meteorological drought in territories with the climatology of Aragon (NE Iberian Peninsula). This region of Spain is characterized by a continental Mediterranean climate with high precipitation variability and marked by very diverse orography throughout its territory that includes areas of high mountains, valleys and steppes (López et al., 2007). In addition, we must consider that previous studies in Aragon have shown that an increase in temperature is one of the variables that will be most noticeable with climate change throughout this century (Gaitan et al., 2019; Ribalaygua et al., 2013a).

As far as we know, drought scenarios in Aragon have not been obtained to date. As has been seen, it is essential to have local scenarios to determine the impact of climate change on the environmental or socioeconomic reality of each region in order to make decisions on adaptation to climate change.

The goal of this study is to obtain, for the first time, meteorological drought scenarios for Aragon (located in NE of Spain) for the 21st century using a statistical methodology to downscale GCMs from CMIP5.

To achieve this goal, the capacity of the GCMs to simulate the past observed climate was assessed (validation) and using CMIP5, precipitation scenarios for Aragon were generated to simulate future daily precipitation.

Finally, as Aragon is a region sensitive to episodes of drought caused by a varying rate of precipitation and high temperatures, the SPI and SPEI meteorological indexes were calculated and the frequency of occurrence of drought and its spatial distribution were simulated to identify the drought vulnerability of the study area. Drought indexes were also verified.

This study provides, for the first time, scenarios of meteorological drought in the NE of Spain according to CMIP5 models, useful for predicting the impacts of climate change on the availability of water at a local scale and which are necessary for stakeholders to make decisions on adaptation and mitigation of climate change. On the other hand, this region of Spain is a good indicator of many characteristic areas of southern Europe (high mountains, river basins, steppes, etc.).

2. Data and methodology

2.1. Study area

The present study was carried out in the region of Aragon (NE of Spain) (Fig. R2.1). Because of its location, Aragon falls within the Western Mediterranean climate area characterized by scarce precipitation with cool winters and hot, dry summers. Differences in latitude between the most northern and most southern points of Aragon (340 km length and 240 km width) along with the influence of the Cantabrian and Mediterranean Seas and the general atmospheric circulation as well as the orographic complexity of the

region (extreme altitude differences of over 3000 m between the plains (the Ebro River valley) and the mountains (the Pyrenees)), give rise to great subclimate variety, with different thermal and pluviometric regimes that condition the local climate (López et al., 2007).

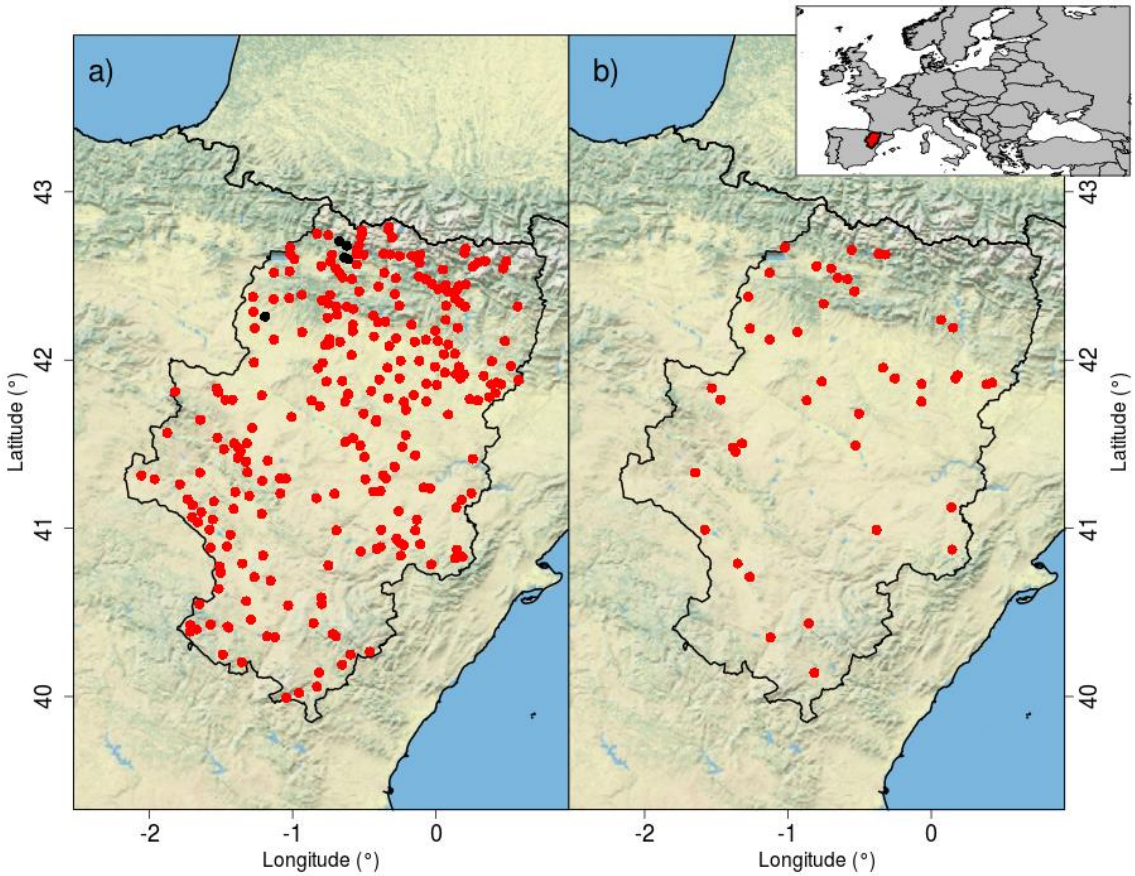

Figure R2.1. Location of the study Area and observatories. Aragon (Spain) in Europe. Points indicate the stations used in the study. a) Stations of precipitation (264) used in the generation of climate regional scenarios of precipitation (verification, validation and scenarios). b) Stations used exclusively on the generation of drought indexes (43). Map source: OpenStreetMap.

Precipitation is scarce in most of Aragon and is distributed clearly according to relief, as the isohyets are arranged in concentric circles decreasing from mountain areas to the centre of the region. Although the average annual total precipitation of the Aragonese territory is around 550 mm, there are regions for which the average is below these values (for example, in the central sector of the Ebro Depression). Only in the Pyrenees and, to a lesser extent, in the Iberian Mountain Range, does precipitation reach important values, 1800–2000 mm, and show positive water balance values (considering the difference between precipitation and AED). On the other hand, more than 60% of the region has average values of AED above 1100 mm, showing a negative water balance, to which contributes not only the scarce rainfall but also the strong wind ("Cierzo") characteristic of the Ebro Valley (López et al., 2007). Therefore, 70% of the Aragonese territory is considered semi-arid (index value proposed by the United Nations Environment Program < 0.5 and even 30% presents values of 0.3) (Cherlet et al., 2018).

2.2. Datasets

2.2.1. Surface observation datasets

In this study, an observational dataset (daily maximum and minimum temperature and precipitation) belonging to the extensive network of instrumental observatories owned by the Spanish Meteorological Agency (AEMET) (http://www.aemet.es) was used (Fig. R2.1). This dataset is the same as the one used in previous studies (Gaitan et al., 2019; Ribalaygua et al., 2013a) in order to work with a set of data that has been subjected to strict quality control (inhomogeneities, gaps, outliers, transcription errors and so on) carried out first by the Government of Aragon (López et al., 2007) and completed, in a second phase, by (Ribalaygua et al., 2013a). As a complement to quality controls, those stations with a large number of data gaps or less than 15 years of daily records were discarded.

For the simulation of future climate scenarios of precipitation, a first set of 263 stations was used (red dots in Fig. R2.1a). Of these 263 stations, just those with data for both variables, temperature and precipitation, were used for the simulation of drought indexes (43 stations, Fig. R2.1b).

2.2.2. Atmospheric dataset

A set of nine climate models were selected from CMIP5, supplied by the Program for Climate Model Diagnosis and Intercomparison (PCMDI) archives.

The global climate models called Earth System Models (ESMs) from the fifth phase of the Coupled Model Intercomparison Project (CMIP5) (Tripathi et al., 2006) have contributed to the acquisition of both dynamic and statistical downscaling techniques with less uncertainty. These models integrate the individual parts of the climate system (atmosphere, ocean, land and sea ice) and the exchange of energy and mass between them (Knutti and Sedlacek, 2013). These models also include chemical processes, land use, plant and ocean ecology and an interactive carbon cycle, which enables integration of biochemical processes into the models (Heavens et al., 2013), constituting a robust set of coordinated climate model experiments (Carvalho et al., 2017; Chen et al., 2016; Perez et al., 2014).

The climate models (Table R2.1) were selected according to the time resolution (daily) of available predictor fields, because it is required for the downscaling method used. All of the models were ESMs (Jones et al., 2011; Wang et al., 2009).

This study used data from two different experiment families of GCMs: the Historical experiment (Taylor et al., 2012), which covers much of the industrial period and can be referred to as ‘twentieth-century’ simulations, and the Representative Concentration Pathway (RCP) family (Moss et al., 2010), which corresponds to different possible ranges of radiative forcing reached in the year 2100 with respect to values of the pre-industrial era. This study used future projections determined by the RCP8.5 ‘high’ scenario and RCP4.5 ‘intermediate’ scenario, the core of IPCC5 experiments.

GFDL-ESM2M	2ºx2,5º daily	National Oceanic and Atmospheric Administration (NOAA), E.E.U.U.	Dunne et al. (2012)
CanESM2	2,8ºx2,8º daily	Canadian Centre for Climate Modeling and Analysis (CC-CMA), Canadá.	Chylek et al. (2011)
CNRM-CM5	1,4ºx1,4º daily	CNRM (Centre National de Recherches Meteorologiques), Meteo-France, Francia.	Voldoire et al. (2013)
BCC-CSM1-1	1,4ºx1,4º daily	Beijing Climate Center (BCC), China Meteorological Administration, China.	Xiao-Ge et al. (2013)
HADGEM2-CC	1,87ºx1,25º daily	Met Office Hadley Center, United Kingdom.	Collins et al. (2008)
MIROC-ESM-CHEM	2,8ºx2,8º daily	Japan Agency for marine-Earth Science and Technology (JAMSTEC), Atmosphere and Ocean Research Institute (AORI), and National Institute for Environmental Studies (NIES), Japan.	Watanabe et al. (2011)
MPI-ESM-MR	1,8ºx1,8º daily	Max-Planck Institute for Meteorology (MPI-M), Germany.	Raddatz et al. (2007); Marsland et al. (2003)
MRI-CGCM3	1,2ºx1,2º daily	Meteorological Research Institute (MRI), Japan.	Yukimoto et al. (2011)
NorESM1-M	2,5ºx1,9º daily	Norwegian Climate Centre (NCC), Norway.	Bentsen et al. (2012); Iversen et al. (2013)

Table R2.1. Information about the nine climate models belonged to the 5 Coupled Model Intercomparison Project (CMIP5) corresponding to the fifth report of the IPCC. Models were supplied by the Program for Climate Model Diagnosis and Intercomparison (PCMDI) archives.

In order to study the behaviour of the CMIP5 model Historical simulations, we used the reanalysis dataset from the European Centre for Medium-Range Weather Forecasts (ECMWF ERA-40; http://www.ecmwf.int/research/era/do/get/) (Uppala et al., 2005) for the period 1958–2000 at 6-hourly time resolution and 125 km spatial resolution. For verification of the methodology, it was necessary to reduce the temporal and spatial scale of the reanalysis in order to compare both ERA-40 and the climate model simulations (Ribalaygua et al., 2013a; Ribalaygua et al., 2013b). The geographical limits of the atmospheric window used were latitudes 31.5°N to 55.1°N and longitudes 27.0°W to 14.6°E, covering not only the geographic area under study but also the surrounding

atmosphere areas which exert a meteorological influence all over the Iberian Peninsula (Ribalaygua et al., 2013a). The use of the ERA-40 data set has allowed us to compare these new results with those published by Ribalaygua et al 2013a.

2.3. Methodologies

2.3.1. Validation and generation of future precipitation scenarios

A two-step analogue/regression statistical downscaling method developed previously (Ribalaygua et al., 2013b) was applied to obtain future scenarios of precipitation and drought. This method has been used in national and international projects, with good verification results (Gaitan et al., 2019; Monjo et al., 2016; Moutahir et al., 2017; Ribalaygua et al., 2018; Rodriguez et al., 2014; Santiago et al., 2017). This methodology offers some advantages: it is computationally inexpensive, provides local information and allows quantifying the uncertainty associated with the downscaling process (Van der Linden and Mitchell, 2009). Other advantages are the application of future simulations consistent with observations (physically coherent between them) and using local scale (because nearby data points in space are not subjected to different climate change conditions) (Ribalaygua et al., 2013b).

Through the validation process we can, on the one hand, evaluate the ability of each ESM to simulate the predictor fields (comparing the downscaled Historical experiment simulation for each model with the downscaled ERA-40 simulation for a common period, 1958–2000) and, on the other, quantify the uncertainties inherent to future climate projections through an ensemble strategy (Monjo et al., 2016).

Bias and standard deviation at seasonal scale have been used as error measures. This validation process presents some limitations related to the observational data available to be considered in the final uncertainty analysis. More information about the validation process can be consulted in (Ribalaygua et al., 2013b).

Future local climate scenarios at local and daily scale for precipitation were produced for nine ESMs (see Table R2.1) and two RCPs (RCP4.5 and RCP8.5) as a previous step to calculate the drought indices. As precipitation is an essential variable in the analysis of drought, these scenarios are a starting point providing initial information on future pluviometric conditions.

The local climatic projections of precipitation belonging to CMIP5 were obtained in this study using the same methodology as that used for temperature scenarios, previously described (Gaitan et al., 2019).

2.3.2. Drought indexes

SPI was developed by McKee et al. (1993) and is based on two assumptions: 1) that the variability of precipitation is greater than that of temperature and AED, and 2) that the rest of the variables are stationary over time. The SPI value is defined as a numerical value that represents the number of standard deviations of precipitation, over the accumulation period in question, with respect to the average, once the original distribution of precipitation has been transformed into a normal distribution (i.e., mean of zero and standard deviation of 1). The SPI values can be interpreted as the number of standard deviations by which the observed anomaly deviates from the long-term mean.

SPEI developed by (Vicente-Serrano et al., 2010a) and revisited by (Begueria et al., 2014) is a variant of the widespread SPI; it has greater potential as a drought index since it considers the climate balance (through the difference between monthly precipitation and AED). SPEI values can be interpreted in the same way as SPI values (number of standard deviations by which the observed anomaly deviates from the long-term mean).

Both indexes were calculated using the R package 'SPEI' (Version 1.7). The SPI was calculated using Gamma distribution to fit the original precipitation series (Organization WMO, 2012) and the SPEI was calculated using log-logistic distribution (Vicente-Serrano et al., 2015; Vicente-Serrano and Beguería, 2016). The parameters of these distributions were obtained by the method of unbiased probabilistic weighted moments (Vicente-Serrano and Beguería, 2016). The scale of SPI and SPEI values used in the study can be seen in Table R2.2.

The period 1976-2005 was used as a reference period, which represents the last 30 years of the Historical period. Based on this reference period, both the SPI and the SPEI were calculated for the period 2006-2100. The choice of the reference period was made to evaluate the future hidroclimatic conditions of the region with respect to the average conditions of the last 30 years of the Historical experiment.

To obtain the AED values used in the calculation of SPEI, both the Hargreaves-Samani (1985) and Thornthwaite (1948), formulas have been used, denominated SPEI-Har and SPEI-Thor, respectively. These formulas were chosen to calculate AED because they are recommended within the SPEI package and they also depend only on temperature and precipitation, unlike other more complex methods such as the Penman–Monteith (Smith M et al., 1998) and Jensen–Haise methods (Jensen and Haise, 1963). Both methods only take into account the temperature, so it is assumed that the calculation of AED trends could have certain limitations (Irmak et al., 2012; McVicar et al., 2012b; Sheffield et al., 2012). For a certain increase in the temperature, the change in the obtained result can be higher than the one really expected according a complete method like Penman-Monteith. Therefore, the role of AED on drought severity would be overestimate and this would have some effect on the drought indices obtained for future scenarios.

The way in which the indexes have been analysed follows the guidelines of the WMO (WMO, 2017) which recommends analysis of a drought episode from three main aspects – magnitude (index values), duration (alternation between positive and negative values) and spatial extent – and all these aspects configure the severity of the episode.

In order to assess the capacity of the downscaling methodology to simulate SPI and SPEI, we analysed the intensity and duration of the different drought episodes shown by both indexes, comparing the SPI and SPEI values calculated from the simulated ERA-40 temperature and precipitation series with those obtained from the observed series for a common period (1970-2000). Verification of the maximum and minimum temperature and precipitation can be seen in a previous study (Ribalaygua et al., 2013a). The statistical measures used in the verification processes were the bias, standard deviation and Pearson correlation. The statistical measures were calculated using R computing software (R Development Core Team, 2010).

From the ESM simulated temperature and precipitation series (nine ESMs and two RCPs), we determined the drought episodes that are expected in Aragon during the upcoming decades of the 21st century. The SPI and SPEI scenarios were compared to a historical period (1976–2005) to analyse the future changes with respect to the actual situation of these extreme events.

To draw future local climate scenario maps, we used Thin Plate Spline (TPS) regression from the R package 'fields' (Nychka et al., 2015).

3. Results

3.1. Validation and precipitation scenarios

The results of the validation process (comparison between the ERA-40 precipitation simulations and the historical precipitation simulations for each ESM for a common period (1958–2000)) are shown in Fig. R2.2, for both absolute (mm) and relative precipitation (%). The results are variable depending on the model and the seasonal period; however, all the models are able to reproduce the annual cycle of precipitation as well as the differences between seasonal periods (maximum values in autumn and spring, followed by winter and summer). The obtained bias and standard deviation are less than ± 1 mm/day, which in relative terms supposes a difference of less than or around ± 10% in the worst of the cases.

In general terms, a big variation in the Aragon precipitation regime is not expected. According to scenario RCP8.5, mean variations in the amount of precipitation are expected to be around ± 10% for all seasons of the year, except for the summer where no precipitation change is expected. Scenario RCP4.5 shows no precipitation fluctuations throughout the 21st century with respect to current values (see support information, Fig. S2.1 to S2.4.

SPEI/SPI	
≥ 2	extremely wet
1.5 a 2	severely wet
0.5 a 1.5	moderately wet
-0.5 a 0.5	normal values
-1.5 ≤ -0.5	moderately dry
-1.5 ≤ -2	severely dry
≤ -2	extremely dry

Table R2.2. SPEI/SPI Intensities Scale (Vicente-Serrano et al 2010a)

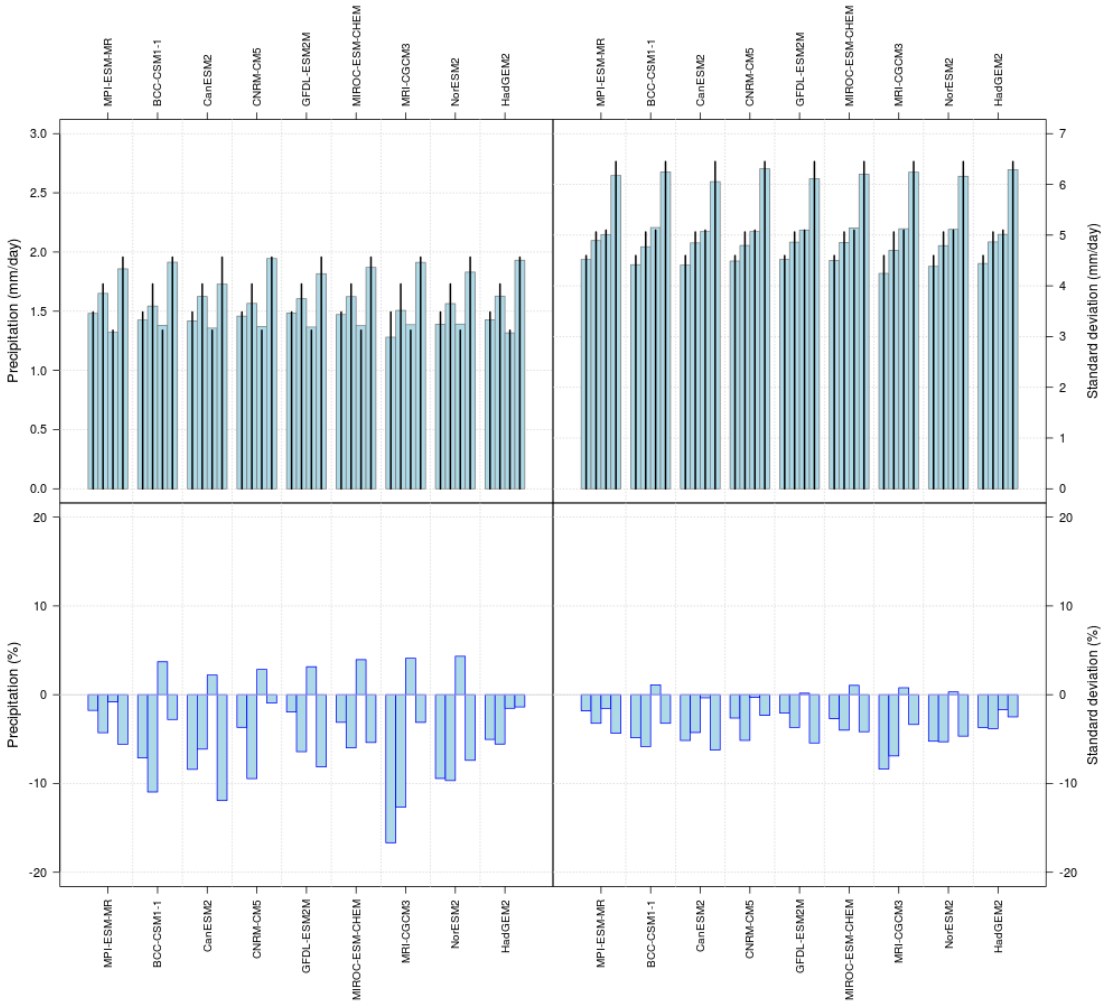

Figure R2.2. Validation of precipitation. Comparison between the precipitations obtained using the downscaled Historical data of the global climate models and the downscaled reanalysis data, for every seasonal period. Two graphs at the top: seasonal comparative between the precipitation simulated using the downscaled Historical data (colour bars) and that of the downscaled reanalysis data (black lines) for each global climate models (see Table R2.1) and for the four seasons: winter (December-February; first bar of each group of four), spring (March–May, second bar), summer (June–August; third bar) and autumn (September–November; four bar). Two graphs at the bottom: relative seasonal differences between the simulated data using the downscaled Historical data and that of the downscaled reanalysis data. Seasonal precipitation amounts are shown on the left columns and seasonal values of the standard deviation on the right

3.2. Generation of future local climate scenarios of drought indexes

3.2.1. Verification of drought index simulation

To verify the simulation of drought indexes, the first step was to compare the SPI and SPEI values obtained from the observations with those calculated from the simulated series of ERA-40.

Fig. R2.3 shows the verification results corresponding to SPI at time scales from 1 month (SPI-1M) to 12 months (SPI-12M) for the period 1970–2000 (Fig. R2.3a and 2.3b). This process allows the identification of episodes of deficit or excess precipitation recorded and simulated from ERA-40. In addition, the number of months in the period 1970–2000 in which SPI values were obtained within different intensity ranges (Table R2.2) for SPI-1M, SPI-3M and SPI-6M are shown (Fig. R2.3c, R2.3d and R2.3e).

As can be seen in Fig. R2.3a and R2.3b, the time series of the simulated SPI for ERA-40 shows, in an acceptable way, the same values presented by the observed SPI, with a correlation of p = 0.75 in the case of SPI-1M, p= 0.72 for SPI- 3M, p = 0.64 for SPI-6M and p = 0.61 for SPI-12M.

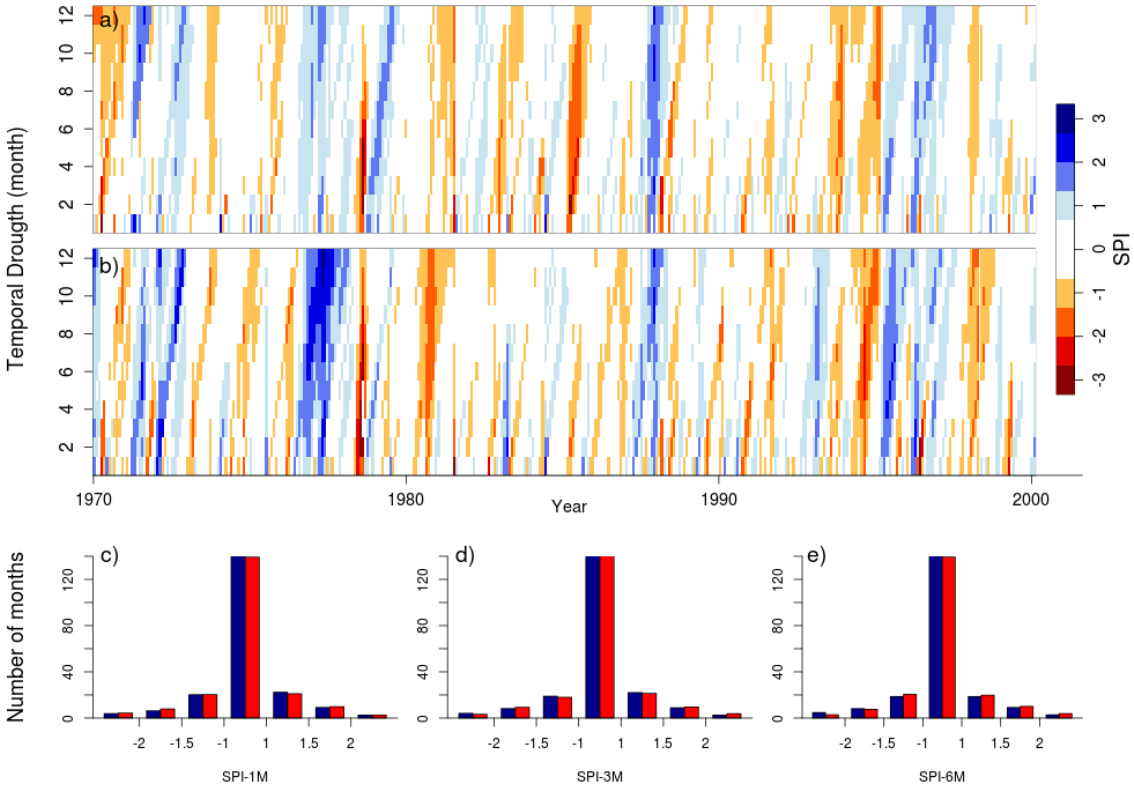

Figure R2.3. SPI verification. Results of the verification process for the SPI. a) time series of the SPI index calculated from observed data at the time-scales from 1 to 12 months for the period 1970-2000, b) time series of the SPI index calculated from downscaled ERA-40 at the time-scales from 1 to 12 months for the period 1970-2000. c), d) and e) number of months within the 1970-2000 period corresponding to each interval of the SPI intensities scale based on observed data (blue columns) and on downscaled ERA-40 (red columns) the time-scales of 1, 3 and 6 months. Average of the all the stations used in the simulations.

The simulated and observed SPI values show dry episodes (negative SPI) in similar periods, for example the periods 1970–1972, 1978, 1981–1982, 1989, 1994–1995 and 1998. The same can be seen for wet episodes (positive SPI) as in, for example, the periods 1976–1977, 1988 and 1996–1997.

Figs. R2.4 and S2.5 show the results of the verification process for SPEI based on SPEI-Har and SPEI-Thor calculations, respectively.

Similar results were obtained for calculation of SPEI based on the Hargreaves method (Fig. R2.4a and R2.4b) although in this case the correlation obtained between the observed and simulated time series of SPEI is slightly higher (0.80 for SPEI-1M, 0.78 for SPEI-3M, 0.72 for SPEI-6M and 0.73 for SPEI-12M).

When the Thornthwaite method is used for calculating AED in SPEI (see Fig. S2.5), the temporal correlations are lower than those obtained with SPEI based on Hargreaves.

On the other hand, for about 65–70% of the period considered, water balance conditions in Aragon was considered normal (SPI/SPEI between −0,5 and 0,5), suffering extreme wet or dry episodes for only 2–4% of the period 1970–2000.

The error (bias) made in the simulation of SPI (Fig. R2.3c to R2.3e) and SPEI (Fig. R2.4c to R2.4e) is quite small for all of the classes considered (< ± 2 months).

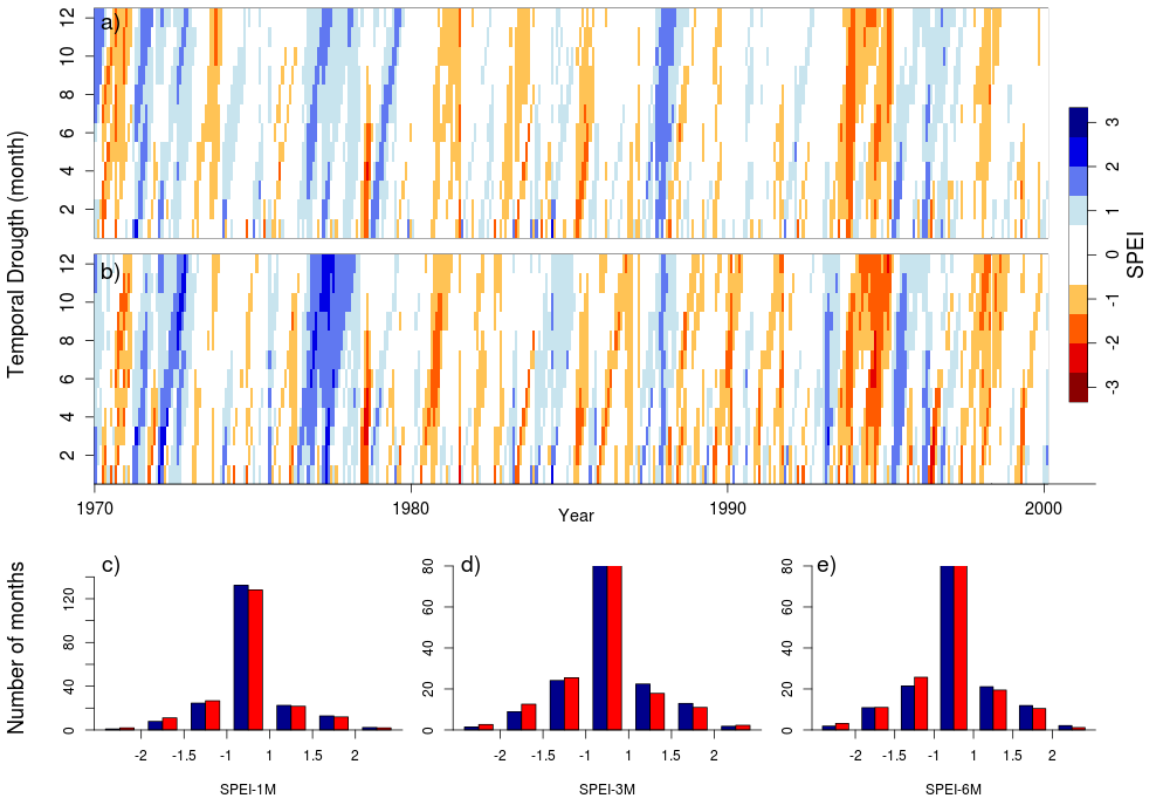

Figure R2.4. SPEI Har verification. Results of the verification process for the SPEI based on Hargreaves Evapotranspiration. a) time series of the SPEI index calculated from observed data at the time-scales from 1 to 12 months for the period 1970-2000, b) time series of the SPEI index calculated from downscaled ERA-40 at the time-scales from 1 to 12 months for the period 1970-2000. c), d) and e) number of months within the 1970-2000 period corresponding to each interval of the SPI intensities scale based on observed data (blue columns) and on downscaled ERA-40 (red columns) for the time-scales of 1, 3 and 6 months. Average of the all the stations used in the simulations.

3.2.2. Local climate scenarios to predict drought indexes

Figs. R2.5 to R2.9 (complemented with Figs. S2.6 and S2.7) show the results obtained for the simulation of SPI and SPEI throughout the 21st century from different perspectives.

Fig. R2.5 shows local climate change scenarios for future SPEI (a, c and d) and SPI (b, d and f) at 3-, 6- and 12-month scale, which have been predicted on the basis of the nine models (see Table R2.2) and here are used to obtain a general vision of the changes in water balance for the Aragon region as a whole. The future projections of SPI and SPEI for the period 2006-2100 have been made based on the reference period (Historical 1976-2005). When working with normalized indexes, the future values of the SPI and SPEI represent anomalies with respect to the average values of the reference period, which allows to evaluate the future evolution of the hydric conditions in Aragon with respect to the average of the last 30 years of the Historical experiment.

The SPI values obtained are hardly modified with respect to the Historical period so, according to these results, the water balance characteristics of the region as a whole would remain similar to the current ones. On the other hand, the SPEI climate change scenarios, considering the effect of AED, show a marked tendency towards increasingly negative values of the index with respect to the Historical period, especially at the end of the century.

Both RCPs show a similar evolution until 2060, with changes of SPEI with respect to the Historical period of −0.6 for SPEI-3M, −0.9 for SPEI-6M and −1.3 for SPEI-12M. For the final period of the century, the variation begins to be more pronounced under the conditions of RCP8.5, with changes of −1.2 for SPEI-3M, −1.8 for SPEI-6M and −2.8 for SPEI-12M, while under scenario RCP4.5, SPEI values vary slightly from those reached in 2060.

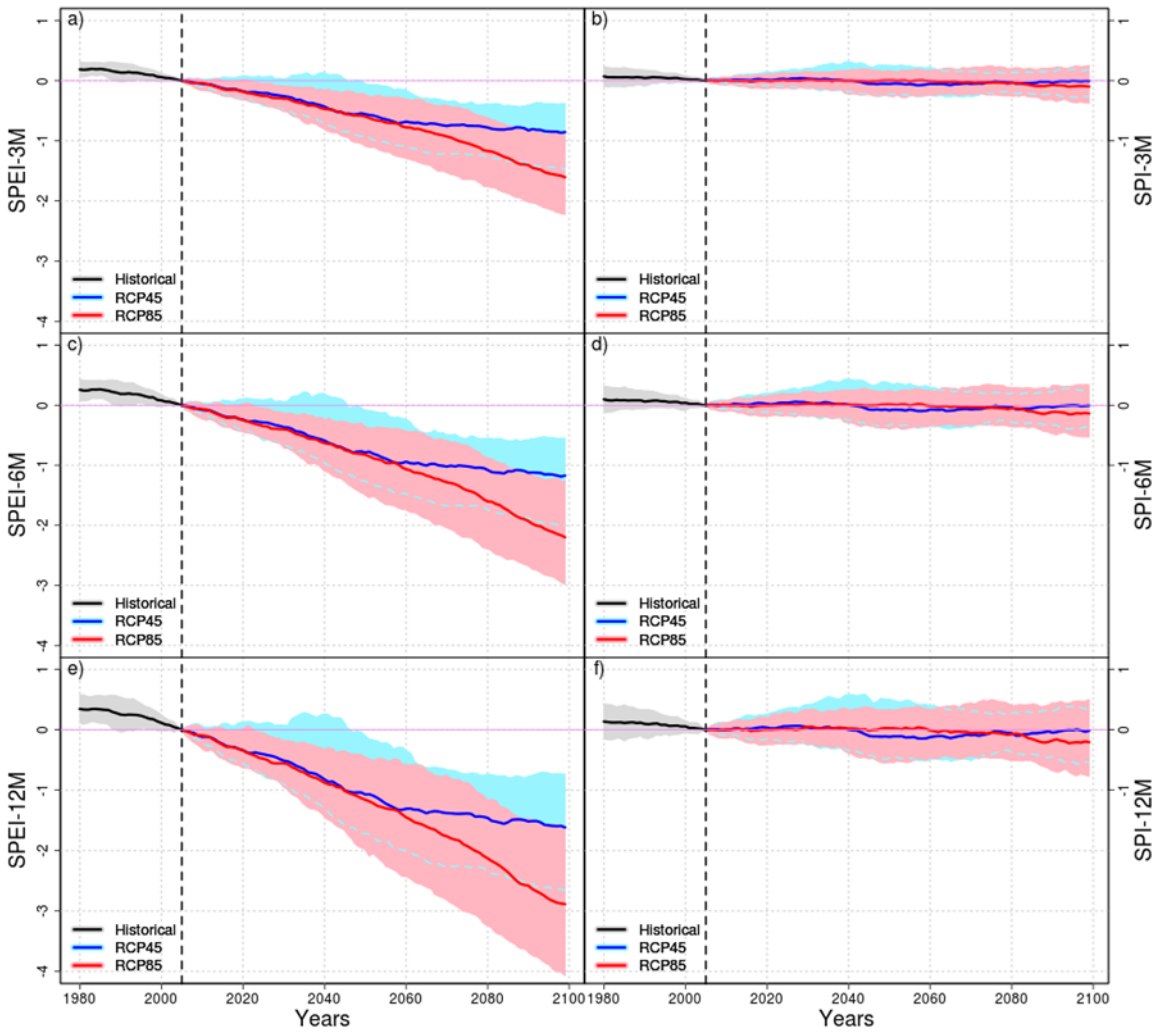

Figure R2.5. Simulated SPEI and SPI for the twenty-first century. Values are displayed as absolute increase compared to the amount simulated for the 1976–2005 Historical period for the time scales 3 months (a and b), 6 months (c and d) and 12 months (e and f). The vertical dotted line marks the end of the Historical data (2005). Data grouped for every RCP simulation of every global climate model selected and for the last 30 years of every station. The ensemble median (solid lines) and the 10th–90th percentile (shaded areas) values are displayed.

These results are very well reflected in the time-scale evolution maps, where the simulated time series from 1976 to 2100 are represented, both for SPEI (Fig. R2.6) and SPI (Fig. R2.7) and under both scenarios, RCP4.5 (Figs. R2.6a and R2.7a) and RCP8.5 (Figs.R2.6b and R2.7b) with respect to different time scales (from 1 to 12 months).

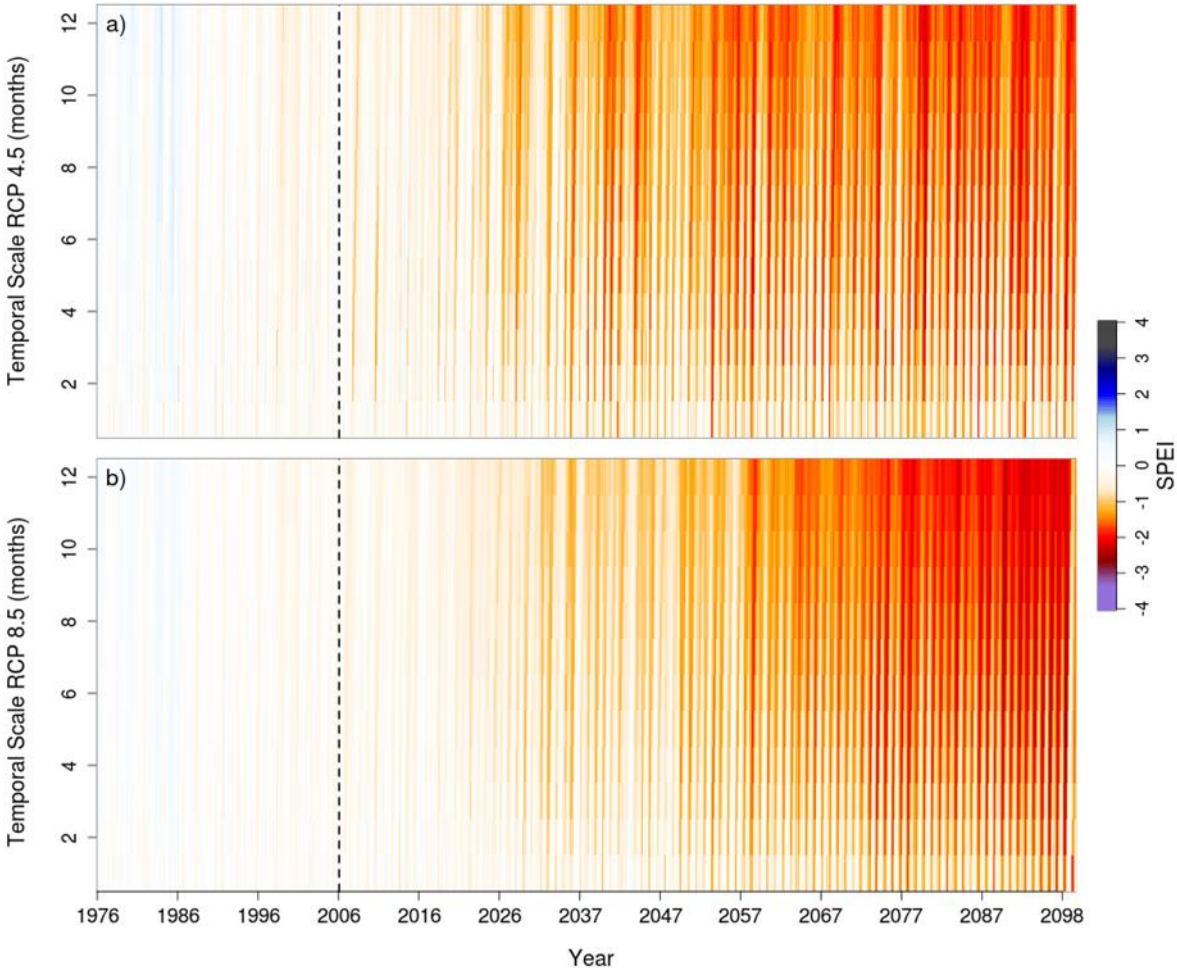

Figure R2.6. SPEI Time series under RCP4.5 and RCP8.5 along the 21st century at time-scales from 1 to 12 months. Data grouped for every RCP simulation of every global climate model and for every station. Both emissions scenarios are represented: RCP4.5 (figure a) and RCP8.5 (figure b)

Fig. R2.6 shows a tendency towards more and more extreme SPEI values, especially in the longer time scales. For time scales of up to 4 months, an alternation between periods considered normal and dry periods is expected (SPEI values between −1,5 and 0,5). For longer time scales, there is a tendency towards more intense and prolonged periods of drought, with SPEI values of up to −3 at the end of the century. The pattern obtained is similar under both RCPs, being more pronounced in the case of RCP8.5.

In the time-scale map corresponding to SPI (Fig. R2.7), the same pattern as that obtained for SPEI is not appreciated; in this case, alternating dry and wet periods are observed for all time scales, these being somewhat more extensive as we move along the time scales. The same pattern is observed under both RCPs, the signal being slightly stronger in the case of RCP8.5.

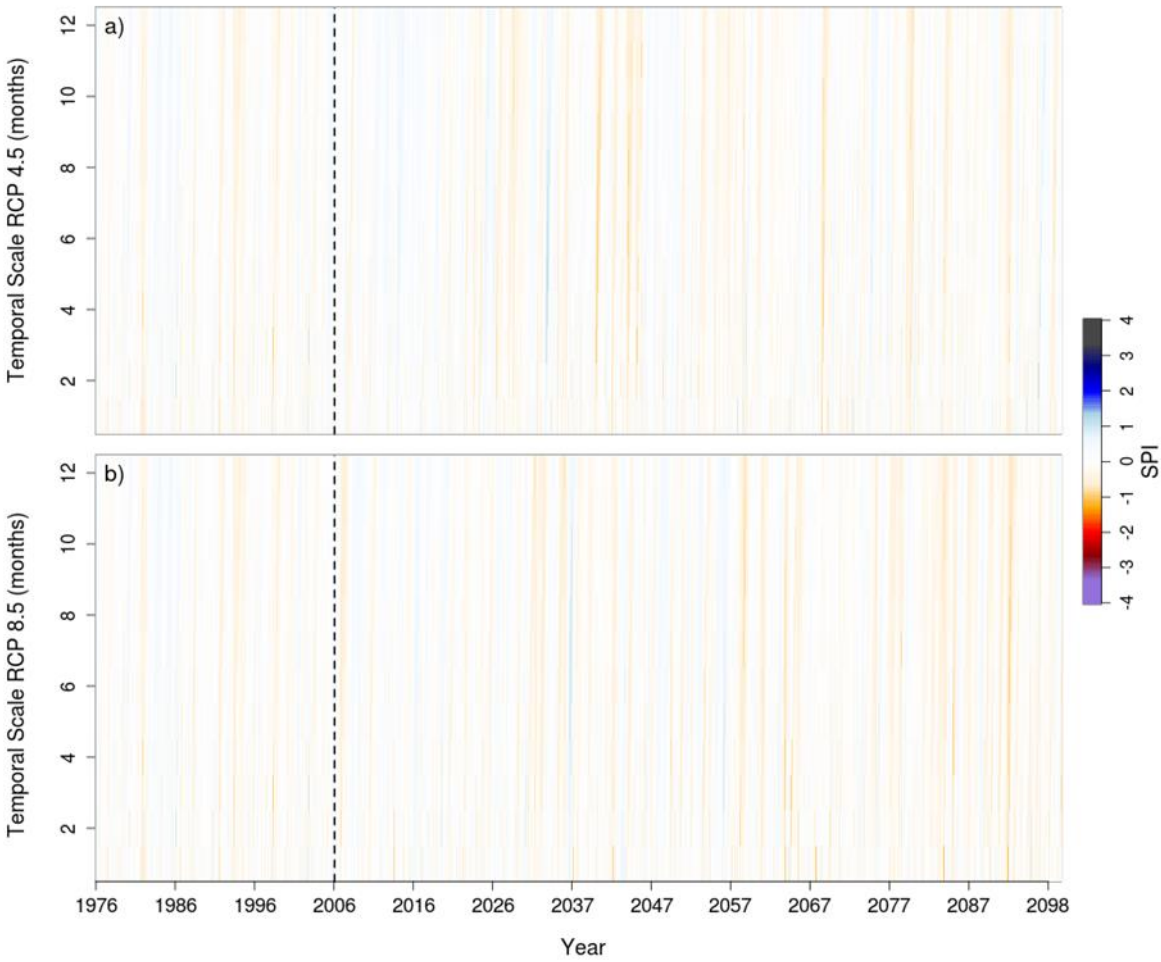

Figure R2.7. SPI Time series under RCP4.5 and RCP8.5 along the 21st century at time-scales from 1 to 12 months. Data grouped for every RCP simulation of every global climate model and for every station. Both emissions scenarios are represented: RCP4.5 (figure a) and RCP8.5 (figure b).

As a complement to the previous results, which allowed the extraction of results for the water regime of Aragon as a whole, the spatial maps of both indexes are shown. Figs. R2.8 and R2.9 show the climate scenarios for mean SPEI according to RCP4.5 and RCP8.5, respectively. These figures show the temporal evolution for four time scales: 1 month (first row), 3 months (second row), 6 months (third row) and 12 months (fourth row). The temporal periods chosen were 2011–2040 (present), 2041–2070 (mid-century) and 2071–2100 (end-century). Figs. S2.6 and S2.7 show the same information but for mean SPI.

The results for SPEI vary considerably between different points in the Aragon region. Coinciding with what was said before, it is observed how the SPEI values become more extreme as the 21st century and time scales advance. The Ebro Valley area is the one that will be subject to more intense episodes of precipitation shortage at the end of the 21st century, with SPEI values from −1 at 3 months to −2 at 12 months according to RCP4.5 and considerably more intense under RCP8.5 with values from −1.8 at 3 months to −4 at 12 months. The north-west area of the region, which is expected to be most affected by drought episodes, deserves special attention. The Pyrenees zone is the one that will clearly suffer the fewest expected drought episodes; under RCP4.5 it is expected

to remain in normal water balance conditions while under RCP8.5, at most, SPEI will reach values of −1.5 (at the end-century and at 12-month time scale).

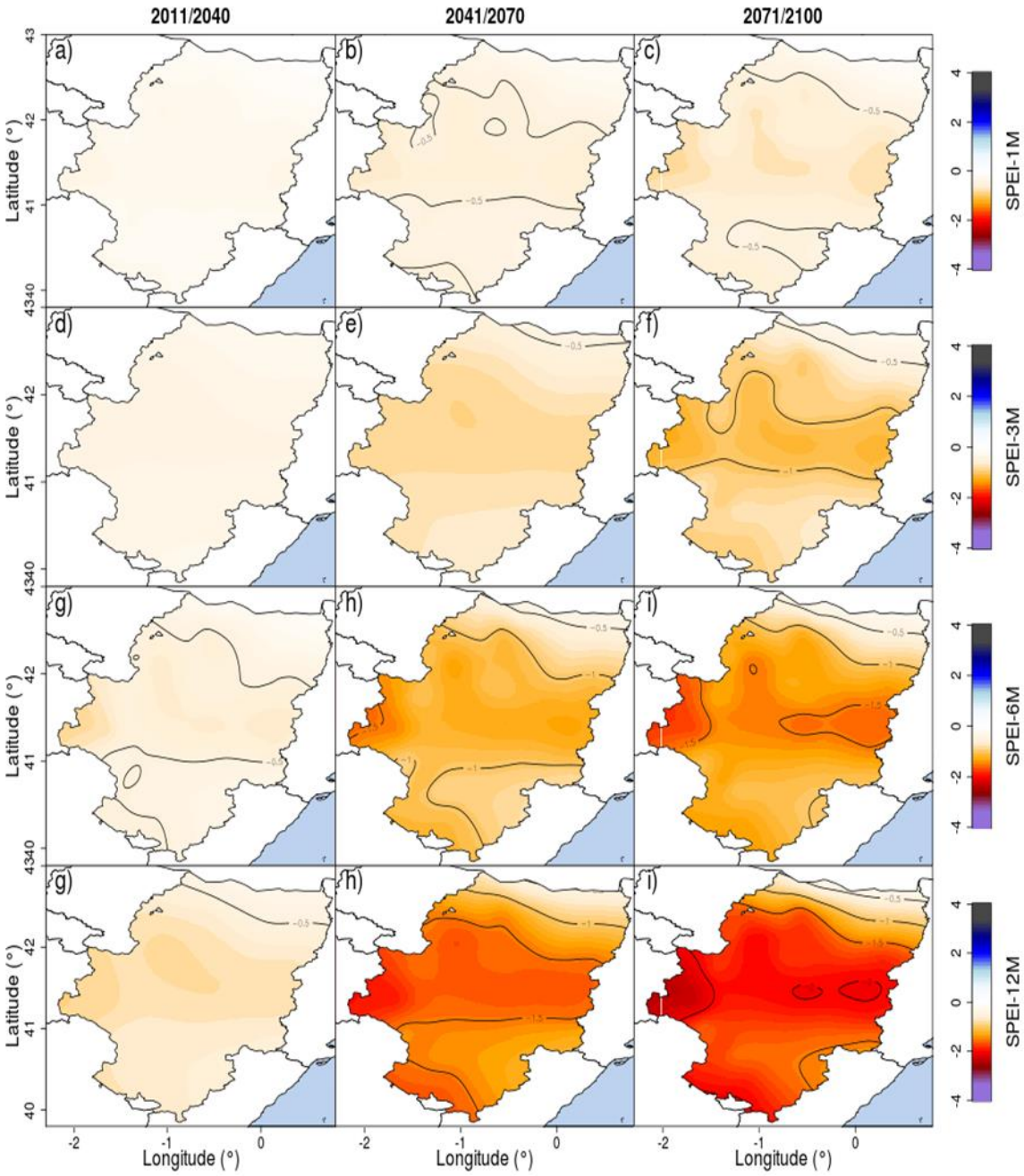

Figure R2.8. Time-scales SPEI maps under RCP4.5. Geographical representation of the expected evolution of the SPEI for Aragon in the periods 2041–2070 and 2071–2100 compared to the reference Historical Period (1971–2000) in terms of absolute values according to the RCP4.5 at different time-scales. The rows show the four time-scales analysed in the study (1 months, 3 months, 6 months and 12 months) and the columns, the three temporal periods (2011-2040, 2041–2070 and 2071–2100). The maps are generated by interpolating the available stations over the territory.

The SPI spatial maps (Figs. S2.6 and S2.7) show how the region will remain under normal water balance conditions, highlighting the Ebro basin at the end of the 21st century and under RCP8.5, where more negative values of SPI (around −1) are appreciated, but which are still within the range considered normal for the region.

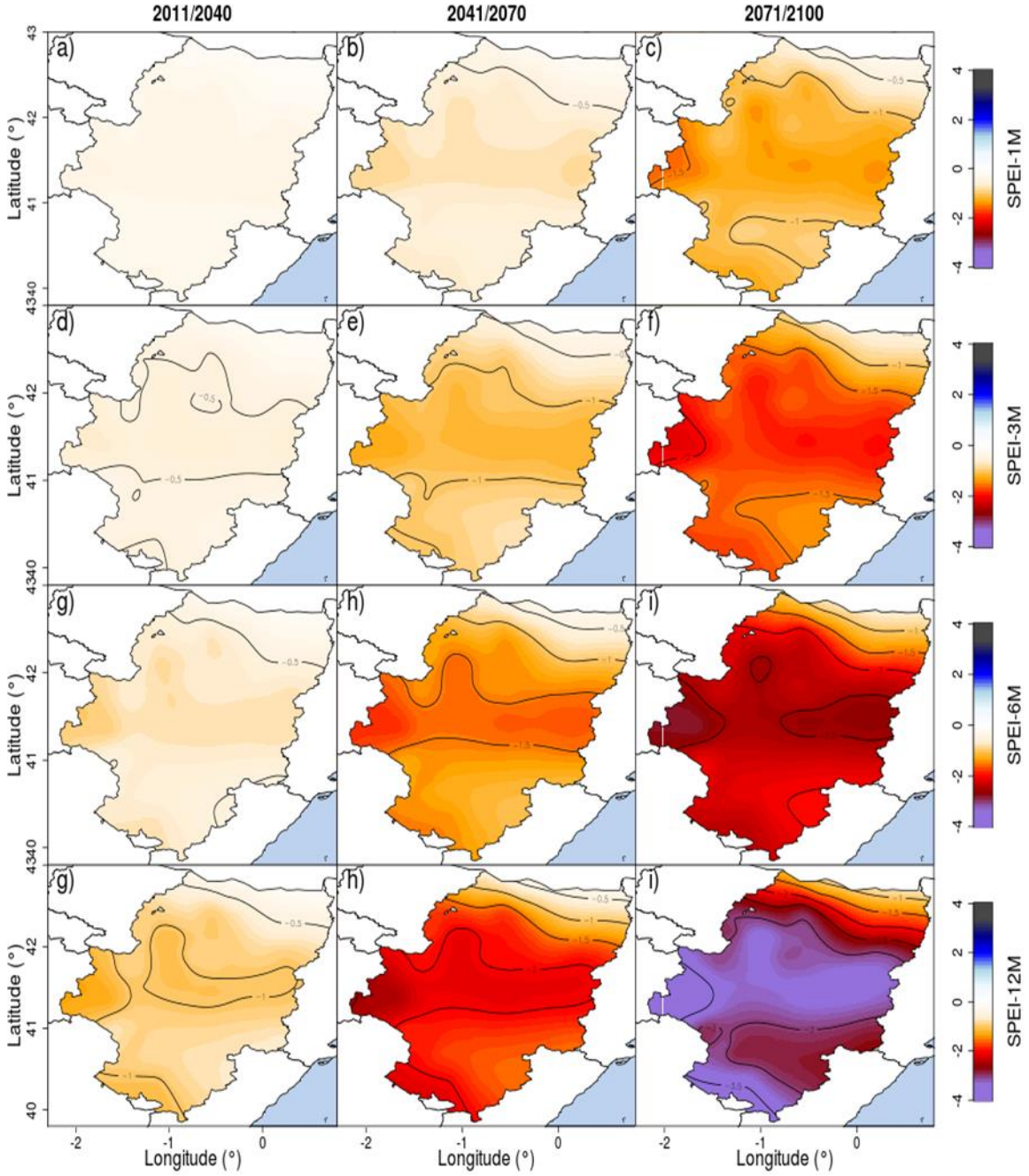

Figure R2.9. Time-scales SPEI maps under RCP8.5. Geographical representation of the expected evolution of the SPEI for Aragon in the periods 2041–2070 and 2071–2100 compared to the reference Historical Period (1971–2000) in terms of absolute values according to the RCP8.5 at different time-scales. The rows show the four time-scales analysed in the study (1 months, 3months, 6 months and 12 months) and the columns the three temporal periods (2011-2040, 2041–2070 and 2071–2100). The maps are generated by interpolating the available stations over the territory.

It is important to emphasize that if the average value of the SPEI/SPI tends to increasingly negative values and if this is a constant trend in the future, the conditions considered normal today will evolve towards new values considered normal (Vicente-Serrano et al. 2020).

This study has been carried out for each of the observatories used in the study and for each of the climatic models, which reveals that the entire region is going to be affected by episodes of drought despite its location and height. As an example, the temporal

evolution of both indexes obtained according to the MPI-ESM-MR climate model and under both RCPs is shown for the observatories of Zaragoza (Figs. R2.10 and R2.11) and Cedrillas-Huesca (Figs. S2.8 and S2.9).

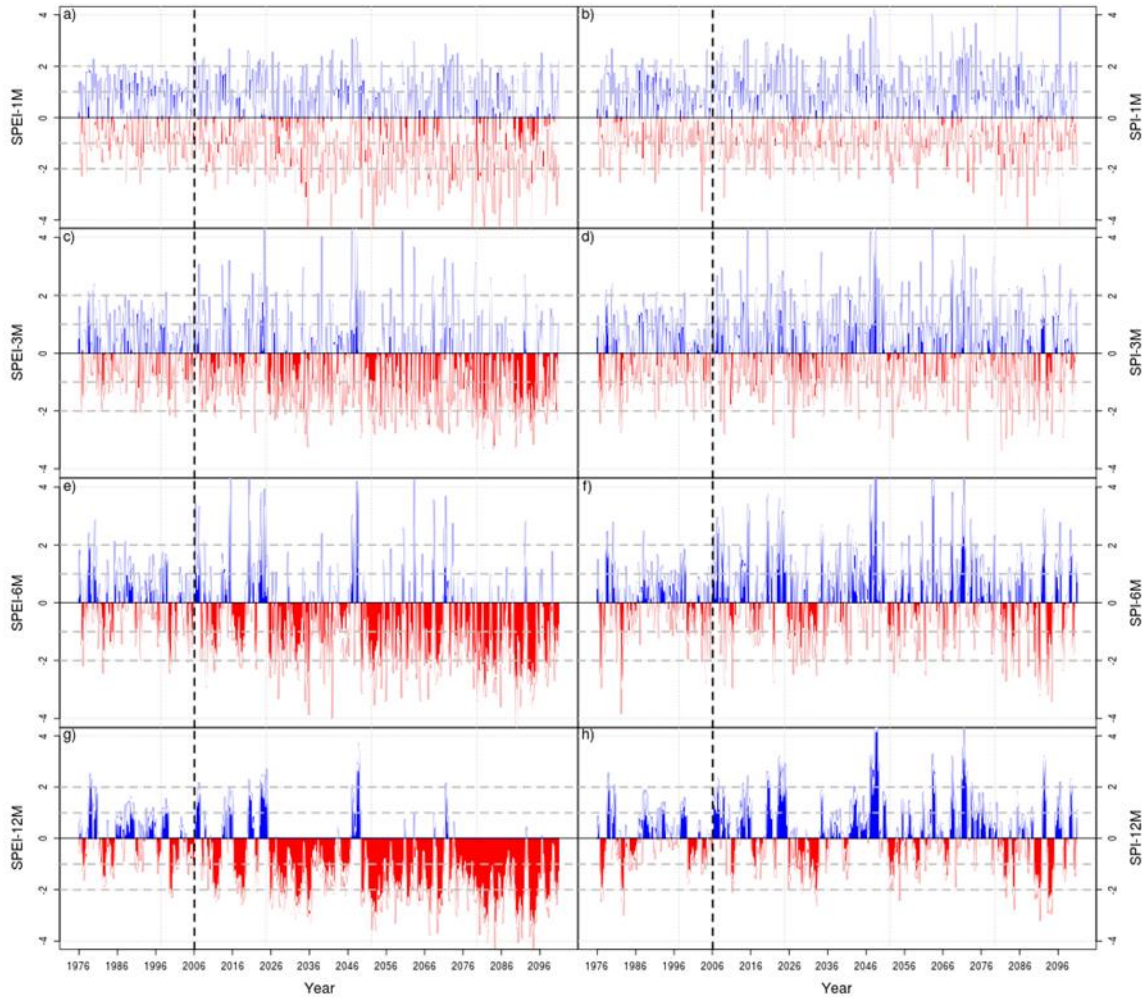

Figure R2.10. Time series for Zaragoza under MPI-ESM-MR RCP4.5. Evolution of the SPEI (first column) and the SPI (second column) based on the MPI-MR-SM model and under the RCP 4.5 at different time-scales - 1 month (first row), 3 months (second row), 6 months (third row) and 12 months (fourth row) - for Zaragoza.

The choice of these observatories was based on the Climate Atlas of Aragon (López et al., 2007), since they are two of the reference points used in the climatic characterization of the region. The choice of these observatories was also made based on their location; the Zaragoza observatory is located in the Zaragoza airport station at a height of 263 m while the Cedrillas-Huesca observatory is located in the northern area of the region at a height of 1347 m. In addition, the Zaragoza airport station is considered representative of the variability of temperatures in Aragon (Roldan et al., 2011).

The expected temporal evolution of SPEI throughout the 21st century is consistent with that explained above, but as it is a single climatic model and uses a single observatory, the alternation between wet and dry periods can be seen more clearly at a time scale of 1 to 3 months. Also, as we move forward in the time scales, this alternation softens, resulting in periods of more intense and prolonged precipitation shortage while, for SPI,

the alternation between wet and dry periods is observed for all time scales. This highlights, as for SPI, how periods with positive SPI for the Cedrillas-Huesca observatory are more intense and prolonged than those predicted for Zaragoza.

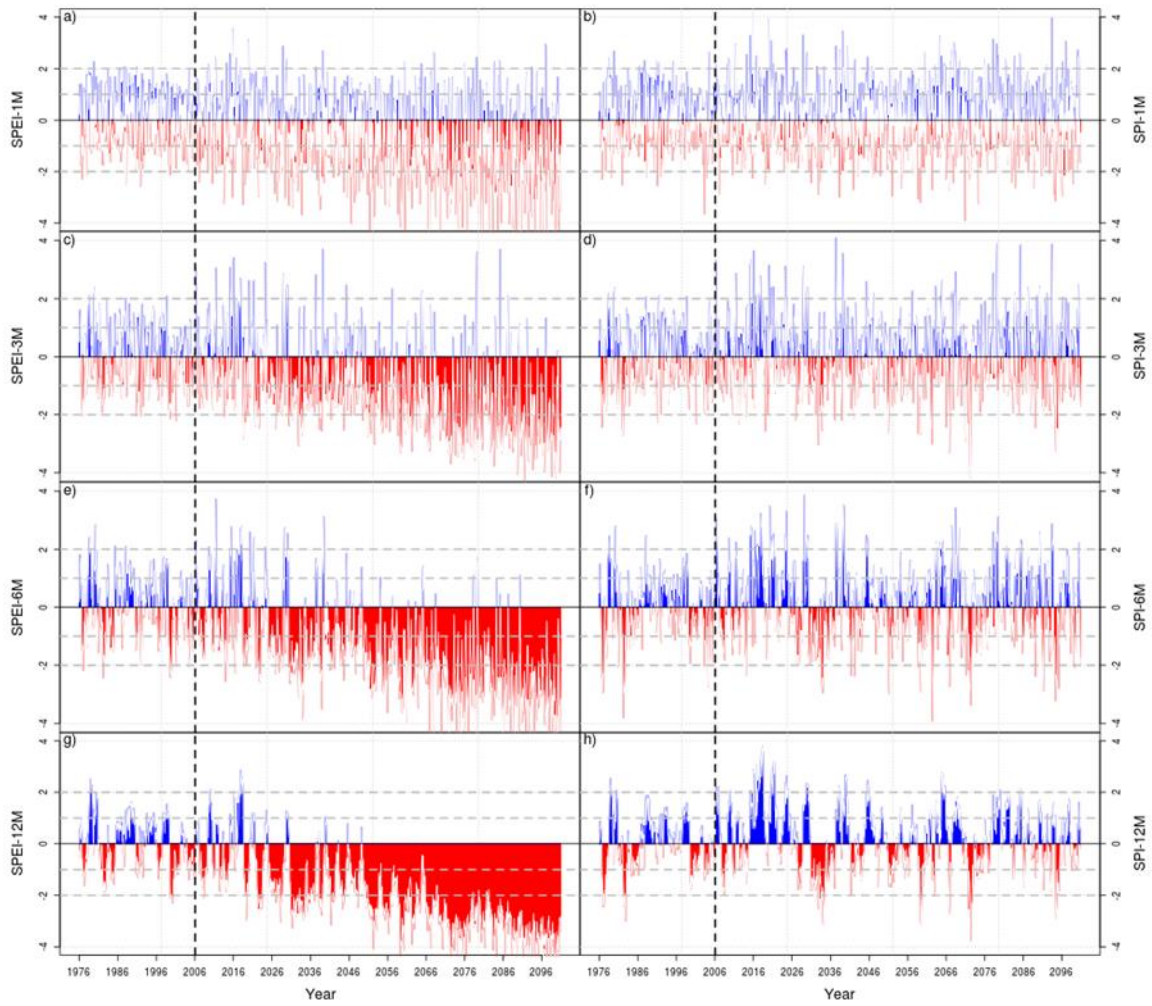

Figure. R2.11. Time series for Zaragoza under MPI-ESM-MR RCP8.5. Evolution of the SPEI (first column) and the SPI (second column) based on the MPI-MR-SM model and under the RCP 8.5 at different time-scales - 1 month (first row), 3 months (second row), 6 months (third row) and 12 months (fourth row) - for Zaragoza.

4. Discussion

These results offer the possibility of having future climate projections based on recently updated data, allowing the evaluation of how drought could affect the region of Aragon, both spatially and temporarily, and can be taken as a reference to analyse its impact on multiple sectors. Temporally, drought increases to the end of the century; at the territory level, the area most affected will be the central area of the Ebro Valley, where most of the population in the area is concentrated.

The difficulty of developing impact studies and quantifying their damage as a result of periods of water scarcity comes mainly from the lack of observed values and studies at a local level with future projections, hence the need to publish studies of these characteristics.

In this study, climate change scenarios of drought indexes for the region of Aragon, Spain, based on nine ESMs corresponding to CMIP5 have been generated for the first time.

The evolution of two indexes, SPI and SPEI, has been obtained throughout this century and also over the territory, which has allowed us to observe that while SPI, which only considers precipitation, shows few changes, SPEI, that considers temperature and incorporates the effects of AED, shows a tendency towards periods of increasingly intense drought, especially when considering accumulated periods of longer duration and those at the end of the century. Therefore, in the current climate change context it is essential to take into account the effect of temperature in the study of droughts.

Figs. R2.6 and R2.7 represent a novel representation of the evolution of drought, allowing identification, simultaneously, of the intensity of the episodes and their duration in different periods of accumulation.

One of the strengths of this study is the use of local climate scenarios (at the observatory level) to generate future drought indexes. Having this information will facilitate decision-making in the face of expected changes based on what is expected to occur at each observatory and not in the region a whole. As an example of the study at local level, the results of future climate scenarios for Zaragoza (representative observatory of Aragon, Roldan et al., 2011) and Cedrillas-Huesca (support information) are shown.

4.1. Precipitation scenarios used for the simulation of drought indexes.

For the simulation of precipitation, ESMs have been used instead of climatic models. ESMs are the most powerful climatic models to date and incorporate significant improvements (Flato et al., 2014) that allow better accuracy in climate simulation, as can be seen in the good results obtained in the validation process.

Validation of the ESMs has shown good results for simulating precipitation. Both the obtained bias and standard deviation are less than ± 1 mm/day, which in relative terms supposes differences of less than or around ± 10% in the worst cases; however, those values are within the order of natural variability of precipitation. These results are better than those obtained for the generation of scenarios of the fourth IPCC report published by (Ribalaygua et al., 2013a) particularly in the summer months, a particularly critical time in Aragon.

The results obtained for the processes of verification of the methodology (Ribalaygua et al., 2013a) and validation of the ESMs are good enough to allow the use of local climatic scenarios generated under these conditions in impact studies and analysis of extreme episodes such as periods of precipitation shortage.

Future precipitation scenarios show, under RCP8.5 conditions, a slight decrease in precipitation throughout the 21st century for all seasons of the year, except for the summer months where there is hardly any variation compared to current values of precipitation in the region. Under RCP4.5 conditions, less pessimistic than the previous one, barely any precipitation changes are expected at any time of the year.

These results are consistent with those published by AEMET (www.aemet.es) and directly by the IPCC (Mukherjee et al., 2018), although the latter show the direct outputs of the ESMs and do not carry the added value of applying downscaling techniques.

4.2. Consideration of the simulation of drought indexes

SPI is considered by experts in this field as one of the few indexes applicable in any region of the world for any time scale (Hayes et al., 2011) and with multiple advantages of application compared to other indexes of widespread use such as PDSI (Dracup et al., 1980; Guttman, 1998; Hayes et al., 2011; Hayes et al., 1999; Vicente-Serrano et al., 2010b). In the context of climate change with significant temperature variations (Gaitan et al., 2019), SPEI has been chosen; its formulation is similar to that of SPI and allows the comparison of both indexes and evaluation of the future behaviour of drought episodes considering the effects of future temperature changes. Both indexes have been verified and used previously in Aragon (Vicente-Serrano et al., 2010a). We have only used the temperature in the calculation of AED because the absence of observed historical data of variables such as radiation or humidity does not allow us a correct validation process of certain indices such as Penman that include these variables.

4.2.1. Verification results

In general, the results of the verification process show good correlations between the observed and simulated time series for both indexes for the period 1970–2000, higher ones being obtained for SPEI. This is consistent with the results published by Vicente-Serrano et al. (2012); they obtained higher correlations for the calculation of SPEI than SPI, especially for the summer months, which are the most critical in the region of Aragon.

The temporal series based on observations are satisfactorily represented by the temporal series based on simulations, recreating almost all dry and wet episodes of importance. It is observed how both the simulated SPI and SPEI tend, for the majority of times, to present dry and humid periods of greater intensity than those observed, especially for longer time scales, as occurred in 1976–1977 for positive values of the indexes and in 1981–1982 for negative ones. In general, the number of months of the period 1970–2000 located within each of the classes defined for SPI/SPEI has been simulated very satisfactorily.

The dry and wet periods detected in this study coincide with or are approximate to those published previously (Vicente-Serrano and Lopez-Moreno, 2005) based on SPI (dry episodes: 1986–1987, 1989 and 1994–1997; wet episodes: 1976–1980), in the Climate Atlas of Aragon (López et al.,2007) based on the precipitation regime (dry episodes: 1970, 1985, 1993 and 1995), by Spinoni (Spinoni et al., 2015) based on a combined 12-month index (dry episodes: 1979–1980 and 1995–1998) and by Tselepidaki (Tselepidaki et al., 1992) from a European study (dry episode: 1989), among others. In some cases, the years are not exactly the same because of the use of different drought and temporal scale indexes.

4.2.2. Future scenarios

The uncertainties associated with both processes, verification and validation, should be considered when interpreting future scenarios. For drought projections the focus should be on changes in the frequency and magnitude of cases located at the lower tail of the distribution as was recommended by Vicente-Serrano et al. (2019).

Future meteorological drought scenarios based on SPI barely show water balance variations with respect to normal values, regardless of the time scale considered and the region of Aragon, except for the Ebro Valley where there is a slight sign of drought at the end of the 21st century and under the conditions of RCP8.5.

These results were expected due to precipitation scenarios barely showing changes throughout the 21st century.

When considering other climatic variables, such as temperature, the drought scenarios based on SPEI show a clear trend towards increasingly dry periods and longer droughts, especially in the Ebro area and south-west of the region. According to the trends shown by the temperature and precipitation scenarios obtained for Aragon, the results obtained were expected. The fact that the results obtained at the 12-month scale are more intense than those of 1-3 months is partly a result of the way in which drought indices are formulated and the autoregressive component of its metric so that when the timescale increases, changes in the frequency of drought conditions increase more in comparison to changes in the mean state. Although, recently, Vicente-Serrano et al (2019) showed that these changes are independent of the metric with which these indices have been calculated, changes in the frequency of drought conditions increase more in comparison to changes in the mean state.

The lack of consideration of variables such as temperature, wind or humidity in the calculation of SPI means that this index presents certain limitations under global warming conditions(Mishra and Singh, 2010; Mishra and Singh, 2011; Vicente-Serrano et al., 2010a) and it is for this reason that, when considering AED in the calculation of SPEI, such different results are obtained, especially at the end of the century and not only under the conditions of RCP8.5, that some authors consider less realistic (Hausfather and Peters, 2020), but also of RCP4.5.

Some studies recommend the use of PET and add value against global warming (Hu and Willson, 2000; Vicente-Serrano et al., 2010a), Tsakiris and Vangelis, 2005). Recent studies (Vicente-Serrano et al. 2019; Vicente-Serrano et al., 2020) suggest using AED in the future study of droughts, as well as analyzing the impact caused by the increase in CO_2 (Yang et al., 2019). Probably, considering the response that vegetation could have to an increase in CO_2 and, therefore, in the evapotranspiration process, could provide some variation in the future evolution of drought episodes that should be explored in future studies.

The results of future drought scenarios presented here show results in line with those obtained in other studies where it is concluded that the Mediterranean regions will experience an increase in the severity and frequency of droughts (Stagge et al., 2015) as a result of a slight decrease in precipitation and an abrupt increase in temperatures (European Environment Agency, 2010; (Stagge et al., 2015) and which represent an increase in water scarcity (Estrela et al., 2012). More specifically in the region of Aragon, the ECCE project, based on dynamic downscaling and scenarios of the fourth IPCC report (Ministerio de Medio Ambiente, 2011), showed a future decline of the Ebro runoff, and Cook (Cook et al., 2014), based on scenarios of the fifth IPCC report but without downscaling, obtained an increase in drought episodes based on SPEI.

4.2.3. Impact on the territory

Although there have been studies on the Aragon area, none present as complete a picture as this study, combining drought evaluation with SPI and SPEI (that is, considering the effect of global warming) based on scenarios of the fifth IPCC report and providing the added value of working at the local scale by applying a downscaling technique.

The scenarios obtained in this study indicate that the Ebro Valley, the most populated area in the region that includes the largest city, Zaragoza with more than 650.000 people, will be most susceptible to future periods of extreme drought and will suffer periods of drought of greater intensity and duration, especially at the end of this century, which will have consequences in sectors such as health, water management, economy and society in general (Lee et al., 2017).

It is remarkable that, in previous publications (Ribalaygua et al., 2013a), we detected that the highest values of maximum temperature, especially at the end of the century and in summer (around 40 °C) as well as the greatest intensity of heat waves will also take place in this area, so it will be especially vulnerable and these data should be considered in the development of specific measures for adapting to climate change.

Adaptation to climate change in each region requires studies applied to the climatic dynamics of each territory, so downscaling quality studies are essential for this. However, these results at the local level are also useful for the whole of the southern Iberian Peninsula and central Europe, since Aragon brings together geographical and climatic features representative also of these other areas.

5. Conclusions

The generation for the first time of climate change scenarios of drought indexes for the region of Aragon (Spain) based on nine ESMs and two RCPs from CMIP5 has allowed us to obtain simultaneously the most accurate representation to date of the magnitude, duration and intensity of meteorological drought episodes and their duration in different periods of accumulation in this area of Spain. The use of different drought indices and drought time-scales and its graphic representation is a relevant novelty in the scientific literature.

This has allowed the detection of a clear trend towards increasingly intense periods of drought, especially at the end of the century when cumulative periods of longer duration are considered. This trend is detected only in the future drought scenarios based on SPEI (which in addition to precipitation, considers AED), while in the SPI-based scenarios it is softened. These results reinforce the need to study these extreme phenomena in a context of climate change, considering the temperature.

At the territory level, spatial representation allowed us to discover that the area that will be most affected by longer and more intense periods of drought, but also the greatest decrease in precipitation (around 10%), is the Ebro Valley, the area that concentrates most of the population as well as the main economic activities of the zone. The results have also allowed, for the first time, the study of future drought indexes at the observatory level, specifically for the most populous city, Zaragoza.

To cope effectively with the impacts of these extreme events that are expected in the present century, it is essential to be able to generate local scenarios that accurately describe climate change at the territory level. On the one hand, our results not only confirm a trend already described in the Mediterranean area of an increase in the severity and frequency of droughts but can also serve as a model and sentinel for similar areas, since it has very varied climatic and orographic conditions.

Material suplementario Resultado 2

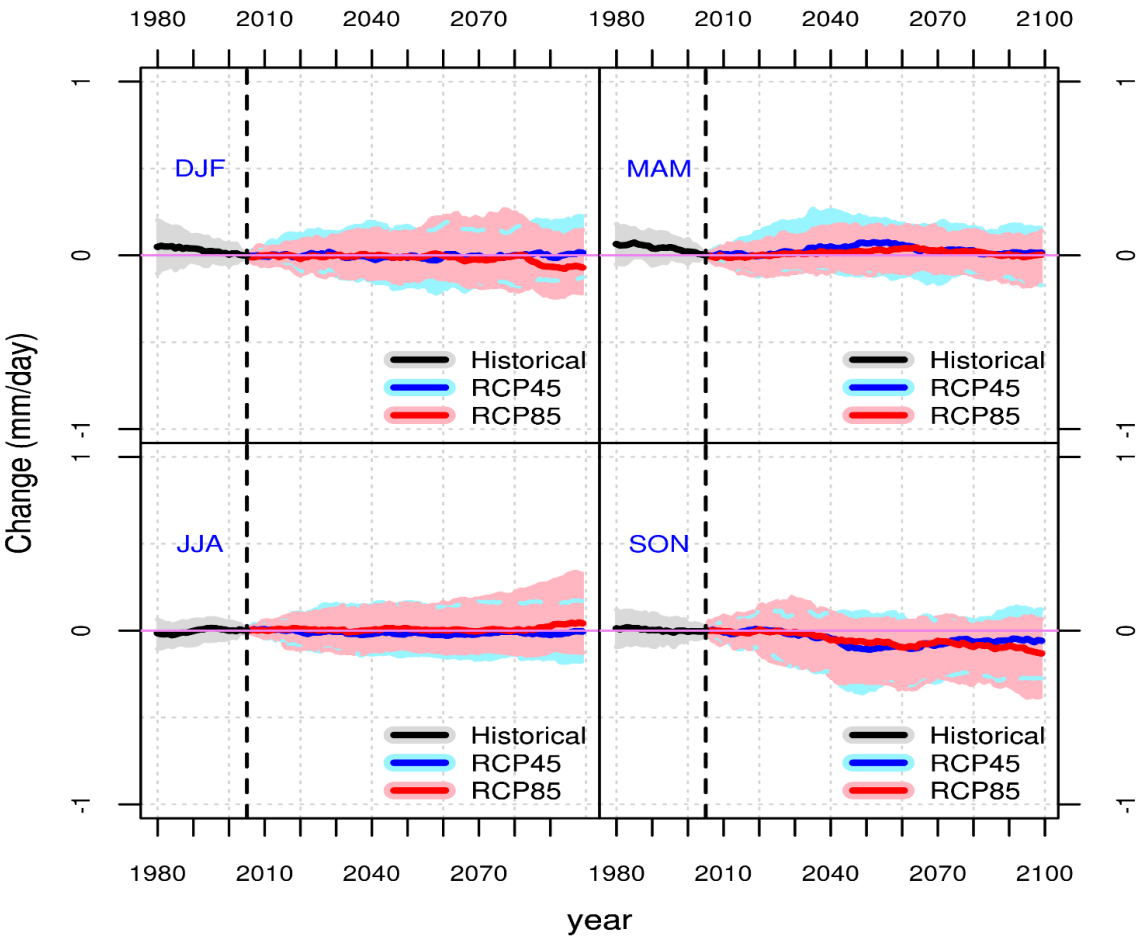

Figure S1.1. Absolute seasonal precipitation in Aragón (mm/day). Simulated precipitation for the twenty-first century displayed as absolute increase compared to the amount simulated for the 1976–2005 Historical period, for the four seasons (winter DJF, spring MAM, summer JJA and autumn SON) The vertical dotted line marks the end of the Historical data (2005). Data grouped for every RCP simulation of every global climate model selected and for the last 30years of every station. The ensemble median (solid lines) and the 10th–90th percentile (shaded areas) values are displayed

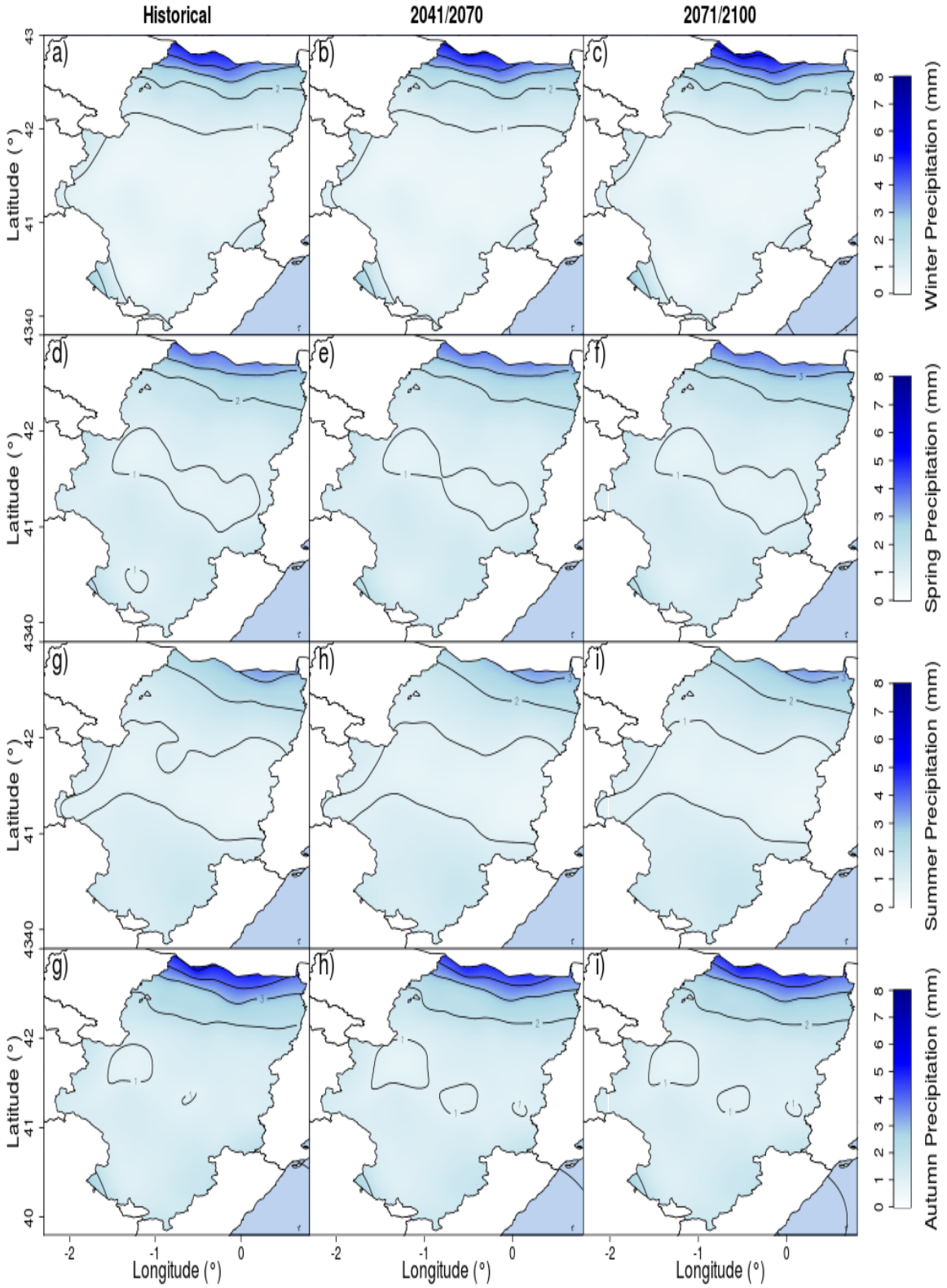

Figure S1.2. Seasonal precipitation maps under RCP4.5 Geographical representation of the expected changes of absolute precipitation in winter, spring, summer and autumn for the periods 2041-2070 and 2071-2100 respect to the reference Historical Period (1976-2005) regarding to the scenario RCP4.5 (ESMs Ensemble mean).

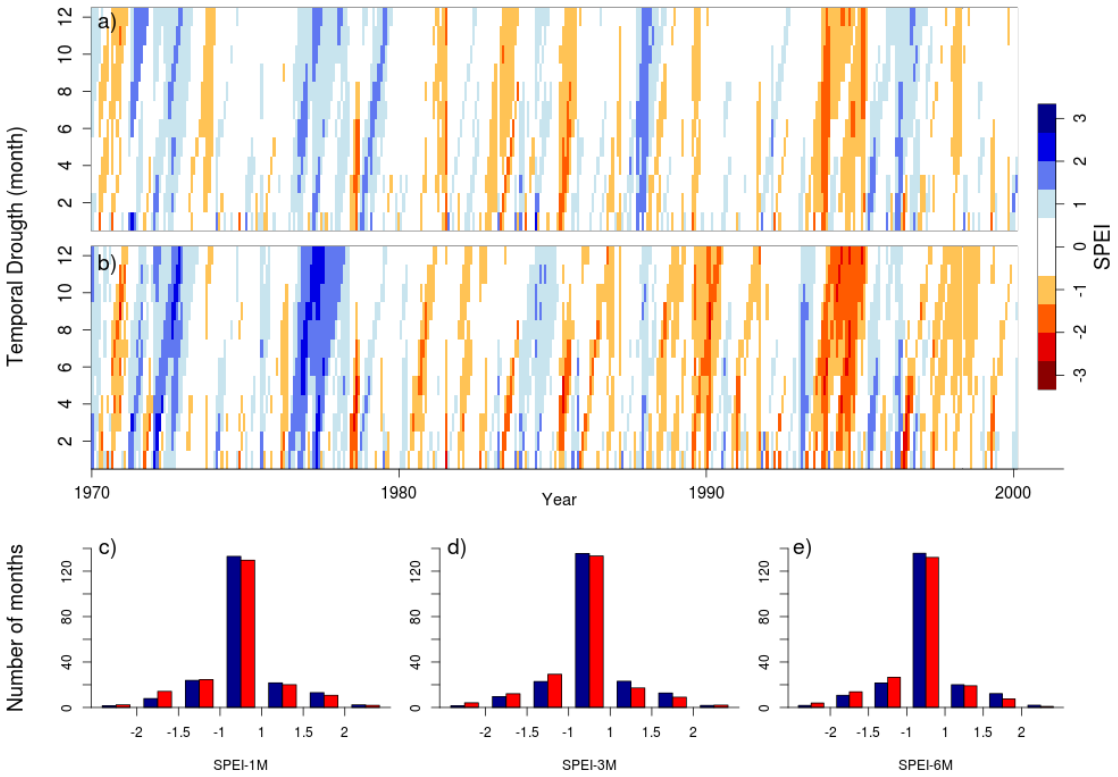

Figure S1.3. SPEI Thor Verification Results of the verification process for the SPEI based on Thornthwaite Evapotranspiration. a) time series of the SPEI index calculated from observed data at the time-scales from 1 to 12 months for the period 1970-2000, b) time series of the SPEI index calculated from downscaled ERA-40 at the time-scales from 1 to 12 months for the period 1970-2000 .c), d) and e) number of months within the 1970-2000 period corresponding to each interval of the SPI intensities scale based on observed data (blue columns) and on downscaled ERA-40 (red columns) for the time-scales of 1, 3 and 6 months. Average of the all the stations used in the simulations.

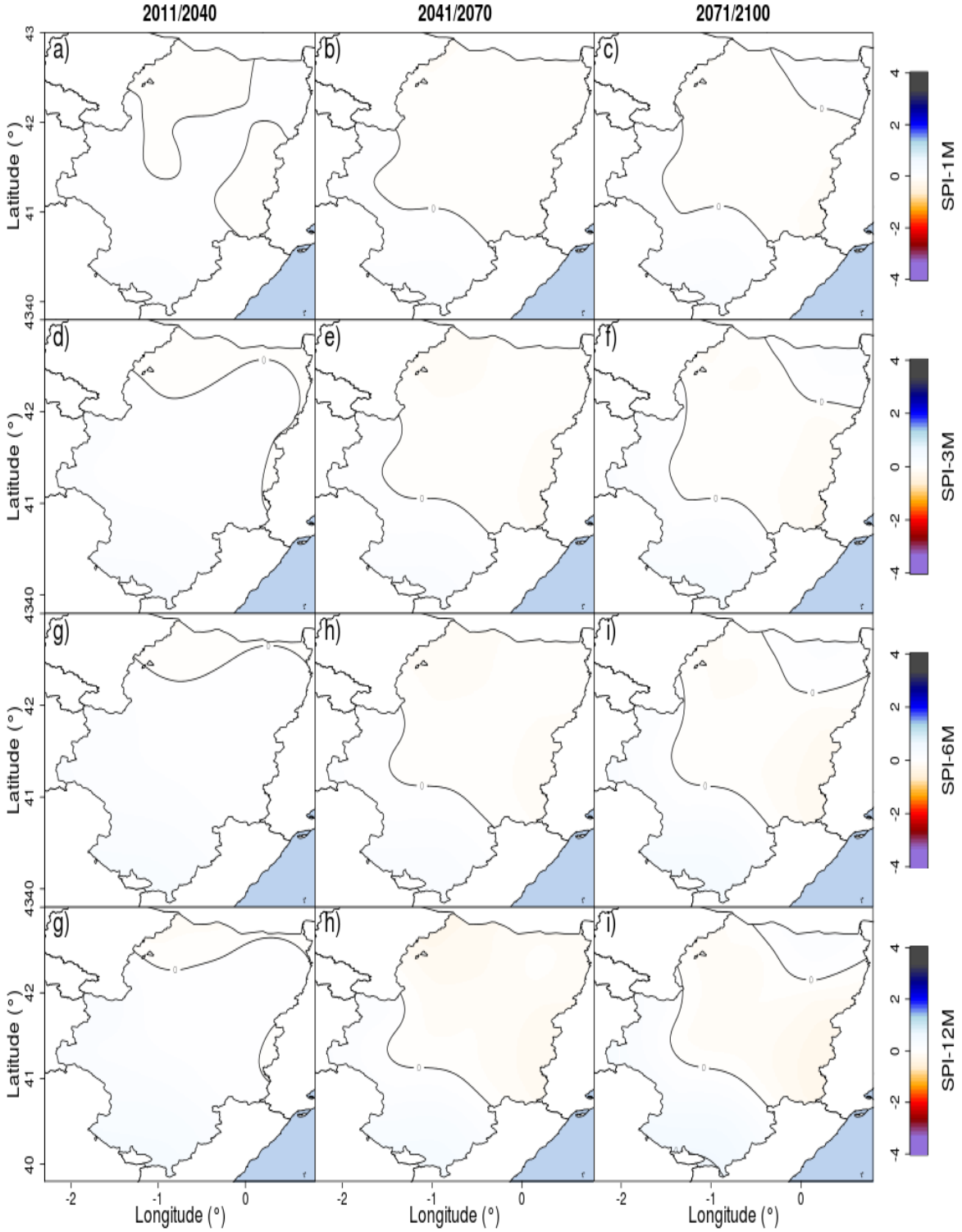

Figure S1.4. Time-scales SPI maps under RCP4.5. Geographical representation of the expected evolution of the SPI for Aragon in the periods 2041–2070 and 2071–2100 compared to the reference Historical Period (1971–2000) in terms of absolute values according to the RCP4.5 at different time-scales. The rows show the four time-scales analysed in the study (1 months, 3months, 6 months and 12 months) and the columns the three temporal periods (2011-2040, 2041–2070 and 2071–2100). The maps are generated by interpolating the available stations over the entire territory.

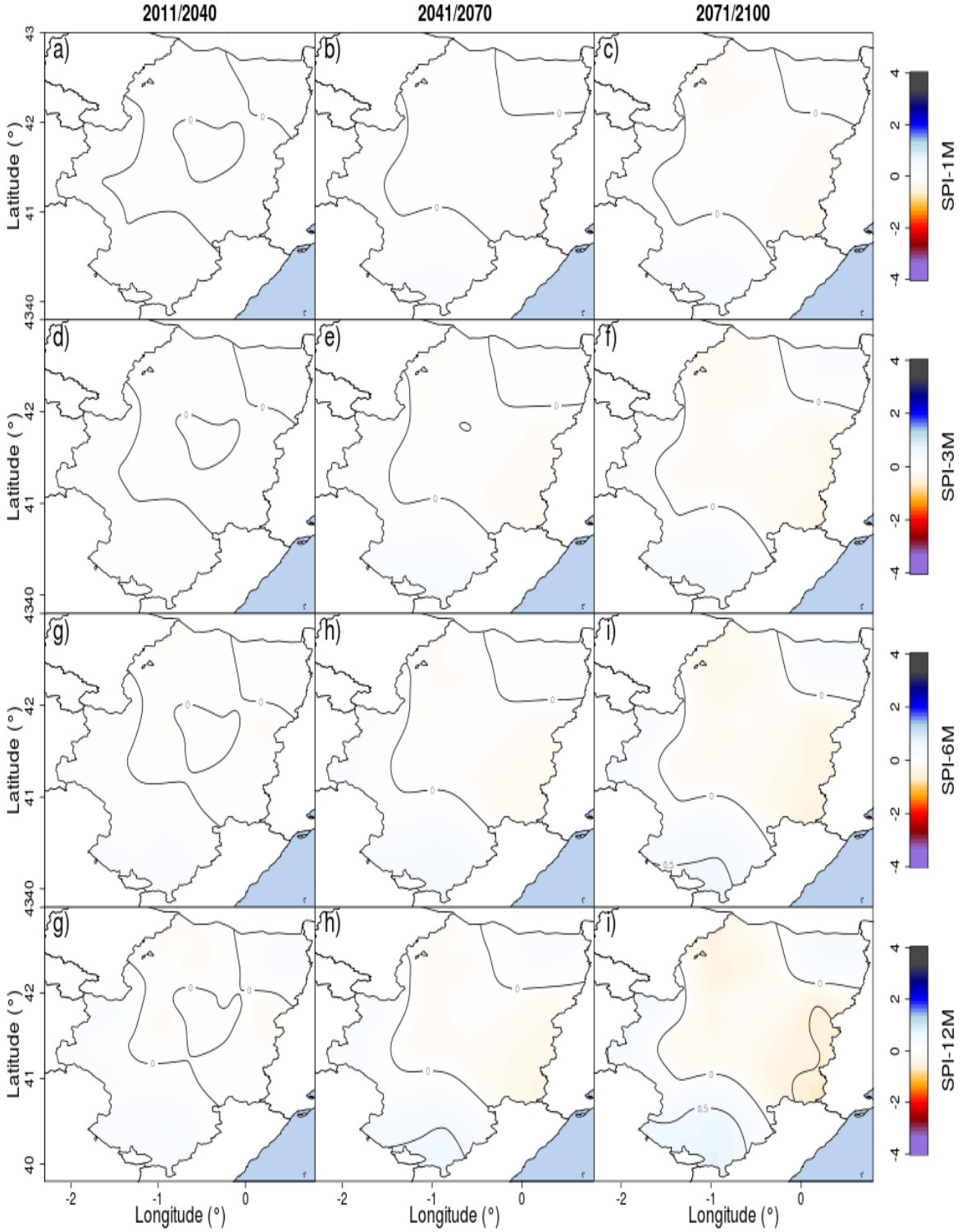

Figure S1.5. Time-scales SPI maps under RCP8.5. Geographical representation of the expected evolution of the SPI for Aragon in the periods 2041–2070 and 2071–2100 compared to the reference Historical Period (1971–2000) in terms of absolute values according to the RCP8.5 at different time-scales. The rows show the four time-scales analysed in the study (1 months, 3months, 6 months and 12 months) and the columns the three temporal periods (2011-2040, 2041–2070 and 2071–2100). The maps are generated by interpolating the available stations over the entire territory.

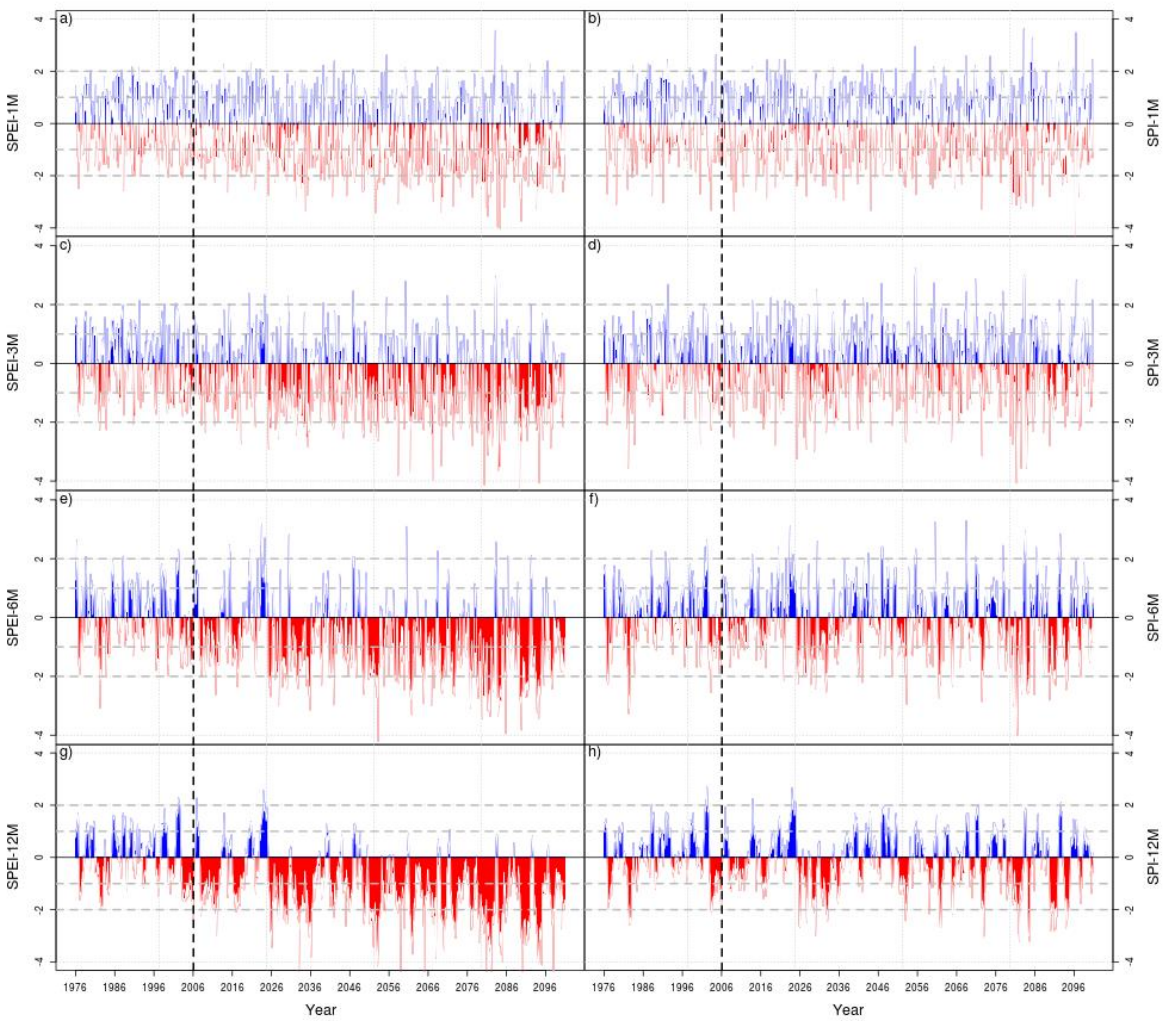

Figure S1.6. Time series for Cedrillas-Huesca under MPI-ESM-MR RCP4.5. Evolution of the SPEI (first column) and the SPI (second column) based on the MPI-MR-SM model and under the RCP 4.5 at different time-scales - 1 month (first row), 3 months (second row), 6 months (third row) and 12 months (fourth row) - for Cedrillas-Huesca.

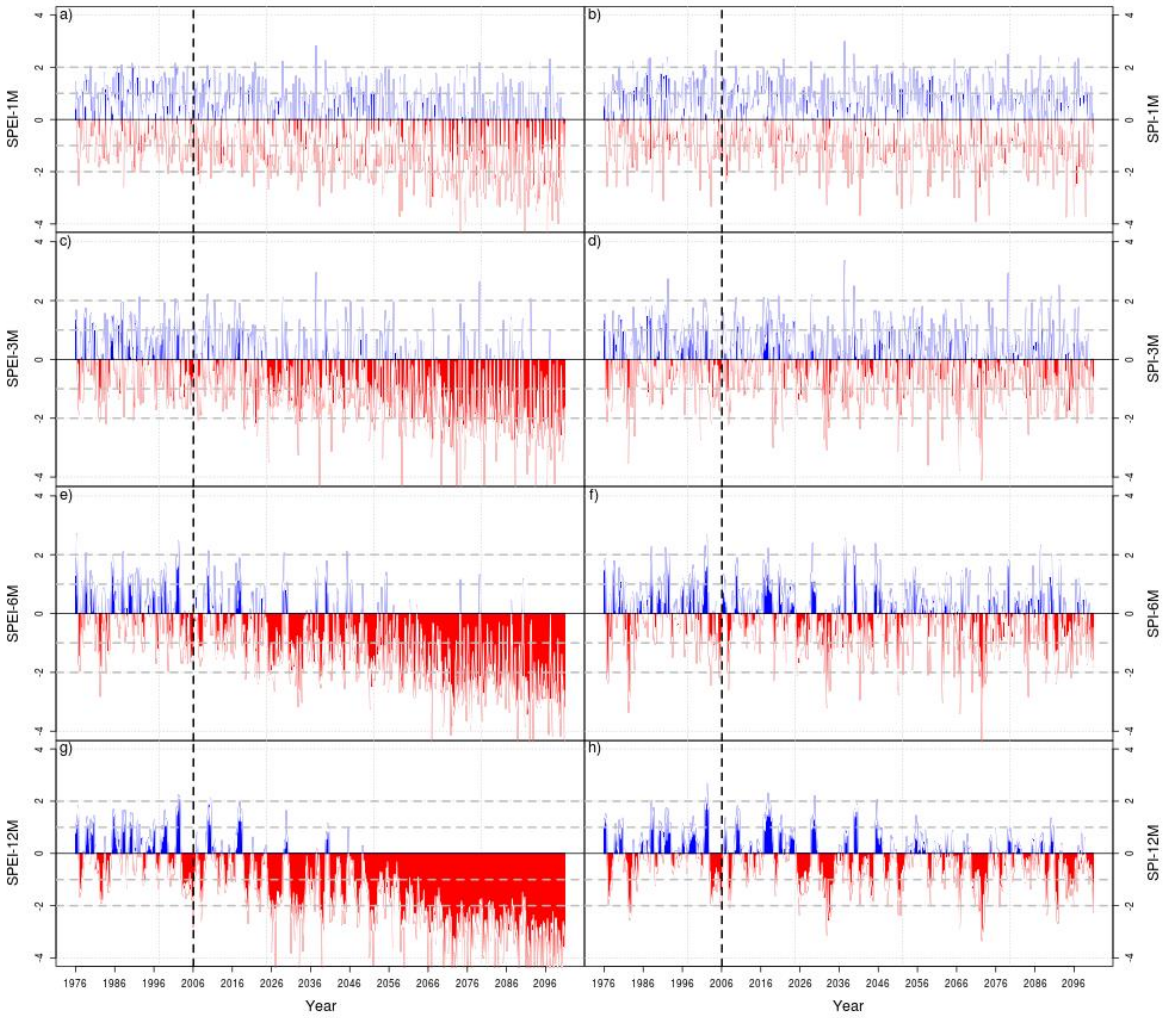

Figure S1.7. Time series for Cedrillas-Huesca under MPI-ESM-MR RCP8.5. Evolution of the SPEI (first column) and the SPI (second column) based on the MPI-MR-SM model and under the RCP 8.5 at different time-scales - 1 month (first row), 3 months (second row), 6 months (third row) and 12 months (fourth row) - for Cedrillas-Huesca.

Anexo resultado 2. Escenarios de precipitación sequía para Península Ibérica y Baleares

En el Anexo Resultado 2 se recogen los resultados de las proyecciones climáticas para todo el territorio español (Península e Islas Baleares) de precipitación y episodios de sequía a partir del SPI y del SPEI.

En las figuras AR1.1 a AR1.2 se muestran los resultados obtenidos para precipitación en base a los escenarios RCP4.5 y RCP8.5. Suponen una representación espacial de la evolución esperada en los periodos 2041-2070 y 2071-2100 comparados con el periodo de referencia (1976-2005) bajo el escenario considerado. Las filas muestran las cuatro estaciones del año (invierno, primavera, verano y otoño) y las columnas los tres periodos temporales (Historical, 2041-2070 and 2071-2100).

En las figuras AR1.5 a AR1.8 se muestran los resultados obtenidos para los episodios de olas de calor y frío en base a los escenarios RCP4.5 y RCP8.5. Suponen una representación espacial de la evolución esperada de cada variable en los periodos 2041-2070 y 2071-2100 comparados con el periodo de referencia (1976-2005) bajo el escenario considerado. Las filas muestran las características principales (intensidad media, intensidad máxima y duración media) y las columnas los tres periodos temporales (Historical, 2041-2070 and 2071-2100).

Los mapas se han generado interpolando todos los observatorios disponibles en el estudio.

En base a los resultados obtenidos y en promedio a todo el territorio (habrá zonas donde los cambios proyectados serán más o menos intensos) se espera:

- Las proyecciones de precipitación para el territorio peninsular y balear apenas muestran ligeros cambios en la cantidad de precipitación (alrededor de un ±5%) acumulada anualmente, aunque con eventos de precipitación más concentrados en el tiempo. Se espera un descenso más acusado en los meses de otoño, pudiendo ser del 5 al 8% a finales de siglo en el caso más desfavorable.
- Según los resultados obtenidos para el SPI (y de acuerdo a los cambios esperados en las precipitaciones) todo el territorio se mantendrá bajo episodios normales de alternancia de episodios secos y húmedos (valores de SPI entre ± 0.5)
- Según los resultados obtenidos para el SPEI, la situación es completamente diferente. En este caso se espera que la región se mueva hacía episodios de sequía cada vez más extremos (SPEI inferior a-3). Intensificándose la sequía según aumentan los periodos considerados. La sequía será especialmente extrema en la meseta central a finales de siglo, con valores de SPEI inferiores a -4, aunque el resto del territorio también se espera que se encuentre en sequía severa o extrema.

Una situación diferente se obtiene al evaluar la sequía meteorológica a partir de escenarios basados en el SPEI (combinando el efecto de la precipitación y la ETP). Los resultados obtenidos muestran que bajo el escenario RCP8.5 y a finales de siglo, la situación se va agravando según se aumentan los periodos considerados. De esta manera, en acumulado a 1 o 3 meses, la mayoría del territorio sufrirá sequía moderada

a severa, mientras que en acumulado de 12 meses, casi todo el territorio se encontrará en situación de sequía severa a muy extrema. A mediados de siglo, la mayor parte del territorio se encontrará en situación de sequía moderada a severa.

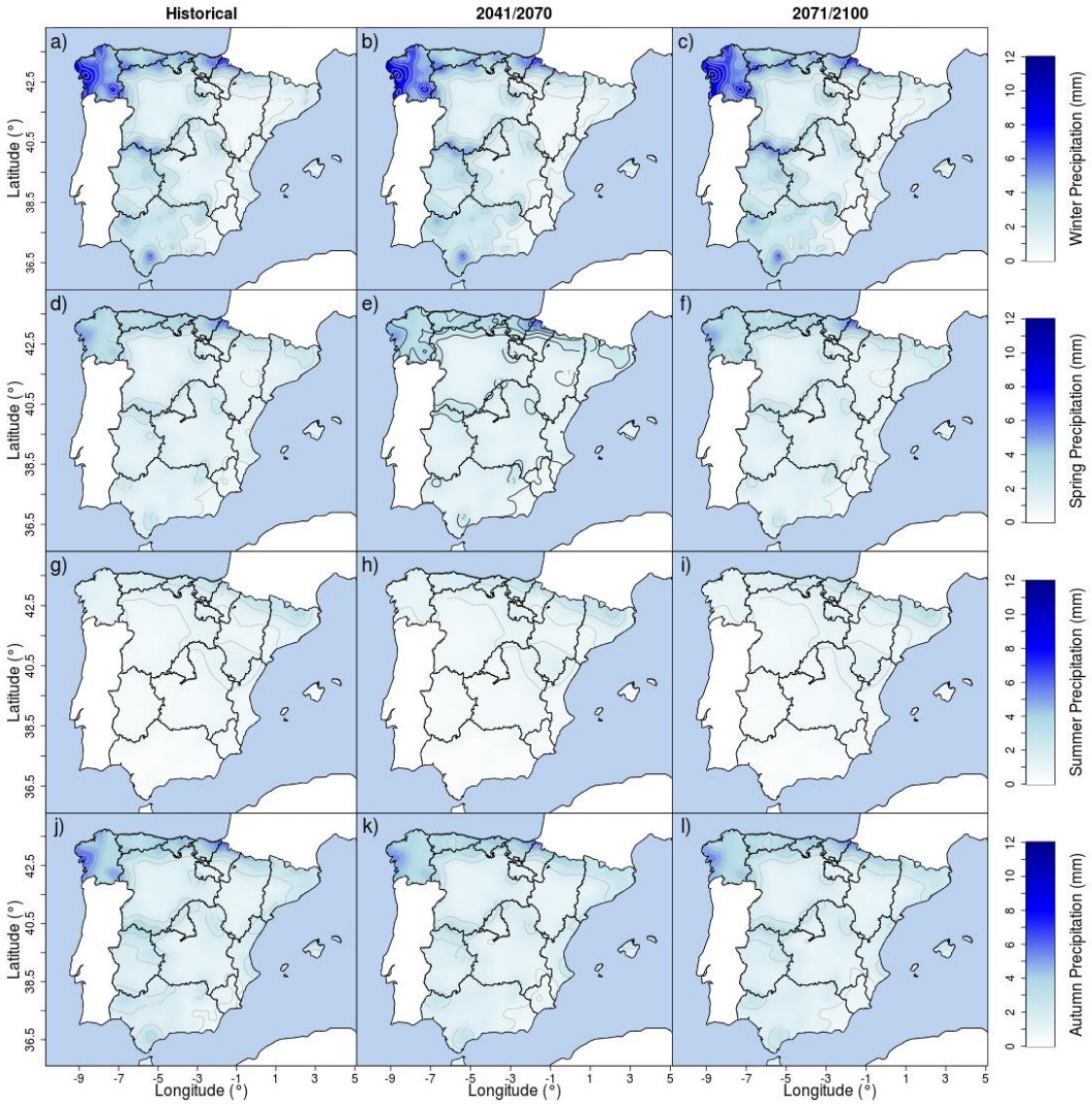

Figura AR2.1. Representación espacial de la evolución esperada de la Precipitación absoluta en los periodos 2041-2070 y 2071-2100 comparados con el periodo de referencia (1976-2005) según el escenario RCP4.5. Las filas muestran las cuatro estaciones del año (invierno, primavera, verano y otoño) y las columnas los tres periodos temporales (Historical, 2041-2070 and 2071-2100). Los mapas se han generado interpolando todos los observatorios disponibles en el estudio.

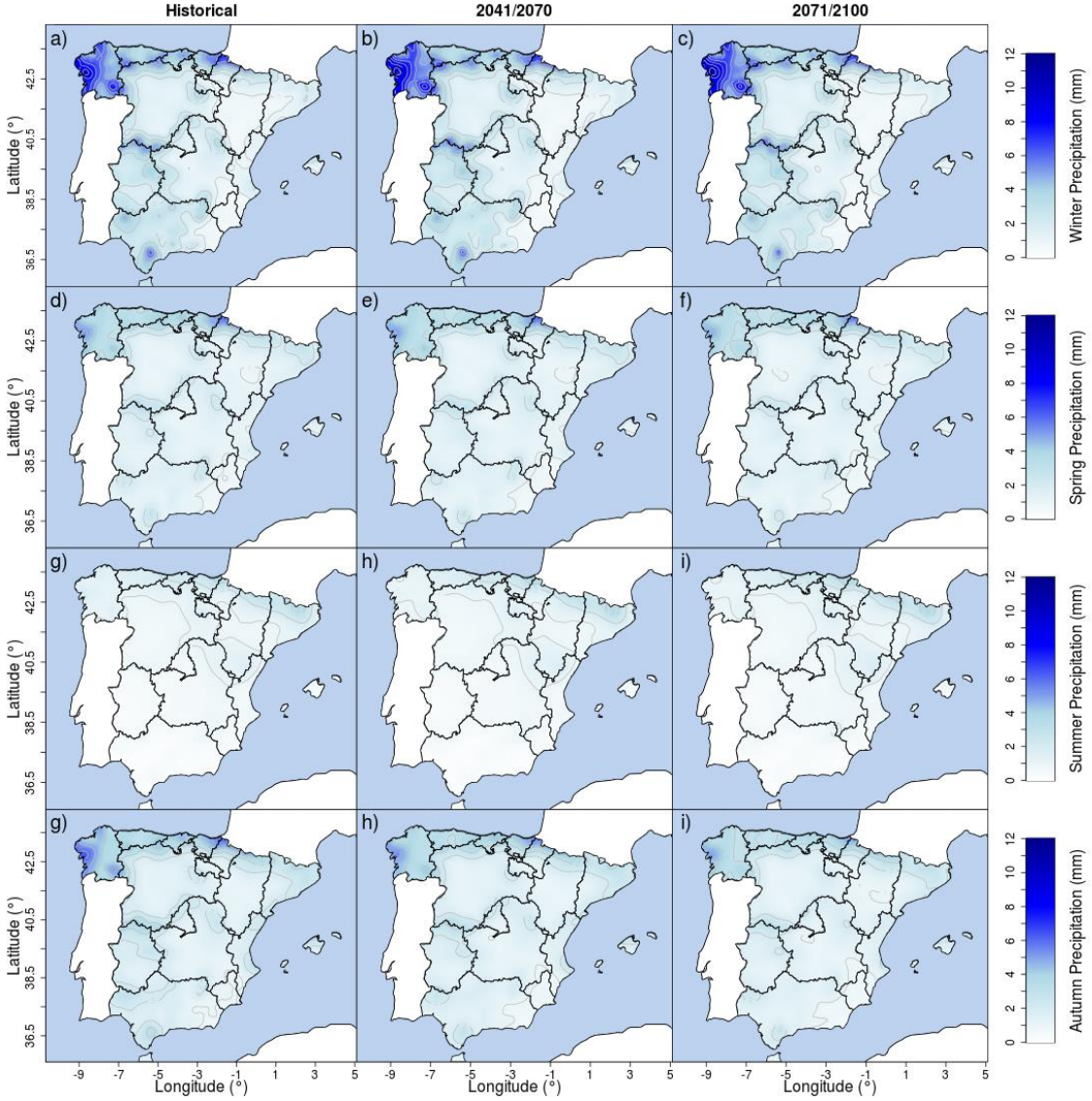

Figura AR2.2. Representación espacial de la evolución esperada de la Precipitación absoluta en los periodos 2041-2070 y 2071-2100 comparados con el periodo de referencia (1976-2005) según el escenario RCP4.5. Las filas muestran las cuatro estaciones del año (invierno, primavera, verano y otoño) y las columnas los tres periodos temporales (Historical, 2041-2070 and 2071-2100). Los mapas se han generado interpolando todos los observatorios disponibles en el estudio.

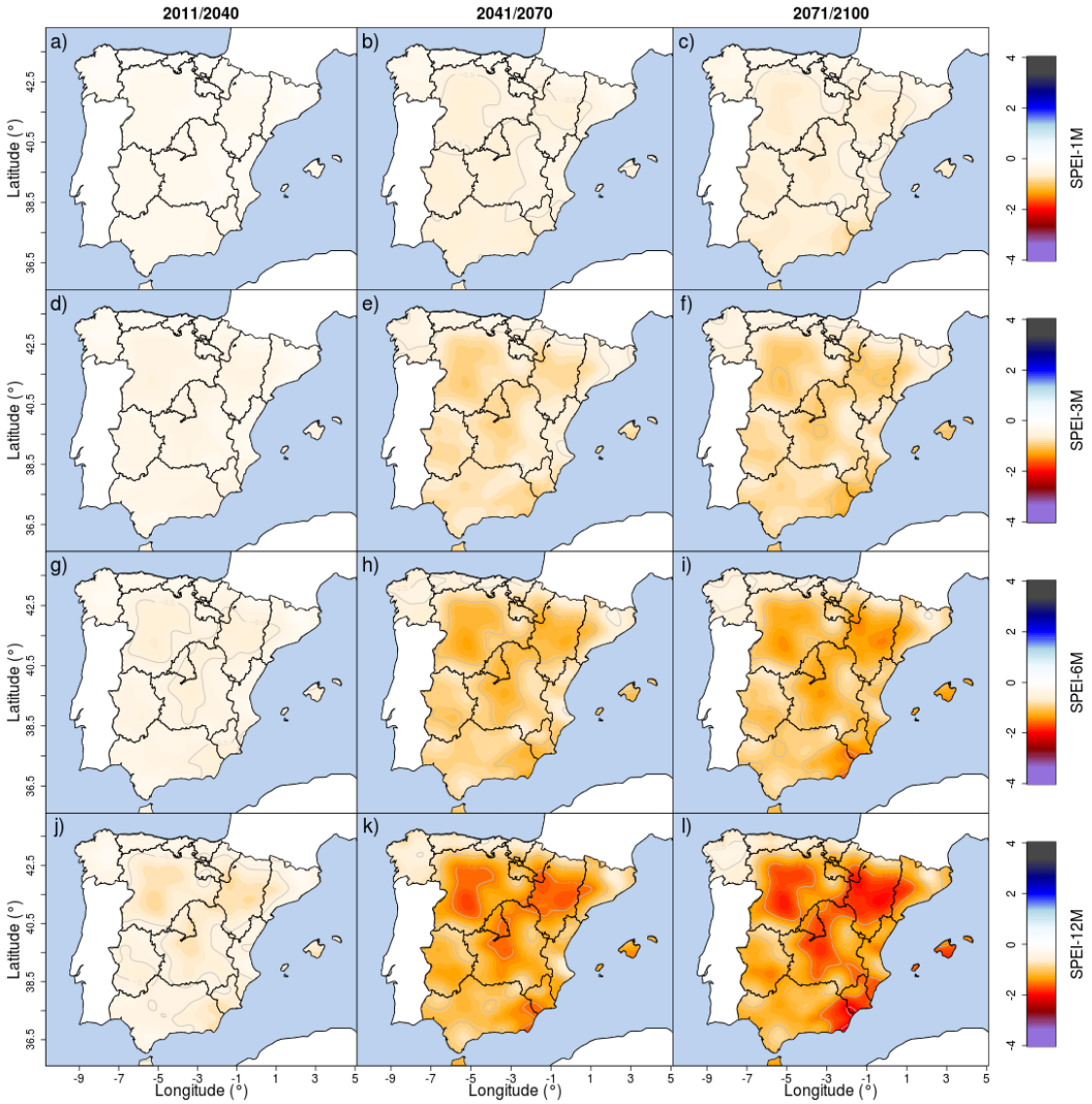

Figura AR2.3. Representación espacial de la evolución especial de la evolución esperada del SPEI en los periodos 2041-2070 y 2071-2100 comparados con el periodo de referencia (1971-2000) según el escenario RCP4.5. Las filas muestran los cuatro periodos acumulados de sequías considerados (6 mes, 12 meses, 24 meses y 60 meses) y las columnas los tres periodos temporales (Historical, 2041-2070 and 2071-2100). Los mapas se han generado interpolando todos los observatorios disponibles en el estudio.

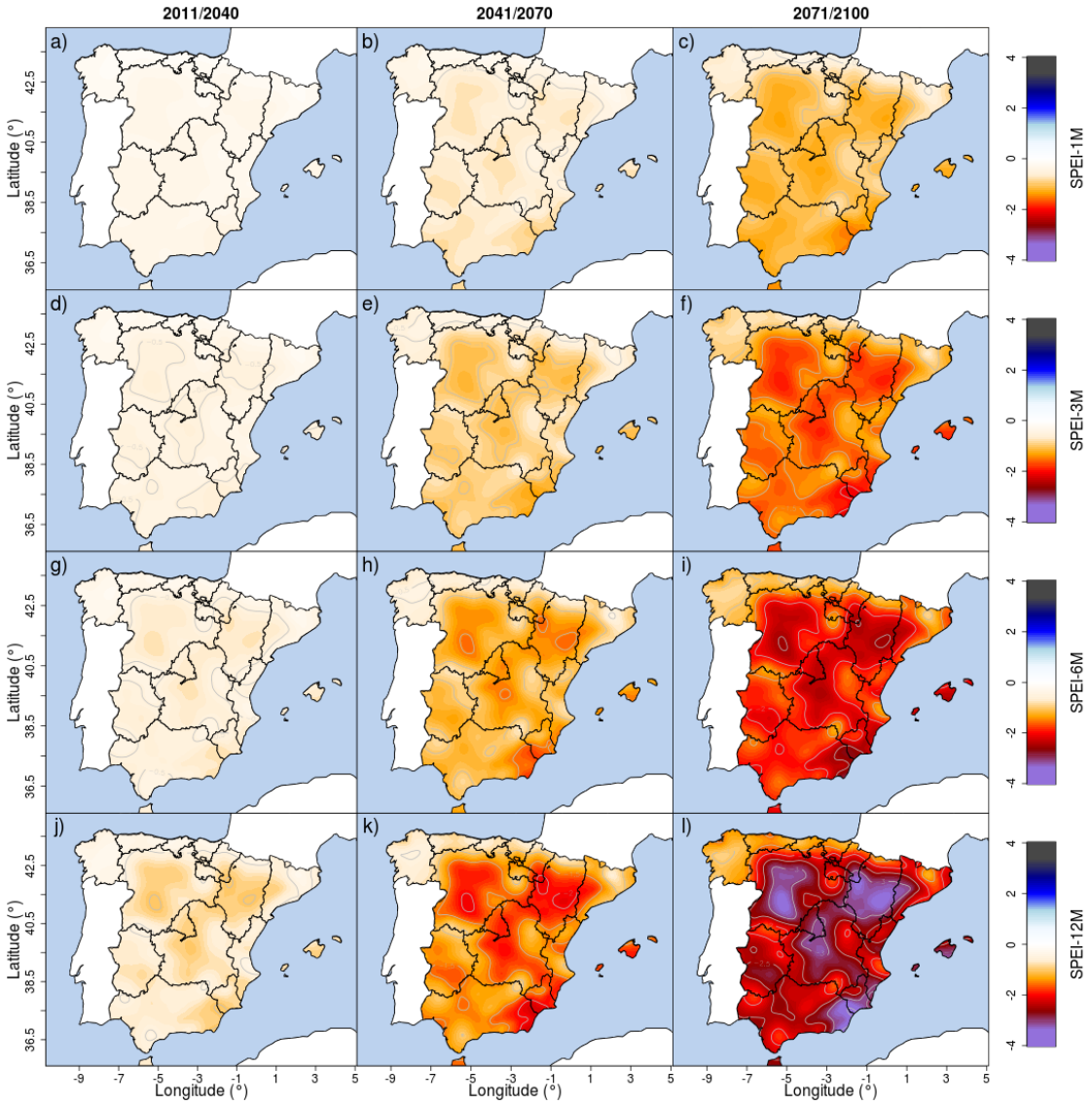

Figura AR2.4. Representación espacial de la evolución especial de la evolución esperada del SPEI en los periodos 2041-2070 y 2071-2100 comparados con el periodo de referencia (1971-2000) según el escenario RCP8.5. Las filas muestran los cuatro periodos acumulados de sequías considerados (6 mes, 12 meses, 24 meses y 60 meses) y las columnas los tres periodos temporales (Historical, 2041-2070 and 2071-2100). Los mapas se han generado interpolando todos los observatorios disponibles en el estudio.

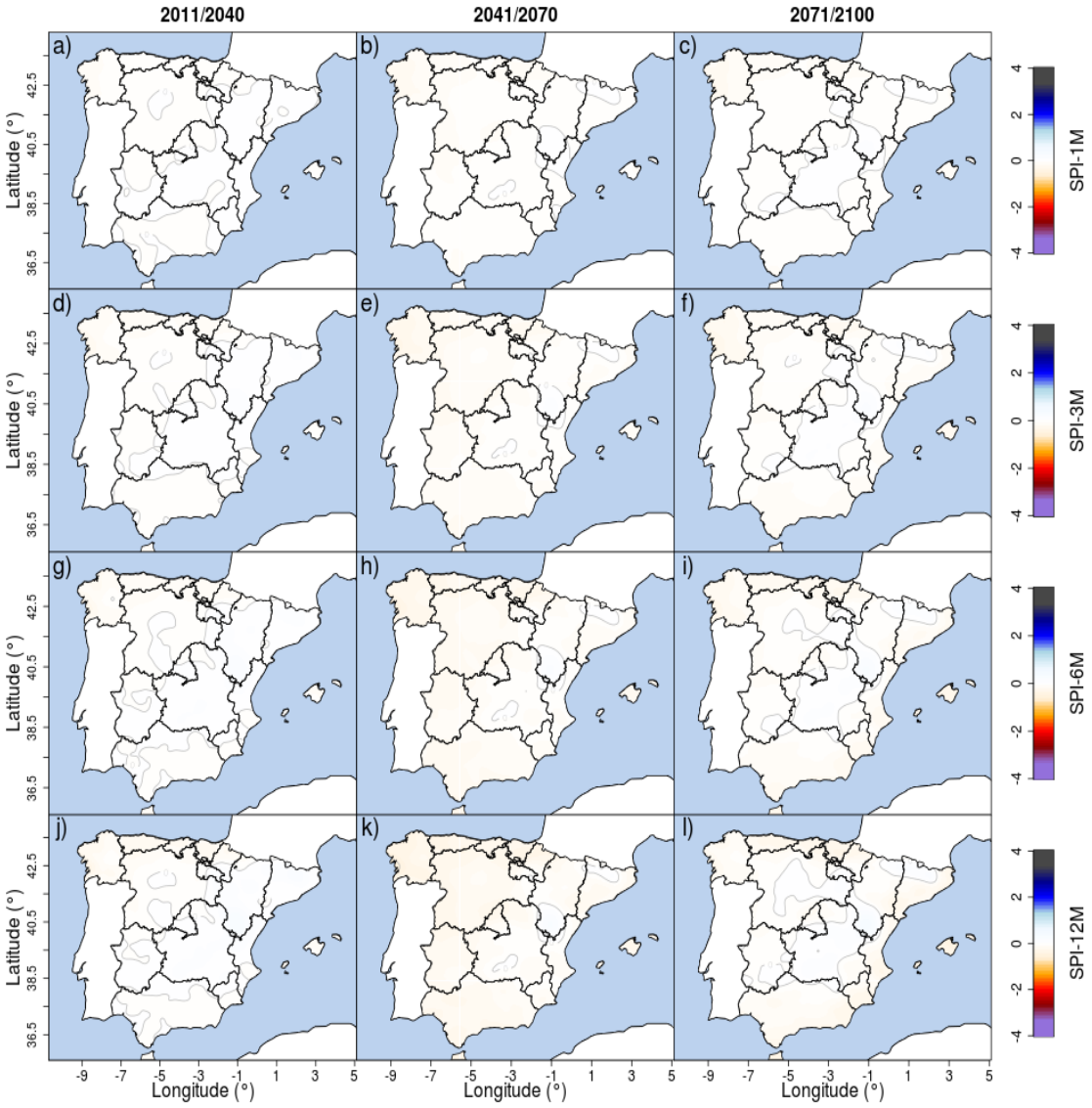

Figura AR2.5. Representación espacial de la evolución especial de la evolución esperada del SPI en los periodos 2041-2070 y 2071-2100 comparados con el periodo de referencia (1971-2000) según el escenario RCP4.5. Las filas muestran los cuatro periodos acumulados de sequías considerados (6 mes, 12 meses, 24 meses y 60 meses) y las columnas los tres periodos temporales (Historical, 2041-2070 and 2071-2100). Los mapas se han generado interpolando todos los observatorios disponibles en el estudio.

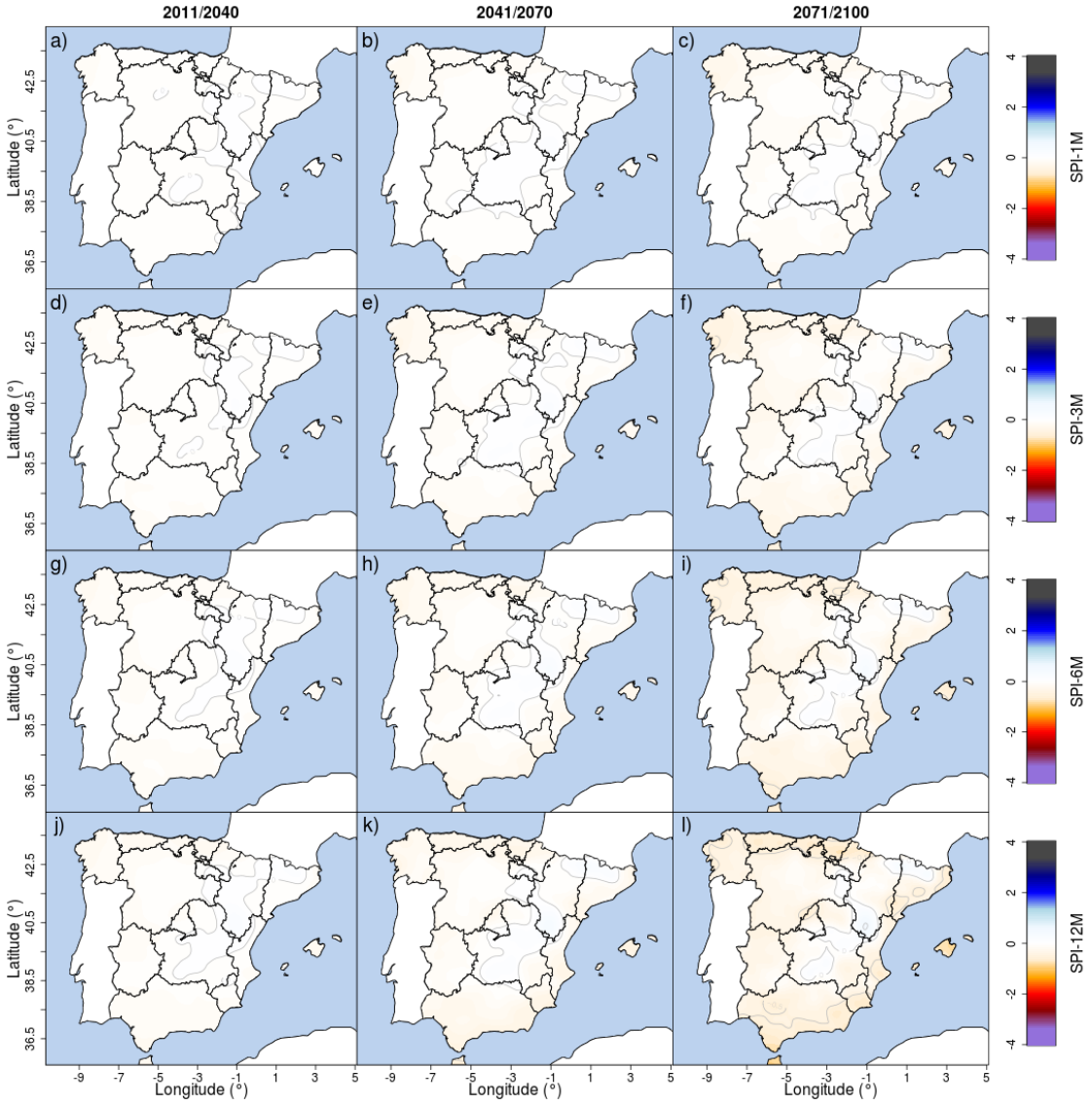

Figura AR2.6. Representación espacial de la evolución especial de la evolución esperada del SPI en los periodos 2041-2070 y 2071-2100 comparados con el periodo de referencia (1971-2000) según el escenario RCP8.5. Las filas muestran los cuatro periodos acumulados de sequías considerados (6 mes, 12 meses, 24 meses y 60 meses) y las columnas los tres periodos temporales (Historical, 2041-2070 and 2071-2100). Los mapas se han generado interpolando todos los observatorios disponibles en el estudio.

Resultado 3
Evaluación del impacto del cambio climático en el sector vitícola español mediante indicadores bioclimáticos

Future climate change impacts for the Spanish wine sector through bioclimatic indicators

Abstract

Grapevine cultivation is an ancestral practice in Mediterranean regions such as Spain. The current climatic characteristics of this region make it a particularly optimal area for its cultivation, and the climatic changes expected in the coming decades may jeopardise this climatic suitability. Therefore, accurate studies of future projections at a local level are essential.

Local climate change scenarios of six bioclimatic indicators (absolute values together with their categorisation) related to vineyards for the Spanish region based on nine Earth System Models (ESMs) as well as two Representative Concentration Pathways (RCPs) corresponding to the fifth phase of the Coupled Model Intercomparison Project (CMIP5) were generated for the first time. These indicators are the Huglin Index (HI), the Cool Index (CI), the Dryness Index (DI) and the Hidrotermic Index. As a complement, two combined indicators were calculated: the Multicriteria Climatic Classification System (MCC System) and the Composite Index (CompI). The whole territory was analysed as well as the areas involved in the Spanish Denominations of Origin.

Our results show that Thermal indicators (HI and CI) will tend to increase through the twenty-first century, while water scarcity (DI) will be more pronounced. The trends found do not have the same repercussions throughout the territory. In the south of the peninsula, with HI values exceeding 3500°C and CI above 20°C and DI below –200 mm, the continuity of the wine-growing sector in its current state is seriously endangered, with a decrease in climatically optimal years as shown by the CompI values. On the contrary, the northern peninsula and mountainous areas, despite the expected increases, with HI below 2500°C, cool nights (CI below 15°C) and sufficient water supply (DI above 150 mm) considerably improve their climatic suitability (CompI) although the risk of mildew disease remains due to the increase in temperature and humidity.

1. Introduction

Over the last decades, changes directly related to the heliothermal and hydric requirements that grapevines need for optimal growth have been observed because of climate change. Among others, increases in temperatures, alterations in the precipitation regime, alterations in potential evapotranspiration or increases in CO_2 concentrations are affecting vineyards worldwide (Alonso and O'Neill, 2011; Battaglini et al., 2009; France and Dubourdieu, 2016).

Grapevine is very sensitive to climate (White et al., 2006, Winkler 1974) and weather conditions over a wide range of time scales (Santos et al., 2020b). Changes in the weather/climate patterns due to climate change are causing numerous impacts on the cultivation of grapes (Jones et al., 2005) with economic repercussions, especially in warmer areas such as Spain. .

Average climate and climatic variability are the environmental factors that most influence wine quality and production (Santos et al., 2011). The results shown by climate projections seem to show a trend towards stronger and stronger impacts (Meehl et al.,

2007) and a shift of the optimal areas for vine cultivation towards the Poles by about 20° by 2050 (Kenny and Harrinson, 1993; Tate, 2001). Many authors have highlighted how climate change will alter current wine-growing regions and the need to act accordingly (Jones and Alves, 2012; Lazoglou et al., 2018; Schultz and Stoll, 2010; White et al., 2006, Olatt et al., 2016).

Europe, as one of the world's major wine-growing regions, is one of the areas most affected by climate change, where extreme events are expected to become more pronounced (Gaitan et al., 2020; Porter and Semenov, 2005). This will lead to increased irrigation demand (Doll, 2002), increased diseases and pests (Alig et al., 2002) and changes in viticultural zoning (Malheiro et al., 2010).

Spain is one of the main wine producers and exporters as well as the world's leading vineyard (with 949,565 ha of vineyards, 13% of the world total, FEV, 2021). Due to its location in southern Europe, it is expected to be one of the regions most affected by the effects of climate change, especially rising temperatures and water stress (Gaitán et al., 2019, Gaitán et al., 2020). Indeed, these impacts are detectable today. In Spain, along with the aforementioned impacts, the area of vineyards has decreased in the north-east of the peninsula as a result of water stress (Odo Camps and Ramos, 2012), an increase in the demand for irrigation (Alonso and O'Neill, 2011) and a reduction in the life expectancy of vines by 30% (Expansión, 2016). According to a study by the University of La Rioja (Expansión, 2019), 90% of professionals associated with a Designation of Origin have felt the effects of climate change and 56% consider that these impacts are affecting them considerably. Among the climatic risks that most affect them are frost, hail, drought and heat waves (Climate change and vineyards in Spain report, 2016). Therefore, determining the relationship between climate and vineyard and assessing its future evolution is of particular interest in regions such as Spain, where the wine sector is not only important in terms of biodiversity but also socio-economic terms.

It is possible to evaluate the relationship between climate/weather and the different factors affecting vines and wine production as a whole by using bioclimatic indices (Fregoni 2003), which make it possible to determine the climatic suitability of a region for growing vines, the most suitable variety or the possibility of the occurrence of certain pests and/or diseases.

Classical studies use individual indices calculated and derived from temperature and precipitation (Carbonneau and Tonietto, 1999; Tonietto 1999, Fraga and Santos, 2017) to assess climate-vineyard relationships (Bindi et al., 1996, Jones 2006) and their impact from different perspectives (Schultz, 2000, Combris et al., 1997).

More recent studies have highlighted the need to work with combined indices as they represent more complete viticultural classification and discrimination and allow wine quality to be characterised (Huglin, 1978; Maglhaes, 2008). This way of working is included in the concept of viticultural zoning and is the first step to evaluate the viticultural potential of a region (Malheiro et al., 2010).

Despite many indications and reports on the effects that climate change has already had on the wine sector, the efforts of the scientific community to identify the relationships between weather variables and vines and the impact of these changes in the future,

there are still few studies focused on how wine producers and growers can adapt to these changes (Holland et al., 2010).

In addition, most studies use dynamic climate projections (which have not taken into account local climatology), direct outputs from climate models or a reduced number of Spanish locations, as they are part of studies covering larger geographical areas. To date, no study assesses the impact of climate change on vineyards in the Ibero-balear Spanish territory using bioclimatic indices calculated based on regionalised climate projections on a local scale with a statistical downscaling technique (considering local climatology) generated from climate models belonging to the fifth phase of the CMIP5.

Therefore, this study aims to generate local future climate scenarios for the twenty-first century for four individual bioclimatic indices of viticultural impact: Huglin Index (HI), Dryness Index (DI), Cool night Index (CI) and Branas, Bernon and Levadoux Hydrotermal Index (HyI), a combined index (CompI) and a viticultural zonation (MCC System) for the Iberian-Peninsular Spanish territory. As a starting point, local daily climate projections generated through a statistical downscaling technique fed with CMPI5 scenarios will be used.

This study will make it possible to assess the suitability of the study area for wine-growing, as well as to determine what areas are going to lose or gain wine-growing potential, which will be very useful information for defining possible adaptation measures and decision making for the wine-growing sector in the face of climate change.

2. Materials and Methods

2.1. Study area

This study was carried out on the Spanish peninsular territory and the Balearic Islands (Fig.R3.1) covering an area of 588,294 km^2. Due to its location close to large bodies of water and its complex orography (from sea level to peaks exceeding 3400 km), the Spanish climate is very varied and complex, so that up to 13 climatic regions can be counted according to the Köppen classification (Köppen and Geiger, 1936), and there are multiple microclimates. The climate of the Iberian Peninsula depends on its location in the extreme southwest of Europe and its complex orography, while the Balearic Islands are located in the western Mediterranean close to the Iberian Peninsula and are relatively mountainous.

The Spanish mainland and the Balearic Islands have very optimal climatic conditions that favour the cultivation of grapevines, as reflected in the almost 950,000 hectares of Spanish territory dedicated to its cultivation.

The Canary Islands have not been included in the study because, due to their climatic characteristics, a consequence of their location in tropical areas, they differ from those of the rest of the Spanish territory and they deserve an individual study that encompasses these differences.

2.2. Spanish Denominations of Origin (DOs)

The Spanish DOs are the system used in Spain for the recognition of a differentiated quality, which is the result of specific and distinguishable characteristics due to the geographical environment in which the raw materials are produced and the products are

made as well as the influence of the human factor involved. In Spain, there is a wide network of recognised quality according to the Government of Spain (2021): 101 Denominations of Origin (occupying an area of more than 900.000 ha), 42 Protected Geographical Indications and 26 “Vinos de Pago” (MAPA, 2022 Ministry of Agriculture, Fisheries and Food).

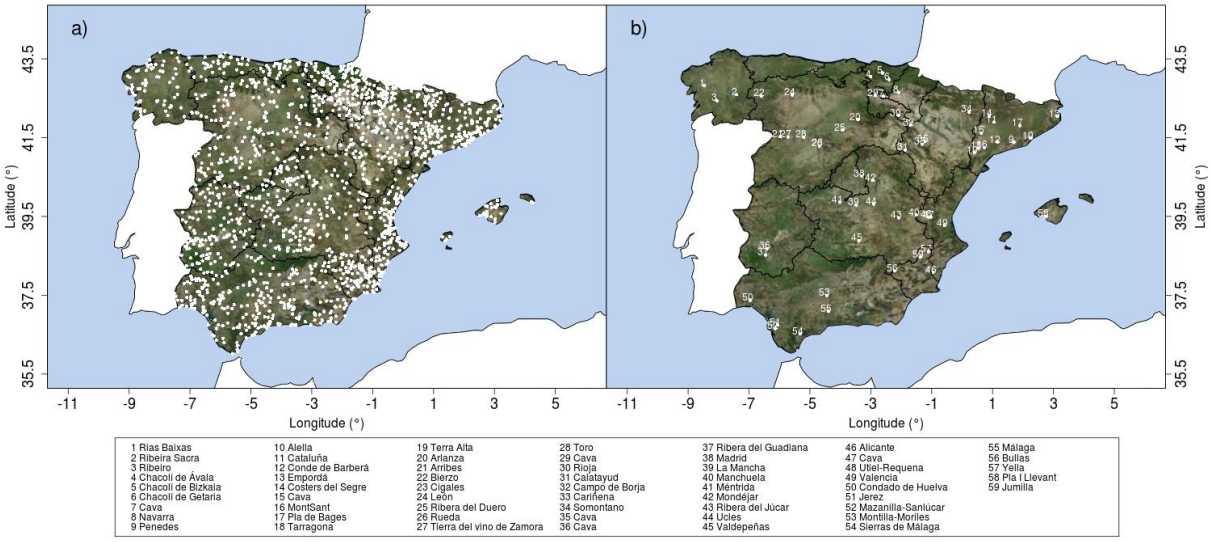

Figure R3.1. Location of the study Area. a) Shows the points corresponding to the observatories used in the complete study with available temperature and precipitation data. b) Shows the location of the denominations of origin “(Map source: OpenStreetMap)”

2.3. Datasets

2.3.1. Surface dataset

The observed data set used in the study consists of a set of time series of daily maximum and minimum temperature and daily precipitation data homogeneously distributed throughout the territory and belonging to the network of observatories of the Spanish Meteorological Agency (AEMET, www.aemet.es).

The selected dataset is the same that has been used in previous studies in the generation of local future climate scenarios for the study area (Gaitan et al., 2019; Gaitan et al., 2020; Gomez-Martinez et al., 2021; Monjo et al., 2016; Ribalaygua et al., 2013b), which have been subjected to strict quality control (p.e. inhomogeneities, gaps and outliers, Lopez et al., 2007).

A total of 1778 observatories with data of both temperature and precipitation were used in the study, covering extensively the entire territory under study (Fig.R3.1a). For the analysis of the results by Denominations of Origin (DOs), we have chosen those observatories that are located within the territory classified as such (Fig.R3.1b). In total, there are 789 observatories within 59 DOs located in the iberian-balearic territory (the DOs where no observatories with information of temperature and precipitation simultaneously or with poor meteorological information were found are left out of the present study).

2.3.2. Local future climate scenarios

A set of daily local future climate projections of temperature (maximum and minimum) and precipitation obtained by applying a two-step analogue/regression statistical downscaling methodology developed by the Climate Research Foundation (FIC) was used (Ribalaygua et al., 2013a; Ribalaygua et al., 2013b). This methodology offers some advantages: it is computationally inexpensive, provides local information at observatory scale and allows quantifying the uncertainty associated with the downscaling process (Van der Linden and Mitchell, 2009). Other advantages are the application of future simulations consistent with observations (physically coherent between them) and using local scale (because nearby data points in space are subjected to different climate change conditions) (Ribalaygua et al., 2013b).The generation of daily future climate local scenarios was based on nine global climate models (Table R3.1), called Earth System Models (ESMs, (Wang et al., 2010), belong to the fifty phase of the Coupled Model Intercomparison Project (CMPI5, Tripathi et al., 2006) and supplied by the Program for Climate Model Diagnosis and Intercomparison (PCMDI) archives. This generation of models has contributed to the acquisition of both dynamical and statistical downscaling techniques with less uncertainty in integrating the individual parts of the climate system (atmosphere, ocean, land and sea ice) and the exchange of energy and mass between them (Knutti and Sedlacek, 2013).

GFDL-ESM2M	2ºx2,5º daily	National Oceanic and Atmospheric Administration (NOAA), E.E.U.U.	Dunne et al. (2012)
CanESM2	2,8ºx2,8º daily	Canadian Centre for Climate Modeling and Analysis (CC-CMA), Canadá.	Chylek et al. (2011)
CNRM-CM5	1,4ºx1,4º daily	CNRM (Centre National de Recherches Meteorologiques), Meteo-France, Francia.	Voldoire et al. (2013)
BCC-CSM1-1	1,4ºx1,4º daily	Beijing Climate Center (BCC), China Meteorological Administration, China.	Xiao-Ge et al. (2013)
HADGEM2-CC	1,87ºx1,25º daily	Met Office Hadley Center, United Kingdom.	Collins et al. (2008)
MIROC-ESM-CHEM	2,8ºx2,8º daily	Japan Agency for marine-Earth Science and Technology (JAMSTEC), Atmosphere and Ocean Research Institute (AORI), and National Institute for Environmental Studies (NIES), Japan.	Watanabe et al. (2011)

MPI-ESM-MR	1,8ºx1,8º daily	Max-Planck Institute for Meteorology (MPI-M), Germany.	Raddatz et al. (2007); Marsland et al. (2003)
MRI-CGCM3	1,2ºx1,2º daily	Meteorological Research Institute (MRI), Japan.	Yukimoto et al. (2011)
NorESM1-M	2,5ºx1,9º daily	Norwegian Climate Centre (NCC), Norway.	Bentsen et al. (2012); Iversen et al. (2013)

Table R3.1. Information about the nine climate models belonged to the 5 Coupled Model Intercomparison Project (CMIP5) corresponding to the fifth report of the IPCC. Models were supplied by the Program for Climate Model Diagnosis and Intercomparison (PCMDI) archives.

This study uses data from two different experiment families of GCMs: the Historical experiment (Taylor et al., 2012), which covers much of the industrial period and can be referred to as "twentieth-century" simulations and the representative concentration pathway (RCP) family (Moss et al., 2010), which corresponds to different possible ranges of radiative forcing reached in the year 2100 for values of the pre-industrial era. This study uses future projections determined by the RCP8.5 'high' scenario and the RCP4.5 'intermediate' scenario.

In total, there is a set of 18 daily climate projections for two emission scenarios, RCP4.5 and RCP8.5 (9 projections for each RCP).

The methodology employed for generating temperature and precipitation projections has been used in national and international projects, with good verification (Gaitan et al., 2019; Monjo et al., 2016; Moutahir et al., 2017; Rodriguez et al., 2014; Santiago et al., 2017, Gutierrez et al., 2019, Ribalaygua et al., 2013a, 2013b, 2018) and validation results (Ribalaygua et al., 2013a, 2013b, Gaitan et. al, 2019, 2020; Monjo et al., 2016). Verification results (goodness of the methodology used) obtained in the above-mentioned studies showed good results for both, temperatures and precipitation. In the case of the temperature, the average bias achieved was below 0.1 ºC while for precipitation, an error of 10-20% was obtained. Validation results obtained in the above-mentioned studies for both the maximum and minimum temperatures, showed a bias of around tenths of a degree in all months, so they were very close to zero. The error was not above half of a degree for any of the cases. Therefore, the results showed that the ESMs were capable of adequately simulating both the maximum and the minimum temperatures on annual and seasonal scales. In the case of the precipitation, the results are variable depending on the model and the seasonal period; however, all the models are able to reproduce the annual cycle of precipitation as well as the differences between seasonal periods (maximum values in autumn and spring, followed by winter and summer). The obtained bias and standard deviation are less than ±1 mm/day, which in relative terms supposes a difference of less than or around ±10% in the worst of the cases.

From the simulated temperature series, future heat and cold wave episodes have been calculated following Gaitán et al., 2019. Heat Waves have been defined at least three consecutive days with a maximum temperature above the 95th percentile of the maximum temperature series calculated between the months of June to September

during the period 1971–2000 and at least three consecutive days with a minimum temperature below the fifth percentile of a minimum temperature series and calculated between the months of November to April during the period 1971–2000.

2.4. Bioclimatic indices

A set of four bioclimatic indices (Huglin Index (HI), Dryness Index (DI), Cool night Index (CI) and Branas, Bernon and Levadoux Hydrotermal Index (HyI)) was used to assess the impact that climate change may have on the suitability of a region for growing grapevines and/or certain grape varieties. In addition, two combinations of these indices were analysed: MCC System and CompI. For a complete explanation of indices' definition see Table R3.2.

The Dryness Index (DI) assesses soil water availability by providing information on water stress conditions. In the absence of information on future land use and other variables, it was decided to use a simplified formula proposed by Tonietto and Carbonneau, 2004 and based on the calculation of the potential evapotranspiration (ETP). According to various studies (Blanco-Ward et al., 2007; Vanderlinden et al., 2004) and specifically Fonseca et al 2012, the Hargreaves formula was chosen for the calculation of ETP instead of other more complex formulations.

Table R3.2. Description of analysed Bioclimatic indicators

Index	Formula	Values	Interpretation	Categories	Description	References
Huglin Index	$\sum_{April}^{Sept.} \frac{(\bar{T}-10)(T_{max}-10)}{2} * k$	≤1200 1200-1500 1500-1800 1800-2100 2100-2400 2400-2700 2700-3000 ≥ 3000	--- HI-3: Very cool HI-2: Cool HI-1: Temperate HI+1: Temperate warm HI+2: Warm HI+3: Very warm ---	0 1 2 3 4 5 6 7	HI is a thermal index based on degree-days, i.e. on the concept of heat accumulation. This index is used to evaluate the basic thermal and radiative demand of the grapevines during the growing period to guarantee a complete and adequate ripening. Each grape variety requires a certain amount of heat accumulation for optimal ripening to occur	Huglin 1978
Dryness Index	$\sum_{April}^{Sept.} (Wo + P - Tv - Es)$	> 150 150-50 50 – (-100) (-100)- (-200) ≤ -200	DI-2: Humid DI-1:Sub-humid DI+1:Moderately Dry DI+2: Dry DI+3: Very dry	5 4 3 2 1	DI assesses soil water availability by providing information on water stress conditions.	Riou et al. 1994 Tonietto and Carbonneau, 2004
Cool night Index	$\bar{T}_{min}$ (sept)	≥25 18-25 14-18 12-14 6-12 ≤6	--- CI1: Warm nights CI2: Temperate nights CI3: Cool nights CI4: Very cool nights ---	5 4 3 2 1 0	CI is a thermal index based on the night temperature during the ripening period (September in the Northern Hemisphere (NH)).	Tonietto, 1999
Hydrotermic Index (HyI)	$\sum_{April}^{Aug} (\bar{T} * P)$	< 2500 2500-5100 5100-7500 >7500	Low risk Medium risk High risk Very high risk	1 2 3 4	HyI is an index that combines the effect of air humidity (through precipitation) and temperature during the growing season to assess the risk of grape exposure to certain diseases such as mildew.	Branas et al. 1946, 1974
CompI Index	$\frac{nº\ optimum\ years}{nº\ years\ for\ a\ period}$ HI ≥ 900 °C DI ≥ -100mm HyI ≤ 7500°C·mm T_{min} > -17 °C (always)	0.0-0.2 0.2-0.4 0.4-0.6 0.6-0.8 0.8-1.0	% means the percentage of years suitable for viticulture		The CompI is an index to evaluate the climatic suitability for grape growth. The CompI is the percentage of optimum years for vine cultivation for a given period. An optimum year is understood as a year in which critical thresholds of the HI, DI, HyI indices and minimum temperature conditions are reached.	Malheiro et al., 2010 Fraga et al.,2013
MCC System classification	Combination of HI, DI and CI	Most optimal categories: HI-3, HI-2, HI + 1 CI + 1; CI +2 DI-1, DI + 1	Least optimal categories: CI-2, CI-1 DI + 2, DI + 3		The MCC System is a climatic classification system for grape-growing regions based on the integration of the different classes of the three climatic indices: DI, HI and CI.	Tonietto and Carbonneau, 2004
$\bar{T} \equiv mean\ temperature\ (°C)$ $T_{max} \equiv maximum\ temperature\ (°C)$ $T_{min} \equiv minimum\ temperature$ $P \equiv Precipitation\ (mm)$ $N \equiv nº\ days\ per\ month$					$Wo \equiv Initial\ available\ soil\ water\ reserve\ (mm) = 200mm$ $Tv \equiv Potential\ transpitarion\ in\ the\ vineyard\ (mm) = ETP * k$ $Es \equiv Direct\ evaporation\ from\ the\ soil\ (mm) = (ETP/N) * (1-k) * JPm$ $JPm = P/5$ $k(month) = 0,0,0,0.1,0.3,0.5,0.5,0.5,0.5,0,0,0)$	

3. Results

3.1. Observed bioclimatic indices and their verification

The observed (categorised) absolute average values of the indices used in the study (HI, DI, CI, HyI, MCC System and CompI) for the period 1971–2000 can be seen in Fig. R3.2 and Support Information R3.1. The results clearly show a north-south and west-east spatial distribution.

Within the Iberian-Balearic territory, we can find HI values (Fig.R3.2a and S3.1a) that cover all the categories defined for this index, from 300 to about 3300°C, accumulated in the period from April to September.

Some regions with climatic characteristics not suitable for growing grapes were detected, either because they are too cold with HI < 1000 (Pyrenees) or too warm with HI > 3000 (some points in the Spanish Southwest).

The areas of the northern peninsula as well as most of the valleys of mountainous areas have characteristics of cold climates with HI values between 1500 and 1800 (category 2). In a smaller proportion, there are regions with temperate climates (HI 1800–2100).

In the mountainous regions of the Central System, the Iberian System and Betic System, we find HI values < 1500 (category 1, very cold), which places them in the lower thermal limit for grapevine. However, most of the territory of Sierra Morena (the mountain range that runs from east to west in the south of the Iberian Peninsula) presents IH values that oscillate between 2700 and 3000 accumulated degrees (category 6), being areas with very warm climates.

The coastal areas of the Mediterranean and the plateau as well as Cádiz (SW Iberian Peninsula) are characterised by being warm areas (category 5) with a high heliothermic potential (HI between 2400 and 2700).

The values observed for the CI (Fig.R3.2b and S13.b) in the ripening month (average minimum temperature in September) range between 4 and 20°C, which is a great difference between regions within the study area. Most of the northern half of the peninsula and the highest points of the Betic system present very cold CI values below 12°C (category 1). The rest of the northern zone and part of the central plateau present cold CI values between 12 and 14°C (category 2). The Mediterranean coast and the south and west areas of the peninsula, as well as the Balearic Islands, are characterised by mild nights (CI between 14 and 18°C, category 3). Very few areas have high minimum temperatures in September (CI > 18, categories 4 and 5).

The DI values obtained (Fig. R3.2c and S3.1c) vary between –260 mm (very dry areas) and 500 mm (super-humid areas). The Cantabrian coast (N) presents the most humid conditions with DI values > 150 mm (category 5), while the Cantabrian mountain range presents DI values higher than 50 mm (category 4), which implies humid and sub-humid characteristics with an absence of drought and a high level of water availability. Most of the northern plateau and the Balearic Islands have DI values between 50 to –100 mm (category 3) and are considered moderately dry areas. The rest of the peninsula is characterised by traditionally dry regions (DI between –100 and –200 mm).

The observed HyI values (Fig.R3. 2d and S3.1d) show that the southern regions have the lowest risk of incidence of diseases such as mildew (which depend on humidity and temperature to a great extent) and that the risk gradually increases towards the north where the precipitations are more abundant during the period of growth of grapevine.

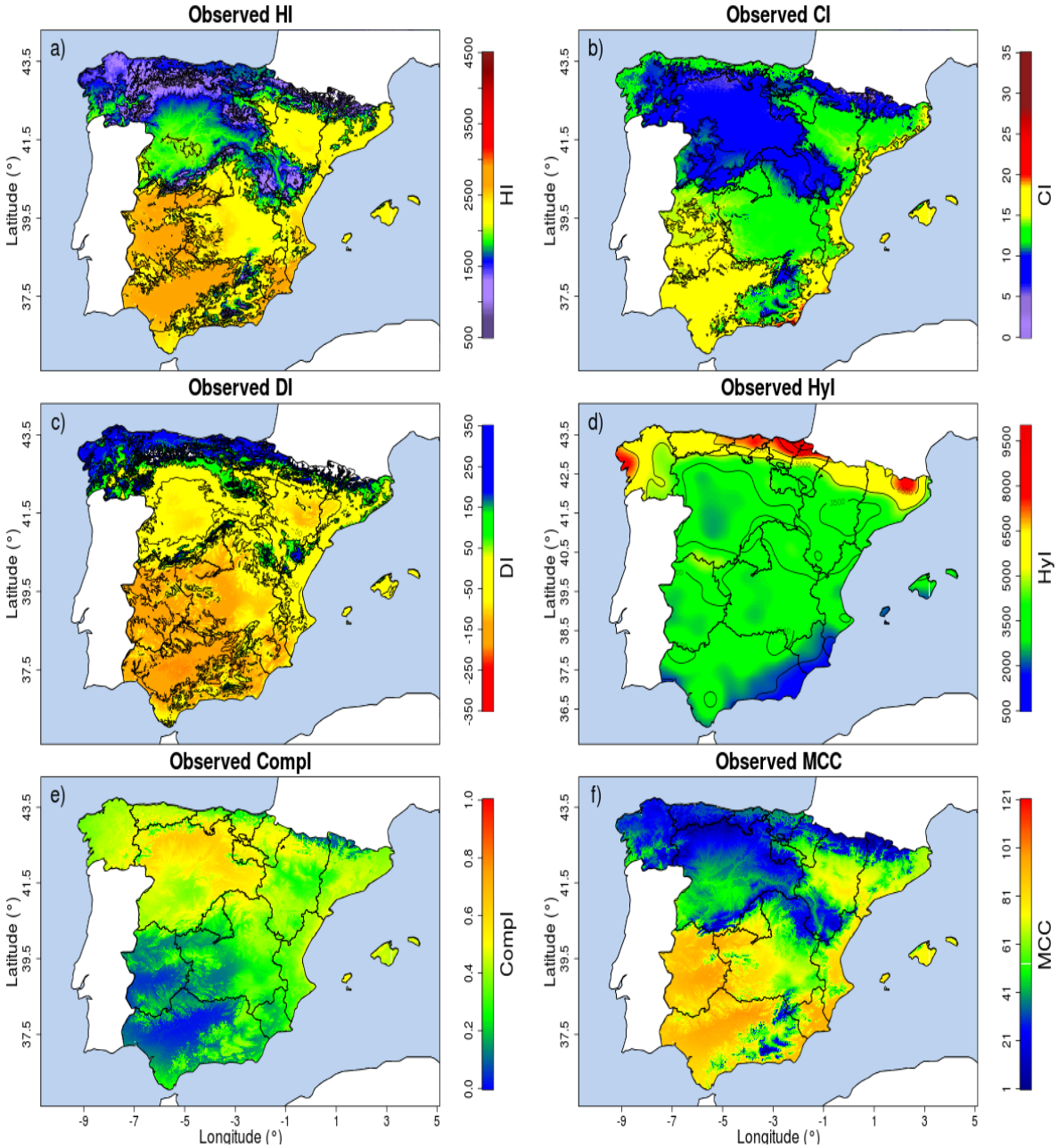

Figure R3. 2. Geographical representation of the observed values of the a) Huglin Index (HI), b) Cool night Index (CI), c) Dryness Index (DI), d) Branas, Bernon and Levadoux Index (HyI), e) Composite Index (CompI) and f) MCC System for the periods 1971-2000

Considering the aforementioned values, there will be years more suitable from the climatic point of view than others will. Fig.R3. 2f shows the CompI index based on thresholds of some of the commented indices (Tmin, HI, DI, CI and HyI, see Table R3.2), which reveals that the southwest regions of the peninsula have an optimal percentage of years, climatically speaking, lower than those of the northern half and the Balearic Islands.

By combining these indices, we can establish within which values of the MCC System climatic classification the study area falls, since each of the indices separately is not a guarantee of viticultural climatic suitability. In total, we defined 120 combinations (see Table S3.1). The northern zone covers the classifications with categories between 1 and 20, the northern plateau belongs to those classifications with categories between 45 and 50, while the Mediterranean and eastern peninsular zones belong to the 70 and90 classes and, finally, the western and southern zones are included in the classes with categories between 90 and 100.

In the verification results (Fig. S3.2), the indices calculated based on observed data are compared with the indices calculated based on data from the temperature and precipitation series of the ERA-40 reanalysis to which downscaling was performed. The verification shows very acceptable bias values for all the indices analysed. In the case of HI the mean Bias is around 104 degrees-day (it supposes at relative error of 4%), for the CI is had been appreciated a mean Bias of 0.16 ºC (corresponding to a relative error of 1.2%), the DI mean Bias is around -10mm (with a relative high error of 45% due to the simulation in very aridity places) and finally, the HyI has showed a mean Bias of -10 ºC*mm (it means a relative error of 0.2%).

3.2. Local future climate scenarios to predict bioclimatic indices

Figures R3.3, R3.5, R3.7 and R3.9 show the expected future evolution for HI, CI, DI and HyI, respectively, in absolute terms starting with the historical reference period (1976–2005) and followed by correlative periods of 30 years from 2011 to 2100 as presentation of short, mid and end-century expected values, which have been predicted based on the nine models (see Table R3.1) and according to the RCP4.5 (top row) and RCP8.5 (bottom row) scenarios.

In addition, the simulated results for the present (Historical period) are displayed to see the expected changes relative to the current state. In the supplementary material, the same information is represented, but in a categorised way (Figs S3.3, S3.5, S3.7 and S3.9).

To examine how the different DOs will be affected, Figures R3.4, R3.6, R3.8 and R3.10 show the expected future evolution for HI, CI, DI and HyI, respectively, considering exclusively those observatories that are located within some DO (Fig. R3.1). The DOs have been represented following a geographical order (north at the bottom of the figure-south on the top). The complementary material represents the same information but in a categorised manner (Figs. S3.4, S3.6, S3.8 and S3.10)

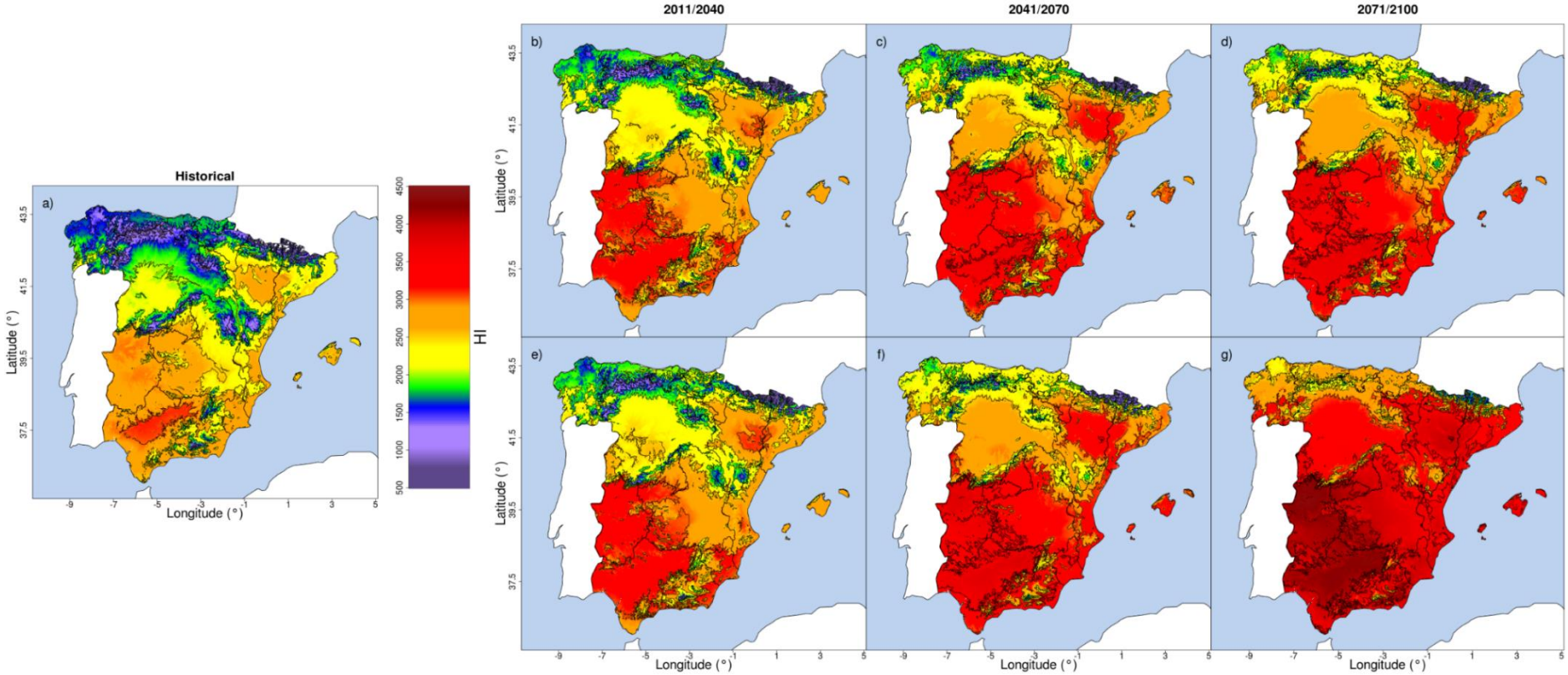

Figure R3.3. Geographical representation of the expected values of the Huglin Index (HI) for the periods 2011-2040, 2041–2070 and 2071–2100. Both emissions scenarios are represented: RCP4.5 (figures b, c and d) and RCP8.5 (figures e, f and g). Fig. R3.3a represents the Historical absolute temperature for the period 1976–2005

In general, all the indices analysed showed a main north-south spatial distribution and a secondary west-east distribution, which, although it fades, tends to remain throughout the twenty-first century.

The entire Iberian-Balearic territory tends towards warmer climates, so that a large part of the territory will show movements towards increasingly warmer HI categories (Fig. R3.3 and S3.3), especially in the last section of the twenty-first century and in the most extreme case of RCP8.5. The highest areas of the territory will go from too-cold climates to optimal climates for any type of grape variety. All ODs show progressive increases in HI throughout the twenty-first century (Fig. R3.4 and S3.4) as evidenced by the gradation of the red colours in the graphs. Although in terms of categorisation it seems that the different territories will not undergo heliothermic variations (as is the case of the DO of the southern territories such as Andalusia or Murcia, see Fig. R3.3 and S3.3), the absolute values reflect these changes perfectly (see Fig. R3.4 and S3.4).

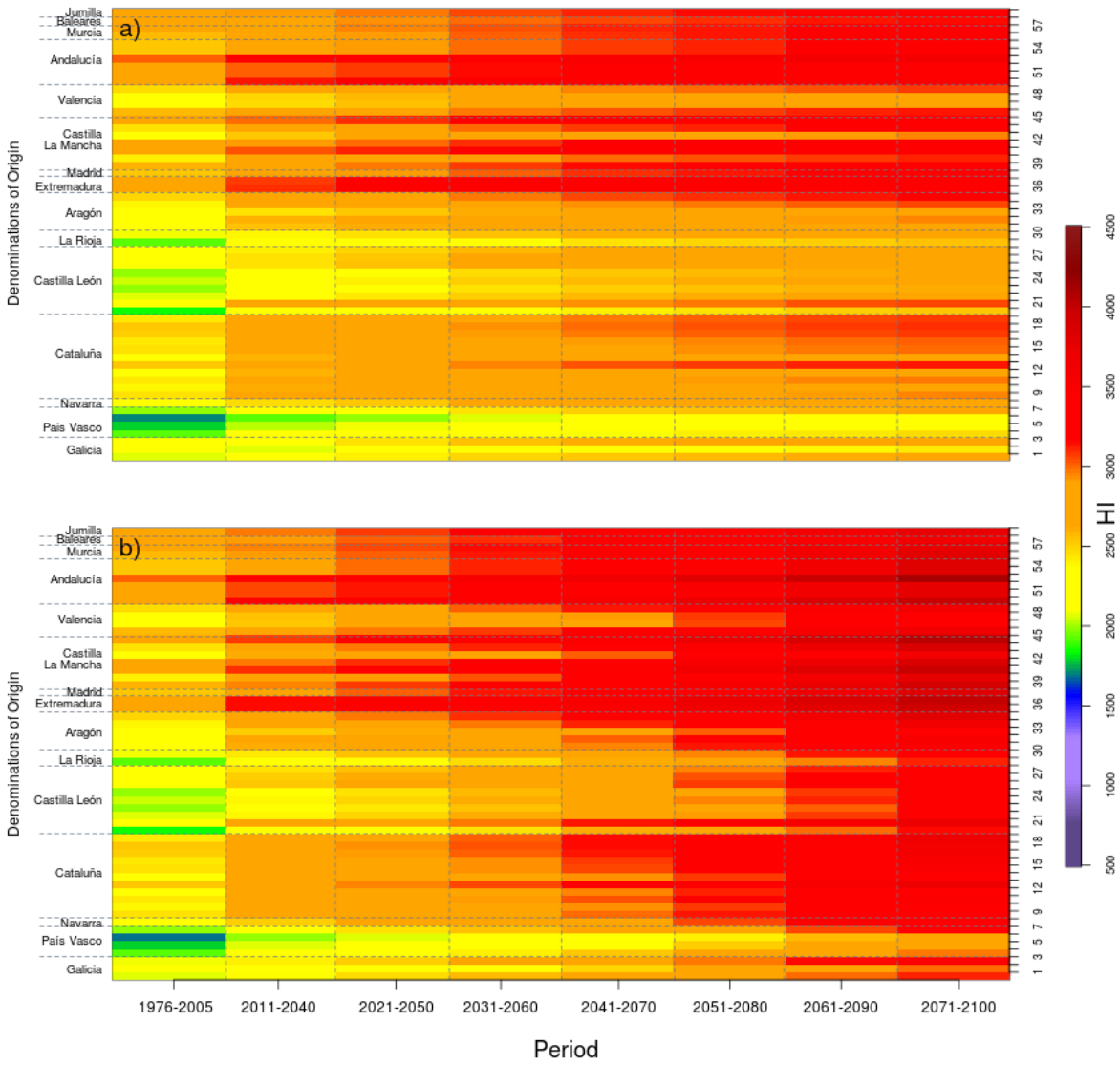

Figure R3.4. Evolution of the expected values of the Huglin Index (HI) for the defined Denominations of origin. Historical period 1976-2005 and 7 correlative periods of 30 years starting on 2011 are showed. Both emissions scenarios are represented: RCP4.5 (figure a) and RCP8.5 (figure b). Each row represents one DO (see Figure R3.1 for number identification) and each column represents a considered period.

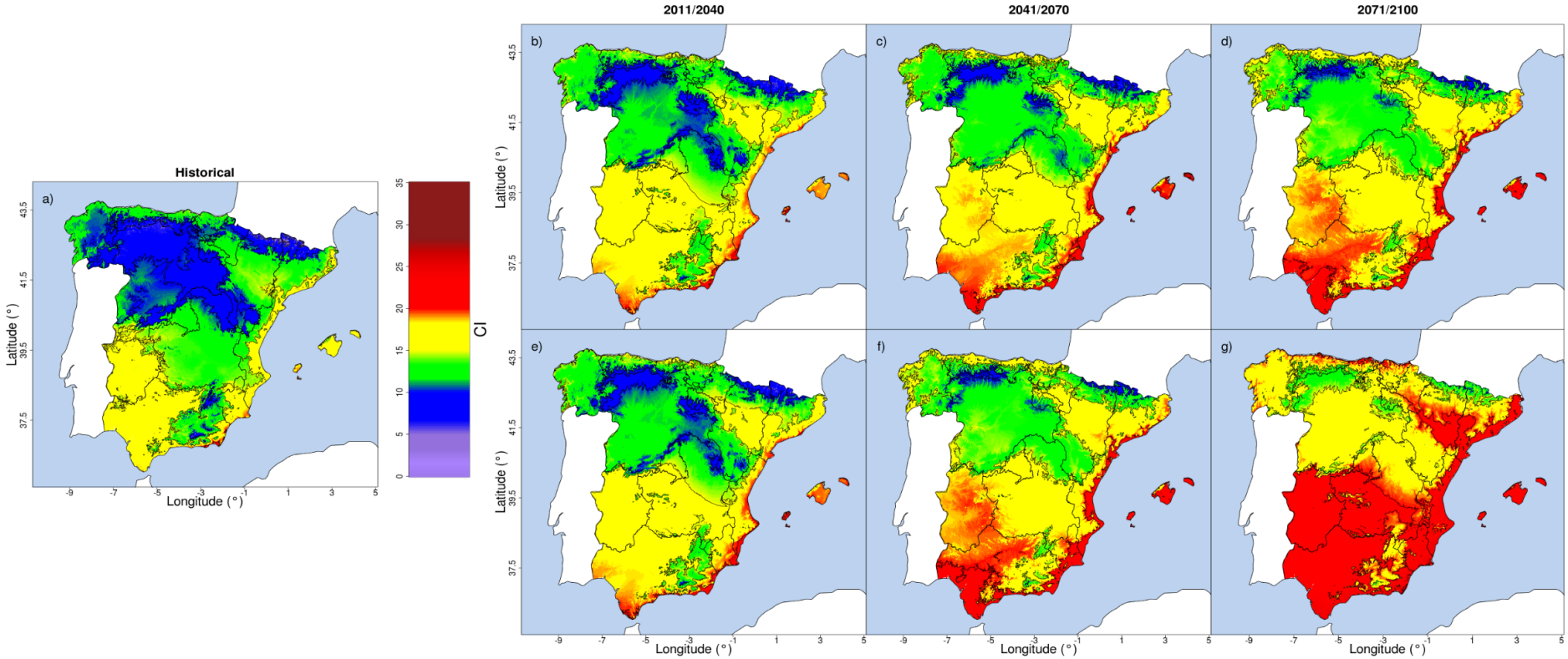

Figure R3.5. Geographical representation of the expected values of the Cool Index (CI) for the periods 2011-2040, 2041–2070 and 2071–2100. Both emissions scenarios are represented: RCP4.5 (figures b, c and d) and RCP8.5 (figures e, f and g). Fig. R3.5a represents the Historical absolute temperature for the period 1976–2005

Under the RCP4.5 scenario, the DOs of the País Vasco are those that start with the lowest HI values, remaining at the end of the century with average HI values. It is followed by the DOs of Galicia and Castilla y León, which gradually become warmer, and they will be the ones that change the most in categorisation throughout the twenty-first century. Under conditions of RCP8.5, the evolutions are much more pronounced, so that almost all DOs will be at the end of the twenty-first century under climates that are too hot, heliothermally speaking, for the cultivation of grapevine.

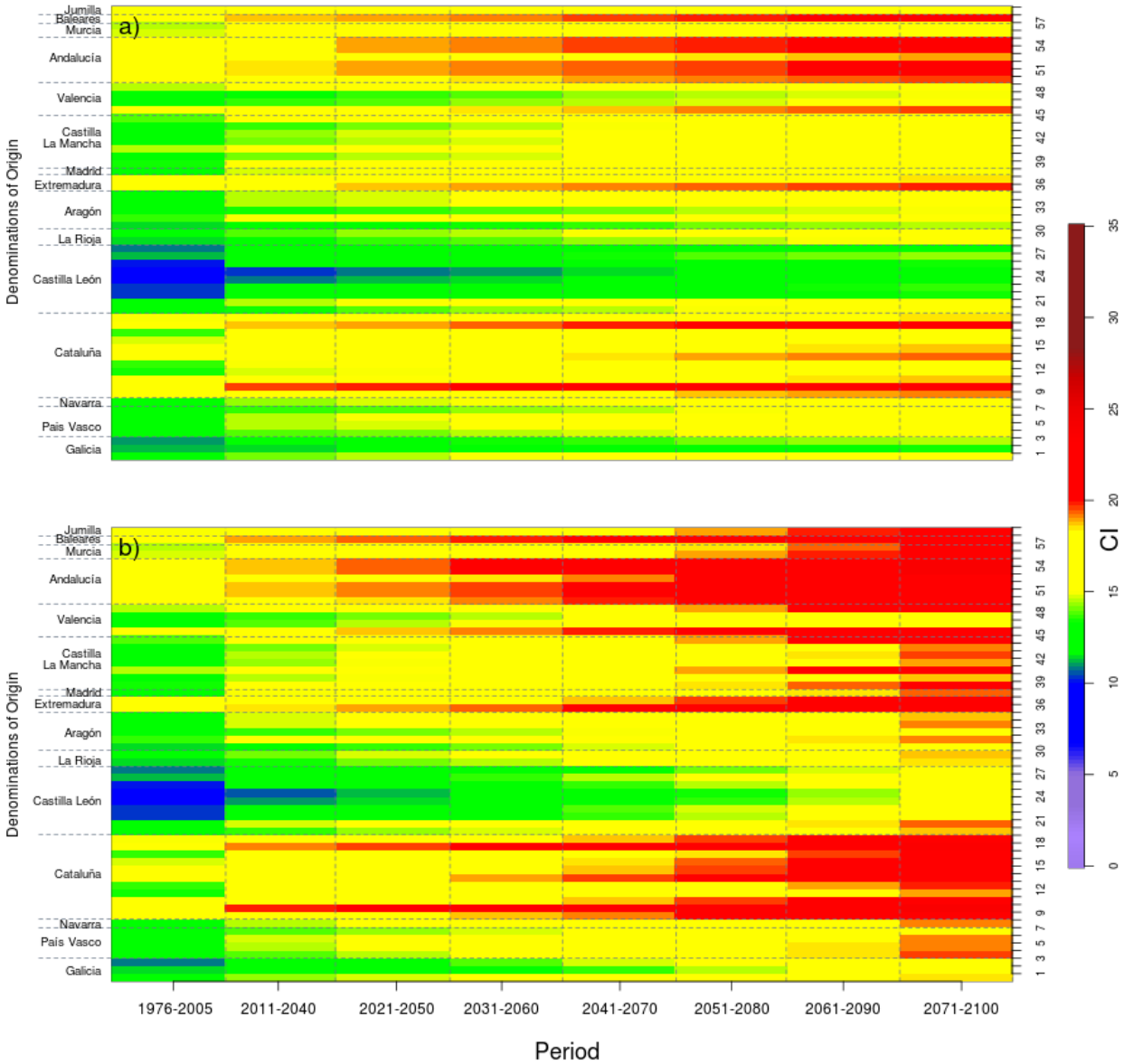

FigureR3. 6. Evolution of the expected values of the Cool Index (CI) for the defined Denominations of origin. Historical period 1976-2005 and 7 correlative periods of 30 years starting on 2011 are showed. Both emissions scenarios are represented: RCP4.5 (figure a) and RCP8.5 (figure b). Each row represents one DO (see Figure R3.1 for number identification) and each column represents a considered period.

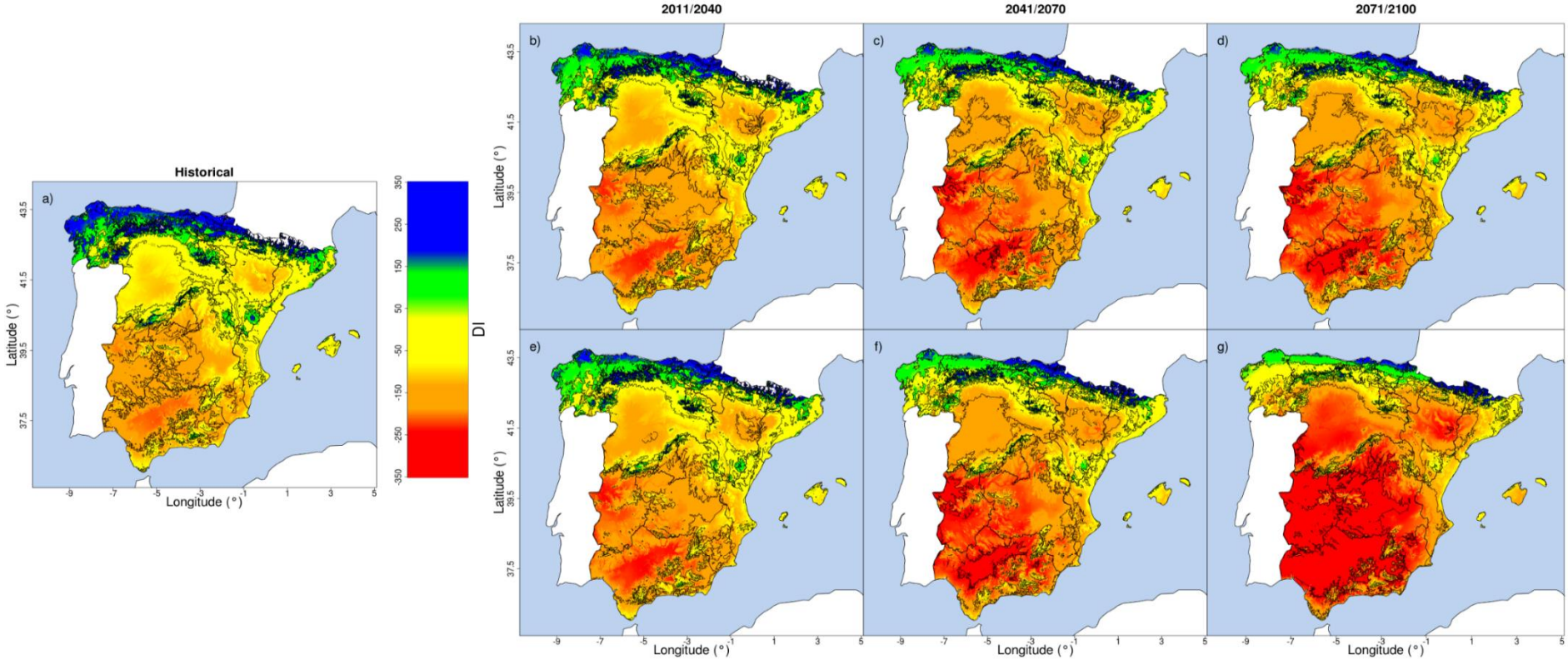

Figure 3.7. Geographical representation of the expected values of the Dryness Index (DI) for the periods 2011-2040, 2041–2070 and 2071–2100. Both emissions scenarios are represented: RCP4.5 (figures b, c and d) and RCP8.5 (figures e, f and g). Fig. R3.7a represents the Historical absolute temperature for the period 1976–2005

It is expected that the CI will increase throughout the twenty-first century in the entire territory studied by at least 1°C (Fig. R3.5 and S3.5), so that those regions that are at the upper limit of any of the categories pass to be included in the category immediately above. In general, all DOs are expected to vary between 3 and 4°C between current CI values and those expected at the end of the twenty-first century in the RCP4.5 scenario (Fig. R3.6a and S3.6b) and between 6 and 8°C under RCP8.5 conditions (Fig. R3.6b and S3.6b). The absolute values of the CI show how this index is expected to increase progressively throughout the twenty-first century. Under the conditions of RCP4.5, the DOs of Andalucía, Murcia and Cataluña are those that are expected to have higher CI values. Cooler nights in September are expected on the other side, for Euskadi, Castilla y León and Valencia.

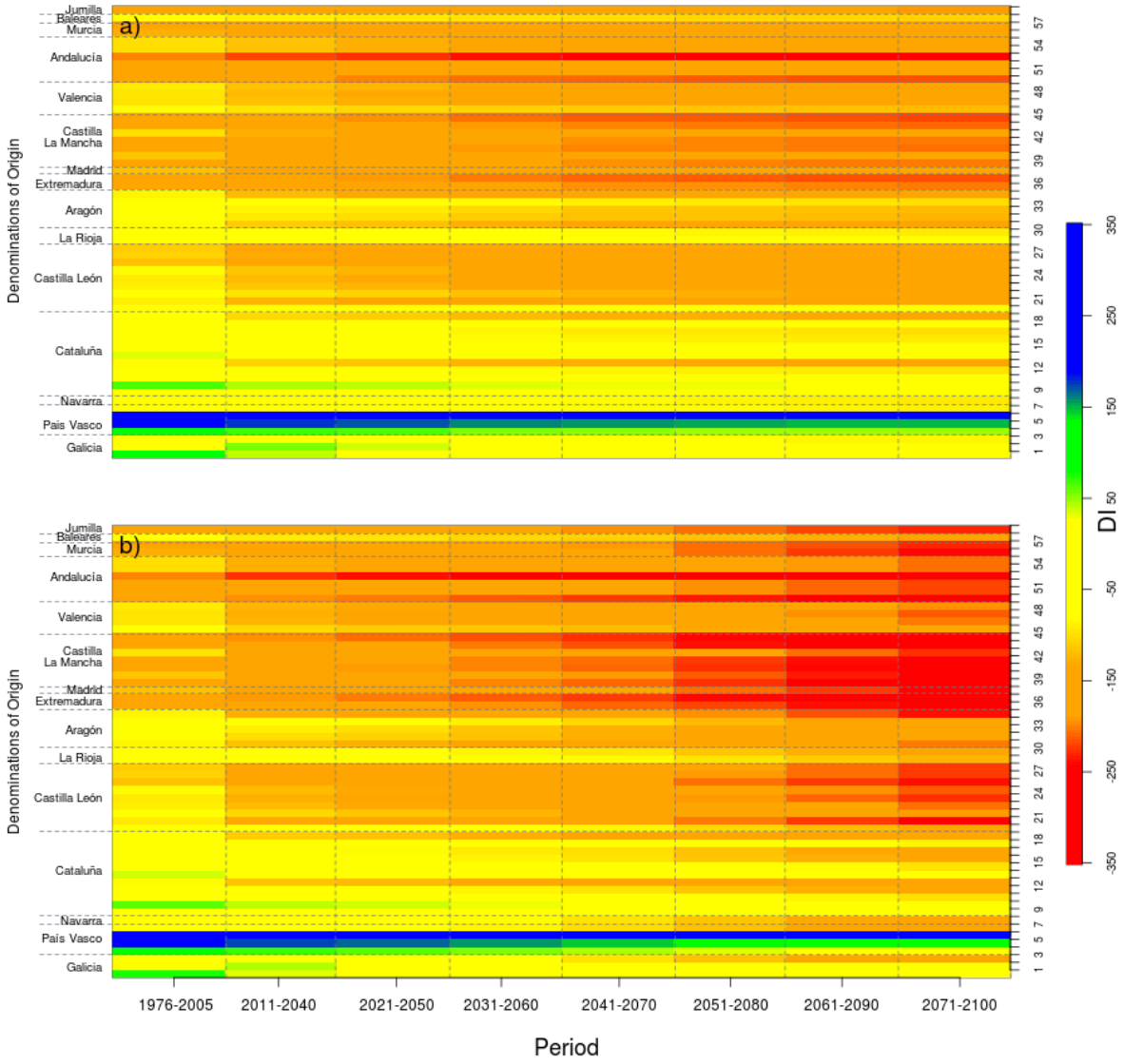

Figure R3.8. Evolution of the expected values of the Dryness Index (DI) for the defined DOs. Historical period 1976-2005 and 7 correlative periods of 30 years starting on 2011 are showed. Both emissions scenarios are represented: RCP4.5 (figure a) and RCP8.5 (figure b). Each row represents one DO (see Figure R3.1 for number identification) and each column represents a considered period.

In the future, it is expected that the DI tends to become increasingly dry values because of the increase in temperatures, and therefore of evapotranspiration, and that most of the peninsula and the Balearic Islands are at risk of water stress (Fig.R3.7 and S3.7). The northern and Mediterranean areas will be the ones that least accrue these changes, staying in humid or not very dry climates. The expected impact on the water balance (Fig. R3.8 and S3.8) shows that only the DO located in the País Vasco will maintain the status of a humid region in the coming decades. Most of the DO will remain at similar hydrological regimens, although the scenarios show a trend towards drier characteristics.

Although the HyI values increase in the coming decades, they remain within the range of medium risk of the presence of diseases such as mildew (Fig. R3.9 and S3.9). Most of the DOs (Fig. R3.10 and S3.10) will be at a low average risk of mildew presence throughout the twenty-first century. The DOs of Andalucía and Murcia are expected to present a low risk of the presence of mildew since their survival is not favoured due to the low precipitation. The DOs of the País Vasco, mainly, and those of Galicia will have the highest risk of suffering from mildew because of the increase in temperatures combined with the increase in the precipitation regime in these regions.

Finally, it is expected that in the coming decades the percentage of climatically optimal years will decrease throughout the territory (Figs. R3.11 and R3.12) a consequence mainly of variations in HyI and DI.

The analysed indices represent the expected changes in climatic characteristics associated with average variables and not with extreme events, such as extreme rainfall, drought or Heat/Cold Waves episodes. The latter, have a strong impact on the vine depending on the phenological stage of the vine at which they occur.

The increase in maximum temperatures will lead to a greater occurrence of heat wave episodes, as well as an increase in their duration, their average intensity and the maximum intensity reached within each heat wave episode (figures S3.13 y S3.14).

One of the most affected area will be the Mediterranean coast, where the average duration of a heat wave episode is expected to increase from 9-12 days to more than 18, increasing the average intensity and maximum intensity by 3-4°C. In the northern part of the Iberian Peninsula, although it will also suffer an increase in heat waves, this will be less pronounced than in the rest of the territory, with average increases in duration of 2-3 days and increases in intensity of 1-2 ºC. In the peninsular plateau and southern zone, the average duration of heat waves is also expected to increase by about 6 days (from 9 to 15 days in duration) with the increase in average and maximum intensity reached during these episodes (between 3-5 ºC) (see supporting information). These results are in line with the conclusions obtained by Molina et al., 2020 in the Mediterranean area, Torres et al., 2021 in the Balearic Islands and by Abaurrea et al., 2018 for the Iberian Peninsula.

The expected increases in minimum temperature will not prevent the occurrence of cold wave episodes (figures S3.15 y S3.16), although the average duration of cold wave episodes is increasingly shorter.

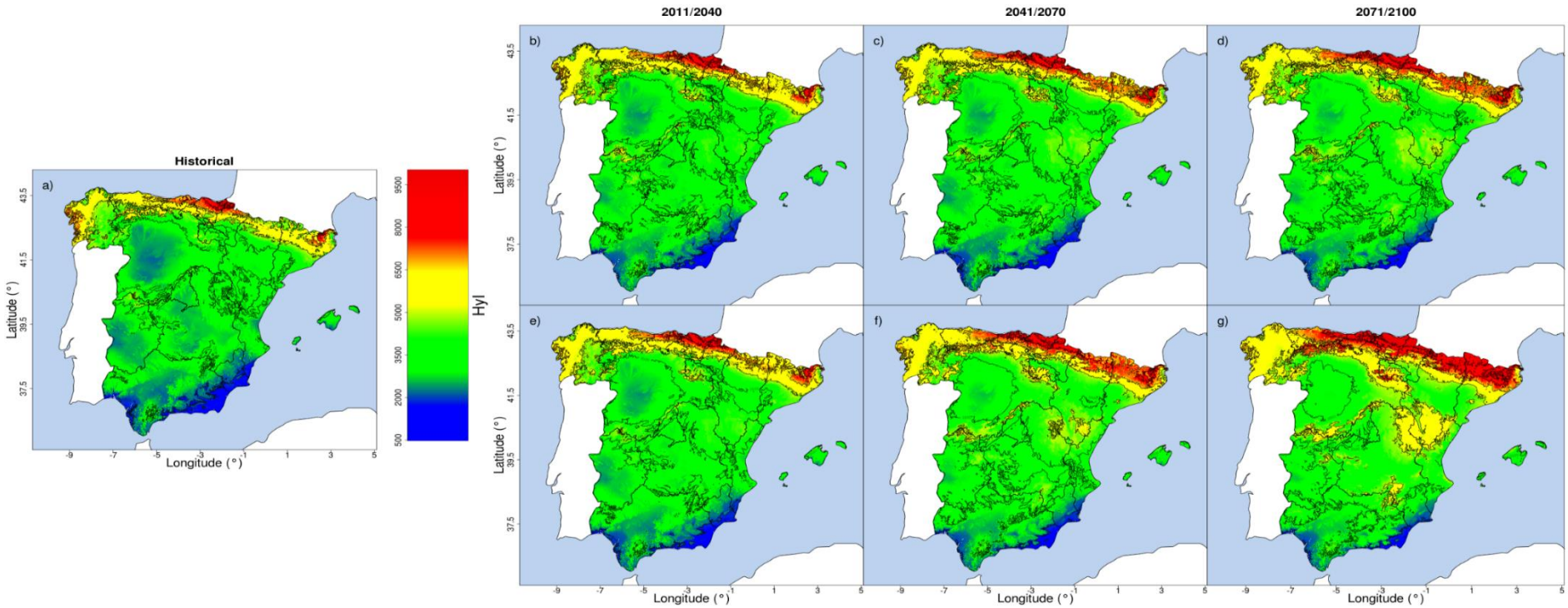

Figure R3.9. Geographical representation of the expected values of the Branas, Bernon and Levadoux Index (HyI) for the periods 2011-2040, 2041–2070 and 2071–2100. Both emissions scenarios are represented: RCP4.5 (figures b, c and d) and RCP8.5 (figures e, f and g). Fig.R3. 9a represents the Historical absolute temperature for the period 1976–2005

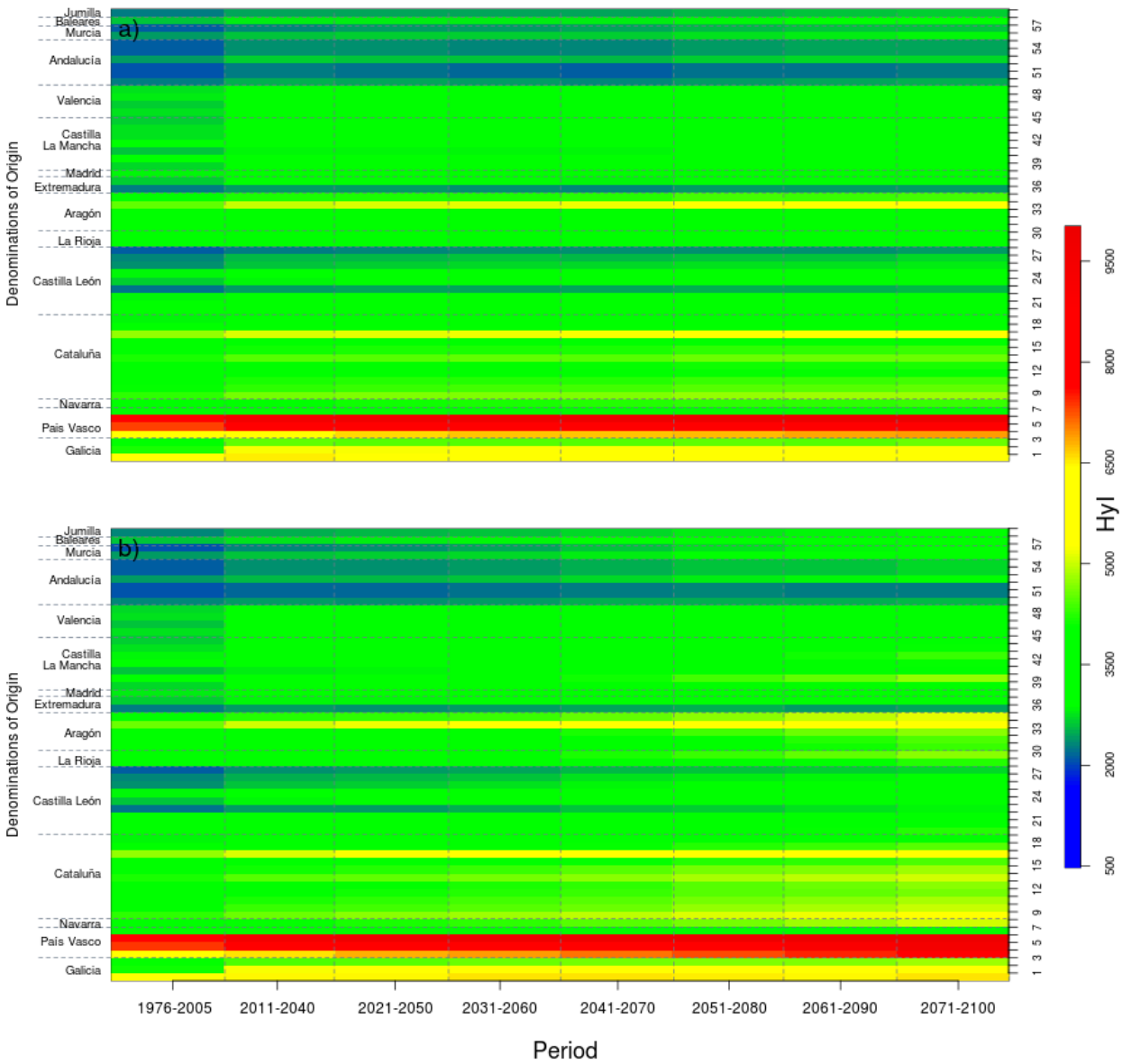

Figure R3.10. Evolution of the expected values of the Branas, Bernon and Levadoux Index (HyI) for the defined DOs. Historical period 1976-2005 and 7 correlative periods of 30 years starting on 2011 are showed. Both emissions scenarios are represented: RCP4.5 (figure a) and RCP8.5 (figure b). Each row represents one DO (see Figure R3.1 for number identification) and each column represents a considered period.

4. Discussion

This study analyses the evolution of climatic suitability for vine cultivation on the Spanish Mainland and the Balearic Islands based on a set of individual and combined bioclimatic indices using, for the first time, local future climate scenarios based on ESMs from the fifth IPCC report. In addition, the nine climate models available under two RCPs, provide a set of future climate projections of 18 possible future evolutions, which allows taking into account uncertainties, as recommended by various authors (Christensen et al., 2010; Fraga et al., 2014; Weigel et al., 2010).

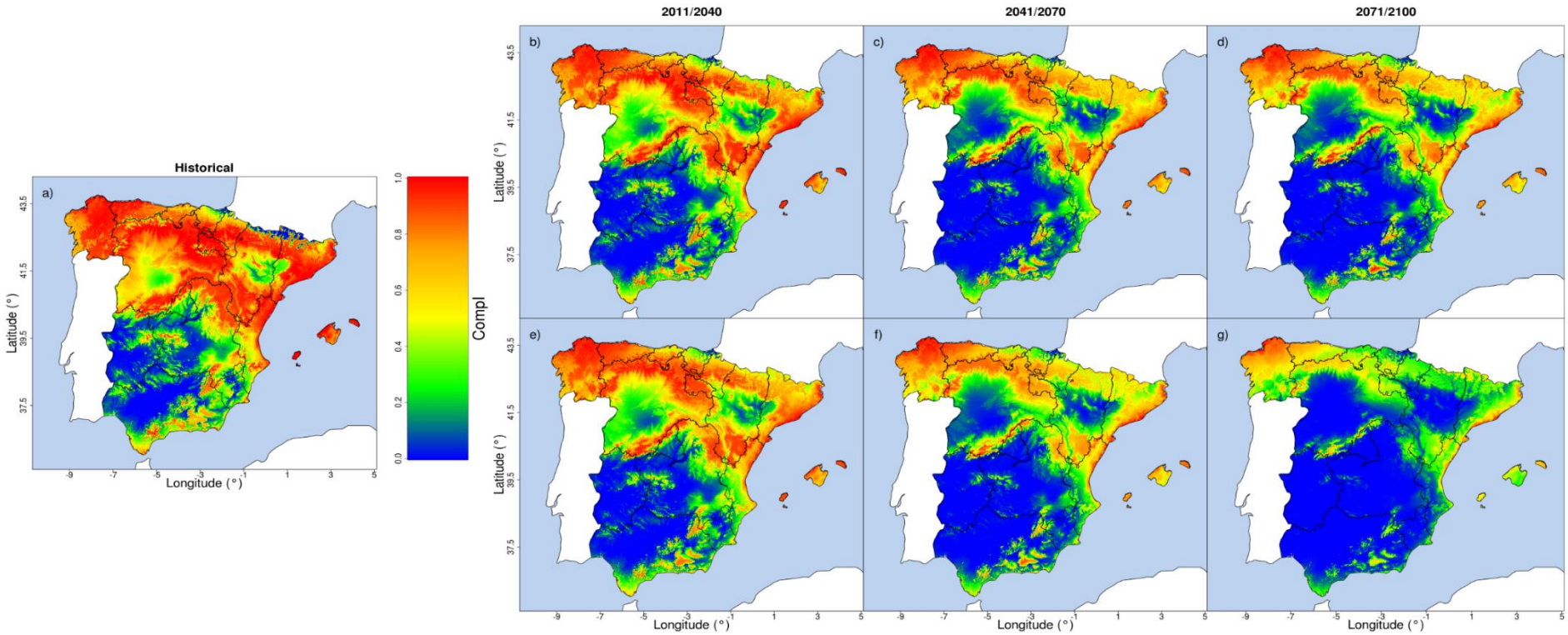

Figure R3.11. Geographical representation of the expected values of the Composite Index (CompI) for the periods 2011-2040, 2041–2070 and 2071–2100. Both emissions scenarios are represented: RCP4.5 (figures b, c and d) and RCP8.5 (figures e, f and g). Fig. R3.11a represents the Historical absolute temperature for the period 1976–2005

Moreover, there are strong differences in assessing climate impact at the regional or local level (Santos et al., 2012). Local studies allow us to establish the origin of the main differences between grape types grown in neighbouring regions as suggested by Ramos, Yones and Juste (2017) and which is evident in the results obtained when considering the future climate scenarios of the bioclimatic indices by denominations of origin. These results reinforce the importance that climatic conditions have on the genuineness and unique character of each designation of origin.

The generation for the first time of future scenarios of bioclimatic indicators of great interest for the wine sector for the 21st century at local scale (considering local microclimatic characteristics) with a wide set of future climate projections using ESMs from the fifth IPCC report, brings novelty to the studies existing so far in the sector.

Therefore, these results offer one of the best snapshots of future climate change, based on currently available data, and the risks that changes in temperature and precipitation regimes could cause in the way grapevines are cultivated.

4.1. Considerations about the simulation of bioclimatic indices

The future climate scenarios at the local scale used as a basis to generate the future scenarios of bioclimatic indices were developed by the FIC with a two-step analogue methodology (Ribalaygua et al., 2013a), which has been verified and validated in various studies in Spanish territory with very good results (Gaitan et al., 2019; Gaitan et al., 2020; Gutierrez et al., 2019; Monjo et al., 2016; Ribalaygua et al., 2013b). Therefore, the future temperature and precipitation scenarios on which the bioclimatic indicators are obtained are robust and reliable. Moreover, it should be noted that there are studies that reinforce the idea that daily changes in atmospheric conditions play an important role in plant phenology (Jones and Davis, 2000), and these changes can be more or less significant depending on the region where they occur. These aspects are considered intrinsically in the type of downscaling's methodology used in this study.

Another factor to consider is the benefits that an increase of CO_2 under future climate conditions plays an important role in the development of the vine (Bindi et al., 2001; Goncalves et al., 2009; Moutinho-Pereira et al., 2009). Although this study does not directly analyse this point, it is taken into account when considering different RCPs.

4.2. Local future climate scenarios of bioclimatic indices

In general terms, there is a positive trend in all thermal indicators (HI and CI) and a negative trend in the water index (DI). This reflects the twenty-first century with progressive increases in temperatures, both maximum and minimum, throughout the Iberian Peninsula, while hardly any changes in precipitation patterns are expected. The combination of the expected changes in both variables will have a strong impact on the vineyard. Similar results have been obtained for areas such as Portugal (Fraga et al., 2012), Italy (Bonfante et al., 2017, 2018), Germany (Neumann and Matzarakis, 2011; Stock et al., 2004), France(Duchene and Schneider, 2005, Duchene 2016, Garcia-Cortazar et at., 2017) and Spain (Gomez-Gesteira et al., 2011, Ramos 2017).

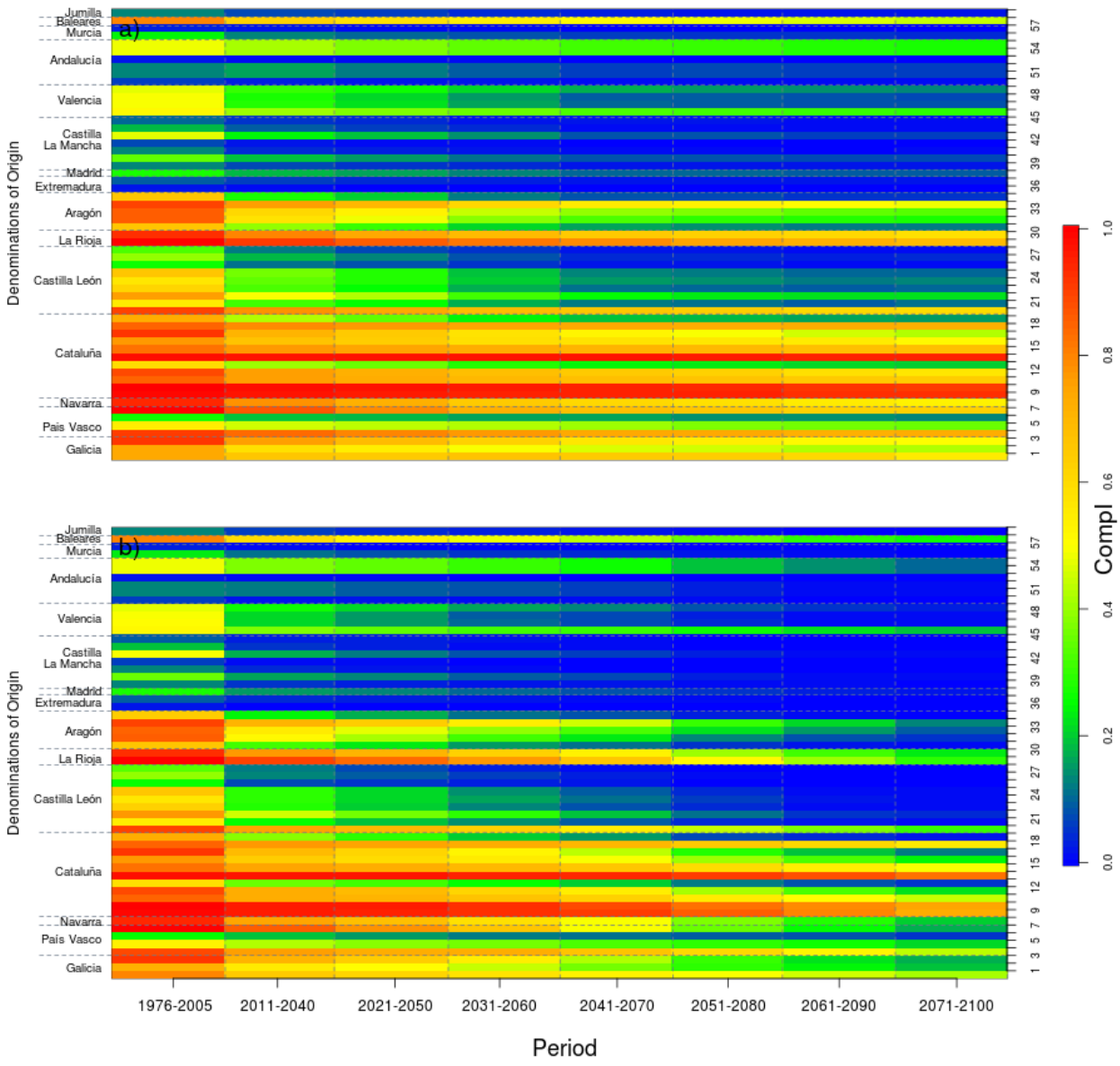

Figure R3.12. Evolution of the expected values of the CompI Index (CompI) for the defined DOs. Historical period 1976-2005 and 7 correlative periods of 30 years starting on 2011 are showed. Both emissions scenarios are represented: RCP4.5 (figure a) and RCP8.5 (figure b). Each row represents one DO and each column represents a considered period.

Consequently, although the northern regions will see their climatic suitability for growing grapes favoured, certain regions of the south and southwest of the Peninsula as well as the Mediterranean coast, that are at the limits of climatic suitability, may be negatively affected. These results confirm those obtained by (Fraga et al., 2012; Resco et al., 2016), among others.

The tendency of the HI values to increase is already in itself a determining factor of the variety of grape that can be grown in each zone since they determine the requirements for heat accumulation so that the ripening of the grape occurs optimally. The gradual change of the entire territory towards warmer climates will cause the necessary levels, in terms of heat, for the ripening of the grapes to occur at earlier times, which translates into an advancement of the ripening date (Molitor and Junk, 2019). This can subject vines to heat stress episodes in many regions. In addition, this index has a strong

correlation with the different phenological states associated with warm conditions(Bock et al., 2011; Jones et al., 2005; Santos et al., 2012) so its increase would imply overtaking of certain phenological properties, which would alter the phenological cycle of the vine.

In this way, in areas that are too cold (according to our results, the Pyrenees area will be the only one that presents these characteristics), only very early varieties could reach maturity, usually white varieties. These regions should opt for a hybrid or American varieties, more resistant than the *Vitis vinífera*, while in the cool regions (high elevation mountainous regions, (category 3) both white and red can be grown. As the climate becomes more temperate (categories 4 and 5, some regions of the northern Peninsula under RCP4.5 and very few areas of the North under RCP8.5), almost any type of grape such as 'Garnacha' or 'Moscatell' can be grown in the first case and 'Pinot Blanc', 'Pinot Noir' or 'Chardonnay' in the second.

The greatest impact will occur in hot or very hot regions (categories 6 and 7), most of the Peninsular territory and the Balearic Islands, where the minimum requirements that the different grape varieties need to ripen, including those with late-ripening, will be exceeded. In very hot climates, there is a high risk of stress due to heat accumulation that can be detrimental to grapevine (most of the study territory, especially under the RCP8.5 scenario). HI values in the northern peninsular plateau are expected to be lower than those expected under RCP4.5, while the southern plateau and the Balearic Islands will reach very high HI values, regardless of the scenario considered.

In addition, it must be considered that within the same category it may be that each variety has different heat requirements to reach maturity (Tonietto and Carbonneau, 1999) and that despite belonging to the same category they could not be cultivated. For example, the 'Cabernet Franc' variety requires an HI of 1800 cumulative degrees while the 'Cabernet Sauvignon' variety requires a HI of 1900 and the 'Ugni Blanc' variety needs a HI of 2000. Although their heliothermic requirements are different, both would be in HI Category 4. Therefore, if we only consider categorised values, we can run the risk of selecting varieties in areas that do not reach the necessary calorific requirements for said variety, hence the need to work with absolute values.

Regarding the CI, the expected increase in minimum temperatures will cause the CI to increase so that in some regions the night coolness necessary for optimal grape ripening will not be achieved. In addition, the advancement of the ripening dates suggests the need to evaluate this index on dates before September (Ramos et al, 2021).

Changes towards very cold night temperatures can have a positive effect on certain varieties of grapes as long as a sufficient heliothermic contribution is guaranteed to guarantee a good level of ripening of the berries. It is not expected that any study region will experience decreases in CI under RCP8.5, but in the case of RCP4.5, areas of the Pyrenees and the Cordillera Cantabria will remain cold at night throughout the twenty-first century.

In those regions with fresh or medium CI values (such as what is expected to occur in most of the Southern Plateau, according to RCP4.5, and in the Northern Plateau, under both RCPs), the results can be both positive as well as negative depending on the cultivated variety, as the late varieties ripen in colder conditions than the early ones.

Finally, if the CI values are higher than 18°C (as will be the case of the Atlantic and Mediterranean coast and the Balearic Islands if RCP4.5 is considered or of the entire Southern Plateau plus the regions previously mentioned according to RCP8.5), the vines can suffer an excess of heat that affects the colour and aromatic potential of the grape.

The changes in the expected DI values condition the region's water supply and, therefore, determine the decisions to be made regarding irrigation. In the entire Iberian-peninsular territory except for the Cantabrian coast and the Pyrenees, regardless of the RCP considered, the DI values will decrease to the lower limit of 50 mm, so these territories will be at the lower limit of water supply, which may give rise to certain restrictions, especially in the summer months. If DI values < –100mm, the region will be excessively dry, requiring an extra water supply.

On the contrary, values higher than 150 mm (as could occur in the areas of the Pyrenees or the Bay of Biscay) can reduce the quality of the wines and have higher quality grapes in wet years.

Intermediate DI values (between 50 and –100 mm) that are expected in regions such as Galicia or Asturias, will suffer certain periods of drought that can become favourable during ripening.

The joint assessment of these indices through the MCC System allows establishing a more complete climatic vision of the suitability of the region. Of all the possible combinations, those that are more suitable for grapevine cultivation are those that combine HI values (categories HI-3, HI-2, HI + 1), CI (categories, CI + 1; CI +2) and DI (categories DI-1, DI + 1). While the least optimal have turned out to be those with CI (categories CI-2, CI-1) and DI (categories DI + 2, DI + 3). In the particular case of this study, it is expected that the optimal regions under this criterion will be found in the north of the peninsula, such as the Cantabrian Mountains and the Pyrenees, as well as in almost the entire Northern Plateau (according to both RCPs in the middle of the century). However, the Northern Plateau will only maintain these conditions under RCP4.5. These results are in line with those obtained by other authors (Fraga et al., 2013; Resco et al., 2016).

The combination of moderately low night temperatures with high daytime temperatures in these areas will favour the production of high-quality wines since the synthesis of some phenological components is favoured.

Regarding Hyl, no major changes are expected in the risk of certain diseases such as mildew, but there may be many differences between regions with very different precipitation patterns. The southern regions have a lower risk, which gradually rises to the north where precipitation will be more abundant during the vine growing season, similar to what other authors found (Fraga et al., 2013; Lazoglou et al., 2018).

The results obtained in the CompI index may seem contradictory since the largest Spanish wine-growing regions, such as Andalusia and Castilla-La Mancha, have a very low percentage of optimal years for growing vines. Similar situations have been found in other studies (Guido, 2015). This is because they are dry regions or with strong periods of drought with DI values < –100 mm, while one of the conditions to consider a climatically optimal year is that the DI > –100mm. The results of this index must be interpreted in the light of multiple socioeconomic factors that determine the success of a

vineyard plantation beyond the climatic conditions. For example, in these regions, this situation is solved by viticultural producers through different management strategies and water management, which allow solving this “climatic problem” and taking full advantage of the rest of the climatic characteristics that favour grapevine. Other factors such as the type of cutting used, the orientation of the vineyard, the field management tasks, the type of soil, among others, will be keys to adapting to the challenges posed by climate change (Alexandrei et al., 2013).

It should also be kept in mind that rising temperatures due to climate change may have indirect effects on these crops, as they are expected to cause an increase in tropospheric ozone concentrations and are also likely to affect the chemistry of ozone precursors (NOx, CO, CH_4, NMHC) (Isaksen and Wang, 2002). This modification of atmospheric pollutant generation can be very detrimental to vineyards. For example, it has been suggested that ozone can cause a loss of productivity and a reduction in the sugar content of grapes (Ascenso et al., 2021). Increased exposure to SO_2, NO_2 can cause a severe reduction in photosynthetic rate, transpiration and stomatal conductance in shoot growth (Popescu et al., 2012).

To all these effects must be added the impact of extreme phenomena, especially heat waves. Heat waves (see figures AR1.5 and AR1.6) combined with summer drought will be the most common abiotic stress combination in the Mediterranean area (Hannah et al., 2013). The response of grapevines to increased temperatures (acceleration of their key phenological stages affecting grape quality and the properties of grape organoleptic components, such as sugar accumulation, pH, acidity, color, aroma and flavor) (Ramos et al., 2008, Leoni et al., 2019), is likely to increase with heat waves and will also depend on its coincidence with grape ripening (Sgubin et al., 2018).

In more humid areas, as the northern part of the Peninsula, new growing areas may become viable, for example in areas of higher altitude (Ramos and Martinez de Toda, 2021) or closer to the coast (Santos et al., 2020a), while low elevation areas would probably be suitable for lower quality varieties, producing wines of high alcohol content (Moriondo et al., 2007).

In almost all the territory (where a significant intensification of heat wave episodes is expected, see support information) all adaptation options must be considered if current crops are to be maintained, such as water application, row orientation or canopy cover. Water availability is the factor, along with high temperatures, that most affects vine development (Fraga et al., 2018, Fraga et al., 2019). In these areas where irrigation water is not available or is too warm, such as the Guadalquivir Valley or Extremadura, it will not be possible for the vines to mature normally, so it will be necessary to make substitutions towards varieties more tolerant to the new climatic conditions (Ramos et al., 2008). The search for adapted grapevine (*Vitis vinifera* L.) varieties will be a priority in the coming years, either through germplasm collections or genetic improvement processes (Duchene et al., 2012).

At the other extreme, cold wave episodes can be especially damaging to primary buds (Gu et al., 2002), although there are not expected to be considerable variations in the average and/or maximum intensities of such episodes in Spain (figures AR1.7 and AR1.8).

Finally, an adaptive evolution with physiological modifications of the wineyard could be expected (Ramos and Martinez de Toda, 2021) especially in those areas where climatic extremes are not so intense or so frequent, as in the northern part of the Peninsula. The adaptation of each variety under the same climatic conditions depends on the peculiarities of each genotype to heat, light or water deficit and the temperature and humidity conditions needed for ripening. The varieties with earlier phenology will be probably the most affected as was described for the Spanish variety "Tempranillo" (Ramos and Martinez de Toda, 2020).

The literature highlights different biochemical, physiological and molecular acclimation mechanisms that grapevine is able to develop in order to adapt to climatic stresses. Changes in photosynthetic efficiency and in the control of electrolyte loss through stomata appear to be frequent mechanisms of adaptation (Zha et al., 2018). For example, adjustment of photosynthesis to elevated temperature has been detected in some cases (Gallo et al., 2021; Kizildeniz et al., 2021). Site-specific stomata and vein traits modulation have been suggested as an acclimation strategy that may influence photosynthetic yield (Damiano et al., 2022). Increasing the heat dissipation capacity by changing the response of its stomata has also been proposed as an adaptation to warmer climatic conditions, since keeping them open allows heat dissipation by evaporative cooling (Costa et al. 2012). Significant changes in the expression pattern of metabolic pathways related to metabolism and hormones have also been detected (Duchene et al., 2012; Kovaleski and Londo, 2019). This opens up opportunities to identify the genetic and physiological traits that make a variety more or less resistant and select varieties which would be suitable to replace the more sensitive ones even in the most affected areas such as those in the south or in the central zone of the country. In Ronda (Málaga, South of the Spain), Petit Verdot (originally from Bordeaux), whose long phenological cycle is perfectly adapted to warm climates, is producing good results in recent experiences. In Extremadura (Southwest of the Spain), Portuguese varieties such as Trincadeira or Touriga National are also being successfully cultivated. In Ribera del Duero (central area of Spain) there is a growing interest in growing Malbec (traditionally grown in areas of Castilla-La Mancha and Castilla y León above 1000 meters) to accompany Tempranillo (traditionally accompanied by Cabernet).

Another option is to include new sub-varieties within a variety rooted in the area, as is the case in the region of Murcia (South of the Spain), where the cultivation of four new Monastrell grape varieties (Gebas, Myrtia, Calnegre and Calblanque), which are more resistant to the new climatic conditions, has recently been approved.

However, the process of incorporating new varieties is complex, not only because it depends strongly on local characteristics (to the meteorological-climatic context must be added the type of soil, orientation, slope of the land and investments in irrigation or other adaptive technologies, among others), but also because it is subject to the legislation in force in each area and the long process involved in incorporating a new variety in a region from which it does not originate.

4.3 Relevance of the results

The results obtained in this study show how the Iberian peninsular territory is one of the wine-growing regions most sensitive to the impact of climate change, not only because of the significant variations in the values obtained in the study, especially in those

dependent thermal indices, but also because these variations place the region within the optimal thermal limits for growing vines. Other European regions such as France and Italy are also expected to suffer variations in their climatic conditions with implications for the vineyard, but the expected impact is not estimated to be as marked (Fraga et al., 2013), and the regions in Northern Europe will even benefit from the expected climate changes (Hannah et al., 2013).

Alterations in climatic requirements (heliothermic and hydric) have a strong impact on the final organoleptic characteristics (sugar, acidity, colour, etc.) of the grape and the characteristics of the wine. Spain has a long viticultural tradition, its wines being recognised worldwide precisely for the characteristics of the wines belonging to each DO, maintaining those own characteristics is of vital importance to guarantee the continuity of the DOs.

Currently, there is a shortage of agricultural models for grapevine (Bindi et al., 1996) or for the quality of grapevine (Webb et al., 2008) as well as tools to support decision-making (Iglesias et al., 2012; Santos et al., 2012). There are some soil suitability models (Escariz et al., 2007) and cereal modelling (STICS, BRIN, WANG04) that combined with a good observed phenological database (Mosedale et al., 2016) and climate projections such as those presented in this study, which would considerably facilitate the adaptation of the wine sector to climate change.

The results obtained can be a starting point to review and update certain factors that under new climatic conditions may be altered. As an example, currently in Spain, only those varieties that are in the register of Commercial Varieties of the Vine of Spain can be cultivated and for the control of plantations the List of Authorised, Recommended and Plant Conservation Varieties is used, both listings could be altered due to new climatic conditions.

The results of this study should be complemented with other limiting factors (White et al., 2006) such as orientation, latitude, longitude, altitude, topography and proximity to water areas as well as orientation and exposure; characteristics that, together with the properties of the soil, the management practices and the iterations between all the factors that make up the system provide grapevine and wine with unique qualities that differentiate them, even within the same DO where different grape varieties, soil types, and field characteristics may coexist. Although these factors play an essential role in the wine creation process, they do not pose as great a challenge as the climate (van Leeuwen et al., 2004), an aspect on which this study was focused.

Finally, the great variety of grape types that are grown in Spain because of the great climatic diversity of the territory, and its long viticultural tradition makes it possible for the studies to be replicated in other regions with very similar climates.

This study has focused on presenting the average climatic conditions that the wine sector will face in the coming decades, allowing winegrowers to have a snapshot of the new changes they will have to face. Therefore, the impacts that some extreme events (such as extreme rainfall, hail, droughts, among others) may have on the sector in the coming decades have not been included. Following this study, it is necessary to go a step further by assessing the impact of extreme events as well as the impact on the phenological stages of the vine through relationships between these and meteorological variables.

On the other hand, future studies should be carried out in the small parts of the island territory not included in this study, such as some iberian-balearic DOs as well as the Canary Islands.

4.4. Conclusions

Our results offer a precise and rigorous picture of the impacts that climate change will cause on the grapevine crop in the Iberian Peninsula based on currently available data applying a set of six bioclimatic indices and using, for the first time, local future climate scenarios based on ESMs from the fifth IPCC report and working locally.

The Iberian-peninsular territory will be the wine-growing region most sensitive to the impact of climate change in the twenty-first century as reflected by the results obtained for the different indices, especially those dependent on thermal and hydric conditions. Progressive increases in temperatures are expected, both maximum and minimum, as indicated by the thermal indicators (HI and CI), while the water shortage (DI) will be more pronounced. The combination of the expected changes of both variables will have a strong impact on the vineyard, modifying the final organoleptic characteristics in the best of cases, but also leaving a large part of the Iberian Peninsula within the optimal thermal limits for growing vines, which it may have dramatic results for grapevine growing

The northern and mountainous areas of the peninsula, having climatic characteristics colder and wetter than in the south, are expected to benefit from climatic variations that will allow them to adapt to climate change in a positive way, either by changing the grape variety or by regulating the water supply, among other measures. The central and southern areas of the peninsula (with strong periods of water scarcity and high temperatures) will have problems in maintaining certain types of grape and tillage techniques. They will not reach the minimum water requirements and will exceed the thermal requirements that the different grape varieties need to ripen. Therefore, these territories will be forced to rethink vineyard management techniques that allow them to counteract these negative effects or assess the economic viability of continuing to cultivate vineyards in the same regions.

These results provide valuable information for decision making in this sector to develop adaptation measures to climate change at the local scale.

Material suplementario Resultado 3

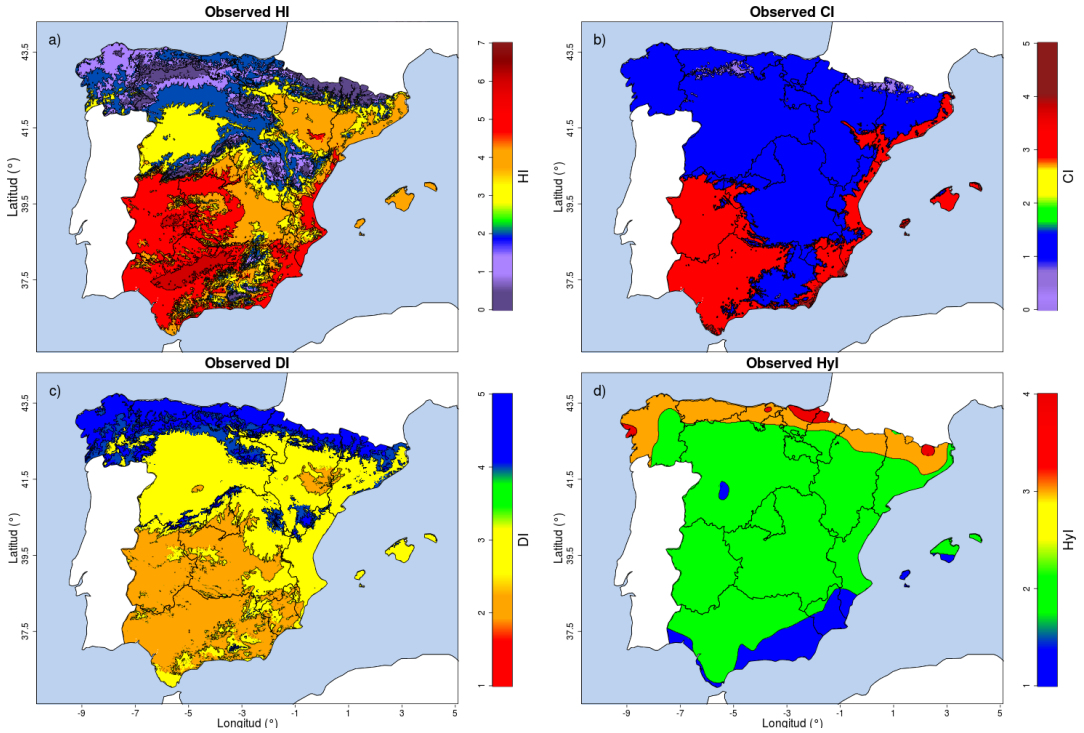

Figure S3.1. Geographical representation of the observed categorised values of the a) Huglin Index (HI), b) Cool night Index (CI), c) Dryness Index (DI) and d) Branas, Bernon and Levadoux Index (HyI) for the periods 1971-2000.

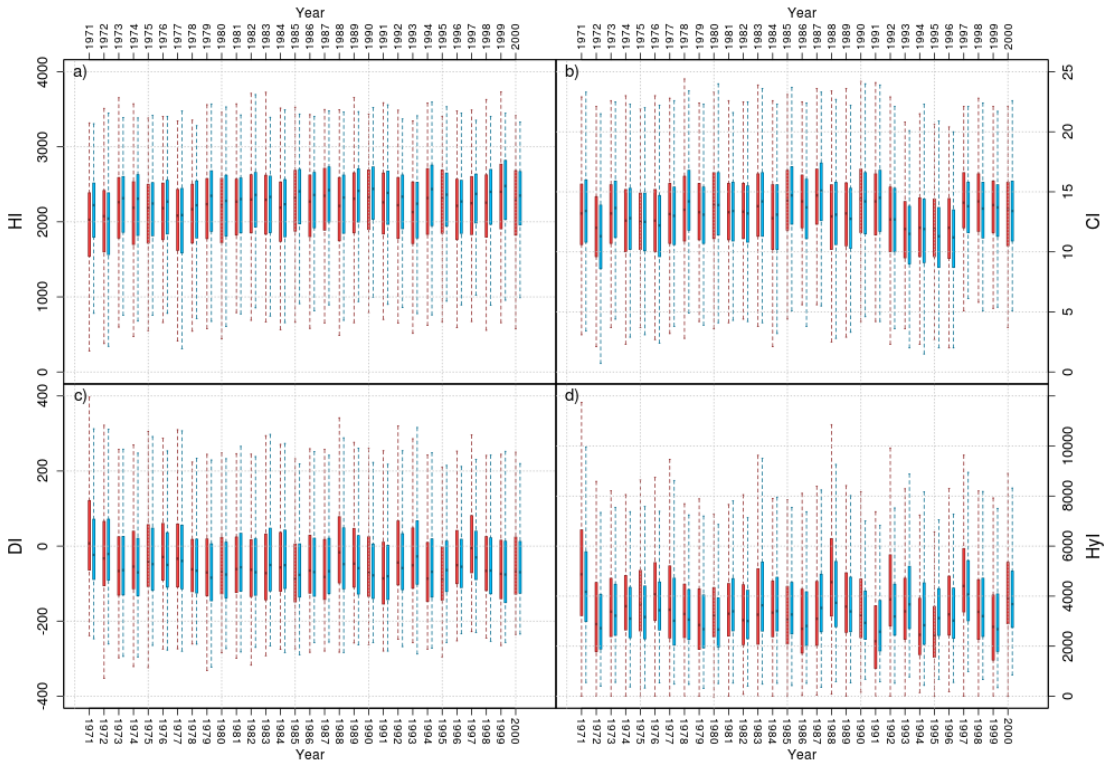

Figure S3.2. Results of the verification process for the a) Huglin Index (HI), b) Cool night Index (CI), c) Dryness Index (DI) and d) Branas, Bernon and Levadoux Index (HyI) for the periods 1971-2000. Boxplots in red correspond to the calculation of the indices based on observed data and boxplots in blue corresponds to the calculation of the indices based on Era40 downscaled data. Boxplots containing data from all observatories used in the study.

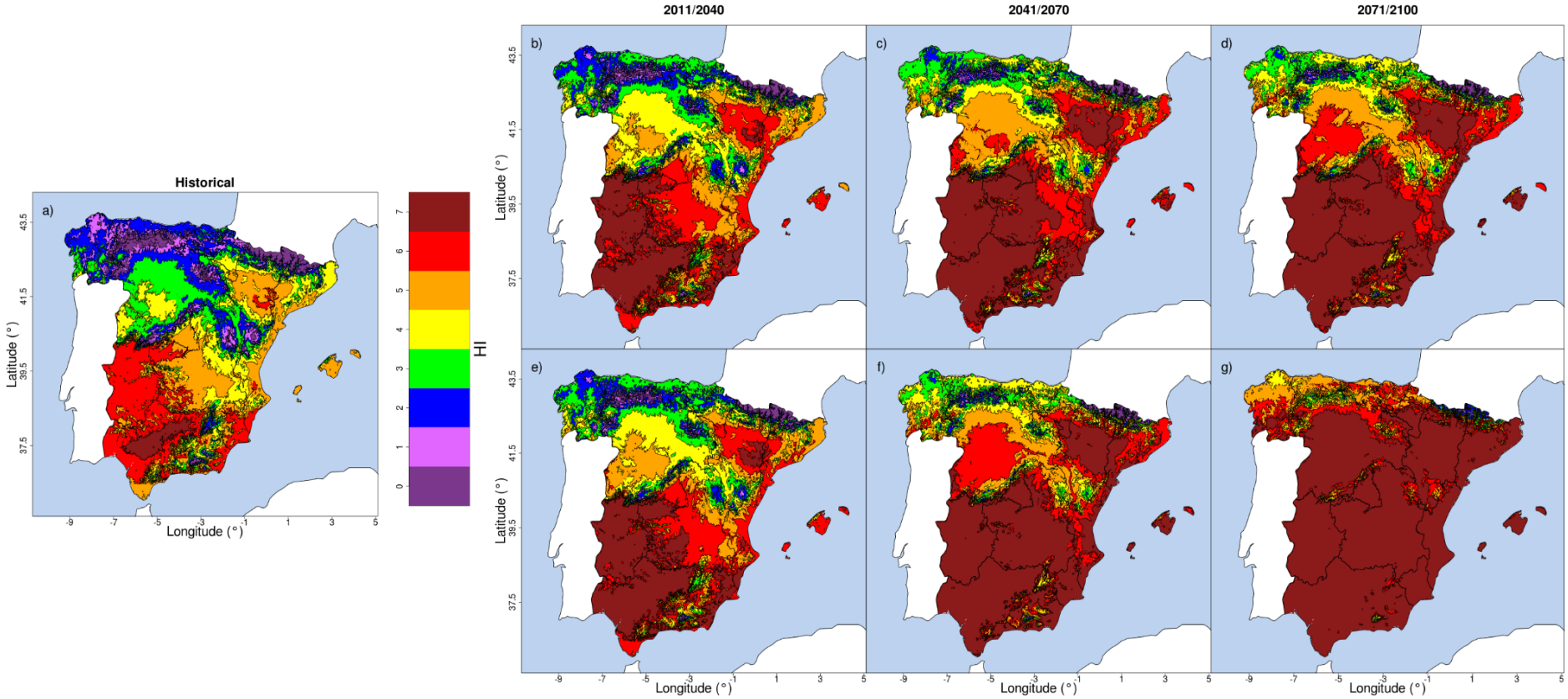

Figure S3.3. Geographical representation of the expected values of the Huglin Index Categories (HI) for the periods 2011-2040, 2041–2070 and 2071–2100. Both emissions scenarios are represented: RCP4.5 (figures b, c and d) and RCP8.5 (figures e, f and g). Fig.S3a represents the Historical absolute temperature for the period 1976–2005

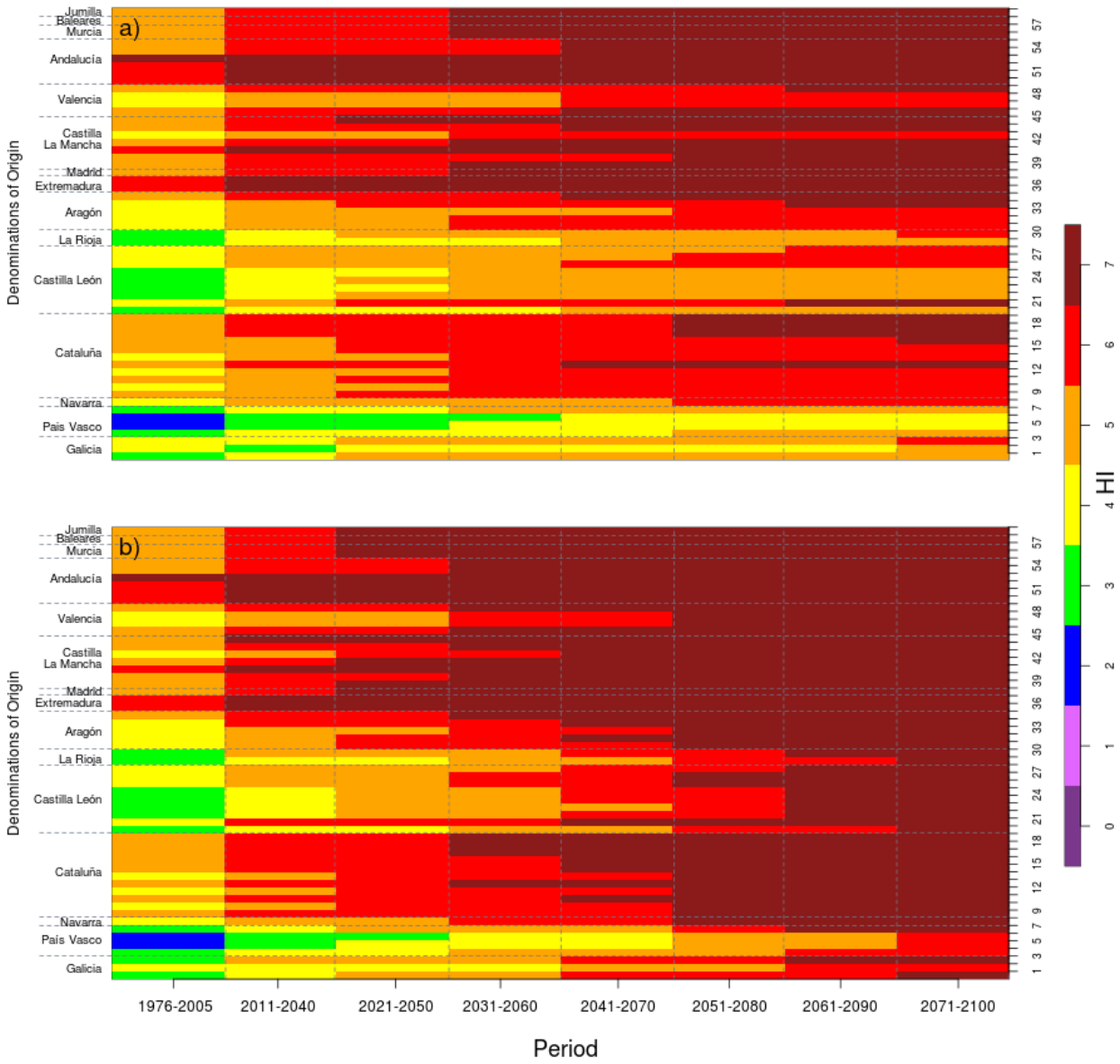

Figure S3.4. Evolution of the expected values of the Huglin Index Categories (HI) for the defined DOs. Historical period 1976-2005 and 7 correlative periods of 30 years starting on 2011 are showed. Both emissions scenarios are represented: RCP4.5 (figure a) and RCP8.5 (figure b). Each row represents one DO (see Figure 1 for number identification) and each column represents a considered period.

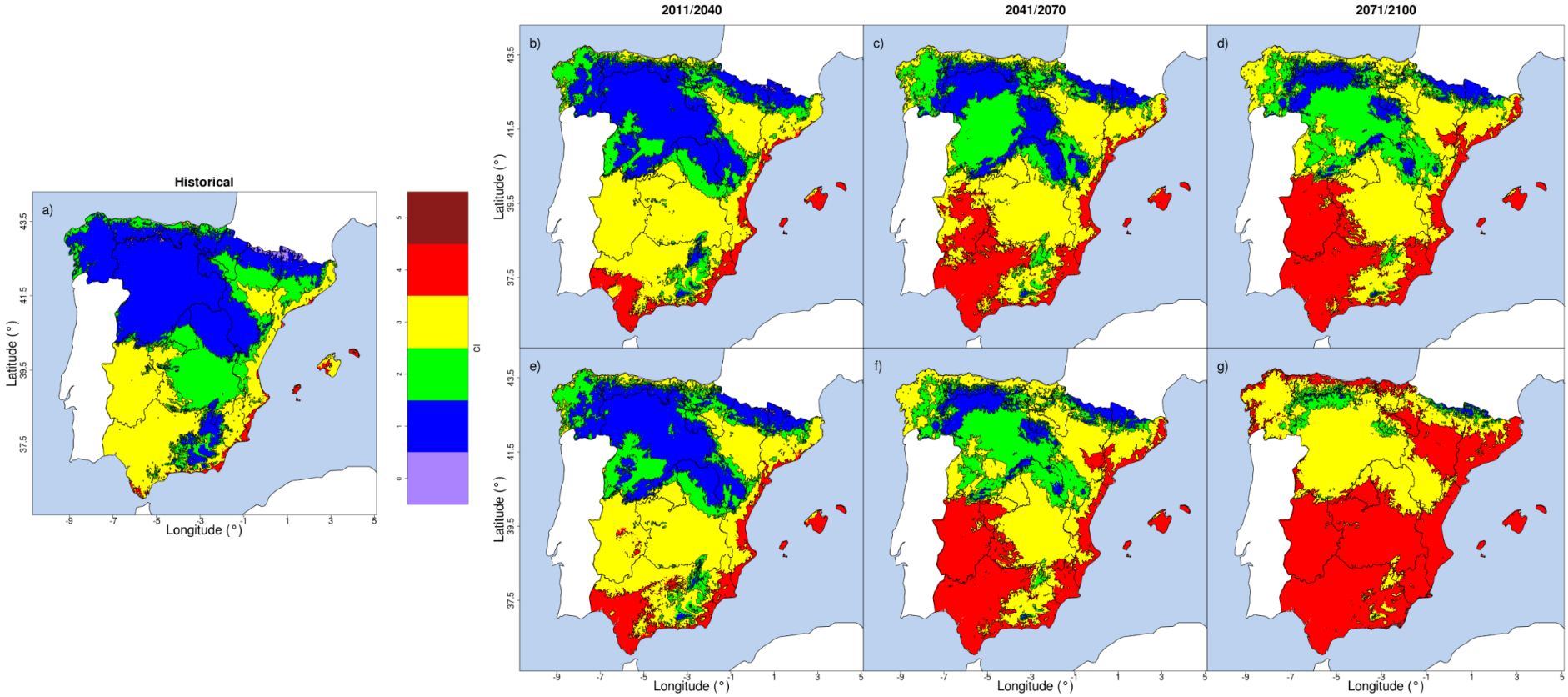

Figure S3.5. Geographical representation of the expected values of the Cool Index Categories (CI) for the periods 2011-2040, 2041–2070 and 2071–2100. Both emissions scenarios are represented: RCP4.5 (figures b, c and d) and RCP8.5 (figures e, f and g). Fig. S5a represents the Historical absolute temperature for the period 1976–2005

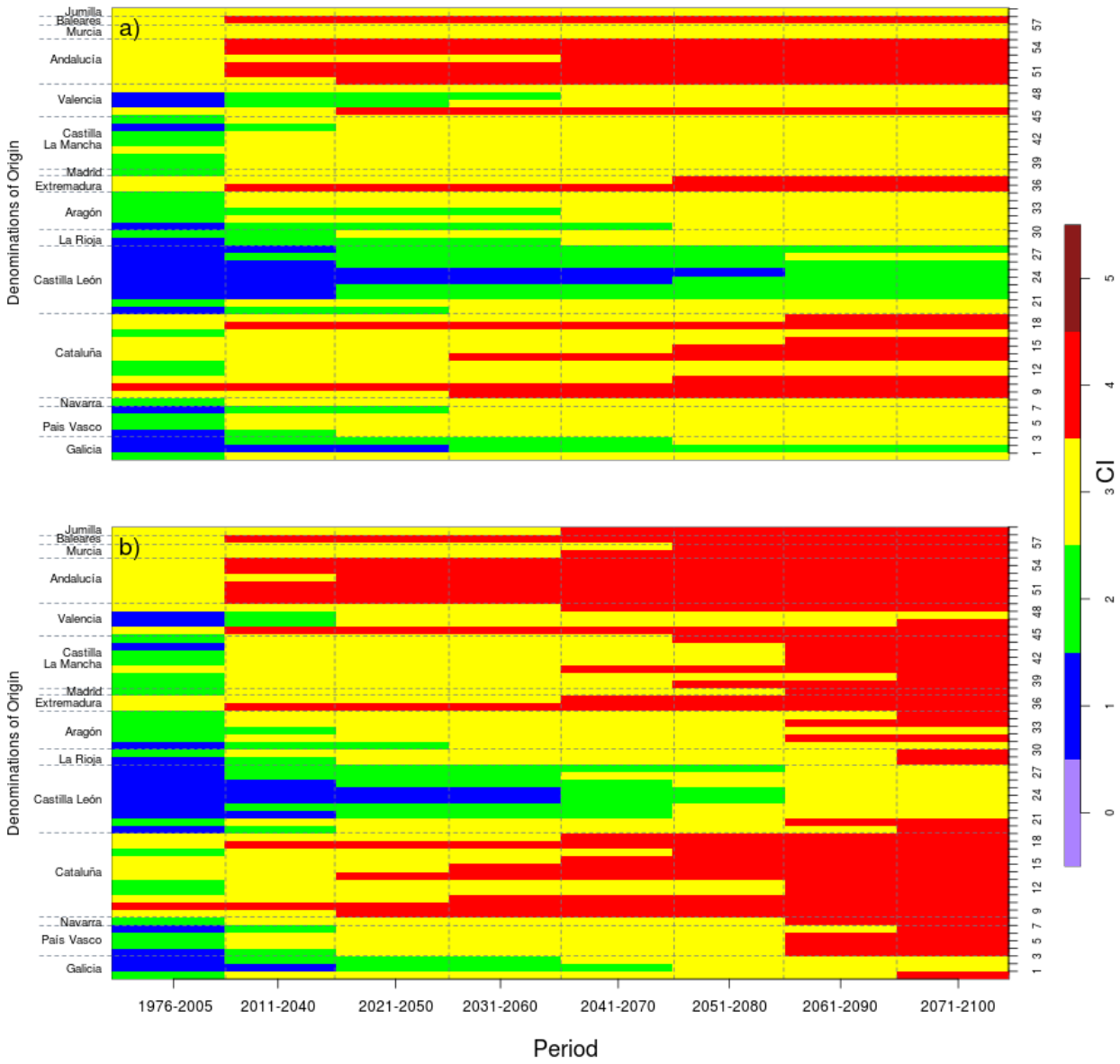

Figure S3.6. Evolution of the expected values of the Cool Index Categories (CI) for the defined DOs. Historical period 1976-2005 and 7 correlative periods of 30 years starting on 2011 are showed. Both emissions scenarios are represented: RCP4.5 (figure a) and RCP8.5 (figure b). Each row represents one DO (see Figure 1 for number identification) and each column represents a considered period.

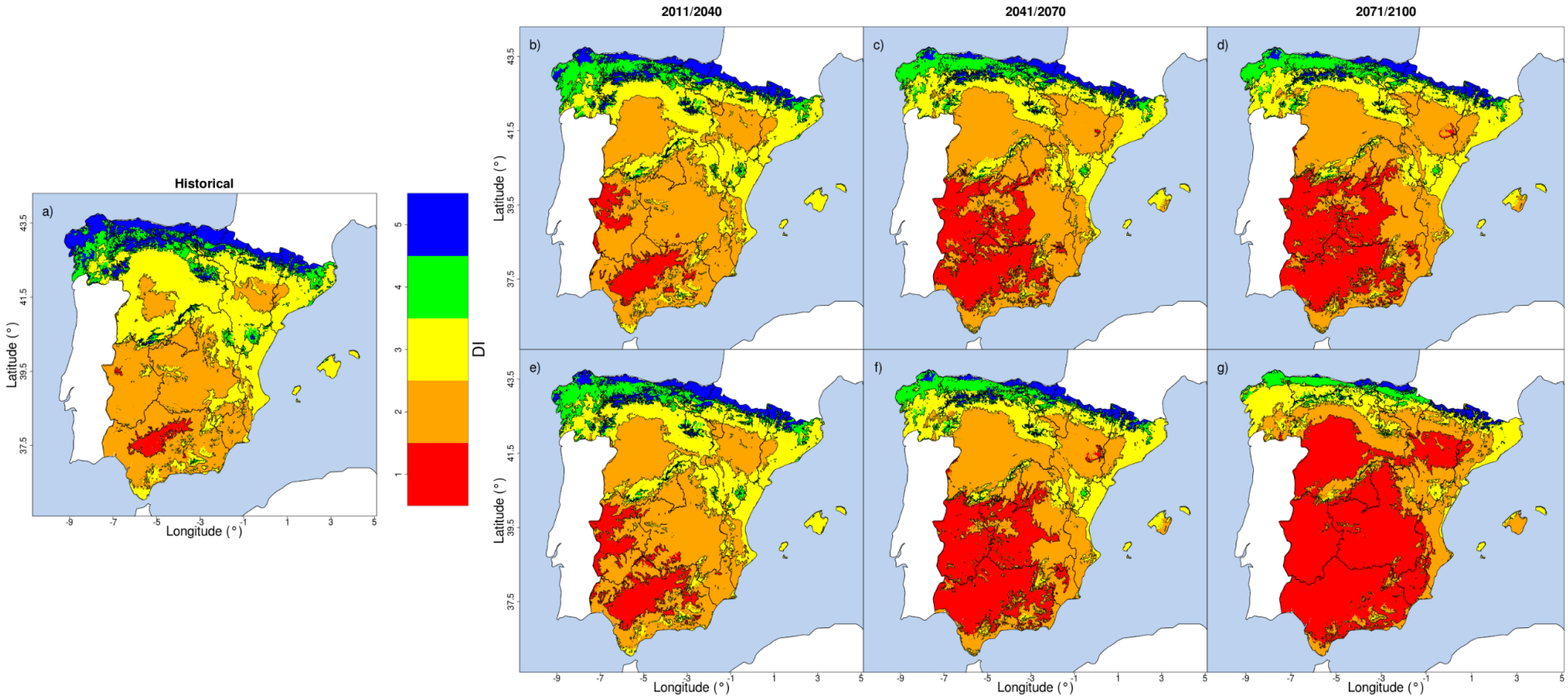

Figure S3.7. Geographical representation of the expected values of the Dryness Index Categories (DI) for the periods 2011-2040, 2041–2070 and 2071–2100. Both emissions scenarios are represented: RCP4.5 (figures b, c and d) and RCP8.5 (figures e, f and g). Fig. S7a represents the Historical absolute temperature for the period 1976–2005

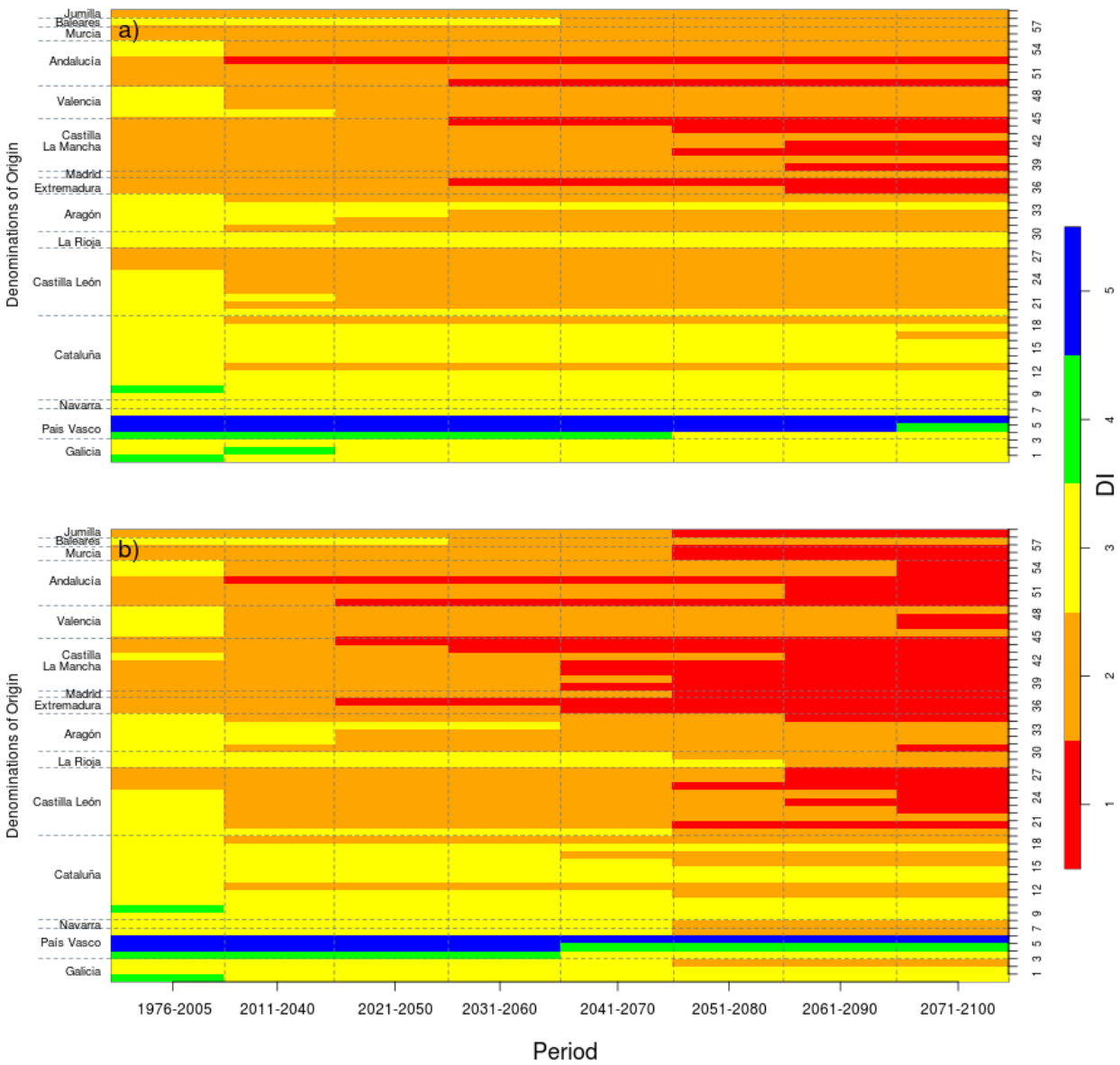

Figure S3.8. Evolution of the expected values of the Dryness Index Categories (DI) for the defined DOs. Historical period 1976-2005 and 7 correlative periods of 30 years starting on 2011 are showed. Both emissions scenarios are represented: RCP4.5 (figure a) and RCP8.5 (figure b). Each row represents one DO (see Figure 1 for number identification) and each column represents a considered period.

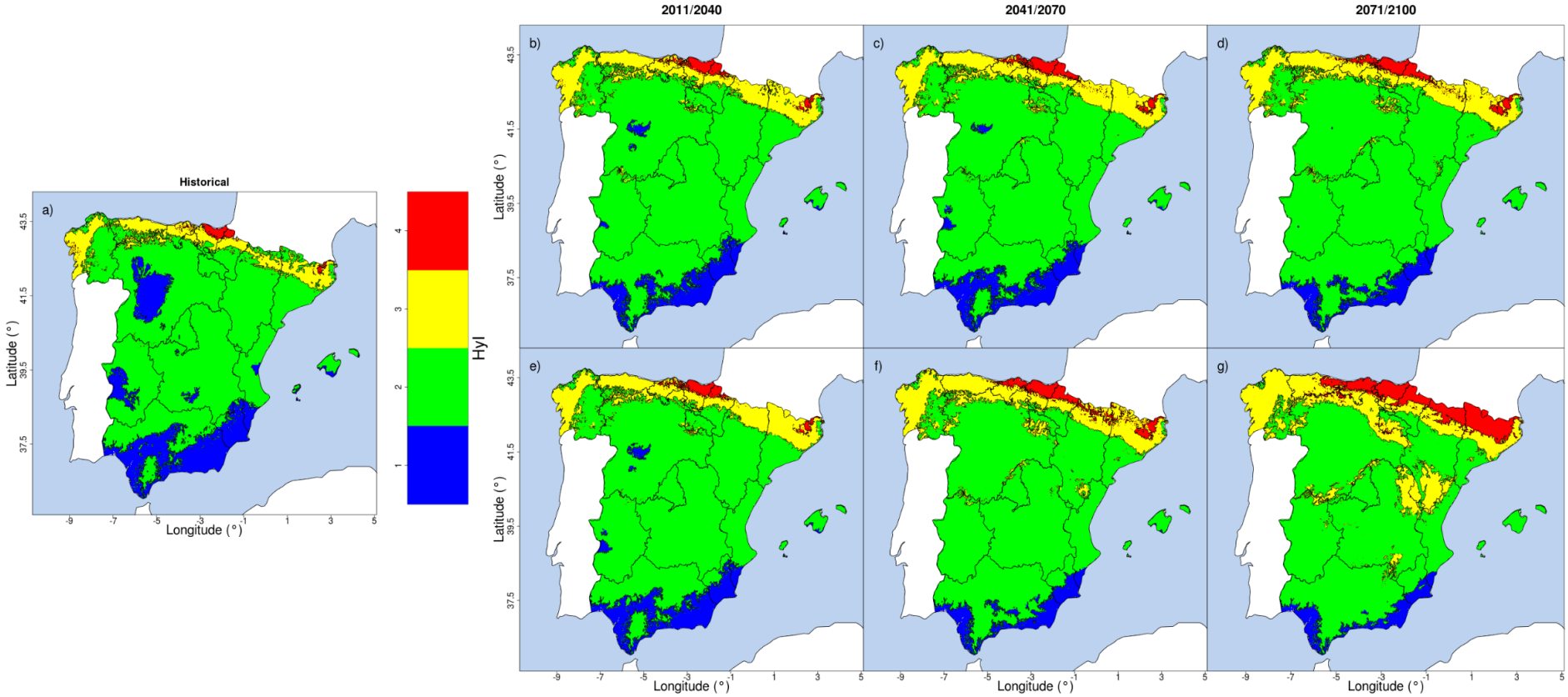

Figure S3.9. Geographical representation of the expected values of the Branas, Bernon and Levadoux Index Categories (HyI) for the periods 2011-2040, 2041–2070 and 2071–2100. Both emissions scenarios are represented: RCP4.5 (figures b, c and d) and RCP8.5 (figures e, f and g). Fig. S9a represents the Historical absolute temperature for the period 1976–2005

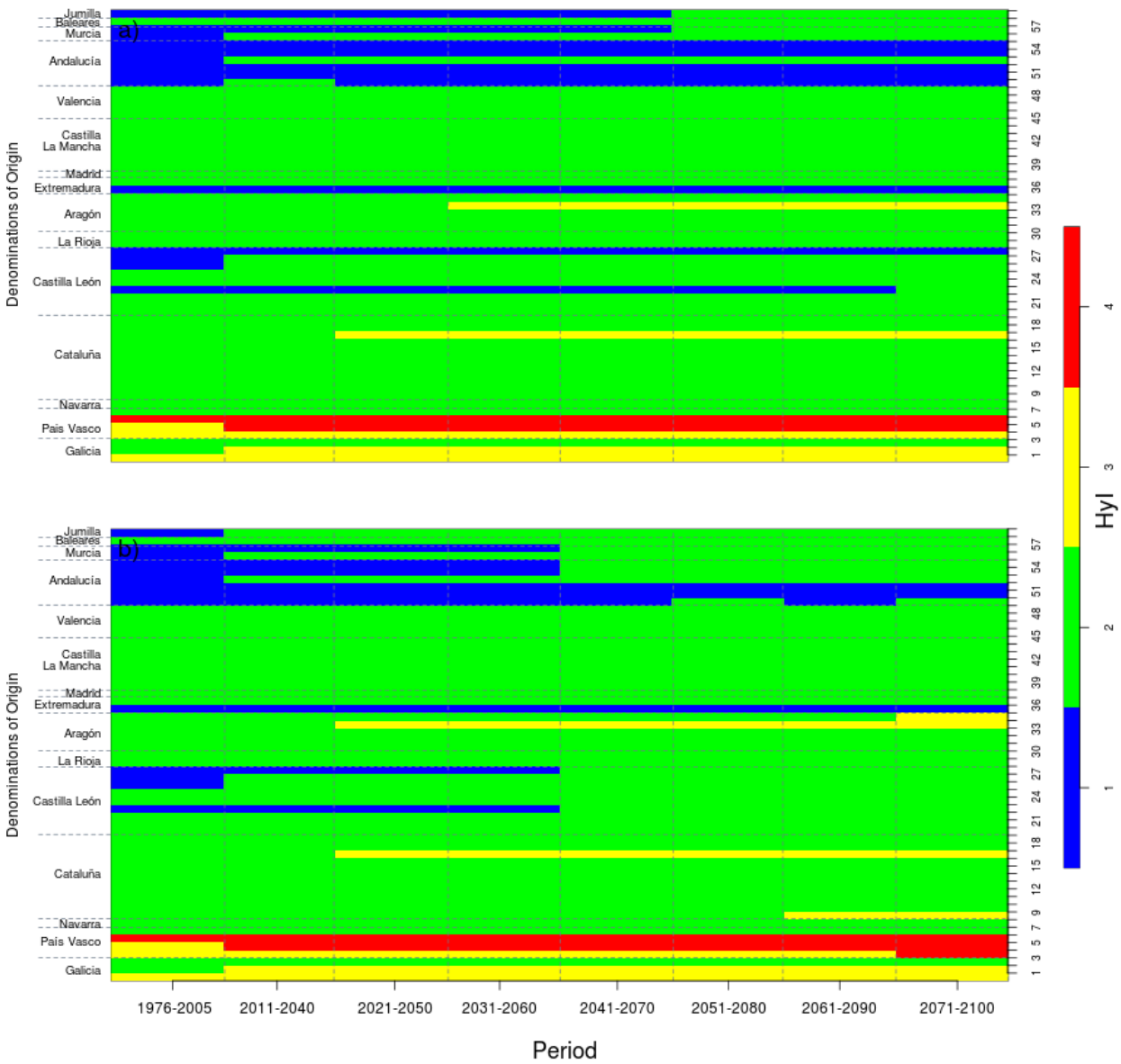

Figure S3.10. Evolution of the expected values of the Branas, Bernon and Levadoux Index Categories (HyI) for the defined DOs. Historical period 1976-2005 and 7 correlative periods of 30 years starting on 2011 are showed. Both emissions scenarios are represented: RCP4.5 (figure a) and RCP8.5 (figure b). Each row represents one DO (see Figure 1 for number identification) and each column represents a considered period.

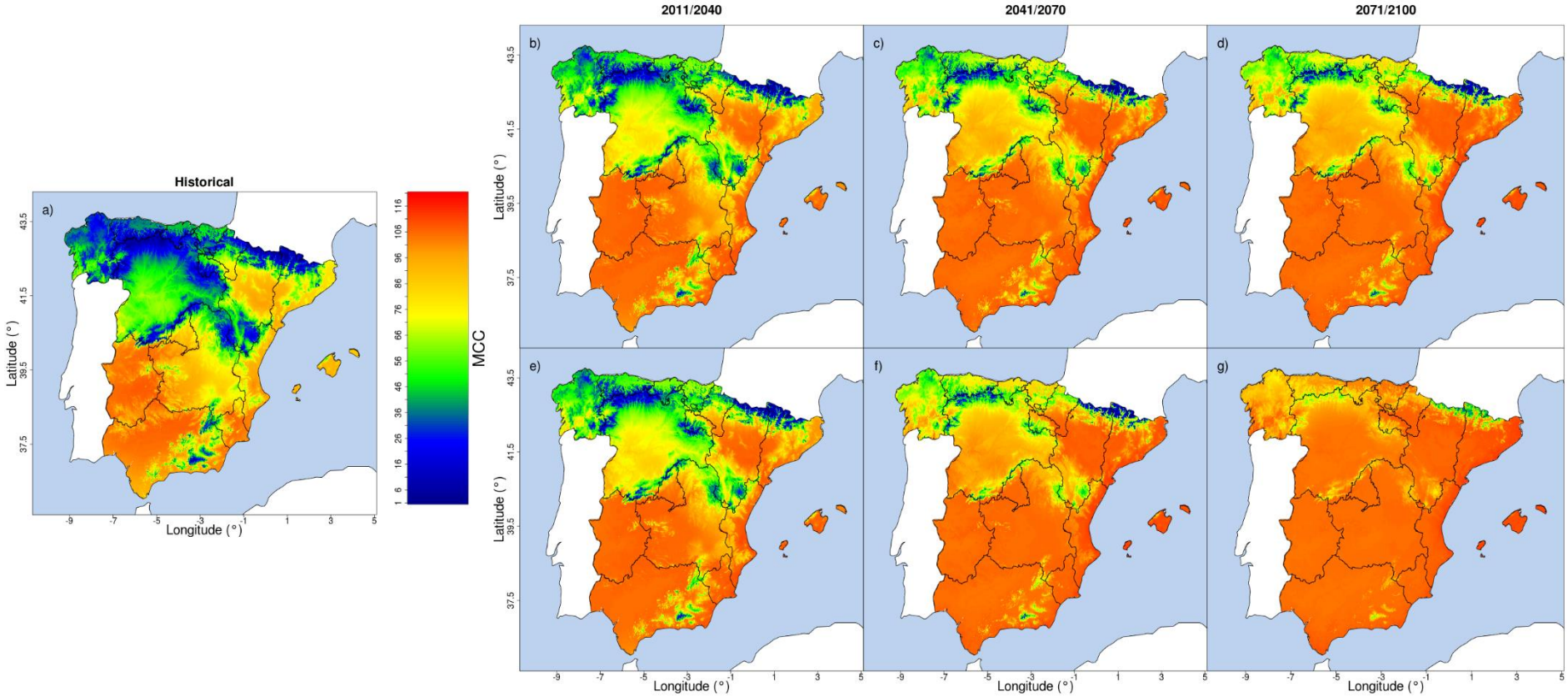

Figure S3.11. Geographical representation of the expected values of the MCC System for the periods 2011-2040, 2041–2070 and 2071–2100. Both emissions scenarios are represented: RCP4.5 (figures b, c and d) and RCP8.5 (figures e, f and g). Fig. S10a represents the Historical absolute temperature for the period 1976–2005

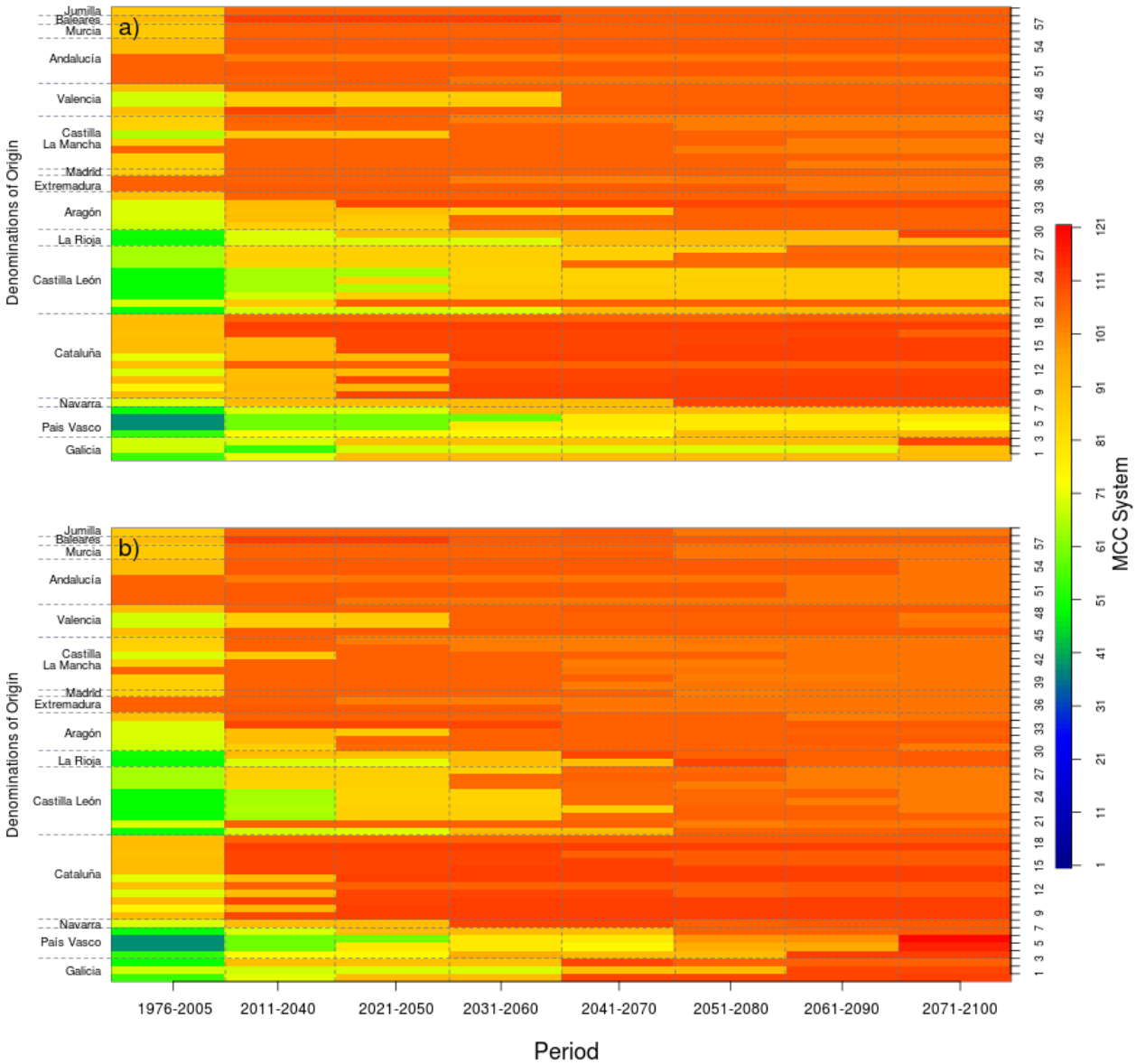

Figure S3.12. Evolution of the expected values of the MCC System for the defined DOs. Historical period 1976-2005 and 7 correlative periods of 30 years starting on 2011 are showed. Both emissions scenarios are represented: RCP4.5 (figure a) and RCP8.5 (figure b). Each row represents one DO (see Figure 1 for number identification) and each column represents a considered period

Table S3.1. List of MCC System Categories

MCC System category	Huglin Index category (HI)	Dryness Index category (DI	Cool Night category (CI)
1	6	5	4
2	6	4	3
3	6	3	2
4	6	2	1
5	6	1	4
6	6	5	3
7	6	4	2
8	6	3	1
9	6	2	4
10	6	1	3
11	6	5	2
12	6	4	1
13	6	3	4
14	6	2	3
15	6	1	2
16	6	5	1
17	6	4	4
18	6	3	3
19	6	2	2
20	6	1	1
21	5	5	4
22	5	4	3
23	5	3	2
24	5	2	1
25	5	1	4
26	5	5	3
27	5	4	2
28	5	3	1
29	5	2	4
30	5	1	3
31	5	5	2
32	5	4	1
33	5	3	4
34	5	2	3
35	5	1	2
36	5	5	1
37	5	4	4
38	5	3	3
39	5	2	2
40	5	1	1
41	4	5	4
42	4	4	3
43	4	3	2
44	4	2	1
45	4	1	4
46	4	5	3

47	4	4	2
48	4	3	1
49	4	2	4
50	4	1	3
51	4	5	2
52	4	4	1
53	4	3	4
54	4	2	3
55	4	1	2
56	4	5	1
57	4	4	4
58	4	3	3
59	4	2	2
60	4	1	1
61	3	5	4
62	3	4	3
63	3	3	2
64	3	2	1
65	3	1	4
66	3	5	3
67	3	4	2
68	3	3	1
69	3	2	4
70	3	1	3
71	3	5	2
72	3	4	1
73	3	3	4
74	3	2	3
75	3	1	2
76	3	5	1
77	3	4	4
78	3	3	3
79	3	2	2
80	3	1	1
81	2	5	4
82	2	4	3
83	2	3	2
84	2	2	1
85	2	1	4
86	2	5	3
87	2	4	2
88	2	3	1
89	2	2	4
90	2	1	3
91	2	5	2
92	2	4	1
93	2	3	4
94	2	2	3
95	2	1	2
96	2	5	1

97	2	4	4
98	2	3	3
99	2	2	2
100	2	1	1
101	1	5	4
102	1	4	3
103	1	3	2
104	1	2	1
105	1	1	4
106	1	5	3
107	1	4	2
108	1	3	1
109	1	2	4
110	1	1	3
111	1	5	2
112	1	4	1
113	1	3	4
114	1	2	3
115	1	1	2
116	1	5	1
117	1	4	4
118	1	3	3
119	1	2	2
120	1	1	1

Como resultado de la presente tesis, se han publicado los siguientes artículos. Los cuales se adjuntan como Anexo.

- **Artículo 1:**

  Gaitan, E., Monjo, R., Pórtoles, J., Pino-Otin, M.R., 2019. Projection of temperatures and heat and cold waves for Aragon (Spain) using a two-step statistical downscaling of CMIP5 model outputs. Sci. Total Environ. 650, 2778–2795.

  Factor de impacto de la revista (2019): 6.551
  Factor de impacto actual: 10.754
  Factor de impacto de los últimos 5 años: 10.237.
  Factor de citación de la revista (2022): 10.753
  Cuartil: Q1 (26/279) en Environmental Sciences

- **Artículo 2:**

  Gaitán, E.; Monjo, R.; Pórtoles, J.; Pino-Otín, M.R. (2020). Impact of climate change on drought in Aragon (NE Spain). / Science of the Total Environment 740. https://doi.org/10.1016/j.scitotenv.2020.140094

  Factor de impacto de la revista (2020): 7.963
  Factor de impacto actual: 10.754
  Factor de impacto de los últimos 5 años: 10.237.
  Factor de citación de la revista (2022): 10.753
  Cuartil: Q1 (26/279) en Environmental Sciences

- **Artículo 3:**

  Gaitán, E. and Pino-Otín, M.R. (2023). Using bioclimatic indicators to assess climate change impacts on the Spanish wine sector. / Atmospheric Research, 2023,106660, ISSN 0169-8095,
  https://doi.org/10.1016/j.atmosres.2023.106660.

  Factor de impacto de la revista (2022): 5.965
  Factor de impacto actual: 5.965
  Factor de impacto de los últimos 5 años: 5.97
  Factor de citación de la revista (2022): 8.5
  Cuartil: Q1 (18/94) en Meteorology and atmospheric sciences

5. DISCUSIÓN GENERAL

En este estudio se han obtenido escenarios climáticos para el Siglo XXI que permiten analizar diferentes impactos del cambio climático sobre Aragón y el territorio español peninsular y balear. Por un lado, se ha analizado cómo las variables meteorológicas, temperatura y precipitación, se van a ver afectadas en las próximas décadas así como la capacidad y fiabilidad de los modelos climáticos y de las técnicas de *downscaling* estadístico para simular el clima pasado y proyectar el clima futuro. En segundo lugar, se ha estudiado cómo los cambios esperados de temperatura y precipitación inciden en la frecuencia e intensidad de eventos de olas de calor y frío así como en la ocurrencia de episodios de sequía meteorológica. Finalmente, se ha analizado dicho impacto en un sector fuertemente ligado a las condiciones climáticas medias de una región y condicionado a las condiciones meteorológicas que se suceden año tras año, como es el sector vitícola, en todo territorio español ibérico-balear.

5.1. Consideraciones generales sobre la generación de escenarios de clima futuro

Se obtienen por primera vez escenarios de clima futuro a escala local basados en ESMs del CMIP5 para todo el siglo XXI de episodios de olas de calor y frío así como de indicadores de sequía (SPI/SPEI) para Aragón. Estos escenarios ofrecen uno de los mejores "*Snapshot*" de escenarios de cambio climático sobre el riesgo que las altas y bajas temperaturas así como alteraciones del régimen pluviométrico pueden causar en la región de Aragón, tanto espacial como temporalmente.

Los escenarios de variables extremas se han generado a partir de las proyecciones futuras de temperatura y precipitación generadas en base a los ESMs anteriormente citados. Para su generación se ha aplicado una técnica de *downscaling* estadístico en dos pasos (selección de análogos y funciones de transferencia) desarrollada por la FIC y aplicada en múltiples estudios nacionales e internacionales con excelentes resultados (Ribalaygua et al., 2013a, 2013b, 2018; Monjo et al., 2016, 2018; Gaitán et al., 2019, 2020; Gutiérrez et al, 2019, Velasco et al., 2020).

Los modelos empleados en el estudio han sido ESMs, considerados como los modelos más potentes que existen en la actualidad. Una de las principales ventajas de los ESMs frente a los MCs es que los primeros presentan una mayor precisión en la simulación de variables climáticas como demostraron los resultados de validación obtenidos en el presente estudio. Los óptimos resultados obtenidos en el proceso de validación de los escenarios de temperatura máxima y mínima hacen posible su uso en futuros estudios relacionados con eventos extremos e indicadores bioclimáticos.

Otro factor clave que justifica el uso de esta generación de escenarios, es la designación por parte del IPCC de los escenarios climáticos más actuales en el momento de la elaboración del presente estudio, los denominados RCPs. Siendo una prioridad trabajar con la información más actual disponible en el momento de la realización de los cálculos.

Aragón se caracteriza por una topografía muy compleja que provoca grandes gradientes climáticos. Las técnicas de reducción de escala fueron necesarias para captar estas características orográficas, permitiendo identificar las áreas más vulnerables a los cambios extremos. La reducción de escala estadística se recomienda especialmente para zonas con topografía compleja (Kattenberg y Amer Meteorol SOC, 1996). Además, Aragón es un territorio representativo de diferentes climas europeos, desde las zonas

bajas del centro de Aragón (la cuenca del Ebro) hasta las regiones montañosas del norte (los Pirineos), lo que lo convierte en un buen indicador de los futuros cambios climáticos europeos.

5.2. Consideraciones sobre los escenarios de clima futuro a escala local en la región de Aragón: temperatura y olas de calor/frío

Los resultados obtenidos para la temperatura muestran una clara tendencia hacía climas cada vez más cálidos en el área estudiada, especialmente durante los meses de verano. Los mayores aumentos de temperatura en Aragón se producirán durante el verano a finales de siglo, alcanzando valores de hasta 7 ºC para el escenario RCP8.5. Los aumentos de las temperaturas mínimas muestran comportamientos similares a los de las máximas, pero con incrementos menos acusados (3 ºC y 5,6 ºC para los escenarios RCP4.5 y RCP8.5 respectivamente en verano a finales de siglo).

Los escenarios obtenidos de olas de calor muestran un aumento de su intensidad media cercano a los 2 ºC (alcanzando temperaturas de hasta 38,8 ºC) y un aumento medio de la intensidad máxima de 3,6 ºC (temperatura de hasta 41,5 ºC) respecto al periodo histórico (1971-2000) para el escenario RCP8.5 a finales de siglo, mientras que la duración de las olas de calor aumentará en 7 días (alcanzando duración media total de 12 días). La intensidad y duración futuras de los episodios de olas de frío se mantendrán estables.

Los resultados obtenidos para la temperatura van en línea con aquellos obtenidos en otros estudios de características similares pero basados en otras técnicas de *downscaling*. Los escenarios futuros de temperatura publicados por el IPCC (IPCC, 2013), AEMET, EURO-CORDEX (https://www.euro-cordex.net/) o Copernicus (www. https://cds.climate.copernicus.eu/) en base al CMIP5 coinciden con los nuestros en que los meses estivales serán los que sufran los mayores incrementos y los meses invernales los que se verán afectados de forma más suave. Nuestros resultados (aumentos de entre 3.6 y 7 ºC a finales de siglo) muestran un calentamiento menos acusado que los publicados por AEMET (entre 4.1 y 8.2 ºC) (www.aemet.es). Respecto a los resultados publicados por el IPCC o Copernicus, éstos provienen de la salida directa de los ESMs, es decir, no tienen el valor añadido de los escenarios regionalizados, condición que sí cumplen los escenarios publicados por AEMET. Uno de los puntos a tener en cuenta en estudios de impacto climático, es el uso de un amplio abanico de proyecciones climáticas (usando el mayor número de modelos climáticos y RCPs así como de metodologías de regionalización). En base a esta hipótesis, surgieron los proyectos EsTcena (Brands et al., 2013, Brands et al., 2011a) o EURO-CORDEX. El primero de ellos, a pesar de basarse en *downscaling* estadístico, se realizó en base a modelos climáticos del CMIP3 y no en ESMs, mientras que el segundo está enfocado en *downscaling* dinámico. Todos estos resultados (incluidos los nuestros) son complementarios entre sí y contribuyen a mejorar el conjunto de proyecciones climáticas disponibles para Aragón.

Estos escenarios se compararon con aquellos publicados por Ribalaygua et al., 2013b, en base al IPCC4, usando la misma metodología, datos observados y reanálisis pero distintos grupos de modelos climáticos. Por un lado, se garantiza el buen comportamiento de la metodología y por otro, los avances proporcionados por los modelos CMPI5 frente a los CMIP3. Los resultados muestran cómo los nuevos

resultados tienden a incrementos mayores de temperatura. En ambos estudios, el patrón espacial se mantiene (mayores incrementos en las regiones noroeste y suroeste). Nuevamente, los resultados de validación ponen de manifiesto que los nuevos escenarios son más precisos que los previos.

En base a los buenos resultados obtenidos en la simulación de temperaturas máximas y mínimas, es posible partir de ellos en el análisis de la evolución futura de los episodios de olas de calor y frío. El cálculo de los episodios de olas de calor y frio se realiza en base a los percentiles 95 de temperatura máxima y 5 de temperatura mínima, respectivamente. Los buenos resultados obtenidos en el proceso de verificación de ambos percentiles permiten asumir que el umbral en el que se basa el cálculo de los episodios de olas se está simulando de forma correcta.

Todos los modelos utilizados en el estudio coinciden en que el número de días de olas de calor aumentará en las próximas décadas y por tanto, el número de episodios de olas de calor. Existen casi tantas maneras de evaluar los episodios extremos relacionados con la temperatura (especialmente los relacionados con temperaturas elevadas) como estudios publicados. La mayoría de los estudios se centran en el análisis de eventos pasados a partir de umbrales de temperatura máxima (Royé et al., 2020), noches cálidas (Royé et al., 2021) o indicadores térmicos (D'Ippoliti et al., 2010). Una línea similar siguen los pocos estudios que evalúan los eventos extremos de calor en el futuro. Por ejemplo, basados en indicadores térmicos como el *Heat Wave Magnitude Index* (Russo et al., 2014; Molina et al., 2020) o el *Excess Heat Factor, EHF* (Lorenzo et al., 2021) o umbrales de temperatura (Lorenzo and Álvarez, 2022). Nuestros resultados (aumento esperados de 7 días en la duración de una ola de calor) van en línea con los obtenidos por muchos de ellos, como los publicados por AEMET (un aumento de entre 5 y 20 días en la duración de las olas de calor y entre un 20 y un 40% en el número de días de calor) o por Lorenzo et al., (2021) con un aumento del 104% de la intensidad de dichos episodios. Los estudios mencionados se basan en modelos del CMIP5 pero o bien interpolan directamente la salida de los ESMs o bien usan modelos dinámicos y en la mayoría de ellos no se contempla nuestra área de estudio. Además, las definiciones empleadas no son exactamente las mismas que las que se han utilizado en este estudio y por tanto no podemos comparar los valores absolutos directamente pero si las tendencias encontradas. Y a pesar de las diferentes maneras de evaluar el problema todos ellos concluyen en que la tendencia esperada es hacía una mayor intensidad, duración, frecuencia y extensión espacial de dichos episodios.

Lo contrario ocurre con los episodios de olas de frio, los cuales se espera que se mantengan similares en frecuencia e intensidad. Son muy pocos los estudios que hacen hincapié en su determinación y análisis, pero los que hay llegan a las mismas conclusiones cualitativas (Carmona et al., 2016; Linares et al., 2015).

Estos resultados se pueden explicar fijándonos en las conclusiones teóricas mostradas por el IPCC (IPCC, 2013) sobre los cambios en la probabilidad de alcanzar ciertos valores de temperatura. La distribución de probabilidad de las temperaturas puede, o bien moverse hacía climas más cálidos (variaciones en la media), puede extenderse (incrementar su varianza) sin variar los valores promedio o puede ser una combinación de ambos. Esta última distribución es la que más se ajusta a los datos observados en las últimas décadas (Hansen et al., 2012, IPCC 2001). Por lo tanto, la nueva distribución

de temperaturas implicaría un cambio menos pronunciado en las temperaturas más frías de la serie y un cambio mucho mayor en las más altas.

Los datos obtenidos para Aragón, muestran que los impactos por altas temperatura y olas de calor más importantes estarán localizados en el Valle del Ebro. Resultado de gran importancia ya que es la zona más poblada y de mayor concentración socioeconómica de la región lo que puede suponer un gran riesgo para la salud, la mortalidad, la movilidad y el bienestar socioeconómico entre otros factores. Aunque el Valle del Ebro se espera que sufra las temperaturas más altas y las olas de calor más intensas, será la zona de los Pirineos la que experimente los mayores incrementos de temperatura y el mayor aumento en intensidad de las olas de calor respecto a los valores actuales. Esta zona también será donde se dé la mayor intensidad de olas de frio, aunque como se ha comentado con anterioridad no sufrirán alteraciones con respeto a los datos actuales. Estos resultados son coincidentes con Lorenzo et al. (2021) que han calculado el EHF a partir de modelos dinámicos pertenecientes a EURO-CORDEX y coinciden en que la zona de los Pirineos será una de las regiones donde más se sentirán los incrementos en los episodios de olas de calor/frío.

La zona de estudio es un área rica desde el punto de vista ecológico, con una alta diversidad de flora y fauna y en la que se encuentran ubicados varios parajes protegidos, como el Parque Nacional de Ordesa y Monte Perdido y los Parques Naturales de los Valles Occidentales y de Posets, de gran riqueza ecológica. Esto la convierte en una zona particularmente vulnerable a los efectos del cambio climático ya que su hábitat puede verse alterado drásticamente a causa de las consecuencias que podría suponer para la biodiversidad aragonesa (OPCC2, 2018). Entre algunas de las complicaciones derivadas del cambio climático destacan: alteraciones en los patrones de migración de ciertas especies (Sanz et al., 2003; Gordo and Sanz, 2006), pérdida de la cubierta vegetal (OPCC2, 2018) y aumento de los incendios forestales (Cardil et al.,2013; Resco de Díos et al.,2021), alteraciones del suelo causadas por la erosión y la desertificación (Magrama, 2016) o cambios en la estratificación en altura de la vegetación (Revuelto et al., 2022).

Mención especial merece la situación en el Pirineo Aragonés, la cual es realmente alarmante. Estudios recientes llevados a cabo por organismos como el Instituto Pirenaico de Ecología y diversas universidades (López-Moreno et al., 2016; Vidaller et al., 2021; OPCC2, 2018) son contundentes y no dejan lugar a duda de la desaparición paulatina del hielo glacial en el Pirineo. La fecha en la cual se pueden extinguir completamente los glaciares pirenaicos se ha ido acortando como consecuencia de las altas temperaturas y periodos cada vez más cálidos. Un ejemplo claro es el año 2022, año en el que ha desaparecido el 20% de la masa de hielo glaciar del Aneto. Esta situación no solo tiene repercusión en la biodiversidad de montaña sino que impacta directamente, a través del deshielo, en el caudal de los ríos de la vertiente izquierda del Valle del Ebro con las consecuentes implicaciones en el aporte hídrico (López-Moreno et al., 2011) o en los episodios de inundaciones (Lastrada et al., 2020), entre otros fenómenos.

Por lo tanto, los cambios en las temperaturas y aumentos en los eventos extremos en las magnitudes calculadas en este estudio, pueden suponer un enorme riesgo para esta área.

5.3. Consideraciones sobre los escenarios de clima futuro a escala local en la región de Aragón: precipitación y sequía meteorológica

Uno de los principales problemas a los que nos enfrentamos en el análisis de estudios de impacto de sequías meteorológicas es la falta de datos observados y de estudios a nivel local que incluyan escenarios futuros y que sirvan de guía para afrontar dicha problemática. En general, los expertos consideran el SPI como uno de los pocos índices aplicable en cualquier región del mundo para cualquier escala (Hayes et al 2011) ofreciendo múltiples ventajas en comparación con otros indicadores usados ampliamente (Dracup et al., 1980; Hayes et al., 2011). En contexto de cambio climático, además, se recomienda el análisis del SPEI- que incluye la ETP- y cuya formulación es similar a la del SPI, lo que permite la comparativa entre ambos. Ambos índices se han aplicado con anterioridad en Aragón (Vicente-Serrano et al., 2010a; Beguería et al., 2014) lo que refuerza su uso en la zona de estudio. Es por ello que en este estudio, tanto el SPI como el SPEI se han calculado en base a las proyecciones climáticas futuras de precipitación (obtenidas en el segundo bloque de resultados) y temperatura (obtenidas en el primer bloque de resultados).

Los escenarios futuros de precipitación muestran un leve descenso (bajo el escenario RCP8.5) a lo largo del siglo XXI y todas las estaciones del año, excepto en verano donde apenas se esperan variaciones con respecto a los valores actuales. Bajo el RCP4.5 apenas se esperan variaciones en el régimen pluviométrico. Estos resultados van en concordancia con los obtenidos en otros proyectos de características similares. Además, los resultados de validación para precipitación muestran valores de ± 1mm/día (alrededor del 10%), estos valores se encuentran dentro de la variabilidad natural de la precipitación por lo que se pueden considerar buenos resultados de validación. Los nuevos escenarios de precipitación, basados en el CMIP5, muestran mejores resultados de validación que los obtenidos en base al CMIP3, especialmente en los meses de verano que es un mes crítico para Aragón (un bias de ±10% para CMIP5 frente a un bias de ±20% en CMIP3).

En el análisis de los episodios de sequía meteorológica calculados a partir del SPI/SPEI, se aprecia que la serie temporal de SPI/SPEI en base a datos observados es bien representada por ambos indicadores calculado en base a datos simulados. Los periodos secos/húmedos son bien recogidos aunque tienden a dar episodios de más intensidad que los observados, especialmente a escalas largas. Estos resultados están en línea con aquellos presentados en otros estudios para la zona y las pequeñas diferencias que se aprecian se deben a la diferencia de metodologías e indicadores empleados así como el periodo histórico observado. Por ejemplo, los periodos húmedos y secos identificados en este estudio coinciden en gran medida con los identificados por Vicente-Serrano and López-Moreno, (2005) basado en SPI (años húmedos: 1976-1980, años secos: 1986-1987,1989, 1994-1997), Spinoni et al., (2015) basado en un índice combinado a 12 meses (años secos:1979-1980,1995-1998) y López et al., (2007) basado en el régimen pluviométrico (años secos: 1970, 1985, 1993 y 1995).

Respecto a los escenarios futuros, en los resultados de SPI no se aprecian cambios en el balance hídrico en ninguna zona de Aragón ni en ninguna de las escalas temporales consideradas, a excepción del RCP8.5 y finales de siglo en la zona del valle del Ebro donde se aprecia una leve tendencia hacía climas más secos. Aunque hasta donde

sabemos no existen estudios similares en nuestra área de estudio, estos resultados van en línea con lo obtenido en los escenarios de precipitación como era de esperar al tratarse de la única variable sobre la que se calcula el SPI. Al considerar otras variables como la temperatura, los escenarios de SPEI muestran una clara tendencia hacía periodos más secos y largos, especialmente en el valle del Ebro y en el suroeste de la región. Algo que se esperaba en base a los escenarios de temperatura y precipitación con los que se han generado. Que los escenarios sean más intensos a escalas de 12 meses que a 1-3 meses es consecuencia de la manera en que los indicadores están formulados. Por lo tanto, en el contexto actual de calentamiento global es esencial tener en cuenta el efecto de la temperatura en los estudios de sequía.

Los resultados muestran que el Valle del Ebro (zona más poblada, incluyendo Zaragoza) será la más susceptible a futuros periodos de sequía extrema con mayor intensidad y duración, especialmente a finales de siglo, con implicaciones en sectores como la salud (Roldán et al., 2016; Carmona et al., 2016), manejo del agua, economía (Pérez and Barreiro-Hurlé, 2009) y sociedad en general (Lee et al., 2017). Estos resultados van en línea con las zonas donde se detectaron los valores más elevados de temperatura y los mayores descensos de precipitación como mostraron los resultados del ECCE Project (Ministerio de Medio Ambiente, 2005) entre otros (Cook et al., 2014; Zambrano-Birgiarini et al., 2010) de manera que la zona del Ebro seguirá siendo una de las más secas y calurosas (Jiménez-Donaire et al., 2020)

Los resultados obtenidos son la representación más precisa hasta la fecha de la magnitud, duración e intensidad de los episodios de sequía meteorológica y su duración en diferentes periodos de acumulación. El uso de diferentes índices de sequía y escalas temporales y su representación gráfica es una novedad relevante en la literatura científica y pueden ser una referencia para el estudio de impactos de sequía en múltiples sectores, especialmente en zonas con climas y orografías complejas como Aragón, algo extrapolable a otras regiones de Europa con características similares.

5.4. Consideraciones sobre los escenarios de indicadores bioclimáticos de interés vitícola a escala local en España

Se han generado escenarios de clima futuro para cuatro índices bioclimáticos individuales de impacto vitícola (HI, CI, DI y HyI), un índice combinado (CompI) y una zonificación vitícola (MCC System).

En este caso, el estudio se ha ampliado a toda la península Ibérica con el objetivo de poder comparar los resultados obtenidos para la región vitícola aragonesa con aquellos obtenidos para otras regiones vitícolas españolas. Además, disponer de información climática en todo el territorio español ibérico-balear supone una herramienta de apoyo en la adaptación al cambio climático. Por un lado, permite comparar medidas llevadas a cabo por regiones climáticas similares (tipos de portainjertos y variedades plantadas, manejo del regadío, etc.) y por otro lado, determinar regiones climáticamente aptas para la vid que actualmente no se usan para tal fin y que pueden ser una alternativa futura a las regiones actuales.

Para poder afrontar el estudio a nivel peninsular y balear, se han tenido que generar proyecciones futuras de temperatura y precipitación para todo el territorio. Estas proyecciones se basan en 9 ESMs del CMIP5 y dos RCPs, siguiendo la misma

metodología empleada para la región de Aragón. Se completa el estudio simulando escenarios futuros de olas de calor/frío y escenarios de sequía mediante los indicadores SPI/SPEI.

Tal como se desprende de los escenarios obtenidos en este estudio (véase Anexo R1), se espera que en las próximas décadas la temperatura media anual ascienda en todo el territorio español entre 2 y 4 °C, siendo los meses estivales los que experimentarán los ascensos más acusados. Para estos meses críticos, se esperan aumentos de hasta 7 ºC a finales de siglo bajo el escenario RCP8.5 en el caso de las temperaturas máximas y 5 ºC para las temperaturas mínimas. Toda la mitad sur peninsular, la zona Mediterránea y las Islas Baleares experimentaran temperaturas máximas estivales por encima de los 32 ºC a mediados de siglo, llegando a superar los 38 ºC a finales del mismo. Estos aumentos de temperatura suponen una intensificación en los episodios de olas de calor en todo el territorio, especialmente en toda la costa Mediterránea dónde se esperan episodios de calor con una duración superior a 20 días (bajo el RCP8.5 y a finales de siglo). A nivel vitícola, el aumento en los episodios de olas de calor supondrá un gran riesgo, no solo de estrés térmico por exceso de calor, sino también de estrés abiótico.

Respecto a las temperaturas mínimas (véase Anexo R1), los mayores aumentos se esperan en los meses estivales, siendo la Costa Mediterránea la zona que experimentará las temperaturas mínimas más elevadas. Aunque se esperan cambios en las temperaturas mínimas medias, no se esperan grandes cambios en los extremos, por lo que no se aprecian alteraciones importantes de los episodios de olas de frío futuros respecto a los actuales. Hay dos aspectos importantes relacionados con la temperatura mínima: las heladas y la temperatura mínima durante la maduración. Estas variables han de ser evaluadas con precaución durante las tareas de mantenimiento del viñedo.

Las proyecciones de precipitación para el territorio peninsular y balear apenas muestran ligeros cambios en la cantidad de precipitación acumulada anualmente, aunque con eventos de precipitación más concentrados en el tiempo (véase Anexo R2). Estas leves variaciones de precipitación ratifican los resultados arrojados por los escenarios de sequía meteorológica basados en SPI (dependiente exclusivamente de la precipitación), los cuáles no muestran una señal significativa de cambio respecto a valores actuales.

Una situación diferente se obtiene al evaluar la sequía meteorológica a partir de escenarios basados en el SPEI (combinando el efecto de la precipitación y la ETP). Los resultados obtenidos muestran que bajo el escenario RCP8.5 y a finales de siglo, la situación se va agravando según se aumentan los periodos considerados. De esta manera, en acumulado a 1 o 3 meses, la mayoría del territorio sufrirá de sequía moderada a severa, mientras que en acumulado de 12 meses, casi todo el territorio se encontrará en situación de sequía severa a muy extrema. A mediados de siglo, la mayor parte del territorio se encontrará en situación de sequía moderada a severa.

Los resultados obtenidos para las proyecciones de temperatura y precipitación así como los de los eventos extremos concuerdan con aquellos publicados de forma oficial por AEMET (www.aemet.es) o el IPCC (estos últimos basados en salidas directas de los MCs) así como los publicados en estudios similares que contemplan o bien, la

información directa de los ESMs (Cos et al., 2022) o bien, el uso aplicado de proyecciones climáticas (Lorenzo et al., 2021; Monjo et al., 2016; Miro et al., 2021)

Las variaciones esperadas en valores medios y extremos de temperatura y precipitación tendrán implicaciones en los resultados obtenidos para los indicadores bioclimáticos.

Los resultados obtenidos ponen de manifiesto cómo los indicadores térmicos (HI y CI) tenderán a aumentar a lo largo del siglo XXI, mientras que la escasez de agua (DI) será más acusada. Las tendencias encontradas no tienen la misma repercusión en todo el territorio, de manera que en el sur de la península, con valores de HI que superan los 3500°C y de CI por encima de los 20°C y de DI por debajo de los -200 mm, la continuidad del sector vitivinícola en su estado actual se ve seriamente amenazada, con una disminución de los años climáticamente óptimos como muestran los valores de CompI. Por el contrario, el norte peninsular y las zonas montañosas, a pesar de los aumentos previstos, con HI inferiores a 2500°C, noches frescas (CI inferior a 15°C) y un aporte hídrico suficiente (DI superior a 150 mm) mejoran considerablemente su aptitud climática (CompI) aunque se mantiene el riesgo de enfermedad de mildiu debido al aumento de la temperatura y la humedad.

Estos cambios puede favorecer de forma positiva a la zona del norte de la península pero regiones como el sur y el suroeste peninsular como el Mediterráneo (que ya se encuentran en el límite de idoneidad vitícola) pueden verse afectados de forma negativa. Estas últimas tendrán que hacer frente a problemas de estrés térmico e hídrico que pueden poner en peligro el cultivo de las vides y por ende la calidad del vino. En aquellas regiones con DO puede ser un problema de gran envergadura ya que son, precisamente, esos factores los que dotan a una región de dicha distinción. Por otro lado, si los cambios climáticos son muy acusados, es posible que muchas regiones deban plantearse cambios a nivel del viñedo (fechas de laboreo, regadío, sombreado, etc.) (Felxas et al., 2010), cambios a nivel de finca (ubicación, variedad de uva, orientación, etc.) viñedo (Hall and Jones 2009, Lobell et al 2006) o cambios en la gestión del (Renée and Thach 2014).

Las principales consecuencias de cambios hacía valores de HI más altos van a estar relacionadas con la variedad de uva a cultivar. Este indicador hace referencia a los requerimientos de acumulación de calor necesarios para que cada tipo de variedad alcance la maduración de forma óptima. Debido a que se espera que se alcancen los valores de requerimiento de calor con anterioridad, la maduración se completará antes de lo que ocurre actualmente. Esto puede llevar a episodios de estrés térmico en muchas regiones. Este índice tiene una fuerte correlación con las etapas fenológicas en las que las condiciones cálidas juegan un papel importante, lo que se traduce en un adelantamiento de las etapas fenológicas y una alteración del ciclo actual de la vid.

Debido al aumento esperado en las temperaturas mínimas se espera que el CI alcance valores que se sitúen fuera de los requerimientos de frescor nocturno necesarios en el periodo de maduración para ciertas variedades de uva. No se espera bajo ningún RCP que los valores de CI desciendan en las próximas décadas. Por otro lado, si se alcanzan los requerimientos térmicos de maduración antes de lo que se hace actualmente, habría que replantearse si el cálculo del CI debe seguir haciéndose en base al mes de septiembre. En el caso de que se garantice que se alcanzan los requerimientos térmicos

necesarios para la maduración, un descenso de las temperaturas nocturnas podría ser beneficioso para ciertas variedades de uva.

Los cambios esperados para el DI van a condicionar el aporte hídrico necesario y por consiguiente las necesidades de riego. En toda la región, a excepción de la cornisa cantábrica y de los Pirineos, e independientemente del RCP considerado, los valores de DI van a descender hasta valores por debajo de los 50 mm (escenario justo en el límite de aporte hídrico), lo que puede suponer la necesidad de tomar medidas de restricción, especialmente en los meses de verano. Si el DI se sitúa por debajo de los -100mm, la región se volverá excesivamente seca y necesitará de aporte hídrico extra para cubrir los requerimientos de la vid. Por el contrario, en aquellas regiones donde se espera que el DI alcance valores por encima de los 150 mm (Pirineos y El Golfo de Vizcaya) se puede comprometer la calidad de la uva y el vino, especialmente en años muy húmedos. En regiones como Galicia y Asturias, donde el DI se moverá en valores intermedios (entre 50 y -100mm) pequeñas épocas de déficit hídrico pueden ser beneficiosas, especialmente durante la maduración.

Bajo las nuevas condiciones climáticas no se espera que aumente el riesgo de presencia del Mildiu, pero sí se aprecia que hay diferencias de riesgo entre regiones con diferentes patrones de precipitación. De esta manera, la zona sur será la que menos riesgo presente, aumentando de forma progresiva hacía el norte, donde el régimen pluviométrico es más abundante, especialmente durante la etapa de crecimiento.

Los resultados obtenidos van en línea con los publicados en otros estudios aplicados sobre algunas de las regiones vitícolas más importante del mundo, como en Portugal (Fraga et al., 2012), Italia (Bonfante et al., 2017), Alemania (Neumann and Matzarakis, 2011), Francia (Duchene and Schneider, 2005) y España (Gomez-Gesteira et al., 2011). Y aunque estos estudios no se basen en las mismas metodologías (no aplican *downscaling*, usan otros indicadores bioclimáticos, son regiones con características climáticas y orográficas diferentes, etc.) obtienen conclusiones similares respecto a cómo el sector vitícola se va a ver afectado por el aumento de las temperaturas y la escasez hídrica.

Las características climáticas definen la idoneidad de una región para cultivar uvas que den vinos de calidad. Se definió el CompI para evaluar si se dan dichas condiciones. Los resultados obtenidos para este índice pueden parecer contradictorios, ya que zonas como Andalucía o Castilla- La Mancha con fuerte tradición vitícola de calidad, presentan un porcentaje muy bajo de años óptimos para el cultivo de la vid (principalmente debido, a la escasez hídrica). En este caso se puede solventar con estrategias que compensen dicha “falta de idoneidad climática”.

Los impactos derivados del cambio climático van a ser importantes a nivel de aclimatización bioquímica, fisiológica y molecular de la uva. Diversos estudios destacan el potencial adaptativo de la vid a nivel molecular para hacer frente al estrés climático (Zha et al., 2018), por ejemplo, mediante un ajuste fotosintético (Gallo et al., 2021; Kizildeniz et al., 2021), un aumento de la capacidad de disipación de calor a través de las estomas (Costa et al. 2012) o alteraciones metabólicas (Duchene et al., 2012; Kovaleski and Londo, 2019). Estos descubrimientos abren una vía para identificar los rasgos genéticos y fisiológicos que hacen que una variedad sea más o menos resistente y seleccionar las variedades que serían adecuadas para sustituir a las más sensibles.

5.5. Consideraciones sobre posibles medidas de adaptación y mitigación

Los cambios observados ponen de manifiesto que existe la posibilidad de que ciertas regiones tradicionales puedan modificarse pasando de ser climáticamente óptimas para el cultivo de la vid a no óptimas y viceversa (Bock et al., 2011; Santos et al., 2012; Fraga et al., 2013; Jones et al., 2006; Jones and Webb, 2010)

Es importante establecer acciones prácticas y relevantes basadas en un análisis que incluya un amplio rango de territorios y diferentes tipos climáticos y vitícolas. Si la industria vitícola, en cualquier región del mundo, quiere sobrevivir debe adaptarse a los retos del cambio climático, es decir, evaluar si es viable en su estado actual o si es necesario hacer cambios (Graça et al 2016). Graça et al 2016 sugieren establecer un marco de trabajo preliminar que permita replicar esfuerzos de planificación, reducir el riesgo y los costes a la hora de implementar medidas de adaptación, aumentar la capacidad de la industria para adaptarse al cambio climático y crear un sistema de estandarización que permita comparar modelos, escenarios y opciones tecnológicas entre regiones. Además es necesario tener en cuenta todos los aspectos que intervienen en la cadena de valor del vino: características biológicas y físicas que se ven afectadas por el cambio climático (Maclaren et al., 2015), prácticas de manejo (Howden et al., 2007; Greenwood et al 2016), factores socioeconómicos y culturales (Grothmann and Patt, 2005; Adger et al. 2008) así como las transformaciones que la industria vitícola ha experimentado en las últimas décadas.

En función del aspecto que se quiera modificar serán necesario aplicar medidas de adaptación inmediatas (medidas a corto plazo) o medidas que perduren en el tiempo (medidas a largo plazo). Además hay que evaluar a que nivel se quieren aplicar. Las medidas a nivel bodega son más fáciles, baratas e inmediatas pero tienen un bajo nivel de adaptación. A nivel viñedo son más caras y presentan mayor dificultad de implementación pero tienen un nivel mayor de adaptación.

En función de la escala temporal en la que se quiere actuar hablaremos de medidas a corto, medio o largo plazo (Santos et al., 2020; Nauellau et al., 2021).

<u>Medidas a corto plazo</u>

Las medidas a corto plazo están centradas en amenazas específicas para optimizar la producción y repercuten en la calidad y el estilo del vino. Estas medidas suponen cambios en las medidas enológicas, mejoras en la calidad del vino, disminución de los efectos en la variabilidad interanual o implicaciones en el seguro agrario. Destacan:

1) Medidas pensadas para retrasar la fecha de maduración: retraso en la fecha de poda que puede retrasarla entre 3 a 5 días, selección clonal que puede retrasarla entre 3 a 8 días, aumentar la altura del tronco, entre 3 a 8 días, la elección del portainjerto entre 3 a 6 días y la elección de la variedad de la uva entre 10 a 25 días.

2) Reducir el estrés debido a la falta de agua, es decir: riego (si el estrés es muy alto alto) (Felxas et al., 2010), variedad de injerto (estrés medio), especies en la cubierta vegetal (estrés débil), labores del suelo y acolchado (estrés débil) y sistema de espalderas (estrés medio).

3) Para realizar durante la época de cosecha destacan la adaptación de las técnicas de cosecha y la adaptación del lagar (por ejemplo, control de la temperatura durante el posproceso para evitar alteraciones bioquímicas).

5) Para aplicar en el manejo del canopy hay varias estrategias. Ralizar la poda tardía (Duchene and Schneider 2005) para retrasar el comienzo de la brotación entre 8 y 11días con respecto a métodos tradicionales es una de ellas, lo que supondría un retraso en la floración y en el envero de entre 4 a 5 días. Otras estrategias serían: aumentar la altura del tronco de la vid, recorte de brotes y/o retirada de hojas para intentar disminuir el ratio área foliar y peso de la fruta (<0,75m2/kg fruta) (Van Leeuwen & Darriet, 2016), o bien aplicar sombreado para reducir la temperatura del fruto y así aumentar la concentración del ácido málico y la acidez en la cosecha (Greer et al., 2011).

6) En la parte relacionada con el suelo, lo principal es controlar el aporte de agua, el vigor de la planta y evitar la erosión del mismo. Para ello se pueden cambiar las técnicas de laboreo. Por ejemplo, buscar alternativas al control químico de las malas hierbas a través de gestión de suelos poco profundos (Pelegrino et al., 2004) o a través de la cubierta de césped (limitamos la ETP del suelo especialmente en verano y en épocas secas).

En conjunto, cambios en las prácticas de manejo, prácticas enológicas e introducción de nuevas tecnologías en toda la cadena de valor (Lobell et al 2006, Olesen et al 2011, Orduna 2010, Renée and Thach 2014).

Medidas de corto a medio plazo

Este tipo de medidas son aquellas que se implantan para momentos concretos que tienen repercusión en el viñedo. Por ejemplo el manejo del riesgo de heladas a través de métodos activos. Sería el caso de los métodos directos que se aplican en el momento justo de la helada como máquinas de viento, calentadores, aspersores sobre la vid y/o pasivos, métodos indirectos que sirven para preparar y reducir el impacto en viñedo.

Medidas a medio y largo plazo

Estas medidas están más pensadas para asegurar la viabilidad económica de la viticultura tradicional y la reducción de gases de efecto invernadero asociados a su actividad y enfocadas, principalmente, a la gestión del viñedo. Estas medidas requieren de cambios de mayor envergadura. Algunas de las medidas que se pueden llevar a cabo son:

1) Cambios en las localizaciones (no solo zonas climáticas sino en latitud y altura) (Fraga et al 2014, White et al 2006, Hall and Jones 2009, Lobell et al 2006, Hannah et al 2013, Moriondo et al 2013). Por otro lado, la proximidad a masas de agua que reducen la amplitud térmica diaria así como la cercanía a los bosques donde la humedad es mayor y por tanto más favorables para la proliferación de algunas enfermedades (Hancock 2005).

2) Cambios en las orientaciones, favoreciendo (Intrieri et al., 1998; Grifoni et al 2008; Hancock 2005) o disminuyendo (Greer et al., 2011) la incidencia de radiación en función de las necesidades.

3) Cambios en las variedades, adaptándose a las nuevas condiciones térmicas y pluviométricas (Jones et al., 2006; Duchene et al., 2012) e intentando mantener las ya existentes que garanticen la biodiversidad natural (Tello et al 2012; Karoglan et al 2018). Realizar la elección de la variedad de uva en función del periodo de maduración eligiendo maduración tardía e incluso sustitución de variedades de blanco a rojo como consecuencia de la demanda de calor (Stock et al., 2004) son otras opciones, siempre y cuando la legislación internacional y nacional lo permitan.

4) Selección clonal (Koundouras et al., 2008; Duchene et al., 2012). En la mayoría de los casos hay una diferencia de entre 8 a 10 días en la fecha de maduración entre clones de la misma variedad de uva y no supone una modificación en la tipicidad del vino.

5) Selección del portainjerto en función de las condiciones hídricas y físicas del suelo (Ozden et al 2010; Pavlousek et al 2011; Harbertson and Keller 2012; Koundouras et al 2008) así como atendiendo a las interacciones entre ambas (Romero et al., 2006; Pelegrino et al., 2004). Esta medida no solo no modifica la tipicidad del vino sino que es respetuosa con el medioambiente, no aumenta los costes de producción y puede suponer un retraso en la maduración de hasta 7-10 días.

6) Establecer un buen diseño del viñedo: densidad de plantación, orientación de las filas, mallas de sombreo, gestión sostenible del agua, estrategias de venta etc. (Renée and Thach 2014)

7) Prevención frente a pestes y enfermedades. Un sondeo realizado sobre las principales adversidades a las que ha tenido que hacer frente el sector vitícola europeo en las últimas décadas (Battaglini et al., 2008) destaca el aumento de las enfermedades y pestes que han afectado a la vid. La intensificación de esta amenaza está ligada al aumento de las temperaturas y de los patrones de humedad.

8) Agrodiversidad como herramienta para la pérdida del cultivo (Morales-Castilla 2020)

9) Introducir sistemas de riego. Esta opción supone un coste económico, social y medioambiental.

La vid es un cultivo muy agradecido que puede crecer en suelos y condiciones edafológicas por lo que gracias a una buena planificación es posible su desarrollo en casi cualquier suelo (Bucelli & Constantini, 2006; Faila et al., 2008). Para poder implementar cualquier medida de adaptación de forma satisfactoria es necesario identificar para cada tarea de cada momento de la cadena vitícola que tipo de impacto climático se produce a corto, medio y largo plazo y actuar en consecuencia (Graça et al., 2016).

Las medidas de mitigación forman parte también de las estrategias del sector para enfrentarse al Cambio Climático. Uno de los planteamientos que se están afrontando desde el mundo vitícola es reducir la huella de carbono: considerando la vid como sumidero de CO_2 y reduciendo el balance de carbono en la viticultura (Jones & Webb 2010), así como analizando el potencial mitigador de algunas prácticas agrarias que sirvan para controlar las emisiones, la erosión, la contaminación difusa, la pérdida de nutrientes o el gasto energético (Iglesias y Moreno 2009).

5.6. Aspectos metodológicos a considerar

Consideraciones sobre la metodología de *downscaling* estadístico

Toda metodología de *downscaling* estadístico presenta ciertas limitaciones que han de tenerse en cuenta a la hora de interpretar los resultados obtenidos (es decir, las proyecciones climáticas):

1) En general, las técnicas de *downscaling* tienden a suavizar las series simuladas respecto a las observadas, es decir, tienen dificultades recogiendo los extremos. Por ejemplo, en el caso de las olas de calor/frío, al ser más larga la serie del reanálisis que la observada, el número de días considerado para calcular el P95 y el P05 es mayor, por lo que la intensidad y duración de dichos episodios es simulada de forma más suave.

Una simulación más suave puede llevar a que en el análisis de eventos extremos categorizados, estos no se sitúen en las mismas categorías considerando evento simulado y evento observado.

2) Un modelo climático no reproduce el clima día a día por lo que la forma de validarlos ha de hacerse en base a estadísticos climáticos sobre periodos de tiempo largos. Estos estudios, en ocasiones, suponen una pérdida de información sobre la variabilidad climática. Además, para evaluar su comportamiento no se puede comparar el periodo *Historical* con las observaciones (estás presentan lagunas en sus series) y ha de hacerse frente a un reanálisis.

Estas dos limitaciones se contemplan en nuestro estudio a la hora de corregir el error sistemático a las series simuladas “brutas” y por tanto suavizar el efecto de ambas.

3) Trabajar con 9 ESMs y 2 RCPs, permite disponer de un conjunto de proyecciones climáticas con las que evaluar las incertidumbres asociadas al proceso de generación de proyecciones climáticas, lo que favorece la toma de decisiones dentro de un rango de actuación.

Consideraciones sobre la simulación de indicadores bioclimáticos

La metodología de *downscaling* empleada ha permitido tener en cuenta dos aspectos importantes en estudios de impacto climático en el viñedo:

1) Hay estudios que refuerzan la idea de que los cambios diarios en las condiciones atmosféricas juegan un papel importante en la fenología de las plantas (Jones y Davis, 2000), y estos cambios pueden ser más o menos significativos dependiendo de la región donde se produzcan. Estos aspectos se consideran intrínsecamente en el tipo de metodología de *downscaling* utilizada en este estudio basada en una estratificación analógica de campos atmosféricos.

2) Un factor a considerar son los beneficios que un aumento de CO_2 en condiciones climáticas futuras tiene en el desarrollo de la vid (Bindi et al., 2001; Goncalves et al., 2009; Moutinho-Pereira et al., 2009). Aunque en este estudio no se analiza directamente este punto, se tiene en cuenta a la hora de considerar los diferentes RCPs (contemplando distintos forzamientos radiativos).

Así mismo, en la evaluación de indicadores bioclimáticos se presentan ciertas limitaciones que se han solventado gracias a la manera en la que se ha abordado el estudio:

3) Las DOs se caracterizan, precisamente, por ser las condiciones locales las que proporcionan los matices que hacen que sus vinos sean únicos y reconocibles. Al trabajar a escala local se están teniendo en cuenta las características micro climáticas que proporcionan dicha especificidad.

4) Evaluar los valores absolutos, tal como se ha hecho en este estudio, permite conocer las particularidades de cada indicador climático a escala de observatorio y por tanto, no perder el valor añadido que proporciona el estudio al trabajar a escala local. Los indicadores climáticos tienen una categorización muy amplia, es decir, el rango de valores que engloba cada categoría es muy grande, y considerar solo dichas categorías supone una pérdida de información de gran valor para la adaptación al cambio climático.

Finalmente, hay ciertas limitaciones que no se han podido considerar dentro del estudio y que son un punto importante a tener en cuenta en estudios futuros:

5) Posibles alteraciones en las concentraciones de ozono y precursores del mismo (NOx, CO, CH4, NMCH), como consecuencia del aumento de las temperaturas en un marco de cambio climático, pueden tener un efecto indirecto en la vid (Isaksen and Wang, 2002). Algunos estudios señalan al ozono como el causante de la pérdida de productividad y el descenso del contenido de azúcar en la vid (Ascenso et al., 2021).

6) Los resultados de este estudio han de completarse con otros factores que complementan a los climáticos como son longitud, latitud, altitud, topografía, proximidad a masas de agua, orientación y exposición, propiedades del suelo, prácticas de manejo e interacción entre todos los actores. Estos factores en conjunto son lo que actúan además del clima para dar lugar a esos vinos únicos que caracterizan cada DO. Dentro de una misma DO pueden diferenciarse diferentes tipos de uvas, suelos y características de campo que juegan un papel importante en la diferenciación vitícola. Aunque estos factores son cruciales no suponen un reto tan importante como el que nos plantea el cambio climático.

6. CONCLUSIONES

CONCLUSIONES

1. Es la primera vez que se generan **escenarios a escala local de temperatura y precipitación** para Aragón en base a las salidas proporcionadas por modelos CMIP5 y usando para ello una metodología de *downscaling* estadístico.

2. Los escenarios de temperatura son más robustos que los que obtuvimos en estudios previos, y publicados en Ribalaygua et al 2013b, en base a fases previas del CMIP5 por lo que resultan más adecuados y fiables para su uso en estudios de adaptación al cambio climático.

3. También los escenarios de precipitación resultado de este estudio proporcionan mayor consenso entre modelos que los obtenidos en estudios previos, donde la dispersión entre las proyecciones climáticas era mayor y por tanto presentaban una mayor incertidumbre.

4. Nuestros resultados en relación **a las temperaturas esperadas** en Aragón para el Siglo XXI, confirman el consenso científico global de un aumento gradual de temperaturas a nivel planetario:
    - los mayores incrementos de temperatura se esperan en Aragón para los meses estivales: hasta 7 ºC y 5.6 ºC en el peor de los escenarios, (RCP8.5) para temperatura máxima y mínima, respectivamente.
    - y los más suaves en invierno: hasta 4-4.2 ºC también de acuerdo con el escenario RCP8.5.
    - las variaciones esperadas en base al CMIP5 se esperan más acusadas que las obtenidas en base a escenarios anteriores, siendo incluso 2 ºC más intensas en los meses estivales bajo el escenario más desfavorable.
    - A nivel del territorio, las regiones noroeste y suroeste de la región son las que se verán más afectadas por estas variaciones.

5. No se esperan grandes cambios en el **régimen pluviométrico de Aragón**. En base a los resultados obtenidos se esperan variaciones medias de alrededor de un ±10% (el equivalente a 1mm/día) en todas las estaciones del año a excepción del verano, donde no se esperan cambios, de acuerdo al escenario más desfavorable.

6. La ampliación del estudio a todo el territorio ibérico-balear se ha realizado con el fin de poder evaluar el impacto del cambio climático sobre la vid para toda España. Entre los resultados obtenidos de las proyecciones climáticas de temperatura y precipitación destacan:
    - Las variaciones de temperatura media en España se esperan graduales a lo largo de todo el Siglo XXI, llegándose a alcanzar incrementos de hasta 4 ºC en el escenario más desfavorable. Respecto a las temperaturas máximas, los mayores incrementos se esperan en los meses estivales (hasta 7 ºC en el caso más desfavorable a finales de siglo) lo que supondrían temperaturas de hasta 38 ºC en gran parte de la

meseta peninsular. Las temperaturas mínimas experimentarán ascensos menos acusados (alrededor de 5 ºC a finales de siglo), siendo, nuevamente, los meses estivales los más afectados.

- No se aprecian variaciones de precipitación destacables respecto a valores actuales. La zona noroeste seguirá siendo la región de mayor pluviometría.
- A nivel de territorio, la meseta sur peninsular, especialmente Andalucía, Extremadura y Murcia, junto con el Valle del Ebro serán las regiones dónde se alcancen lpos mayores incrementos de temperatura.

7. Es la primera vez que se generan **escenarios a escala local de episodios de olas de calor/frío para la zona de Aragón** en base a proyecciones climáticas locales de temperatura generadas con una metodología de *dowsncaling* estadístico y en base a la información proporcionada por el CMIP5.

8. Los escenarios de **olas de calor** muestran episodios cada vez más largos e intensos a lo largo de las próximas décadas en Aragón:
    - En promedio para todo el territorio, se espera un aumento en la intensidad media cercano a los 2 ºC y a los 3.6 ºC en el caso de la intensidad máxima (alcanzándose temperaturas medias de casi 39 ºC y máximas superiores a 41.5 ºC) a finales de siglo bajo el escenario RCP8.5.
    - Respecto a la duración de la ola de calor hemos estimado que aumentará en 7 días, lo que supone una duración media de las olas de calor de 12 días.
    - Los episodios más intensos se esperan en la zona del Valle del Ebro, con episodios de olas de calor que pueden alcanzar valores máximos de 46 ºC, con una intensidad media de 41 ºC y una duración media de 11 días. Esto provocará los impactos socioeconómicos y sobre la salud más importantes al concentrarse en esta zona la mayor parte de la población.
    - Por otra parte, los cambios extremos en relación a la duración de las olas de calor, con respecto al clima actual, se observarán en los Pirineos, con un aumento en la duración de las olas de calor de 10 días, haciendo que su duración se extienda hasta 17 días y con temperaturas medias superiores a los 30 ºC. Esto sin duda impactará en la biodiversidad de esta zona sensible, así como en el régimen hídrico de toda la comunidad.

9. **Los escenarios de olas de frío** se esperan que se mantengan en intensidad y duración similares a los actuales en todo el territorio. Estos resultados van en línea con la teoría, ampliamente contrastada, de que las variaciones en la distribución de la temperatura afectan tanto a la media como a la varianza, por lo que las variaciones en las temperaturas mínimas extremas serán muy poco acusados.

10. Es la primera vez que se generan escenarios a escala local de episodios de sequía calculados a partir de los indicadores SPI/SPEI para la zona de Aragón en base a proyecciones climáticas locales de temperatura generadas con una

metodología de *dowsncaling* estadístico y en base a la información proporcionada por el CMIP5.

11. Estos escenarios de SPI/SPEI suponen una manera novedosa de representar la magnitud, duración y la intensidad de los episodios de **sequía meteorológica** en base a distintas escalas temporales y su representación gráfica.

12. Nuestros resultados muestran una clara tendencia hacía episodios de sequía más intensos, especialmente a finales de siglo y cuando se consideran periodos acumulativos más largos. Esta tendencia se aprecia sólo en escenarios de SPEI (sequía severa a extrema) mientras que en los escenarios SPI esta tendencia es muy suave (sequía normal).

13. A nivel de impactos en territorio, el área más afectada por episodios de sequía y descenso de precipitación es la zona del Valle de Ebro. Estos resultados no solo coinciden con estudios previos realizados sobre la zona sino que además van en línea con los resultados históricos, que ponen de manifiesto cómo la zona del Valle del Ebro se ha visto afectada por episodios de sequía cada vez más recurrentes e intensos en las últimas décadas.

14. Los escenarios futuros de eventos extremos (olas de calor/frío y sequía) en el territorio español ibérico-peninsular muestran las siguientes conclusiones generales:
    - Intensificación de los episodios de olas de calor en todo el territorio, especialmente en toda la costa Mediterránea, con episodios de más de 20 días de duración (bajo el RCP8.5 a finales de siglo).
    - Aunque se esperan cambios en las temperaturas mínimas medias, no se esperan grandes cambios en los extremos, por lo que no se aprecian alteraciones importantes de los episodios de olas de frío futuros respecto a los actuales.
    - Al no apreciarse cambios significativos en el régimen pluviométrico, los escenarios de SPI no muestran alteraciones significativas con respecto al periodo actual, por lo que según estos escenarios toda la región se encontraría bajo un estado de sequía considerado normal (debido a la propia variabilidad climática).
    - Los escenarios de SPEI, bajo el escenario RCP8.5 y a finales de siglo, ponen de manifiesto como toda la región se mueve hacía episodios de sequía cada vez más extrema y extensa en el tiempo.

15. Se obtienen por primera vez resultados rigurosos y a escala local de los **impactos que el cambio climático supone para el sector vitícola español (peninsular y balear)** en base a proyecciones climáticas regionalizadas del CMIP5.

16. Por primera vez, se analizan los indicadores climáticos en base a valores absolutos junto con valores categorizados. Esta manera de evaluar los resultados permite tomar decisiones mucho más precisas considerando el valor añadido que supone tener en cuenta las condiciones micro climáticas locales.

17. Los resultados obtenidos a través de la simulación de diferentes indicadores bioclimáticos reflejan que el territorio ibérico-balear será uno de los más afectados a nivel, tanto térmico como hídrico. Estos datos concuerdan con los que ponen de manifiesto estudios similares pero aplicados en áreas más extensas, como Europa o el Mediterráneo, sin tener en cuenta las condiciones locales muestran tendencias similares.

18. Se aprecia un aumento en los valores termales (como indican el HI y el CI), mientras que se espera un descenso las reservas de almacenamiento hídrico (como pone de manifiesto el DI). La combinación de ambas situaciones compromete el cultivo de la vid que verá alteradas sus condiciones hidrotermales actuales.

19. Estos cambios supondrán alteraciones en las características organolépticas de la uva y posiciona a gran parte del territorio (especialmente la meseta central y el sur peninsular) en los límites térmicos óptimos para el cultivo de la vid.

20. A nivel del territorio el impacto es heterogéneo:
    - En el sur de la península, con valores de HI superiores a 3500°C y CI por encima de 20°C y DI inferior a -200 mm, la continuidad del sector vitícola en su estado actual se verá seriamente amenazada, con una disminución de los años climáticamente óptimos como muestran los valores de CompI.
    - El norte peninsular y las zonas montañosas, a pesar de los aumentos previstos, con HI inferiores a 2500°C, noches frescas (IC inferior a 15°C) y suministro de agua suficiente (DI superior a 150 mm) mejorarán considerablemente su aptitud climática (CompI), aunque el riesgo de enfermedad de mildiu se mantiene debido al aumento de la temperatura y la humedad.

21. Para poder mantener los niveles de calidad de las vides y los vinos, lo más probable es que los productores vitícolas se vean obligados a adoptar medidas de adaptación al cambio climático y replantearse la manera actual en la que funcionan sus viñedos y buscar como potenciar los efectos positivos y minimizar los negativos asociados al cambio climático.

22. Estos resultados proporcionan información de gran valor añadido para la toma de decisiones, nos solo en el sector vitícola, sino también en otros sectores sensibles a los eventos extremos (olas de calor/frío y sequía meteorológica).

23. Así mismo, estos resultados, no solo sirven para el territorio objeto de estudio, sino que debido a la gran variedad climática y orográfica tanto de Aragón como de toda España, pueden ser de utilidad para áreas similares como la zona del Mediterráneo (Italia, Grecia), la zona atlántica (Portugal) e incluso las regiones vitícolas de Napa en California o las grandes regiones vitícolas de Chile y Argentina (ubicadas en regiones climáticas de latitudes medias).

BIBLIOGRAFÍA

Abaurrea J., Asín J. and Cebrián A.C., Modelling the occurrence of heat waves in maximum and minimum temperatures over Spain and projections for the period 2031-60, Global and Planetary Change, Volume 161, 2018, Pages 244-260, ISSN 0921-8181, https://doi.org/10.1016/j.gloplacha.2017.11.015.

Adger WN, Dessai S, Goulden M et al. Are there social limits to adaptation to climate change? Climatic Change, 2008 93, 335–354.

Alary V, Messad S, Aboul-Naga A, Osman MA, Daoud I, Bonnet P, et al. Livelihood strategies and the role of livestock in the processes of adaptation to drought in the Coastal Zone of Western Desert (Egypt). Agricultural Systems 2014; 128: 44-54.

Aleixandre JL, Giner JF, Aleixandre–Tudó JL. Evaluación del efecto terroir sobre la calidad de la uva y el vino. Enoviticultura N20. 2013.

Alig RJ, Adams DM, McCarl BA. Projecting impacts of global climate change on the US forest and agriculture sectors and carbon budgets. Forest Ecology and Management 2002; 169: 3-14.

Alonso AD, O'Neill MA. Climate change from the perspective of Spanish wine growers: a three-region study. British Food Journal 2011; 113: 205-221.

Anderson BG, Bell ML. Weather-Related Mortality How Heat, Cold, and Heat Waves Affect Mortality in the United States. Epidemiology 2009; 20: 205-213.

Andrés, S., Pascual, N, Diago, M.P., Miranda, J., Ramalle-Gomara, E., Bengoechea, C., Arpón, L. and Zúñiga Crespo, J. Impacto, adaptación y percepción del cambio climático en la DOCa Rioja, 2020.

Ascenso A, Gama C, Blanco-Ward D, Monteiro A, Silveira C, Viceto C, et al. Assessing Douro Vineyards Exposure to Tropospheric Ozone. Atmosphere 2021; 12.

Ashenfelter, O., Ashmore, D., Lalonde, R., Bordeaux wine vintage quality and the weather. In: Chance, 1995 Vol. 8, No. 4, 7 pp.

Asong ZE, Khaliq MN, Wheater HS. Projected changes in precipitation and temperature over the Canadian Prairie Provinces using the Generalized Linear Model statistical downscaling approach. Journal of Hydrology 2016; 539: 429-446.

Barbeau G.,. Climat et vigne en moyenne vallée de la Loire, France. In : Proceedings of the Conference on Climate and Viticulture, Zaragoza (Spain),2007, pp. 106- 111.

Barrera-Escoda A, Goncalves M, Guerreiro D, Cunillera J, Baldasano JM. Projections of temperature and precipitation extremes in the North Western Mediterranean Basin by dynamical downscaling of climate scenarios at high resolution (1971-2050). Climatic Change 2014; 122: 567-582.

Bates B, Kundzewicz Z, Wu S, Palutikof J. Climate Change and water. 2008. Eds. IPCC Secretariat, Geneva, 210 pp

Battaglini A, Barbeau G, Bindi M, Badeck F-W. European winegrowers' perceptions of climate change impact and options for adaptation. Regional Environmental Change 2009; 9: 61-73.

Begueria S, Vicente-Serrano SM, Reig F, Latorre B. Standardized precipitation evapotranspiration index (SPEI) revisited: parameter fitting, evapotranspiration models, tools, datasets and drought monitoring. International Journal of Climatology 2014; 34: 3001-3023.

Bellia S., Douguedroit A. and Seguin B.,. Impacts du réchauffement sur les étapes phénologiques du Grenache et de la Syrah dans les Côtes du Rhône méridionales et les Côtes de Provence (1976-2000). 2008 In : Journées de Climatologie, Nantes (France), Climat et société : climat et végétation, pp. 45-55.

Bender MA, Knutson TR, Tuleya RE, Sirutis JJ, Vecchi GA, Garner ST, et al. Modeled Impact of Anthropogenic Warming on the Frequency of Intense Atlantic Hurricanes. Science 2010; 327: 454-458.

Benestad RE, Hanssen-Bauer I, Forland EJ. An evaluation of statistical models for downscaling precipitation and their ability to capture long-term trends. International Journal of Climatology 2007; 27.

Beniston M, Stephenson DB, Christensen OB, Ferro CAT, Frei C, Goyette S, et al. Future extreme events in European climate: an exploration of regional climate model projections. Climatic Change 2007; 81: 71-95.

Bentsen M, Bethke I, Debernard JB, Iversen T, Kirkevag A, Seland O, et al. The Norwegian Earth System Model, NorESM1-M - Part 1: Description and basic evaluation of the physical climate. Geoscientific Model Development 2013; 6: 687-720.

Berg A, Sheffield J. Climate Change and Drought: the Soil Moisture Perspective. Current Climate Change Reports 2018; 4: 180-191.

Berg A, Sheffield J, Milly PCD. Divergent surface and total soil moisture projections under global warming. Geophysical Research Letters 2017; 44: 236-244.

Bernetti, I., Menghini, S., Marinelli, N., Sacchelli, S., Alampi Sottini, V., 2012. Assessment of climate change impact on viticulture: economic evaluations and adaptation strategies analysis for the Tuscan wine sector. Wine Economics and Policy 2012,1, 73-86.

Bindi M, Fibbi L, Gozzini B, Orlandini S, Miglietta F. Modelling the impact of future climate scenarios on yield and yield variability of grapevine. Climate Research 1996; 7: 213-224.

Bindi M, Fibbi L, Lanini M, Miglietta F. Free Air CO2 Enrichment (FACE) of grapevine (Vitis vinifera L.): I. Development and testing of the system for CO2 enrichment. European Journal of Agronomy 2001; 14: 135-143.

Blanco-Ward D, Garcia Queijeiro JM, Jones GV. Spatial climate variability and viticulture in the Mino River Valley of Spain. Vitis 2007; 46: 63-70.

Blenkinsop S, Fowler HJ. Changes in European drought characteristics projected by the PRUDENCE regional climate models. International Journal of Climatology 2007; 27: 1595-1610.

Bock A, Sparks T, Estrella N, Menzel A. Changes in the phenology and composition of wine from Franconia, Germany. Climate Research 2011; 50: 69-81.

Bois, B., M. Moriondo, and G. V. Jones,: Thermal risk assessment for viticulture using monthly temperature data. In : Proceedings of the 10th International Terroir Congress, 2014, Vol. 2. Corvinus University of Budapest

Bois B., Cartographie agroclimatique à méso-échelle : méthodologie et application à la variabilité spatiale en Gironde viticole. Conséquences pour le développement de la vigne et la maturation du raisin. Thèse de Doctorat, Université Bordeaux1 (France). 2007

Bonfante, A.; Alfieri, S.M.; Albrizio, R.; Basile, A.; De Mascellis, R.; Gambuti, A.; Giorio, P.; Langella, G.; Manna, P.; Monaco, E.; et al. Evaluation of the effects of future climate change on grape quality through a physically based model application: A case study for the Aglianico grapevine in Campania region, Italy. Agric. Syst. 2017, 152, 100–109

Bonfante, A.; Monaco, E.; Langella, G.; Mercogliano, P.; Bucchignani, E.; Manna, P.; Terribile, F. A dynamic viticultural zoning to explore the resilience of terroir concept under climate change. Sci. Total Environ. 2018, 624, 294–308

Bonnefoy C., Quénol H., Bonnardot V., Barbeau G., Madelin M., Planchon O. and Neethling E.,. Temporal and spatial analyses of temperature in a French wine-producing area: the Loire Valley. Int. J. Climatol., 2013. 33, 1849-1862 (DOI : 10.1002/joc.3552).

Branas J. Viticulture générale. Dehan, Montpellier. 1974; 990 p

Branas J, Bernon G, Levadoux L. □léments de viticulture générale 1946.

Brands S, Herrera S, Fernandez J, Gutierrez JM. How well do CMIP5 Earth System Models simulate present climate conditions in Europe and Africa? Climate Dynamics 2013; 41: 803-817.

Brands S, Herrera S, San-Martin D, Gutierrez JM. Validation of the ENSEMBLES global climate models over southwestern Europe using probability density functions, from a downscaling perspective. Climate Research 2011a; 48: 145-161.

Brands S, Taboada JJ, Cofino AS, Sauter T, Schneider C. Statistical downscaling of daily temperatures in the NW Iberian Peninsula from global climate models: validation and future scenarios. Climate Research 2011b; 48.

Breshears D. An ecologist's perspective of ecohydrology, Bull. Ecol. Soc. Am., 2005; 86: 296 – 300.

Brixner, G.F., Schöffel, E.R. and Tonietto, J. Determinacao da evapotranspiracaao por diferentes métodos e sua aplicacao no índice de seca na campnha Gaúcha, Brasil. Rev. Bras.Fructi., Jaboticabal-SP, 2014, V.36, n4, p780-793

Bryant. EA. Natural hazards. International Journal of Climatology, E. Cambridge University Press, Cambridge. ISBN 0 521 37295 X. 1993; 13:344-346. https://doi.org/10.1002/joc.3370130310

Bryant. EA. Natural hazards. International Journal of Climatology, E. Cambridge University Press, Cambridge. ISBN 0 521 37295 X. 1993; 13:344-346. https://doi.org/10.1002/joc.3370130310

Bucelli, P., & Costantini, E. Vite da vino e zonazioni vitivinicole. In Metodi di valutazione dei suoli e delle terre (p. 922). 2006. Siena: Edizioni Cantagalli.

Buerger CM, Kolditz O, Fowler HJ, Blenkinsop S. Future climate scenarios and rainfall-runoff modelling in the Upper Gallego catchment (Spain). Environmental Pollution 2007; 148.

Bureau, S. M., A. J. Razungles, and R. L. Baumes. The aroma of Muscat of Frontignan grapes: effect of the light environment of vine or bunch on volatiles and glycoconjugates. J. Sci. Food Agric. 2000, 80:2012–2020

Burke EJ, Brown SJ. Evaluating uncertainties in the projection of future drought. Journal of Hydrometeorology 2008; 9: 292-299.

Buttrose, M. S., C. R. Hale, and W. M. Kliewer. Effect of temperature on composition of cabernet-sauvignon berries. Am. J. Enol. Vitic. 1971,22:71–75.

Calbo J. Possible Climate Change Scenarios with Specific Reference to Mediterranean Regions. In: Sabater S, Barcelo D, editors. Water Scarcity in the Mediterranean: Perspectives under Global Change. 8, 2010, pp. 1-13.

Camps, J. O., and M. C. Ramos. Grape harvest and yield responses to inter-annual changes in temperature and precipitation in an area of north-east Spain with a Mediterranean climate. Int. J. Biometeorol. 2012, 56:853–864.

Carbonneau, A. Ecophysiologie de la vigne et terroir. Terroir, zonazione, viticoltura. Trattato internazionale, 2003. Phytoline 1:61–102.

Carbonneau A, Tonietto J. La géoviticulture: de la géographie viticole aux évolutions climatiques et technologiques à l'échelle mondiale. Rev. Oenol. Tech.Vitivin. Oenol.1998; 87, 16-18.

Cardil, A., Molina Terrén, D., Ramirez, J. and Vega-Garcia, C. Trends in adverse weather patterns and large wildland fires in Aragón (NE Spain) from 1978 to 2010. Natural Hazards and Earth System Sciences, 2013; 13. 1393-1399. 10.5194/nhess-13-1393-2013.

Carmona, R., Díaz, J., Miron, I., Ortiz, C., Luna, M. Y., Linares, C. Mortality attributable to extreme temperatures in Spain: A comparative analysis by city. Environment International, 2016; 91. 22-28. 10.1016/j.envint.2016.02.018.

Carvalho D, Rocha A, Gomez-Gesteira M, Santos CS. Potential impacts of climate change on European wind energy resource under the CMIP5 future climate projections. Renewable Energy 2017; 101: 29-40.

Carvalho, D., Pereira, S. and Rocha, A. Future surface temperature changes for the Iberian Peninsula according to EURO-CORDEX climate projections. Climate Dynamics. 56. 2021 1-16. 10.1007/s00382-020-05472-3.

Cheeseman, John. Food Security in the Face of Salinity, Drought, Climate Change, and Population Growth, 2016. 10.1016/B978-0-12-801854-5.00007-8.

Chen YD, Li JF, Zhang Q. Changes in site-scale temperature extremes over China during 2071-2100 in CMIP5 simulations. Journal of Geophysical Research-Atmospheres 2016; 121: 2732-2749.

Cherlet M, Hutchinson C, Reynolds J, Hill J, Sommer S, von Maltitz G. (Eds.), World Atlas of Desertification, Publication Office of the European Union, Luxembourg, 2018. United Nations Environment Program

Christensen JH, Kjellstrom E, Giorgi F, Lenderink G, Rummukainen M. Weight assignment in regional climate models. Climate Research 2010; 44: 179-194.

Chuine, I., Yiou, P., Viovy, N., Seguin, B., Daux, V., and Ladurie, E. L. Historical phenology: Grape ripening as a past climate indicator. Nature, 2014. 432, 289–290.

Chylek P, Li J, Dubey MK, Wang M, Lesins G. Observed and model simulated 20th century Arctic temperature variability: Canadian Earth System Model CanESM2. Atmos. Chem. Phys. Discuss. 2011; 11: 22893–22907, doi: 10.5194/acpd-11-22893-2011

Clark, J.S., Iverson, L., Woodall, C.W., Allen, C.D., Bell, D.M., Bragg, D.C., D'Amato, A.W., Davis, F.W., Hersh, M.H., Ibanez, I., Jackson, S.T., Matthews, S., Pederson, N., Peters, M., Schwartz, M.W., Waring, K.M. and Zimmermann, N.E. (2016), The impacts of increasing drought on forest dynamics, structure, and biodiversity in the United States. Glob Change Biol, 22: 2329-2352. https://doi.org/10.1111/gcb.13160

Collados-Lara AJ, Pulido-Velazquez D, Pardo-Iguzquiza E. An Integrated Statistical Method to Generate Potential Future Climate Scenarios to Analyse Droughts. Water 2018; 10.

Collins W, Bellouin N, Doutriaux-Boucher M, Gedney N, Hinton T, Jones CD, Liddicoat S, Martin G, O'Connor F, Rae J, Senior C, Totterdell I, Woodward S, Reichler T, Kim J, Halloran P. 2008.Evaluation of the HadGEM2 model. Hadley Centre Technical Note. HCTN 74, Met Office Hadley Centre, Exeter, UK.

Combris P, Lecocq S, Visser, M. 1997. Estimation of a hedonic price equation for Bordeaux wine: does quality matter? Econom. J. 1997; 107:3-390

Cook J, Nuccitelli D, Green SA, Richardson M, Winkler B, Painting R, Way R, Jacobs P, Skuce A. Quantifying the consensus on anthropogenic global warming in the scientific literature. Environ Res Lett 8:024024. 2013. doi:10.1088/1748-9326/8/2/024024

Cos, J., Doblas-Reyes, F., Jury, M., Marcos, R., Bretonnière, P.-A., and Samsó, M.: The Mediterranean climate change hotspot in the CMIP5 and CMIP6 projections, Earth Syst. Dynam., 13, 321–340, https://doi.org/10.5194/esd-13-321-2022, 2022.

Costa JM, Ortuño MF, Lopes CM, Chaves MM. Grapevine varieties exhibiting differences in stomatalresponse to water deficit. Funct Plant Biol 39: 179–189, 2012

Dai, A. G., T. B. Zhao, and J. Chen. 2018. "Climate Change and Drought: A Precipitation and Evaporation Perspective." Current Climate Change Reports 4, no. 3 (Sep): 301-312. http://dx.doi.org/10.1007/s40641-018-0101-6.

Dai AG. Drought under global warming: a review. Wiley Interdisciplinary Reviews-Climate Change 2011; 2: 45-65.

Dai AG. Increasing drought under global warming in observations and models (vol 3, pg 52, 2013). Nature Climate Change 2013; 3: 171-171.

Damiano N, Arena C, Bonfante A, Caputo R, Erbaggio A, Cirillo C, et al. How Leaf Vein and Stomata Traits Are Related with Photosynthetic Efficiency in Falanghina Grapevine in Different Pedoclimatic Conditions. Plants-Basel 2022; 11.

De Martino G, De Paola F, Fontana N, Marini G, Ranucci A. Experimental assessment of level pool routing in preliminary design of floodplain storage. Science of the Total Environment 2012; 416: 142-147.

De Salvo, M., Raffaelli, R., Moser, R. The impact of climate change on permanent crops in an Alpine region: A Ricardian analysis. Agricultural Systems, 2013. 118, 23-32

Déqué M, Somot S, Sanchez-Gomez E, Goodess CM, Jacob D, Lenderink G, Christensen OB. The spread amongst ENSEMBLES regional scenarios: regional climate models, driving general circulation models and inter-annual variability. Clim Dyn, 2012. 38:951–964. doi:10.1007/s00382-011-1053-x

Diaz, Henry & Murnane, Richard. Preface: The significance of weather and climate extremes to society: An introduction. xiii-xvi. 2008 10.1017/CBO9780511535840.002.

D'Ippoliti, D., Michelozzi, P., Marino, C. et al. The impact of heat waves on mortality in 9 European cities: results from the EuroHEAT project. Environ Health, 2010; 9, 37. https://doi.org/10.1186/1476-069X-9-37

Doll P. Impact of climate change and variability on irrigation requirements: A global perspective. Climatic Change 2002; 54: 269-293.

Dosio A. Projection of temperature and heat waves for Africa with an ensemble of CORDEX Regional Climate Models. Climate Dynamics 2017; 49: 493-519.

Downey, M. O., N. K. Dokoozlian, and M. P. Krstic. Cultural practice and environmental impacts on the flavonoid composition of grapes and wine: a review of recent research. Am. J. Enol. Vitic., 2006. 57:257–268.

Dracup JA, Lee KS, Paulson EG. ON THE STATISTICAL CHARACTERISTICS OF DROUGHT EVENTS. Water Resources Research 1980; 16: 289-296.

Duchene E, Huard F, Dumas V, Schneider C, Merdinoglu D. The challenge of adapting grapevine varieties to climate change. Climate Research 2010; 41: 193-204.

Duchene E, Schneider C. Grapevine and climatic changes: a glance at the situation in Alsace. Agronomy for Sustainable Development 2005; 25: 93-99.

Duchene, E. How can grapevine genetics contribute to the adaptation to climate change? OENO One 2016, 50

Duchene E, Butterlin G, Dumas V, Merdinoglu D. Towards the adaptation of grapevine varieties to climate change: QTLs and candidate genes for developmental stages. Theor. Appl. Genet. 2012. 124(4): 623–635, doi: 10.1007/s00122-011-1734-1

Dunne JP, John JG, Adcroft AJ, Griffies SM, Hallberg RW, Shevliakova E, et al. GFDL's ESM2 Global Coupled Climate-Carbon Earth System Models. Part I: Physical Formulation and Baseline Simulation Characteristics. Journal of Climate 2012; 25: 6646-6665.

Easterling, D.R., Evans, J.L., Groisman, P. Ya., Karl, T.R., Kunkel, K.E. and Ambenje, P. Observed variability and trends in extreme climate events: A brief review. Bull. Amer. Meteorol. Soc. 2000. 81:417-425.

Escariz A, Blanco J, Miranda D, Crecente R. Zonificación y metodología para la delimitación de comarcas vitícolas. Aplicación a la ampliación de vino de la tierra de Betanzos. XI congreso internacional de Ingenieria de proyectos Lugo 2007.

Estrela T, Perez-Martin MA, Vargas E. Impacts of climate change on water resources in Spain. Hydrological Sciences Journal-Journal Des Sciences Hydrologiques 2012; 57: 1154-1167.

Estrella N, Menzel A. Recent and future climate extremes arising from changes to the bivariate distribution of temperature and precipitation in Bavaria, Germany. International Journal of Climatology 2013; 33: 1687-1695.

EXPANSIÓN, 2016. https://www.expansion.com/economia/2019/12/16/5df6afff468aebed0c8b467f.html

EXPANSIÓN 2019 https://www.researchgate.net/publication/345973796_Impacto_adaptacion_y_percepcion_del_cambio_climatico_en_la_DOCa_Rioja

Eyring, V., Bony, S., Meehl, G. A., Senior, C. A., Stevens, B., Stouffer, R. J., and Taylor, K. E.: Overview of the Coupled Model Intercomparison Project Phase 6 (CMIP6) experimental design and organization, Geosci. Model Dev.,2016, 9, 1937-1958

Failla, O., Mariani, L., & Toninato, L. Viticoltura di territorio, 2008. In La vite e il vino (p. 624). Milano: Bayer CropScience.

Fernandez-Montes S, Rodrigo FS. Trends in seasonal indices of daily temperature extremes in the Iberian Peninsula, 1929-2005. International Journal of Climatology 2012; 32: 2320-2332.

Feyen L, Dankers R. Impact of global warming on streamflow drought in Europe. Journal of Geophysical Research-Atmospheres 2009; 114.

FEV, 2021. https://www.expansion.com/economia/2019/12/16/5df6afff468aebed0c8b467f.html

Field, C.B., Barros, V., Stocker, T.F., Qin, D., Dokken, D.J., Ebi, K.L., Mastrandrea, M.D., Mach, K.J., Plattner, G.K., Allen, S.K., Tignor, M., Midgley, P.M., IPCC, 2012. Managing the Risks of Extreme Events and Disasters to Advance Climate Change Adaptation. Cambridge University Press, Cambridge, United Kingdom and New York, NY, USA, p. 582 pp.

Fischer EM, Schar C. Consistent geographical patterns of changes in high-impact European heatwaves. Nature Geoscience 2010; 3: 398-403.

Flato G, Marotzke J, Abiodun B, Braconnot P, Chou SC, Collins W, et al. Evaluation of Climate Models, 2014.

Flexas J, Galmes J, Galle A, Gulias J, Pou A, Ribas-Carbo M, Tomas M, Medrano H. Improving water use efficiency in grapevines: potential physiological targets for biotechnological improvement. Aust. J. Grape Wine Res., 2010. 16: 106–121, doi: 10.1111/j.1755-0238.2009.00057.x.

Fonseca Conceicao MA, Tonietto J, Fialho FB. Using temperature to calculate the dryness index of grape production regions. Revista Brasileira De Fruticultura 2012; 34: 175-182.

Fonseca D, Carvalho MJ, Marta-Almeida M, Melo-Goncalves P, Rocha A. Recent trends of extreme temperature indices for the Iberian Peninsula. Physics and Chemistry of the Earth 2016; 94: 66-76.

Forzieri G, Feyen L, Rojas R, Florke M, Wimmer F, Bianchi A. Ensemble projections of future streamflow droughts in Europe. Hydrology and Earth System Sciences 2014; 18: 85-108.

Fragoso M, Carraca MD, Alcoforado MJ. Droughts in Portugal in the 18th century: A study based on newly found documentary data. International Journal of Climatology 2018; 38: 5522-5541.

Fraga, H.; García de Cortázar Atauri, I.; Santos, J.A. Viticultural irrigation demands under climate change scenarios in Portugal. Agric. Water Manag. 2018, 196, 66–74

Fraga H, Malheiro AC, Moutinho-Pereira J, Jones GV, Alves F, Pinto JG, et al. Very high resolution bioclimatic zoning of Portuguese wine regions: present and future scenarios. Regional Environmental Change 2014; 14: 295-306.

Fraga H, Malheiro AC, Moutinho-Pereira J, Santos JA. Future scenarios for viticultural zoning in Europe: ensemble projections and uncertainties. International Journal of Biometeorology 2013; 57: 909-925.

Fraga H, Santos JA, Malheiro AC, Moutinho-Pereira J. Climate change projections for the portuguese viticulture using a multi-model ensemble. Ciencia E Tecnica Vitivinicola 2012; 27: 39-48.

Fraga, H.; Santos, J.A. Daily prediction of seasonal grapevine production in the Douro wine region based on favourable meteorological conditions. Aust. J. Grape Wine Res. 2017

Fraga, H.; Pinto, J.G.; Santos, J.A. Climate change projections for chilling and heat forcing conditions in European vineyards and olive orchards: A multi-model assessment. Clim. Chang. 2019, 152, 179–193

France I, Dubourdieu AD. Climate Change: Field Reports from Leading Winemakers. Journal of Wine Economics 2016; 11: 5-47.

Fregoni, M. L'indice bioclimatico di qualitá Fregoni. Terroir, Zonazione Viticoltura 2003; 115-127.

Frias MD, Fernandez J, Saenz J, Rodriguez-Puebla C. Operational predictability of monthly average maximum temperature over the Iberian Peninsula using DEMETER simulations and downscaling. Tellus Series a-Dynamic Meteorology and Oceanography 2005; 57.

Frias MD, Herrera S, Cofino AS, Gutierrez JM. Assessing the Skill of Precipitation and Temperature Seasonal Forecasts in Spain: Windows of Opportunity Related to ENSO Events. Journal of Climate 2010; 23.

Caffarra, A., Rinaldi, M., Eccel, E., Rossi, V., Pertot, I. Modelling the impact of climate change on the interaction between grapevine and its pests and pathogens: European grapevine moth and powdery mildew. Agriculture, Ecosystems and Environment, 2012. 148, 89-101.

Gaitan E, Monjo R, Portoles J, Pino-Otin MR. Projection of temperatures and heat and cold waves for Aragon (Spain) using a two-step statistical downscaling of CMIP5 model outputs. Science of the Total Environment 2019; 650: 2778-2795.

Gaitan E, Monjo R, Portoles J, Rosa Pino-Otin M. Impact of climate change on drought in Aragon (NE Spain). Science of the Total Environment 2020; 740.

Gallego MC, Trigo RM, Vaquero JM, Brunet M, Garcia JA, Sigro J, et al. Trends in frequency indices of daily precipitation over the Iberian Peninsula during the last century. Journal of Geophysical Research-Atmospheres 2011; 116.

Gallo AE, Perez Pena JE, Prieto JA. Mechanisms underlying photosynthetic acclimation to high temperature are different between Vitis vinifera cv. Syrah and Grenache. Functional Plant Biology 2021; 48: 342-357

Galbreath J. Climate Change Response: Evidence from the Margaret River Wine Region of Australia. Business Strategy and the Environment, 2014. 23, 89–104.

Ganichot, B. Evolution de la date des vendanges dans les Côtes du Rhône méridionales. In 6emes Recontres Rhodaniennes, 2002 (pp. 38–41). Orange, France: Institut Rhodanien.

García de Cortázar-Atauri, I.; Duchêne, E.; Destrac-Irvine, A.; Barbeau, G.; de Rességuier, L.; Lacombe, T.; Parker, A.K.; Saurin, N.; van Leeuwen, C. Grapevine phenology in France: From past observations to future evolutions in the context of climate change. OENO One 2017, 51

Garcia-Barron L, Aguilar M, Sousa A. Evolution of annual rainfall irregularity in the southwest of the Iberian Peninsula. Theoretical and Applied Climatology 2011; 103: 13-26.

Garcia-Herrera R, Diaz J, Trigo RM, Hernandez E. Extreme summer temperatures in Iberia: health impacts and associated synoptic conditions. Annales Geophysicae 2005; 23: 239-251.

Carroll, N., Frijters, P., and Shields, M. A. Quantifying the Costs of Drought: New Evidence from Life Satisfaction Data. Journal of Population Economics, 2009, 22(2), 445–461. http://www.jstor.org/stable/40344739

Choat, Brendan & Jansen, Steven & Brodribb, Tim & Cochard, Hervé & Delzon, Sylvain & Bhaskar, Radika & Bucci, Sandra & Feild, Taylor & Gleason, Sean & Hacke, Uwe & Jacobsen, Anna & Lens, Frederic & Maherali, Hafiz & Martinez Vilalta, Jordi & Mayr, Stefan & Mencuccini, Maurizio & Mitchell, Patrick & Nardini, Andrea

& Pittermann, Jarmila & Zanne, Amy. (2012). Global convergence in the vulnerability of forests to drought. Nature. 491. 10.1038/nature11688.
Gilaberte-Burdalo M, Lopez-Martin F, Pino-Otin MR, Lopez-Moreno JI. Impacts of climate change on ski industry. Environmental Science & Policy 2014; 44: 51-61.
Gilaberte-Burdalo M, Lopez-Moren JI, Moran-Tejeda E, Jerez S, Alonso-Gonzalez E, Lopez-Martin F, et al. Assessment of ski condition reliability in the Spanish and Andorran Pyrenees for the second half of the 20th century. Applied Geography 2017; 79: 127-142.
Giorgi F, Jones C, Asrar GR. Addressing climate information needs at the regional level: the CORDEX framework. WMO Bull. 2009; 58(3):175–183
Giorgi F, Gutowski WJ. Regional Dynamical Downscaling and the CORDEX Initiative. Annual Review of Environment and Resources, Vol 40 2015; 40: 467-490.
Giorgi F, Mearns LO. Approaches to the simulation of regional climate change - a review. Reviews of Geophysics 1991; 29: 191-216.
Gladstones, J. Viticulture and environment. Winetitles ed. Winetitles; Underdale, South Australia, 1992; Australia.
Gobiet A, Kotlarski S, Beniston M, Heinrich G, Rajczak J, Stoffel M. 21st century climate change in the European Alps-A review. Science of the Total Environment 2014; 493: 1138-1151.
Gomez-Gesteira M, Gimeno L, deCastro M, Lorenzo MN, Alvarez I, Nieto R, et al. The state of climate in NW Iberia. Climate Research 2011; 48: 109-144.
Gomez-Martinez G, Galiano L, Rubio T, Prado-Lopez C, Redolat D, Blazquez CP, et al. Effects of Climate Change on Water Quality in the Jucar River Basin (Spain). Water 2021; 13
Gommes, R., and Petrassi, F. Rainfall variability and drought in sub-Saharan Africa since 1960. Agrometeorology Series Working Paper 9, Food and Agriculture Organization, 1994, Rome, Italy, 100 pp.
Goncalves B, Falco V, Moutinho-Pereira J, Bacelar E, Peixoto F, Correia C. Effects of Elevated CO2 on Grapevine (Vitis vinifera L.): Volatile Composition, Phenolic Content, and in Vitro Antioxidant Activity of Red Wine. Journal of Agricultural and Food Chemistry 2009; 57: 265-273.
Goncalves M, Barrera-Escoda A, Guerreiro D, Baldasano JM, Cunillera J. Seasonal to yearly assessment of temperature and precipitation trends in the North Western Mediterranean Basin by dynamical downscaling of climate scenarios at high resolution (1971-2050). Climatic Change 2014; 122: 243-256.
González, J., and Valdés, J. 2006. New drought frequency index: Definition and comparative performance analysis. Water Resour. Res. 42 (11): W11421. doi:10.1029/2005WR004308.
Gordo, O. and Sanz, J.J. Climate change and bird phenology: a long-term study in the Iberian Peninsula. Global Change Biology, 2006; 12: 1993-2004. https://doi.org/10.1111/j.1365-2486.2006.01178.x
Graça, A., Gishen, M. and Jones, G. Proposal for the development of a framework for a globally relevant wine sector climate change adaptation strategy 2016. 10.13140/RG.2.2.11875.14883.
Greenwood O, Mossman HL, Suggitt AJ, Curtis RJ, Maclean IMD (2016) Using in situ management to conserve biodiversity under climate change. Journal of Applied Ecology, doi: 10.1111/1365-2664.12602.
Greer, D. H., M. M. Weedon, and C. Weston. Reductions in biomass accumulation, photosynthesis in situ and net carbon balance are the costs of protecting Vitis vinifera “Semillon” grapevines from heat stress with shade covering, 2011. AoB plants. 2011: plr023.
Grifoni, D., G. Carreras, G. Zipoli, F. Sabatini, A. Dalla Marta, and S. Orlandini. Row orientation effect on UV-B, UV-A and PAR solar irradiation components in vineyards at Tuscany, 2008. Italy. Int. J. Biometeorol. 52:755–763.

Gross MH, Alexander LV, Macadam I, Green D, Evans JP. The representation of health-relevant heatwave characteristics in a Regional Climate Model ensemble for New South Wales and the Australian Capital Territory, Australia. International Journal of Climatology 2017; 37: 1195-1210.

Gu, S., Ding, P. and Howard, S. Effect of temperature and exposure time on cold hardiness of primary buds during the dormant season in 'Concord', 'Norton', 'Vignoles' and 'St. Vincent' grapevines. Journal of Horticultural Science and Biotechnology 2002.77. 635-639. 10.1080/14620316.2002.11511550.

Gudmundsson L, Rego F C, Rocha M and Seneviratne S I. Environ. Res. Lett., 2014. 9

Guerreiro SB, Dawson RJ, Kilsby C, Lewis E, Ford A. Future heat-waves, droughts and floods in 571 European cities. Environmental Research Letters 2018; 13.

Guido V, Impact of Climate Change on Vitis Vinifera L. over Mediterranean Area. Tesi di Dottorato in Agrometeorologia ed Ecofisiologia dei Sistemi Agrari e Forestali, Università degli Studi di Sassari. 2015.

Gutierrez JM, Maraun D, Widmann M, Huth R, Hertig E, Benestad R, et al. An intercomparison of a large ensemble of statistical downscaling methods over Europe: Results from the VALUE perfect predictor cross-validation experiment. International Journal of Climatology 2019; 39: 3750-3785.

Guttman NB. Comparing the Palmer Drought Index and the standardized precipitation index. Journal of the American Water Resources Association 1998; 34: 113-121.

Hagman G. Prevention better than cure: report on human and natural disasters in the Third World, 1984. Swedish Red Cross, Stockholm, Sweden.

Hall, A., and G. V. Jones. Effect of potential atmospheric warming on temperature-based indices describing Australian winegrape growing conditions. Aust. J. Grape Wine R, 2009, 15:97– 119

Hannah L, Roehrdanz PR, Ikegami M, Shepard AV, Shaw MR, Tabor G, et al. Climate change, wine, and conservation. Proceedings of the National Academy of Sciences of the United States of America 2013; 110: 6907-6912.

Hansen J, Sato M, Ruedy R. Perception of climate change. Proceedings of the National Academy of Sciences of the United States of America 2012; 109: E2415-E2423.

Hancock J.M. Feature Review – `Terrior. The Role of Geology, Climate, and Culture in Making of French Wines' by Wilson J.E. Journal of Wine Research 10, 1999. (1), 43–49.

Hancock J.M. Geology of wine. In Selley R.C. et al., (Eds.). The Encyclopaedia of Geology Volume III, Elsevier, Amsterdam, 2005. 85–90.

Hao ZC, Hao FH, Singh VP, Ouyang W. Quantitative risk assessment of the effects of drought on extreme temperature in eastern China. Journal of Geophysical Research-Atmospheres 2017; 122: 9050-9059.

Harbertson, J. F., and M. Keller. Rootstock effects on deficit-irrigated winegrapes in a dry climate: grape and wine composition. Am. J. Enol. Vitic., 2012. 63:40–48.

Hargreaves GL, Samani ZA. Reference crop evapotranspiration from temperature. Appl. Eng. Agric. 1985;1: 96–99.

Hartmann, D.L., Klein Tank, A.M.G., Rusticucci, M., Alexander, L.V., Brönnimann, S., Kaplan,A., Soden, B.J., Thorne, P.W., Wild, M., Zhai, P.M. Observations: Atmosphere and Surface. In T.F. Stocker, D. Qin, G.K. Plattner, M. Tignor, S.K. Allen, J. Boschung, A. Nauels, Y. Xia, V. Bex, P.M. Midgley (eds.), Climate Change 2013: The Physical Science Basis. Contribution of Working Group I to the Fifth Assessment Report of the Intergovernmental Panel on Climate Change, Cambridge University Press, Cambridge, United Kingdom and New York, NY, USA. 2013.

Hausfather Z, Peters GP. Emissions - the 'business as usual' story is misleading. Nature 2020; 577: 618-620.

Hidalgo, T. and Togores, J. EL concepto de "Terroir" en el viñedo. Ponencia en el XII curso de verano, Innovación vitivinícola en la ribera del Duero, sostenibilidad

II.2012. Editado por el consejo regulador de la denominación de origen Ribera del Duero, pp 9-45
Hayes M, Svoboda M, Wall N, Widhalm M. The lincoln declaration on drought indices. Bulletin of the American Meteorological Society 2011; 92: 485-488.
Hayes MJ, Svoboda MD, Wilhite DA, Vanyarkho OV. Monitoring the 1996 drought using the standardized precipitation index. Bulletin of the American Meteorological Society 1999; 80: 429-438.
Heavens N, Ward D and Natalie M. Studying and Projecting Climate Change with Earth System Models. Nature Education Knowledge.2013; 4(5):4
Hertig E, Seubert S, Jacobeit J. Temperature extremes in the Mediterranean area: trends in the past and assessments for the future. Natural Hazards and Earth System Sciences 2010; 10: 2039-2050.
Hervada-Sala C, Pawlowsky-Glahn V, Jarauta-Bragulat E. A statistical method to downscale temperature forecasts. A case study in Catalonia. Meteorological Applications 2000; 7.
Hoerling M, Eischeid J, Perlwitz J, Quan XW, Zhang T, Pegion P. On the Increased Frequency of Mediterranean Drought. Journal of Climate 2012; 25: 2146-2161.
Holland, T., Smit, B., 2010. Climate change and the wine industry: current research themes and new directions. Journal of Wine Research 21, 125-136.
Holland T, Smit B. Climate change and the wine industry: current research themes and new directions. J. Wine Res. 2010; 21:125-136.
Howden SM, Soussana J-F, Tubiello FN, Chhetri N, Dunlop M, Meinke H. Adapting agriculture to climate change. Proceedings of the National Academy of Sciences, 2007, 104, 19691-19696.
Hu Q, Willson GD. Effects of temperature anomalies on the Palmer Drought Severity Index in the central United States. International Journal of Climatology 2000; 20: 1899-1911.
Huglin P. Nouveau Mode d'Évaluation des Possibilités Héliothermiques d'un Milieu Viticole. C. R. Acad. Agr. France, 1978; 1117-1126.
Hunter J.J., Volschenk C.G. and Bonnardot V., 2010. Linking grapevine row orientation to a changing climate in South Africa. In : Proceedings of the Inter vitis Interfructa Conference, Stuttgart (Germany), pp. 60-70
Hussein M, Cholette S, Castaldi RM. An Analysis of Globalization Forces in the Wine Industry. Journal of Global Marketing, 2008, 21, 33-47.
Ibacache, A., Martínez, L. and Sturla, C. Zonificación del territorio de la denominación de origen Pisco. Instituto Nacional de Investigaciones Agropecuarias INIA: La Serena (Chile). 2010
Iglesias A, Garrote L, Flores F, Moneo M. Challenges to manage the risk of water scarcity and climate change in the Mediterranean. Water Resources Management 2007; 21: 775-788.
Iglesias A. y Medina F. (2009). Consecuencias del cambio climático para la agricultura: ¿un problema de hoy o del futuro?. Revista española de Estudios Agrosociales y Pesqueros, nº 221, 2009.
Iglesias A, Quiroga S, Moneo M, Garrote L. From climate change impacts to the development of adaptation strategies: Challenges for agriculture in Europe. Climatic Change 2012; 112: 143-168
Imbert A, Benestad RE. An improvement of analog model strategy for more reliable local climate change scenarios. Theoretical and Applied Climatology 2005; 82: 245-255.
Intrieri, C., S. Poni, B. Rebucci, and E. Magnanini. 1998. Row orientation effects on whole-canopy gas exchange of potted and field-grown grapevines. JKI, Siebeldingen, Germany, 37
IPCC, 2021a: Climate Change 2021: The Physical Science Basis. Contribution of Working Group I to the Sixth Assessment Report of the Intergovernmental Panel on Climate Change [Masson-Delmotte, V., P. Zhai, A. Pirani, S.L. Connors, C.

Péan, S. Berger, N. Caud, Y. Chen, L. Goldfarb, M.I. Gomis, M. Huang, K. Leitzell, E. Lonnoy, J.B.R. Matthews, T.K. Maycock, T. Waterfield, O. Yelekçi, R. Yu, and B. Zhou (eds.)]. Cambridge University Press. In Press

IPCC, 2021b: Summary for Policymakers. In: Climate Change 2021: The Physical Science Basis. Contribution of Working Group I to the Sixth Assessment Report of the Intergovernmental Panel on Climate Change [MassonDelmotte, V., P. Zhai, A. Pirani, S.L. Connors, C. Péan, S. Berger, N. Caud, Y. Chen, L. Goldfarb, M.I. Gomis, M. Huang, K. Leitzell, E. Lonnoy, J.B.R. Matthews, T.K. Maycock, T. Waterfield, O. Yelekçi, R. Yu, and B. Zhou (eds.)]. Cambridge University Press. In Press.

IPCC, 2014a Climate Change 2014: Impacts, Adaptation, and Vulnerability. Part A: Global and Sectoral Aspects. Contribution of Working Group II to the Fifth Assessment Report of the Intergovernmental Panel on Climate Change. Cambridge University Press, Cambridge, United Kingdom and New York, NY, USA, p. 1132

IPCC, 2014b Climate Change 2014: Synthesis Report. Contribution of Working Groups I, II and III to the Fifth Assessment Report of the Intergovernmental Panel on Climate Change [Core Writing Team, R.K. Pachauri and L.A. Meyer (eds.)]. IPCC, Geneva, Switzerland, 151 pp.

IPCC, 2013 In: Stocker TF, Qin D, Plattner G-K, Tignor M, Allen SK, Boschung J, Nauels A, Xia Y, Bex V, Midgley PM (eds) Climate Change 2013: the Physical Science Basis. Contribution of Working Group I to the Fifth Assessment Report of the Intergovernmental PanelonClimateChange. Cambridge UniversityPress, Cambridge. doi:10.1017/CBO9781107415324

IPCC, 2013: Glosario [Planton, S. (ed.)]. En: Cambio Climático 2013. Bases físicas. Contribución del Grupo de trabajo I al Quinto Informe de Evaluación del Grupo Intergubernamental de Expertos sobre el Cambio Climático [Stocker, T.F., D. Qin, G.-K. Plattner, M. Tignor, S.K. Allen, J. Boschung, A. Nauels, Y. Xia, V. Bex y P.M. Midgley (eds.)]. Cambridge University Press, Cambridge, Reino Unido y Nueva York, NY, Estados Unidos de América.

IPCC, 2007: Contribution of Working Group I to the Fourth Assessment Report of the Intergovernmental Panel on Climate Change, 2007. Solomon, S., D.Qin, M.Manning, Z.Chen, M.Marquis, K.B. Averyt, M. Tiggnor and H.L. Miller (eds) Cambridge University Press, Cambridge, United Kingdom and New York, NY, USA.

IPCC, 2001: climate change 2001: the scientific basis. Contribution of Working Group 1 to the Third Assessment Report of the Intergovernmental Panel on Climate Change, edited by J. T. Houghton, Y. Ding, D. J. Griggs, M. Noguer, P. J. van der Linden, X. Dai, K. Maskell and C. A. Johnson (eds). Cambridge University Press, Cambridge, UK, and New York, USA, 2001

IPCC, 2000. Special report on emissions scenarios, Cambridge University Press, Cambridge, UK. ISBN 0 521 80493 0

Irimia, L., Patriche, C., and Quénol, H. Viticultural zoning: A comparative study regarding the accuracy of different approaches in vineyards climate suitability assessment. Cercetari agronomice in Moldova, 2013, 46(3), 95-106.

Irmak S, Kabenge I, Skaggs KE, Mutiibwa D. Trend and magnitude of changes in climate variables and reference evapotranspiration over 116-yr period in the Platte River Basin, central Nebraska-USA. Journal of Hydrology 2012; 420: 228-244.

Isaksen ISA, Wang WC. Atmospheric ozone and climate change. 3rd International Symposium on Non-CO2 Greenhouse Gases, Maastricht, Netherlands, 2002, pp. 319-330.

Iversen T, Bentsen M, Bethke I, Debernard JB, Kirkevag A, Seland O, et al. The Norwegian Earth System Model, NorESM1-M - Part 2: Climate response and scenario projections. Geoscientific Model Development 2013; 6: 389-415.

Jensen M and Haise H. Estimating Evapotranspiration from Solar Radiation. Journal

Jeong DI, Sushama L, Diro GT, Khaliq MN, Beltrami H, Caya D. Projected changes to high temperature events for Canada based on a regional climate model ensemble. Climate Dynamics 2016; 46: 3163-3180.

Jiménez-Donaire, M.d.P.; Giráldez, J.V.; Vanwalleghem, T. Impact of Climate Change on Agricultural Droughts in Spain. *Water* 2020, *12*, 3214. https://doi.org/10.3390/w12113214

Jones, Gregory V. and Webb, Leanne B. 'Climate Change, Viticulture, and Wine: Challenges and Opportunities', Journal of Wine Research, 2010, 21: 2, 103 — 106

Jones, G.V. and Davis, R.E. Climate influences on grapevine phenology, grape composition, and wine production and quality for Bordeaux, France. American Journal of Enology and Viticulture, 2000, 51, 249–261

Jones CD, Hughes JK, Bellouin N, Hardiman SC, Jones GS, Knight J, et al. The HadGEM2-ES implementation of CMIP5 centennial simulations. Geoscientific Model Development 2011; 4: 543-570.

Jones GV, Alves F. Impact of climate change on wine production: a global overview and regional assessment in the Douro Valley of Portugal. International Journal of Global Warming 2012; 4: 383-406.

Jones GV, Davis RE. Climate influences on grapevine phenology, grape composition, and wine production and quality for Bordeaux, France. American Journal of Enology and Viticulture 2000; 51: 249-261.

Jones GV, White MA, Cooper OR, Storchmann K. Climate change and global wine quality. Climatic Change 2005; 73: 319-343.

Jones, G.V. Climate and Terroir: Impacts of Climate Variability and Change on Win, in Fine Wine and Terroir - The Geoscience Perspective. Macqueen, R.W., and Meinert, L.D., (eds.), Geoscience Canada Reprint Series Number 9, Geological Association of Canada, St. John's, Newfoundland, 2006. 247 p.

Kattenberg A, Amer Meteorol SOC. Climate models: Projections of future climate. Seventh Symposium on Global Change Studies 1996.

Kenny GH, Harrison PA. The effects of climatic variability and change on grape suitability in Europe. J Wine Res 1993; 4:163–183.

Kent ST, McClure LA, Zaitchik BF, Smith TT, Gohlke JM. Heat Waves and Health Outcomes in Alabama (USA): The Importance of Heat Wave Definition. Environmental Health Perspectives 2014; 122: 151-158.

Khalili M, Nguyen VTV. An efficient statistical approach to multi-site downscaling of daily precipitation series in the context of climate change. Climate Dynamics 2017; 49: 2261-2278.

Kim S, Sinclair VA, Raisanen J, Ruuhela R. Heat waves in Finland: present and projected summertime extreme temperatures and their associated circulation patterns. International Journal of Climatology 2018; 38: 1393-1408.

Kizildeniz T, Pascual I, Irigoyen JJ, Morales F. Future CO2, warming and water deficit impact white and red Tempranillo grapevine: Photosynthetic acclimation to elevated CO2 and biomass allocation. Physiologia Plantarum 2021; 172: 1779-1794.

Knutti R, Sedlacek J. Robustness and uncertainties in the new CMIP5 climate model projections. Nature Climate Change 2013; 3: 369-373.

Koufos G, Mavromatis T, Koundouras S, Fyllas MN, Jones GV. 2014. Viticulture–climate relationships in Greece: the impact of recent climate trends on harvest dates variation. Int. J. Climatol. 34(5): 1445–1459

Koufos, G., Mavromatis, T., Koundouras, S. and Jones, G. Response of viticulture-related climatic indices and zoning to historical and future climate conditions in Greece: response of viticulture-related climatic indices and zoning in greece. International Journal of Climatology, 2017. 38. 10.1002/joc.5320.

Koundouras, S., C. Van Leeuwen, G. Seguin, and Y. Glories. Influence of water status on vine vegetative growth, berry ripening and wine characteristics in

mediterranean zone (example of Nemea, Greece, variety Saint-George, 1997). J. Int. Sci. Vigne. Vin. 1999. 33:149–160.
Koundouras, S., I. T. Tsialtas, E. Zioziou, and N. Nikolaou. Rootstock effects on the adaptive strategies of grapevine (Vitis vinifera L. cv. Cabernet-Sauvignon) under contrasting water status: leaf physiological and structural responses. Agric. Ecosyst. Environ., 2008, 128:86–96

Kovaleski AP, Londo JP. Tempo of gene regulation in wild and cultivated Vitis species shows coordination between cold deacclimation and budbreak. Plant Science 2019; 287
Köppen W, Geiger R. Das geographische System der Klimate, 1936.
Kuglitsch FG, Toreti A, Xoplaki E, Della-Marta PM, Zerefos CS, Turkes M, et al. Heat wave changes in the eastern Mediterranean since 1960. Geophysical Research Letters 2010; 37.
Kulakowski D, Seidl R, Holeksa J, Kuuluvainen T, Nagel TA, Panayotov M, et al. A walk on the wild side: Disturbance dynamics and the conservation and management of European mountain forest ecosystems. Forest Ecology and Management 2017; 388: 120-131.
Lastrada, E.; Cobos, G.; Torrijo, F.J. Analysis of Climate Change's Effect on Flood Risk. Case Study of Reinosa in the Ebro River Basin. *Water* 2020, *12*, 1114. https://doi.org/10.3390/w12041114
Lavaysse C, Vrac M, Drobinski P, Lengaigne M, Vischel T. Statistical downscaling of the French Mediterranean climate: assessment for present and projection in an anthropogenic scenario. Natural Hazards and Earth System Sciences 2012; 12: 651-670.
Lazoglou G, Anagnostopoulou C, Koundouras S. Climate change projections for Greek viticulture as simulated by a regional climate model. Theoretical and Applied Climatology 2018; 133: 551-567.
Lee SH, Yoo SH, Choi JY, Bae S. Assessment of the Impact of Climate Change on Drought Characteristics in the Hwanghae Plain, North Korea Using Time Series SPI and SPEI: 1981-2100. Water 2017; 9.
Lemos MC, Kirchhoff CJ, Ramprasad V. Narrowing the climate information usability gap. Nature Climate Change, 2012, 2, 789–794.
Leolini, L.; Moriondo, M.; Romboli, Y.; Gardiman, M.; Costafreda-Aumedes, S.; de Cortazar-Atauri, I.G.; Bindi, M.; Granchi, L.; Brilli, L. Modelling sugar and acid content in Sangiovese grapes under future climates: An Italian case study. Clim. Res. 2019, 78, 211–224
Lereboullet A-L, Beltrando G, Bardsley DK. Socio-ecological adaptation to climate change: A comparative case study from the Mediterranean wine industry in France and Australia. Agriculture, Ecosystems & Environment, 2013a, 164, 273–285.
Lesk C, Rowhani P, Ramankutty N. Influence of extreme weather disasters on global crop production. Nature 2016; 529: 84-+
Lewis, S.L., Brando, P.M., Phillips, O.L., van der Heijden, G.M.F., Nepstad, D., The 2010 Amazon drought. Science, 2011. 331 (6017), 554. http://dx.doi.org/10.1126/science.1200807.
Linares, C., Diaz, J., Tobías, A. et al. Impact of heat and cold waves on circulatory-cause and respiratory-cause mortality in Spain: 1975–2008. Stoch Environ Res Risk Assess, 2015; 29, 2037–2046. https://doi.org/10.1007/s00477-014-0976-2
Lin S, Luo M, Walker RJ, Liu X, Hwang SA, Chinery R. Extreme High Temperatures and Hospital Admissions for Respiratory and Cardiovascular Diseases. Epidemiology 2009; 20: 738-746.
Livneh B, Hoerling MP. The Physics of Drought in the US Central Great Plains. Journal of Climate 2016; 29: 6783-6804.

Lloyd-Hughes B, Saunders MA. A drought climatology for Europe. International Journal of Climatology 2002; 22: 1571-1592.

Lobell, D.; Field, C.; Cahill, K. y Bonfils, C. “Impacts of future climate change on California perennial crop yields: Model projections with climate and crop uncertainties“. Agric For Meteorol., 2006, 141 (2-4), pgs.208-218

Lopes, J., J. E. Eiras-Dias, F. Abreu, P. Climaco, J. P. Cunha, and J. Silvestre. Thermal requirements, duration and precocity of phenological stages of grapevine cultivars of the Portuguese collection. Ci^encia Tec. Vitiv., 2008, 23:61–71.

Lopez-Bustins JA, Pascual D, Pla E, Retana J. Future variability of droughts in three Mediterranean catchments. Natural Hazards 2013; 69: 1405-1421.

López F, Cabrera M, Cuadrat JM. Atlas Climático de Aragón. First ed.Spain: J. Factory; 2007.

Lopez-Moreno JI, Goyette S, Vicente-Serrano SM, Beniston M. Effects of climate change on the intensity and frequency of heavy snowfall events in the Pyrenees. Climatic

López-Moreno, J. I., Revuelto, J., Rico, I., Chueca-Cía, J., Julián, A., Serreta, A., Serrano, E., Vicente-Serrano, S. M., Azorin-Molina, C., Alonso-González, E., and García-Ruiz, J. M.: Thinning of the Monte Perdido Glacier in the Spanish Pyrenees since 1981, The Cryosphere, 2016; 10, 681–694, https://doi.org/10.5194/tc-10-681-2016,

López-Moreno, J. I., Vicente-Serrano, S. M., Moran-Tejeda, E., Zabalza, J., Lorenzo-Lacruz, J., and García-Ruiz, J. M.: Impact of climate evolution and land use changes on water yield in the Ebro basin, Hydrol. Earth Syst. Sci.,2011; 15, 311–322, https://doi.org/10.5194/hess-15-311-2011

Lorenzo, M. N.; Taboada, J. J.; Lorenzo, J. F.; Ramos, A. M. Influence of climate on grape production and wine quality in the Rías Baixas, north-western Spain. Regional Environmental Change, 2013, 13(4), 887–896. doi:10.1007/s10113-012-0387-1

Lorenzo, M.N. and Alvarez, I., Climate change patterns in precipitation over Spain using CORDEX projections for 2021–2050, Science of The Total Environment, Volume 723,2020,138024,ISSN 0048-9697, https://doi.org/10.1016/j.scitotenv.2020.138024.

Lorenzo M.N., Díaz-Poso, A. and Dominic R. Heatwave intensity on the Iberian Peninsula: Future climate projections. Atmospheric Research, 2021. doi:10.1016/j.atmosres.2021.105655

Lorenzo, M.N. and Alvarez, I. Future changes of hot extremes in Spain: towards warmer conditions. Natural Hazards. 2022, 113. 10.1007/s11069-022-05306-x.

Lorenzo MN, Taboada JJ, Lorenzo JF, Ramos AM (2013) Influence of climate on grape production and wine quality in the Rı´as Baixas, north-western Spain. Reg Environ Change 13:887–896. doi:10.1007/s10113-012-0387-1

Lorenzo, Nieves & Ramos, Alexandre & Brands, Swen. (2016). Present and future climate conditions for winegrowing in Spain. Regional Environmental Change. 2016. 617. 10.1007/s10113-015-0883-1.

Machado MJ, Benito G, Barriendos M, Rodrigo FS. 500 Years of rainfall variability and extreme hydrological events in southeastern Spain drylands. Journal of Arid Environments 2011; 75: 1244-1253.

Maclean IMD, Hopkins JJ, Bennie J, Lawson CR and Wilson RJ. Microclimates buffer the responses of plant communities to climate change. Global Ecology and Biogeography, 2015, 24, 1340–1350

Magalhaes, N. Tratado de viticultura: a videira, a vinha e o terroir. Chaves Ferreira Publicacoes, Lisboa, Portugal 2008.

MAGRAMA, 2016 : Análisis de los procesos de desertificación en España en función de los distintos escenarios climáticos.

Makra, L., B. Vitanyi, A. Gal, J. Mika, I. Matyasovszky, and T. Hirsch. Wine quantity and quality variations in relation to climatic factors in the Tokaj (Hungary), 2009.

Malheiro AC, Santos JA, Fraga H, Pinto JG. Climate change scenarios applied to viticultural zoning in Europe. Climate Research 2010; 43: 163-177.

Marcos-Garcia P, Lopez-Nicolas A, Pulido-Velazquez M. Combined use of relative drought indices to analyze climate change impact on meteorological and hydrological droughts in a Mediterranean basin. Journal of Hydrology 2017; 554: 292-305.

Marko, K., Prtenjak, M., Šimon, S., Osrečak, M., Anić, M.,Karoglan Kontic, J., Andabaka, Ž., Tomaz, I., Grisogono, B., Belušić Vozila, A., Marki, A., Prša, Ž., Omazić, B., Jelić, D., Večenaj, Ž., Vučetić, V., Počakal, D., Petric, I., Leder, R. and Prša, Ivan. Classification of Croatian winegrowing regions based on bioclimatic indices. E3S Web of Conferences, 2018, 50. 01032. 10.1051/e3sconf/20185001032.

Marsland SJ, Haak H, Jungclaus JH, Latif M, Roske F. The Max-Planck-Institute global ocean/sea ice model with orthogonal curvilinear coordinates. Ocean Modelling 2003; 5: 91-127.

Martínez-Casasnovas JA, Ramos MC, Ribes-Dasi M. Soil erosion caused by extreme rainfall events: mapping and quantification in agricultural plots from very detailed digital elevation models. Geoderma, 2002, 105:125–140

Maxwell, J. T., Darren L. F., Grant Logan H. and Gregory V. J.. “Projecting future winegrape yields using a combination of Vitis vinifera L. growth rings and soil moisture simulations, northern California, USA.” *Australian Journal of Grape and Wine Research* 22, 2016, 73-80.

McVicar TR, Roderick ML, Donohue RJ, Li LT, Van Niel TG, Thomas A, et al. Global review and synthesis of trends in observed terrestrial near-surface wind speeds: Implications for evaporation. Journal of Hydrology 2012a; 416: 182-205.

McVicar TR, Roderick ML, Donohue RJ, Van Niel TG. Less bluster ahead? Ecohydrological implications of global trends of terrestrial near-surface wind speeds. Ecohydrology 2012b; 5: 381-388.

Mckee T, Doesken N and Kleist J. The Relationship of Drought Frequency and Duration Times Scales. American Meteorological Society. 8th Conference on Applied Climatology. 1993: January 17–22 Anaheim, California, pp. 179–184.

Meehl GA, Stocker TF, Collins WD, Friedlingstein P, Gaye AT, Gregory JM et al. Global climate projections 2007: the physical science basis 2007; 747–845

Menzel A, Seifert H, Estrella N. Effects of recent warm and cold spells on European plant phenology. Int. J. Biometeorol., 2011, 55(6): 921–932, doi: 10.1007/s00484-011-0466-x

Michael A, S.J, Enke W, Deutschländer Th, M. G. Impact of expected increase in precipitation intensities on soil loss — results of comparative model simulations. Catena, 2005, 61:155–164

Ministerio de Medio Ambiente, 2005. Assessment report of the preliminary impacts in Spain due to Climate Change. Centro de publicaciones del Ministerio de Medio Ambiente, Madrid.

Miró JJ, Estrela MJ, Caselles V, Olcina-Cantos J. Fine-scale estimations of bioclimatic change in the Valencia region, Spain. Atmospheric Research 2016; 180: 150-164.

Miró J.J.; Estrela, M.J.; Olcina-Cantos, J.; Martin-Vide, J. Future Projection of Precipitation Changes in the Júcar and Segura River Basins (Iberian Peninsula) by CMIP5 GCMs Local Downscaling. Atmosphere 2021, 12, 879. https://doi.org/10.3390/atmos12070879

Mishra AK, Singh VP. A review of drought concepts. Journal of Hydrology 2010; 391: 204-216.

Mishra AK, Singh VP. Drought modeling - A review. Journal of Hydrology 2011; 403: 157-175.

Molina, M.O., Sánchez, E. & Gutiérrez, C. Future heat waves over the Mediterranean from an Euro-CORDEX regional climate model ensemble. Sci Rep 10, 8801 2020. https://doi.org/10.1038/s41598-020-65663-0

Molitor, D.; Junk, J. Climate change is implicating a two-fold impact on air temperature increase in the ripening period under the conditions of the Luxembourgish grapegrowing region. OENO One 2019, 53, 409–422.

Monjo R, Gaitan E, Portoles J, Ribalaygua J, Torres L. Changes in extreme precipitation over Spain using statistical downscaling of CMIP5 projections. International Journal of Climatology 2016; 36: 757-769.

Monjo R., Paradinas C., Gaitán E., Redolat D., Paradinas C., Prado C., Portolés J., Torres L., Ribalaygua J. Russo B., Velasco M., Pouget L., Vela S., David M. L., Morais M., Ribalaygua J. Report on extreme events predictions. Deliverable 1.3 RESCCUE Project. Grant Agreement No. 700174, 2018

Morales-Castilla, I.; García de Cortázar-Atauri, I.; Cook, B.I.; Lacombe, T.; Parker, A.; van Leeuwen, C.; Nicholas, K.A.; Wolkovich, E.M. Diversity buffers winegrowing regions from climate change losses. Proc. Natl. Acad. Sci. USA 2020

Moral García, F. J., Rebollo, F., Paniagua, L., Garcia, A. and Salazar, Enrique. Application of climatic indices to analyse viticultural suitability in Extremadura, south-western Spain. Theoretical and Applied Climatology, 2015, 123. 10.1007/s00704-014-1363-0.

Moriondo M, Maselli F, Bindi M. A simple model of regional wheat yield based on NDVI data. European Journal of Agronomy 2007; 26: 266-274.

Mosedale JR, Abernethy KE, Smart RE, Wilson RJ, Maclean IMD. Climate change impacts and adaptive strategies: lessons from the grapevine. Global Change Biology 2016; 22: 3814-3828.

Moss RH, Edmonds JA, Hibbard KA, Manning MR, Rose SK, van Vuuren DP, et al. The next generation of scenarios for climate change research and assessment. Nature 2010; 463: 747-756.

Moutahir H, Bellot P, Monjo R, Bellot J, Garcia M, Touhami I. Likely effects of climate change on groundwater availability in a Mediterranean region of Southeastern Spain. Hydrological Processes 2017; 31: 161-176.

Moutinho-Pereira, J., N. Magalh~aes, B. Goncalves, E. Bacelar, M. Brito, and C. Correia. Gas exchange and water relations of three Vitis vinifera L. cultivars growing under Mediterranean climate. Photosynthetica, 2007, 45:202–207

Moutinho-Pereira J, Goncalves B, Bacelar E, Cunha JB, Coutinho J, Correia CM. Effects of elevated CO2 on grapevine (Vitis vinifera L.): Physiological and yield attributes. Vitis 2009; 48: 159-165.

Mukherjee S, Mishra A, Trenberth KE. Climate Change and Drought: a Perspective on Drought Indices. Current Climate Change Reports 2018; 4: 145-163.

Naulleau, A,. Gary, C., Prevot, L. and Hossard, L. Evaluating Strategies for Adaptation to Climate Change in Grapevine Production–A Systematic Review. Frontiers in Plant Science 2021. 11. 10.3389/fpls.2020.607859.

Neethling E., Barbeau G., Bonnefoy C. and Quénol H., 2012. Change in climate and berry composition for grapevine varieties cultivated in the Loire Valley. Clim. Res., 53, 89-101.

Neumann PA, Matzarakis A. Viticulture in southwest Germany under climate change conditions. Climate Research 2011; 47: 161-169

Nychka D, Furrer R, Paige J and Sain S (2015). Fields: Tools for spatial data. R package version 9.0 doi: 10.5065/D6W957CT (URL: http://doi.org/10.5065/D6W957CT) <URL: www.image.ucar.edu/fields>.

Odo Camps J, Ramos MC. Grape harvest and yield responses to inter-annual changes in temperature and precipitation in an area of north-east Spain with a Mediterranean climate. International Journal of Biometeorology 2012; 56: 853-864.

Ollat, N.; Touzard, J.M.; van Leeuwen, C. Climate Change Impacts and Adaptations: New Challenges for the Wine Industry. J. Wine Econ. 2016, 11, 139–149

Olesen JE, Trnka M, Kersebaum KC, Skjelvag AO, Seguin B, Peltonen-Sainio P, et al. Impacts and adaptation of European crop production systems to climate change. European Journal of Agronomy 2011; 34: 96-112.

Orduna, R. M. Climate change associated effects on grape and wine quality and production. Food Res. Int., 2010, 43:1844–1855

OPCC2, 2018: Climate change in the Pyrenees: impacts, vulnerability and adaptation. Executive summary of the OPCC-CTP 2018 report.

Ojeda MGV, Gamiz-Fortis SR, Castro-Diez Y, Esteban-Parra MJ. Evaluation of WRF capability to detect dry and wet periods in Spain using drought indices. Journal of Geophysical Research-Atmospheres 2017; 122: 1569-1594.

Ojeda MGV, Gámiz-Fortis SR, Romero-Jiménez, E., Rosa-Cánovas, J.J., Yeste, P., Castro-Díez, Y., Esteban-Parra, M.J. Projected changes in the Iberian Peninsula drought characteristics, Science of The Total Environment (2021), ,Volume 757,2021,143702,ISSN 0048-9697, https://doi.org/10.1016/j.scitotenv.2020.143702.

Ozden, M., Vardin, H., Simsek, M., and Karaaslan, M. Effects of rootstocks and irrigation levels on grape quality of Vitis vinifera L. cv. Shiraz. Afr. J. Biotechnol., 2010. 9:3801–380

Palmer W. «Meteorological Drought». Research paper no.45, U.S. Department of Commerce Weather Bureau, febrero de 1965 (58 páginas). Available in National Climatic Data Center de NOAA: http://www.ncdc.noaa.gov/temp-and-precip/drought/docs/palmer.pdf

Paparrizos S, Maris F, Weiler M, Matzarakis A. Analysis and mapping of present and future drought conditions over Greek areas with different climate conditions. Theoretical and Applied Climatology 2018; 131: 259-270.

Parry ML, Canziani OF, Palutikof JP, Van der Linden PJ,Hanson CE, editors. IPCC impacts, adaptation and vulnerability contribution of Working Group II to the Fourth Assessment Report of the IPCC. Cambridge University Press; 2007.Patz JA, Campbell-Lendrum D, Holloway T, Foley JA. Impact of regional climate change on human health. Nature 2005; 438: 310-317.

Pavlousek, P. Evaluation of drought tolerance of new grapevine rootstock hybrids. J. Environ. Biol., 2011. 32:543–549.

Pedro-Monzonís, M., Solera, A., Ferrer, J., Estrela, T., and Paredes-Arquiola, J. A review of water scarcity and drought indexes in water resources planning and management. Journal of Hydrology, 2015. 527, 482–493. https://doi.org/10.1016/j.jhydrol.2015.05.003

Pellegrino, A., E. Lebon, M. Voltz, and J. Wery. Relationships between plant and soil water status in vine (Vitis vinifera L.). Plant Soil, 2004. 266:129–142.

Pereira, S.C.; Carvalho, D.; Rocha, A. Temperature and Precipitation Extremes over the Iberian Peninsula under Climate Change Scenarios: A Review. Climate 2021, 9, 139. https://doi.org/ 10.3390/cli9090139

Pereira, Susana & Marta-Almeida, Martinho & Carvalho, Ana cristina. (2017). Heat Waves and Cold Spells changes in Iberia for a future climate scenario. International Journal of Climatology. 37. 10.1002/joc.5158.

Perez J, Menendez M, Mendez FJ, Losada IJ. Evaluating the performance of CMIP3 and CMIP5 global climate models over the north-east Atlantic region. Climate Dynamics 2014; 43: 2663-2680.

Perez, L. and Barreiro-Hurlé, J. Assessing the socio-economic impacts of drought in the Ebro River Basin. Spanish Journal of Agricultural Research, 2009. 7. 269. 10.5424/sjar/2009072-418.

Petgen, M. Möglichkeiten und Grenzen der Reifesteuerung: Wie flexibel reagiert die Rebe? Das Deutsche Weinmagazin, 2007. 7/8, 42–47

Pieri P. Changement climatique et culture de la vigne: l'essentiel des impacts. In: Changement Climatique, Agriculture et Forêt en France : Simulations d'Impacts sur les Principales Espèces. Le Livre Vert du projet CLIMATOR (2007-2010), ANR and INRA (eds), 2010. Ademe Editions, pp. 213-223.

Planton S, Deque M, Chauvin F, Terray L. Expected impacts of climate change on extreme climate events. Comptes Rendus Geoscience 2008; 340: 564-574.

Pons M, Lopez-Moreno JI, Rosas-Casals M, Jover E. The vulnerability of Pyrenean ski resorts to climate-induced changes in the snowpack. Climatic Change 2015; 131: 591-605.

Porter JR, Semenov MA. Crop responses to climatic variation. Philosophical Transactions of the Royal Society B-Biological Sciences 2005; 360: 2021-2035.

PricewaterhouseCoopers 2009. Efectos del cambio climático sobre la industria vitivinícola de la Argentina y Chile

R Development Core Team (2010): R: a language and environment for statistical computing. R Foundation for Statistical Computing, Vienna, Austria. http://www.R-project.org. ISBN: 3-900051-07-0. Accessed 6 July 2011

Raddatz TJ, Reick CH, Knorr W, Kattge J, Roeckner E, Schnur R, et al. Will the tropical land biosphere dominate the climate-carbon cycle feedback during the twenty-first century? Climate Dynamics 2007; 29: 565-574.

Ramos MC, Jones GV, Yuste J. Variability of Tempranillo grape quality within the Ribera del Duero do (Spain) and relationships with climatic characteristics. Journal of Viticulture and Enology 2017; N 12/1

Ramos, M.C. Projection of phenology response to climate change in rainfed vineyards in north-east Spain. Agric. For. Meteorol. 2017, 247, 104–115

Ramos MC, Jones GV, Martinez-Casasnovas JA. Structure and trends in climate parameters affecting winegrape production in northeast Spain. Climate Research 2008; 38: 1-15.

Ramos MC, Martinez de Toda F. Variability in the potential effects of climate change on phenology and on grape composition of Tempranillo in three zones of the Rioja DOCa (Spain). European Journal of Agronomy 2020; 115

Ramos MC, Martinez de Toda F. Interannual and spatial variability of grape composition in the Rioja DOCa show better resilience of cv. Graciano than cv. Tempranillo under a warming scenario. Oeno One 2021; 55: 85-100.

Rebetez M, Mayer H, Dupont O, Schindler D, Gartner K, Kropp JP, et al. Heat and drought 2003 in Europe: a climate synthesis. Annals of Forest Science 2006; 63: 569-577.

Renée Mozell, M. and Thach, E. The impact of climate change on the global wine industry: Challenges & Solutions. Wine Economics and Policy.2014. 3. 10.1016/j.wep.2014.08.001

Resco P, Iglesias A, Bardaji I, Sotes V. Exploring adaptation choices for grapevine regions in Spain. Regional Environmental Change 2016; 16: 979-993.

Resco de Dios, J.H., Cunill Camprubí, A., Thapa, P., Martínez del Castillo, E., Martínez de Aragón, J., Bonet, J.A., Balaguer-Romano, R., Díaz-Sierra, R., Yebra, M., Boer, M.M., Climate change induced declines in fuel moisture may turn currently fire-free Pyrenean mountain forests into fire-prone ecosystems, Science of The Total Environment, Volume 797, 2021, 149104, ISSN 0048-9697, https://doi.org/10.1016/j.scitotenv.2021.149104.

Revuelto, J., Gómez, D., Alonso-González, E. et al. Intermediate snowpack melt-out dates guarantee the highest seasonal grasslands greening in the Pyrenees. Sci Rep, 2022, 12, 18328. https://doi.org/10.1038/s41598-022-22391-x https://www.sciencedirect.com/science/article/pii/S0048969721041760

Ribalaygua J, Gaitan E, Portoles J, Monjo R. Climatic change on the Gulf of Fonseca (Central America) using two-step statistical downscaling of CMIP5 model outputs. Theoretical and Applied Climatology 2018; 132: 867-883.

Ribalaygua J, Rosa Pino M, Portoles J, Roldan E, Gaitan E, Chinarro D, et al. Climate change scenarios for temperature and precipitation in Aragon (Spain). Science of the Total Environment 2013a; 463: 1015-1030.

Ribalaygua J, Torres L, Portoles J, Monjo R, Gaitan E, Pino MR. Description and validation of a two-step analogue/regression downscaling method. Theoretical and Applied Climatology 2013b; 114: 253-269.

Riou CH, Becker N, Sotes Ruiz V, Gomez-Miguel V, Carbonneau A, Panagiotou M, Calo A, Costacurta A, Castro de R, Pinto A, Lopes C, Carneiro L, Climaco P. Le déterminisme climatique de la maturation du raisin: application au zonage de la teneur em sucre dans la communauté européenne. Office des Publications Officielles des Communautés Européennes, Luxembourg, 1994; 322 pp

Robine JM, Cheung SLK, Le Roy S, Van Oyen H, Griffiths C, Michel JP, et al. Death toll exceeded 70,000 in Europe during the summer of 2003. Comptes Rendus Biologies 2008; 331: 171-U5.

Roderick, M. L., P. Greve, and G. D. Farquhar. 2015. "On the Assessment of Aridity with Changes in Atmospheric Co2." Water Resources Research 51, no. 7 (Jul): 5450-5463. http://dx.doi.org/10.1002/2015wr017031.

Rodriguez R, Navarro X, Casas MC, Ribalaygua J, Russo B, Pouget L, et al. Influence of climate change on IDF curves for the metropolitan area of Barcelona (Spain). International Journal of Climatology 2014; 34: 643-654.

Roldan E, Gomez M, Pino MR, Diaz J. The impact of extremely high temperatures on mortality and mortality cost. International Journal of Environmental Health Research 2015; 25: 277-287.

Roldan E, Gomez M, Pino MR, Portoles J, Linares C, Diaz J. The effect of climate-change-related heat waves on mortality in Spain: uncertainties in health on a local scale. Stochastic Environmental Research and Risk Assessment 2016; 30: 831-839.

Romero, P., J. M. Navarro, J. Perez-Perez, F. Garcia-Sanchez, A. Gomez-Gomez, I. Porras, et al. 2006. Deficit irrigation and rootstock: their effects on water relations, vegetative development, yield, fruit quality and mineral nutrition of Clemenules mandarin. Tree Physiol. 26:1537–1548.

Royé, D., Codesido, R., Tobías, A. and Taracido, M. Heat wave intensity and daily mortality in four of the largest cities of Spain, Environmental Researc, 2020; Volume 182, 109027, ISSN 0013-9351

https://doi.org/10.1016/j.envres.2019.109027.

Royé, D., Sera, F. Tobías, A., Lowe, R., Gasparrini, A., Pascal, M., Donato, F. Nunes, B., Teixeira, J.P. Effects of Hot Nights on Mortality in Southern Europe. Epidemiology: July 2021 - Volume 32 - Issue 4 - p 487-498 doi: 10.1097/EDE.0000000000001359

Ruml, M., A. Vukovic, M. Vujadinovic, V. Djurdjevic, Z. Rankovic-Vasic, Z. Atanackovic, et al. 2012. On the use of regional climate models: implications of climate change for viticulture in Serbia. Agric. For. Meteorol. 158:53–62.

Russo S, Sillmann J, Sterl A. Humid heat waves at different warming levels. Scientific Reports 2017; 7.

Russo, S., Dosio, A., Graversen, R. G., Sillmann, J., Carrao, H., Dunbar, M. B., Singleton, A., Montagna, P., Barbola, P., and Vogt, J. V. Magnitude of extreme heat waves in present climate and their projection in a warming world, J. Geophys. Res. Atmos.,2014, 119, 12,500– 12,512, doi:10.1002/2014JD022098.

Saeed F, Almazroui M, Islam N, Khan MS. Intensification of future heat waves in Pakistan: a study using CORDEX regional climate models ensemble. Natural Hazards 2017; 87: 1635-1647.

Santiago JM, Munoz-Mas R, Solana-Gutierrez J, de Jalon DG, Alonso C, Martinez-Capel F, et al. Waning habitats due to climate change: the effects of changes in streamflow and temperature at the rear edge of the distribution of a cold-water fish. Hydrology and Earth System Sciences 2017; 21.

Santos JA, Malheiro AC, Karremann MK, Pinto JG. Statistical modelling of grapevine yield in the Port Wine region under present and future climate conditions. International Journal of Biometeorology 2011; 55: 119-131.

Santos JA, Malheiro AC, Pinto JG, Jones GV. Macroclimate and viticultural zoning in Europe: observed trends and atmospheric forcing. Climate Research 2012; 51: 89-103.

Santos, M., Fonseca, A., Helder, F., Jones, G..; Santos, João A. Bioclimatic conditions of the Portuguese wine denominations of origin under changing climates. International Journal of Climatology, 2019, joc.6248–. doi:10.1002/joc.6248

Santos M, Fonseca A, Fraga H, Jones GV, Santos JA. Bioclimatic conditions of the Portuguese wine denominations of origin under changing climates. International Journal of Climatology 2020a; 40: 927-941.

Santos, J., Fraga, H., Malheiro, A., Moutinho Pereira, J., L-T, Dinis, Correia, C., Moriondo, M., Leolini, L., Dibari, C., Costafreda-Aumedes, S., Kartschall, T., Menz, C., Molitor, D., Junk, J., Beyer, M., Schultz, H. A Review of the Potential Climate Change Impacts and Adaptation Options for European Viticulture. Applied Sciences.2020b 10. 10.3390/app10093092. INTRO

Sanz, J.J., Potti, J., Moreno, J., Merino, S. and Frías, O. Climate change and fitness components of a migratory bird breeding in the Mediterranean region. Global Change Biology, 2003, 9: 461-472. https://doi.org/10.1046/j.1365-2486.2003.00575.x

Schoetter R, Cattiaux J, Douville H. Changes of western European heat wave characteristics projected by the CMIP5 ensemble. Climate Dynamics 2015; 45: 1601-1616.

Schroter D, Cramer W, Leemans R, Prentice IC, Araujo MB, Arnell NW, et al. Ecosystem service supply and vulnerability to global change in Europe. Science 2005; 310.

Schultz HR, Stoll M. Some critical issues in environmental physiology of grapevines: future challenges and current limitations. Australian Journal of Grape and Wine Research 2010; 16: 4-24.

Schultz HR. Climate change and viticulture: a European perspective on climatology, carbon dioxide and UV-B effects. Aust J Grape Wine Res 2000; 6:2–12

Seager, R., Hoerling, M., Schubert, S., Wang, H., Lyon, B., Kumar, A., Henderson, N. (2015). Causes of the 2011–14 California drought. Journalof Climate, 28(18), 6997–7024. https://doi.org/10.1175/JCLI-D-14-00860.1

Semenov MA, Stratonovitch P. Use of multi-model ensembles from global climate models for assessment of climate change impacts. Climate Research 2010; 41: 1-14.

Sepulcre-Canto, G., Horion, S., Singleton, A., Carrao, H., & Vogt, J. Development of a Combined Drought Indicator to detect agricultural drought in Europe. Natural Hazards and Earth System Sciences, () 12(11), 3519–3531. https://doi.org/10.5194/nhess-12-3519-2012

Seubert S, Fernandez-Montes S, Philipp A, Hertig E, Jacobeit J, Vogt G, et al. Mediterranean climate extremes in synoptic downscaling assessments. Theoretical and Applied Climatology 2014; 117: 257-275.

Sgubin, G.; Swingedouw, D.; Dayon, G.; Garcia de Cortazar-Atauri, I.; Ollat, N.; Pagé, C.; Van Leeuwen, C. The risk of tardive frost damage in French vineyards in a changing climate. Agric. For. Meteorol. 2018, 250–251, 226–242.

Sheffield J, Wood EF, Roderick ML. Little change in global drought over the past 60 years. Nature 2012; 491: 435-+.

Sheffield J, Wood EF. Projected changes in drought occurrence under future global warming from multi-model, multi-scenario, IPCC AR4 simulations. Climate Dynamics 2008; 31: 79-105.

Sigler, J. In den Zeiten des Klimawandels: Von der Süßreserve zur Sauerreserve? Der Badische Winzer, 2008. 33, 21–25.

Sillmann J, Donat MG, Fyfe JC, Zwiers FW. Observed and simulated temperature extremes during the recent warming hiatus. Environmental Research Letters 2014; 9.

Skaugen T, Astrup M, Roald LA, Forland E. Scenarios of extreme daily precipitation for Norway under climate change. Nordic Hydrology 2004; 35: 1-13.

Smith M, Allen R, Pereira L. Revised FAO methodology for crop-water requirements. Management of nutrients and water in rainfed arid and semi-arid areas. Proceedings of a consultants meeting. International Atomic Energy Agency (IAEA). 1998; IAEA-TECDOC--1026. Ref. number: 29062763.

Smith TT, Zaitchik BF, Gohlke JM. Heat waves in the United States: definitions, patterns and trends. Climatic Change 2013; 118: 811-825.

Spain Government. Mapa de las Denominaciones de Origen Protegidas de Vinos de España (Map of Protected Designations of Origin of Wines of Spain). 2014. (https://www.mapa.gob.es/es/cartografia-y-sig/publicaciones/alimentacion/mapa_dop_vinos.aspx)

Soares PMM, Cardoso RM, Miranda PMA, de Medeiros J, Belo-Pereira M, Espirito-Santo F. WRF high resolution dynamical downscaling of ERA-Interim for Portugal. Climate Dynamics 2012; 39: 2497-2522.

Sonmez FK, Komuscu AU, Erkan A, Turgu E. An analysis of spatial and temporal dimension of drought vulnerability in Turkey using the standardized precipitation index. Natural Hazards 2005; 35: 243-264.

Sotés Ruiz, V.; Gómez-Miguel, V.; Almorox, J.; Vidal Ragout, J. y Vida Navarro, L. “Clima, zonificación; tipicidad del vino en España“. In J. Tonietto, V. Sotés Ruiz, y V. GómezMiguel (Eds.), Clima, zonificación; tipicidad del vino en regiones vitivinícolas Iberoamericanas (Vols. ISBN 978-84-15413-10-3), 2012. Madrid: CYTED

Spellman G. Wine, weather and climate, 1999. Weather 54:230–239

Spinoni J, Naumann G, Vogt JV, Barbosa P. The biggest drought events in Europe from 1950 to 2012. Journal of Hydrology-Regional Studies 2015; 3: 509-524.

Stagge JH, Kohn I, Tallaksen LM, Stahl K. Modeling drought impact occurrence based on meteorological drought indices in Europe. Journal of Hydrology 2015; 530: 37-50.

Stahl, Kerstin & Blauhut, Veit & Kohn, Irene & Acácio, V. & Assimacopoulos, D. & Bifulco, Carlo & De Stefano, Lucia & Dias, Susana & Eilertz, D. & Frielingsdorf, B. & Hegdahl, Trine & Kampragou, E. & Kourentzis, V. & Melsen, L.A. & Van Lanen, Henny & Van Loon, Anne & Massarutto, Antonio & Musolino, Dario & Paoli, L. & Urquijo Reguera, Julia. (2012). A European Drought Impact Report Inventory (EDII): Design and Test for Selected Recent Droughts in Europe.

Stanke C, Kerac M, Prudhomme C, Medlock J, Murray V. Health effects of drought: a systematic review of the evidence. PLoS Curr. 2013 Jun 5;5. pii: ecurrents.dis.7a2cee9e980f91ad7697b570bcc4b004.

Stegehuis AI, Vautard R, Ciais P, Teuling AJ, Miralles DG, Wild M. An observation-constrained multi-physics WRF ensemble for simulating European mega heat waves. Geoscientific Model Development 2015; 8: 2285-2298.

Stephenson, D. B. (2008). Definition, diagnosis, and origin of extreme weather and climate events. In H. F. Diaz & R. J. Murnane (Eds.), Climate Extremes and Society (pp. 11–23). Cambridge, England: Cambridge University Press. Retrieved from http://ebooks.cambridge .org/ref/id/CBO9780511535840A011

Steul KS, Latasch L, Jung HG, Heudorf U. Health Impact of the Heatwave of 2015: Hospital Admissions in Frankfurt/Main, Germany. Gesundheitswesen 2018; 80: 353-359.

Stock M, Gerstengarbe FW, Kartschall T, Werner PC. Reliability of climate change impact assessments for viticulture. 7th International Symposium on Grapevine Physiology and Biotechnology, Davis, CA, 2004, pp. 29-39.

Subrahmanyam, V.P., and Subramaniam, A.R.. Application of water balance concepts for a climatic study of droughts in South India.1964 I.J.M.G., 15, 393-402.
Tate AB. Global warming's impact on wine. J Wine Res 2001; 12:95–109
Taylor KE, Stouffer RJ, Meehl GA. AN OVERVIEW OF CMIP5 AND THE EXPERIMENT DESIGN. Bulletin of the American Meteorological Society 2012; 93: 485-498.
Teixeira, A.H. de C.; Tonietto, J.; Pereira, G.A.; Angelloti, F. Delimitação da aptidão agroclimática para videira sob irrigação no Nordeste brasileiro. Revista Brasileira de Engenharia Agrícola e Ambiental, v.16, p.399-407, 2012. DOI: 10.1590/S1415-43662012000400010.
Thornthwaite C. An approach toward a rational classification of climate. Geogr. Rev.1948; 38: 55–94.
Tobías, A., Armstrong, B., Gasparrini, A. et al. Effects of high summer temperatures on mortality in 50 Spanish cities. Environ Health 2014; 13, 48 https://doi.org/10.1186/1476-069X-13-48
Tomozeiu R, Cacciamani C, Pavan V, Morgillo A, Busuioc A. Climate change scenarios for surface temperature in Emilia-Romagna (Italy) obtained using statistical downscaling models. Theoretical and Applied Climatology 2007; 90: 25-47.
Tonietto J, Carbonneau A. A multicriteria climatic classification system for grape-growing regions worldwide. Agricultural and Forest Meteorology 2004; 124: 81-97.
Tonietto, J. Les Macroclimats Viticoles Mondiaux et l'Influence du Mésoclimat sur la Typicité de la Syrah et du Muscat de Hambourg dans le Sud de la France: Méthodologie de Caráctérisation. Thèse Doctorat. Ecole Nationale Supérieure Agronomique, Montpellier 1999.
Tonietto, J., Sotés, V., Zanus, M., Montes, C., Uliarte, E., Antelo, L., Carbonneau, A. L'effet du climat viticole sur la typicité des vins rouges- Caractérisation au niveau des régions viticoles Ibéro-Americaines. In VIII International Terroirs Congress (Vol. 3, p. 17-22), 2010. Soave, Italy: CRA-VIT Centro di Ricerca per la Viticoltura.
Tonietto J, Carbonneau A. Análise mundial do clima das regiões vit´ıcolase de sua influencia sobre a tipicidade dos vinhos: a posição da viticultura brasileira comparada a 100 regiões em 30 paıses. Anais do Congresso Brasileiro de Viticultura e Enologia, Embrapa Uva e Vinho. Bento Gonçalves, 1999; 75–90.
Torres C, Jordà G, de Vílchez P, Vaquer-Sunyer R, Rita J, Canals V, Cladera A, Escalona JM, Miranda MÁ. Climate change and their impacts in the Balearic Islands: a guide for policy design in Mediterranean regions. Reg Environ Change. 2021;21(4):107. doi: 10.1007/s10113-021-01810-1. Epub 2021 Oct 23. PMID: 34720740; PMCID: PMC8536903.
Trenberth, K.E., Dai, A., Van der Schrier, G., Jones, P.D., Barichivich, J., Briffa, K.R., Sheffield, J. Global warming and changes in drought. Nature Climate Change, 2014. 4, 17-22. Doi:10.1038/nclimate2067
Tripathi S, Srinivas VV, Nanjundiah RS. Dowinscaling of precipitation for climate change scenarios: A support vector machine approach. Journal of Hydrology 2006; 330: 621-640.
Tsakiris, G., and Vangelis, H. 2005. Establishing a drought index incorporating evapotranspiration. European Water 2005; 9 (10): 3–11.
Tselepidaki I, Zarifis B, Asimakopoulos DN. LOW PRECIPITATION OVER GREECE DURING 1989-1990. Theoretical and Applied Climatology 1992; 46: 115-121.
Turco, M., Quintana Seguí, P., Llasat, M., Herrera García, S. and Gutiérrez, J. Testing MOS precipitation downscaling for ENSEMBLES regional climate models over Spain. Journal of Geophysical Research, 2011. 116. 10.1029/2011JD016166.
Turco M, Marcos R, Quintana-Segui P, Llasat MC. Testing instrumental and downscaled reanalysis time series for temperature trends in NE of Spain in the last century. Regional Environmental Change 2014; 14: 1811-1823.
Uppala SM, Kallberg PW, Simmons AJ, Andrae U, Bechtold VD, Fiorino M, et al. The ERA-40 re-analysis. Quarterly Journal of the Royal Meteorological Society 2005; 131: 2961-3012.

Van Leeuwen, C., & Darriet, P. The Impact of Climate Change on Viticulture and Wine Quality. Journal of Wine Economics, 2016, 11(1), 150-167. doi:10.1017/jwe.2015.21

Van Leeuwen C, Friant P, Chone X, Tregoat O, Koundouras S, Dubourdieu D. Influence of climate, soil, and cultivar on terroir. American Journal of Enology and Viticulture 2004; 55: 207-217.

Vanderlinden K, Giraldez JV, Van Meirvenne M. Assessing reference evapotranspiration by the Hargreaves method in southern Spain. Journal of Irrigation and Drainage Engineering 2004; 130: 184-191.

Van der Linden P, Mitchell JFB (eds) 2009: ENSEMBLES: Climate change and its impacts: summary of research and results from the ENSEMBLES project. Met Office Hadley Centre, UK, 160 pp.http://ensembles-eu.metoffice.com/docs/Ensembles_final_report_Nov09.pdf. (see p 68). Accessed 10 Feb 2012

Van-Rooy, M.P. 1965. A rainfall anomaly index (RAI) independent of time and space. Notos, 14: 43–48.

Vautard R, Gobiet A, Jacob D, Belda M, Colette A, Deque M, et al. The simulation of European heat waves from an ensemble of regional climate models within the EURO-CORDEX project. Climate Dynamics 2013; 41: 2555-2575.

Velasco, M, Russo, B.; Monjo, R et al. Increased Urban Resilience to Climate Change. Key Outputs from the RESCCUE Project. Sustainability, 2020, 12(23), 9881 doi:10.3390/su12239881

Vicente-Serrano SM, McVicar TR, Miralles DG, Yang YT, Tomas-Burguera M. Unraveling the influence of atmospheric evaporative demand on drought and its response to climate change. Wiley Interdisciplinary Reviews-Climate Change 2020; 11.

Vicente-Serrano, M., Beguería, S., Reig, F., Latorre, B., Peña-Gallardo, M., Luna, M.Y., Morata, A. and González-Hidalgo, J. C. A High Resolution Dataset of Drought Indices for Spain. Data 2017, 2, 22; doi:10.3390/data2030022

Vicente-Serrano SM, Dominguez-Castro F, McVicar TR, Tomas-Burguera M, Pena-Gallardo M, Noguera I, et al. Global characterization of hydrological and meteorological droughts under future climate change: The importance of timescales, vegetation-CO2 feedbacks and changes to distribution functions. International Journal of Climatology. 2019. https://doi.org/10.1002/joc.6350

Vicente-Serrano SM, Begueria S. Comment on 'Candidate distributions for climatological drought indices (SPI and SPEI)' by James H. Stagge et al. International Journal of Climatology 2016; 36: 2120-2131.

Vicente-Serrano SM, Van der Schrier G, Begueria S, Azorin-Molina C, Lopez-Moreno JI. Contribution of precipitation and reference evapotranspiration to drought indices under different climates. Journal of Hydrology 2015; 526: 42-54.

Vicente-Serrano, S.M. Spatial and temporal evolution of precipitation droughts in Spain in the last century in Adverse Weather in Spain; Martínez, C.C.-L.; Rodríguez, F.V., Eds.; WCRP Spanish Committee: Madrid, Spain, 2013; 283–296.

Vicente-Serrano SM, Begueria S, Lopez-Moreno JI. A Multiscalar Drought Index Sensitive to Global Warming: The Standardized Precipitation Evapotranspiration Index. Journal of Climate 2010a; 23: 1696-1718.

Vicente-Serrano SM, Begueria S, Lopez-Moreno JI, Angulo M, El Kenawy A. A New Global 0.5 degrees Gridded Dataset (1901-2006) of a Multiscalar Drought Index: Comparison with Current Drought Index Datasets Based on the Palmer Drought Severity Index. Journal of Hydrometeorology 2010b; 11: 1033-1043.

Vicente-Serrano SM, Gonzalez-Hidalgo JC, de Luis M, Raventos J. Drought patterns in the Mediterranean area: the Valencia region (eastern Spain). Climate Research 2004; 26: 5-15.

Vicente-Serrano SM, Lasanta T, Gracia C. Aridification determines changes in forest growth in Pinus halepensis forests under semiarid Mediterranean climate conditions. Agricultural and Forest Meteorology 2010c; 150: 614-628.

Vicente-Serrano SM, Lopez-Moreno JI. Hydrological response to different time scales of climatological drought: an evaluation of the Standardized Precipitation Index in a mountainous Mediterranean basin. Hydrology and Earth System Sciences 2005; 9: 523-533.

Vicente-Serrano, S.M.; Beguería, S. Comment on "Candidate Distributions for Climatological Drought Indices (SPI and SPEI)" by James H. Stagge et al. Int. J. Clim. 2016, 36, 2120–2131.

Vidaller, I., Revuelto, J., Izagirre, E., Rojas-Heredia, F., Alonso-González, E., Gascoin, S., et al. Toward an ice-free mountain range: Demise of Pyrenean glaciers during 2011–2020. Geophysical Research Letters, 2021, 48, e2021GL094339. https://doi.org/10.1029/2021GL094339

Voldoire A, Sanchez-Gomez E, Melia DSY, Decharme B, Cassou C, Senesi S, et al. The CNRM-CM5.1 global climate model: description and basic evaluation. Climate Dynamics 2013; 40: 2091-2121.

Vuković, A., Vujadinović, M., Djurdjević, V., Ranković-Vasić, Z., Marković, N., Atanacković, Z., . . . Petrović, N. Appliance of climate projections for climate change study in serbian vineyard regions. In VIII International Terroirs Congress, 2010. (Vol. 3, p. 36-41). Soave, Italy: CRAVIT Centro di Ricerca per la Viticoltura.

Wang B, Zhou TJ, Yu YQ. A View of Earth System Model Development. Acta Meteorologica Sinica 2009; 23: 1-17.

Wang, Xueqiu & Wang, Hua & Li, Hua. (2020). The influence of recent climate variability on viticultural zoning and variety regionalization of Vitis vinifera in China. OENO One. 54. 523-541. 10.20870/oeno-one.2020.54.3.2971.

Watanabe S, Hajima T, SudNagashima T, Takemura T, Okajima H, et al. MIROC-ESM 2010: model description and basic results of CMIP5-20c3m experiments. Geoscientific Model Development 2011; 4: 845-872.

Webb LB, Whetton PH, Barlow EWR. Modelling the relationship between climate, winegrape price and winegrape quality in Australia. Climate Research 2008; 36: 89-98.

Weigel AP, Knutti R, Liniger MA, Appenzeller C. Risks of Model Weighting in Multimodel Climate Projections. Journal of Climate 2010; 23: 4175-4191.

Westerling AL, Hidalgo HG, Swetnam TW . Warming and earlier spring increase Western U.S. forest wildfire activity. Science, 2006. 313, 940–943.

Westphalen, S.L. and Maluf, J.R.T. Caracterização das áreas bioclimáticas para o cultivo de Vitis vinifera L.: regiões da Serra do Nordeste e Planalto do Estado do Rio Grande do Sul. Brasília: Embrapa Comunicação para Transferência de Tecnologia, 2000. 99p.

White MA, Diffenbaugh NS, Jones GV, Pal JS, Giorgi F. Extreme heat reduces and shifts United States premium wine production in the 21st century. Proceedings of the National Academy of Sciences of the United States of America 2006; 103: 11217-11222.

Wild, M., Folini, D., Schaer, C., Loeb, N., Dutton, E.G., Koning-Langlo, G. 2013. The global energy balance from a surface perspective. Climate Dynamics 40 (11), 3107-3134. Doi:10.1007/s00382-012-1569-8.

Wilhite D. Drought as a natural hazard: concepts and definitions. In: Wilhite DA, ed. Droughts: Global Assessment. London: Routledge; 2000; 3–18.

Wilhite, D.A., Glantz, M.H. Understanding the drought phenomenon: The role of definitions. Water International 10(3): 111-120, 1985

Wilhite, D. Drought, Encyclopaedia of Earth System Science. San Diego,. CA: Academic Press.1992; 2: 81–92.

Willett KM, Dunn RJH, Thorne PW, Bell S, de Podesta M, Parker DE, et al. HadISDH land surface multi-variable humidity and temperature record for climate monitoring. Climate of the Past 2014; 10: 1983-2006.

Winkler AJ. General Viticulture. University of California Press, CA 1974

WMO (World Meteorological Organization), 2010. No. 1055. ISBN 978-92-63-11055-8. Switzerland www.wmo.int

WMO (World Meteorological Organization), 2012. In: Svoboda, M., Hayes, M. and Wood, D.(Eds.) Standardized Precipitation Index User Guide. Geneva: WMO

WMO (World Meteorological Organization), 2015. Guidelines on the Definition and Monitoring of Extreme Weather and Climate Events.

WMO (World Meteorological Organization), 2017. Statement on the State of the Global Climate in 2016.Nº 1189.2017. ISBN 978-92-63-11189-0

Xiao-Ge X, Tong-Wen W, Jie Z. Introduction of CMIP5 experiments carried out with the climate system models of Beijing Climate Center. Adv. Clim. Chang. Res. 2013; 4:41–49. https://doi.org/10.3724/SP.J.1248.2013.041

Yang YT, Roderick ML, Zhang SL, McVicar TR, Donohue RJ. Hydrologic implications of vegetation response to elevated CO2 in climate projections. Nature Climate Change 2019; 9: 44-+.

Yang YT, Zhang SL, McVicar TR, Beck HE, Zhang YQ, Liu B. Disconnection Between Trends of Atmospheric Drying and Continental Runoff. Water Resources Research 2018; 54: 4700-4713.

Yu S, Eder B, Dennis R, Chu S-H, Schwartz SE. New unbiased symmetric metrics for evaluation of air quality models. Atmospheric Science Letters 2006; 7.

Yukimoto S, Yoshimura H, Hosaka M, Sakami T, Tsujino H, Hirabara M, Tanaka T, Deushi M, Obata A, Nakano H, Adachi Y, Shindo E, Yabu S, Ose T, Kitoh A. 2011. Meteorological research institute- earth system model v1 (MRI-ESM1)—model description. Technical Report of MRI. vol 64.

Zargar A., Rehan Sadiq, Bahman Naser, and Faisal I. Khan (2011) A review of drought indices. Environ. Rev. 19: 333–349. doi:10.1139/A11-013

Zambrano-Bigiarini, M., Majone, B., Bellin, A., Bovolo, C., Blenkinsop, S. and Fowler, H. Hydrological Impacts of Climate Change on the Ebro River Basin, 2010. 10.1007/698_2010_85.

Zittis G, Hadjinicolaou P, Fnais M, Lelieveld J. Projected changes in heat wave characteristics in the eastern Mediterranean and the Middle East. Regional Environmental Change 2016; 16: 1863-1876.

Zha Q, Xi X, He Y, Jiang A. Comprehensive evaluation of heat resistance in 68 Vitis germplasm resources. Vitis 2018; 57: 75-81.

Zorita, Eduardo & Von Storch, Hans. (1999). The Analog Method as a Simple Statistical Downscaling Technique: Comparison With More Complicated Methods. J. Climate. 12. 2474-2489. 10.1175/1520-0442(1999)012<2474:TAMAAS>2.0.CO;2.

ANEXO DE PUBLICACIONES

Science of the Total Environment 650 (2019) 2778–2795

Contents lists available at ScienceDirect

Science of the Total Environment

journal homepage: www.elsevier.com/locate/scitotenv

Projection of temperatures and heat and cold waves for Aragón (Spain) using a two-step statistical downscaling of CMIP5 model outputs

Emma Gaitán [a,b], Robert Monjo [b], Javier Pórtoles [b], Mª. Rosa Pino-Otín [a,*]

[a] Universidad San Jorge, Villanueva de Gállego, 50830, Zaragoza, Spain
[b] Fundación para la Investigación del Clima, C/Tremps 11, 28040 Madrid, Spain

HIGHLIGHTS

- Future temperature and heat and cold wave scenarios are obtained for Aragón, Spain.
- All scenarios are obtained using Earth System Models from CMIP5 for the first time.
- Intensity and duration of the cold waves will remain stable during this century.
- Intensity and duration of the heat waves will increase (3.6 °C, 7 days).
- The maximum temperature may increase up to 7 °C in summer at the end of the century.

GRAPHICAL ABSTRACT

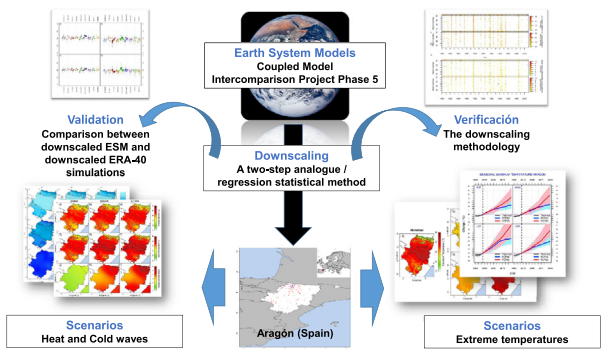

ARTICLE INFO

Article history:
Received 6 July 2018
Received in revised form 18 September 2018
Accepted 28 September 2018
Available online 04 October 2018

Editor: Pavlos Kassomenos

Keywords:
Climate change
Heat wave
Cold wave
Extreme temperatures
Downscaling
Spain

ABSTRACT

Heat- and cold-wave scenarios and temperature scenarios during the 21st century were obtained for Aragón (Spain), using, for the first time, nine Earth System Models (ESM) and two Representative Concentration Pathway (RCP) scenarios – RCP4.5 and RCP8.5 - belonging to the 5th Coupled Model Intercomparison Project (CMIP5).
Local climate heat-wave scenarios show an increase of its mean intensity close to 2 °C (reaching temperatures of up to 38.8 °C) and an average increase of the maximum intensity of 3.6 °C (temperature of up to 41.5 °C) with respect to a historic period (1971–2000) for the RCP8.5 scenario at the end of the century. The duration of heat waves will increase by 7 days at the end of the century (total average duration of 12 days). The future intensity and duration of cold-wave episodes will remain stable.
Local climate change scenarios for daily maximum temperatures show a gradual increase throughout the 21st century. The greatest increases will occur during the summer at the end of the century, reaching values of up to 7 °C for the RCP 8.5 scenario. The minimum temperature increases show similar behaviours to the maximum temperatures, but with less marked increases (3 °C and 5.6 °C for the RCP4.5 and RCP8.5 scenarios respectively in summer at the end of the century).
The highest temperatures and the intensity of the heat waves will be especially intense in the Ebro Valley, the most populated area. In addition, the Pyrenees will suffer the longest heat waves, especially at the end of the century, and the greatest increases in maximum temperatures.
The downscaling of the CMIP5 models, offers accurate scenarios -both spatially and temporally- of extreme temperatures and heat and cold waves, useful for decision-making for local adaptation to climate change but also as a reference for other European regions.

* Corresponding author at: Universidad San Jorge, Campus Universitario Villanueva de Gállego Autovía A-23 Zaragoza-Huesca, km. 510, 50830 Villanueva de Gállego, Zaragoza, Spain
E-mail address: rpino@usj.es (M.ªR. Pino-Otín).

https://doi.org/10.1016/j.scitotenv.2018.09.352
0048-9697/

1. Introduction

There is widespread agreement in the scientific literature that the most severe effects of global warming will be related not only to a change in the mean climate, but especially to an increase in the frequency and intensity of extreme events, such as floods, droughts and heat waves as is reflected in the conclusions provided by the Intergovernmental Panel on Climate Change (IPCC) and in independent studies (Cook et al., 2013). Heat waves (i.e, a period of consecutive days with extreme hot temperatures) are one form of extreme weather that is likely to increase in frequency, intensity and duration under the influence of a changing climate during upcoming years (IPCC, 2013; Field et al., 2012). Extreme temperature events can impact many aspects of human life, such as mortality, health, comfort, agriculture and hydrology (Garcia-Herrera et al., 2005; Patz et al., 2005; Roldan et al., 2016). For example, in 2003, an extraordinary "mega heat wave" occurred in Central Europe, which had important consequences on society.

One of the main problems when evaluating extreme episodes of temperature (that is, cold or heat waves) is that there are no universal definitions of these phenomena. Some definitions use a fixed term (5 days >30 °C or 3 days >35 °C in the case of a heat wave); some include humidity, spatial extent or accumulated heat ((Anderson and Bell, 2009; Russo et al., 2017; Suparta and Yatim, 2017); some set their threshold according to a specific percentile (Anderson and Bell, 2009; Kent et al., 2014; Smith et al., 2013); and some are based on combined indexes of different meteorological variables, such as World Meteorological Organization member guidelines (WMO, 2010).

Although large-scale and small-scale processes involved in the development of European heat waves, such as interactions between land surface and atmosphere and the influence of large-scale atmospheric circulation, are not fully understood (Vautard et al., 2013), climate models could be a suitable tool for providing accurate heat-wave assessments for future adaptation strategies.

Global climate models (GCMs) are fundamental tools for the study of future climate, and they are able to provide data to estimate large-scale aspects of climate change, to drive regional climate models or to be used directly by impact models. GCM outputs are also used for projections of temperature extremes around the world (Dosio, 2017; Gross et al., 2017; Jeong et al., 2016; Saeed et al., 2017; Sillmann et al., 2014).

Recently, efforts to reduce model uncertainty have led to a new generation of global climate models called Earth System Models (ESM) that integrate the individual parts of the climate system (atmosphere, ocean, land and sea ice) and the exchange of energy and mass between them (Knutti and Sedlacek, 2013). They also include chemical processes, land use, plant and ocean ecology and an interactive carbon cycle, which enables integration of biochemical processes into the models (Heavens et al., 2013). These models are the basis of the fifth phase of the Coupled Model Intercomparison Project (CMIP5) (Taylor et al., 2012), constituting the most current set of coordinated climate model experiments (Brands et al., 2013; Carvalho et al., 2017; Chen et al., 2016; Perez et al., 2014).

The CMIP5 models and their predecessors have become an important resource for climate scientists and others investigating possible future impacts. However, the spatial resolution of these models remains too low for many impact assessments at a local scale, on which policy and management decisions need to be made. These models are run at coarse spatial resolutions, which is also a major limitation in projecting extreme events because projections of climate extremes and simulations of heat-wave characteristics on regional scales are very sensitive to spatial resolution and the interpretation of gridded outputs (Chen et al., 2016).

The deficiency in scale is addressed through downscaling techniques involving either statistical approaches or dynamic approaches. In the statistical approach, high-resolution predictands (surface variables) are obtained by applying relationships that are identified from the observed climate data to these predictands and to large-scale predictors of GCM outputs (Asong et al., 2016; Benestad et al., 2007; Semenov and Stratonovitch, 2010). In dynamical downscaling, a time-varying regional climate model (RCM) of atmospheric boundary conditions is nested within the GCM (Giorgi and Gutowski, 2015; Giorgi and Mearns, 1991;). Both methods have been widely used and both have advantages and disadvantages. The main advantages of statistical downscaling techniques are that they are computationally inexpensive, they provide local information and they allow quantifying the uncertainty associated to the downscaling process and to the climatic models.

Several studies have been carried out to explore present temperature extremes in Europe (Soares et al., 2012) and in the Mediterranean region (Kuglitsch et al., 2010; Seubert et al., 2014), and other studies have developed scenarios of temperature extremes in the same areas (Estrella and Menzel, 2013; Hertig et al., 2010; Lavaysse et al., 2012). However, none of them have applied the downscaling CMIP5 models.

Although many climate models have difficulties in properly reproducing climate extremes, such as heat-wave conditions (Stegehuis et al., 2015), a few studies have reported on heat-wave scenarios in Europe (Fischer and Schar, 2010; Schoetter et al., 2015), or located in in the Mediterranian region (Zittis et al., 2016), in France (Planton et al., 2008), Italy (Tomozeiu et al., 2007) or Finland (Kim et al., 2018). Schoetter et al. (2015) and Kim et al. (2018) are one of the few studies that already use the models from the IPPC5. As a part of the European Coordinated Regional Downscaling Experiment (EUROCORDEX) (Giorgi et al., 2009), the EUROCORDEX initiative provides regional climate projections for Europe. (Vautard et al., 2013) used the EUROCORDEX project to simulate heat waves at the European regional scale, providing a downscaling of CMIP5 simulations. These European-scale studies only featured a few locations in Spain. Several downscaling studies have been specifically conducted on temperature in Spain (Brands et al., 2011b; Frias et al., 2005; Frias et al., 2010; Hervada-Sala et al., 2000; Miro et al., 2016; Turco et al., 2014), but very few studies have explored temperature extremes in Spain (Fernandez-Montes and Rodrigo, 2012; Fonseca et al., 2016) and they do it in past periods (1925–2006 and 1986–2005, respectively).

Only a few studies have developed temperature scenarios in the Aragón region (northeastern Spain) (Buerger et al., 2007; Goncalves et al., 2014; Ribalaygua et al., 2013a), but none of them developed temperature-extreme or heat-wave scenarios. Only (Barrera-Escoda et al., 2014) developed scenarios of extreme temperatures in the Ebro basin. That study showed that the projected increase in the number of tropical nights and extreme temperatures could have a negative effect on human health and comfort conditions. Other studies have also analysed the possible impacts of climate change in this region on human health (Roldan et al., 2016). Both studies used the climate models associated to the 4th assessment report of the IPCC.

Aragón is characterised by a highly complex topography that causes large climate gradients. Downscaling techniques were required to capture these orographic features, allowing for the areas that were most vulnerable to extreme changes to be identified. Statistical downscaling is particularly recommended for areas with complex topography (Kattenberg and Amer Meteorol SOC, 1996). Nevertheless, downscaling of CMIP5 simulations has not been used to date, and heat-wave scenarios cannot be found in this sensible area of Spain.

Therefore, the objectives of this study were:

- Generate local heat- and cold-wave scenarios of the 21st century to downscale GCMs from CMIP5 using a statistical methodology in the area of Aragón, Spain.
- In addition, generate new climate scenarios using CMIP5 models for Aragón to simulate the future daily maximum and minimum temperatures in order to analyse the differences with respect to the scenarios we generated in 2013 for the 21st century using the Special Report on Emissions Scenarios, SRES (IPCC, 2000) previous to CMIP5.

Aragón, moreover, is a representative territory of different European climates, from the low-land areas in the centre of Aragón (the Ebro

River Basin) to the mountain regions in the north (the Pyrenees) which makes it a good indicator of future European climate changes. Finally, an original two-step analogue/regression statistical downscaling method developed by the Climate Research Foundation was carried out.

The information used in the present study was based on the most current data available. It was useful for identifying the areas that were most vulnerable to extreme temperature changes in Aragón, and for helping decision makers to design mitigation and adaptation strategies in response to territorial environmental impacts derived from climate change.

2. Material and methods

2.1. Study area and datasets

2.1.1. Study area

The present study was carried out in the region of Aragón (Fig. 1), which is located in the northeast part of the Iberian Peninsula in Spain and which has an area of approximately 47,720 km^2 (340 km length and 240 km width). Because of its location, Aragón falls within the Western Mediterranean climate area, with cool winters and hot, dry summers. However, the extreme altitude differences of over 3000 m between the plains (the Ebro River Basin) and the mountains (the Pyrenees), together with the specific topography of the Ebro River Basin and the mountain chains (the Pyrenees to the north of the basin and the Iberian Mountains to the south), modify the local climate. As a result, the climate characteristics of the area are somewhat different from a standard Western Mediterranean climate, and they typically consist of dryness of the land along the banks of the Ebro River, random rain patterns, high thermal contrast between winter and summer as a consequence of the strong continental characteristics of the region and the typical northeast "mistral" winds, which are frequent in the region.

2.1.2. Surface observation dataset (predictands)

The observational dataset used in the present study consists of a time series of the daily maximum and minimum temperatures distributed, quite homogeneously, throughout the Aragón territory (Fig. 1). This dataset it is the same as the one used in a previous study (Ribalaygua et al., 2013a) in order to facilitate comparison of the results.

Data were obtained from the extensive network of instrumental observatories owned by the Spanish Meteorological Agency (AEMET) (http://www.aemet.es). The stations are subject to strict data quality control, which includes detecting and correcting multiple aberrant points in the long-term climate time series, covering the gaps, assessing the homogeneity of the climate series and correcting any inhomogeneities found. This process was carried out by the Aragón Government (López et al., 2007) To guarantee the quality of the data, stations with a large number of data gaps or without at least 15 years of daily records were discarded. Second, we analysed the dataset for the presence of extreme data points that could be considered suspect observations or transcription errors (we considered data points to be extreme if they were separated from the monthly average by more than four times the value of the standard deviation). Third, we verified that the data did not contain inhomogeneities that could introduce bias into any records that were not related to the climate, (Ribalaygua et al., 2013a).

The first set of data (composed of 103 stations) was used to analyse and produce the regional climate scenarios of maximum and minimum temperatures (Fig. 1a). Of these 103 stations, those that had at least 75% of maximum temperature data collected from June to September (i.e, the reference period for the calculation of heat waves) between 1980 and 2000 and stations that had at least 75% of minimum temperature data collected from November to April (that is, the reference period for the calculation of cold waves) between 1980 and 2000 perform a second set of data selected for the study of extreme events. In both cases, the number of observatories was 71 (Fig. 1b).

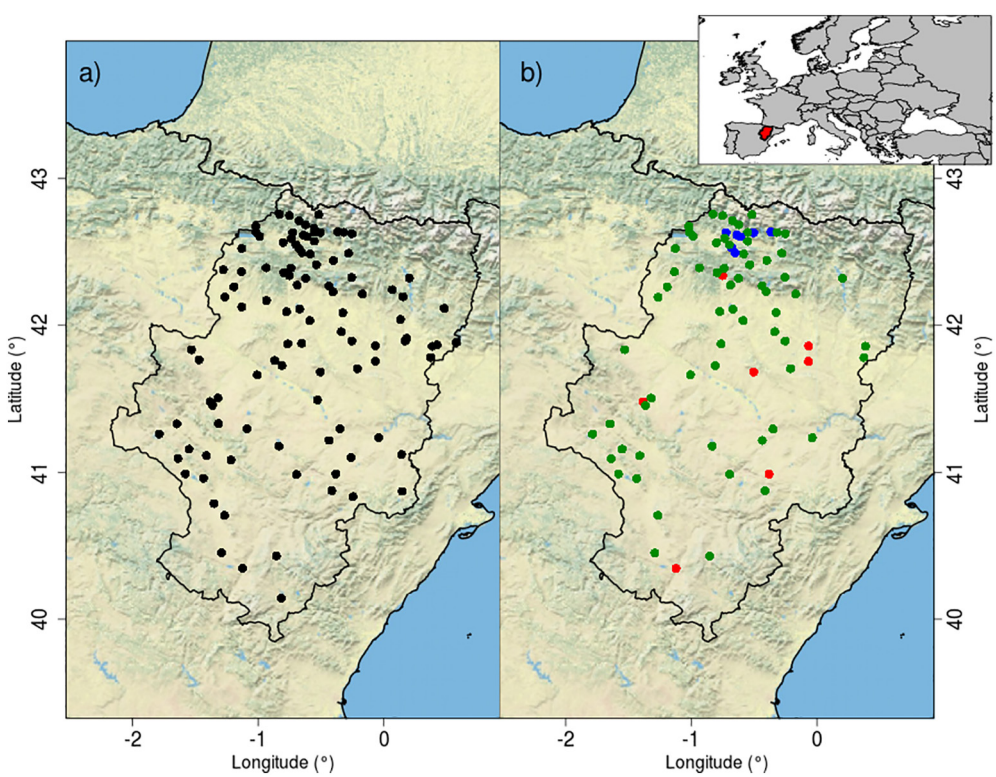

Fig. 1. Location of the study Area: Aragon (Spain) in Europe. Points indicate the stations used in the study. a) Stations of temperature (103) used in the generation of climate regional scenarios of maximum and minimum temperature (verification, validation and scenarios). b) Stations used exclusively on the generation of heat waves (7, red), used exclusively on the generation of cold waves (7, blue) and those used in both extreme events (64, green). "(Map source: OpenStreetMap)". (For interpretation of the references to colour in this figure legend, the reader is referred to the web version of this article.)

2.1.3. Atmospheric dataset (predictors)

2.1.3.1. Reanalysis. As a reference dataset, we used the reanalysis from the European Centre for Medium-Range Weather Forecasts (ECMWF ERA-40; http://www.ecmwf.int/research/era/do/get/era-40) (Uppala et al., 2005) for the period 1958–2000. For the atmospheric window, we used geographical limits from 31.5°N to 55.1°N latitude and from 27.0°W to 14.6°E longitude, covering not only the geographic area under study, but also the surrounding atmosphere areas, which exert a meteorological influence all over the Iberian Peninsula (Ribalaygua et al., 2013a).

For verification of the methodology, it was necessary to reduce the temporal (six hourly) and spatial (125 km) scale of the reanalysis to that of the different climate models in order to compare both, ERA-40 and the climate model simulations (Ribalaygua et al., 2013a, 2013b).

2.1.3.2. Climate model data. In the present study, we worked with a set of nine climate models that belong to the CMIP5 and that were provided by the Program for Climate Model Diagnosis and Intercomparison (PCMDI) archives (Table 1). The number of models chosen was limited to the availability of data with daily time frequencies. All of the models were ESMs.

To generate the model predictor fields, we took the daily values of several large-scale fields of interest (that is, geopotential height, specific humidity and wind) at different pressure levels for the nine ESMs showed in the Table 1 associated with the CMIP5 (Taylor et al., 2012). Moreover, we used an historical experiment (Taylor et al., 2012) which generated simulations of the past 20th century and which was useful for the evaluation of model performance against the present climate. Finally, the representative concentration pathway (RCP) families were considered (Moss et al., 2010), specifically the RCP8.5 'high' scenario and the RCP4.5 'intermediate' scenario, both of which corresponded to different possible ranges of radiative forcing reached in the year 2100 with respect to values of the pre-industrial era (4.5 and 8.5 W/m^2, respectively).

2.2. Methodologies

2.2.1. Description of the downscaling methodology

The methodology of statistical downscaling used in this study was chosen according to three main advantages:

1) Allows easier quantification of the main uncertainties associated with the generation of future climate scenarios (Van der Linden and Mitchell, 2009).
2) It is a key for the achievement of climate simulations that are consistent with observations which, in turn, are physically coherent (Ribalaygua et al., 2013b).
3) Provides local detail, which is useful information because nearby data points in space can evolve under different future climate conditions (Ribalaygua et al., 2013b).

A two-step analogue/regression statistical downscaling method that was developed by the Climate Research Foundation (FIC) (Ribalaygua et al., 2013b) was applied to obtain future scenarios of the maximum and minimum temperatures at a local scale in the region of Aragón. This methodology consisted of a two-step analogue/regression statistical method, which has been used in national and international projects with good verification results. In the present paper, we present a summary of the two-step method (more details can be found in Ribalaygua et al., 2013b).

The first step was analogous stratification. An analogue method was applied based on the hypothesis that 'analogue' atmospheric patterns (predictors) should cause analogue local effects (predictands), which means that the number of days that were most similar to the day to be downscaled were selected (Benestad et al., 2007; Zorita and von Storch, 1999). The similarity between any two days was measured using a pseudo-Euclidean distance between the large-scale fields used as predictors. For each predictor, the weighted Euclidean distance was calculated and standardised by substituting it with the closest percentile of a reference population of weighted Euclidean distances for that predictor. This method is a good method for reproducing nonlinear relationships between predictors and the predictands, but it could not be used to simulate values outside of the range of observed values ((Imbert and Benestad, 2005). In order to overcome this problem and to obtain a better simulation, a second step was required.

The second step focuses on temperature. To determine the temperature, a multiple linear regression analysis for the selected number of most analogous days was performed for each station and for each problem day. From a group of potential predictors, the linear regression selected those with the highest correlation, using a forward and backward stepwise approach.

About the accuracy in simulating temperatures of our downscaling technique, in our previous work about climate change in Aragón we achieved an average bias below 0.1 °C″ (Ribalaygua et al., 2013a).

Table 1
Information about the nine climate models belonged to the 5 Coupled Model Intercomparison Project (CMIP5) corresponding to the fifth report of the IPCC. Models were supplied by the Program for Climate Model Diagnosis and Intercomparison (PCMDI) archives.

Climatic model	SPATIAL/TEMPORAL resolution	Research centre	References
GFDL-ESM2M	2°×2,5° daily	National Oceanic and Atmospheric Administration (NOAA), E.E.U.U.	Dunne et al. (2012)
CanESM2	2,8°×2,8° daily	Canadian Centre for Climate Modeling and Analysis (CC-CMA), Canadá.	Chylek et al. (2011)
CNRM-CM5	1,4°×1,4° daily	CNRM (Centre National de Recherches Meteorologiques), Meteo-France, Francia.	Voldoire et al. (2013)
BCC-CSM1-1	1,4°×1,4° daily	Beijing Climate Center (BCC), China Meteorological Administration, China.	Xiao-Ge et al. (2013)
HADGEM2-CC	1,87°×1,25° daily	Met Office Hadley Center, United Kingdom.	Collins et al. (2008)
MIROC-ESM-CHEM	2,8°×2,8° daily	Japan Agency for marine-Earth Science and Technology (JAMSTEC), Atmosphere and Ocean Research Institute (AORI), and National Institute for Environmental Studies (NIES), Japan.	Watanabe et al. (2011)
MPI-ESM-MR	1,8°×1,8° daily	Max-Planck Institute for Meteorology (MPI-M), Germany.	Raddatz et al. (2007); Marsland et al. (2003)
MRI-CGCM3	1,2°×1,2° daily	Meteorological Research Institute (MRI), Japan.	Yukimoto et al. (2011)
NorESM1-M	2,5°×1,9° daily	Norwegian Climate Centre (NCC), Norway.	Bentsen et al. (2013); Iversen et al. (2013)

2.2.2. Validation and climate simulation of temperature

In order to determine the ability of each ESM to simulate the predictor fields, absolute and relative temperatures from the downscaled ESM simulation of the historical experiment was compared with the downscaled ERA-40 simulation (previously verified against the observations) during a common historical period (1958–2000).

Due to the characteristics of the ESMs, the validation process presents certain limitations. First, as climate models do not reproduce day-to-day meteorology, validation cannot be performed on a daily scale and it must be done using climate statistics over long periods of time, resulting in a loss of information on climate variability. Second, we could not compare the climate characteristics obtained from the ESM historical simulation with those obtained from the observations because the latter had missing data and large gaps; therefore, we had to compare ESMs simulations with simulations from the re-anlaysis of a dataset (previously validated in the verification process). Both sources of error should be considered in the final uncertainty analysis.

As error measures, bias and standard deviation were analysed on a seasonal scale for both maximum and minimum temperatures. An ensemble strategy was used to quantify the uncertainties inherent in future climate projections (IPCC, 2013). For each scenario (i.e, RCP4.5 and RCP8.5), an ensemble of the approved downscaled ESMs was used to estimate the mean change (compared to 1976–2005) and to quantify the main contributions to the uncertainty.

Future local climate scenarios for maximum and minimum temperature, for nine GCMs and two RCPs have been produced at the daily scale. To draw the temperature maps, we used Thin Plate Spline regression (TPS) from the R-Package "fields" (Nychka et al., 2015).

2.2.3. Definition of hot- and cold-wave episodes

There are many and varied terms used to define a heat wave. For example, the AEMET defines a heat wave as an "episode of at least three consecutive days, in which at least 10% of the stations considered record maximums above the 95% percentile of their series of maxima daily temperatures of the months of July and August of the period 1971–2000." The WMO defines a heat wave as an extreme event with marked warmed of the air or the invasion of very warm air over a large area, it usually last from a few days to a few weeks. The IPCC defines a heat wave as "a period [of] abnormally and uncomfortably hot weather". Those definitions are not the only ones accepted in the

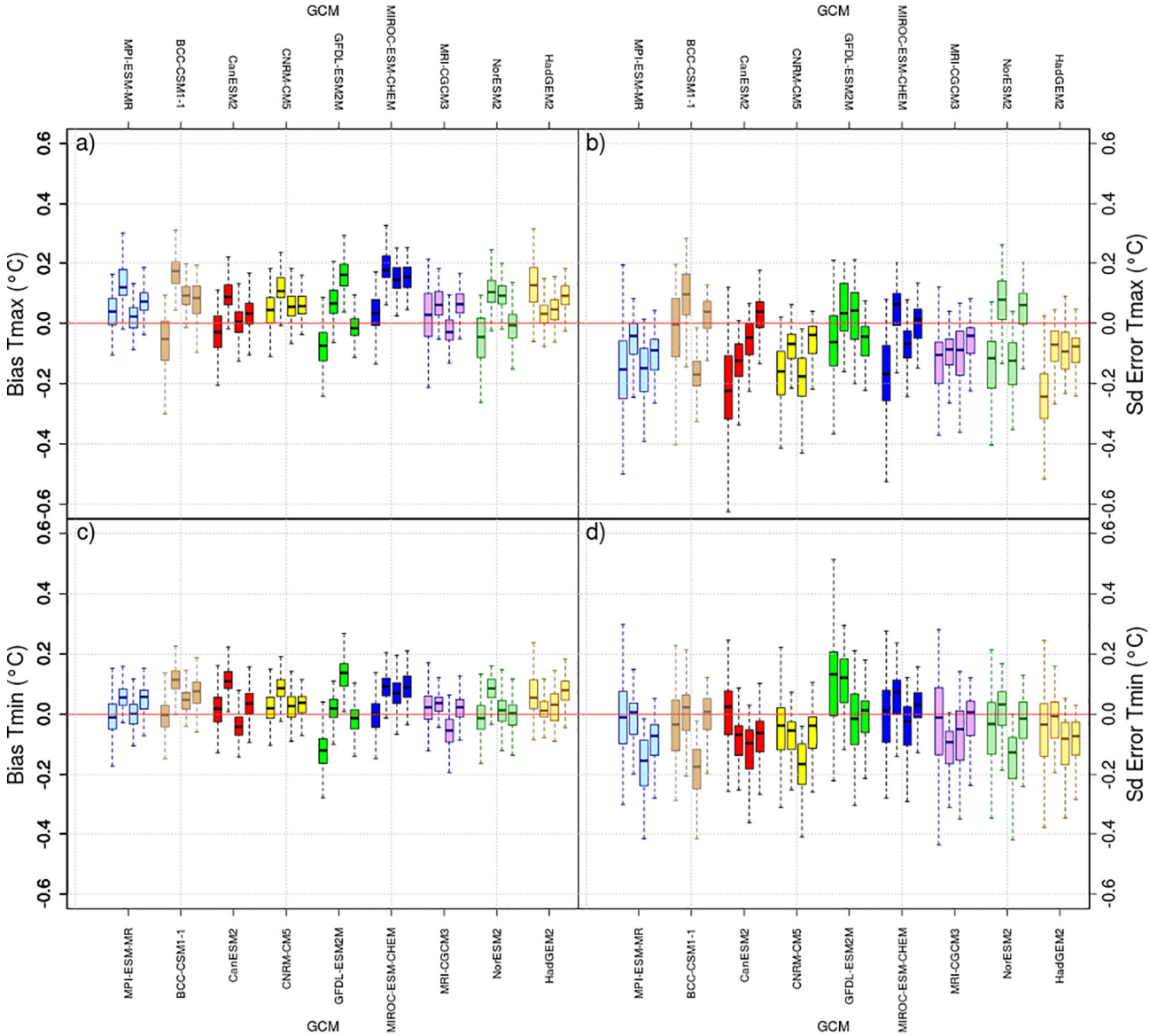

Fig. 2. Validation of the GCMs used for the simulation of temperatures. Absolute Bias for a) maximum and c) minimum temperature and absolute standard deviations for b) maximum and d) minimum temperature, between the results obtained by downscaling the Historical scenario of each GCM used in the study with those obtained by downscaling the reanalysis ERA-40 for a common period (1958–2000). There are four boxplots, representing a season of the year (winter, spring, summer and autumn), for each GCM.

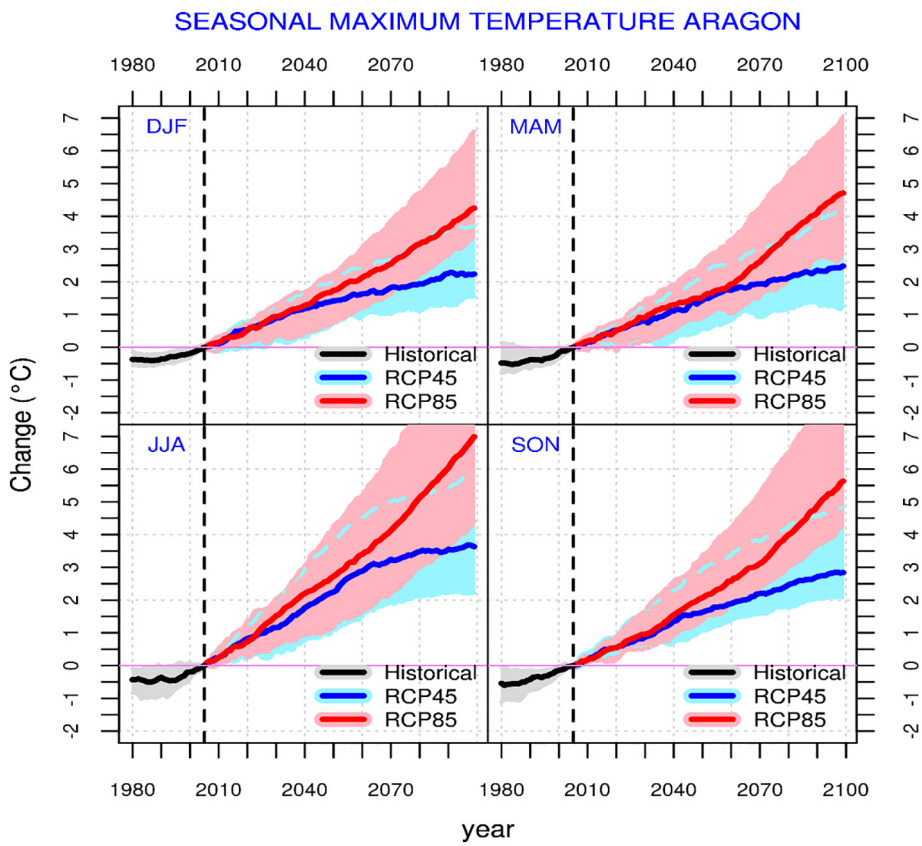

Fig. 3. For the four seasons (winter, spring, summer and autumn) simulated maximum temperature for the twenty-first century displayed as absolute increase against the value simulated for the 1976–2005 Historical period. The vertical dotted line marks the end of the Historical data (2005). Data grouped for every RCP simulation of every global climate model used and for the last 30 years of every station. The ensemble median (solid lines) and the 10th–90th percentile (shaded areas) values are displayed.

scientific literature. Some heat-wave definitions have been used to identify heat waves in a time series of temperature data (Smith et al., 2013;), and the choice of the heat wave definition can influence both projected heat-wave trends (Smith et al., 2013) and estimates of health risks during events (Anderson and Bell, 2009; Chen et al., 2015; Kent et al., 2014).

According to the recommendations of the WMO, (2010), a practical and qualitative definition of a heat wave must consider marked and unusual hot weather over a region during at least two consecutive days in the hot period of the year, based on local climate conditions, with thermal conditions recorded above given thresholds. On the basis of these recommendations and the characteristics of the Aragón climatology, we defined a heat wave as follows: at least three consecutive days with a maximum temperature above the 95th percentile of the maximum temperature series and calculated between the months of June to September during the period 1980–2000.

In broad terms, a cold wave can be defined as a meteorological event characterised by a sharp drop of air temperature near the surface, leading to extremely low values. According to the IPCC 2007, (Parry et al., 2007) a cold wave is an event that often causes problems and severe impacts on the population, especially in northern altitudes. However, there is still a lack of a clear and consistent definition for cold-wave events in the world.

In the WMO's Meteoterm vocabulary, a cold wave is defined as "marked cooling of the air, or the invasion of very cold air, over a large area." For the AEMET, a cold wave is "an episode of at least three consecutive days, in which at least 10% of the considered stations register minimums below the 5% percentile of their series of minima daily temperatures for the months of January and February of the period 1971–2000". The WMO's members guideline define a cold wave as "marked and unusual cold weather characterised by a sharp and significant drop of air temperatures near the surface (max, min and daily average) over a large area and persisting below certain thresholds for at least two consecutive days during the cold season".

Considering the climate characteristics of Aragón, we defined a cold wave as follows: at least three consecutive days with a minimum temperature below the fifth percentile of a minimum temperature series and calculated between the months of November to April during the period 1980–2000.

To better identify a heat or cold wave, we evaluated average duration, maximum intensity and average intensity as it is recommended by the WMO in the Guidelines on the definition and monitoring of extreme weather and Climate Events. The average duration refers to the average number of days the heat wave lasted. The average intensity represents the average value of the temperature during the heat wave. The maximum intensity is equal to the maximum value that the temperature reached during the heat wave.

2.2.4. Verification and simulation of heat and cold waves

In order to assess the capacity of the downscaling methodology to simulate heat and cold waves observed in the past, we evaluated how the downscaling methodology simulated the 95th percentile of maximum temperatures and the 5th percentile of minimum temperatures, which are the thresholds that indicate the existence of an episode of a heat and cold wave, respectively. In addition, we analysed the intensity of the wave (average and maximum) and the average duration, comparing the heat and cold waves calculated from the simulated ERA-40 temperature series with those obtained from the observed series. Verification of the maximum and minimum temperatures can be seen in a previous study by Ribalaygua et al. (2013a). The statistical measures used in the verification processes were the bias, the standard deviation and the Pearson correlation at the daily scale. The statistical

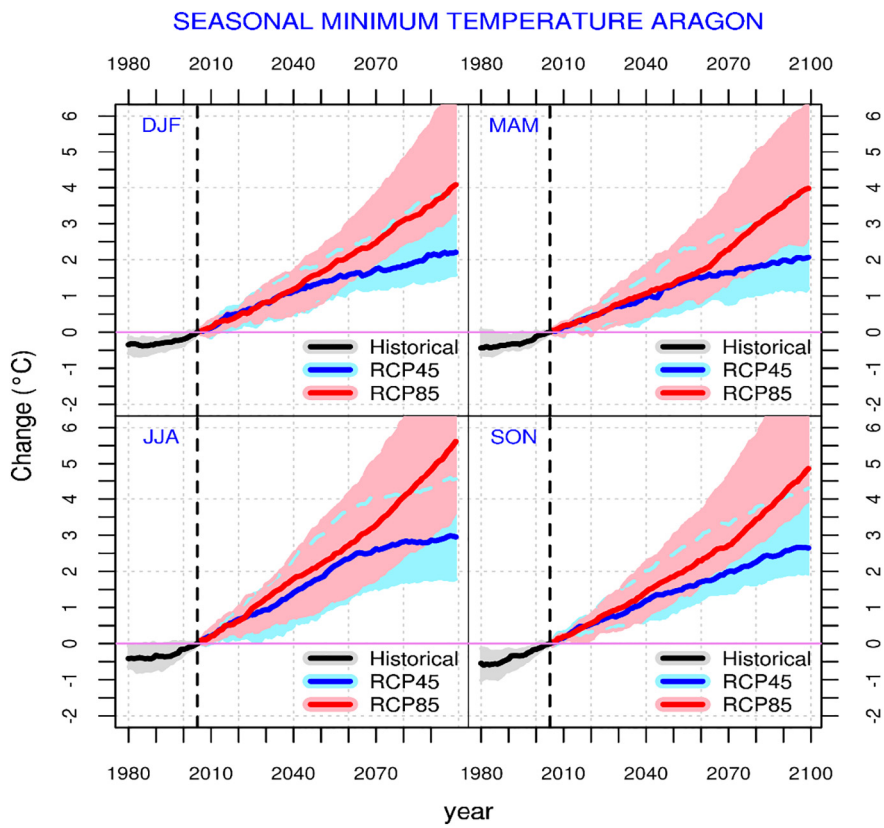

Fig. 4. For the four seasons (winter, spring, summer and autumn) simulated minimum temperature for the twenty-first century displayed as absolute increase against the value simulated for the 1976–2005 Historical period. The vertical dotted line marks the end of the Historical data (2005). Data grouped for every RCP simulation of every global climate model used and for the last 30 years of every station. The ensemble median (solid lines) and the 10th–90th percentile (shaded areas) values are displayed.

measures were calculated using R-cran package computing software (R Development Core Team, 2010).

From the ESM simulated temperature series (nine ESMs and two RCPs), we determined the heat- and cold-wave episodes that were expected in Aragón during the upcoming decades of the 21st century. The heat- and cold-wave scenarios were compared to a historical period (1976–2005) to analyse the future changes with respect to the actual situation of these extreme events.

3. Results

3.1. Validation of the CMIP5 model statistical downscaling to predict temperatures

The seasonal bias that result from a comparison between the ERA-40 temperature simulations and the historical temperature simulations for each ESM for a common period (1958–2000) are shown in Fig. 2 for absolute temperatures (that is, the difference between simulated Historical ESM data and simulated ERA-40 data). For both the maximum and minimum temperatures, the obtained bias was around tenths of a degree in all months, so they were very close to zero. The error was not above half of a degree for any of the cases. Therefore, the results showed that the ESMs were capable of adequately simulating both the maximum and the minimum temperatures on annual and seasonal scales.

3.2. Local climate scenarios to predict future temperatures

Figs. 3 and 4 show local climate-change scenarios for future daily maximum and minimum temperatures respectively, that have been predicted on the basis of the nine models (see Table 1). Figs. 3 and 4 allowed for the establishment of a general view of the changes expected in Aragón. In addition, Figs. 5 and 6 represent the summer maximum and winter minimum temperature changes expected for the periods 2041–2070 and 2071–2100 as presentation of mid- and end-century expected changes, which were calculated according to the scenarios RCP4.5 and RCP8.5.

Expected changes in the average temperature for the rest of the seasons of the year can be found in the supplementary material for maximum temperatures increase (Figs. S1–S3) and minimum temperatures increase (Fig. S4–S6). In addition, Fig. S7–S9 showed the maximum and Figs. S10–S12, minimum temperatures expected in this century.

Fig. 3 shows a gradual increase in the maximum temperatures throughout the 21st century. During the mid-century, the least significant changes are expected during the winter and springs months (around 1.5 and 1.7 °C for the RCP4.5 and RCP8.5, respectively), and the most significant changes are expected for the summer months, with values of 2.1 °C for the RCP4.5 and 2.7 °C for the RCP8.5. At the end of the century, the expected changes are more marked and differ notably between the two RCPs. During winter and spring months, the expected values are around 2.3 °C and 2.4 °C for the RPC4.5 and 4.3 °C and 4.7 °C for the RCP8.5, respectively. The greatest changes are expected for summer months, reaching values of 7 °C for the RCP8.5 and 3.6 °C for the RCP4.5.

The areas most affected by the maximum temperature increases are expected to be the Pyrenees and the areas in the southwest and north of Aragón during all the 21th century for the months of summer, spring and autumn, especially in the RCP8.5 scenario (Fig. 5). In contrast, in the winter months, the highest temperature increases at the end of the century are expected in the Pyrenees area and the Ebro Valley (Fig. S1).

Scenarios of maximum temperatures of the 21st century (Figs. 5 and S7–S9) point that expected maximum temperatures are not proportional to the expected increases shown before (Figs. 5 and S1–S3).

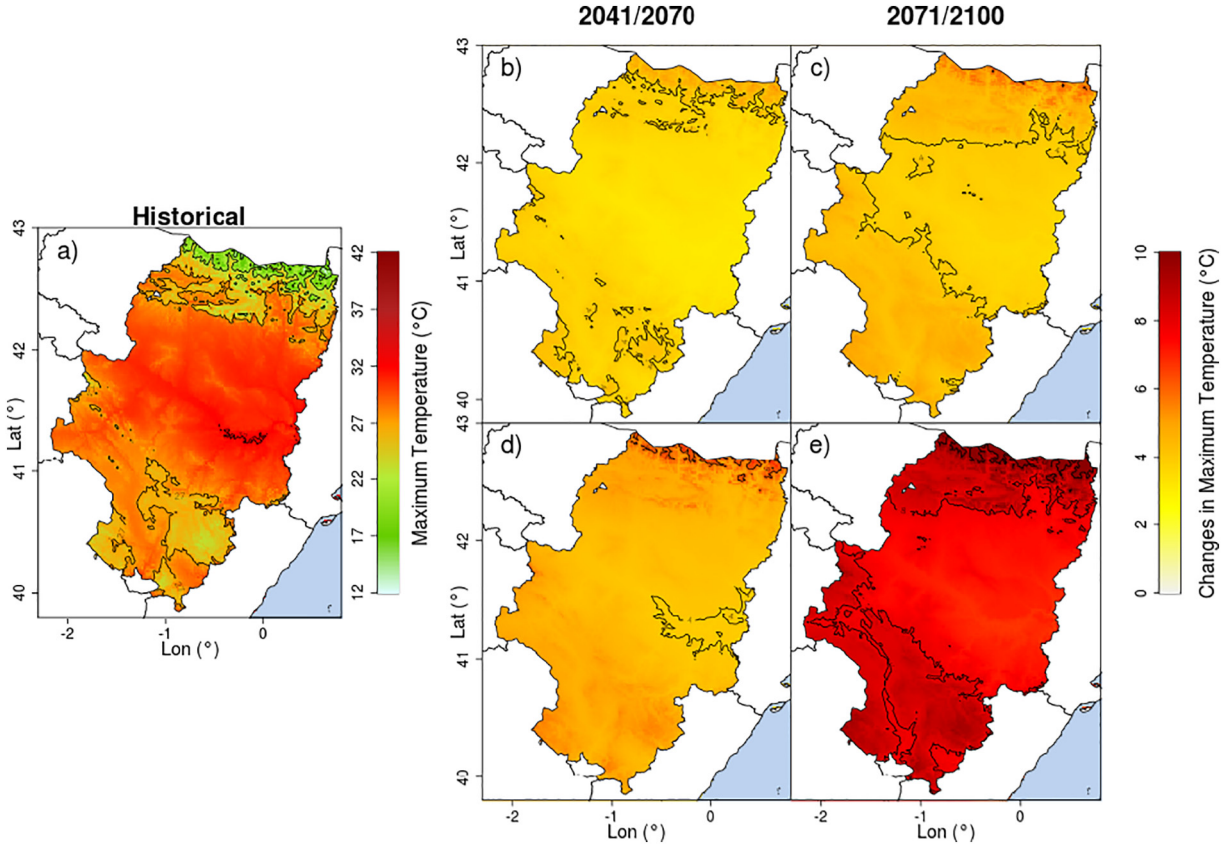

Fig. 5. Geographical representation of the expected changes of maximum temperature in summer for the periods 2041–2070 and 2071–2100 respect to the reference Historical Period (1976–2005). Both emissions scenarios are represented: RCP4.5 (figures b and c) and RCP8.5 (figures d and e). Fig. 5a represents the Historical absolute temperature for the period 1976–2005.

The evolution of the minimum temperature increases throughout the 21st century demonstrate similar behaviours to the maximum temperatures, but with less marked increases, especially at the end of the century (Figs. 6 and S4–S6). By the middle of the century, all of the seasons of the year, except for the summer, are expected to show increases in the minimum temperature of <2.0 °C, and even in the spring, the increases are expected to be close to 1.0–1.2 °C. The summer months are expected to show the greatest increases in minimum temperatures, varying from 1.8 °C for the RCP4.5 to 2.3 °C for the RCP8.5. At the end of the century, increases in the minimum temperatures during the summer months are expected to range from 3.0 °C (RCP4.5) to 5.6 °C (RCP8.5. Winter months are expected to show an increase between 2.8 °C and 4.1 °C, spring months between 2.1 °C and 4 °C and autumn months between 2.6 °C and 5 °C for the RCP4.5 and RCP8.5 scenarios, respectively.

The increases in the minimum temperature in are expected to be quite homogeneous throughout the region and the seasons according to the RCP4.5. In contrast, according to RCP8.5 (Fig. 6c,d), these changes will be more pronounced in the Ebro Valley at the end of the 21st century. The highest minimum temperatures are expected to be recorded in the central zone of Aragón during all seasons of the year (see supporting information, Figs. S10–S12).

3.3. Verification of hot- and cold-wave episodes

To verify the simulation of both of heat waves and cold waves, we compared the wave episodes obtained from ERA-40 simulations against the episodes recorded by the observations.

The first step was to verify that the methodology correctly simulated both percentiles, the 95th percentile of the maximum temperature and the 5th percentile of the minimum temperature. Both cases have been well simulated by applying the downscaling methodology to the ERA-40 series (Fig. 7). Data from the simulated ERA-40 series and the observed series were very close, and the error committed by simulating the ERA-40 series respect to the observed one was very low, especially in the 95th percentile. For example, we found error values around 0.36 °C for summer months and around 0.69 °C for the winter months in the 95th percentile, and 0.6 °C for summer months and around 0.68 °C for the winter months in the 5th percentile.

Regarding the verification of the identification parameters of a heat wave, Fig. 8 shows the results obtained for the duration of a heat wave, its temporary occurrence and its average intensity (maximum intensity is not shown here, but it was also taken into account in the present study and can be seen in Support Information (S13)).

As can be seen in Fig. 8a and b the average intensity of observed heat waves and ERA-40 simulations are very similar in the 71 observatories. We found a high correlation between the average intensity of a heat wave and the results from the observed and the simulated ERA-40 scenarios ($p = 0.9889$). A similarly high correlation was obtained in terms of the maximum intensity of a heat wave ($p = 0.9883$, not shown here).

Regarding to the average duration of heat waves episodes, Fig. 8c and d showed a similar pattern of temporal and spatial distribution and a strong correlation ($p = 0.8976$). For example, both datasets showed a clear signal of heat waves during the years 1982, 1987, 1990, 1994 and 1998, and they both showed no heat wave during the years 1986, 1987, 1996 and 1997.

Similar results are present in Fig. 9 for cold waves. In this case, the correlation obtained between the average duration of the observed cold waves (Fig. 9c) and those simulated for ERA-40 (Fig. 9d) was $p = 0.8593$, which was lower than the p-value obtained for heat waves. The correlations of the intensities between both groups of data were strong ($p = 0.8849$ and $p = 0.792$ for maximum intensity and average

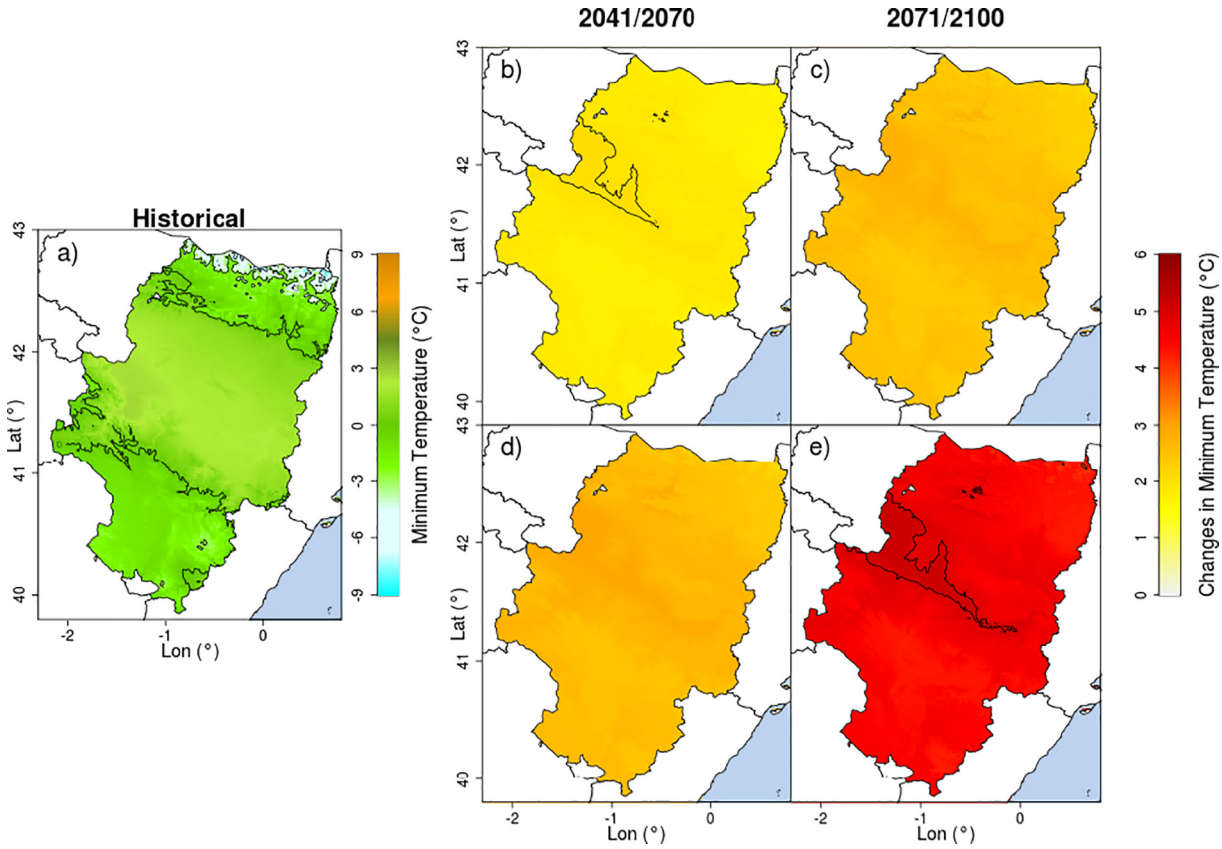

Fig. 6. Geographical representation of the expected changes of minimum temperature in winter for the periods 2041–2070 and 2071–2100 respect to the reference Historical Period (1976–2005). Both emissions scenarios are represented: RCP4.5 (up, figures b and c and RCP8.5 (figures d and e). Panel a represents the Historical absolute temperature for the period 1976–2005.

intensity, respectively), but lower than those obtained for the heat waves. The cold-wave pattern (that is, duration, average intensities and maximum intensities) were very similar in both datasets, marking episodes of cold waves during the same time periods.

3.4. Local future climate scenarios of hot- and cold-waves episodes

Figs. 10 and 11 show the climate scenarios for heat waves in Aragón according to the RCP4.5 and the RCP8.5scenarios, respectively. The figures show the temporal evolution (from historical data to 2100) for three main features of the heat waves: average intensity (first row), maximum intensity (second row) and average duration (third row). The temporal periods analysed were 1976–2005 (historical; first column), 2041–2070 (second column) and 2071–2100 (third column). These periods were chosen as representative of the present, mid-century and end-century periods. Figs. 12 and 13 show the same information but for cold waves.

In addition, in Support information heat and cold waves are represented as increments in temperature for heat waves (S15 and S16 for RCP4.5 and the RCP8.5 scenarios, respectively) and for cold waves (S17 and S18 for RCP4.5 and the RCP8.5 scenarios, respectively).

During the coming decades, an increase in the duration of heat waves is expected. According to the RPC4.5, sharp increases in the average intensity of heat waves are not expected with respect to the values corresponding to the historical period (an average of approximately 0.8 °C). This means that a mean intensity of 37.6 °C is expected at mid-century and 37.8 °C at the end of the century. According to the RCP8.5, the average intensity would increase an average of approximately 1–1.2 °C during the middle of the century (reaching 38 °C) and close to 2 °C at the end of the century (reaching 38.8 °C).

In the case of the maximum intensity of the heat waves, the average increases with respect to the expected historical period were somewhat more pronounced than those expected for the average intensity, especially in the case of RCP8.5. According to RCP4.5, average increases of 1.4 °C and 1.7 °C (reaching 39.3 °C and 39.6 °C) are expected in the maximum intensity during the middle and end of the century, respectively. In the case of RCP8.5, those average increases are expected to rise to 2 °C and 3.6 °C (reaching 39.9 °C and 41.5 °C) during the middle and end of the century, respectively.

Note that for the average (maximum) intensity, there was a difference between observatories, such that in some of them the intensity could reach 46 °C (48 °C), while in other parts of the region it would not exceed 32 °C (34 °C) according to the RCP8.5.

The average and maximum intensity of the heat waves will be especially intense in the Ebro Valley in the middle of the century, and it will spread throughout the entire territory toward the end of the century, except for the Pyrenean area further north.

According to RCP4.5, an average increase in the number of days that lasts a heat waves (duration) compared to the historical period of about 2 days is expected during mid-century (2041–2070), with a maximum increase of 11 days, which would mean that the average duration of heat waves it would be around 7 days, with durations that vary between 4 and 18 days according to the station. At the end of the century, very sharp variations are not expected with respect to half a century. Results from the RCP8.5 predict that the average duration of heat waves will increase by 3 days in the middle of the century and by 7 days at the end of the century, which means that heat waves would have an average duration of between 8 and 12 days, respectively. Note that according to the RCP8.5 scenario, some observatories are expected to experience sharp increases during the historic period of up to 16 and 44 days for the period 2041–2070 and 2071–2100 respectively, so there would be

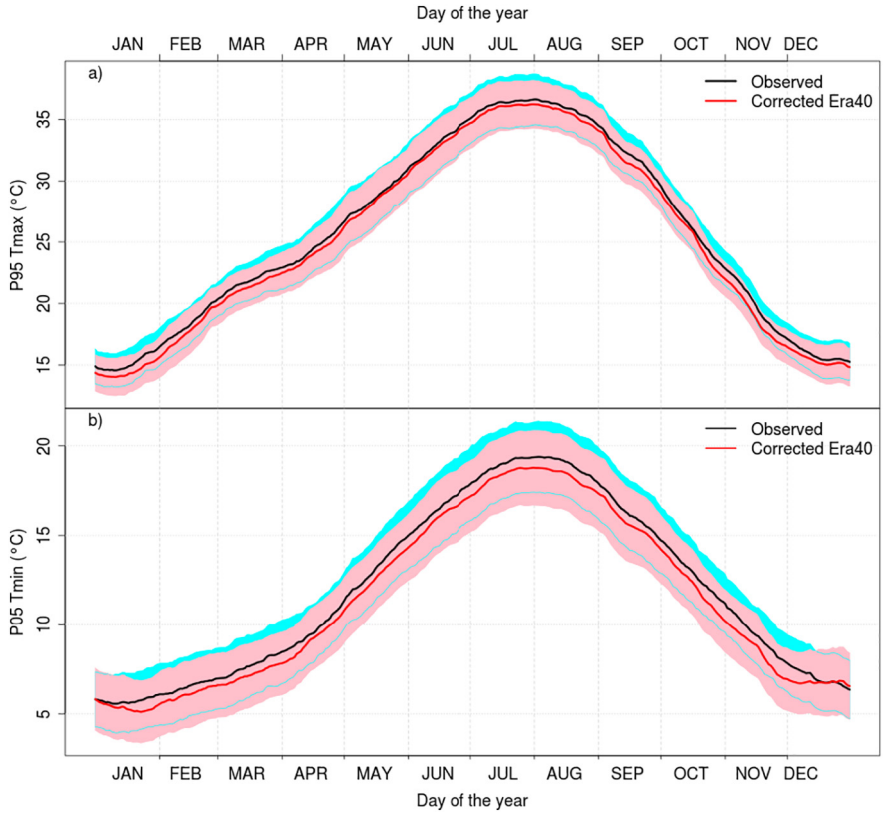

Fig. 7. Results of the verification process obtained for a) the 95th percentile of maximum temperature and b) the 05th percentile of minimum temperature comparing the results obtained by downscaling the reanalysis ERA-40 (black) along the observations (red) for a common (1980–2000). The solid lines represent the median and the shaded areas the 10-90th percentile of the values. (For interpretation of the references to colour in this figure legend, the reader is referred to the web version of this article.)

observatories where the consecutive days that exceed the "hot-day" threshold would be 23 and 52 days, for the same periods.

In this case, the Pyrenees to the north and the Iberian to the south of Aragón are the zones that would suffer longer heat waves; although, as we have seen, they would be the least affected by the intensity of the expected heat waves.

On the other hand, the episodes of cold waves would not change either the average or maximum intensity values (see Figs. 12 and S17 for the RCP4.5 scenario and Figs. 13 and S18 for the RCP8.5). The variations of average intensity with respect to the historic period are, on average, ±0.5 °C, and in some observatories they could reach ±1.0–1.°5 °C, independent of the RCP.

A similar pattern is expected for the maximum intensity of the cold waves (Figs. 12b and 13b), with few variations with respect to the historical period and similar patterns to those expected for the mean intensity. The north and the south of the territory are the regions that are expected to be the most affected by the intensity of the cold waves.

During the upcoming decades, an increase in the duration of cold-wave episodes is not expected. Both RCP4.5 (Figs. 12h and S17h) and RCP8.5 (Figs. 13h and S18h) predict that by the middle of the century, the average duration of cold waves will remain around 4 to 5 days, with episodes of 3 to 7 days in the middle of the century and 11 days at the end of the century. This would mean that the average duration of cold waves would not be modified with respect to the historical period, unlike what is expected in the case of heat waves, and in the most severe cases, the increase would be about three days at the end of the century. No differences of this pattern are expected in the territory.

4. Discussion

In the present study, heat- and cold-wave scenarios for the 21st century were obtained for the first time in the region of Aragón, Spain, using new ESMs belonging to the CMIP5. In addition, the climate scenarios for temperatures in this region were reconstructed with the new ESMs in order to assess differences with respect to the models used prior to CMIP5. These results offer one of the best snapshots of future climate change based on currently available data on the risks that extreme temperatures can cause in the Aragón region, both spatially and temporally.

4.1. Considerations of the temperature scenarios

The new models used in the present study to obtain climate scenarios in Aragón are ESMs, not climate models. The improvements incorporated in the ESMs allow for greater precision in the simulation of climate variables, which provides evidence that the results of the validation are good.

The validation of the ESMs was good for both maximum and minimum temperatures. The differences between seasonal means were practically negligible (below a few tenths of a degree in temperature), and the differences between seasonal standard deviations were almost always below the reference values for every ESM (the standard deviation of the downscaled reanalysis data).

The validation results obtained in the present study show lower error rates than those obtained by the scenarios described in the fourth IPCC report and presented in previous studies (Ribalaygua et al., 2013a). In that case, the error was 1 °C, and even in some models (for example, the CNCM3 model in the summer), it was around 1.5 °C; in contrast, the results presented here did not reach such high values. Likewise, the values of the standard deviation are lower than those obtained in the previous study (5–10% in the present study vs 15–20% in a previous study (Ribalaygua et al., 2013a).

Another key point that justifies the generation of new climate scenarios for Aragón is the current designation of climate scenarios

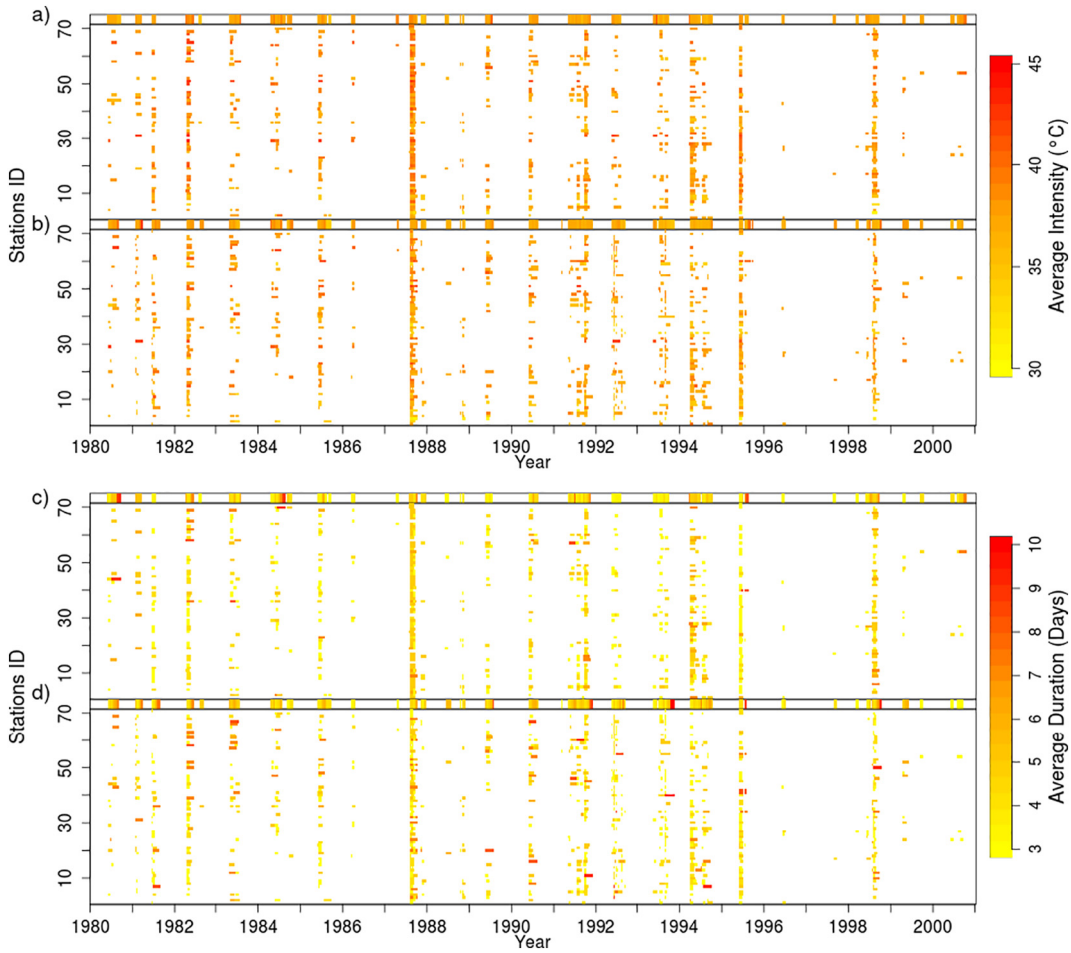

Fig. 8. Results of the verification process for heat waves obtained comparing the simulated heat waves for the reanalysis Era40 along the observed heat waves for a common period (1980–2000). a) Average intensity of the heat waves registered in the 71 stations used in the study against b) the average intensity obtained by downscaling of the reanalysis ERA-40 in these stations for the period 1980–2000. The colour of each pixel shows the average intensity that corresponds to each heat wave (°C), each column represents one year of the considered period and each row one station The upper row shows the mean of the average intensity from the whole observatories. Down, c) and d) same as a) and b) but for the duration of the heat waves. The colour of each pixel shows the duration corresponding to each heat wave (number of days).

provided by IPCC experts—that is, RCPs. Therefore, obtaining local climate scenarios that are based on the most current information is a priority.

The results obtained in the present study, both in the validation process and in the verification process, allow for the maximum and minimum temperature scenarios to be possibly used in subsequent studies of extreme events and bioclimatic variables. Future climate scenarios (maximum and minimum temperatures) show an evolution toward warmer climates throughout the Aragón region. These results agree with those obtained from the CMIP5 models by the IPCC (IPCC, 2013) and by the AEMET (www.Aemet.es). Previous data collected by other authors and assembled by the IPCC (IPCC, 2013) expect that the greatest temperature increases will occur during the summer months. The results of the present study showed that increases in temperature (both maximum and minimum) were less marked than those published by the AEMET (for example, our results showed changes of 3.6 and 7 °C at the end of the century, while the AEMET results predicted changes of 4.1 and 8.2 °C under RPC4.5 and RCP8.5 scenarios, respectively), although both our results and the AEMET results suggest that the summer months will be the time during which the most abrupt changes in temperature will be observed, while the winter months will be the time during which the least abrupt changes will be observed.

Results presented by the IPCC came from the ESMs, so they do not have the added value of applying downscaling techniques to obtain results at a local scale. On the other hand, one of the advantages of working with climate-change scenarios is to have the widest range of future projections (using the greatest possible number of climate scenarios and downscaling methodologies). Therefore, the scenarios generated by the AEMET are complementary to those presented here because different statistical downscaling methodologies, as well as different ESMs, have been applied.

Similar processes were carried out in the generation of climate scenarios for Spain published by the AEMET (www.Aemet.es) and in the EsTcena project (Brands et al., 2013; Brands et al., 2011a). Results that were generated by different centres were presented on the basis of different methodologies, including the one used in the present study.

We compared the new scenarios that were based on the models of the fifth report of the IPCC with those published by Ribalaygua (Ribalaygua et al., 2013a), which correspond to the fourth report of the IPCC. We observed that the most recent scenarios trended toward higher temperatures than what was expected in (Ribalaygua et al., 2013a), with greater increases occurring during summer months compared to winter months. For example, for the summer months, the new results expect that for the period 2071–2100, the maximum temperature in the most extreme case will reach up to 7 °C, while those presented by Ribalaygua (Ribalaygua et al., 2013a) for the same period were estimated to reach 5 °C. However, both studies agreed that the northwest and southwest regions would be the most affected by these variations.

In both cases, maximum and minimum temperatures, in view of the validation results and in the face of the same reanalysis of ERA-40, it is justified that the scenarios generated for the fifth IPCC report are more

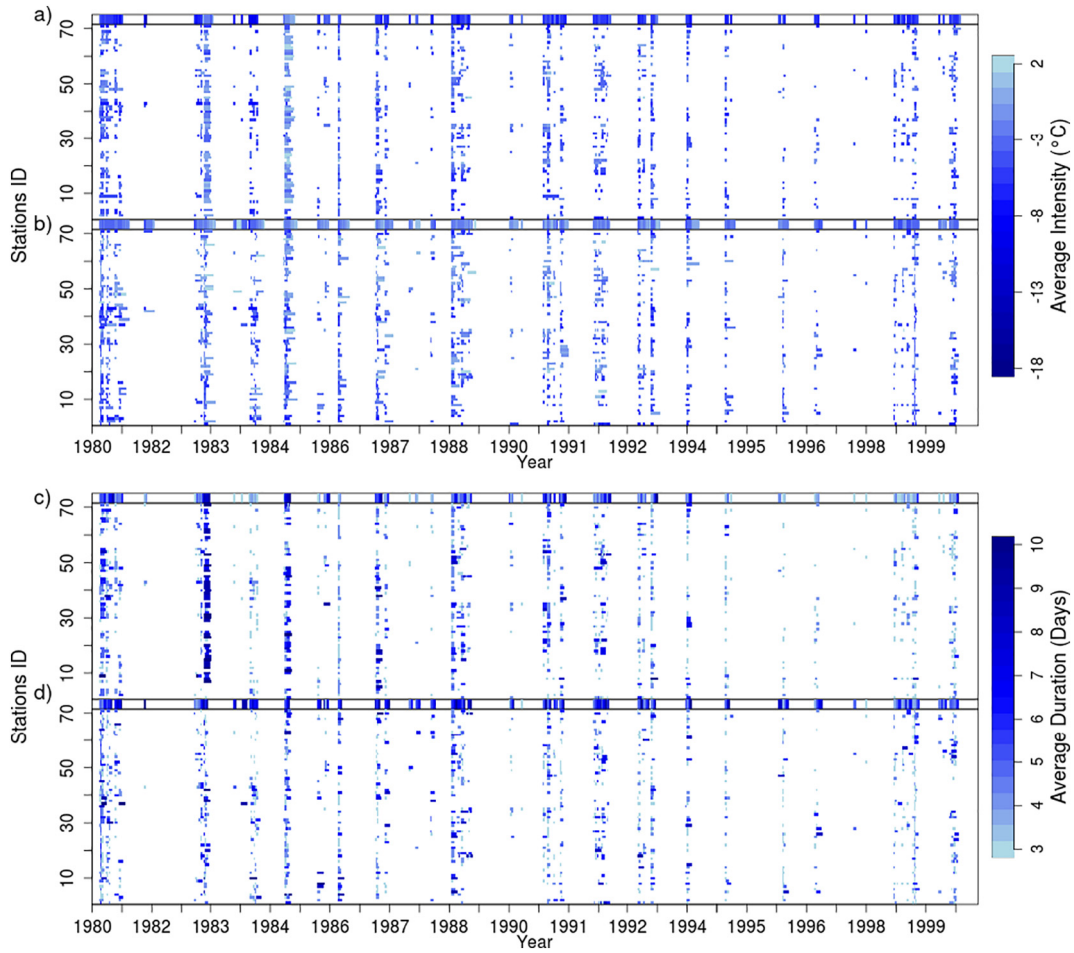

Fig. 9. Results of the verification process for cold waves obtained comparing the simulated cold waves for the reanalysis Era40 along the observed cold waves for a common period (1980–2000). a) Average intensity of the heat waves registered in the 71 stations used in the study against b) the average intensity obtained by downscaling of the reanalysis ERA-40 in these stations for the period 1980–2000. The colour of each pixel shows the average intensity that corresponds to each cold wave (°C), each column represents one year of the considered period and each row one station. The upper row shows the mean of the average intensity from the whole observatories. Down, c) and d) same as a) and b) but for the duration of the cold wave. The colour of each pixel shows the duration corresponding to each cold wave (number of days).

precise than those that already exist for the Aragón region. Having a range of climate-scenario projections in Aragón facilitates the evaluation of extreme phenomena of interest, such as heat and cold waves, which have strong impacts in the region.

4.2. Consideration about the simulation of heat and cold waves

Our results allow for the simulation of episodes of heat and cold waves throughout the 21st century and prove the validity of the simulations, as is evident by the good verification and validation results. As the methodology is able to adequately simulate the 95th percentile of maximum temperatures and the 5th percentile of minimum temperatures, it is assumed that the thresholds that define the heat or cold waves are being simulated in an appropriate way.

The downscaling methodology that was used was able to successfully simulate heat and cold waves reported by the observations, as shown by the results of the verification process. The ESMs were also successful at simulating the maximum and minimum temperatures during the validation process. However, in the verification process of heat and cold waves, were identified some limitations that must be considered in the simulation of future scenarios:

1) There were gaps in the observed series. The lack of data in the observed series reduced the length of observed data compared to the reanalysed ERA-40 series (that is, the full series without gaps) for the same period of time. Therefore, the number of days included in the 95th percentile (or 5th percentile) of the maximum (or minimum) temperature was greater in the ERA-40 series compared to the observed series.
2) In general, downscaling techniques tend to soften the simulated temperature series with respect to the observed values, which implies that certain episodes of hot or cold waves are softened in their duration or intensity compared to the observed data and would therefore be classified differently. In the present study, it was appreciated that the average and maximum intensities of the observed cold and heat waves was greater than that simulated for the ERA-40 reanalysis.

In summary, the uncertainties associated with both verification and validation must be considered when interpreting future scenarios.

The results of this study about heat and cold waves are consistent with the results published by both the IPCC (IPCC, 2013) and the AEMET (www.Aemet.es). All models agree that the number of days considered as “hot days” will increase in the coming decades and, therefore, the heat waves will be more frequent. On the other hand, the number of “cold days” will be maintained and, in some cases, will even decrease so, on the contrary of what is expected for heat waves, the frequency of cold waves will remain at its current frequency.

What is stated in the previous paragraph is plausible with one of the main theoretical conclusions about the trend of temperatures reported by the IPCC (IPCC, 2013), which is based on the change in the probability

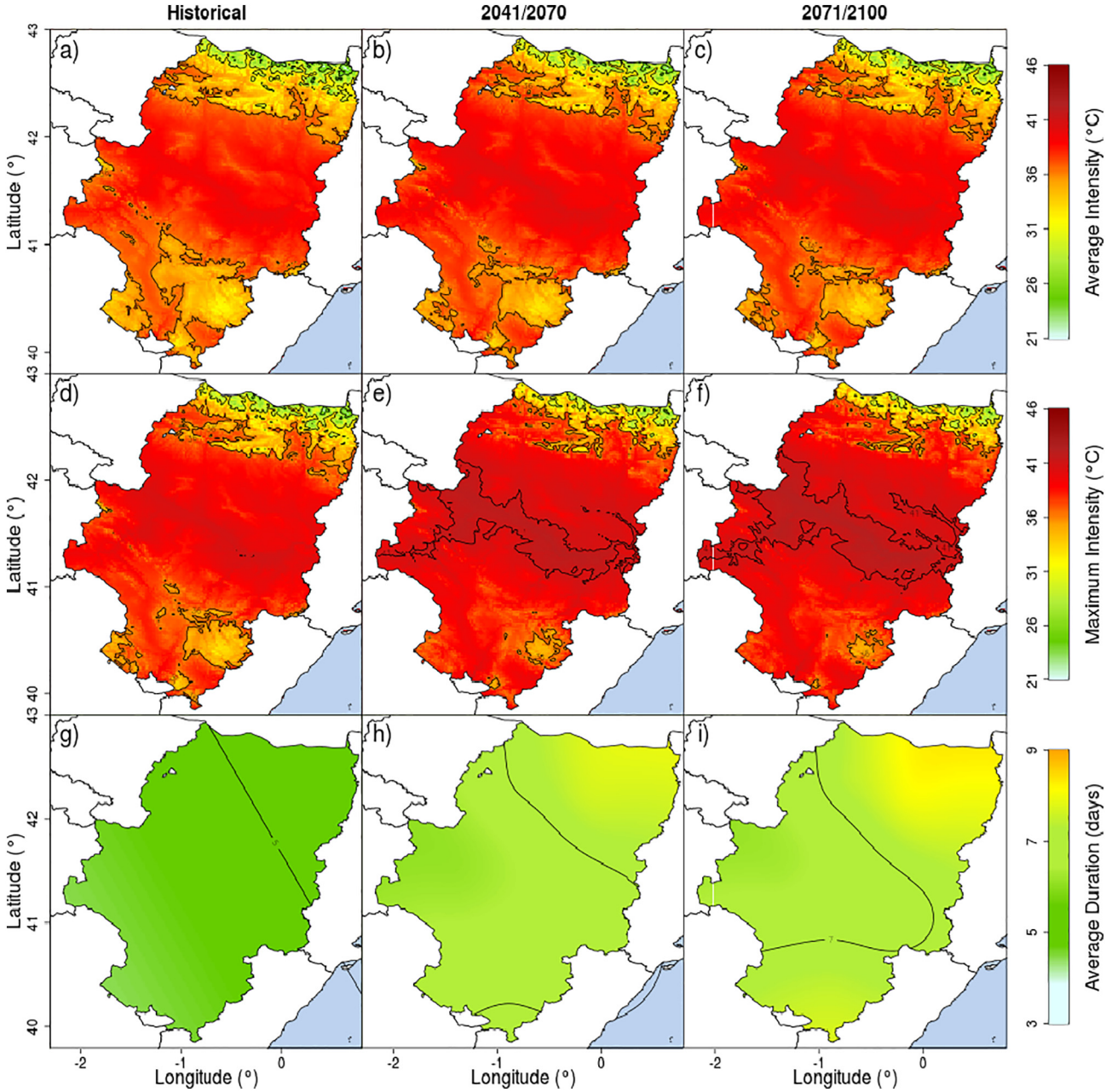

Fig. 10. Geographical representation of the expected evolution of the heat waves for Aragon in the periods 2041–2070 and 2071–2100 compared to the reference Historical Period (1971–2000) in terms of absolute values according to the RCP4.5. The rows show the three parameters analysed in the study (average intensity, maximum intensity and duration) and the columns the three temporal periods (Historical, 2041–2070 and 2071–2100). The maps are generated by interpolating the available stations over the entire territory.

of reaching certain temperature values. The probability distribution of temperatures can either move to warmer climates without undergoing changes, can be extended or a combination of both. The third situation is the one that has been observed in recent decades in different studies (Hansen et al., 2012) IPCC, 2001) and is the most plausible situation in the context of the observed data. The new distribution of temperatures implies a less pronounced change in the colder temperatures of the series, a much more marked change in the warmer temperatures and a greater number of warm extreme events. These conclusions support the results anticipated for the coming decades—i.e, the maintenance of cold waves (in number and intensity) and an increase of heat waves.

Regarding the territory of Aragón, the scenarios obtained in the present study indicate that the Ebro valley, the most populated area in the region, will observe the highest maximum temperatures, especially at the end of the century and in the summer (around 40 °C), as well as the greatest intensity of heat waves. This can have important impacts on the health of the population. The health risks associated with heat waves are well known, both in terms of mortality (Robine et al., 2008; Roldan et al., 2016) and mobility (Lin et al., 2009; Steul et al., 2018), as well as health costs (Roldan et al., 2015). Moreover, these extreme events will cause significant socio-economic impacts because a large part of Aragonese industry and farming is situated in this zone (Olesen et al., 2011).

In addition, the Pyrenees will suffer the longest heat waves (but not the most intense ones), especially at the end of the century, and the greatest increases in maximum temperatures with respect to the values recorded during the historical period (1971–2000). The northern zone is where the greatest intensity of cold waves will also be located, although their durations will not change much compared to the current

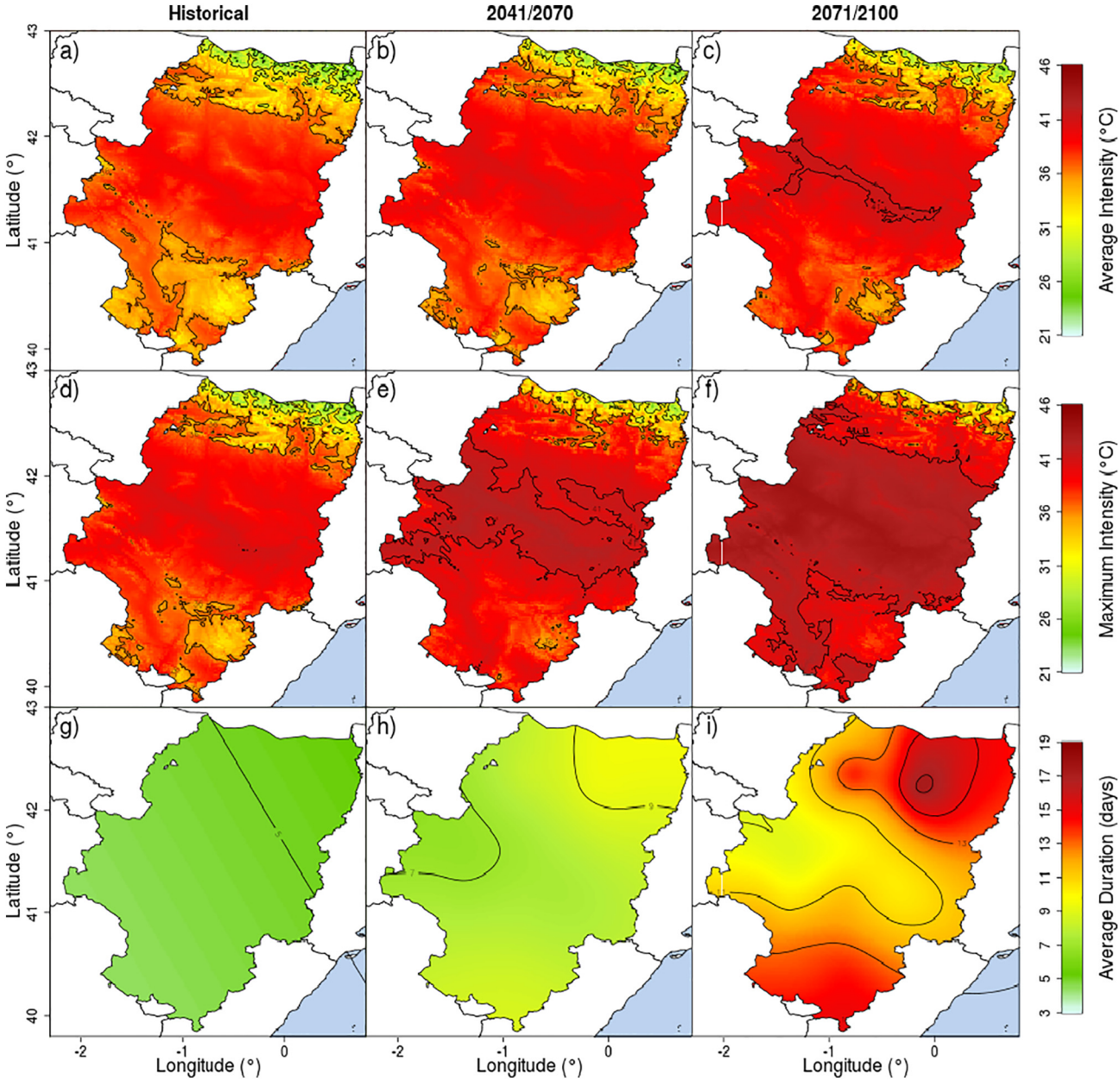

Fig. 11. Geographical representation of the expected evolution of the heat waves for Aragon in the periods 2041–2070 and 2071–2100 compared to the reference Historical Period (1971–2000) in terms of absolute values according to the RCP8.5. The rows show the three parameters analysed in the study (average intensity, maximum intensity and duration) and the columns the three temporal periods (Historical, 2041–2070 and 2071–2100). The maps are generated by interpolating the available stations over the entire territory.

cold waves. Therefore, it is the heat that is the most outstanding future risk for these ecosystems.

Changes in temperature (even if they are moderate) and warming are potential risks to this rich ecological area, which is characterised by a diversity of species and a wealth of native plants and animals, giving rise to national parks such as Ordesa and Monte Perdido (high mountains). Therefore, these areas are particularly vulnerable to any changes in climate that could lead to radical alterations in habitats or cause losses in their rich biodiversity, as has been previously described (Kulakowski et al., 2017).

Furthermore, the Pyrenees area decides the amount of water available for urban and agricultural use, with a direct effect on hydrology and agriculture in the Ebro Valley. Changes in temperature and snow accumulation could seriously threaten the sustainability and the equilibrium between available resources and water demand. On the other hand, abrupt temperature changes can lead to accelerated thawing that could cause flooding in populated areas near the river, a risk that has been well evaluated in the literature (Gobiet et al., 2014; Guerreiro et al., 2018) and that will demand new and innovative adaptation strategies (De Martino et al., 2012).

Finally, the disappearance of snow due to a rise in temperature in the area could lead to a negative impact on the winter tourism industry and the Pyrenean ski resorts, which are currently an important part of the region's economy, especially in the Pyrenean valleys (Gilaberte-Burdalo et al., 2014; Gilaberte-Burdalo et al., 2017; Lopez-Moreno et al., 2011; Pons et al., 2015).

5. Conclusions

Our study of data from Aragón, Spain, is the first to simulate episodes of heat and cold waves throughout the 21st century in a valid way, based on the good verification and validation results. In addition, we used

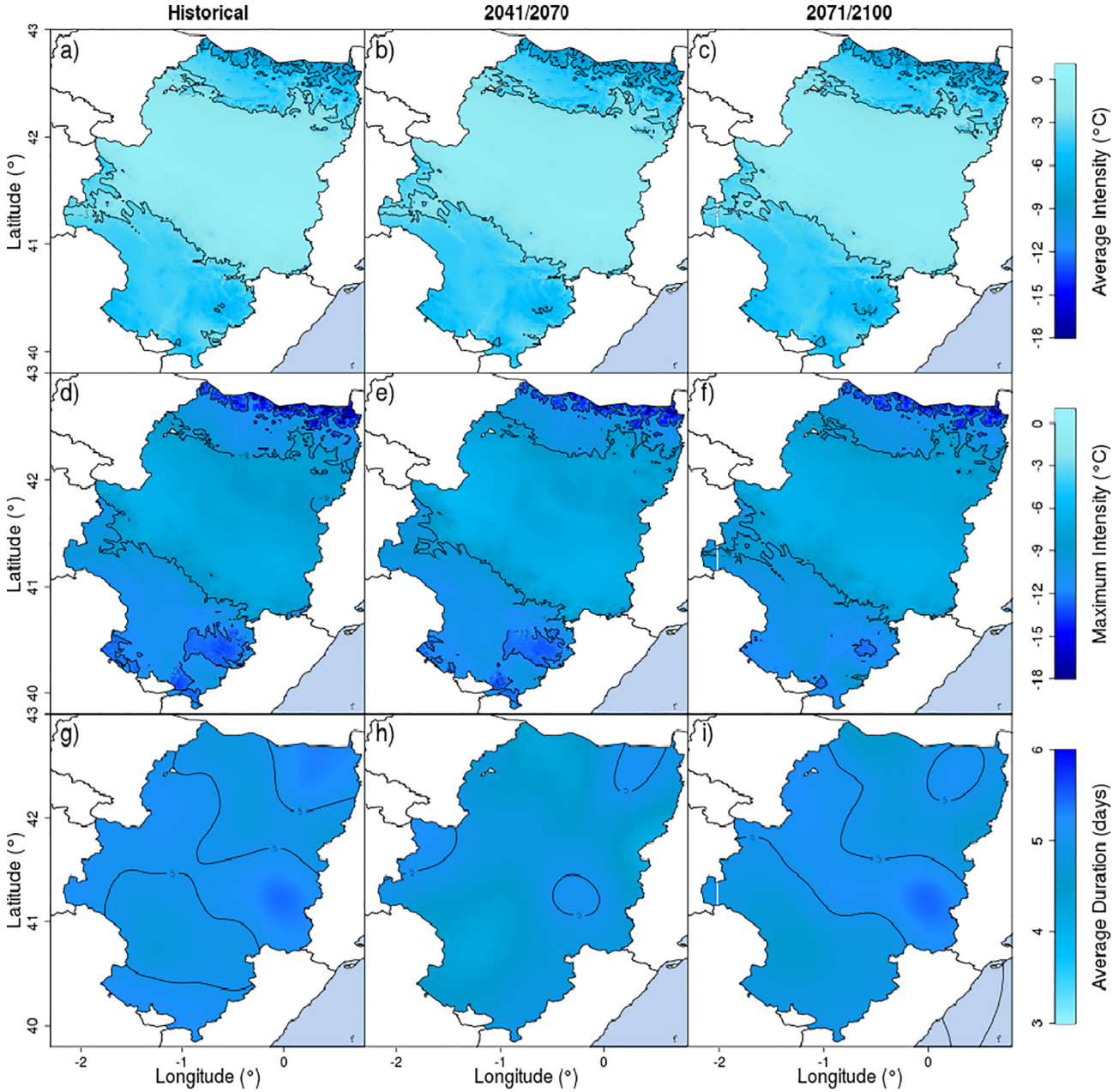

Fig. 12. Geographical representation of the expected evolution of the cold waves for Aragon in the periods 2041–2070 and 2071–2100 compared to the reference Historical Period (1971–2000) in terms of absolute values according to the RCP4.5. The rows show the three parameters analysed in the study (average intensity, maximum intensity and duration) and the columns the three temporal periods (Historical, 2041–2070 and 20,712,100). The maps are generated interpolating the available observatories over the entire territory.

climate models to obtain more precise climate scenarios for the temperatures in this territory compared to previously available scenarios.

The use of ESMs from the fifth report of the IPCC and a methodology of downscaling has proven to be effective, allowing us to obtain greater precision in the simulation of the climate variables in this territory and to predict a realistic picture of the risks that extreme temperatures can cause in the Aragón region, both spatially and temporally. The climate scenarios predict higher maximum temperatures compared to previous scenarios. The greatest increases will occur during summer at the end of the century, reaching values of up to 7 °C in the most unfavourable scenario.

Climate heat- and cold-wave scenarios showed that heat waves will be longer and more intense in upcoming decades. However, intensity and duration of cold waves will not change much compared to the current cold waves. The temperatures and heat-wave intensities will be especially high in the Ebro Valley, the most populated area. However, the Pyrenees will suffer the longest heat waves, especially at the end of the century, and the greatest increases in maximum temperatures.

The present study provides useful information coming from the downscaling for the first time in Aragón of models from IPCC5 to support decision-making and in the development of specific measures to prevent socio-economic, environmental and human health impacts due climate change in Aragón, a territory that can be a good indicator of the impacts of climate change in southern Europe.

Appendix A. Supplementary data

Supplementary data to this article can be found online at https://doi.org/10.1016/j.scitotenv.2018.09.352.

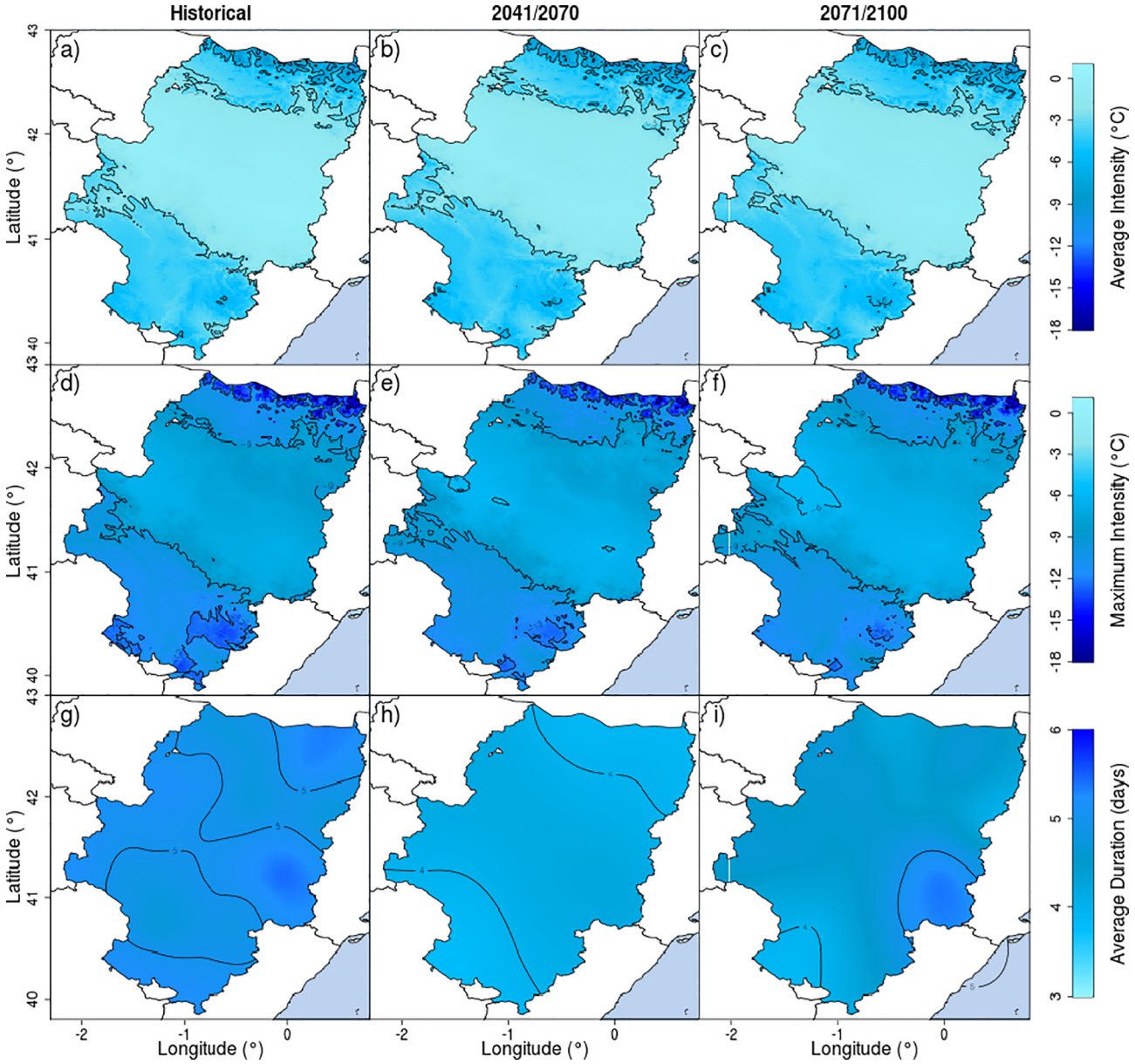

Fig. 13. Geographical representation of the expected evolution of the cold waves for Aragon in the periods 2041–2070 and 2071–2100 compared to the reference Historical Period (1971–2000) in terms of absolute values according to the RCP8.5. The rows show the three parameters analysed in the study (average intensity, maximum intensity and duration) and the columns the three temporal periods (Historical, 2041–2070 and 20,712,100). The maps are generated interpolating the available observatories over the entire territory.

References

Anderson, B.G., Bell, M.L., 2009. Weather-related mortality how heat, cold, and heat waves affect mortality in the United States. Epidemiology 20, 205–213.

Asong, Z.E., Khaliq, M.N., Wheater, H.S., 2016. Projected changes in precipitation and temperature over the Canadian prairie provinces using the generalized linear model statistical downscaling approach. J. Hydrol. 539, 429–446.

Barrera-Escoda, A., Goncalves, M., Guerreiro, D., Cunillera, J., Baldasano, J.M., 2014. Projections of temperature and precipitation extremes in the North Western Mediterranean Basin by dynamical downscaling of climate scenarios at high resolution (1971–2050). Clim. Chang. 122, 567–582.

Benestad, R.E., Hanssen-Bauer, I., Forland, E.J., 2007. An evaluation of statistical models for downscaling precipitation and their ability to capture long-term trends. Int. J. Climatol. 27.

Bentsen, M., Bethke, I., Debernard, J.B., Iversen, T., Kirkevag, A., Seland, O., et al., 2013. The Norwegian Earth System Model, NorESM1-M - part 1: description and basic evaluation of the physical climate. Geosci. Model Dev. 6, 687–720.

Brands, S., Herrera, S., San-Martin, D., Gutierrez, J.M., 2011a. Validation of the ENSEMBLES global climate models over southwestern Europe using probability density functions, from a downscaling perspective. Clim. Res. 48, 145–161.

Brands, S., Taboada, J.J., Cofino, A.S., Sauter, T., Schneider, C., 2011b. Statistical downscaling of daily temperatures in the NW Iberian Peninsula from global climate models: validation and future scenarios. Clim. Res. 48.

Brands, S., Herrera, S., Fernandez, J., Gutierrez, J.M., 2013. How well do CMIP5 Earth System Models simulate present climate conditions in Europe and Africa? Clim. Dyn. 41, 803–817.

Buerger, C.M., Kolditz, O., Fowler, H.J., Blenkinsop, S., 2007. Future climate scenarios and rainfall-runoff modelling in the Upper Gallego catchment (Spain). Environ. Pollut. 148.

Carvalho, D., Rocha, A., Gomez-Gesteira, M., Santos, C.S., 2017. Potential impacts of climate change on European wind energy resource under the CMIP5 future climate projections. Renew. Energy 101, 29–40.

Chen, K., Bi, J., Chen, J., Chen, X., Huang, L., Zhou, L., 2015. Influence of heat wave definitions to the added effect of heat waves on daily mortality in Nanjing, China. Sci. Total Environ. 506-507, 18–25. https://doi.org/10.1016/j.scitotenv.2014.10.092 PMID: 25460935.

Chen, Y.D., Li, J.F., Zhang, Q., 2016. Changes in site-scale temperature extremes over China during 2071–2100 in CMIP5 simulations. J. Geophys. Res.-Atmos. 121, 2732–2749.

Chylek, P., Li, J., Dubey, M.K., Wang, M., Lesins, G., 2011. Observed and model simulated 20th century Arctic temperature variability: Canadian Earth System Model CanESM2. Atmos. Chem. Phys. Discuss. 11, 22893–22907. https://doi.org/10.5194/acpd-11-22893-2011.

Collins, W.J., Bellouin, N., Doutriaux-Boucher, M., Gedney, N., Hinton, T., Jones, C.D., Liddicoat, S., Martin, G., O'Connor, F., Rae, J., Senior, C., Totterdell, I., Woodward, S., Reichler, T., Kim, J., Halloran, P., 2008. Evaluation of the HadGEM2 model. Hadley Centre Technical Note HCTN. vol 74. Met Office Hadley Centre, Exeter, UK.

Cook, J., Nuccitelli, D., Green, S.A., Richardson, M., Winkler, B., Painting, R., Way, R., Jacobs, P., Skuce, A., 2013. Quantifying the consensus on anthropogenic global warming in the scientific literature. Environ. Res. Lett. 8, 024024. https://doi.org/10.1088/1748-9326/8/2/024024.

De Martino, G., De Paola, F., Fontana, N., Marini, G., Ranucci, A., 2012. Experimental assessment of level pool routing in preliminary design of floodplain storage. Sci. Total Environ. 416, 142–147.

Dosio, A., 2017. Projection of temperature and heat waves for Africa with an ensemble of CORDEX regional climate models. Clim. Dyn. 49, 493–519.

Dunne, J.P., John, J.G., Adcroft, A.J., Griffies, S.M., Hallberg, R.W., Shevliakova, E., et al., 2012. GFDL's ESM2 global coupled climate-carbon Earth System Models. Part I: physical formulation and baseline simulation characteristics. J. Clim. 25, 6646–6665.

Estrella, N., Menzel, A., 2013. Recent and future climate extremes arising from changes to the bivariate distribution of temperature and precipitation in Bavaria, Germany. Int. J. Climatol. 33, 1687–1695.

Fernandez-Montes, S., Rodrigo, F.S., 2012. Trends in seasonal indices of daily temperature extremes in the Iberian Peninsula, 1929–2005. Int. J. Climatol. 32, 2320–2332.

Field, C.B., Barros, V., Stocker, T.F., Qin, D., Dokken, D.J., Ebi, K.L., Mastrandrea, M.D., Mach, K.J., Plattner, G.K., Allen, S.K., Tignor, M., Midgley, P.M., IPCC, 2012. Managing the Risks of Extreme Events and Disasters to Advance Climate Change Adaptation. Cambridge University Press, Cambridge, United Kingdom and New York, NY, USA, p. 582.

Fischer, E.M., Schar, C., 2010. Consistent geographical patterns of changes in high-impact European heatwaves. Nat. Geosci. 3, 398–403.

Fonseca, D., Carvalho, M.J., Marta-Almeida, M., Melo-Goncalves, P., Rocha, A., 2016. Recent trends of extreme temperature indices for the Iberian Peninsula. Phys. Chem. Earth 94, 66–76.

Frias, M.D., Fernandez, J., Saenz, J., Rodriguez-Puebla, C., 2005. Operational predictability of monthly average maximum temperature over the Iberian Peninsula using DEMETER simulations and downscaling. Tellus Ser. A Dyn. Meteorol. Oceanogr. 57.

Frias, M.D., Herrera, S., Cofino, A.S., Gutierrez, J.M., 2010. Assessing the skill of precipitation and temperature seasonal forecasts in Spain: windows of opportunity related to ENSO events. J. Clim. 23.

Garcia-Herrera, R., Diaz, J., Trigo, R.M., Hernandez, E., 2005. Extreme summer temperatures in Iberia: health impacts and associated synoptic conditions. Ann. Geophys. 23, 239–251.

Gilaberte-Burdalo, M., Lopez-Martin, F., Pino-Otin, M.R., Lopez-Moreno, J.I., 2014. Impacts of climate change on ski industry. Environ. Sci. Pol. 44, 51–61.

Gilaberte-Burdalo, M., Lopez-Moren, J.I., Moran-Tejeda, E., Jerez, S., Alonso-Gonzalez, E., Lopez-Martin, F., et al., 2017. Assessment of ski condition reliability in the Spanish and Andorran Pyrenees for the second half of the 20th century. Appl. Geogr. 79, 127–142.

Giorgi, F., Gutowski, W.J., 2015. Regional dynamical downscaling and the CORDEX initiative. Annu. Rev. Environ. Resour. 40, 467–490.

Giorgi, F., Mearns, L.O., 1991. Approaches to the simulation of regional climate change - a review. Rev. Geophys. 29, 191–216.

Giorgi, F., Jones, C., Asrar, G.R., 2009. Addressing climate information needs at the regional level: the CORDEX framework. WMO Bull. 58 (3), 175–183.

Gobiet, A., Kotlarski, S., Beniston, M., Heinrich, G., Rajczak, J., Stoffel, M., 2014. 21st century climate change in the European Alps-a review. Sci. Total Environ. 493, 1138–1151.

Goncalves, M., Barrera-Escoda, A., Guerreiro, D., Baldasano, J.M., Cunillera, J., 2014. Seasonal to yearly assessment of temperature and precipitation trends in the North Western Mediterranean Basin by dynamical downscaling of climate scenarios at high resolution (1971–92050). Clim. Chang. 122, 243–256.

Gross, M.H., Alexander, L.V., Macadam, I., Green, D., Evans, J.P., 2017. The representation of health-relevant heatwave characteristics in a regional climate model ensemble for New South Wales and the Australian Capital Territory, Australia. Int. J. Climatol. 37, 1195–1210.

Guerreiro, S.B., Dawson, R.J., Kilsby, C., Lewis, E., Ford, A., 2018. Future heat-waves, droughts and floods in 571 European cities. Environ. Res. Lett. 13.

Hansen, J., Sato, M., Ruedy, R., 2012. Perception of climate change. Proc. Natl. Acad. Sci. U. S. A. 109, E2415–E2423.

Heavens, N., Ward, D., Natalie, M., 2013. Studying and projecting climate change with earth System Models. Nat. Educ. Knowl. 4 (5), 4.

Hertig, E., Seubert, S., Jacobeit, J., 2010. Temperature extremes in the Mediterranean area: trends in the past and assessments for the future. Nat. Hazards Earth Syst. Sci. 10, 2039–2050.

Hervada-Sala, C., Pawlowsky-Glahn, V., Jarauta-Bragulat, E., 2000. A statistical method to downscale temperature forecasts. A case study in Catalonia. Meteorol. Appl. 7.

Imbert, A., Benestad, R.E., 2005. An improvement of analog model strategy for more reliable local climate change scenarios. Theor. Appl. Climatol. 82, 245–255.

IPCC, 2000. Special Report on Emissions Scenarios. Cambridge University Press, Cambridge, UK 0 521 80493 0.

IPCC, 2001. In: Houghton, J.T., Ding, Y., Griggs, D.J., Noguer, M., van der Linden, P.J., Dai, X., Maskell, K., Johnson, C.A. (Eds.), Climate Change 2001: The Scientific Basis. Contribution of Working Group 1 to the Third Assessment Report of the Intergovernmental Panel on Climate Change. Cambridge University Press, Cambridge, UK, and New York, USA.

IPCC, 2013. In: Stocker, T.F., Qin, D., Plattner, G.-K., Tignor, M., Allen, S.K., Boschung, J., Nauels, A., Xia, Y., Bex, V., Midgley, P.M. (Eds.), Climate Change 2013: The Physical Science Basis. Contribution of Working Group I to the Fifth Assessment Report of the Intergovernmental Panelon Climate Change. Cambridge University Press, Cambridge https://doi.org/10.1017/CBO9781107415324.

Iversen, T., Bentsen, M., Bethke, I., Debernard, J.B., Kirkevag, A., Seland, O., et al., 2013. The Norwegian Earth System Model, NorESM1-M - part 2: climate response and scenario projections. Geosci. Model Dev. 6, 389–415.

Jeong, D.I., Sushama, L., Diro, G.T., Khaliq, M.N., Beltrami, H., Caya, D., 2016. Projected changes to high temperature events for Canada based on a regional climate model ensemble. Clim. Dyn. 46, 3163–3180.

Kattenberg, A., Amer Meteorol SOC, 1996. Climate models: projections of future climate. Seventh Symposium on Global Change Studies.

Kent, S.T., McClure, L.A., Zaitchik, B.F., Smith, T.T., Gohlke, J.M., 2014. Heat waves and health outcomes in Alabama (USA): the importance of heat wave definition. Environ. Health Perspect. 122, 151–158.

Kim, S., Sinclair, V.A., Raisanen, J., Ruuhela, R., 2018. Heat waves in Finland: present and projected summertime extreme temperatures and their associated circulation patterns. Int. J. Climatol. 38, 1393–1408.

Knutti, R., Sedlacek, J., 2013. Robustness and uncertainties in the new CMIP5 climate model projections. Nat. Clim. Chang. 3, 369–373.

Kuglitsch, F.G., Toreti, A., Xoplaki, E., Della-Marta, P.M., Zerefos, C.S., Turkes, M., et al., 2010. Heat wave changes in the eastern Mediterranean since 1960. Geophys. Res. Lett. 37.

Kulakowski, D., Seidl, R., Holeksa, J., Kuuluvainen, T., Nagel, T.A., Panayotov, M., et al., 2017. A walk on the wild side: disturbance dynamics and the conservation and management of European mountain forest ecosystems. For. Ecol. Manag. 388, 120–131.

Lavaysse, C., Vrac, M., Drobinski, P., Lengaigne, M., Vischel, T., 2012. Statistical downscaling of the French Mediterranean climate: assessment for present and projection in an anthropogenic scenario. Nat. Hazards Earth Syst. Sci. 12, 651–670.

Lin, S., Luo, M., Walker, R.J., Liu, X., Hwang, S.A., Chinery, R., 2009. Extreme high temperatures and hospital admissions for respiratory and cardiovascular diseases. Epidemiology 20, 738–746.

López, F., Cabrera, M., Cuadrat, J.M., 2007. Atlas Climático de Aragón. First ed. J. Factory, Spain.

Lopez-Moreno, J.I., Goyette, S., Vicente-Serrano, S.M., Beniston, M., 2011. Effects of climate change on the intensity and frequency of heavy snowfall events in the Pyrenees. Clim. Chang. 105, 489–508.

Marsland, S.J., Haak, H., Jungclaus, J.H., Latif, M., Roske, F., 2003. The Max-Planck-Institute global ocean/sea ice model with orthogonal curvilinear coordinates. Ocean Model 5, 91–127.

Miro, J.J., Estrela, M.J., Caselles, V., Olcina-Cantos, J., 2016. Fine-scale estimations of bioclimatic change in the Valencia region, Spain. Atmos. Res. 180, 150–164.

Moss, R.H., Edmonds, J.A., Hibbard, K.A., Manning, M.R., Rose, S.K., van Vuuren, D.P., et al., 2010. The next generation of scenarios for climate change research and assessment. Nature 463, 747–756.

Nychka, D., Furrer, R., Paige, J., Sain, S., 2015. Fields: tools for spatial data. R package version 9.0. (URL: http://doi.org/10.5065/D6W957CT). www.image.ucar.edu/fields.

Olesen, J.E., Trnka, M., Kersebaum, K.C., Skjelvag, A.O., Seguin, B., Peltonen-Sainio, P., et al., 2011. Impacts and adaptation of European crop production systems to climate change. Eur. J. Agron. 34, 96–112.

Parry, M.L., Canziani OF, Palutikof, J.P., Van der Linden, P.J., Hanson, C.E. (Eds.), 2007. IPCC Impacts, Adaptation and Vulnerability Contribution of Working Group II to the Fourth Assessment Report of the IPCC. Cambridge University Press.

Patz, J.A., Campbell-Lendrum, D., Holloway, T., Foley, J.A., 2005. Impact of regional climate change on human health. Nature 438, 310–317.

Perez, J., Menendez, M., Mendez, F.J., Losada, I.J., 2014. Evaluating the performance of CMIP3 and CMIP5 global climate models over the north-east Atlantic region. Clim. Dyn. 43, 2663–2680.

Planton, S., Deque, M., Chauvin, F., Terray, L., 2008. Expected impacts of climate change on extreme climate events. Compt. Rendus Geosci. 340, 564–574.

Pons, M., Lopez-Moreno, J.I., Rosas-Casals, M., Jover, E., 2015. The vulnerability of Pyrenean ski resorts to climate-induced changes in the snowpack. Clim. Chang. 131, 591–605.

R Development Core Team, 2010. R: A Language and Environment for Statistical Computing. R Foundation for Statistical Computing, Vienna, Austria 3-900051-07-0 http://www.R-project.org, Accessed date: 6 July 2011.

Raddatz, T.J., Reick, C.H., Knorr, W., Kattge, J., Roeckner, E., Schnur, R., et al., 2007. Will the tropical land biosphere dominate the climate-carbon cycle feedback during the twenty-first century? Clim. Dyn. 29, 565–574.

Ribalaygua, J., Rosa Pino, M., Portoles, J., Roldan, E., Gaitan, E., Chinarro, D., et al., 2013a. Climate change scenarios for temperature and precipitation in Aragon (Spain). Sci. Total Environ. 463, 1015–1030.

Ribalaygua, J., Torres, L., Portoles, J., Monjo, R., Gaitan, E., Pino, M.R., 2013b. Description and validation of a two-step analogue/regression downscaling method. Theor. Appl. Climatol. 114, 253–269.

Robine, J.M., SLK, Cheung, Le Roy, S., Van Oyen, H., Griffiths, C., Michel, J.P., et al., 2008. Death toll exceeded 70,000 in Europe during the summer of 2003. C. R. Biol. 331, 171-U5.

Roldan, E., Gomez, M., Pino, M.R., Diaz, J., 2015. The impact of extremely high temperatures on mortality and mortality cost. Int. J. Environ. Health Res. 25, 277–287.

Roldan, E., Gomez, M., Pino, M.R., Portoles, J., Linares, C., Diaz, J., 2016. The effect of climate-change-related heat waves on mortality in Spain: uncertainties in health on a local scale. Stoch. Env. Res. Risk A. 30, 831–839.

Russo, S., Sillmann, J., Sterl, A., 2017. Humid heat waves at different warming levels. Sci. Rep. 7.

Saeed, F., Almazroui, M., Islam, N., Khan, M.S., 2017. Intensification of future heat waves in Pakistan: a study using CORDEX regional climate models ensemble. Nat. Hazards 87, 1635–1647.

Schoetter, R., Cattiaux, J., Douville, H., 2015. Changes of western European heat wave characteristics projected by the CMIP5 ensemble. Clim. Dyn. 45, 1601–1616.

Semenov, M.A., Stratonovitch, P., 2010. Use of multi-model ensembles from global climate models for assessment of climate change impacts. Clim. Res. 41, 1–14.

Seubert, S., Fernandez-Montes, S., Philipp, A., Hertig, E., Jacobeit, J., Vogt, G., et al., 2014. Mediterranean climate extremes in synoptic downscaling assessments. Theor. Appl. Climatol. 117, 257–275.

Sillmann, J., Donat, M.G., Fyfe, J.C., Zwiers, F.W., 2014. Observed and simulated temperature extremes during the recent warming hiatus. Environ. Res. Lett. 9.

Smith, T.T., Zaitchik, B.F., Gohlke, J.M., 2013. Heat waves in the United States: definitions, patterns and trends. Clim. Chang. 118, 811–825.

Soares, P.M.M., Cardoso, R.M., Miranda, P.M.A., de Medeiros, J., Belo-Pereira, M., Espirito-Santo, F., 2012. WRF high resolution dynamical downscaling of ERA-interim for Portugal. Clim. Dyn. 39, 2497–2522.

Stegehuis, A.I., Vautard, R., Ciais, P., Teuling, A.J., Miralles, D.G., Wild, M., 2015. An observation-constrained multi-physics WRF ensemble for simulating European mega heat waves. Geosci. Model Dev. 8, 2285–2298.

Steul, K.S., Latasch, L., Jung, H.G., Heudorf, U., 2018. Health impact of the heatwave of 2015: hospital admissions in Frankfurt/Main, Germany. Gesundheitswesen 80, 353–359.

Suparta, W., Yatim, A.N.M., 2017. An analysis of heat wave trends using heat index in East Malaysia. In: Suparta, W., Ismail, M., Abdullah, M. (Eds.), 2017 International Conference on Space Science and Communication. 852.

Taylor, K.E., Stouffer, R.J., Meehl, G.A., 2012. An overview of CMIP5 and the experiment design. Bull. Am. Meteorol. Soc. 93, 485–498.

Tomozeiu, R., Cacciamani, C., Pavan, V., Morgillo, A., Busuioc, A., 2007. Climate change scenarios for surface temperature in Emilia-Romagna (Italy) obtained using statistical downscaling models. Theor. Appl. Climatol. 90, 25–47.

Turco, M., Marcos, R., Quintana-Segui, P., Llasat, M.C., 2014. Testing instrumental and downscaled reanalysis time series for temperature trends in NE of Spain in the last century. Reg. Environ. Chang. 14, 1811–1823.

Uppala, S.M., Kallberg, P.W., Simmons, A.J., Andrae, U., Bechtold, V.D., Fiorino, M., et al., 2005. The ERA-40 re-analysis. Q. J. R. Meteorol. Soc. 131, 2961–3012.

Van der Linden, P., JFB, Mitchell (Eds.), 2009. ENSEMBLES: Climate Change and Its Impacts: Summary of Research and Results From the ENSEMBLES Project. Met Office Hadley Centre, UK , p. 68 160 pp. http://ensembles-eu.metoffice.com/docs/Ensembles_final_report_Nov09.pdf, Accessed date: 10 February 2012.

Vautard, R., Gobiet, A., Jacob, D., Belda, M., Colette, A., Deque, M., et al., 2013. The simulation of European heat waves from an ensemble of regional climate models within the EURO-CORDEX project. Clim. Dyn. 41, 2555–2575.

Voldoire, A., Sanchez-Gomez, E., Melia, D.S.Y., Decharme, B., Cassou, C., Senesi, S., et al., 2013. The CNRM-CM5.1 global climate model: description and basic evaluation. Clim. Dyn. 40, 2091–2121.

Watanabe, S., Hajima, T., Sudo, K., Nagashima, T., Takemura, T., Okajima, H., et al., 2011. MIROC-ESM 2010: model description and basic results of CMIP5-20c3m experiments. Geosci. Model Dev. 4, 845–872.

World Meteorological Organization, 2010. No. 1055. 978-92-63-11055-8 (Switzerland). www.wmo.int.

Xiao-Ge, X., Tong-Wen, W., Jie, Z., 2013. Introduction of CMIP5 experiments carried out with the climate system models of Beijing Climate Center. Adv. Clim. Chang. Res. 4, 41–49. https://doi.org/10.3724/SP.J.1248.2013.041.

Yukimoto, S., Yoshimura, H., Hosaka, M., Sakami, T., Tsujino, H., Hirabara, M., Tanaka, T.Y., Deushi, M., Obata, A., Nakano, H., Adachi, Y., Shindo, E., Yabu, S., Ose, T., Kitoh, A., 2011. Meteorological research institute- earth system model v1 (MRI-ESM1)—model description. Technical Report of MRI. vol 64.

Zittis, G., Hadjinicolaou, P., Fnais, M., Lelieveld, J., 2016. Projected changes in heat wave characteristics in the eastern Mediterranean and the Middle East. Reg. Environ. Chang. 16, 1863–1876.

Zorita, E., von Storch, H., 1999. The analog method as a simple statistical downscaling technique: comparison with more complicated methods. J. Clim. 12, 2474–2489.

Science of the Total Environment 740 (2020) 140094

Contents lists available at ScienceDirect

Science of the Total Environment

journal homepage: www.elsevier.com/locate/scitotenv

Impact of climate change on drought in Aragon (NE Spain)

Emma Gaitán [a,b], Robert Monjo [b], Javier Pórtoles [b], María Rosa Pino-Otín [a,*]

[a] Universidad San Jorge, Villanueva de Gállego, 50830, Zaragoza, Spain
[b] Fundación para la Investigación del Clima, C/ Tremps 11, 28040 Madrid, Spain

HIGHLIGHTS

- Future SPI and SPEI scenarios for Aragon (Spain) were downscaled.
- Scenarios were based on the most recent Earth System Models (CMPI5) at first time.
- The SPI, considering only precipitation, shows no changes in the water balance.
- The SPEI, considering the global warming, shows an increase of the drought episodes.
- Hydroclimatic conditions of Aragon will change towards a drier climate.

GRAPHICAL ABSTRACT

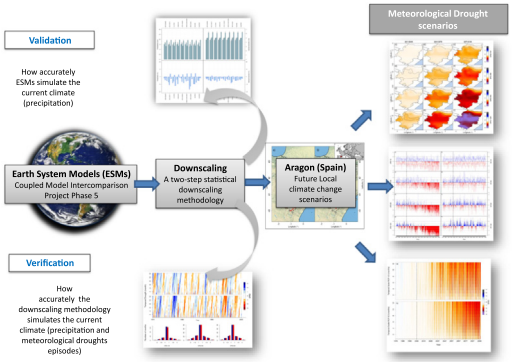

ARTICLE INFO

Article history:
Received 12 December 2019
Received in revised form 4 June 2020
Accepted 7 June 2020
Available online 10 June 2020

Editor: Martin Drews

ABSTRACT

Droughts are one of the extreme climatic phenomena with the greatest and most persistent impact on health, economic activities and ecosystems and are poorly understood due to their complexity. The exacerbation of global warming throughout this century probably will cause an increase in droughts, so accurate studies of future projections at a local level, not done so far, are essential.

Climate change scenarios of drought indexes for the region of Aragon (Spain) based on nine Earth System Models (ESMs) and two Representative Concentration Pathways (RCPs) corresponding to the fifth phase of the Coupled Model Intercomparison Project (CMIP5) have been generated for the first time. Meteorological Drought episodes were analysed from three main aspects: magnitude (index values), duration and spatial extent. The evolution of drought is also represented in a novel way, allowing identification, simultaneously, of the intensity of the episodes as well as their duration in different periods of accumulation and, for the first time, at the observatory level. Future meteorological drought scenarios based on the Standardized Precipitation Index (SPI) hardly show variations in water balance with respect to normal values. However, the Standardized Precipitation Evapotranspiration Index (SPEI) which, in addition to precipitation, considers evapotranspiration, shows a clear trend towards increasingly intense periods of drought, especially when considering cumulative periods and those at the end of the century.

Representation of the territory of the drought indexes reflects that the most populated areas (Ebro Valley and SW of the region), will suffer the longest and most intense drought episodes. These results are key in the development of specific measures for adapting to climate change.

* Corresponding author at: Universidad San Jorge, Campus Universitario Villanueva de Gállego Autovía A-23 Zaragoza-Huesca, km. 510, 50830 Villanueva de Gállego, Zaragoza, Spain.
E-mail addresses: emma@ficlima.org (E. Gaitán), robert@ficlima.org (R. Monjo), javier@ficlima.org (J. Pórtoles), rpino@usj.es, *URL:* https://www.usj.es (M.R. Pino-Otín).

https://doi.org/10.1016/j.scitotenv.2020.140094
0048-9697/

1. Introduction

Drought is probably one of the extreme climatic phenomena with the greatest impact on the world's population and that can affect millions of people every year around the planet (Bryant, 1993; Wilhite, 2000). It also has serious effects on the availability of water and therefore on economic activities such as agriculture (Lesk et al., 2016) and tourism and profound impacts on human health (Stanke et al., 2013) and ecosystems (Alary et al., 2014) that may persist over time. (Dai, 2011). However, drought is a phenomenon that is not well understood due to its complexity and lack of historical records (Wilhite, 2000) and because it depends on numerous factors.

For this reason, the scientific community and institutions are putting a lot of effort into understanding, identifying, documenting and monitoring this phenomenon more exhaustively. Examples are the drought databases of the European Drought Observatory, the National Drought Mitigation Center and, the historical database of the Standardized Precipitation Evapotranspiration Index (SPEI) (http://spei.csic.es/database.html).

1.1. Droughts types and indexes

Precipitation is the primary controlling factor of drought but other meteorological phenomena, such as temperature (Cook et al., 2014; Hao et al., 2017; Livneh and Hoerling, 2016), wind (McVicar et al., 2012a) and relative humidity (Willett et al., 2014), can modulate its intensity (Bates et al., 2008). Through potential evapotranspiration (PET), it is possible to evaluate the amount of water that would evaporate and transpire if there was enough water available, which is very important in the evaluation of meteorological droughts.

Because drought affects so many different aspects (environmental, economic, social, health), a single 'drought' does not really exist. Drought is often classified into four types (Wilhite, 2000; Wilhite and Glantz, 1985): meteorological, agricultural, hydrological and socioeconomic drought.

The main subject of the current study is meteorological drought, a type of drought characterized by below-normal precipitation over a period of months to years and that should be defined as a condition relative to the normal local condition (Dai, 2011; Paparrizos et al., 2018; Wilhite, 2000).

On the other hand, to characterize droughts, standardized drought indexes are used in the literature. These indexes are direct indicators based on climate information, defined so that the results are comparable in time and space since droughts of the same magnitude can have very different effects depending on the time of year and the place where they occur (Hayes et al., 1999; Vicente-Serrano, 2016; Wilhite, 2000).

Some of these indexes are well established and have been used to monitor climatic conditions across different locations; these include the Palmer Drought Severity Index (PDSI; Palmer, 1965) and Standardized Precipitation Index (SPI; Mckee et al., 1993), for example. The Lincoln Declaration on Drought Indexes (Hayes et al., 2011) determined that SPI is the only index, from the point of view of meteorological drought, valid for any region of the world and any time scale, being one of the most used in Europe (Spinoni et al., 2015). It is able to provide better spatial standardization than PDSI (Lloyd-Hughes and Saunders, 2002) and indicate drought initiation and termination because they are implicit parts of the index (Sonmez et al., 2005).

SPI, however, presents some limitations such as that it neglects the effect of temperature increase and, therefore, the effect that an increase in PET (Vicente-Serrano et al., 2010a) or in the atmospheric evaporative demand (AED) (Vicente-Serrano et al., 2020) can have on droughts, which may affect prediction of the impact of global warming in future drought conditions. It should be noted, however, that other meteorological variables as wind speed, solar radiation and air humidity, can also affect PET changes linked to climate change.

To avoid this problem, (Vicente-Serrano et al., 2010a) proposed a new climatic drought index, SPEI, which considers the difference between monthly precipitation and AED. Thus, SPEI best reflects climate change as it makes a more realistic measurement of water availability by incorporating the effect of temperature on changes in evaporation demand as does PDSI. On the other hand, it maintains the multitemporal nature and simplicity of SPI (Marcos-Garcia et al., 2017).

According to the latest report of the Intergovernmental Panel on Climate Change (IPCC, 2014), analysis of the precipitation regime (Calbo, 2010; Lavaysse et al., 2012), droughts (Burke and Brown, 2008; Lopez-Bustins et al., 2013) and the extreme temperatures that drastically increase evapotranspiration (ET) (Rebetez et al., 2006) and decrease soil moisture (Sheffield and Wood, 2008) suggest that drought episodes could become more severe around the world in the 21st century (Dai, 2013).

There are some studies that emphasize that future projections of drought may overestimate drought episodes if future soil moisture (Berg et al., 2017) and runoff (Yang et al., 2018) simulations are not taken into account (Berg and Sheffield, 2018), which can affect AED. In addition, recent studies highlight the need to include CO_2 concentration in the analysis of AED under climate conditions since an increase of the CO_2 acts contributing to the increase in temperatures that in turn affect the Vapour-Pressure Deficit (VPD). On the other hand, CO_2 could increase water use efficiency by plants reducing AED and therefore mitigate the drying (Dai et al., 2018; Roderick et al., 2015).

In this context, most European areas and the Mediterranean region seem to be prominent regional climate change hotspots where an increment in the occurrence of extreme events is expected (Beniston et al., 2007; Skaugen et al., 2004). Specifically, a possible rise in the intensity and frequency of extreme drought events is expected (Forzieri et al., 2014; Hoerling et al., 2012; Iglesias et al., 2007; Marcos-Garcia et al., 2017; Paparrizos et al., 2018), especially in the summer months (Vicente-Serrano et al., 2010c), and will have significant environmental, social and economic impacts (Blenkinsop and Fowler, 2007).

The global climate models used today reproduce temperature trends very well, but the level of precision for large-scale precipitation patterns is lower than for temperature (IPCC, 2014). This has caused the climatic projections of droughts to show great uncertainty and therefore we cannot know with precision the effects of climatic change on drought severity at the regional level in the future (Burke and Brown, 2008). This is especially problematic in areas with high precipitation variability, such as the Mediterranean region, where the drought patterns derived from the results of global climate models are not consistent (Vicente-Serrano et al., 2004).

1.2. Drought in NE Spain (Aragón)

In Spain, as in the rest of Europe (Feyen and Dankers, 2009), different series of major droughts have been happening in recent decades. In addition, the literature seems to indicate a trend towards an increase in meteorological water scarcity in the Iberian Peninsula, either due to an increase in the frequency of drought episodes or due to a change in the precipitation regime (Fragoso et al., 2018; Gallego et al., 2011; Garcia-Barron et al., 2011; Machado et al., 2011; Ojeda et al., 2017; Vicente-Serrano et al., 2004). This makes necessary studies at a local level and the development of future scenarios of droughts which are adequate as possible for evaluating the local impacts of climate change.

Drought scenarios in Spain are also scarce: either they are from studies conducted prior to the Fifth Assessment Report of the United Nations Intergovernmental Panel on Climate Change (IPCC5) and in very small areas (Lopez-Bustins et al., 2013) or they use IPCC5 models but use dynamic downscaling information from the European Coordinated Regional Downscaling Experiment EUROCORDEX; (Collados-Lara et al., 2018; Marcos-Garcia et al., 2017). The latter also evaluates only SPI and SPEI at the 12-month scale. However, these studies agree that the

combined use of SPI and SPEI is adequate for studying drought episodes in the future (Lopez-Bustins et al., 2013; Marcos-Garcia et al., 2017).

The combined study of both indexes, SPEI and SPI could be an effective formula for an adequate study of meteorological drought in territories with the climatology of Aragon (NE Iberian Peninsula). This region of Spain is characterized by a continental Mediterranean climate with high precipitation variability and marked by very diverse orography throughout its territory that includes areas of high mountains, valleys and steppes (López et al., 2007). In addition, we must consider that previous studies in Aragon have shown that an increase in temperature is one of the variables that will be most noticeable with climate change throughout this century (Gaitan et al., 2019; Ribalaygua et al., 2013a).

As far as we know, drought scenarios in Aragon have not been obtained to date. As has been seen, it is essential to have local scenarios to determine the impact of climate change on the environmental or socioeconomic reality of each region in order to make decisions on adaptation to climate change.

The goal of this study is to obtain, for the first time, meteorological drought scenarios for Aragon (located in NE of Spain) for the 21st century using a statistical methodology to downscale GCMs from CMIP5.

To achieve this goal, the capacity of the GCMs to simulate the past observed climate was assessed (validation) and using CMIP5, precipitation scenarios for Aragon were generated to simulate future daily precipitation.

Finally, as Aragon is a region sensitive to episodes of drought caused by a varying rate of precipitation and high temperatures, the SPI and SPEI meteorological indexes were calculated and the frequency of occurrence of drought and its spatial distribution were simulated to identify the drought vulnerability of the study area. Drought indexes were also verified.

This study provides, for the first time, scenarios of meteorological drought in the NE of Spain according to CMIP5 models, useful for predicting the impacts of climate change on the availability of water at a local scale and which are necessary for stakeholders to make decisions on adaptation and mitigation of climate change. On the other hand, this region of Spain is a good indicator of many characteristic areas of southern Europe (high mountains, river basins, steppes, etc.).

2. Data and methodology

2.1. Study area

The present study was carried out in the region of Aragon (NE of Spain) (Fig. 1). Because of its location, Aragon falls within the Western Mediterranean climate area characterized by scarce precipitation with cool winters and hot, dry summers. Differences in latitude between the most northern and most southern points of Aragon (340 km length and 240 km width) along with the influence of the Cantabrian and Mediterranean Seas and the general atmospheric circulation as well as the orographic complexity of the region (extreme altitude differences of over 3000 m between the plains (the Ebro River valley) and the mountains (the Pyrenees)), give rise to great subclimate variety, with different thermal and pluviometric regimes that condition the local climate (López et al., 2007).

Precipitation is scarce in most of Aragon and is distributed clearly according to relief, as the isohyets are arranged in concentric circles decreasing from mountain areas to the centre of the region. Although the average annual total precipitation of the Aragonese territory is around 550 mm, there are regions for which the average is below these values (for example, in the central sector of the Ebro Depression). Only in the Pyrenees and, to a lesser extent, in the Iberian Mountain Range, does precipitation reach important values, 1800–2000 mm, and show positive water balance values (considering the difference between precipitation and AED). On the other hand, >60% of the region has average values of AED above 1100 mm, showing a negative water balance, to which contributes not only the scarce rainfall but also the strong wind ("Cierzo") characteristic of the Ebro Valley (López et al., 2007). Therefore, 70% of the Aragonese territory is considered semi-arid (index value proposed by the United Nations Environment Program <0.5 and even 30% presents values of 0.3) (Cherlet et al., 2018).

2.2. Datasets

2.2.1. Surface observation datasets

In this study, an observational dataset (daily maximum and minimum temperature and precipitation) belonging to the extensive network of instrumental observatories owned by the Spanish Meteorological Agency (AEMET) (http://www.aemet.es) was used (Fig. 1). This dataset is the same as the one used in previous studies (Gaitan et al., 2019; Ribalaygua et al., 2013a) in order to work with a set of data that has been subjected to strict quality control (inhomogeneities, gaps, outliers, transcription errors and so on) carried out first by the Government of Aragon (López et al., 2007) and completed, in a second phase, by (Ribalaygua et al., 2013a). As a complement to quality controls, those stations with a large number of data gaps or <15 years of daily records were discarded.

For the simulation of future climate scenarios of precipitation, a first set of 263 stations was used (red dots in Fig. 1a). Of these 263 stations, just those with data for both variables, temperature and precipitation, were used for the simulation of drought indexes (43 stations, Fig. 1b).

2.2.2. Atmospheric dataset

A set of nine climate models were selected from CMIP5, supplied by the Program for Climate Model Diagnosis and Intercomparison (PCMDI) archives.

The global climate models called Earth System Models (ESMs) from the fifth phase of the Coupled Model Intercomparison Project (CMIP5) (Tripathi et al., 2006) have contributed to the acquisition of both dynamic and statistical downscaling techniques with less uncertainty. These models integrate the individual parts of the climate system (atmosphere, ocean, land and sea ice) and the exchange of energy and mass between them (Knutti and Sedlacek, 2013). These models also include chemical processes, land use, plant and ocean ecology and an interactive carbon cycle, which enables integration of biochemical processes into the models (Heavens et al., 2013), constituting a robust set of coordinated climate model experiments (Carvalho et al., 2017; Chen et al., 2016; Perez et al., 2014).

The climate models (Table 1) were selected according to the time resolution (daily) of available predictor fields, because it is required for the downscaling method used. All of the models were ESMs (Jones et al., 2011; Wang et al., 2009).

This study used data from two different experiment families of GCMs: the Historical experiment (Taylor et al., 2012), which covers much of the industrial period and can be referred to as 'twentieth-century' simulations, and the Representative Concentration Pathway (RCP) family (Moss et al., 2010), which corresponds to different possible ranges of radiative forcing reached in the year 2100 with respect to values of the pre-industrial era. This study used future projections determined by the RCP8.5 'high' scenario and RCP4.5 'intermediate' scenario, the core of IPCC5 experiments.

In order to study the behaviour of the CMIP5 model Historical simulations, we used the reanalysis dataset from the European Centre for Medium-Range Weather Forecasts (ECMWF ERA-40; http://www.ecmwf.int/research/era/do/get/) (Uppala et al., 2005) for the period 1958–2000 at 6-hourly time resolution and 125 km spatial resolution. For verification of the methodology, it was necessary to reduce the temporal and spatial scale of the reanalysis in order to compare both ERA-40 and the climate model simulations (Ribalaygua et al., 2013a; Ribalaygua et al., 2013b). The geographical limits of the atmospheric window used were latitudes 31.5°N to 55.1°N and longitudes 27.0°W to 14.6°E, covering not only the geographic area under study but also the surrounding atmosphere areas which exert a meteorological influence all over the

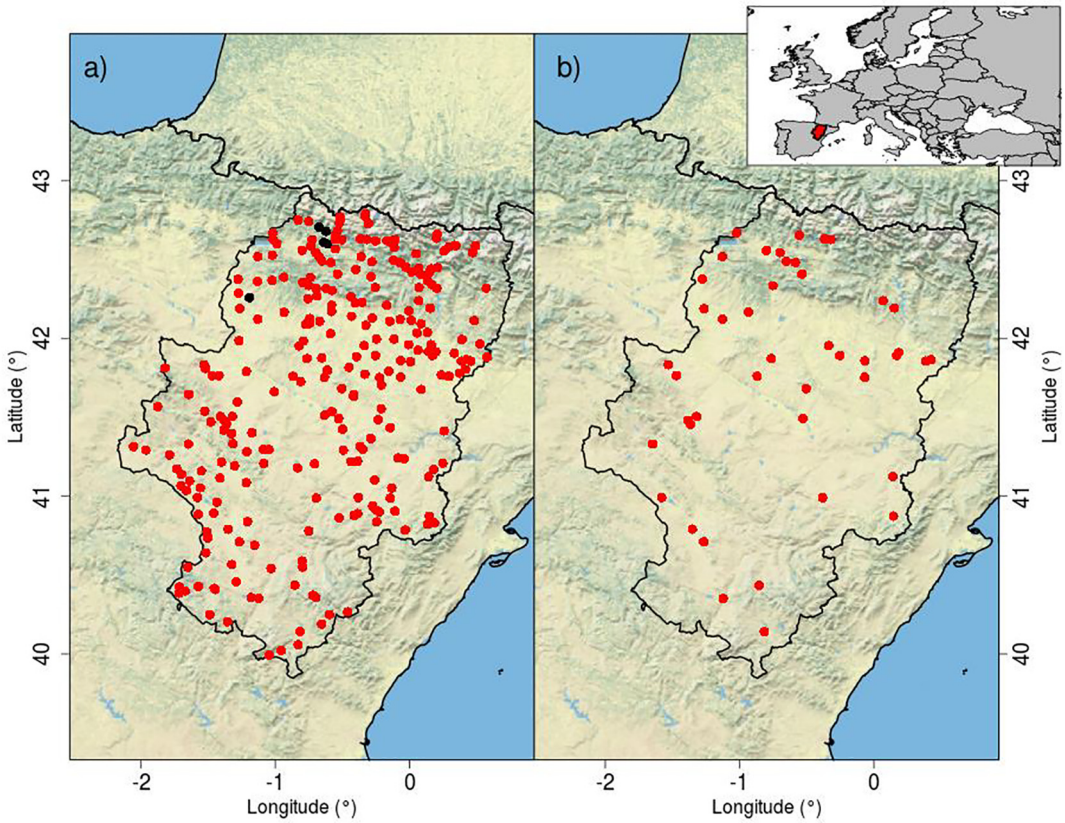

Fig. 1. Location of the study area and observatories. Aragon (Spain) in Europe. Points indicate the stations used in the study. a) Stations of precipitation (264) used in the generation of climate regional scenarios of precipitation (verification, validation and scenarios). b) Stations used exclusively on the generation of drought indexes (43).
Map source: OpenStreetMap.

Iberian Peninsula (Ribalaygua et al., 2013a). The use of the ERA-40 data set has allowed us to compare these new results with those published by Ribalaygua et al., 2013a.

2.3. Methodologies

2.3.1. Validation and generation of future precipitation scenarios

A two-step analogue/regression statistical downscaling method developed previously (Ribalaygua et al., 2013b) was applied to obtain future scenarios of precipitation and drought. This method has been used in national and international projects, with good verification results (Gaitan et al., 2019; Monjo et al., 2016; Moutahir et al., 2017; Ribalaygua et al., 2018; Rodriguez et al., 2014; Santiago et al., 2017). This methodology offers some advantages: it is computationally inexpensive, provides local information and allows quantifying the uncertainty associated with the downscaling process (Van der Linden and Mitchell, 2009). Other advantages are the application of future simulations consistent with observations (physically coherent between them) and using local scale (because nearby data points in space are not subjected to different climate change conditions) (Ribalaygua et al., 2013b).

Through the validation process we can, on the one hand, evaluate the ability of each ESM to simulate the predictor fields (comparing the downscaled Historical experiment simulation for each model with the

Table 1
Information about the nine climate models belonged to the 5 Coupled Model Intercomparison Project (CMIP5) corresponding to the fifth report of the IPCC. Models were supplied by the Program for Climate Model Diagnosis and Intercomparison (PCMDI) archives.

GFDL-ESM2M	2°x2,5° daily	National Oceanic and Atmospheric Administration (NOAA), E.E.U.U.	Dunne et al. (2012)
CanESM2	2,8°x2,8° daily	Canadian Centre for Climate Modeling and Analysis (CC-CMA), Canadá.	Chylek et al. (2011)
CNRM-CM5	1,4°x1,4° daily	CNRM (Centre National de Recherches Meteorologiques), Meteo-France, Francia.	Voldoire et al. (2013)
BCC-CSM1-1	1,4°x1,4° daily	Beijing Climate Center (BCC), China Meteorological Administration, China.	Xiao-Ge et al. (2013)
HADGEM2-CC	1,87°x1,25° daily	Met Office Hadley Center, United Kingdom.	Collins et al. (2008)
MIROC-ESM-CHEM	2,8°x2,8° daily	Japan Agency for marine-Earth Science and Technology (JAMSTEC), Atmosphere and Ocean Research Institute (AORI), and National Institute for Environmental Studies (NIES), Japan.	Watanabe et al. (2011)
MPI-ESM-MR	1,8°x1,8° daily	Max-Planck Institute for Meteorology (MPI-M), Germany.	Raddatz et al. (2007); Marsland et al. (2003)
MRI-CGCM3	1,2°x1,2° daily	Meteorological Research Institute (MRI), Japan.	Yukimoto et al. (2011)
NorESM1-M	2,5°x1,9° daily	Norwegian Climate Centre (NCC), Norway.	Bentsen et al. (2013); Iversen et al. (2013)

downscaled ERA-40 simulation for a common period, 1958–2000) and, on the other, quantify the uncertainties inherent to future climate projections through an ensemble strategy (Monjo et al., 2016).

Bias and standard deviation at seasonal scale have been used as error measures. This validation process presents some limitations related to the observational data available to be considered in the final uncertainty analysis. More information about the validation process can be consulted in (Ribalaygua et al., 2013b).

Future local climate scenarios at local and daily scale for precipitation were produced for nine ESMs (see Table 1) and two RCPs (RCP4.5 and RCP8.5) as a previous step to calculate the drought indices. As precipitation is an essential variable in the analysis of drought, these scenarios are a starting point providing initial information on future pluviometric conditions.

The local climatic projections of precipitation belonging to CMIP5 were obtained in this study using the same methodology as that used for temperature scenarios, previously described (Gaitan et al., 2019).

2.3.2. Drought indexes

SPI was developed by Mckee et al. (1993) and is based on two assumptions: 1) that the variability of precipitation is greater than that of temperature and AED, and 2) that the rest of the variables are stationary over time. The SPI value is defined as a numerical value that represents the number of standard deviations of precipitation, over the accumulation period in question, with respect to the average, once the original distribution of precipitation has been transformed into a normal distribution (i.e., mean of zero and standard deviation of 1). The SPI values can be interpreted as the number of standard deviations by which the observed anomaly deviates from the long-term mean.

SPEI developed by (Vicente-Serrano et al., 2010a) and revisited by (Begueria et al., 2014) is a variant of the widespread SPI; it has greater potential as a drought index since it considers the climate balance (through the difference between monthly precipitation and AED). SPEI values can be interpreted in the same way as SPI values (number of standard deviations by which the observed anomaly deviates from the long-term mean).

Both indexes were calculated using the R package 'SPEI' (Version 1.7). The SPI was calculated using Gamma distribution to fit the original precipitation series (Organization WMO, 2012) and the SPEI was calculated using log-logistic distribution (Vicente-Serrano et al., 2015; Vicente-Serrano and Begueria, 2016). The parameters of these distributions were obtained by the method of unbiased probabilistic weighted moments (Vicente-Serrano and Begueria, 2016). The scale of SPI and SPEI values used in the study can be seen in Table 2.

The period 1976–2005 was used as a reference period, which represents the last 30 years of the Historical period. Based on this reference period, both the SPI and the SPEI were calculated for the period 2006–2100. The choice of the reference period was made to evaluate the future hidroclimatic conditions of the region with respect to the average conditions of the last 30 years of the Historical experiment.

To obtain the AED values used in the calculation of SPEI, both the Hargreaves and Samani (1985) and Thornthwaite (1948), formulas have been used, denominated SPEI-Har and SPEI-Thor, respectively. These formulas were chosen to calculate AED because they are recommended within the SPEI package and they also depend only on temperature and precipitation, unlike other more complex methods such as the Penman–Monteith (Smith et al., 1998) and Jensen–Haise methods (Jensen and Haise, 1963). Both methods only take into account the temperature, so it is assumed that the calculation of AED trends could have certain limitations (Irmak et al., 2012; McVicar et al., 2012b; Sheffield et al., 2012). For a certain increase in the temperature, the change in the obtained result can be higher than the one really expected according a complete method like Penman-Monteith. Therefore, the role of AED on drought severity would be overestimate and this would have some effect on the drought indices obtained for future scenarios.

The way in which the indexes have been analysed follows the guidelines of the WMO (WMO, 2017) which recommends analysis of a drought episode from three main aspects – magnitude (index values), duration (alternation between positive and negative values) and spatial extent – and all these aspects configure the severity of the episode.

In order to assess the capacity of the downscaling methodology to simulate SPI and SPEI, we analysed the intensity and duration of the different drought episodes shown by both indexes, comparing the SPI and SPEI values calculated from the simulated ERA-40 temperature and precipitation series with those obtained from the observed series for a common period (1970–2000). Verification of the maximum and minimum temperature and precipitation can be seen in a previous study (Ribalaygua et al., 2013a). The statistical measures used in the verification processes were the bias, standard deviation and Pearson correlation. The statistical measures were calculated using R computing software (R Development Core Team, 2010).

From the ESM simulated temperature and precipitation series (nine ESMs and two RCPs), we determined the drought episodes that are expected in Aragon during the upcoming decades of the 21st century. The SPI and SPEI scenarios were compared to a historical period (1976–2005) to analyse the future changes with respect to the actual situation of these extreme events.

To draw future local climate scenario maps, we used Thin Plate Spline (TPS) regression from the R package 'fields' (Nychka et al., 2015).

Table 2
SPEI/SPI Intensities Scale (Vicente-Serrano et al., 2010a).

SPEI/SPI	
≥2	Extremely wet
1.5 a 2	Severely wet
0.5 a 1.5	Moderately wet
−0.5 a 0.5	Normal values
−1.5 ≤ −0.5	Moderately dry
−1.5 ≤ −2	Severely dry
≤−2	Extremely dry

3. Results

3.1. Validation and precipitation scenarios

The results of the validation process (comparison between the ERA-40 precipitation simulations and the historical precipitation simulations for each ESM for a common period (1958–2000)) are shown in Fig. 2, for both absolute (mm) and relative precipitation (%). The results are variable depending on the model and the seasonal period; however, all the models are able to reproduce the annual cycle of precipitation as well as the differences between seasonal periods (maximum values in autumn and spring, followed by winter and summer). The obtained bias and standard deviation are less than ±1 mm/day, which in relative terms supposes a difference of less than or around ±10% in the worst of the cases.

In general terms, a big variation in the Aragon precipitation regime is not expected. According to scenario RCP8.5, mean variations in the amount of precipitation are expected to be around ±10% for all seasons of the year, except for the summer where no precipitation change is expected. Scenario RCP4.5 shows no precipitation fluctuations throughout the 21st century with respect to current values (see Support information, Figs. S1 to S4).

3.2. Generation of future local climate scenarios of drought indexes

3.2.1. Verification of drought index simulation

To verify the simulation of drought indexes, the first step was to compare the SPI and SPEI values obtained from the observations with those calculated from the simulated series of ERA-40.

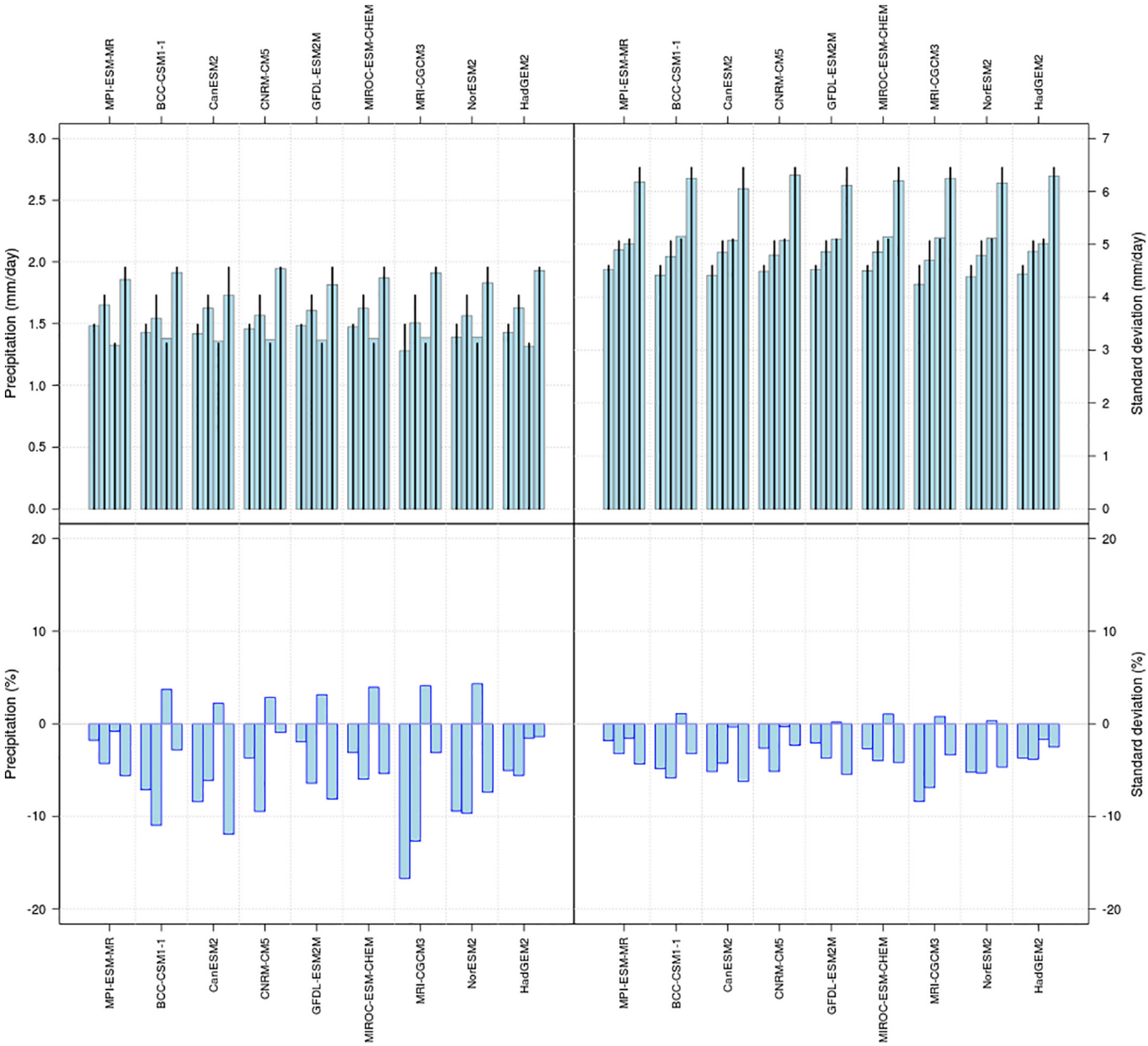

Fig. 2. Validation of precipitation. Comparison between the precipitations obtained using the downscaled Historical data of the global climate models and the downscaled reanalysis data, for every seasonal period. Two graphs at the top: seasonal comparative between the precipitation simulated using the downscaled Historical data (colour bars) and that of the downscaled reanalysis data (black lines) for each global climate models (see Table 1) and for the four seasons: winter (December–February; first bar of each group of four), spring (March–May, second bar), summer (June–August; third bar) and autumn (September–November; four bar). Two graphs at the bottom: relative seasonal differences between the simulated data using the downscaled Historical data and that of the downscaled reanalysis data. Seasonal precipitation amounts are shown on the left columns and seasonal values of the standard deviation on the right columns. (For interpretation of the references to colour in this figure legend, the reader is referred to the web version of this article.)

Fig. 3 shows the verification results corresponding to SPI at time scales from 1 month (SPI-1 M) to 12 months (SPI-12 M) for the period 1970–2000 (Fig. 3a and b). This process allows the identification of episodes of deficit or excess precipitation recorded and simulated from ERA-40. In addition, the number of months in the period 1970–2000 in which SPI values were obtained within different intensity ranges (Table 1) for SPI-1 M, SPI-3 M and SPI-6 M are shown (Fig. 3c, d and e).

As can be seen in Fig. 3a and b, the time series of the simulated SPI for ERA-40 shows, in an acceptable way, the same values presented by the observed SPI, with a correlation of $p = 0.75$ in the case of SPI-1 M, $p = 0.72$ for SPI- 3 M, $p = 0.64$ for SPI-6 M and $p = 0.61$ for SPI-12 M.

The simulated and observed SPI values show dry episodes (negative SPI) in similar periods, for example the periods 1970–1972, 1978, 1981–1982, 1989, 1994–1995 and 1998. The same can be seen for wet episodes (positive SPI) as in, for example, the periods 1976–1977, 1988 and 1996–1997.

Figs. 4 and S5 show the results of the verification process for SPEI based on SPEI-Har and SPEI-Thor calculations, respectively.

Similar results were obtained for calculation of SPEI based on the Hargreaves method (Fig. 4a and b) although in this case the correlation obtained between the observed and simulated time series of SPEI is slightly higher (0.80 for SPEI-1 M, 0.78 for SPEI-3 M, 0.72 for SPEI-6 M and 0.73 for SPEI-12 M).

When the Thornthwaite method is used for calculating AED in SPEI (see Fig. S5), the temporal correlations are lower than those obtained with SPEI based on Hargreaves.

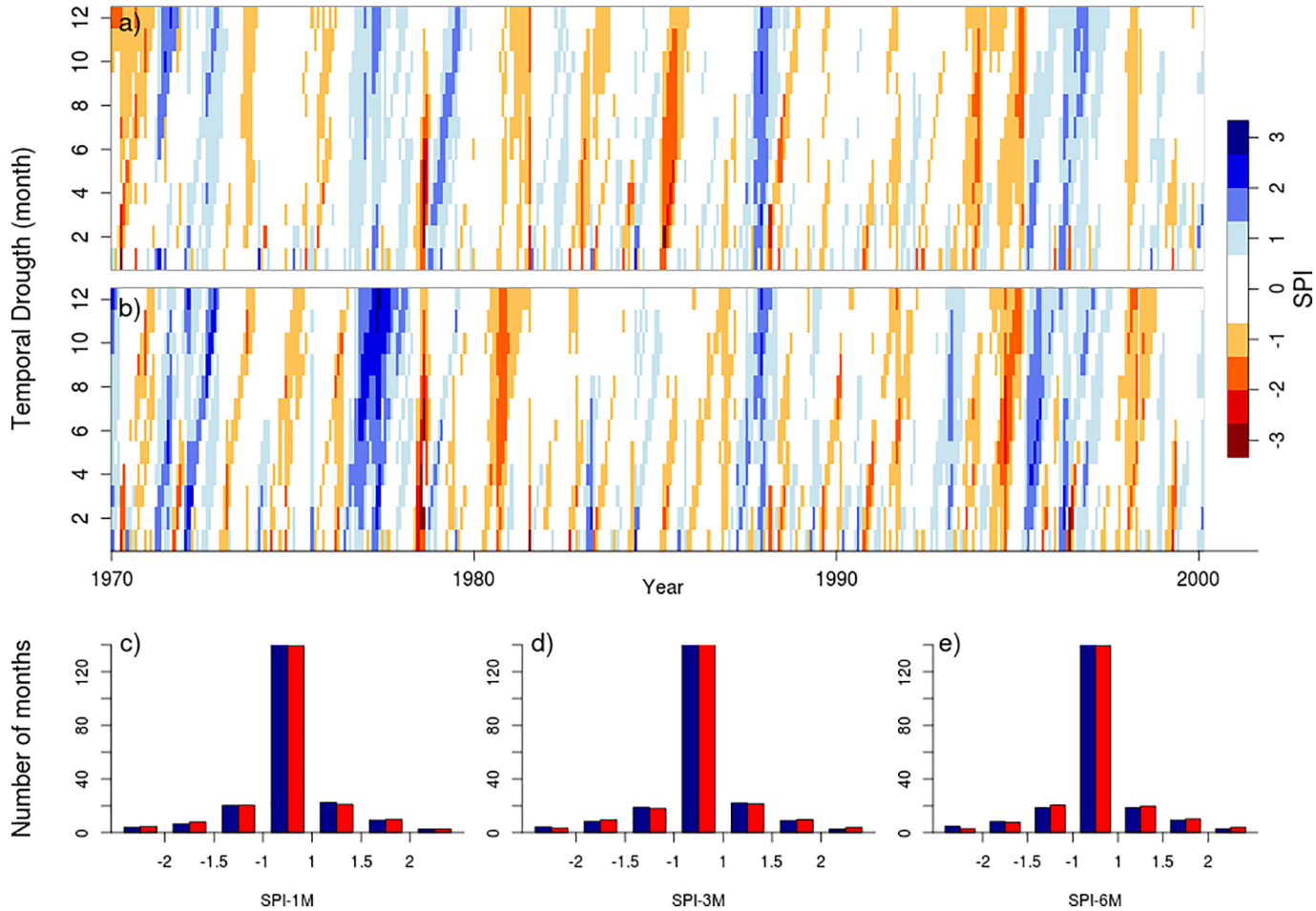

Fig. 3. SPI verification. Results of the verification process for the SPI. a) Time series of the SPI index calculated from observed data at the time-scales from 1 to 12 months for the period 1970–2000, b) time series of the SPI index calculated from downscaled ERA-40 at the time-scales from 1 to 12 months for the period 1970–2000. c), d) and e) number of months within the 1970–2000 period corresponding to each interval of the SPI intensities scale based on observed data (blue columns) and on downscaled ERA-40 (red columns) for the time-scales of 1, 3 and 6 months. Average of the all the stations used in the simulations. (For interpretation of the references to colour in this figure legend, the reader is referred to the web version of this article.)

On the other hand, for about 65–70% of the period considered, water balance conditions in Aragon was considered normal (SPI/SPEI between −0,5 and 0,5), suffering extreme wet or dry episodes for only 2–4% of the period 1970–2000.

The error (bias) made in the simulation of SPI (Fig. 3c to e) and SPEI (Fig. 4c to e) is quite small for all of the classes considered (< ± 2 months).

3.2.2. Local climate scenarios to predict drought indexes

Figs. 5 to 9 (complemented with Figs. S6 and S7) show the results obtained for the simulation of SPI and SPEI throughout the 21st century from different perspectives.

Fig. 5 shows local climate change scenarios for future SPEI (a, c and d) and SPI (b, d and f) at 3-, 6- and 12-month scale, which have been predicted on the basis of the nine models (see Table 2) and here are used to obtain a general vision of the changes in water balance for the Aragon region as a whole. The future projections of SPI and SPEI for the period 2006–2100 have been made based on the reference period (Historical 1976–2005). When working with normalized indexes, the future values of the SPI and SPEI represent anomalies with respect to the average values of the reference period, which allows to evaluate the future evolution of the hydric conditions in Aragon with respect to the average of the last 30 years of the Historical experiment.

The SPI values obtained are hardly modified with respect to the Historical period so, according to these results, the water balance characteristics of the region as a whole would remain similar to the current ones. On the other hand, the SPEI climate change scenarios, considering the effect of AED, show a marked tendency towards increasingly negative values of the index with respect to the Historical period, especially at the end of the century.

Both RCPs show a similar evolution until 2060, with changes of SPEI with respect to the Historical period of −0.6 for SPEI-3 M, −0.9 for SPEI-6 M and − 1.3 for SPEI-12 M. For the final period of the century, the variation begins to be more pronounced under the conditions of RCP8.5, with changes of −1.2 for SPEI-3 M, −1.8 for SPEI-6 M and − 2.8 for SPEI-12 M, while under scenario RCP4.5, SPEI values vary slightly from those reached in 2060.

These results are very well reflected in the time-scale evolution maps, where the simulated time series from 1976 to 2100 are represented, both for SPEI (Fig. 6) and SPI (Fig. 7) and under both scenarios, RCP4.5 (Figs. 6a and 7a) and RCP8.5 (Figs. 6b and 7b) with respect to different time scales (from 1 to 12 months).

Fig. 6 shows a tendency towards more and more extreme SPEI values, especially in the longer time scales. For time scales of up to 4 months, an alternation between periods considered normal and dry periods is expected (SPEI values between −1,5 and 0,5). For longer time scales, there is a tendency towards more intense and prolonged periods

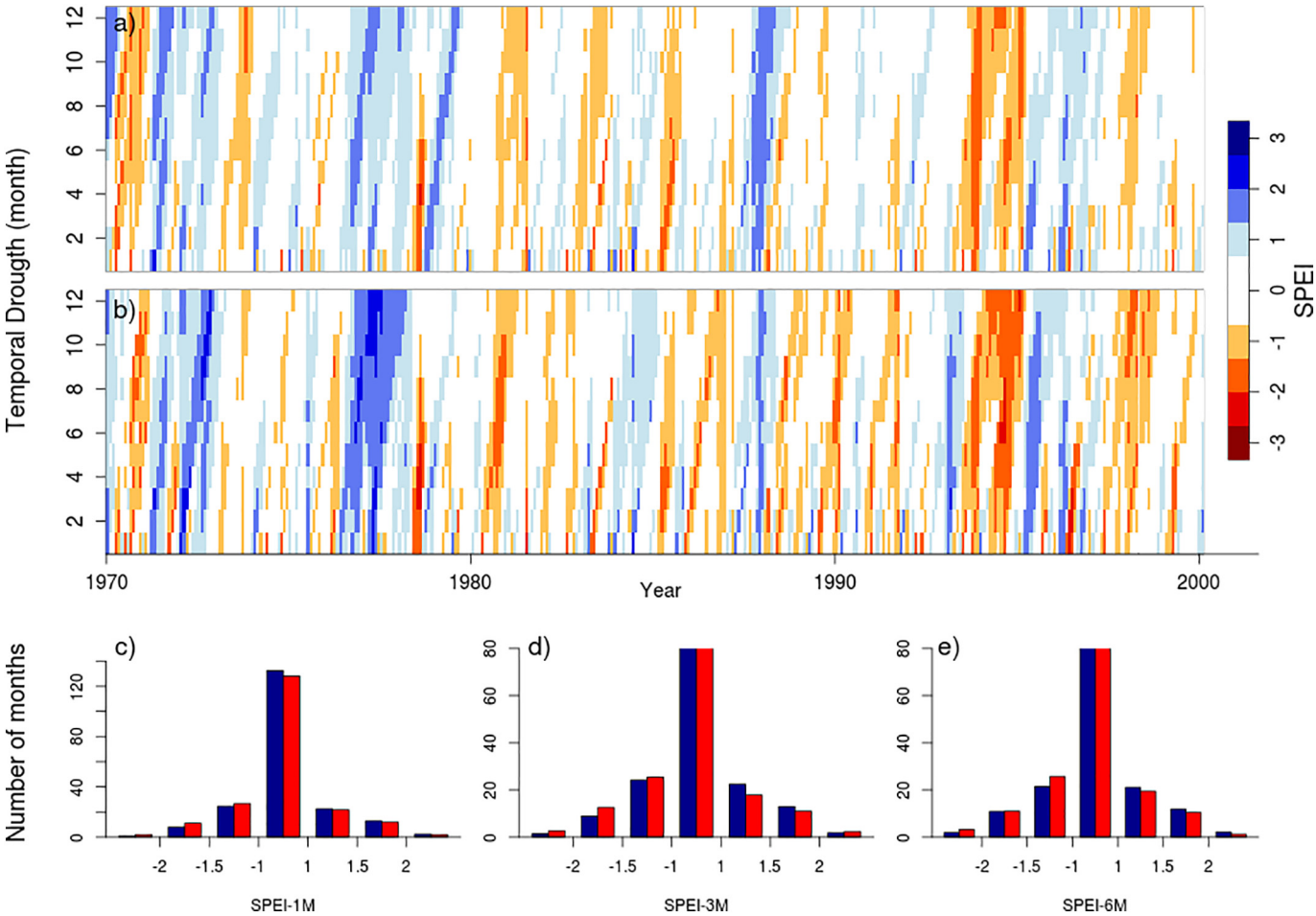

Fig. 4. SPEI Har verification. Results of the verification process for the SPEI based on Hargraves Evapotranspiration. a) Time series of the SPEI index calculated from observed data at the time-scales from 1 to 12 months for the period 1970–2000, b) time series of the SPEI index calculated from downscaled ERA-40 at the time-scales from 1 to 12 months for the period 1970–2000. c), d) and e) number of months within the 1970–2000 period corresponding to each interval of the SPI intensities scale based on observed data (blue columns) and on downscaled ERA-40 (red columns) for the time-scales of 1, 3 and 6 months. Average of the all the stations used in the simulations. (For interpretation of the references to colour in this figure legend, the reader is referred to the web version of this article.)

of drought, with SPEI values of up to −3 at the end of the century. The pattern obtained is similar under both RCPs, being more pronounced in the case of RCP8.5.

In the time-scale map corresponding to SPI (Fig. 7), the same pattern as that obtained for SPEI is not appreciated; in this case, alternating dry and wet periods are observed for all time scales, these being somewhat more extensive as we move along the time scales. The same pattern is observed under both RCPs, the signal being slightly stronger in the case of RCP8.5.

As a complement to the previous results, which allowed the extraction of results for the water regime of Aragon as a whole, the spatial maps of both indexes are shown. Figs. 8 and 9 show the climate scenarios for mean SPEI according to RCP4.5 and RCP8.5, respectively. These figures show the temporal evolution for four time scales: 1 month (first row), 3 months (second row), 6 months (third row) and 12 months (fourth row). The temporal periods chosen were 2011–2040 (present), 2041–2070 (mid-century) and 2071–2100 (end-century). Figs. S6 and S7 show the same information but for mean SPI.

The results for SPEI vary considerably between different points in the Aragon region. Coinciding with what was said before, it is observed how the SPEI values become more extreme as the 21st century and time scales advance. The Ebro Valley area is the one that will be subject to more intense episodes of precipitation shortage at the end of the 21st century, with SPEI values from −1 at 3 months to −2 at 12 months according to RCP4.5 and considerably more intense under RCP8.5 with values from −1.8 at 3 months to −4 at 12 months. The north-west area of the region, which is expected to be most affected by drought episodes, deserves special attention. The Pyrenees zone is the one that will clearly suffer the fewest expected drought episodes; under RCP4.5 it is expected to remain in normal water balance conditions while under RCP8.5, at most, SPEI will reach values of −1.5 (at the end-century and at 12-month time scale).

The SPI spatial maps (Figs. S6 and S7) show how the region will remain under normal water balance conditions, highlighting the Ebro basin at the end of the 21st century and under RCP8.5, where more negative values of SPI (around −1) are appreciated, but which are still within the range considered normal for the region.

It is important to emphasize that if the average value of the SPEI/SPI tends to increasingly negative values and if this is a constant trend in the future, the conditions considered normal today will evolve towards new values considered normal (Vicente-Serrano et al., 2020).

This study has been carried out for each of the observatories used in the study and for each of the climatic models, which reveals that the entire region is going to be affected by episodes of drought despite its location and height. As an example, the temporal evolution of both indexes obtained according to the MPI-ESM-MR climate model and under both RCPs is shown for the observatories of Zaragoza (Figs. 10 and 11) and Cedrillas-Huesca (Figs. S8 and S9).

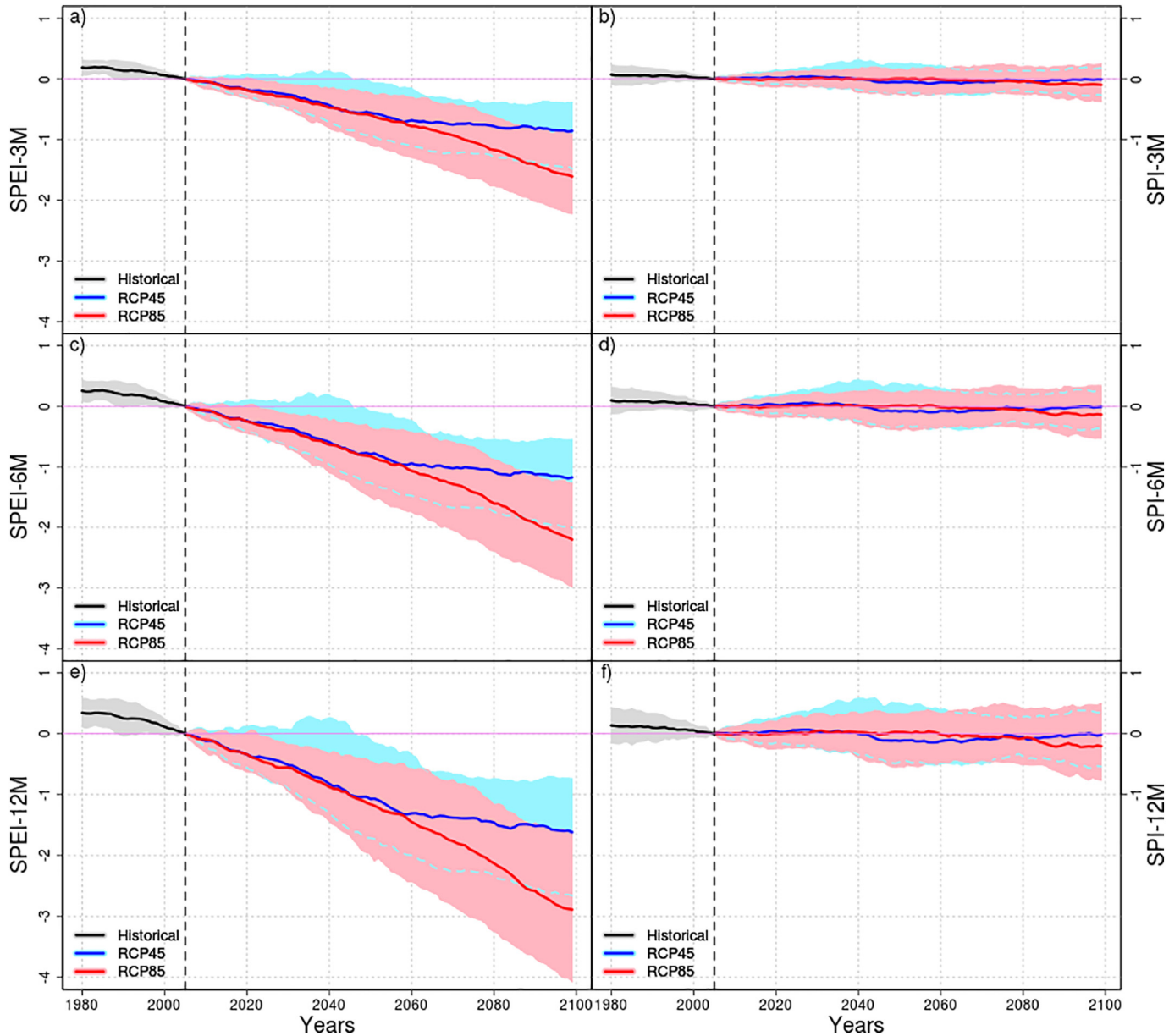

Fig. 5. Simulated SPEI and SPI for the twenty-first century. Values are displayed as absolute increase compared to the amount simulated for the 1976–2005 Historical period for the time scales 3 months (a and b), 6 months (c and d) and 12 months (e and f). The vertical dotted line marks the end of the Historical data (2005). Data grouped for every RCP simulation of every global climate model selected and for the last 30 years of every station. The ensemble median (solid lines) and the 10th–90th percentile (shaded areas) values are displayed.

The choice of these observatories was based on the Climate Atlas of Aragon (López et al., 2007), since they are two of the reference points used in the climatic characterization of the region. The choice of these observatories was also made based on their location; the Zaragoza observatory is located in the Zaragoza airport station at a height of 263 m while the Cedrillas-Huesca observatory is located in the northern area of the region at a height of 1347 m. In addition, the Zaragoza airport station is considered representative of the variability of temperatures in Aragon (Roldán et al., 2011).

The expected temporal evolution of SPEI throughout the 21st century is consistent with that explained above, but as it is a single climatic model and uses a single observatory, the alternation between wet and dry periods can be seen more clearly at a time scale of 1 to 3 months. Also, as we move forward in the time scales, this alternation softens, resulting in periods of more intense and prolonged precipitation shortage while, for SPI, the alternation between wet and dry periods is observed for all time scales. This highlights, as for SPI, how periods with positive SPI for the Cedrillas-Huesca observatory are more intense and prolonged than those predicted for Zaragoza.

4. Discussion

These results offer the possibility of having future climate projections based on recently updated data, allowing the evaluation of how drought could affect the region of Aragon, both spatially and temporarily, and can be taken as a reference to analyse its impact on multiple sectors. Temporally, drought increases to the end of the century; at the territory level, the area most affected will be the central area of the Ebro Valley, where most of the population in the area is concentrated.

The difficulty of developing impact studies and quantifying their damage as a result of periods of water scarcity comes mainly from the lack of observed values and studies at a local level with future projections, hence the need to publish studies of these characteristics.

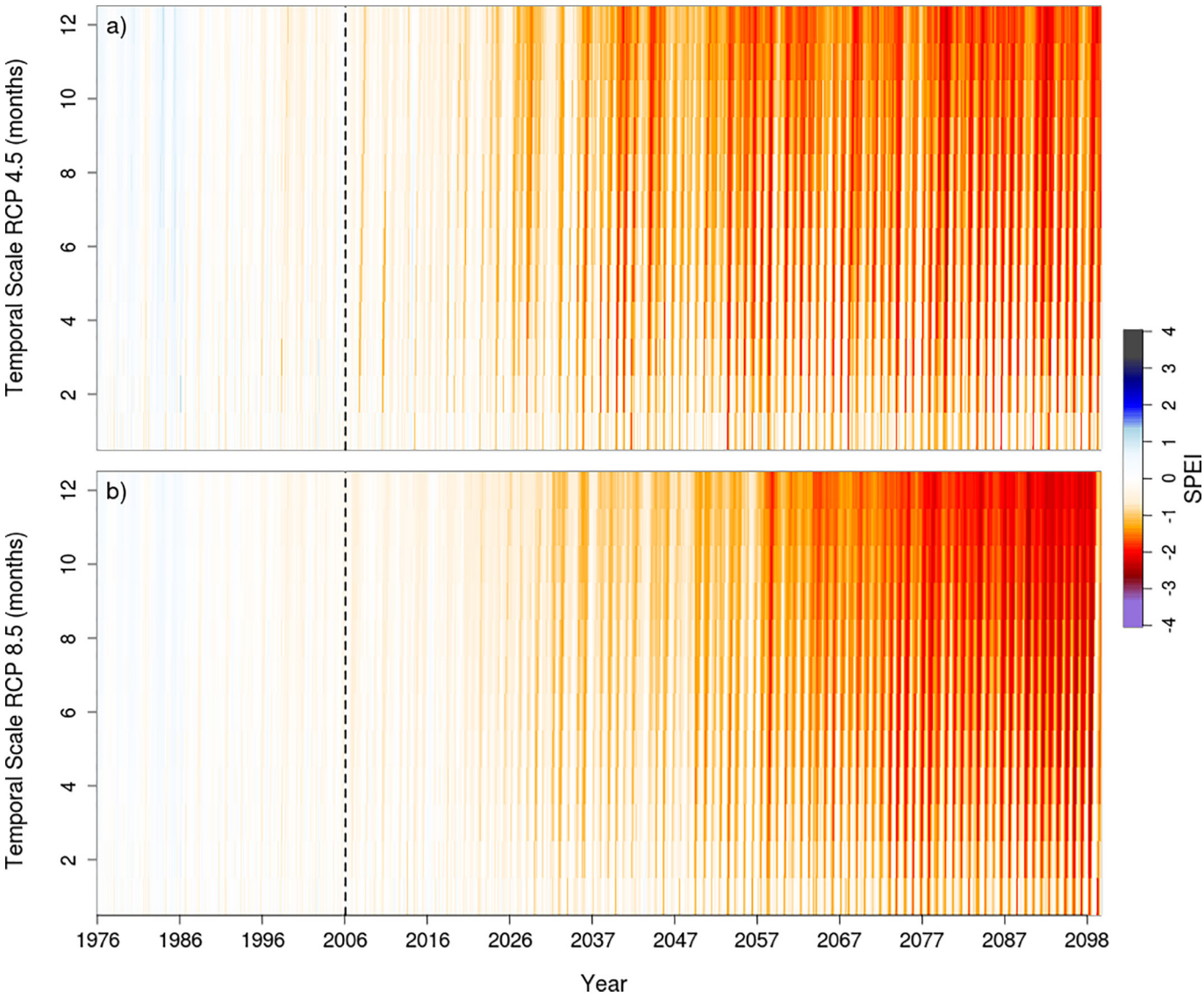

Fig. 6. SPEI Time series under RCP4.5 and RCP8.5 along the 21st century at time-scales from 1 to 12 months. Data grouped for every RCP simulation of every global climate model and for every station. Both emissions scenarios are represented: RCP4.5 (figure a) and RCP8.5 (figure b).

In this study, climate change scenarios of drought indexes for the region of Aragon, Spain, based on nine ESMs corresponding to CMIP5 have been generated for the first time.

The evolution of two indexes, SPI and SPEI, has been obtained throughout this century and also over the territory, which has allowed us to observe that while SPI, which only considers precipitation, shows few changes, SPEI, that considers temperature and incorporates the effects of AED, shows a tendency towards periods of increasingly intense drought, especially when considering accumulated periods of longer duration and those at the end of the century. Therefore, in the current climate change context it is essential to take into account the effect of temperature in the study of droughts.

Figs. 6 and 7 represent a novel representation of the evolution of drought, allowing identification, simultaneously, of the intensity of the episodes and their duration in different periods of accumulation.

One of the strengths of this study is the use of local climate scenarios (at the observatory level) to generate future drought indexes. Having this information will facilitate decision-making in the face of expected changes based on what is expected to occur at each observatory and not in the region a whole. As an example of the study at local level, the results of future climate scenarios for Zaragoza (representative observatory of Aragon, Roldán et al., 2011) and Cedrillas-Huesca (Support information) are shown.

4.1. Precipitation scenarios used for the simulation of drought indexes

For the simulation of precipitation, ESMs have been used instead of climatic models. ESMs are the most powerful climatic models to date and incorporate significant improvements (Flato et al., 2014) that allow better accuracy in climate simulation, as can be seen in the good results obtained in the validation process.

Validation of the ESMs has shown good results for simulating precipitation. Both the obtained bias and standard deviation are less than ± 1 mm/day, which in relative terms supposes differences of less than or around $\pm 10\%$ in the worst cases; however, those values are within the order of natural variability of precipitation. These results are better than those obtained for the generation of scenarios of the fourth IPCC report published by (Ribalaygua et al., 2013a) particularly in the summer months, a particularly critical time in Aragon.

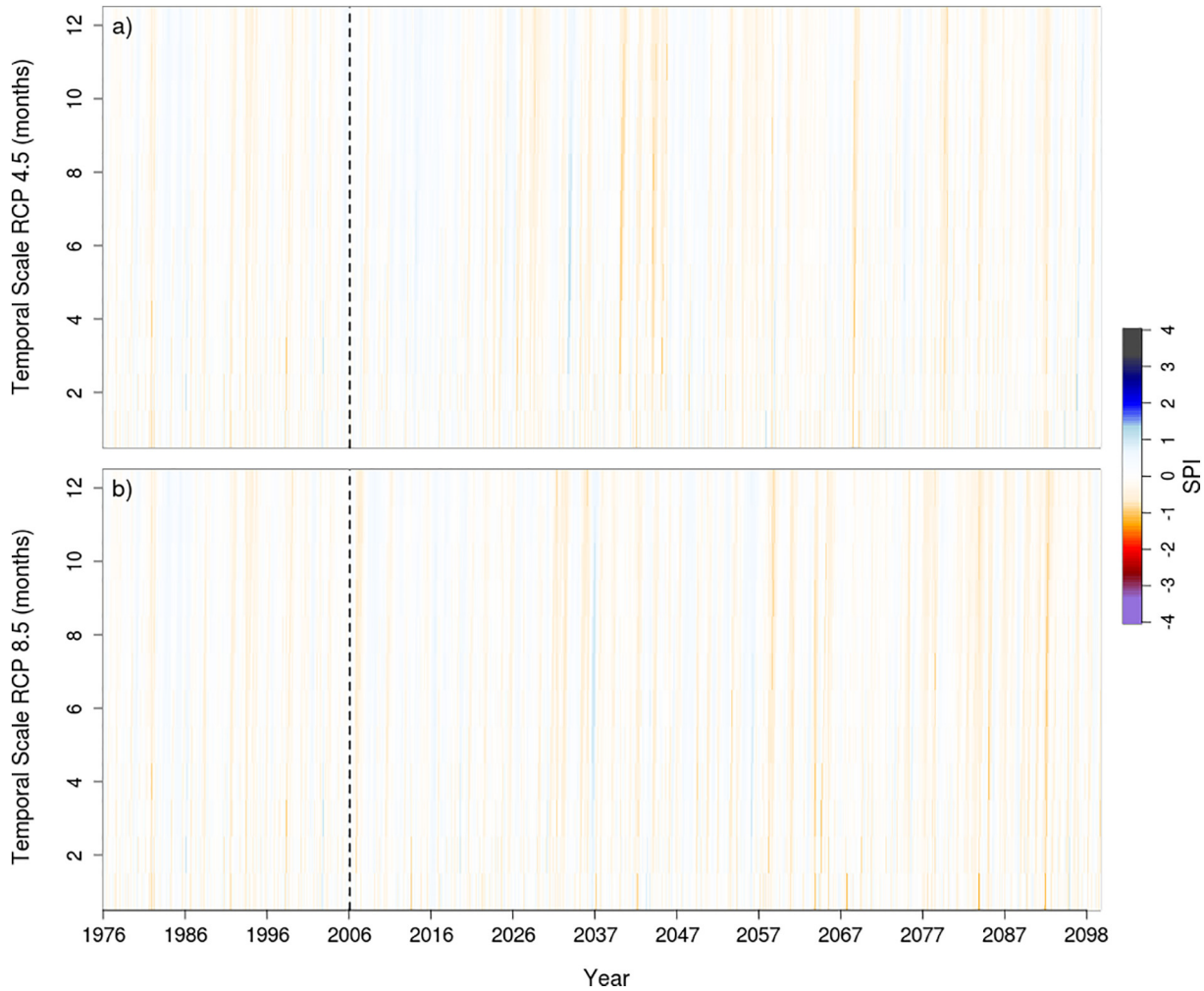

Fig. 7. SPI Time series under RCP4.5 and RCP8.5 along the 21st century at time-scales from 1 to 12 months. Data grouped for every RCP simulation of every global climate model and for every station. Both emissions scenarios are represented: RCP4.5 (figure a) and RCP8.5 (figure b).

The results obtained for the processes of verification of the methodology (Ribalaygua et al., 2013a) and validation of the ESMs are good enough to allow the use of local climatic scenarios generated under these conditions in impact studies and analysis of extreme episodes such as periods of precipitation shortage.

Future precipitation scenarios show, under RCP8.5 conditions, a slight decrease in precipitation throughout the 21st century for all seasons of the year, except for the summer months where there is hardly any variation compared to current values of precipitation in the region. Under RCP4.5 conditions, less pessimistic than the previous one, barely any precipitation changes are expected at any time of the year.

These results are consistent with those published by AEMET (www.aemet.es) and directly by the IPCC (Mukherjee et al., 2018), although the latter show the direct outputs of the ESMs and do not carry the added value of applying downscaling techniques.

4.2. Consideration of the simulation of drought indexes

SPI is considered by experts in this field as one of the few indexes applicable in any region of the world for any time scale (Hayes et al., 2011) and with multiple advantages of application compared to other indexes of widespread use such as PDSI (Dracup et al., 1980; Guttman, 1998; Hayes et al., 2011; Hayes et al., 1999; Vicente-Serrano et al., 2010b). In the context of climate change with significant temperature variations (Gaitan et al., 2019), SPEI has been chosen; its formulation is similar to that of SPI and allows the comparison of both indexes and evaluation of the future behaviour of drought episodes considering the effects of future temperature changes. Both indexes have been verified and used previously in Aragon (Vicente-Serrano et al., 2010a). We have only used the temperature in the calculation of AED because the absence of observed historical data of variables such as radiation or humidity does not allow us a correct validation process of certain indices such as Penman that include these variables.

4.2.1. Verification results

In general, the results of the verification process show good correlations between the observed and simulated time series for both indexes for the period 1970–2000, higher ones being obtained for SPEI. This is consistent with the results published by Vicente-Serrano (2013); they obtained higher correlations for the calculation of SPEI than SPI, especially for the summer months, which are the most critical in the region of Aragon.

The temporal series based on observations are satisfactorily represented by the temporal series based on simulations, recreating almost all dry and wet episodes of importance. It is observed how both the simulated SPI and SPEI tend, for the majority of times, to present dry and humid periods of greater intensity than those observed, especially for longer time scales, as occurred in 1976–1977 for positive

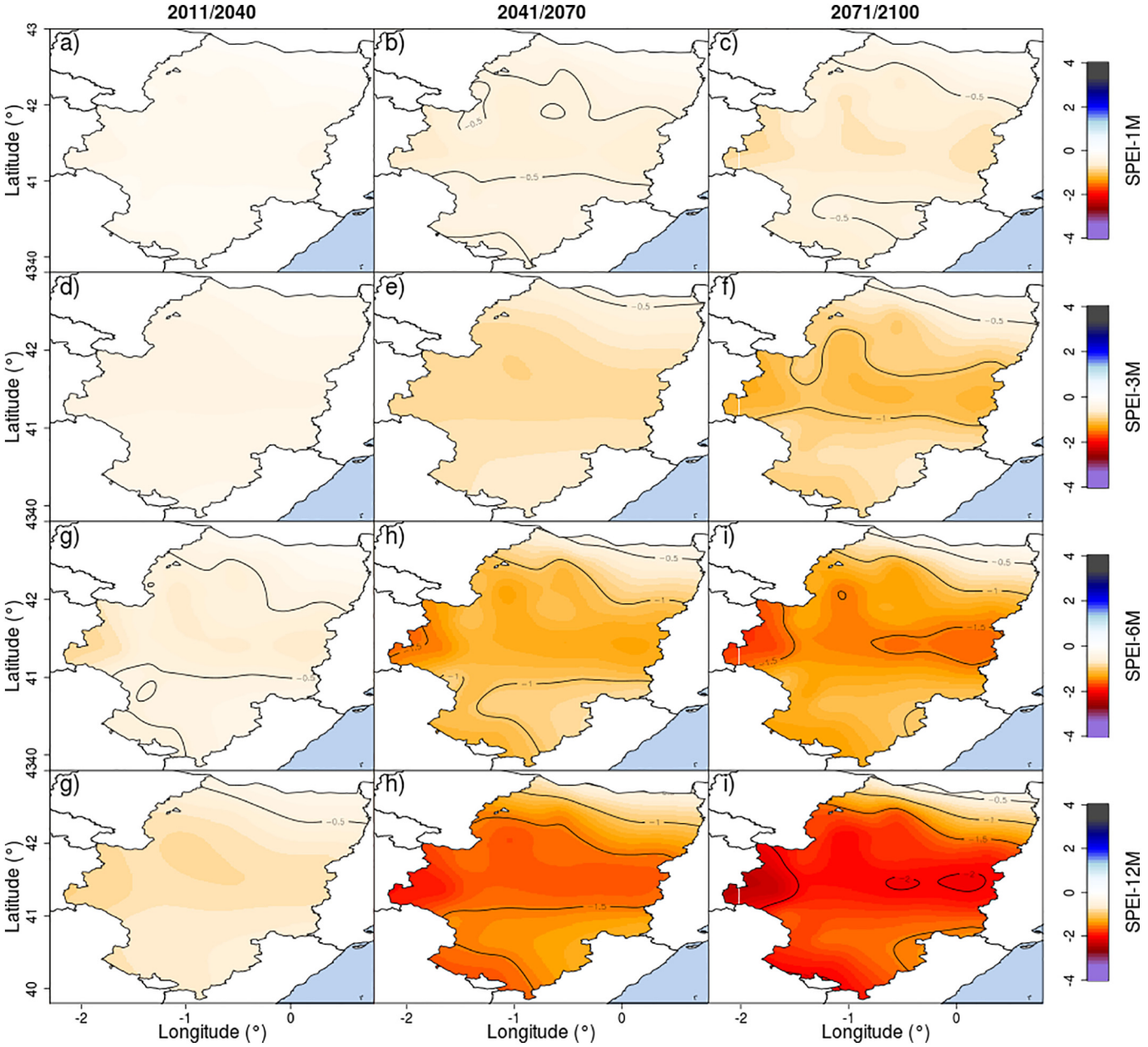

Fig. 8. Time-scales SPEI maps under RCP4.5. Geographical representation of the expected evolution of the SPEI for Aragon in the periods 2041–2070 and 2071–2100 compared to the reference Historical Period (1971–2000) in terms of absolute values according to the RCP4.5 at different time-scales. The rows show the four time-scales analysed in the study (1 months, 3 months, 6 months and 12 months) and the columns, the three temporal periods (2011–2040, 2041–2070 and 2071–2100). The maps are generated by interpolating the available stations over the territory.

values of the indexes and in 1981–1982 for negative ones. In general, the number of months of the period 1970–2000 located within each of the classes defined for SPI/SPEI has been simulated very satisfactorily.

The dry and wet periods detected in this study coincide with or are approximate to those published previously (Vicente-Serrano and Lopez-Moreno, 2005) based on SPI (dry episodes: 1986–1987, 1989 and 1994–1997; wet episodes: 1976–1980), in the Climate Atlas of Aragon (López et al., 2007) based on the precipitation regime (dry episodes: 1970, 1985, 1993 and 1995), by Spinoni (Spinoni et al., 2015) based on a combined 12-month index (dry episodes: 1979–1980 and 1995–1998) and by Tselepidaki (Tselepidaki et al., 1992) from a European study (dry episode: 1989), among others. In some cases, the years are not exactly the same because of the use of different drought and temporal scale indexes.

4.2.2. Future scenarios

The uncertainties associated with both processes, verification and validation, should be considered when interpreting future scenarios. For drought projections the focus should be on changes in the frequency and magnitude of cases located at the lower tail of the distribution as was recommended by Vicente-Serrano et al. (2019).

Future meteorological drought scenarios based on SPI barely show water balance variations with respect to normal values, regardless of the time scale considered and the region of Aragon, except for the Ebro Valley where there is a slight sign of drought at the end of the 21st century and under the conditions of RCP8.5.

These results were expected due to precipitation scenarios barely showing changes throughout the 21st century.

When considering other climatic variables, such as temperature, the drought scenarios based on SPEI show a clear trend towards

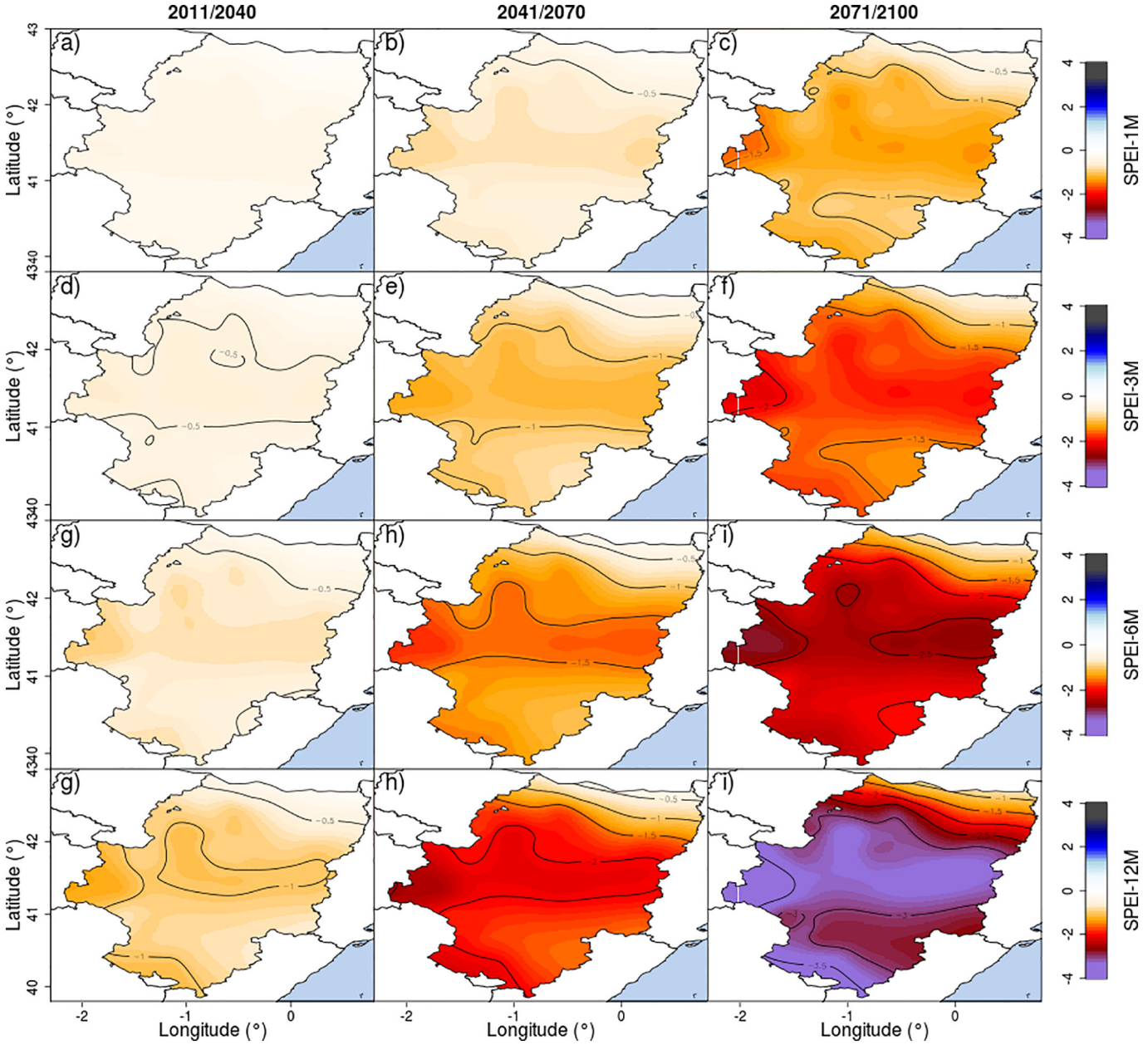

Fig. 9. Time-scales SPEI maps under RCP8.5. Geographical representation of the expected evolution of the SPEI for Aragon in the periods 2041–2070 and 2071–2100 compared to the reference Historical Period (1971–2000) in terms of absolute values according to the RCP8.5 at different time-scales. The rows show the four time-scales analysed in the study (1 months, 3 months, 6 months and 12 months) and the columns the three temporal periods (2011–2040, 2041–2070 and 2071–2100). The maps are generated by interpolating the available stations over the territory.

increasingly dry periods and longer droughts, especially in the Ebro area and south-west of the region. According to the trends shown by the temperature and precipitation scenarios obtained for Aragon, the results obtained were expected. The fact that the results obtained at the 12-month scale are more intense than those of 1–3 months is partly a result of the way in which drought indices are formulated and the autoregressive component of its metric so that when the timescale increases, changes in the frequency of drought conditions increase more in comparison to changes in the mean state. Although, recently, Vicente-Serrano et al. (2019) showed that these changes are independent of the metric with which these indices have been calculated, changes in the frequency of drought conditions increase more in comparison to changes in the mean state.

The lack of consideration of variables such as temperature, wind or humidity in the calculation of SPI means that this index presents certain limitations under global warming conditions(Mishra and Singh, 2010; Mishra and Singh, 2011; Vicente-Serrano et al., 2010a) and it is for this reason that, when considering AED in the calculation of SPEI, such different results are obtained, especially at the end of the century and not only under the conditions of RCP8.5, that some authors consider less realistic (Hausfather and Peters, 2020), but also of RCP4.5.

Some studies recommend the use of PET and add value against global warming (Hu and Willson, 2000; Vicente-Serrano et al., 2010a, Tsakiris and Vangelis, 2005). Recent studies (Vicente-Serrano et al., 2019; Vicente-Serrano et al., 2020) suggest using AED in the future study of droughts, as well as analyzing the impact caused by the increase in CO_2 (Yang et al., 2019). Probably, considering the response that vegetation could have to an increase in CO_2 and, therefore, in the evapotranspiration process, could provide some variation in the future evolution of drought episodes that should be explored in future studies.

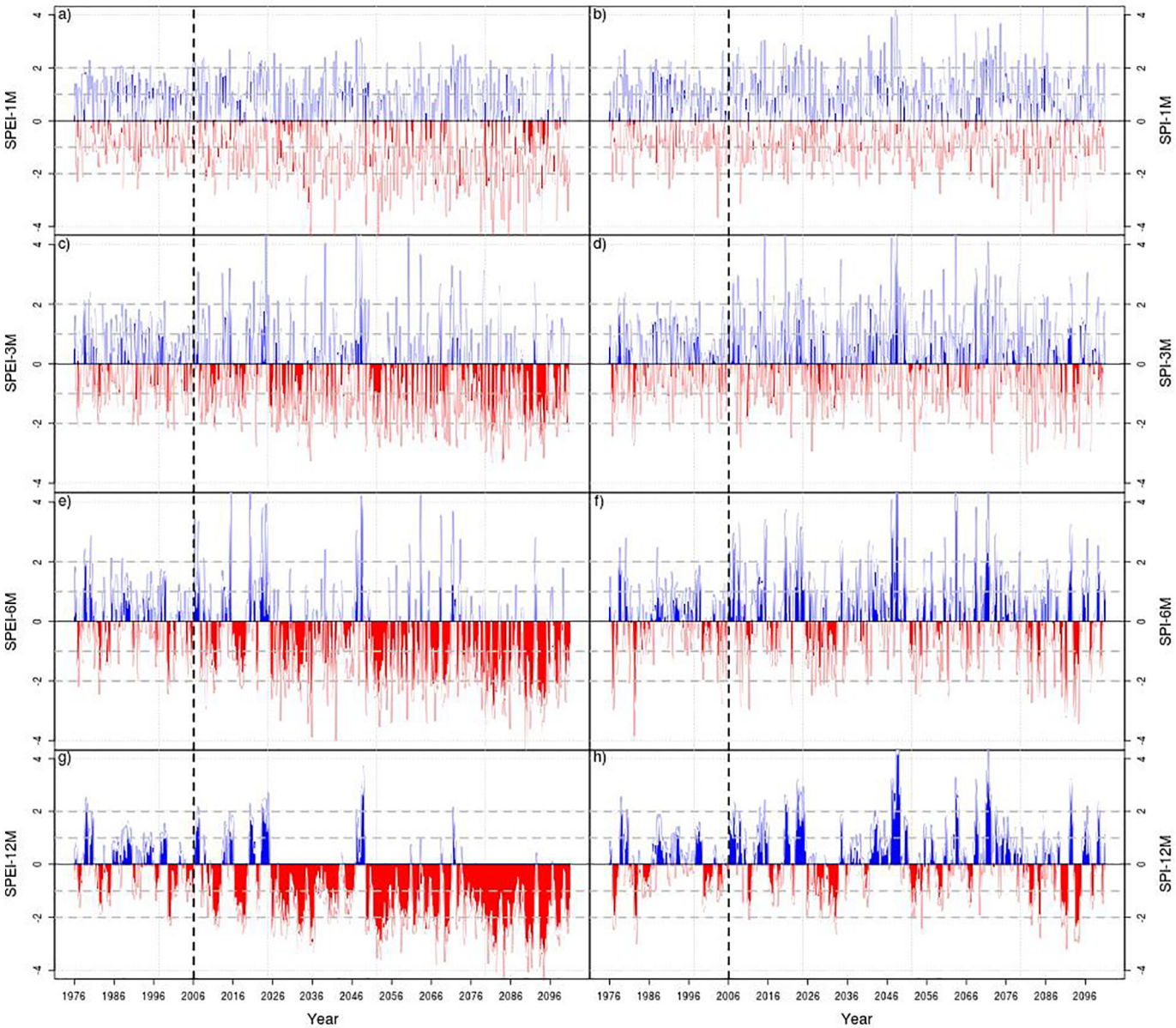

Fig. 10. Time series for Zaragoza under MPI-ESM-MR RCP4.5. Evolution of the SPEI (first column) and the SPI (second column) based on the MPI-MR-SM model and under the RCP 4.5 at different time-scales - 1 month (first row), 3 months (second row), 6 months (third row) and 12 months (fourth row)- for Zaragoza.

The results of future drought scenarios presented here show results in line with those obtained in other studies where it is concluded that the Mediterranean regions will experience an increase in the severity and frequency of droughts (Stagge et al., 2015) as a result of a slight decrease in precipitation and an abrupt increase in temperatures (EEA, 2010; Stagge et al., 2015) and which represent an increase in water scarcity (Estrela et al., 2012). More specifically in the region of Aragon, the ECCE project, based on dynamic downscaling and scenarios of the fourth IPCC report (Ministerio de Medio Ambiente, 2005), showed a future decline of the Ebro runoff, and Cook (Cook et al., 2014), based on scenarios of the fifth IPCC report but without downscaling, obtained an increase in drought episodes based on SPEI.

4.2.3. Impact on the territory

Although there have been studies on the Aragon area, none present as complete a picture as this study, combining drought evaluation with SPI and SPEI (that is, considering the effect of global warming) based on scenarios of the fifth IPCC report and providing the added value of working at the local scale by applying a downscaling technique.

The scenarios obtained in this study indicate that the Ebro Valley, the most populated area in the region that includes the largest city, Zaragoza with >650.000 people, will be most susceptible to future periods of extreme drought and will suffer periods of drought of greater intensity and duration, especially at the end of this century, which will have consequences in sectors such as health, water management, economy and society in general (Lee et al., 2017).

It is remarkable that, in previous publications (Ribalaygua et al., 2013a), we detected that the highest values of maximum temperature, especially at the end of the century and in summer (around 40 °C) as well as the greatest intensity of heatwaves will also take place in this area, so it will be especially vulnerable and these data should be considered in the development of specific measures for adapting to climate change.

Adaptation to climate change in each region requires studies applied to the climatic dynamics of each territory, so downscaling quality

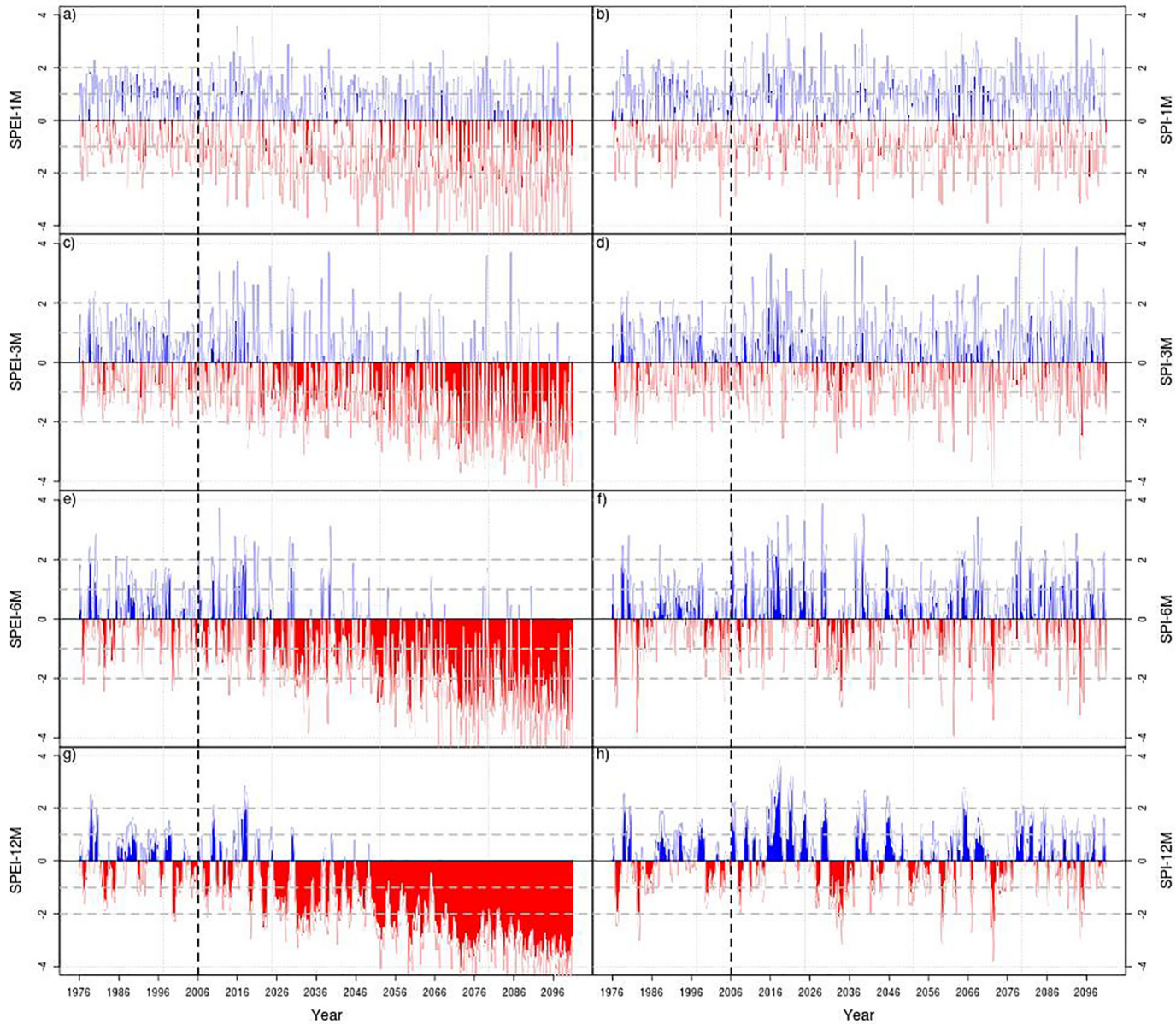

Fig. 11. Time series for Zaragoza under MPI-ESM-MR RCP8.5. Evolution of the SPEI (first column) and the SPI (second column) based on the MPI-MR-SM model and under the RCP 8.5 at different time-scales - 1 month (first row), 3 months (second row), 6 months (third row) and 12 months (fourth row)- for Zaragoza.

studies are essential for this. However, these results at the local level are also useful for the whole of the southern Iberian Peninsula and central Europe, since Aragon brings together geographical and climatic features representative also of these other areas.

5. Conclusions

The generation for the first time of climate change scenarios of drought indexes for the region of Aragon (Spain) based on nine ESMs and two RCPs from CMIP5 has allowed us to obtain simultaneously the most accurate representation to date of the magnitude, duration and intensity of meteorological drought episodes and their duration in different periods of accumulation in this area of Spain. The use of different drought indices and drought time-scales and its graphic representation is a relevant novelty in the scientific literature.

This has allowed the detection of a clear trend towards increasingly intense periods of drought, especially at the end of the century when cumulative periods of longer duration are considered. This trend is detected only in the future drought scenarios based on SPEI (which in addition to precipitation, considers AED), while in the SPI-based scenarios it is softened. These results reinforce the need to study these extreme phenomena in a context of climate change, considering the temperature.

At the territory level, spatial representation allowed us to discover that the area that will be most affected by longer and more intense periods of drought, but also the greatest decrease in precipitation (around 10%), is the Ebro Valley, the area that concentrates most of the population as well as the main economic activities of the zone. The results have also allowed, for the first time, the study of future drought indexes at the observatory level, specifically for the most populous city, Zaragoza.

To cope effectively with the impacts of these extreme events that are expected in the present century, it is essential to be able to generate local scenarios that accurately describe climate change at the territory level. On the one hand, our results not only confirm a trend already

described in the Mediterranean area of an increase in the severity and frequency of droughts but can also serve as a model and sentinel for similar areas, since it has very varied climatic and orographic conditions.

Declaration of competing interest

The authors declare that they have no known competing financial interests or personal relationships that could have appeared to influence the work reported in this paper.

Appendix A. Supplementary data

Supplementary data to this article can be found online at https://doi.org/10.1016/j.scitotenv.2020.140094.

References

Alary, V., Messad, S., Aboul-Naga, A., Osman, M.A., Daoud, I., Bonnet, P., et al., 2014. Livelihood strategies and the role of livestock in the processes of adaptation to drought in the Coastal Zone of Western Desert (Egypt). Agric. Syst. 128, 44–54.

Bates, B., Kundzewicz, Z., Wu, S., Palutikof, J., 2008. Climate Change and Water. IPCC Secretariat, Geneva (210 pp).

Begueria, S., Vicente-Serrano, S.M., Reig, F., Latorre, B., 2014. Standardized precipitation evapotranspiration index (SPEI) revisited: parameter fitting, evapotranspiration models, tools, datasets and drought monitoring. Int. J. Climatol. 34, 3001–3023.

Beniston, M., Stephenson, D.B., Christensen, O.B., Ferro, C.A.T., Frei, C., Goyette, S., et al., 2007. Future extreme events in European climate: an exploration of regional climate model projections. Clim. Chang. 81, 71–95.

Bentsen, M., Bethke, I., Debernard, J.B., Iversen, T., Kirkevag, A., Seland, O., et al., 2013. The Norwegian Earth System Model, NorESM1-M - part 1: description and basic evaluation of the physical climate. Geosci. Model Dev. 6, 687–720.

Berg, A., Sheffield, J., 2018. Climate change and drought: the soil moisture perspective. Current Climate Change Reports 4, 180–191.

Berg, A., Sheffield, J., Milly, P.C.D., 2017. Divergent surface and total soil moisture projections under global warming. Geophys. Res. Lett. 44, 236–244.

Blenkinsop, S., Fowler, H.J., 2007. Changes in European drought characteristics projected by the PRUDENCE regional climate models. Int. J. Climatol. 27, 1595–1610.

Bryant, E.A., 1993. Natural hazards. Int. J. Climatol. 13, 344–346. https://doi.org/10.1002/joc.3370130310 E. Cambridge University Press, Cambridge. ISBN 0 521 37295 X.

Burke, E.J., Brown, S.J., 2008. Evaluating uncertainties in the projection of future drought. J. Hydrometeorol. 9, 292–299.

Calbo, J., 2010. Possible climate change scenarios with specific reference to Mediterranean regions. In: Sabater, S., Barcelo, D. (Eds.), Water Scarcity in the Mediterranean: Perspectives Under Global Change. 8, pp. 1–13.

Carvalho, D., Rocha, A., Gomez-Gesteira, M., Santos, C.S., 2017. Potential impacts of climate change on European wind energy resource under the CMIP5 future climate projections. Renew. Energy 101, 29–40.

Chen, Y.D., Li, J.F., Zhang, Q., 2016. Changes in site-scale temperature extremes over China during 2071-2100 in CMIP5 simulations. J. Geophys. Res.-Atmos. 121, 2732–2749.

Cherlet, M., Hutchinson, C., Reynolds, J., Hill, J., Sommer, S., von Maltitz, G. (Eds.), 2018. World Atlas of Desertification. Publication Office of the European Union, Luxembourg (United Nations Environment Program).

Chylek, P., Li, J., Dubey, M., Wang, M., Lesins, G., 2011. Observed and model simulated 20th century Arctic temperature variability: Canadian Earth System Model CanESM2. Atmos. Chem. Phys. Discuss. 11, 22893–22907. https://doi.org/10.5194/acpd-11-22893-2011.

Collados-Lara, A.J., Pulido-Velazquez, D., Pardo-Iguzquiza, E., 2018. An integrated statistical method to generate potential future climate scenarios to analyse droughts. Water 10.

Collins, W., Bellouin, N., Doutriaux-Boucher, M., Gedney, N., Hinton, T., Jones, C.D., Liddicoat, S., Martin, G., O'Connor, F., Rae, J., Senior, C., Totterdell, I., Woodward, S., Reichler, T., Kim, J., Halloran, P., 2008. Evaluation of the HadGEM2 Model. Hadley Centre Technical Note. HCTN 74. Met Office Hadley Centre, Exeter, UK.

Cook, B.I., Smerdon, J.E., Seager, R., Coats, S., 2014. Global warming and 21st century drying. Clim. Dyn. 43, 2607–2627.

Dai, A.G., 2011. Drought under global warming: a review. Wiley Interdisciplinary Reviews-Climate Change 2, 45–65.

Dai, A.G., 2013. Increasing drought under global warming in observations and models (vol 3, pg 52, 2013). Nat. Clim. Chang. 3, 171.

Dai, A.G., Zhao, T.B., Chen, J., 2018. Climate change and drought: a precipitation and evaporation perspective. Current Climate Change Reports 4 (3), 301–312. https://doi.org/10.1007/s40641-018-0101-6 Sep.

Dracup, J.A., Lee, K.S., Paulson, E.G., 1980. On the statistical characteristics of drought events. Water Resour. Res. 16, 289–296.

Dunne, J.P., John, J.G., Adcroft, A.J., Griffies, S.M., Hallberg, R.W., Shevliakova, E., et al., 2012. GFDL'sESM2global coupled climate carbon Earth System Models. PartI:physical formulation and baseline simulation characteristics. J. Clim. 25, 6646–6665.

EEA, 2010. The European environment: State and outlook 2010: Thematic assessment – Adapting to Climate Change. European Environment Agency, Copenhagen http://www.eea.europa.eu/soer/europe/adapting-to-climate-change.

Estrela, T., Perez-Martin, M.A., Vargas, E., 2012. Impacts of climate change on water resources in Spain. Hydrological Sciences Journal-Journal Des Sciences Hydrologiques 57, 1154–1167.

Feyen, L., Dankers, R., 2009. Impact of global warming on streamflow drought in Europe. J. Geophys. Res.-Atmos. 114.

Flato, G., Marotzke, J., Abiodun, B., Braconnot, P., Chou, S.C., Collins, W., et al., 2014. Evaluation of Climate Models.

Forzieri, G., Feyen, L., Rojas, R., Florke, M., Wimmer, F., Bianchi, A., 2014. Ensemble projections of future streamflow droughts in Europe. Hydrol. Earth Syst. Sci. 18, 85–108.

Fragoso, M., Carraca, M.D., Alcoforado, M.J., 2018. Droughts in Portugal in the 18th century: a study based on newly found documentary data. Int. J. Climatol. 38, 5522–5541.

Gaitan, E., Monjo, R., Portoles, J., Pino-Otin, M.R., 2019. Projection of temperatures and heat and cold waves for Aragon (Spain) using a two-step statistical downscaling of CMIP5 model outputs. Sci. Total Environ. 650, 2778–2795.

Gallego, M.C., Trigo, R.M., Vaquero, J.M., Brunet, M., Garcia, J.A., Sigro, J., et al., 2011. Trends in frequency indices of daily precipitation over the Iberian Peninsula during the last century. J. Geophys. Res.-Atmos. 116.

Garcia-Barron, L., Aguilar, M., Sousa, A., 2011. Evolution of annual rainfall irregularity in the southwest of the Iberian Peninsula. Theor. Appl. Climatol. 103, 13–26.

Guttman, N.B., 1998. Comparing the Palmer Drought Index and the standardized precipitation index. J. Am. Water Resour. Assoc. 34, 113–121.

Hao, Z.C., Hao, F.H., Singh, V.P., Ouyang, W., 2017. Quantitative risk assessment of the effects of drought on extreme temperature in eastern China. J. Geophys. Res.-Atmos. 122, 9050–9059.

Hargreaves, G.L., Samani, Z.A., 1985. Reference crop evapotranspiration from temperature. Appl. Eng. Agric. 1985 (1), 96–99.

Hausfather, Z., Peters, G.P., 2020. Emissions - the 'business as usual' story is misleading. Nature 577, 618–620.

Hayes, M., Svoboda, M., Wall, N., Widhalm, M., 2011. The Lincoln Declaration on Drought Indices. Bull. Am. Meteorol. Soc. 92, 485–488.

Hayes, M.J., Svoboda, M.D., Wilhite, D.A., Vanyarkho, O.V., 1999. Monitoring the 1996 drought using the standardized precipitation index. Bull. Am. Meteorol. Soc. 80, 429–438.

Heavens, N., Ward, D., Natalie, M., 2013. Studying and projecting climate change with Earth System Models. Nat. Educ. Knowl. 4 (5), 4.

Hoerling, M., Eischeid, J., Perlwitz, J., Quan, X.W., Zhang, T., Pegion, P., 2012. On the increased frequency of Mediterranean drought. J. Clim. 25, 2146–2161.

Hu, Q., Willson, G.D., 2000. Effects of temperature anomalies on the Palmer Drought Severity Index in the central United States. Int. J. Climatol. 20, 1899–1911.

Iglesias, A., Garrote, L., Flores, F., Moneo, M., 2007. Challenges to manage the risk of water scarcity and climate change in the Mediterranean. Water Resour. Manag. 21, 775–788.

IPCC, 2014. Climate change 2014: impacts, adaptation, and vulnerability. Part A: global and sectoral aspects. Contribution of Working Group II to the Fifth Assessment Report of the Intergovernmental Panel on Climate Change. Cambridge University Press, Cambridge, United Kingdom and New York, NY, USA, p. 1132.

Irmak, S., Kabenge, I., Skaggs, K.E., Mutiibwa, D., 2012. Trend and magnitude of changes in climate variables and reference evapotranspiration over 116-yr period in the Platte River Basin, central Nebraska-USA. J. Hydrol. 420, 228–244.

Iversen, T., Bentsen, M., Bethke, I., Debernard, J.B., Kirkevag, A., Seland, O., et al., 2013. The Norwegian Earth System Model, NorESM1-M - part 2: climate response and scenario projections. Geosci. Model Dev. 6, 389–415.

Jensen, M.E., Haise, H.R., 1963. Estimating evapotranspiration from solar radiation. J. Irrig. Drain. Div. 89, 15–41.

Jones, C.D., Hughes, J.K., Bellouin, N., Hardiman, S.C., Jones, G.S., Knight, J., et al., 2011. The HadGEM2-ES implementation of CMIP5 centennial simulations. Geosci. Model Dev. 4, 543–570.

Knutti, R., Sedlacek, J., 2013. Robustness and uncertainties in the new CMIP5 climate model projections. Nat. Clim. Chang. 3, 369–373.

Lavaysse, C., Vrac, M., Drobinski, P., Lengaigne, M., Vischel, T., 2012. Statistical downscaling of the French Mediterranean climate: assessment for present and projection in an anthropogenic scenario. Nat. Hazards Earth Syst. Sci. 12, 651–670.

Lee, S.H., Yoo, S.H., Choi, J.Y., Bae, S., 2017. Assessment of the impact of climate change on drought characteristics in the Hwanghae Plain, North Korea using time series SPI and SPEI: 1981-2100. Water 9.

Lesk, C., Rowhani, P., Ramankutty, N., 2016. Influence of extreme weather disasters on global crop production. Nature 529, 84.

Livneh, B., Hoerling, M.P., 2016. The physics of drought in the US Central Great Plains. J. Clim. 29, 6783–6804.

Lloyd-Hughes, B., Saunders, M.A., 2002. A drought climatology for Europe. Int. J. Climatol. 22, 1571–1592.

López, F., Cabrera, M., Cuadrat, J.M., 2007. Atlas Climático de Aragón. first ed. J. Factory, Spain.

Lopez-Bustins, J.A., Pascual, D., Pla, E., Retana, J., 2013. Future variability of droughts in three Mediterranean catchments. Nat. Hazards 69, 1405–1421.

Machado, M.J., Benito, G., Barriendos, M., Rodrigo, F.S., 2011. 500 Years of rainfall variability and extreme hydrological events in southeastern Spain drylands. J. Arid Environ. 75, 1244–1253.

Marcos-Garcia, P., Lopez-Nicolas, A., Pulido-Velazquez, M., 2017. Combined use of relative drought indices to analyze climate change impact on meteorological and hydrological droughts in a Mediterranean basin. J. Hydrol. 554, 292–305.

Marsland, S.J., Haak, H., Jungclaus, J.H., Latif, M., Roske, F., 2003. The Max-Planck-Institute global ocean/sea ice model with orthogonal curvilinear coordinates. Ocean Model 5, 91–127.
Mckee, T., Doesken, N., Kleist, J., 1993. The relationship of drought frequency and duration times scales. 8th Conference on Applied Climatology. American Meteorological Society, Anaheim, California, pp. 179–184 January 17–22.
McVicar, T.R., Roderick, M.L., Donohue, R.J., Li, L.T., Van Niel, T.G., Thomas, A., et al., 2012a. Global review and synthesis of trends in observed terrestrial near-surface wind speeds: implications for evaporation. J. Hydrol. 416, 182–205.
McVicar, T.R., Roderick, M.L., Donohue, R.J., Van Niel, T.G., 2012b. Less bluster ahead? Ecohydrological implications of global trends of terrestrial near-surface wind speeds. Ecohydrology 5, 381–388.
Ministerio de Medio Ambiente, 2005. Assessment Report of the Preliminary Impacts in Spain Due to Climate Change. Centro de publicaciones del Ministerio de Medio Ambiente, Madrid.
Mishra, A.K., Singh, V.P., 2010. A review of drought concepts. J. Hydrol. 391, 204–216.
Mishra, A.K., Singh, V.P., 2011. Drought modeling - a review. J. Hydrol. 403, 157–175.
Monjo, R., Gaitan, E., Portoles, J., Ribalaygua, J., Torres, L., 2016. Changes in extreme precipitation over Spain using statistical downscaling of CMIP5 projections. Int. J. Climatol. 36, 757–769.
Moss, R.H., Edmonds, J.A., Hibbard, K.A., Manning, M.R., Rose, S.K., van Vuuren, D.P., et al., 2010. The next generation of scenarios for climate change research and assessment. Nature 463, 747–756.
Moutahir, H., Bellot, P., Monjo, R., Bellot, J., Garcia, M., Touhami, I., 2017. Likely effects of climate change on groundwater availability in a Mediterranean region of Southeastern Spain. Hydrol. Process. 31, 161–176.
Mukherjee, S., Mishra, A., Trenberth, K.E., 2018. Climate change and drought: a perspective on drought indices. Current Climate Change Reports 4, 145–163.
Nychka D, Furrer R, Paige J, Sain S, 2015. Fields: tools for spatial data. R package version 9.0. (URL: https://doi.org/10.5065/D6W957CT). www.image.ucar.edu/fields.
Ojeda, M.G.V., Gamiz-Fortis, S.R., Castro-Diez, Y., Esteban-Parra, M.J., 2017. Evaluation of WRF capability to detect dry and wet periods in Spain using drought indices. J. Geophys. Res.-Atmos. 122, 1569–1594.
Organization WMO, 2012. In: Svoboda, M., Hayes, M., Wood, D. (Eds.), Standardized Precipitation Index User Guide. WMO, Geneva.
Palmer, W., 1965. «Meteorological Drought». Research Paper No. 45. U.S. Department of Commerce Weather Bureau febrero de. (58 páginas). Available in National Climatic Data Center de NOAA. http://www.ncdc.noaa.gov/temp-and-precip/drought/docs/palmer.pdf.
Paparrizos, S., Maris, F., Weiler, M., Matzarakis, A., 2018. Analysis and mapping of present and future drought conditions over Greek areas with different climate conditions. Theor. Appl. Climatol. 131, 259–270.
Perez, J., Menendez, M., Mendez, F.J., Losada, I.J., 2014. Evaluating the performance of CMIP3 and CMIP5 global climate models over the north-east Atlantic region. Clim. Dyn. 43, 2663–2680.
R Development Core Team, 2010. R: A Language and Environment for Statistical Computing. R Foundation for Statistical Computing, Vienna, Austria 3-900051-07-0. http://www.R-project.org (Accessed date: 6 July 2011).
Raddatz, T.J., Reick, C.H., Knorr, W., Kattge, J., Roeckner, E., Schnur, R., et al., 2007. Will the tropical land biosphere dominate the climate-carbon cycle feedback during the twenty-first century? Clim. Dyn. 29, 565–574.
Rebetez, M., Mayer, H., Dupont, O., Schindler, D., Gartner, K., Kropp, J.P., et al., 2006. Heat and drought 2003 in Europe: a climate synthesis. Ann. For. Sci. 63, 569–577.
Ribalaygua, J., Rosa Pino, M., Portoles, J., Roldan, E., Gaitan, E., Chinarro, D., et al., 2013a. Climate change scenarios for temperature and precipitation in Aragon (Spain). Sci. Total Environ. 463, 1015–1030.
Ribalaygua, J., Torres, L., Portoles, J., Monjo, R., Gaitan, E., Pino, M.R., 2013b. Description and validation of a two-step analogue/regression downscaling method. Theor. Appl. Climatol. 114, 253–269.
Ribalaygua, J., Gaitan, E., Portoles, J., Monjo, R., 2018. Climatic change on the Gulf of Fonseca (Central America) using two-step statistical downscaling of CMIP5 model outputs. Theor. Appl. Climatol. 132, 867–883.
Roderick, M.L., Greve, P., Farquhar, G.D., 2015. On the assessment of aridity with changes in atmospheric CO2. Water Resour. Res. 51 (7), 5450–5463. https://doi.org/10.1002/2015wr017031 Jul.
Rodriguez, R., Navarro, X., Casas, M.C., Ribalaygua, J., Russo, B., Pouget, L., et al., 2014. Influence of climate change on IDF curves for the metropolitan area of Barcelona (Spain). Int. J. Climatol. 34, 643–654.
Roldán, E., Gómez, M., Pino-Otín, R., Esteban, M., Díaz, J., 2011. Determinación de zonas isotérmicas y selección de estaciones meteorológicas representativas en Aragón como base para la estimación del impacto del cambio climático sobre la posible relación entre mortalidad y temperatura. Rev Esp Salud Pública 85, 457–469.
Santiago, J.M., Munoz-Mas, R., Solana-Gutierrez, J., de Jalon, D.G., Alonso, C., Martinez-Capel, F., et al., 2017. Waning habitats due to climate change: the effects of changes in streamflow and temperature at the rear edge of the distribution of a cold-water fish. Hydrol. Earth Syst. Sci. 21.
Sheffield, J., Wood, E.F., 2008. Projected changes in drought occurrence under future global warming from multi-model, multi-scenario, IPCC AR4 simulations. Clim. Dyn. 31, 79–105.
Sheffield, J., Wood, E.F., Roderick, M.L., 2012. Little change in global drought over the past 60 years. Nature 491, 435.
Skaugen, T., Astrup, M., Roald, L.A., Forland, E., 2004. Scenarios of extreme daily precipitation for Norway under climate change. Nord. Hydrol. 35, 1–13.
Smith, M., Allen, R., Pereira, L., 1998. Revised FAO Methodology for Crop-water Requirements. Management of Nutrients and Water in Rainfed Arid and Semi-arid Areas. Proceedings of a Consultants Meeting. International Atomic Energy Agency (IAEA) (IAEA-TECDOC–1026. Ref. number: 29062763).
Sonmez, F.K., Komuscu, A.U., Erkan, A., Turgu, E., 2005. An analysis of spatial and temporal dimension of drought vulnerability in Turkey using the standardized precipitation index. Nat. Hazards 35, 243–264.
Spinoni, J., Naumann, G., Vogt, J.V., Barbosa, P., 2015. The biggest drought events in Europe from 1950 to 2012. Journal of Hydrology-Regional Studies 3, 509–524.
Stagge, J.H., Kohn, I., Tallaksen, L.M., Stahl, K., 2015. Modeling drought impact occurrence based on meteorological drought indices in Europe. J. Hydrol. 530, 37–50.
Stanke, C., Kerac, M., Prudhomme, C., Medlock, J., Murray, V., 2013. Health effects of drought: a systematic review of the evidence. PLoS Curr., 5 Jun 5. pii: ecurrents.dis.7a2cee9e980f91ad7697b570bcc4b004. https://doi.org/10.1371/currents.dis.7a2cee9e980f91ad7697b570bcc4b004.
Taylor, K.E., Stouffer, R.J., Meehl, G.A., 2012. An overview of CMIP5 and the experiment design. Bull. Am. Meteorol. Soc. 93, 485–498.
Thornthwaite, C., 1948. An approach toward a rational classification of climate. Geogr. Rev. 38, 55–94.
Tripathi, S., Srinivas, V.V., Nanjundiah, R.S., 2006. Dowinscaling of precipitation for climate change scenarios: a support vector machine approach. J. Hydrol. 330, 621–640.
Tsakiris, G., Vangelis, H., 2005. Establishing a drought index incorporating evapotranspiration. European Water 9 (10), 3–11 2005.
Tselepidaki, I., Zarifis, B., Asimakopoulos, D.N., 1992. Low precipitation over Greece during 1989–1990. Theor. Appl. Climatol. 46, 115–121.
Uppala, S.M., Kallberg, P.W., Simmons, A.J., Andrae, U., Bechtold, V.D., Fiorino, M., et al., 2005. The ERA-40 re-analysis. Q. J. R. Meteorol. Soc. 131, 2961–3012.
Van der Linden, P., Mitchell, J. (Eds.), 2009. ENSEMBLES: Climate Change and Its Impacts. Summary of Research and Results From the ENSEMBLES Project. Met Office Hadley Centre, FitzRoy Road, Exeter EX1 3PB, UK 160 pp.
Vicente-Serrano, S.M., 2013. In: Martínez, C.C.-L., Rodríguez, F.V. (Eds.), Spatial and Temporal Evolution of Precipitation Droughts in Spain in the Last Century in Adverse Weather in Spain. WCRP Spanish Committee, Madrid, Spain, pp. 283–296.
Vicente-Serrano, S.M., 2016. Foreword: drought complexity and assessment under climate change conditions. Cuadernos De Investigacion Geografica 42, 7–11.
Vicente-Serrano, S.M., Begueria, S., 2016. Comment on 'Candidate distributions for climatological drought indices (SPI and SPEI)' by James H. Stagge et al. Int. J. Climatol. 36, 2120–2131.
Vicente-Serrano, S.M., Lopez-Moreno, J.I., 2005. Hydrological response to different time scales of climatological drought: an evaluation of the Standardized Precipitation Index in a mountainous Mediterranean basin. Hydrol. Earth Syst. Sci. 9, 523–533.
Vicente-Serrano, S.M., Gonzalez-Hidalgo, J.C., de Luis, M., Raventos, J., 2004. Drought patterns in the Mediterranean area: the Valencia region (eastern Spain). Clim. Res. 26, 5–15.
Vicente-Serrano, S.M., Begueria, S., Lopez-Moreno, J.I., 2010a. A multiscalar drought index sensitive to global warming: the standardized precipitation evapotranspiration index. J. Clim. 23, 1696–1718.
Vicente-Serrano, S.M., Begueria, S., Lopez-Moreno, J.I., Angulo, M., El Kenawy, A., 2010b. A new global 0.5 degrees gridded dataset (1901–2006) of a multiscalar drought index: comparison with current drought index datasets based on the Palmer Drought Severity Index. J. Hydrometeorol. 11, 1033–1043.
Vicente-Serrano, S.M., Lasanta, T., Gracia, C., 2010c. Aridification determines changes in forest growth in Pinus halepensis forests under semiarid Mediterranean climate conditions. Agric. For. Meteorol. 150, 614–628.
Vicente-Serrano, S.M., Van der Schrier, G., Begueria, S., Azorin-Molina, C., Lopez-Moreno, J.I., 2015. Contribution of precipitation and reference evapotranspiration to drought indices under different climates. J. Hydrol. 526, 42–54.
Vicente-Serrano, S.M., Dominguez-Castro, F., McVicar, T.R., Tomas-Burguera, M., Pena-Gallardo, M., Noguera, I., et al., 2019. Global characterization of hydrological and meteorological droughts under future climate change: the importance of timescales, vegetation-CO2 feedbacks and changes to distribution functions. Int. J. Climatol. https://doi.org/10.1002/joc.6350.
Vicente-Serrano, S.M., McVicar, T.R., Miralles, D.G., Yang, Y.T., Tomas-Burguera, M., 2020. Unraveling the influence of atmospheric evaporative demand on drought and its response to climate change. Wiley Interdisciplinary Reviews-Climate Change 11.
Voldoire, A., Sanchez-Gomez, E., Melia, D.S.Y., Decharme, B., Cassou, C., Senesi, S., et al., 2013. The CNRM-CM5.1 global climate model: description and basic evaluation. Clim. Dyn. 40, 2091–2121.
Wang, B., Zhou, T.J., Yu, Y.Q., 2009. A view of earth system model development. Acta Meteorologica Sinica 23, 1–17.
Watanabe, S., Hajima, T., Sudo, K., Nagashima, T., Takemura, T., Okajima, H., et al., 2011. MIROC-ESM 2010: model description and basic results of CMIP5-20c3m experiments. Geosci. Model Dev. 4, 845–872.
Wilhite, D., 2000. Drought as a natural hazard: concepts and definitions. In: Wilhite, D.A. (Ed.), Droughts: Global Assessment. Routledge, London, pp. 3–18.
Wilhite, D.A., Glantz, M.H., 1985. Understanding the drought phenomenon: the role of definitions. Water Int. 10 (3), 111–120.
Willett, K.M., Dunn, R.J.H., Thorne, P.W., Bell, S., de Podesta, M., Parker, D.E., et al., 2014. HadISDH land surface multi-variable humidity and temperature record for climate monitoring. Clim. Past 10, 1983–2006.
WMO (World Meteorological Organization), 2017. Statement on the State of the Global Climate in 2016.N° 1189.2017. 978-92-63-11189-0.
Xiao-Ge, X., Tong-Wen, W., Jie, Z., 2013. Introduction of CMIP5 experiments carried out with the climate system models of Beijing Climate Center. Adv. Clim. Chang. Res. 4, 41–49. https://doi.org/10.3724/SP.J.1248.2013.041.

Yang, Y.T., Zhang, S.L., McVicar, T.R., Beck, H.E., Zhang, Y.Q., Liu, B., 2018. Disconnection between trends of atmospheric drying and continental runoff. Water Resour. Res. 54, 4700–4713.

Yang, Y.T., Roderick, M.L., Zhang, S.L., McVicar, T.R., Donohue, R.J., 2019. Hydrologic implications of vegetation response to elevated CO2 in climate projections. Nat. Clim. Chang. 9, 44.

Yukimoto, S., Yoshimura, H., Hosaka, M., Sakami, T., Tsujino, H., Hirabara, M., Tanaka, T., Deushi, M., Obata, A., Nakano, H., Adachi, Y., Shindo, E., Yabu, S., Ose, T., Kitoh, A., 2011. Meteorological research institute- earth system model v1 (MRI-ESM1)—model description. Technical Report of MRI. vol. 64.

Atmospheric Research 286 (2023) 106660

Contents lists available at ScienceDirect

Atmospheric Research

journal homepage: www.elsevier.com/locate/atmosres

Invited review article

Using bioclimatic indicators to assess climate change impacts on the Spanish wine sector

Emma Gaitán [a,b], Mª. Rosa Pino-Otín [b,*]

[a] Fundación para la Investigación del Clima, C/ Tremps 11, 28040 Madrid, Spain
[b] Universidad San Jorge, Villanueva de Gállego, 50830 Zaragoza, Spain

ARTICLE INFO

Keywords:
Grapevine
Climate change
Spain
Impacts
CMIP5
Statistical downscaling

ABSTRACT

Grapevine cultivation is an ancestral practice in Mediterranean regions such as Spain. The current climatic characteristics of this region make it a particularly optimal area for its cultivation, and the climatic changes expected in the coming decades may jeopardise this climatic suitability. Therefore, accurate studies of future projections at a local level are essential.

Local climate change scenarios of six bioclimatic indicators (absolute values together with their categorisation) related to vineyards for the Spanish region based on nine Earth System Models (ESMs) as well as two Representative Concentration Pathways (RCPs) corresponding to the fifth phase of the Coupled Model Intercomparison Project (CMIP5) were generated for the first time. These indicators are the Huglin Index (HI), the Cool Index (CI), the Dryness Index (DI) and the Hidrotermic Index. As a complement, two combined indicators were calculated: the Multicriteria Climatic Classification System (MCC System) and the Composite Index (CompI). The whole territory was analysed as well as the areas involved in the Spanish Denominations of Origin (DOs).

Our results show that Thermal indicators (HI and CI) will tend to increase through the twenty-first century, while water scarcity (DI) will be more pronounced. The trends found do not have the same repercussions throughout the territory. In the south of the peninsula, with HI values exceeding 3500°C and CI above 20°C and DI below −200 mm, the continuity of the wine-growing sector in its current state is seriously endangered, with a decrease in climatically optimal years as shown by the CompI values. On the contrary, the northern peninsula and mountainous areas, despite the expected increases, with HI below 2500°C, cool nights (CI below 15°C) and sufficient water supply (DI above 150 mm) considerably improve their climatic suitability (CompI) although the risk of mildew disease remains due to the increase in temperature and humidity.

1. Introduction

Over the last decades, changes directly related to the heliothermal and hydric requirements that grapevines need for optimal growth have been observed because of climate change. Among others, increases in temperatures, alterations in the precipitation regime, alterations in potential evapotranspiration or increases in CO_2 concentrations are affecting vineyards worldwide (Alonso and O'Neill, 2011; Battaglini et al., 2009; France and Dubourdieu, 2016).

Grapevine is very sensitive to climate (White et al., 2006; Winkler, 1974) and weather conditions over a wide range of time scales (Santos et al., 2020). Changes in the weather/climate patterns due to climate change are causing numerous impacts on the cultivation of grapes (Jones et al., 2005) with economic repercussions, especially in warmer areas such as Spain.

Average climate and climatic variability are the environmental factors that most influence wine quality and production (Santos et al., 2011). The results shown by climate projections seem to show a trend towards stronger and stronger impacts (Meehl et al., 2007) and a shift of the optimal areas for vine cultivation towards the Poles by about 20° by 2050 (Kenny and Harrison, 1993; Tate, 2001). Many studies have highlighted how climate change will alter current wine-growing regions and the need to act accordingly (Jones and Alves, 2012; Lazoglou et al., 2018; Schultz and Stoll, 2010; White et al., 2006, Ollat et al., 2016).

* Corresponding author at: Universidad San Jorge, Campus Universitario Villanueva de Gállego Autovía A-23 Zaragoza-Huesca, km. 510 50830 Villanueva de Gállego, Zaragoza, Spain.

E-mail addresses: emma@ficlima.org (E. Gaitán), rpino@usj.es (Mª.R. Pino-Otín).

https://doi.org/10.1016/j.atmosres.2023.106660
Received 28 November 2022; Received in revised form 2 February 2023; Accepted 6 February 2023
Available online 10 February 2023

Europe, as one of the world's major wine-growing regions, is one of the areas most affected by climate change, where extreme events are expected to become more pronounced (Gaitan et al., 2020; Porter and Semenov, 2005). This will lead to increased irrigation demand (Doll, 2002), increased diseases and pests (Alig et al., 2002) and changes in viticultural zoning (Malheiro et al., 2010).

Spain is one of the main wine producers and exporters as well as the world's leading vineyard (with 949,565 ha of vineyards, 13% of the world total, FEV, 2021). Due to its location in southern Europe, it is expected to be one of the regions most affected by climate change, especially rising temperatures and water stress (Gaitan et al., 2019, Gaitan et al., 2020). Indeed, these impacts are detectable today. In Spain, along with the aforementioned impacts, the area of vineyards has decreased in the north-east of the peninsula as a result of water stress (Odo Camps and Ramos, 2012), an increase in the demand for irrigation (Alonso and O'Neill, 2011) and a reduction in the life expectancy of vines by 30% (EXPANSIÓN, 2016). According to a study by the University of La Rioja (EXPANSIÓN, 2019), 90% of professionals associated with a Designation of Origin have felt the effects of climate change and 56% consider that these impacts are affecting them considerably. Among the climatic risks that most affect them are frost, hail, drought and heat waves (Climate change and vineyards in Spain report, 2016). Therefore, determining the relationship between climate and vineyard and assessing its future evolution is of particular interest in regions such as Spain, where the wine sector is not only important in terms of biodiversity but also socio-economic terms.

It is possible to evaluate the relationship between climate/weather and the different factors affecting vines and wine production as a whole by using bioclimatic indices (Fregoni, 2003), which make it possible to determine the climatic suitability of a region for growing vines, the most suitable variety or the possibility of the occurrence of certain pests and/or diseases.

Classical studies use individual indices calculated and derived from temperature and precipitation (Carbonneau and Tonietto, 1998; Tonietto, 1999; Fraga and Santos, 2017) to assess climate-vineyard relationships (Bindi et al., 1996, Jones, 2006) and their impact from different perspectives (Schultz, 2000, Combris et al., 1997).

More recent studies have highlighted the need to work with combined indices as they represent more complete viticultural classification and discrimination and allow wine quality to be characterised (Huglin, 1978; Magalhaes, 2008). This way of working is included in the concept of viticultural zoning and is the first step to evaluate the viticultural potential of a region (Malheiro et al., 2010).

Despite many indications and reports on the effects that climate change has already had on the wine sector, the efforts of the scientific community to identify the relationships between weather variables and vines and the impact of these changes in the future, there are still few studies focused on how wine producers and growers can adapt to these changes (Holland and Smit, 2010).

In addition, most studies use dynamic climate projections (which have not taken into account local climatology), direct outputs from climate models or a limited number of Spanish locations, as they are part of studies covering larger geographical areas. To date, no study assesses the impact of climate change on vineyards in the Ibero-balear Spanish territory using bioclimatic indices calculated based on regionalised climate projections on a local scale with a statistical downscaling technique (considering local climatology) generated from climate models belonging to CMIP5.

Therefore, this study aims to generate local future climate scenarios for the twenty-first century for four individual bioclimatic indices of viticultural impact: Huglin Index (HI), Dryness Index (DI), Cool night Index (CI) and Branas, Bernon and Levadoux Hydrotermal Index (HyI), a combined index (CompI) and a viticultural zonation (MCC System, Tonietto and Carbonneau, 2004) for the Iberian-Peninsular Spanish territory. As a starting point, local daily climate projections generated through a statistical downscaling technique fed with CMIP5 scenarios will be used.

This study will make it possible to assess the suitability of the study area for wine-growing, as well as to determine what areas are going to lose or gain wine-growing potential, which will be very useful information for defining possible adaptation measures and decision making for the wine-growing sector in the face of climate change.

2. Materials and methods

2.1. Study area

This study was carried out on the Spanish peninsular territory and the Balearic Islands (Fig. 1) covering an area of 588,294 km^2. Due to its location close to large bodies of water and its complex orography (from sea level to peaks exceeding 3400 km), the Spanish climate is very varied and complex, so that up to 13 climatic regions can be counted according to the Köppen classification (Köppen and Geiger, 1936), and there are multiple local climate. The climate of the Iberian Peninsula depends on its location in the extreme southwest of Europe and its complex orography, while the Balearic Islands are located in the western Mediterranean close to the Iberian Peninsula and are relatively mountainous.

The Spanish mainland and the Balearic Islands have very optimal climatic conditions that favour the cultivation of grapevines, as reflected in the almost 950,000 ha of Spanish territory dedicated to its cultivation.

The Canary Islands have not been included in the study because, due to their climatic characteristics, a consequence of their location in tropical areas, they differ from those of the rest of the Spanish territory and they deserve an individual study that encompasses these differences.

2.2. Spanish Denominations of Origin (DOs)

The Spanish DOs are the system used in Spain for the recognition of a differentiated quality, which is the result of specific and distinguishable characteristics due to the geographical environment in which the raw materials are produced and the products are made as well as the influence of the human factor involved. In Spain, there is a wide network of recognised quality according to the Government of Spain (2021): 101 Denominations of Origin (occupying an area of >900.000 ha), 42 Protected Geographical Indications and 26 “Vinos de Pago” (MAPA, 2022 Ministry of Agriculture, Fisheries and Food).

2.3. Datasets

2.3.1. Surface dataset

The observed data set used in the study consists of a set of time series of daily maximum and minimum temperature and daily precipitation data homogeneously distributed throughout the territory and belonging to the network of observatories of the Spanish Meteorological Agency (AEMET, www.aemet.es).

The selected dataset is the same that has been used in previous studies in the generation of local future climate scenarios for the study area (Gaitan et al., 2019; Gaitan et al., 2020; Gomez-Martinez et al., 2021; Monjo et al., 2016; Ribalaygua et al., 2013b), which have been subjected to strict quality control (p.e. inhomogeneities, gaps and outliers, López et al., 2007).

A total of 1778 observatories with data of both temperature and precipitation were used in the study, covering extensively the entire territory under study (Fig. 1a). For the analysis of the results by Denominations of Origin (DOs), we have chosen those observatories that are located within the territory classified as such (Fig. 1b). In total, there are 789 observatories within 59 DOs located in the iberian-balearic territory (the DOs where no observatories with information of temperature and precipitation simultaneously or with poor meteorological information were found are left out of the present study).

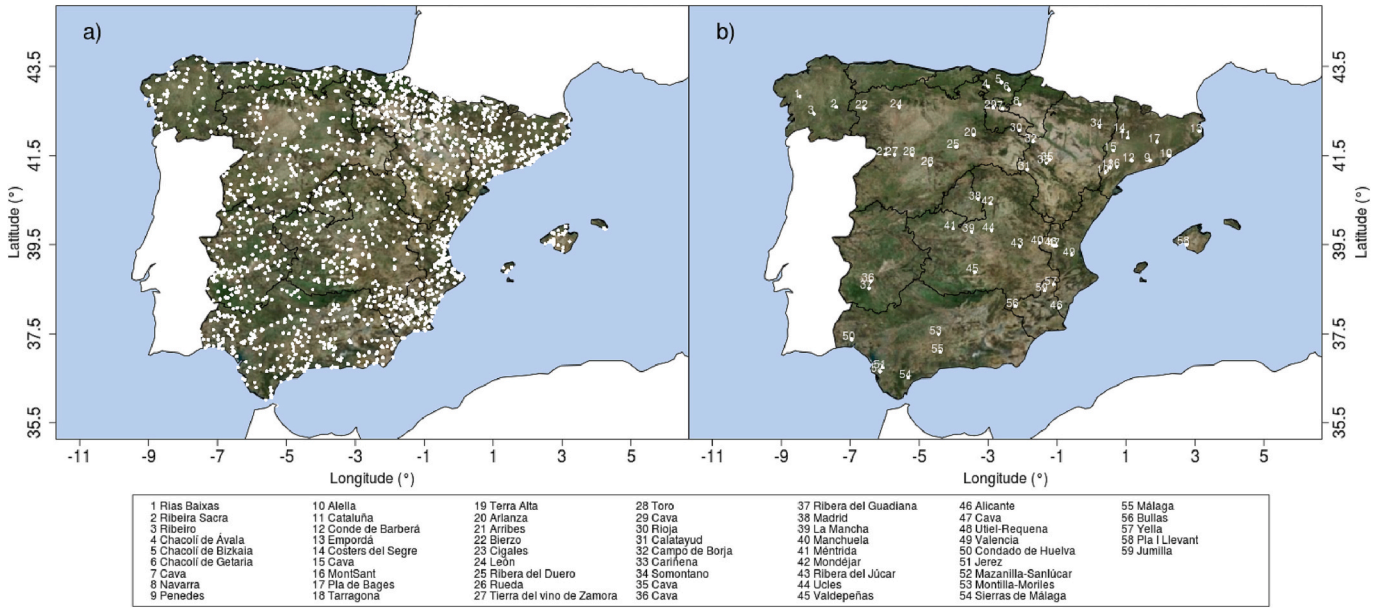

Fig. 1. Location of the study Area. a) Shows the points corresponding to the observatories used in the complete study with available temperature and precipitation data. b) Shows the location of the denominations of origin "(Map source: OpenStreetMap)".

2.3.2. Local future climate scenarios

A set of daily local future climate projections of temperature (maximum and minimum) and precipitation obtained by applying a two-step analogue/regression statistical downscaling methodology developed by the Climate Research Foundation (FIC) was used (Ribalaygua et al., 2013a; Ribalaygua et al., 2013b). This methodology offers some advantages: it is computationally inexpensive, provides local information at observatory scale and allows quantifying the uncertainty associated with the downscaling process (Van der Linden and Mitchell, 2009). Other advantages are the application of future simulations consistent with observations (physically coherent between them) and using local scale (because nearby data points in space are subjected to different climate change conditions) (Ribalaygua et al., 2013b).The generation of daily future climate local scenarios was based on nine global climate models (Table 1), called Earth System Models (ESMs, (Wang et al., 2010), belong to the fifty phase of the Coupled Model Intercomparison Project (CMIP5, Tripathi et al., 2006) and supplied by the Program for Climate Model Diagnosis and Intercomparison (PCMDI) archives. This generation of models has contributed to the acquisition of both dynamical and statistical downscaling techniques with less uncertainty in integrating the individual parts of the climate system (atmosphere, ocean, land and sea ice) and the exchange of energy and mass between them (Knutti and Sedlacek, 2013).

This study uses data from two different experiment families of GCMs: the Historical experiment (Taylor et al., 2012), which covers much of the industrial period and can be referred to as "twentieth-century" simulations and the representative concentration pathway (RCP) family (Moss et al., 2010), which corresponds to different possible ranges of radiative forcing reached in the year 2100 for values of the pre-industrial era. This study uses future projections determined by the RCP8.5 'high' scenario and the RCP4.5 'intermediate' scenario.

In total, there is a set of 18 daily climate projections for two emission scenarios, RCP4.5 and RCP8.5 (9 projections for each RCP).

The methodology employed for generating temperature and precipitation projections has been used in national and international projects, with good verification (Gaitan et al., 2019; Monjo et al., 2016; Moutahir et al., 2017; Rodriguez et al., 2014; Santiago et al., 2017; Gutierrez et al., 2019; Ribalaygua et al., 2013a, 2013b, 2018) and validation results (Ribalaygua et al., 2013a, 2013b; Gaitan et al., 2019, 2020; Monjo et al., 2016). Verification results (goodness of the methodology used) obtained in the above-mentioned studies showed good results for both, temperatures and precipitation. In the case of the temperature, the average bias achieved was below 0.1°C (which is an error of the simulated climate mean, so it does not accumulate from one

Table 1
Information about the nine climate models belonged to the 5 Coupled Model Intercomparison Project (CMIP5) corresponding to the fifth report of the IPCC. Models were supplied by the Program for Climate Model Diagnosis and Intercomparison (PCMDI) archives.°

Climatic model	Spatial /temporal resolution	Research center	References
GFDL-ESM2M	2° x2,5° daily	National Oceanic and Atmospheric Administration (NOAA), E.E.U.U.	Dunne et al. (2013)
CanESM2	2,8° x2,8° daily	Canadian Centre for Climate Modeling and Analysis (CCCMA), Canadá	Chylek et al. (2011)
CNRM-CM5	1,4° x1,4° daily	CNRM (Centre National de Recherches Meteorologiques), Meteo-France, Francia	Voldoire et al. (2013)
BCC-CSM1–1	1,4°x1,4° daily	Beijing Climate Center (BCC), China Meteorological Administration, China	Xiao-Ge et al. (2013)
HADGEM2-CC	1,87° x1,25° daily	Met Office Hadley Center, United Kingdom	Collins et al. (2008)
MIROC-ESM-CHEM	2,8°x2,8° daily	Japan Agency for marine-Earth Science and Technology (JAMSTEC), Atmosphere and Ocean Research Institute (AORI), and National Institute for Environmental Studies (NIES), Japan	Watanabe et al. (2011)
MPI-ESM-MR	1,8° x1,8° daily	Max-Planck Institute for Meteorology (MPI-M), Germany	Raddatz et al. (2007); Marsland et al. (2003)
MRI-CGCM3	1,2° x1,2° daily	Meteorological Research Institute (MRI), Japan	Yukimoto et al. (2011)
NorESM1-M	2,5° x1,9° daily	Norwegian Climate Centre (NCC), Norway	Bentsen et al. (2013); Iversen et al. (2013)

day to the next) while for precipitation, an error of 10–20% was obtained. The signal of climate change in mean precipitation is always weaker due to natural climate variability but the combination of precipitation and evapotranspiration makes the water balance clearly negative despite these uncertainties. Validation results obtained in the above-mentioned studies for both the maximum and minimum temperatures, showed a bias of around tenths of a degree in all months, so they were very close to zero. The error was not above half of a degree for any of the cases. Therefore, the results showed that the ESMs were capable of adequately simulating both the maximum and the minimum temperatures on annual and seasonal scales. In the case of the precipitation, the results are variable depending on the model and the seasonal period; however, all the models are able to reproduce the annual cycle of precipitation as well as the differences between seasonal periods (maximum values in autumn and spring, followed by winter and summer). The obtained bias and standard deviation are less than ±1 mm/day, which in relative terms supposes a difference of less than or around ±10% in the worst of the cases. Systematic errors (commented in previous paragraphs) have been corrected on a daily scale and do not affect the climate change signal of the bioclimatic indicators.

From the simulated temperature series, future heat and cold wave episodes have been calculated following Gaitan et al., 2019. Heat Waves have been defined at least three consecutive days with a maximum temperature above the 95th percentile of the maximum temperature series calculated between the months of June to September during the period 1971–2000 and at least three consecutive days with a minimum temperature below the fifth percentile of a minimum temperature series and calculated between the months of November to April during the period 1971–2000.

2.4. Bioclimatic indices

A set of four bioclimatic indices (Huglin Index (HI), Dryness Index (DI), Cool night Index (CI) and Branas, Bernon and Levadoux Hydrotermal Index (HyI)) was used to assess the impact that climate change may have on the suitability of a region for growing grapevines and/or certain grape varieties. In addition, two combinations of these indices were analysed: MCC System and CompI. For a complete explanation of indices' definition see Table 2.

The Dryness Index (DI) assesses soil water availability by providing information on water stress conditions. In the absence of information on future land use and other variables, it was decided to use a simplified formula proposed by Tonietto and Carbonneau, 2004 and based on the calculation of the potential evapotranspiration (ETP). According to various studies (Blanco-Ward et al., 2007; Vanderlinden et al., 2004) and specifically Fonseca Conceicao et al., 2012, the Hargraves formula was chosen for the calculation of ETP instead of other more complex formulations.

Table 2
Description of analysed bioclimatic indicators.

Index	Formula	Values or Categories		Interpretation	Description	References
Huglin Index	$\sum_{Abril}^{Sept.}\frac{(\overline{T}-10)(T_{max}-10)}{2}*k$	≤1200	0	—	HI is a thermal index based on degree-days, i.e. on the concept of heat accumulation. This index is used to evaluate the basic thermal and radiative demand of the grapevines during the growing period to guarantee a complete and adequate ripening. Each grape variety requires a certain amount of heat accumulation for optimal ripening to occur	Huglin, 1978
		1200–1500	1	HI-3: Very cool		
		1500–1800	2	HI-2: Cool		
		1800–2100	3	HI-1: Temperate		
		2100–2400	4	HI+1: Temperate warm		
		2400–2700	5	HI+2: Warm		
		2700–3000	6	HI+3: Very warm		
		≥ 3000	7	—		
Dryness Index	$\sum_{April}^{Sept.}(Wo+P-Tv-Es)$	> 150	5	DI-2: Humid	DI assesses soil water availability by providing information on water stress conditions	Riou et al., 1994 Tonietto and Carbonneau, 2004
		150–50	4	DI-1:Sub-humid		
		50–(−100)	3	DI+1:Moderately Dry		
		(−100)–(−200)	2	DI+2: Dry		
		≤ −200	1	DI+3: Very dry		
Cool night Index	$\overline{T}_{\min}$ (sept)	≥25	5	—	CI is a thermal index based on the night temperature during the ripening period (September in the Northern Hemisphere (NH))	Tonietto, 1999
		18–25	4	CI1: Warm nights		
		14–18	3	CI2: Temperate nights		
		12–14	2	CI3: Cool nights		
		6–12	1	CI4: Very cool nights		
		≤6	0	—		
Hydrotermic Index (HyI)	$\sum_{April}^{Aug}(\overline{T}*P)$	< 2500	1	Low risk	HyI is an index that combines the effect of air humidity (through precipitation) and temperature during the growing season to assess the risk of grape exposure to certain diseases such as mildew	Branas et al., 1946, Branas, 1974
		2500–5100	2	Medium risk		
		5100–7500	3	High risk		
		>7500	4	Very high risk		
CompI Index	$\frac{n^{\circ}\ optimum\ years}{n^{\circ}\ years\ for\ a\ period}$ HI ≥ 900 °C DI ≥ −100mm HyI ≤ 7500°C·mm $T_{\min}$ > −17 °C (always)	0.0–0.2 0.2–0.4 0.4–0.6 0.6–0.8 0.8–1.0		% means the percentage of years suitable for viticulture	The CompI is an index to evaluate the climatic suitability for grape growth. The CompI is the percentage of optimum years for vine cultivation for a given period. An optimum year is understood as a year in which critical thresholds of the HI, DI, HyI indices and minimum temperature conditions are reached	Malheiro et al., 2010 Fraga et al., 2013
MCC System classification	Combination of HI, DI and CI	Most optimal categories: HI-3, HI-2, HI+1 CI+1; CI+2 DI-1, DI+1		Least optimal categories: CI-2, CI-1 DI+2, DI+3	The MCC System is a climatic classification system for grape-growing regions based on the integration of the different classes of the three climatic indices: DI, HI and CI	Tonietto and Carbonneau, 2004
	$\overline{T}$ ≡ *mean temperature* (°C) T_{max} ≡ *maximum temperature* (°C) T_{min} ≡ *minimum temperature* P ≡ *Precipitation* (mm) N ≡ *n° days per month*				Wo ≡ *Initial available soil water reserve* (mm) = 200mm Tv ≡ *Potential transpitarion in the vineyard* (mm) = $ETP * k$ Es ≡ *Direct evaporation from the soil* (mm) = $(ETP/N) * (1-k) * JPm$ $JPm = P/5$ $k(month)$ = 0, 0, 0,0.1,0.3,0.5,0.5,0.5,0.5,0, 0, 0)	

3. Results

3.1. Observed bioclimatic indices and their verification

The observed (categorised) absolute average values of the indices used in the study (HI, DI, CI, HyI, MCC System and CompI) for the period 1971–2000 can be seen in Fig. 2 and Support Information 1. The results clearly show a north-south and west-east spatial distribution.

Within the Iberian-Balearic territory, we can find HI values (Figs. 2a and S1a) that cover all the categories defined for this index, from 300 to about 3300°C, accumulated in the period from April to September.

Some regions with climatic characteristics not suitable for growing grapes were detected, either because they are too cold with HI < 1000 (Pyrenees) or too warm with HI > 3000 (some points in the Spanish Southwest).

The areas of the northern peninsula as well as most of the valleys of mountainous areas have characteristics of cold climates with HI values between 1500 and 1800 (category 2). In a smaller proportion, there are regions with temperate climates (HI 1800–2100).

In the mountainous regions of the Central System, the Iberian System and Betic System, we find HI values <1500 (category 1, very cold), which places them in the lower thermal limit for grapevine. However, most of the territory of Sierra Morena (the mountain range that runs from east to west in the south of the Iberian Peninsula) presents IH values that oscillate between 2700 and 3000 accumulated degrees (category 6), being areas with very warm climates.

The coastal areas of the Mediterranean and the plateau as well as Cádiz (SW Iberian Peninsula) are characterised by being warm areas (category 5) with a high heliothermic potential (HI between 2400 and 2700).

The values observed for the CI (Figs. 2b and S1b) in the ripening month (average minimum temperature in September) range between 4 and 20°C, which is a great difference between regions within the study area. Most of the northern half of the peninsula and the highest points of the Betic system present very cold CI values below 12°C (category 1). The rest of the northern zone and part of the central plateau present cold CI values between 12 and 14°C (category 2). The Mediterranean coast and the south and west areas of the peninsula, as well as the Balearic Islands, are characterised by mild nights (CI between 14 and 18°C, category 3). Very few areas have high minimum temperatures in

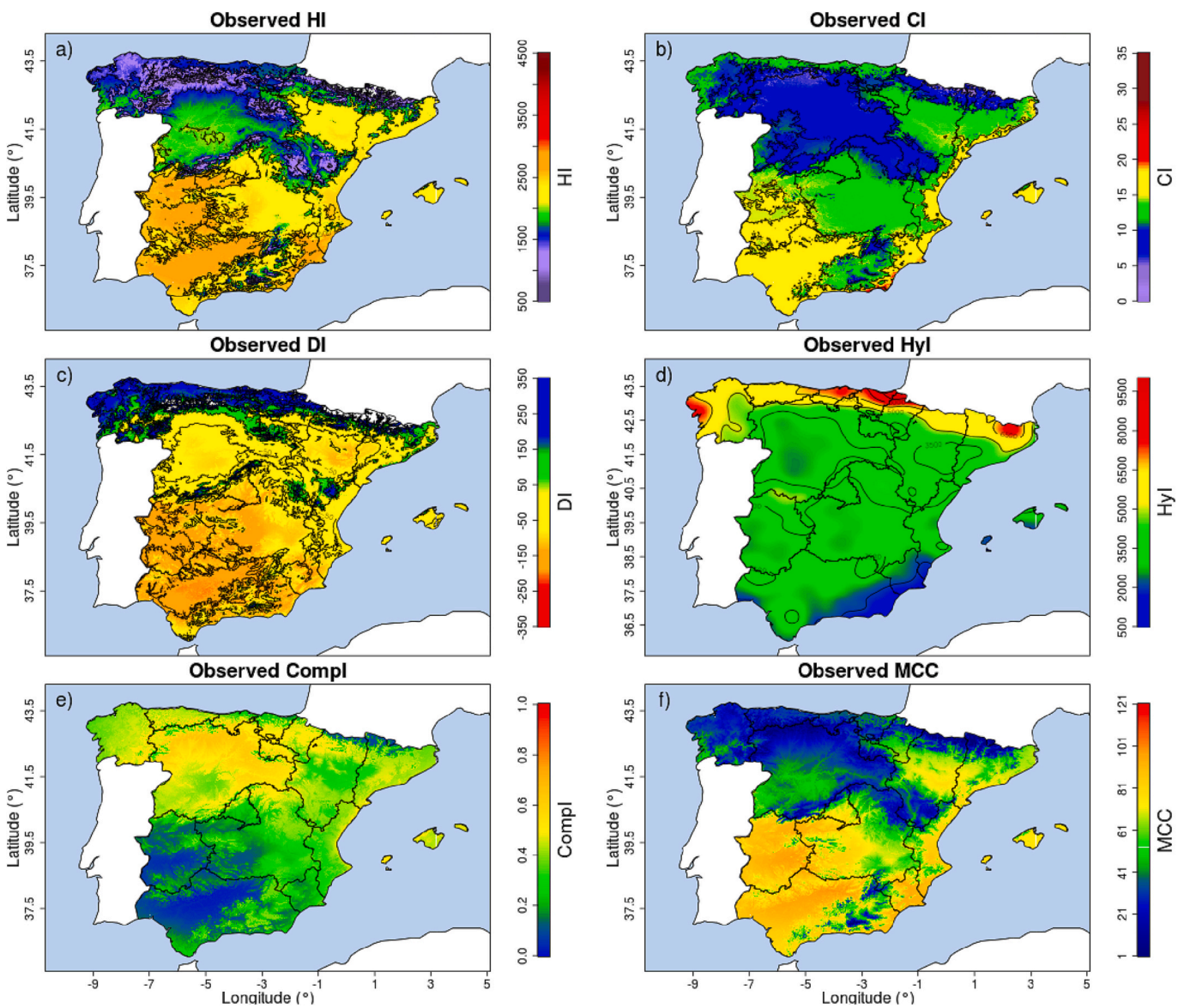

Fig. 2. Geographical representation of the observed values of the a) Huglin Index (HI), b) Cool night Index (CI), c) Dryness Index (DI), d) Branas, Bernon and Levadoux Index (HyI), e) Composite Index (CompI) and f) MCC System for the periods 1971–2000.

September (CI > 18, categories 4 and 5).

The DI values obtained (Figs. 2c and S1c) vary between −260 mm (very dry areas) and 500 mm (super-humid areas). The Cantabrian coast (N) presents the most humid conditions with DI values >150 mm (category 5), while the Cantabrian mountain range presents DI values higher than 50 mm (category 4), which implies humid and sub-humid characteristics with an absence of drought and a high level of water availability. Most of the northern plateau and the Balearic Islands have DI values between 50 to −100 mm (category 3) and are considered moderately dry areas. The rest of the peninsula is characterised by traditionally dry regions (DI between −100 and − 200 mm).

The observed HyI values (Figs. 2d and S1d) show that the southern regions have the lowest risk of incidence of diseases such as mildew (which depend on humidity and temperature to a great extent) and that the risk gradually increases towards the north where the precipitations are more abundant during the period of growth of grapevine.

Considering the aforementioned values, there will be years more suitable from the climatic point of view than others will. Fig. 2f shows the CompI index based on thresholds of some of the commented indices (Tmin, HI, DI, CI and HyI, see Table 2), which reveals that the southwest regions of the peninsula have an optimal percentage of years, climatically speaking, lower than those of the northern half and the Balearic Islands.

By combining these indices, we can establish within which values of the MCC System climatic classification the study area falls, since each of the indices separately is not a guarantee of viticultural climatic suitability. In total, we defined 120 combinations (see Table S1). The northern zone covers the classifications with categories between 1 and 20, the northern plateau belongs to those classifications with categories between 45 and 50, while the Mediterranean and eastern peninsular zones belong to the 70 and90 classes and, finally, the western and southern zones are included in the classes with categories between 90 and 100.

In the verification results (Fig. S2), the indices calculated based on observed data are compared with the indices calculated based on data the downscaled temperature and precipitation series of the ERA40 reanalysis. The verification shows very acceptable bias values for all the indices analysed. In the case of HI the mean Bias is around 104°-day (it supposes at relative error of 4%), for the CI is had been appreciated a mean Bias of 0.16°C (corresponding to a relative error of 1.2%), the DI mean Bias is around −10 mm (with a relative high error of 45% due to the simulation in very aridity places) and finally, the HyI has showed a mean Bias of −10°C *mm (it means a relative error of 0.2%).

3.2. Local future climate scenarios to predict bioclimatic indices

Figs. 3, 5, 7 and 9 show the expected future evolution for HI, CI, DI and HyI, respectively, in absolute terms starting with the historical reference period (1976–2005) and followed by correlative periods of 30 years from 2011 to 2100 as presentation of short, mid and end-century expected values, which have been predicted based on the nine models (see Table 1) and according to the RCP4.5 (top row) and RCP8.5 (bottom row) scenarios.

In addition, the simulated results for the present (Historical period) are displayed to see the expected changes relative to the current state. In the supplementary material, the same information is represented, but in a categorised way (Figs. S3, S5, S7 and S9).

To examine how the different DOs will be affected, Figs. 4, 6, 8 and 10 show the expected future evolution for HI, CI, DI and HyI, respectively, considering exclusively those observatories that are located within some DO (Fig. 1). The DOs have been represented following a geographical order (north at the bottom of the figure-south on the top). The complementary material represents the same information but in a categorised manner (Figs. S4, S6, S8 and S10).

In general, all the indices analysed showed a main north-south spatial distribution and a secondary west-east distribution, which, although it fades, tends to remain throughout the twenty-first century.

The entire Iberian-Balearic territory tends towards warmer climates, so that a large part of the territory will show movements towards increasingly warmer HI categories (Figs. 3 and S3), especially in the last section of the twenty-first century and in the most extreme case of RCP8.5. The highest areas of the territory will go from too-cold climates to optimal climates for any type of grape variety. All DOs show progressive increases in HI throughout the twenty-first century (Figs. 4 and S4) as evidenced by the gradation of the red colours in the graphs. Although in terms of categorisation it seems that the different territories will not undergo heliothermic variations (as is the case of the DO of the southern territories such as Andalusia or Murcia, see Figs. 3 and S3), the absolute values reflect these changes perfectly (see Figs. 4 and S4).

Under the RCP4.5 scenario, the DOs of the País Vasco are those that start with the lowest HI values, remaining at the end of the century with average HI values. It is followed by the DOs of Galicia and Castilla y

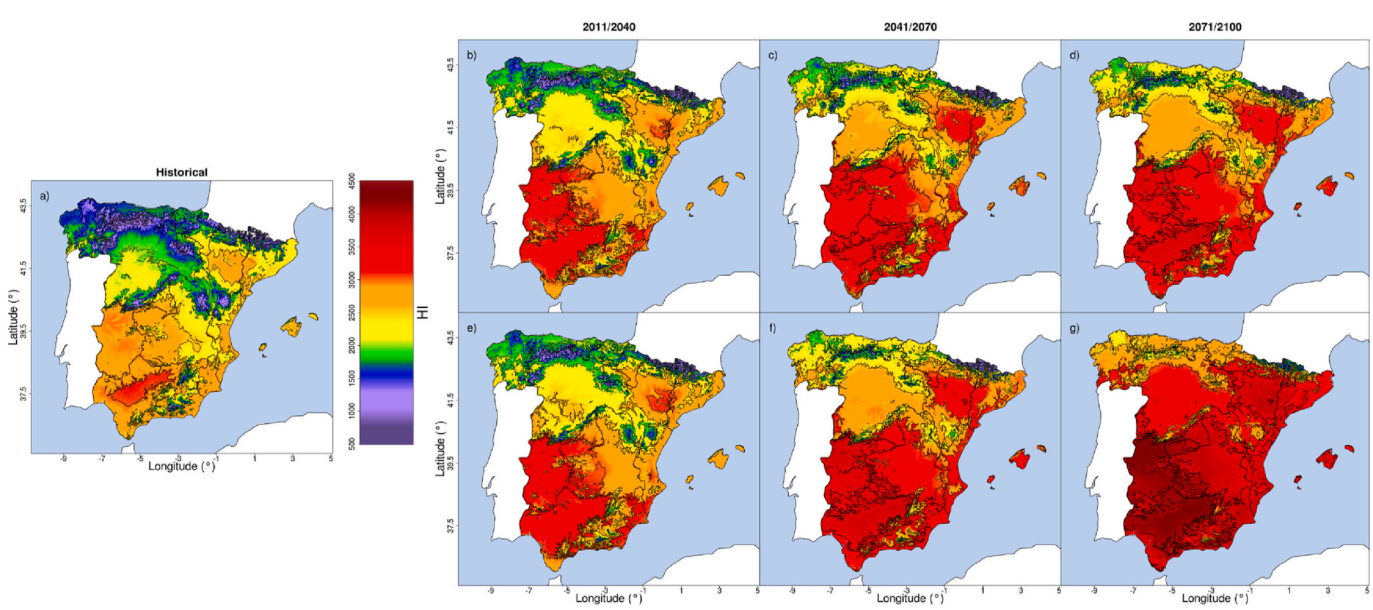

Fig. 3. Geographical representation of the expected values of the Huglin Index (HI) for the periods 2011–2040, 2041–2070 and 2071–2100. Both emissions scenarios are represented: RCP4.5 (figures b, c and d) and RCP8.5 (figures e, f and g). Fig. 3a represents the Historical absolute temperature for the period 1976–2005.

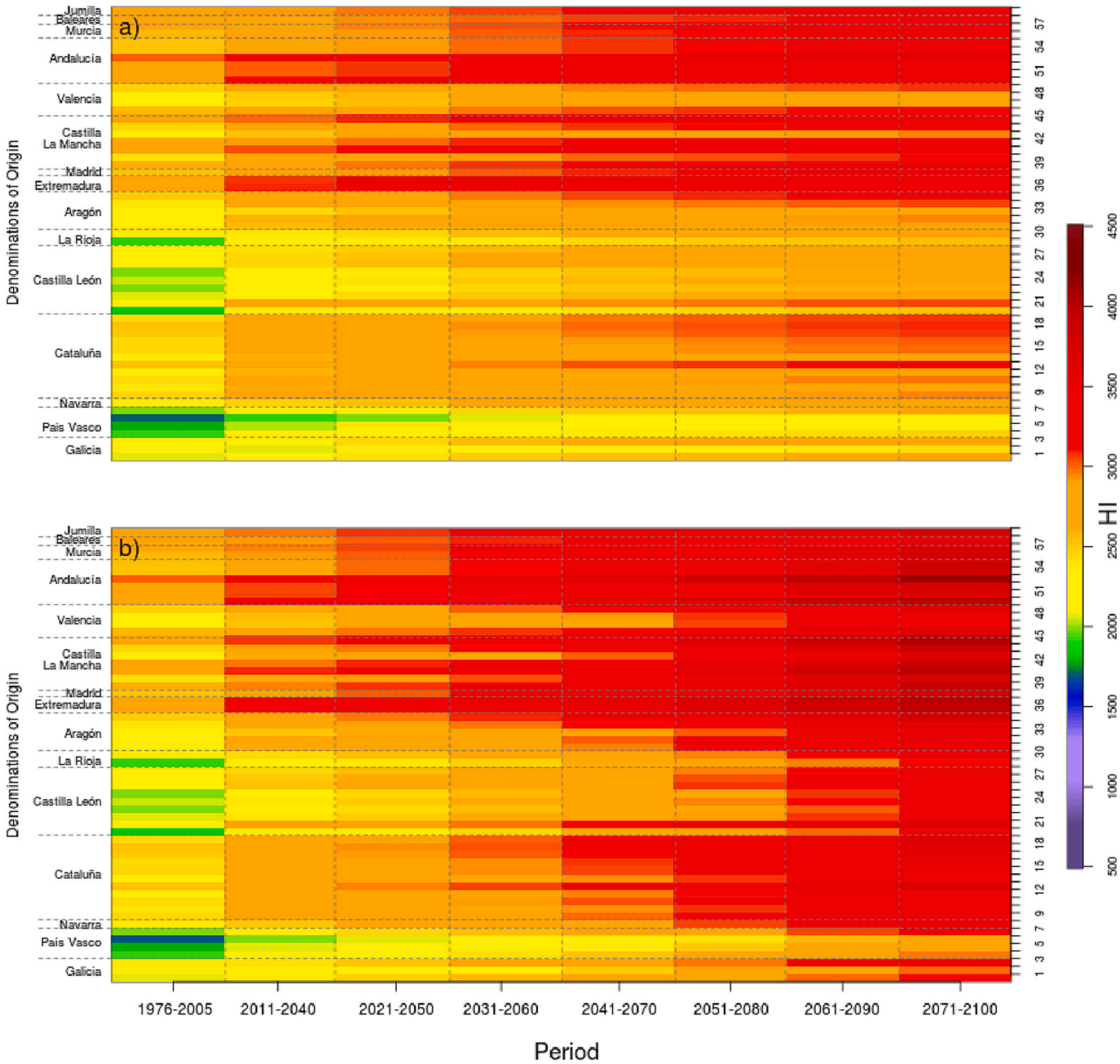

Fig. 4. Evolution of the expected values of the Huglin Index (HI) for the defined Denominations of origin (DOs). Historical period 1976–2005 and 7 correlative periods of 30 years starting on 2011 are showed. Both emissions scenarios are represented: RCP4.5 (figure a) and RCP8.5 (figure b). Each row represents one DO (see Fig. 1 for number identification) and each column represents a considered period.

León, which gradually become warmer, and they will be the ones that change the most in categorisation throughout the twenty-first century. Under conditions of RCP8.5, the evolutions are much more pronounced, so that almost all DOs will be at the end of the twenty-first century under climates that are too hot, heliothermally speaking, for the cultivation of grapevine.

It is expected that the CI will increase throughout the twenty-first century in the entire territory studied by at least 1°C (Figs. 5 and S5), so that those regions that are at the upper limit of any of the categories pass to be included in the category immediately above. In general, all DOs are expected to vary between 3 and 4°C between current CI values and those expected at the end of the twenty-first century in the RCP4.5 scenario (Figs. 6a and S6b) and between 6 and 8°C under RCP8.5 conditions (Figs. 6b and S6b). The absolute values of the CI show how this index is expected to increase progressively throughout the twenty-first century. Under the conditions of RCP4.5, the DOs of Andalucía, Murcia and Cataluña are those that are expected to have higher CI values. Cooler nights in September are expected on the other side, for Euskadi, Castilla y León and Valencia.

In the future, it is expected that the DI tends to become increasingly dry values because of the increase in temperatures, and therefore of evapotranspiration, and that most of the peninsula and the Balearic Islands are at risk of water stress (Figs. 7 and S7). The northern and Mediterranean areas will be the ones that least accrue these changes, staying in humid or not very dry climates. The expected impact on the water balance (Figs. 8 and S8) shows that only the DO located in the País Vasco will maintain the status of a humid region in the coming decades. Most of the DO will remain at similar hydrological regimens, although

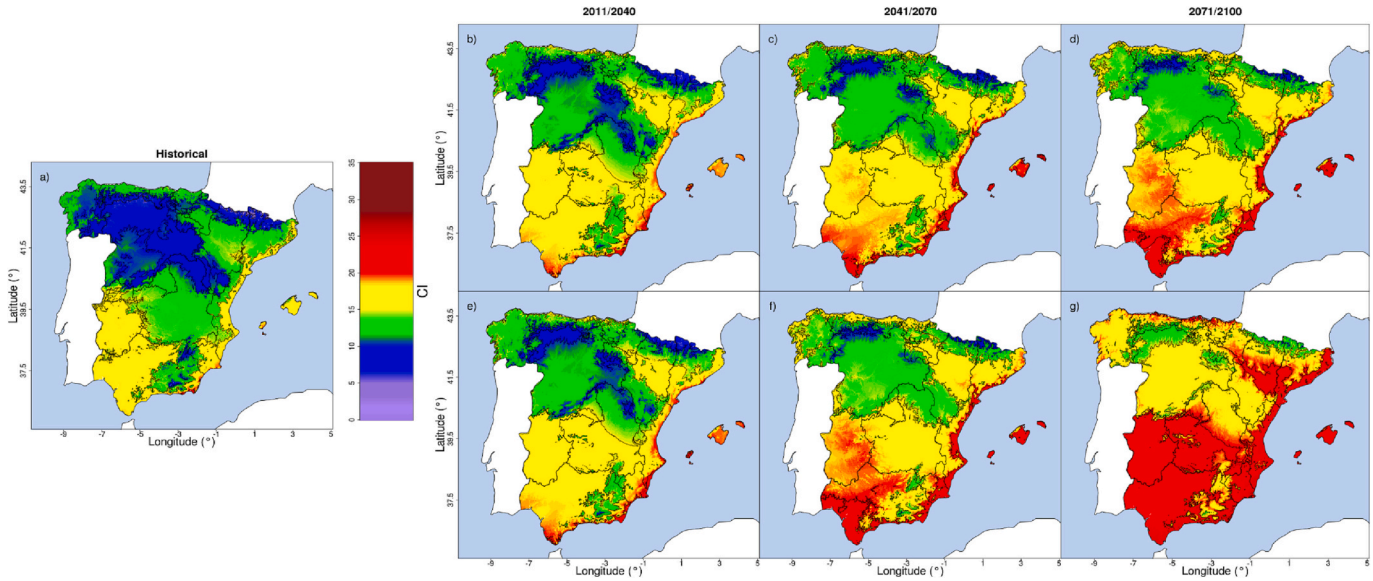

Fig. 5. Geographical representation of the expected values of the Cool Index (CI) for the periods 2011–2040, 2041–2070 and 2071–2100. Both emissions scenarios are represented: RCP4.5 (figures b, c and d) and RCP8.5 (figures e, f and g). Fig. 5a represents the Historical absolute temperature for the period 1976–2005.

the scenarios show a trend towards drier characteristics.

Although the HyI values increase in the coming decades, they remain within the range of medium risk of the presence of diseases such as mildew (Figs. 9 and S9). Most of the DOs (Figs. 10 and S10) will be at a low average risk of mildew presence throughout the twenty-first century. The DOs of Andalucía and Murcia are expected to present a low risk of the presence of mildew since their survival is not favoured due to the low precipitation. The DOs of the País Vasco, mainly, and those of Galicia will have the highest risk of suffering from mildew because of the increase in temperatures combined with the increase in the precipitation regime in these regions.

Finally, it is expected that in the coming decades the percentage of climatically optimal years will decrease throughout the territory (Figs. 11 and 12) a consequence mainly of variations in HyI and DI.

The analysed indices represent the expected changes in climatic characteristics associated with average variables and not with extreme events, such as extreme rainfall, drought or Heat/Cold Waves episodes. The latter, have a strong impact on the vine depending on the phenological stage of the vine at which they occur.

The increase in maximum temperatures will lead to a greater occurrence of heat wave episodes, as well as an increase in their duration, their average intensity and the maximum intensity reached within each heat wave episode (Figs. S13 and S14).

One of the most affected area will be the Mediterranean coast, where the average duration of a heat wave episode is expected to increase from 9 to 12 days to >18, increasing the average intensity and maximum intensity by 3–4°C. In the northern part of the Iberian Peninsula, although it will also suffer an increase in heat waves, this will be less pronounced than in the rest of the territory, with average increases in duration of 2–3 days and increases in intensity of 1–2°C. In the peninsular plateau and southern zone, the average duration of heat waves is also expected to increase by about 6 days (from 9 to 15 days in duration) with the increase in average and maximum intensity reached during these episodes (between 3 and 5°C) (see supporting information). These results are in line with the conclusions obtained by Molina et al., 2020 in the Mediterranean area, Torres et al., 2021 in the Balearic Islands and by Abaurrea et al., 2018 for the Iberian Peninsula.

The expected increases in minimum temperature will not prevent the occurrence of cold wave episodes (Figs. S15 and S16), although the average duration of cold wave episodes is increasingly shorter.

4. Discussion

This study analyses the evolution of climatic suitability for vine cultivation on the Spanish Mainland and the Balearic Islands based on a set of individual and combined bioclimatic indices using, for the first time, local future climate scenarios based on ESMs from the fifth IPCC report. In addition, the nine climate models available under two RCPs, provide a set of future climate projections of 18 possible future evolutions, which allows taking into account uncertainties, as recommended by various authors (Christensen et al., 2010; Fraga et al., 2014; Weigel et al., 2010).

Moreover, there are strong differences in assessing climate impact at the regional or local level (Santos et al., 2012). Local studies allow us to establish the origin of the main differences between grape types grown in neighbouring regions as suggested by Ramos et al. (2017) and which is evident in the results obtained when considering the future climate scenarios of the bioclimatic indices by DOs. These results reinforce the importance that climatic conditions have on the genuineness and unique character of each designation of origin.

The generation for the first time of future scenarios of bioclimatic indicators of great interest for the wine sector for the 21st century at local scale (considering local climatic characteristics) with a wide set of future climate projections using ESMs from the fifth IPCC report, brings novelty to the studies existing so far in the sector.

Therefore, these results offer one of the best snapshots of future climate change, based on currently available data, and the risks that changes in temperature and precipitation regimes could cause in the way grapevines are cultivated.

4.1. Considerations about the simulation of bioclimatic indices

The future climate scenarios at the local scale used as a basis to generate the future scenarios of bioclimatic indices were developed by the FIC with a two-step analogue methodology (Ribalaygua et al., 2013a), which has been verified and validated in various studies in Spanish territory with very good results (Gaitan et al., 2019; Gaitan et al., 2020; Gutierrez et al., 2019; Monjo et al., 2016; Ribalaygua et al., 2013b). Therefore, the future temperature and precipitation scenarios on which the bioclimatic indicators are obtained are robust and reliable. Moreover, it should be noted that there are studies that reinforce the idea that daily changes in atmospheric conditions play an important role

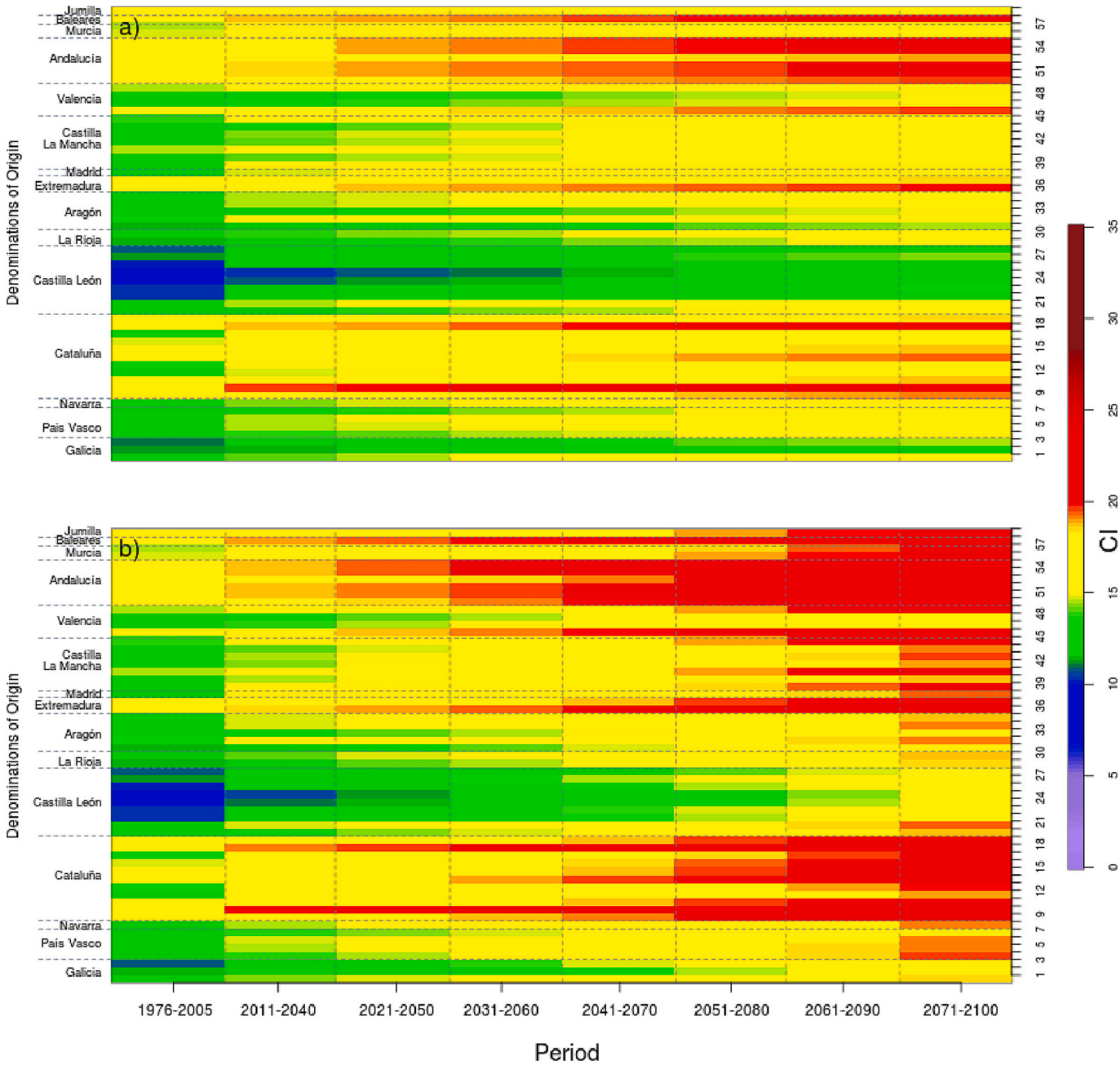

Fig. 6. Evolution of the expected values of the Cool Index (CI) for the defined Denominations of origin (DOs). Historical period 1976–2005 and 7 correlative periods of 30 years starting on 2011 are showed. Both emissions scenarios are represented: RCP4.5 (figure a) and RCP8.5 (figure b). Each row represents one DO (see Fig. 1 for number identification) and each column represents a considered period.

in plant phenology (Jones and Davis, 2000), and these changes can be more or less significant depending on the region where they occur. These aspects are considered intrinsically in the type of downscaling's methodology used in this study.

Another factor to consider is the benefits that an increase of CO_2 under future climate conditions plays an important role in the development of the vine (Bindi et al., 2001; Goncalves et al., 2009; Moutinho-Pereira et al., 2009) which has only been indirectly considered in this study.

4.2. Local future climate scenarios of bioclimatic indices

In general terms, there is a positive trend in all thermal indicators (HI and CI) and a negative trend in the water index (DI). This reflects the twenty-first century with progressive increases in temperatures, both maximum and minimum, throughout the Iberian Peninsula, while hardly any changes in precipitation patterns are expected. The combination of the expected changes in both variables will have a strong impact on the vineyard. Similar results have been obtained for areas such as Portugal (Fraga et al., 2012), Italy (Bonfante et al., 2017, Bonfante et al., 2018), Germany (Neumann and Matzarakis, 2011; Stock et al., 2004), France(Duchene and Schneider, 2005, Duchene, 2016, García de Cortázar-Atauri et al., 2017) and Spain (Gomez-Gesteira et al., 2011; Ramos, 2017).

Consequently, although the northern regions will see their climatic suitability for growing grapes favoured, certain regions of the south and southwest of the Peninsula as well as the Mediterranean coast, that are at the limits of climatic suitability, may be negatively affected. These

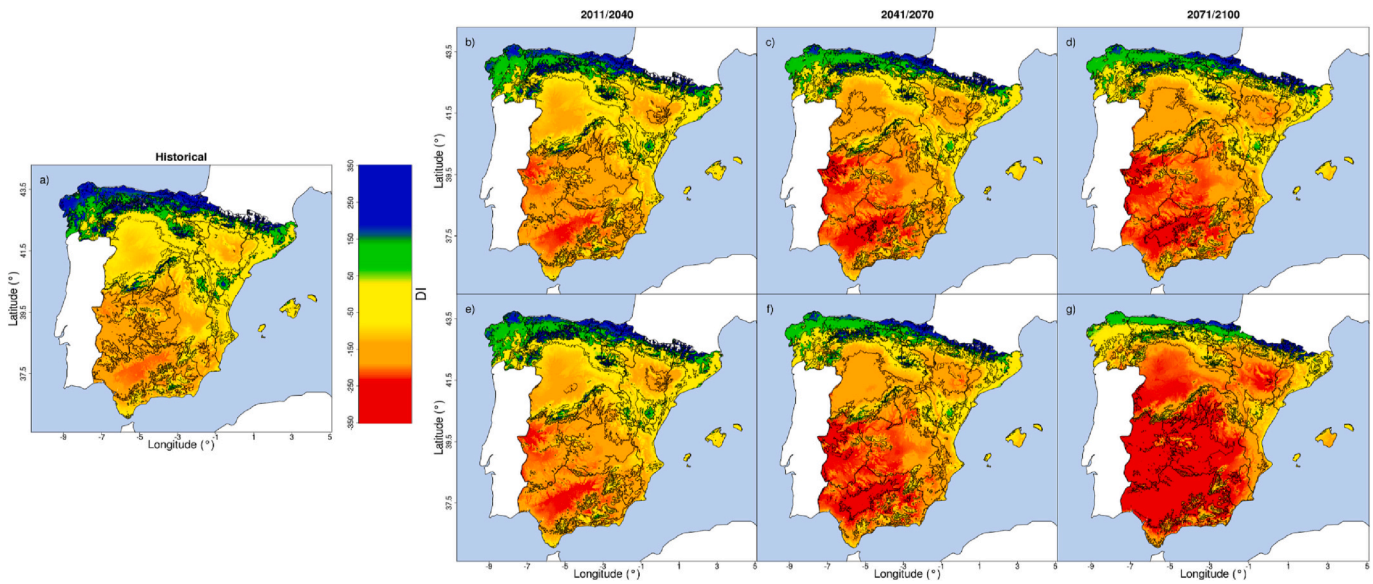

Fig. 7. Geographical representation of the expected values of the Dryness Index (DI) for the periods 2011–2040, 2041–2070 and 2071–2100. Both emissions scenarios are represented: RCP4.5 (figures b, c and d) and RCP8.5 (figures e, f and g). Fig. 7a represents the Historical absolute temperature for the period 1976–2005.

results confirm those obtained by (Fraga et al., 2012; Resco et al., 2016), among others.

The tendency of the HI values to increase is already in itself a determining factor of the variety of grape that can be grown in each zone since they determine the requirements for heat accumulation so that the ripening of the grape occurs optimally. The gradual change of the entire territory towards warmer climates will cause the necessary levels, in terms of heat, for the ripening of the grapes to occur at earlier times, which translates into an advancement of the ripening date (Molitor and Junk, 2019). This can subject vines to heat stress episodes in many regions. In addition, this index has a strong correlation with the different phenological states associated with warm conditions(Bock et al., 2011; Jones et al., 2005; Santos et al., 2012) so its increase would imply overtaking of certain phenological properties, which would alter the phenological cycle of the vine.

In this way, in areas that are too cold (according to our results, the Pyrenees area will be the only one that presents these characteristics), only very early varieties could reach maturity, usually white varieties. These regions should opt for a hybrid or American varieties, more resistant than the *Vitis vinifera*, while in the cool regions (high elevation mountainous regions, (category 3) both white and red can be grown. As the climate becomes more temperate (categories 4 and 5, some regions of the northern Peninsula under RCP4.5 and very few areas of the North under RCP8.5), almost any type of grape such as 'Garnacha' or 'Moscatell' can be grown in the first case and 'Pinot Blanc', 'Pinot Noir' or 'Chardonnay' in the second.

The greatest impact will occur in hot or very hot regions (categories 6 and 7), most of the Peninsular territory and the Balearic Islands, where the minimum requirements that the different grape varieties need to ripen, including those with late-ripening, will be exceeded. In very hot climates, there is a high risk of stress due to heat accumulation that can be detrimental to grapevine (most of the study territory, especially under the RCP8.5 scenario). HI values in the northern peninsular plateau are expected to be lower than those expected under RCP4.5, while the southern plateau and the Balearic Islands will reach very high HI values, regardless of the scenario considered.

In addition, it must be considered that within the same category it may be that each variety has different heat requirements to reach maturity (Tonietto, 1999) and that despite belonging to the same category they could not be cultivated. For example, the 'Cabernet Franc' variety requires an HI of 1800 cumulative degrees while the 'Cabernet Sauvignon' variety requires a HI of 1900 and the 'Ugni Blanc' variety needs a HI of 2000. Although their heliothermic requirements are different, both would be in HI Category 4. Therefore, if we only consider categorised values, we can run the risk of selecting varieties in areas that do not reach the necessary calorific requirements for said variety, hence the need to work with absolute values.

Regarding the CI, the expected increase in minimum temperatures will cause the CI to increase so that in some regions the night coolness necessary for optimal grape ripening will not be achieved. In addition, the advancement of the ripening dates suggests the need to evaluate this index on dates before September (Ramos and Martinez de Toda, 2021).

Changes towards very cold night temperatures can have a positive effect on certain varieties of grapes as long as a sufficient heliothermic contribution is guaranteed to ensure a good level of ripening of the berries. It is not expected that any study region will experience decreases in CI under RCP8.5, but in the case of RCP4.5, areas of the Pyrenees and the Cordillera Cantábrica will remain cold at night throughout the twenty-first century.

In those regions with fresh or medium CI values (such as what is expected to occur in most of the Southern Plateau, according to RCP4.5, and in the Northern Plateau, under both RCPs), the results can be both positive as well as negative depending on the cultivated variety, as the late varieties ripen in colder conditions than the early ones.

Finally, if the CI values are higher than 18°C (as will be the case of the Atlantic and Mediterranean coast and the Balearic Islands if RCP4.5 is considered or of the entire Southern Plateau plus the regions previously mentioned according to RCP8.5), the vines can suffer an excess of heat that affects the colour and aromatic potential of the grape.

The changes in the expected DI values condition the region's water supply and, therefore, determine the decisions to be made regarding irrigation. In the entire Iberian-peninsular territory except for the Cantabrian coast and the Pyrenees, regardless of the RCP considered, the DI values will decrease to the lower limit of 50 mm, so these territories will be at the lower limit of water supply, which may give rise to certain restrictions, especially in the summer months. If DI values < -100 mm, the region will be excessively dry, requiring an extra water supply.

On the contrary, values higher than 150 mm (as could occur in the areas of the Pyrenees or the Bay of Biscay) can reduce the quality of the wines and have higher quality grapes in wet years.

Intermediate DI values (between 50 and − 100 mm) that are expected in regions such as Galicia or Asturias, will suffer certain periods

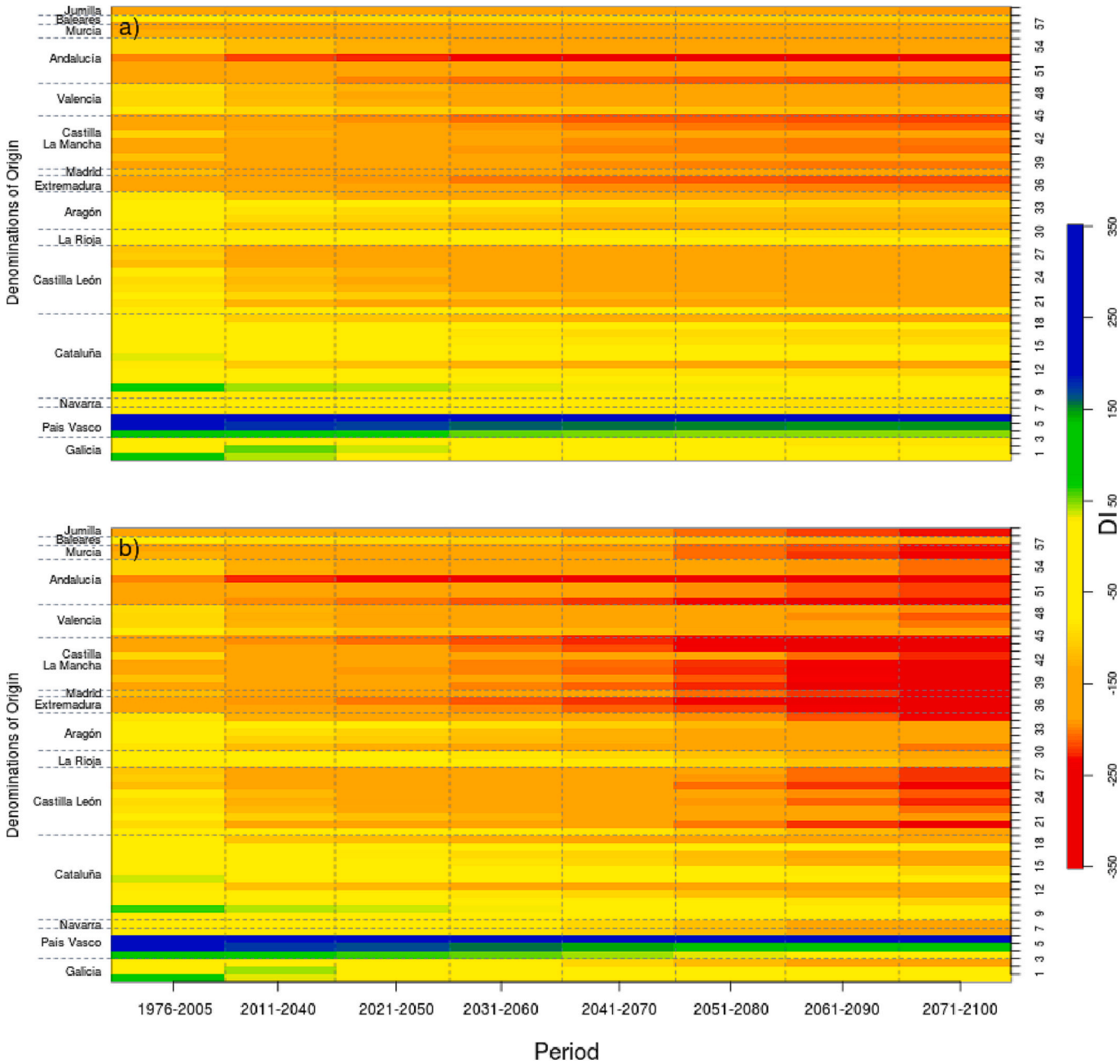

Fig. 8. Evolution of the expected values of the Dryness Index (DI) for the defined Denominations of origin (DOs). Historical period 1976–2005 and 7 correlative periods of 30 years starting on 2011 are showed. Both emissions scenarios are represented: RCP4.5 (figure a) and RCP8.5 (figure b). Each row represents one DO (see Fig. 1 for number identification) and each column represents a considered period.

of drought that can become favourable during ripening.

The joint assessment of these indices through the MCC System allows establishing a more complete climatic vision of the suitability of the region. Of all the possible combinations, those that are more suitable for grapevine cultivation are those that combine HI values (categories HI-3, HI-2, HI + 1), CI (categories, CI + 1; CI +2) and DI (categories DI-1, DI + 1). While the least optimal have turned out to be those with CI (categories CI-2, CI-1) and DI (categories DI + 2, DI + 3). In the particular case of this study, it is expected that the optimal regions under this criterion will be found in the north of the peninsula, such as the Cantabrian Mountains and the Pyrenees, as well as in almost the entire Northern Plateau (according to both RCPs in the middle of the century). However, the Northern Plateau will only maintain these conditions under RCP4.5. These results are in line with those obtained by other authors (Fraga et al., 2013; Resco et al., 2016).

The combination of moderately low night temperatures with high daytime temperatures in these areas will favour the production of high-quality wines since the synthesis of some phenological components is favoured.

Regarding Hyl, no major changes are expected in the risk of certain diseases such as mildew, but there may be many differences between regions with very different precipitation patterns. The southern regions have a lower risk, which gradually rises to the north where precipitation will be more abundant during the vine growing season, similar to what other authors found (Fraga et al., 2013; Lazoglou et al., 2018).

The results obtained in the CompI index may seem contradictory since the largest Spanish wine-growing regions, such as Andalusia and Castilla-La Mancha, have a very low percentage of optimal years for

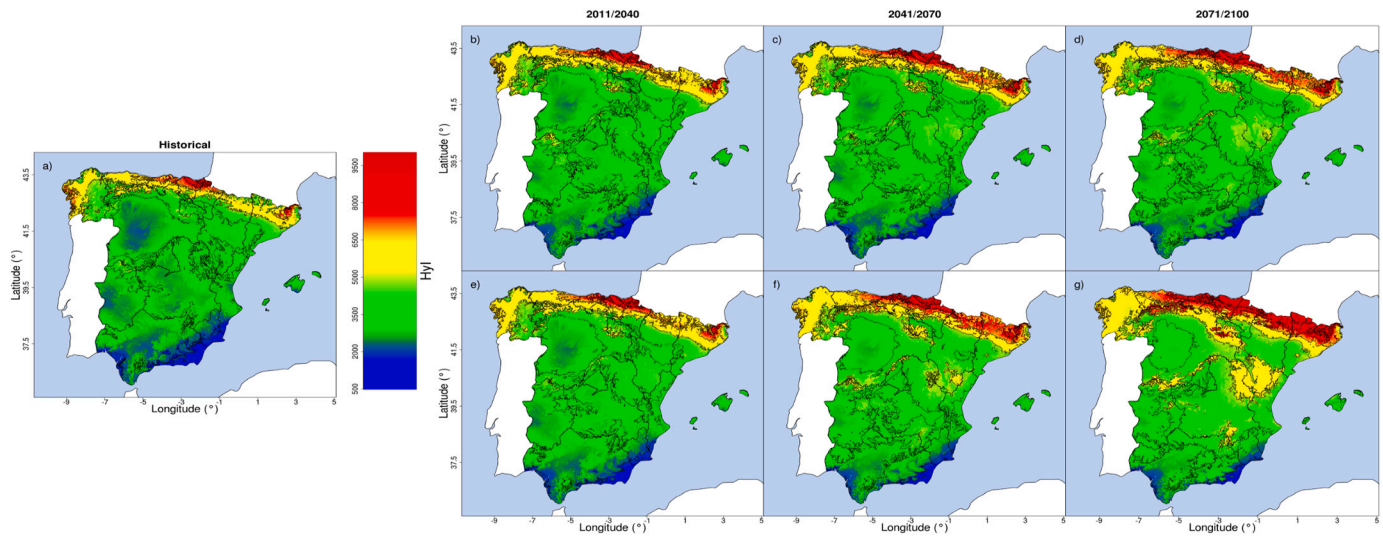

Fig. 9. Geographical representation of the expected values of the Branas, Bernon and Levadoux Index (HyI) for the periods 2011–2040, 2041–2070 and 2071–2100. Both emissions scenarios are represented: RCP4.5 (figures b, c and d) and RCP8.5 (figures e, f and g). Fig. 9a represents the Historical absolute temperature for the period 1976–2005.

growing vines. Similar situations have been found in other studies (Guido, 2015). This is because they are dry regions or with strong periods of drought with DI values < -100 mm, while one of the conditions to consider a climatically optimal year is that the DI > -100 mm. The results of this index must be interpreted in the light of multiple socio-economic factors that determine the success of a vineyard plantation beyond the climatic conditions. For example, in these regions, this situation is solved by viticultural producers through different management strategies and water management, which allow solving this "climatic problem" and taking full advantage of the rest of the climatic characteristics that favour grapevine. Other factors such as the type of cutting used, the orientation of the vineyard, the field management tasks, the type of soil, among others, will be keys to adapting to the challenges posed by climate change (Aleixandre et al., 2013).

It should also be kept in mind that rising temperatures due to climate change may have indirect effects on these crops, as they are expected to cause an increase in tropospheric ozone concentrations and are also likely to affect the chemistry of ozone precursors (NOx, CO, CH_4, NMHC) (Isaksen and Wang, 2002). This modification of atmospheric pollutant generation can be very detrimental to vineyards. For example, it has been suggested that ozone can cause a loss of productivity and a reduction in the sugar content of grapes (Ascenso et al., 2021). Increased exposure to SO_2, NO_2 can cause a severe reduction in photosynthetic rate, transpiration and stomatal conductance in shoot growth (Popescu et al., 2012).

To all these effects must be added the impact of extreme phenomena, especially heat waves. Heat waves (see Figs. S13 and S14) combined with summer drought will be the most common abiotic stress combination in the Mediterranean area (Hannah et al., 2013). The response of grapevines to increased temperatures (acceleration of their key phenological stages affecting grape quality and the properties of grape organoleptic components, such as sugar accumulation, pH, acidity, colour, aroma and flavor) (Ramos et al., 2008, Leolini et al., 2019), is likely to increase with heat waves and will also depend on its coincidence with grape ripening (Sgubin et al., 2018).

In more humid areas, as the northern part of the Peninsula, new growing areas may become viable, for example in areas of higher altitude (Ramos and Martinez de Toda, 2021) or closer to the coast (Santos et al., 2020), while low elevation areas would probably be suitable for lower quality varieties, producing wines of high alcohol content (Moriondo et al., 2007).

In almost all the territory (where a significant intensification of heat wave episodes is expected, see support information) all adaptation options must be considered if current crops are to be maintained, such as water application, row orientation or canopy cover. Water availability is the factor, along with high temperatures, that most affects vine development (Fraga et al., 2018; Fraga et al., 2019). In these areas where irrigation water is not available or is too warm, such as the Guadalquivir Valley or Extremadura, it will not be possible for the vines to mature normally, so it will be necessary to make substitutions towards varieties more tolerant to the new climatic conditions (Ramos et al., 2008). The search for adapted grapevine (*Vitis vinifera* L.) varieties will be a priority in the coming years, either through germplasm collections or genetic improvement processes (Duchene et al., 2010).

At the other extreme, cold wave episodes can be especially damaging to primary buds (Gu et al., 2002), although there are not expected to be considerable variations in the average and/or maximum intensities of such episodes in Spain (Figs. S15 and S16).

Finally, an adaptive evolution with physiological modifications of the wineyard could be expected (Ramos and Martinez de Toda, 2021) especially in those areas where climatic extremes are not so intense or so frequent, as in the northern part of the Peninsula. The adaptation of each variety under the same climatic conditions depends on the peculiarities of each genotype to heat, light or water deficit and the temperature and humidity conditions needed for ripening. The varieties with earlier phenology will be probably the most affected as was described for the Spanish variety "Tempranillo" (Ramos and Martinez de Toda, 2020).

The literature highlights different biochemical, physiological and molecular acclimation mechanisms that grapevine is able to develop in order to adapt to climatic stresses. Changes in photosynthetic efficiency and in the control of electrolyte loss through stomata appear to be frequent mechanisms of adaptation (Zha et al., 2018). For example, adjustment of photosynthesis to elevated temperature has been detected in some cases (Gallo et al., 2021; Kizildeniz et al., 2021). Site-specific stomata and vein traits modulation have been suggested as an acclimation strategy that may influence photosynthetic yield (Damiano et al., 2022). Increasing the heat dissipation capacity by changing the response of its stomata has also been proposed as an adaptation to warmer climatic conditions, since keeping them open allows heat dissipation by evaporative cooling (Costa et al., 2012). Significant changes in the expression pattern of metabolic pathways related to metabolism and hormones have also been detected (Duchene et al., 2010; Kovaleski and Londo, 2019). This opens up opportunities to identify the genetic and physiological traits that make a variety more or less resistant and select

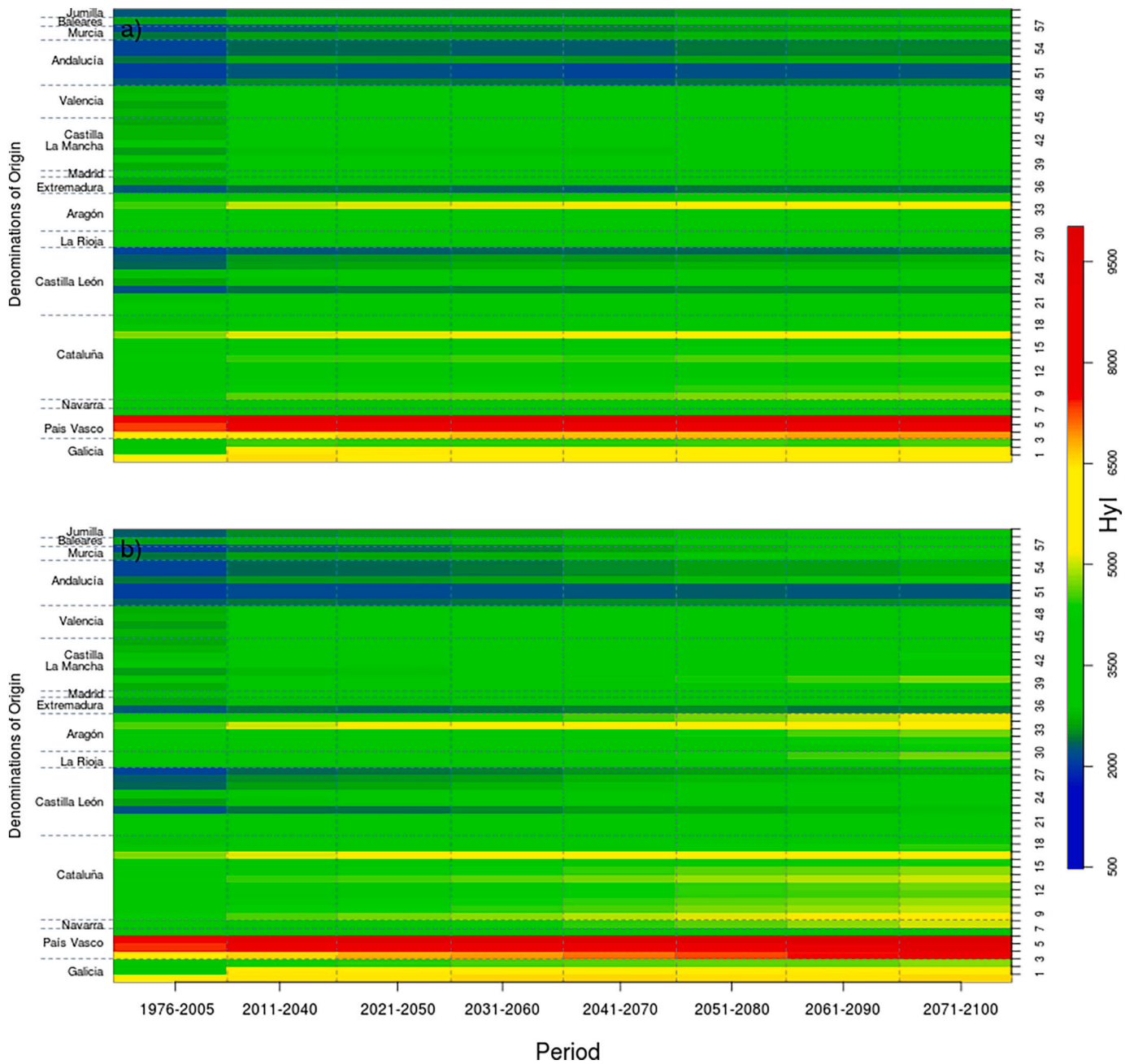

Fig. 10. Evolution of the expected values of the Branas, Bernon and Levadoux Index (HyI) for the defined Denominations of origin (DOs). Historical period 1976–2005 and 7 correlative periods of 30 years starting on 2011 are showed. Both emissions scenarios are represented: RCP4.5 (figure a) and RCP8.5 (figure b). Each row represents one DO (see Fig. 1 for number identification) and each column represents a considered period.

varieties which would be suitable to replace the more sensitive ones even in the most affected areas such as those in the south or in the central zone of the country. In Ronda (Málaga, South of the Spain), Petit Verdot (originally from Bordeaux), whose long phenological cycle is perfectly adapted to warm climates, is producing good results in recent experiences. In Extremadura (Southwest of the Spain), Portuguese varieties such as Trincadeira or Touriga Nacional are also being successfully cultivated. In Ribera del Duero (central area of Spain) there is a growing interest in growing Malbec (traditionally grown in areas of Castilla-La Mancha and Castilla y León above 1000 m) to accompany Tempranillo (traditionally accompanied by Cabernet).

Another option is to include new sub-varieties within a variety rooted in the area, as is the case in the region of Murcia (South of the Spain), where the cultivation of four new Monastrell grape varieties (Gebas, Myrtia, Calnegre and Calblanque), which are more resistant to the new climatic conditions, has recently been approved.

It is also worth mentioning the efforts being made in Spain to recover local varieties. These vines have adaptive characteristics to the area where they have been cultivated for hundreds of years, so they can be more resilient to climate change at the local level. A recent ambitious project (Munoz-Organero et al., 2022) has studied the phenological characteristics of 53 Spanish minority grape varieties, mostly from the vine collection of El Encín (Alcalá de Henares, Madrid) to determine their possible adaptation to climate change conditions, concluding that many white (Planta nova, Zurieles, Albana, Hebén, Tortozón, and Aúrea among others) and red varieties (Cornifesto, Negreda, Benedicto, among others) present characteristics for a greater chance of success under more extreme climatic conditions.

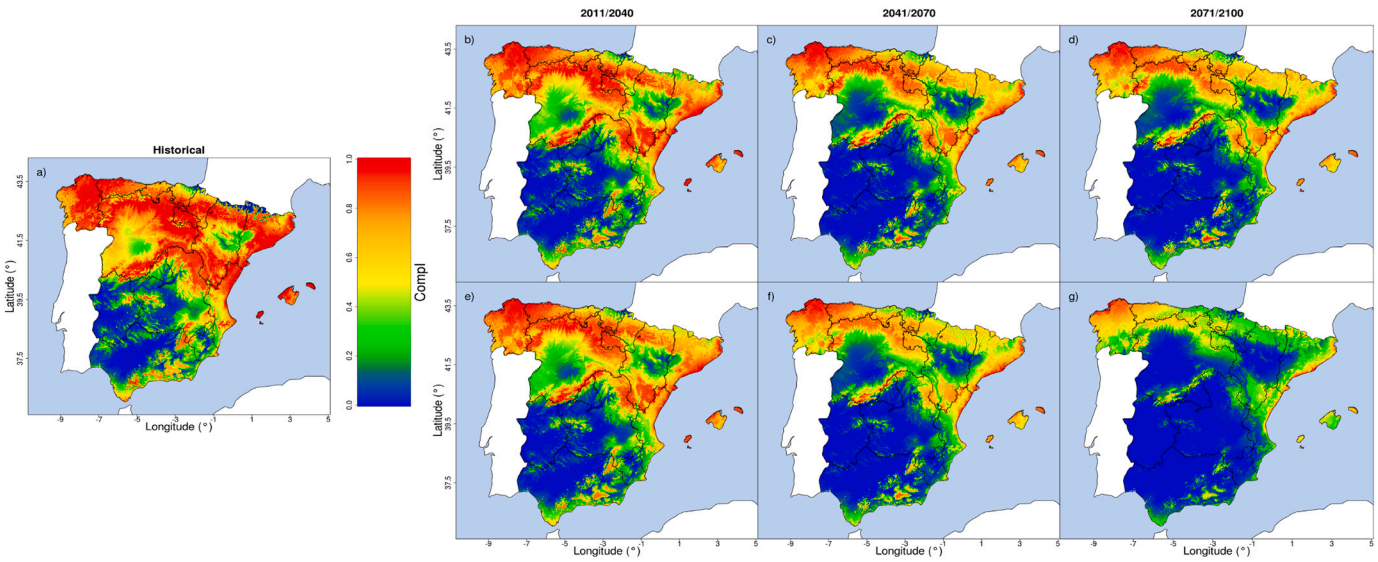

Fig. 11. Geographical representation of the expected values of the Composite Index (CompI) for the periods 2011–2040, 2041–2070 and 2071–2100. Both emissions scenarios are represented: RCP4.5 (figures b, c and d) and RCP8.5 (figures e, f and g). Fig. 11a represents the Historical absolute temperature for the period 1976–2005.

Other studies describe the local red grapevine Pasera (PAS), a variety from northern Spain (Navarra), as a potential candidate to be exploited under climate change, as it can maintain wine quality under warming and increased CO_2 (Goicoechea et al., 2021). Other local minor Mediterranean grapevine varieties (Alicante, Spain) such as Arcos and Forcallat have been studied for their ability to withstand water stress and show higher intrinsic water use efficiency (Gisbert et al., 2022).

Encouraging the cultivation of these local varieties can contribute to the adaptation of vines to climate change, but also to the local economy and to avoid the loss of genetic diversity.

However, the process of incorporating new varieties is complex, not only because it depends strongly on local characteristics (to the meteorological-climatic context must be added the type of soil, orientation, slope of the land and investments in irrigation or other adaptive technologies, among others), but also because it is subject to the legislation in force in each area and the long process involved in incorporating a new variety in a region from which it does not originate.

A final aspect that may play an additional role in the adaptation of the grapevine crop to stress generated by increased temperatures, drought or increased CO_2 and, perhaps less studied, is the protective role of soil microflora and, in particular, of mycorrhiza, a plant-fungus symbiosis (Trouvelot et al., 2015). Increasing heat tolerance by inoculating the plant with endophytic microorganisms, such as arbuscular mycorrhizal fungi (AMF), may be a new strategy to overcome the impact of high temperatures on grapevines(Fraga et al., 2016). In fact, there are already experiences that show that AMF inoculation could also help sustain grape growth under thermal stress conditions, especially after heat shocks(Nogales et al., 2020). AMF also increase the tolerance to water stress improving water uptake(Kohler et al., 2008). It seems that during periods of water stress, grapevines compensate for a lower density of fine roots by stimulating the colonization of arbuscular mycorrhizal fungi (Schreiner et al., 2007) which allow the plant to absorb water more efficiently, enabling the grapevine to cope with water stress. The grapevines inoculated with mycorrhiza not only improved leaf water status, but also photosynthetic capacity, stomatal conductance, and transpiration rate and decreased the intercellular CO_2 concentration making the plant more resistant to abiotic stresses(Ye et al., 2022).

4.3. Relevance of the results

The results obtained in this study show how the Iberian peninsular territory is one of the wine-growing regions most sensitive to the impact of climate change, not only because of the significant variations in the values obtained in the study, especially in those dependent thermal indices, but also because these variations place the region within the optimal thermal limits for growing vines. Other European regions such as France and Italy are also expected to suffer variations in their climatic conditions with implications for the vineyard, but the expected impact is not estimated to be as marked (Fraga et al., 2013), and the regions in Northern Europe will even benefit from the expected climate changes (Hannah et al., 2013).

Alterations in climatic requirements (heliothermic and hydric) have a strong impact on the final organoleptic characteristics (sugar, acidity, colour, etc.) of the grape and the characteristics of the wine. Spain has a long viticultural tradition, its wines being recognised worldwide precisely for the characteristics of the wines belonging to each DO, maintaining those own characteristics is of vital importance to guarantee the continuity of the DOs.

Currently, there is a shortage of agricultural models for grapevine (Bindi et al., 1996) or for the quality of grapevine (Webb et al., 2008) as well as tools to support decision-making (Iglesias et al., 2012; Santos et al., 2012). There are some soil suitability models (Escariz et al., 2007) and cereal modeling (STICS, BRIN, WANG04) that combined with a good observed phenological database (Mosedale et al., 2016) and climate projections such as those presented in this study, which would considerably facilitate the adaptation of the wine sector to climate change.

The results obtained can be a starting point to review and update certain factors that under new climatic conditions may be altered. As an example, currently in Spain, only those varieties that are in the register of Commercial Varieties of the Vine of Spain can be cultivated and for the control of plantations the List of Authorised, Recommended and Plant Conservation Varieties is used, both listings could be altered due to new climatic conditions.

The results of this study should be complemented with other limiting factors (White et al., 2006) such as orientation, latitude, longitude, altitude, topography and proximity to water areas as well as orientation and exposure; characteristics that, together with the properties of the soil, the management practices and the iterations between all the factors that make up the system provide grapevine and wine with unique qualities that differentiate them, even within the same DO where different grape varieties, soil types, and field characteristics may coexist.

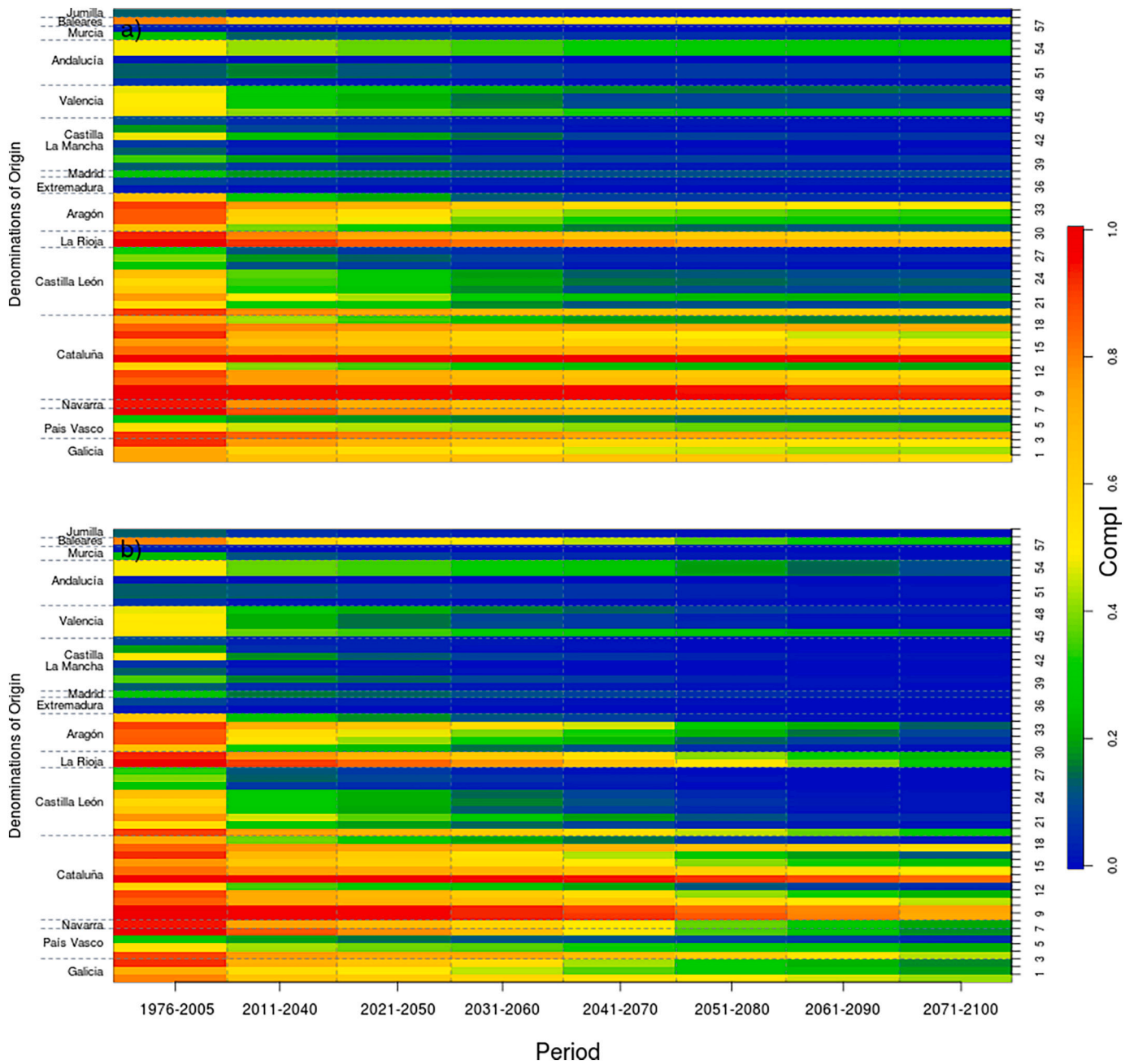

Fig. 12. Evolution of the expected values of the CompI Index (CompI) for the defined Denominations of origin (DOs). Historical period 1976–2005 and 7 correlative periods of 30 years starting on 2011 are showed. Both emissions scenarios are represented: RCP4.5 (figure a) and RCP8.5 (figure b). Each row represents one DO and each column represents a considered period.

Although these factors play an essential role in the wine creation process, they do not pose as great a challenge as the climate (Van Leeuwen et al., 2004), an aspect on which this study was focused.

Finally, the great variety of grape types that are grown in Spain because of the great climatic diversity of the territory, and its long viticultural tradition makes it possible for the studies to be replicated in other regions with very similar climates.

This study has focused on presenting the average climatic conditions that the wine sector will face in the coming decades, allowing winegrowers to have a snapshot of the new changes they will have to face. Therefore, the impacts that some extreme events (such as extreme rainfall, hail, droughts, among others) may have on the sector in the coming decades have not been included. Following this study, it is necessary to go a step further by assessing the impact of extreme events as well as the impact on the phenological stages of the vine through relationships between these and meteorological variables.

On the other hand, future studies should be carried out in the small parts of the island territory not included in this study, such as some iberian-balearic DOs as well as the Canary Islands.

4.4. Conclusions

Our results offer a precise and rigorous picture of the impacts that climate change will cause on the grapevine crop in the Iberian Peninsula based on currently available data applying a set of six bioclimatic indices and using, for the first time, local future climate scenarios based on ESMs from the fifth IPCC report and working locally.

The Iberian-peninsular territory will be the wine-growing region

most sensitive to the impact of climate change in the twenty-first century as reflected by the results obtained for the different indices, especially those dependent on thermal and hydric conditions. Progressive increases in temperatures are expected, both maximum and minimum, as indicated by the thermal indicators (HI and CI), while the water shortage (DI) will be more pronounced. The combination of the expected changes of both variables will have a strong impact on the vineyard, modifying the final organoleptic characteristics in the best of cases, but also leaving a large part of the Iberian Peninsula within the optimal thermal limits for growing vines, which it may have dramatic results for grapevine growing.

The northern and mountainous areas of the peninsula, having climatic characteristics colder and wetter than in the south, are expected to benefit from climatic variations that will allow them to adapt to climate change in a positive way, either by changing the grape variety or by regulating the water supply, among other measures. The central and southern areas of the peninsula (with strong periods of water scarcity and high temperatures) will have problems in maintaining certain types of grape and tillage techniques. They will not reach the minimum water requirements and will exceed the thermal requirements that the different grape varieties need to ripen. Therefore, these territories will be forced to rethink vineyard management techniques that allow them to counteract these negative effects or assess the economic viability of continuing to cultivate vineyards in the same regions.

These results provide valuable information for decision making in this sector to develop adaptation measures to climate change at the local scale.

Funding

This study has been partially supported by the Ministry for the Ecological Transition and the Demographic Challenge (MITECO) of the Spanish Government under the projects “Spanish VITicultural characterisation under conditions of CLIMAte change (VITCLIMA)” and “Impacts on AGROecology due to CLImate Change and Climate Variability EXtreme (AGROCLIMEX)”.

CRediT authorship contribution statement

Emma Gaitán: Conceptualization, Formal analysis, Methodology, Investigation, Writing – original draft. **Mª. Rosa Pino-Otín:** Conceptualization, Formal analysis, Investigation, Project administration, Resources, Supervision, Validation, Writing – original draft, Writing – review & editing.

Declaration of Competing Interest

The authors declare that they have no known competing financial interests or personal relationships that could have appeared to influence the work reported in this paper.

Data availability

Data will be made available on request.

Acknowledgements

We are grateful to the Spanish State Meteorological Agency (Aemet) for providing the data from the weather stations used in the study as well as to the Coupled Model Intercomparision phase 5 (CMIP5) for making the outputs of the climate models available.

Appendix A. Supplementary data

Supplementary data to this article can be found online at https://doi.org/10.1016/j.atmosres.2023.106660.

References

Abaurrea, J., Asín, J., Cebrián, A.C., 2018. Modelling the occurrence of heat waves in maximum and minimum temperatures over Spain and projections for the period 2031-60. Glob. Planet. Chang. 161, 244–260. ISSN 0921-8181,. https://doi.org/10.1016/j.gloplacha.2017.11.015.

Aleixandre, J.L., Giner, J.F., Aleixandre–Tudó, J.L., 2013. Evaluación del efecto terroir sobre la calidad de la uva y el vino. Enoviticultura N20.

Alig, R.J., Adams, D.M., McCarl, B.A., 2002. Projecting impacts of global climate change on the US forest and agriculture sectors and carbon budgets. For. Ecol. Manag. 169, 3–14.

Alonso, A.D., O'Neill, M.A., 2011. Climate change from the perspective of Spanish wine growers: a three-region study. Br. Food J. 113, 205–221.

Ascenso, A., Gama, C., Blanco-Ward, D., Monteiro, A., Silveira, C., Viceto, C., et al., 2021. Assessing Douro vineyards exposure to tropospheric ozone. Atmosphere 12.

Battaglini, A., Barbeau, G., Bindi, M., Badeck, F.-W., 2009. European winegrowers' perceptions of climate change impact and options for adaptation. Reg. Environ. Chang. 9, 61–73.

Bentsen, M., Bethke, I., Debernard, J.B., Iversen, T., Kirkevag, A., Seland, O., et al., 2013. The Norwegian earth system model, NorESM1-M - part 1: description and basic evaluation of the physical climate. Geosci. Model Dev. 6, 687–720.

Bindi, M., Fibbi, L., Gozzini, B., Orlandini, S., Miglietta, F., 1996. Modelling the impact of future climate scenarios on yield and yield variability of grapevine. Clim. Res. 7, 213–224.

Bindi, M., Fibbi, L., Lanini, M., Miglietta, F., 2001. Free air CO_2 enrichment (FACE) of grapevine (*Vitis vinifera* L.): I. Development and testing of the system for CO_2 enrichment. Eur. J. Agron. 14, 135–143.

Blanco-Ward, D., Garcia Queijeiro, J.M., Jones, G.V., 2007. Spatial climate variability and viticulture in the Mino River Valley of Spain. Vitis 46, 63–70.

Bock, A., Sparks, T., Estrella, N., Menzel, A., 2011. Changes in the phenology and composition of wine from Franconia, Germany. Clim. Res. 50, 69–81.

Bonfante, A., Alfieri, S.M., Albrizio, R., Basile, A., De Mascellis, R., Gambuti, A., Giorio, P., Langella, G., Manna, P., Monaco, E., et al., 2017. Evaluation of the effects of future climate change on grape quality through a physically based model application: a case study for the Aglianico grapevine in Campania region, Italy. Agric. Syst. 152, 100–109.

Bonfante, A., Monaco, E., Langella, G., Mercogliano, P., Bucchignani, E., Manna, P., Terribile, F., 2018. A dynamic viticultural zoning to explore the resilience of terroir concept under climate change. Sci. Total Environ. 624, 294–308.

Branas, J., 1974. Viticulture générale. Dehan, Montpellier, p. 990.

Branas, J., Bernon, G., Levadoux, L., 1946. eléments de viticulture générale.

Carbonneau, A., Tonietto, J., 1998. La géoviticulture: de la géographie viticole aux évolutions climatiques et technologiques à l'échelle mondiale. Rev. Oenol. Tech. Vitivin. Oenol. 87, 16–18.

Christensen, J.H., Kjellstrom, E., Giorgi, F., Lenderink, G., Rummukainen, M., 2010. Weight assignment in regional climate models. Clim. Res. 44, 179–194.

Chylek, P., Li, J., Dubey, M.K., Wang, M., Lesins, G., 2011. Observed and model simulated 20th century Arctic temperature variability: Canadian Earth System Model CanESM2. Atmos. Chem. Phys. Discuss. 11, 22893–22907.

Collins, W.J., Bellouin, N., Doutriaux-Boucher, M., Gedney, N., Hinton, T., Jone, C.D., Liddicoat, S., Martin, G., O'Connor, F., Rae, J., Senior, C., Totterdell, I., Woodward, S., Reichler, T., Kim, J., Halloran, P., 2008. Evaluation of the HadGEM2 Model. Hadley Centre Technical Note HCTN. Met Office Hadley Centre, Exeter, UK, p. 74.

Combris, P., Lecocq, S., Visser, M., 1997. Estimation of a hedonic price equation for Bordeaux wine: does quality matter? Econ. J. 1997 (107), 3–390.

Costa, J.M., Ortuño, M.F., Lopes, C.M., Chaves, M.M., 2012. Grapevine varieties exhibiting differences in stomatal response to water deficit. Funct. Plant Biol. 39, 179–189.

Damiano, N., Arena, C., Bonfante, A., Caputo, R., Erbaggio, A., Cirillo, C., et al., 2022. How leaf vein and stomata traits are related with photosynthetic efficiency in Falanghina grapevine in different pedoclimatic conditions. Plants-Basel 11.

Doll, P., 2002. Impact of climate change and variability on irrigation requirements: a global perspective. Clim. Chang. 54, 269–293.

Duchene, E., 2016. How can grapevine genetics contribute to the adaptation to climate change? OENO One 50.

Duchene, E., Schneider, C., 2005. Grapevine and climatic changes: a glance at the situation in Alsace. Agron. Sustain. Dev. 25, 93–99.

Duchene, E., Huard, F., Dumas, V., Schneider, C., Merdinoglu, D., 2010. The challenge of adapting grapevine varieties to climate change. Clim. Res. 41, 193–204.

Dunne, J.P., John, J.G., Shevliakova, E., Stouffer, R.J., Krasting, J.P., Malyshev, S.L., et al., 2013. GFDL's ESM2 global coupled climate-carbon earth system models. Part II: Carbon system formulation and baseline simulation characteristics. J. Clim. 26, 2247–2267.

Escariz, A., Blanco, J., Miranda, D., Crecente, R., 2007. Zonificación y metodología para la delimitación de comarcas vitícolas. Aplicación a la ampliación de vino de la tierra de Betanzos. In: XI congreso internacional de Ingenieria de proyectos Lugo.

EXPANSIÓN, 2016. https://www.expansion.com/economia/2019/12/16/5df6afff468aebed0c8b467f.html.

EXPANSIÓN, 2019. https://www.researchgate.net/publication/345973796_Impacto_adaptacion_y_percepcion_del_cambio_climatico_en_la_DOCa_Rioja.

FEV, 2021. https://www.expansion.com/economia/2019/12/16/5df6afff468aebed0c8b467f.html.

Fonseca Conceicao, M.A., Tonietto, J., Fialho, F.B., 2012. Using temperature to calculate the dryness index of grape production regions. Rev. Bras. Frutic. 34, 175–182.

Fraga, H., Santos, J.A., 2017. Daily prediction of seasonal grapevine production in the Douro wine region based on favourable meteorological conditions. Aust. J. Grape Wine Res.
Fraga, H., Santos, J.A., Malheiro, A.C., Moutinho-Pereira, J., 2012. Climate change projections for the portuguese viticulture using a multi-model ensemble. Cienc. Tec. Vitivinic. 27, 39–48.
Fraga, H., Malheiro, A.C., Moutinho-Pereira, J., Santos, J.A., 2013. Future scenarios for viticultural zoning in Europe: ensemble projections and uncertainties. Int. J. Biometeorol. 57, 909–925.
Fraga, H., Malheiro, A.C., Moutinho-Pereira, J., Jones, G.V., Alves, F., Pinto, J.G., et al., 2014. Very high resolution bioclimatic zoning of Portuguese wine regions: present and future scenarios. Reg. Environ. Chang. 14, 295–306.
Fraga, H., Santos, J.A., Malheiro, A.C., Oliveira, A.A., Moutinho-Pereira, J., Jones, G.V., 2016. Climatic suitability of Portuguese grapevine varieties and climate change adaptation. Int. J. Climatol. 36, 1–12.
Fraga, H., de Cortázar, García, Atauri, I., Santos, J.A., 2018. Viticultural irrigation demands under climate change scenarios in Portugal. Agric. Water Manag. 196, 66–74.
Fraga, H., Pinto, J.G., Santos, J.A., 2019. Climate change projections for chilling and heat forcing conditions in European vineyards and olive orchards: a multi-model assessment. Clim. Chang. 152, 179–193.
France, I., Dubourdieu, A.D., 2016. Climate change: field reports from leading winemakers. J. Wine Econ. 11, 5–47.
Fregoni, M., 2003. L'indice bioclimatico di qualitá Fregoni. Terroir, Zonazione Viticoltura 2003, 115–127.
Gaitan, E., Monjo, R., Portoles, J., Rosa, Pino-Otin M., 2019. Projection of temperatures and heat and cold waves for Aragon (Spain) using a two-step statistical downscaling of CMIP5 model outputs. Sci. Total Environ. 650, 2778–2795.
Gaitan, E., Monjo, R., Portoles, J., Rosa, Pino-Otin M., 2020. Impact of climate change on drought in Aragon (NE Spain). Sci. Total Environ. 740.
Gallo, A.E., Perez Pena, J.E., Prieto, J.A., 2021. Mechanisms underlying photosynthetic acclimation to high temperature are different between *Vitis vinifera* cv. Syrah and Grenache. Funct. Plant Biol. 48, 342–357.
García de Cortázar-Atauri, I., Duchêne, E., Destrac-Irvine, A., Barbeau, G., de Rességuier, L., Lacombe, T., Parker, A.K., Saurin, N., van Leeuwen, C., 2017. Grapevine phenology in France: from past observations to future evolutions in the context of climate change. OENO One 51.
Gisbert, C., Soler, J.X., Fos, M., Intrigliolo, D.S., Yuste, A., Pico, B., et al., 2022. Characterization of local Mediterranean grapevine varieties for their resilience to semi-arid conditions under a rain-fed regime. Agronomy-Basel 12.
Goicoechea, N., Jimenez, L., Prieto, E., Gogorcena, Y., Pascual, I., Irigoyen, J.J., et al., 2021. Assessment of nutritional and quality properties of leaves and musts in three local Spanish grapevine varieties undergoing controlled climate change scenarios. Plants-Basel 10.
Gomez-Gesteira, M., Gimeno, L., deCastro, M., Lorenzo, M.N., Alvarez, I., Nieto, R., et al., 2011. The state of climate in NW Iberia. Clim. Res. 48, 109–144.
Gomez-Martinez, G., Galiano, L., Rubio, T., Prado-Lopez, C., Redolat, D., Blazquez, C.P., et al., 2021. Effects of climate change on water quality in the Jucar River Basin (Spain). Water 13.
Goncalves, B., Falco, V., Moutinho-Pereira, J., Bacelar, E., Peixoto, F., Correia, C., 2009. Effects of elevated CO_2 on grapevine (*Vitis vinifera* L.): volatile composition, phenolic content, and in vitro antioxidant activity of red wine. J. Agric. Food Chem. 57, 265–273.
Gu, S., Ding, P., Howard, S., 2002. Effect of temperature and exposure time on cold hardiness of primary buds during the dormant season in 'Concord', 'Norton', 'Vignoles' and 'St. Vincent' grapevines. J. Hortic. Sci. Biotechnol. 77, 635–639. https://doi.org/10.1080/14620316.2002.11511550.
Guido, V., 2015. Impact of climate change on *Vitis Vinifera* L. over Mediterranean area. In: Tesi di Dottorato in Agrometeorologia ed Ecofisiologia dei Sistemi Agrari e Forestali. Università degli Studi di Sassari.
Gutierrez, J.M., Maraun, D., Widmann, M., Huth, R., Hertig, E., Benestad, R., et al., 2019. An intercomparison of a large ensemble of statistical downscaling methods over Europe: results from the VALUE perfect predictor cross-validation experiment. Int. J. Climatol. 39, 3750–3785.
Hannah, L., Roehrdanz, P.R., Ikegami, M., Shepard, A.V., Shaw, M.R., Tabor, G., et al., 2013. Climate change, wine, and conservation. Proc. Natl. Acad. Sci. U. S. A. 110, 6907–6912.
Holland, T., Smit, B., 2010. Climate change and the wine industry: current research themes and new directions. J. Wine Res. 21, 125–136.
Huglin, P., 1978. Nouveau Mode d'Évaluation des Possibilités Héliothermiques d'un Milieu Viticole. C. R. Acad. Agr. France 1117–1126.
Iglesias, A., Quiroga, S., Moneo, M., Garrote, L., 2012. From climate change impacts to the development of adaptation strategies: challenges for agriculture in Europe. Clim. Chang. 112, 143–168.
Isaksen, I.S.A., Wang, W.C., 2002. Atmospheric ozone and climate change. In: 3rd International Symposium on Non-CO_2 Greenhouse Gases, Maastricht, Netherlands, pp. 319–330.
Iversen, T., Bentsen, M., Bethke, I., Debernard, J.B., Kirkevag, A., Seland, O., et al., 2013. The Norwegian earth system model, NorESM1-M - part 2: climate response and scenario projections. Geosci. Model Dev. 6, 389–415.
Jones, G.V., 2006. Climate and Terroir: Impacts of Climate Variability and Change on Win, in Fine Wine and Terroir - The Geoscience Perspective. In: Macqueen, R.W., Meinert, L.D. (Eds.), Geoscience Canada Reprint Series Number 9. Geological Association of Canada, St. John's, Newfoundland, p. 247.
Jones, G.V., Alves, F., 2012. Impact of climate change on wine production: a global overview and regional assessment in the Douro Valley of Portugal. Int. J. Glob. Warm. 4, 383–406.
Jones, G.V., Davis, R.E., 2000. Climate influences on grapevine phenology, grape composition, and wine production and quality for Bordeaux, France. Am. J. Enol. Vitic. 51, 249–261.
Jones, G.V., White, M.A., Cooper, O.R., Storchmann, K., 2005. Climate change and global wine quality. Clim. Chang. 73, 319–343.
Kenny, G.H., Harrison, P.A., 1993. The effects of climatic variability and change on grape suitability in Europe. J. Wine Res. 4, 163–183.
Kizildeniz, T., Pascual, I., Irigoyen, J.J., Morales, F., 2021. Future CO_2, warming and water deficit impact white and red Tempranillo grapevine: photosynthetic acclimation to elevated CO_2 and biomass allocation. Physiol. Plant. 172, 1779–1794.
Knutti, R., Sedlacek, J., 2013. Robustness and uncertainties in the new CMIP5 climate model projections. Nat. Clim. Chang. 3, 369–373.
Kohler, J., Hernandez, J.A., Caravaca, F., Roldan, A., 2008. Plant-growth-promoting rhizobacteria and arbuscular mycorrhizal fungi modify alleviation biochemical mechanisms in water-stressed plants. Funct. Plant Biol. 35, 141–151.
Köppen, W., Geiger, R., 1936. Das geographische System der Klimate.
Kovaleski, A.P., Londo, J.P., 2019. Tempo of gene regulation in wild and cultivated *Vitis* species shows coordination between cold deacclimation and budbreak. Plant Sci. 287.
Lazoglou, G., Anagnostopoulou, C., Koundouras, S., 2018. Climate change projections for Greek viticulture as simulated by a regional climate model. Theor. Appl. Climatol. 133, 551–567.
Leolini, L., Moriondo, M., Romboli, Y., Gardiman, M., Costafreda-Aumedes, S., de Cortazar-Atauri, I.G., Bindi, M., Granchi, L., Brilli, L., 2019. Modelling sugar and acid content in Sangiovese grapes under future climates: an Italian case study. Clim. Res. 78, 211–224.
López, F., Cabrera, M., Cuadrat, J.M., 2007. Atlas Climático de Aragón, First ed. J. Factory, Spain.
Magalhaes, N., 2008. Tratado de viticultura: a videira, a vinha e o terroir. Chaves Ferreira Publicacoes, Lisboa, Portugal.
Malheiro, A.C., Santos, J.A., Fraga, H., Pinto, J.G., 2010. Climate change scenarios applied to viticultural zoning in Europe. Clim. Res. 43, 163–177.
Marsland, S.J., Haak, H., Jungclaus, J.H., Latif, M., Roske, F., 2003. The Max-Planck-Institute global ocean/sea ice model with orthogonal curvilinear coordinates. Ocean Model. 5, 91–127.
Meehl, G.A., Stocker, T.F., Collins, W.D., Friedlingstein, P., Gaye, A.T., Gregory, J.M., et al., 2007. Global Climate Projections 2007: The Physical Science Basis, pp. 747–845.
Molina, M.O., Sánchez, E., Gutiérrez, C., 2020. Future heat waves over the Mediterranean from an Euro-CORDEX regional climate model ensemble. Sci. Rep. 10, 8801. https://doi.org/10.1038/s41598-020-65663-0.
Molitor, D., Junk, J., 2019. Climate change is implicating a two-fold impact on air temperature increase in the ripening period under the conditions of the Luxembourgish grapegrowing region. OENO One 53, 409–422.
Monjo, R., Gaitan, E., Portoles, J., Ribalaygua, J., Torres, L., 2016. Changes in extreme precipitation over Spain using statistical downscaling of CMIP5 projections. Int. J. Climatol. 36, 757–769.
Moriondo, M., Maselli, F., Bindi, M., 2007. A simple model of regional wheat yield based on NDVI data. Eur. J. Agron. 26, 266–274.
Mosedale, J.R., Abernethy, K.E., Smart, R.E., Wilson, R.J., Maclean, I.M.D., 2016. Climate change impacts and adaptive strategies: lessons from the grapevine. Glob. Chang. Biol. 22, 3814–3828.
Moss, R.H., Edmonds, J.A., Hibbard, K.A., Manning, M.R., Rose, S.K., van Vuuren, D.P., et al., 2010. The next generation of scenarios for climate change research and assessment. Nature 463, 747–756.
Moutahir, H., Bellot, P., Monjo, R., Bellot, J., Garcia, M., Touhami, I., 2017. Likely effects of climate change on groundwater availability in a Mediterranean region of Southeastern Spain. Hydrol. Process. 31, 161–176.
Moutinho-Pereira, J., Goncalves, B., Bacelar, E., Cunha, J.B., Coutinho, J., Correia, C.M., 2009. Effects of elevated CO_2 on grapevine (*Vitis vinifera* L.): physiological and yield attributes. Vitis 48, 159–165.
Munoz-Organero, G., Espinosa, F.E., Cabello, F., Zamorano, J.P., Urbanos, M.A., Puertas, B., et al., 2022. Phenological study of 53 Spanish minority grape varieties to search for adaptation of vitiviniculture to climate change conditions. Horticulturae 8.
Neumann, P.A., Matzarakis, A., 2011. Viticulture in Southwest Germany under climate change conditions. Clim. Res. 47, 161–169.
Nogales, A., Ribeiro, H., Nogales-Bueno, J., Hansen, L.D., Goncalves, E.F., Coito, J.L., et al., 2020. Response of mycorrhizal 'touriga nacional' variety grapevines to high temperatures measured by calorespirometry and near-infrared spectroscopy. Plants-Basel 9.
Odo Camps, J., Ramos, M.C., 2012. Grape harvest and yield responses to inter-annual changes in temperature and precipitation in an area of north-East Spain with a Mediterranean climate. Int. J. Biometeorol. 56, 853–864.
Ollat, N., Touzard, J.M., van Leeuwen, C., 2016. Climate change impacts and adaptations: new challenges for the wine industry. J. Wine Econ. 11, 139–149.
Popescu, Simona, Popa, Aurel, Gavrilescu, Elena, Marius, Gruia, 2012. The effects of air pollution on the main physiological processes of the grapevine grown in the vicinity of a power plant. Carpathian J. Earth Environ. Sci. 7, 61–70.
Porter, J.R., Semenov, M.A., 2005. Crop responses to climatic variation. Philos. Trans. R. Soc. B Biol. Sci. 360, 2021–2035.

Raddatz, T.J., Reick, C.H., Knorr, W., Kattge, J., Roeckner, E., Schnur, R., et al., 2007. Will the tropical land biosphere dominate the climate-carbon cycle feedback during the twenty-first century? Clim. Dyn. 29, 565–574.
Ramos, M.C., 2017. Projection of phenology response to climate change in rainfed vineyards in north-East Spain. Agric. For. Meteorol. 247, 104–115.
Ramos, M.C., Martinez de Toda, F., 2020. Variability in the potential effects of climate change on phenology and on grape composition of Tempranillo in three zones of the Rioja DOCa (Spain). Eur. J. Agron. 115.
Ramos, M.C., Martinez de Toda, F., 2021. Interannual and spatial variability of grape composition in the Rioja DOCa show better resilience of cv. Graciano than cv. Tempranillo under a warming scenario. Oeno One 55, 85–100.
Ramos, M.C., Jones, G.V., Martinez-Casasnovas, J.A., 2008. Structure and trends in climate parameters affecting winegrape production in Northeast Spain. Clim. Res. 38, 1–15.
Ramos, M.C., Jones, G.V., Yuste, J., 2017. Variability of Tempranillo grape quality within the Ribera del Duero do (Spain) and relationships with climatic characteristics. J. Vitic. Enol. N 12/1.
Resco, P., Iglesias, A., Bardaji, I., Sotes, V., 2016. Exploring adaptation choices for grapevine regions in Spain. Reg. Environ. Chang. 16, 979–993.
Ribalaygua, J., Rosa Pino, M., Portoles, J., Roldan, E., Gaitan, E., Chinarro, D., et al., 2013a. Climate change scenarios for temperature and precipitation in Aragon (Spain). Sci. Total Environ. 463, 1015–1030.
Ribalaygua, J., Torres, L., Portoles, J., Monjo, R., Gaitan, E., Pino, M.R., 2013b. Description and validation of a two-step analogue/regression downscaling method. Theor. Appl. Climatol. 114, 253–269.
Ribalaygua, J., Gaitan, E., Portoles, J., Monjo, R., 2018. Climatic change on the Gulf of Fonseca (Central America) using two-step statistical downscaling of CMIP5 model outputs. Theor. Appl. Climatol. 132, 867–883.
Riou, C.H., Becker, N., Sotes Ruiz, V., Gomez-Miguel, V., Carbonneau, A., Panagiotou, M., Calo, A., Costacurta, A., Castro de, R., Pinto, A., Lopes, C., Carneiro, L., Climaco, P., 1994. Le déterminisme climatique de la maturation du raisin: application au zonage de la teneur em sucre dans la communauté européenne. Office des Publications Officielles des Communautés Européennes, Luxembourg, p. 322.
Rodriguez, R., Navarro, X., Casas, M.C., Ribalaygua, J., Russo, B., Pouget, L., et al., 2014. Influence of climate change on IDF curves for the metropolitan area of Barcelona (Spain). Int. J. Climatol. 34, 643–654.
Santiago, J.M., Munoz-Mas, R., Solana-Gutierrez, J., de Jalon, D.G., Alonso, C., MartinezCapel, F., et al., 2017. Waning habitats due to climate change: the effects of changes in streamflow and temperature at the rear edge of the distribution of a cold-water fish. Hydrol. Earth Syst. Sci. 21.
Santos, J.A., Malheiro, A.C., Karremann, M.K., Pinto, J.G., 2011. Statistical modelling of grapevine yield in the Port Wine region under present and future climate conditions. Int. J. Biometeorol. 55, 119–131.
Santos, J.A., Malheiro, A.C., Pinto, J.G., Jones, G.V., 2012. Macroclimate and viticultural zoning in Europe: observed trends and atmospheric forcing. Clim. Res. 51, 89–103.
Santos, M., Fonseca, A., Fraga, H., Jones, G.V., Santos, J.A., 2020. Bioclimatic conditions of the Portuguese wine denominations of origin under changing climates. Int. J. Climatol. 40, 927–941.
Schreiner, R.P., Tarara, J.M., Smithyman, R.P., 2007. Deficit irrigation promotes arbuscular colonization of fine roots by mycorrhizal fungi in grapevines (*Vitis vinifera* L.) in an arid climate. Mycorrhiza 17, 551–562.
Schultz, H.R., 2000. Climate change and viticulture: a European perspective on climatology, carbon dioxide and UV-B effects. Aust. J. Grape Wine Res. 6, 2–12.
Schultz, H.R., Stoll, M., 2010. Some critical issues in environmental physiology of grapevines: future challenges and current limitations. Aust. J. Grape Wine Res. 16, 4–24.
Sgubin, G., Swingedouw, D., Dayon, G., Garcia de Cortazar-Atauri, I., Ollat, N., Pagé, C., Van Leeuwen, C., 2018. The risk of tardive frost damage in French vineyards in a changing climate. Agric. For. Meteorol. 250–251, 226–242.
Stock, M., Gerstengarbe, F.W., Kartschall, T., Werner, P.C., 2004. Reliability of climate change impact assessments for viticulture. In: 7th International Symposium on Grapevine Physiology and Biotechnology, Davis, CA, pp. 29–39.
Tate, A.B., 2001. Global warming's impact on wine. J. Wine Res. 12, 95–109.
Taylor, K.E., Stouffer, R.J., Meehl, G.A., 2012. An overview of CMIP5 and the experiment design. Bull. Am. Meteorol. Soc. 93, 485–498.
Tonietto, J., 1999. Les Macroclimats Viticoles Mondiaux et l'Influence du Mésoclimat sur la Typicité de la Syrah et du Muscat de Hambourg dans le Sud de la France: Méthodologie de Caráctérisation. Thèse Doctorat. Ecole Nationale Supérieure Agronomique, Montpellier.
Tonietto, J., Carbonneau, A., 2004. A multicriteria climatic classification system for grape-growing regions worldwide. Agric. For. Meteorol. 124, 81–97.
Torres, C., Jordà, G., de Vílchez, P., Vaquer-Sunyer, R., Rita, J., Canals, V., Cladera, A., Escalona, J.M., Miranda, M.Á., 2021. Climate change and their impacts in the Balearic Islands: a guide for policy design in Mediterranean regions. Reg. Environ. Change 21 (4), 107. https://doi.org/10.1007/s10113-021-01810-1. Epub 2021 Oct 23. 34720740. PMC8536903.
Tripathi, S., Srinivas, V.V., Nanjundiah, R.S., 2006. Dowinscaling of precipitation for climate change scenarios: a support vector machine approach. J. Hydrol. 330, 621–640.
Trouvelot, S., Bonneau, L., Redecker, D., van Tuinen, D., Adrian, M., Wipf, D., 2015. Arbuscular mycorrhiza symbiosis in viticulture: a review. Agron. Sustain. Dev. 35, 1449–1467.
ENSEMBLES: climate change and its impacts. In: Van der Linden, P., Mitchell, J. (Eds.), 2009. Summary of Research and Results from the ENSEMBLES Project. Met Office Hadley Centre, FitzRoy Road, Exeter EX1 3PB, UK, p. 160.
Van Leeuwen, C., Friant, P., Chone, X., Tregoat, O., Koundouras, S., Dubourdieu, D., 2004. Influence of climate, soil, and cultivar on terroir. Am. J. Enol. Vitic. 55, 207–217.
Vanderlinden, K., Giraldez, J.V., Van Meirvenne, M., 2004. Assessing reference evapotranspiration by the Hargreaves method in southern Spain. J. Irrig. Drain. Eng. 130, 184–191.
Voldoire, A., Sanchez-Gomez, E., Salas y Melia, D., Decharme, B., Cassou, C., Senesi, S., et al., 2013. The CNRM-CM5.1 global climate model: description and basic evaluation. Clim. Dyn. 40, 2091–2121.
Wang, B., Zhou, T., Yu, Y., 2010. A view of earth system model development (vol 23, pg 1, 2009). Acta Meteorol. Sin. 24, 547.
Watanabe, S., Hajima, T., Sudo, K., Nagashima, T., Takemura, T., Okajima, H., et al., 2011. MIROC-ESM 2010: model description and basic results of CMIP5-20c3m experiments. Geosci. Model Dev. 4, 845–872.
Webb, L.B., Whetton, P.H., Barlow, E.W.R., 2008. Modelling the relationship between climate, winegrape price and winegrape quality in Australia. Clim. Res. 36, 89–98.
Weigel, A.P., Knutti, R., Liniger, M.A., Appenzeller, C., 2010. Risks of model weighting in multimodel climate projections. J. Clim. 23, 4175–4191.
White, M.A., Diffenbaugh, N.S., Jones, G.V., Pal, J.S., Giorgi, F., 2006. Extreme heat reduces and shifts United States premium wine production in the 21st century. Proc. Natl. Acad. Sci. U. S. A. 103, 11217–11222.
Winkler, A.J., 1974. General Viticulture. University of California Press, CA.
Xiao-Ge, X., Tong-Wen, W., Jie, Z., 2013. Introduction of CMIP5 experiments carried out with the climate system models of Beijing climate Center. Adv. Clim. Chang. Res. 4, 41–49. https://doi.org/10.3724/SP.J.1248.2013.041.
Ye, Q., Wang, H., Li, H., 2022. Arbuscular mycorrhizal fungi improve growth, photosynthetic activity, and chlorophyll fluorescence of *Vitis vinifera* L. cv. ecolly under drought stress. Agronomy-Basel 12.
Yukimoto, S., Yoshimura, H., Hosaka, M., Sakami, T., Tsujino, H., Hirabara, M., Tanaka, T.Y., Deushi, M., Obata, A., Nakano, H., Adachi, Y., Shindo, E., Yabu, S., Ose, T., Kitoh, A., 2011. Meteorological Research Institute- Earth System Model v1 (MRI-ESM1)— Model Description. Technical Report of MRI, p. 64.
Zha, Q, Xi, X, He, Y, Jiang, A, 2018. Comprehensive evaluation of heat resistance in 68 Vitis germplasm resources. Vitis 57, 75–81.